

UNCLASSIFIED
AD

227876

FOR
MICRO-CARD
CONTROL ONLY

1

OF

9

Reproduced by

Armed Services Technical Information Agency

ARLINGTON HALL STATION; ARLINGTON 12 VIRGINIA

UNCLASSIFIED

"NOTICE: When Government or other drawings, specifications or other data are used for any purpose other than in connection with a definitely related Government procurement operation, the U.S. Government thereby incurs no responsibility, nor any obligation whatsoever; and the fact that the Government may have formulated, furnished, or in any way supplied the said drawings, specifications or other data is not to be regarded by implication or otherwise as in any manner licensing the holder or any other person or corporation, or conveying any rights or permission to manufacture, use or sell any patented invention that may in any way be related thereto."

THE
MECHANICS
OF
AEROSOLS
FUCK

227876

CWLS 12
PUB. 4 12

U.S.
CHEM.
CO.

FILE COPY

Return to (9)

ASTIA

ARLINGTON HALL STATION

ARLINGTON 12, VIRGINIA

ATTN: TISSO

CWL Special Publication 4-12

THE MECHANICS OF AEROSOLS

by

N. A. FUKS
Academy of Sciences of the U. S. S. R.
Institute of Scientific Information
1955

Translated from the Russian by
MSP. E. Tachowicz

Technical Information Division
Directorate of Technical Services
U. S. ARMY CHEMICAL WARFARE LABORATORIES
Army Chemical Center, Maryland

FOREWORD

Translated 1958 under sponsorship of the CWL Technical Library, Technical Information Division, by MSP. E. Lachowicz, U. S. Army Chemical Warfare Laboratories, from the original in Russian by N. A. Fuks, Academy of Sciences of the U. S. S. R. - Institute of Scientific Information, Moscow 1955.

Corrections of printing errors listed by the author on page 353 were absorbed in course of translation of this book.

The primary technical review of the translation was made by Dr. Leo Finkelstein, consultant to the C. W. Laboratories on aerosols, and for many years, prior to retirement, in charge of aerosol investigations. Other technical reviewers include Dr. W. Ranz, Penn State University and Mr. Robert D. Kracke of these Laboratories. Editorial reviewer was Mrs. Meirel K. Salamon of these Laboratories.

Editor-in-Chief

B. V. DERYAGIN

Associate Correspondent of

The Academy of Sciences of the U. S. S. R.

CONTENTS

	<u>Page</u>
The Most Important Symbols	vii
Introduction	1

Chapter I.

Classification of Aerosols. Dimensions and Shape of Particles in Aerosols.

§ 1. - Classification of Aerosols	7
§ 2. - Dimensions of Particles in Aerosols	9
§ 3. - Distribution of Particle Dimensions in Aerosols	13
§ 4. - "Average" Sizes of Aerosol Particles	26
§ 5. - Shape and Formation of Aerosol Particles	30

Chapter II.

Rectilinear, Uniform Motion of Aerosol Particles

§ 6. - Resistance of a Gaseous Medium to Motion of Very Small Particles	37
§ 7. - STOKES' Law Equation	39
§ 8. - Resistance of the Medium in a Transitional Region	43
§ 9. - Experimental Proof of STOKES' Law and Its Exactness ..	48
§ 10. - Resistance of the Medium Within Ultra-STOKES' Region .	50
§ 11. - General Properties of Motion of Non-Spherical Particles	54
§ 12. - Resistance of a Medium to Motion of Non-Spherical Particles	58
§ 13. - Settling of Clouds	68
§ 14. - Motion of Aerosols in a Confined Space	72
§ 15. - Vertical and Horizontal Electrical Field Methods and Their Application	74
§ 16. - Radiometric Forces in Aerosols (Thermophoresis)	82

Chapter III.

Rectilinear Irregular Motion of Aerosol Particles.

§ 17. - Nonuniform Motion of Particles With Small Re Numbers .	93
--	----

§ 18. - Nonuniform Motion of Particles at Greater Re Numbers	101
§ 19. - Oscillations of Aerosol Particles Actuated by a Periodical External Force	104
§ 20. - Oscillations of Aerosol Particles Actuated by Sonic Waves	109
§ 21. - Sonic Pressure Upon Aerosol Particles	114
§ 22. - Dispersion and Absorption of Sonic Waves by Aerosols	116
§ 23. - Hydrodynamic Interaction Between Aerosol Particles ...	123
§ 24. - Electrostatic Dispersion of Aerosols	129

Chapter IV

Curvilinear Motion of Aerosol Particles

§ 25. - General Theory of a Curvilinear Motion of Particles. Precipitation of Aerosols in an Alternating Horizontal Electrical Field	133
§ 26. - Precipitation of Aerosols During Laminar Flow Under the Influence of Gravity	136
§ 27. - Precipitation of Aerosols During Laminar Flow Under the Influence of an Electrical Field	140
§ 28. - Precipitation of Aerosols in a Field of Centrifugal Force. Aerosolic Centrifuge	154
§ 29. - Cyclones	158
§ 30. - Determination of Trajectories of Aerosol Particles in Curvilinear Flow	167
§ 31. - Theory of Similarity in the Mechanics of Aerosols	170
§ 32. - Theory of Procurement of Aerosol Specimens	177
§ 33. - Slit Instruments	183
§ 34. - Inertial Precipitation of Aerosols Upon Substances of Ordinary Shape	189

Chapter V

Brownian Movement and Diffusion in Aerosols

§ 35. - Brownian Movement in Aerosols	201
§ 36. - Experimental Study of the Brownian Movement in Aerosols	207
§ 37. - Probabilities of Transition. Occurrence and Arrival at a Boundary of Particles	212

§ 38. - Diffusible Precipitation of Aerosol in an Immobile Medium	220
§ 39. - Diffusion of Aerosols in Laminar Flow	233
§ 40. - Cloth and Fibrous Filters	240
§ 41. - Precipitation of Aerosols in Respiratory Tracts	258
§ 42. - Absorption of Aerosols During Bubbling	266
§ 43. - Brownian Spinning. Orientation of Aerosol Particles in an Electrical Field	272

Chapter VI

Convective and Turbulent Diffusion in Aerosols

§ 44. - Precipitation of Aerosols During Convection and Turbulence	279
§ 45. - Movement of Aerosol Particles in Turbulent Flow	290
§ 46. - Precipitation of Aerosols in Turbulent Flow	297
§ 47. - Spreading of Aerosols in the Atmosphere	308
§ 48. - Fall-out of Aerosols From the Atmosphere	325

Chapter VII

Coagulation of Aerosols

§ 49. - Thermal (Brownian) Coagulation of Aerosols With Spherical Particles	329
§ 50. - Coagulation of Aerosols With Particles of Elongated Shape	347
§ 51. - Thermal Coagulation of Aerosols With Charged Particles. Influence of Molecular Forces Upon Rapidity of Coagulation	352
§ 52. - Coagulation of Aerosols in an Electrical Field. "Directed" Coagulation	358
§ 53. - Coagulation of Aerosols Under the Influence of Ultrasonic Oscillations	365
§ 54. - Kinematic (Gravitational) Coagulation of Aerosols	370
§ 55. - Coagulation of Aerosols During Agitation and in Turbulent Flow	383
§ 56. - Effectiveness of Collisions Between Aerosol Particles	390

The Most Important Symbols

A	coefficient in CUNNINGHAM'S equation .
B	particle mobility.
C_E	electrical capacity.
D	coefficient of diffusion.
D_t	coefficient of turbulent diffusion.
E	field potential.
Erf	KRAMP'S function.
3	effectiveness of precipitation in a filter, etc.
F	force.
F_M	medium's resistance.
F(r)	calculated integral function of distribution.
Φ	volumetric velocity of gas; number of particles precipitating or passing in 1 sec. over a surface; yield of a point source.
Φ'	number of particles precipitating in 1 sec. for a unit length. of a cylinder; yield of a line source (per cm length).
G	velocity of thermal movement of a particle.
G_g	velocity of thermal movement of gaseous molecules.
G(r)	gravimetric integral function of distribution.
∇	gradient (of velocity, temperature).
I	strength of current; flow (of particles, energy) in 1 sec. per cm ²
K	coagulation constant.
L	length.

M	molecular weight.
N	total number of particles.
P	moment of force; dipole moment.
Π	potential difference.
Q	LONDON'S equation constant.
R	radius of a sphere, cylinder.
R_g	gas constant.
Re	REYNOLD'S number for particles.
Re_f	REYNOLD'S number for flow.
S	area.
$Sc = \nu/D$	SCHMIDT'S number.
$Stk = l_i/2R$	STOKES' number.
T	temperature.
U	velocity of flow, current.
U_0	amplitude of velocity of medium's oscillation.
U^*	drag velocity.
V	velocity of a particle.
V_s	terminal velocity of settling of a particle.
V_E	velocity of a particle in an electrical field.
V_R	velocity of a particle in relation to a medium.
$W(x, t)$	probability of occurrence.
$W^*(x, t)$	probability of arrival at a boundary.

a	equatorial semi-axis of a spinning ellipsoid.
c	weight concentration; polar semi-axis of a spinning ellipsoid.
c_p	specific heat.
c_s	velocity of sound.
β	coefficient of settling, of capture.
$f(r)$	calculated function of distribution.
$g(r)$	gravimetric function of distribution.
g	acceleration of gravity.
k	BOLTZMANN'S constant.
l	mean length of gaseous molecular free path.
l_B	mean apparent length of particle free path.
l_i	inertial run-down of particles.
\ln	natural logarithm.
\lg	decimal logarithm.
m	mass of a particle.
m'	mass of a medium displaced by a particle.
m_g	mass of a gaseous molecule.
n	number of particles in 1 cm^3 .
p	pressure.
q	charge.
r	particle's radius.
r_e	equivalent radius.

r_s	sedimentation radius.
t	time.
t_p	oscillation period.
u	electrical mobility; mean quadratic fluctuation of a medium.
v	volume; mean quadratic fluctuation rate of a particle.
$w(x_0, x, t)$	probability of occurrence.
α	coefficient of accommodation, absorption (of aerosol, of sound).
γ	density of particle.
γ_g	density of a medium (gas).
δ	thickness of a layer, distance from a wall.
\mathcal{E}	elemental charge; energy dissipated in 1 sec. in 1 cm ³ of a medium.
ϵ_K	dielectric constant.
η	viscosity of a medium.
θ	polar angle.
κ	shape factor; KARMAN'S constant.
λ	wave length; scale of turbulent fluctuation.
λ_0	internal scale of turbulence.
ν	whole number; oscillation frequency; kinematic viscosity.
ρ	distance from a center, from an axis.
σ	specific free surface energy; electrical density.

- τ relaxation time, force of internal friction per cm^2 .
- τ_0 force of gas friction against wall per cm^2 .
- ϕ phase difference of oscillations.
- ϕ coefficient of apparent volume (volume of the dispersed phase in 1 cm^3 system).
- χ heat conductivity.
- ψ coefficient of drag resistance.
- $\psi(\rho)$ potential function.
- ω angular velocity, angular frequency.
- Ω energy.

Introduction

Aero-dispersion systems, or aerosols, which consist of solid or liquid particles suspended in a gaseous media, play a very important role in nature and in human life. It is sufficient to mention that the circulation of water has its beginning in a voluminous condensation of water-vapor, followed by formations of clouds, which subsequently result in rainfall. Furthermore, the resultant overcast which influences the climate to a great extent, protects the earth's surface from excessive heat from the sun rays and from cooling off by heat radiation. The processes of suspending, carrying-off, and depositing solid particles by the wind are even of greater importance. In the course of many centuries the action of "aerial carriers" formed huge loessic deposits (e.g., HWANG PU river basin). Desert sand carried by wind induces a constant conflict with cultivated and irrigated terrains, and if man ceased his struggle against this dreadful enemy, whole towns would soon be buried. Winds also cause great damage by erosion of loose arable land. Therefore, forest belts are of particular importance in the contest against dry winds: they protect fields, orchards, and canals from being buried, and top-soil from being carried away. The struggle against snow drifts is conducted in the same manner by the use of snow screens and fences.

At the time of cross-pollination of many plants (grasses and numerous trees) pollen is spread by winds as an aerosol. The dissemination of a considerable number of seeds and spores is effected in a similar manner. Many microorganisms floating in the air preserve their germinative power for a long time within the environs of colloidal substrata which are present there. Thus, the "atmospheric microflora" represents a large number of various fungi and bacteria which must be embraced in medicine and in fermentation work. Very many infectious diseases (grippe, whooping cough, pulmonary plague, and tuberculosis) are undoubtedly transmitted by air.

Dust, which contains loose or combined silicates and which is formed in the course of boring siliceous rocks as well as during a mechanical processing of silica, is harmful to the lungs. Silicosis, which is caused by such dust, is a very dangerous and most common occupational disease. Radioactive aerosols which are formed during explosions of atomic bombs and during the operation of atomic industry involve a great danger. On the other hand certain medicinal compounds are particularly effective when applied in aerosol form (inhalation).

Aerosols also gained their enormous importance with regard to technical sciences. The process of winnowing grain has been known to man from time immemorial: grain and chaff mixed together are subjected to an aerosol stage and their separation is effected by fanning. As a rule, a liquid fuel prior to burning is converted into a fog by mechanical atomization; the utilization of solid fuels in a form of dust has also been widely accepted. Even some types of mineral raw materials (pyrites) spark when they are pulverized. A pulverized siccative of viscous liquids is also of great importance when in a state of suspension. In recent times greater attention has been directed toward the utilization of "fluidized" catalyzers, namely those which are in a state of suspension within a gas current. Means of combatting blights in agriculture and malaria-carrying mosquitos are almost exclusively in the aerosol category and as such contain pulverized solid or liquid combinations. Screening smokes and fogs play an important part in military usage.

Of no less importance than a transition of matter to an aerosol condition is the course of the inverse problem, i. e., that of aerosolic condensations which occur in numerous industrial processes in spite of precautions. Among those we include smoke and fly-ash, which are discharged upon combustion of fuel (solids in particular) and during smelting processes of various metals, where soot is produced; then follows fog, which is formed in the course of manufacture of sulphuric acid and from electrolysis; and finally dust, which is produced by grinding various hard materials (e. g., cement), etc. Fall-out of aerosols consists of valuable substances (e. g., metallurgic smokes), or they can effect harmful reactions to people and to the surrounding country-side (sulphurous-acid fog); they can also cause corrosion and pollute surrounding localities. In order to combat industrial aerosols there are available numerous effective methods and devices, which cause precipitation of aerosols; there are also in use highly improved smoke filters for individual protection. Great significance is attached to the problem of fog dispersion because of difficulties in landing airplanes on airfields. The prevention of dust explosions in coal mines, grain mills, sugar refineries, etc. also poses a serious problem. In the above-quoted instances, detonation waves convert dust deposits into an aerosolic condition. A very realistic problem is the prevention of ice formation on airplanes, telegraph lines, etc. caused by freezing fog and rain.

Aerosols are of very important significance to science, especially in the field of experimental physics. The electron charge and the AVOGADRO number were exactly determined for the first time when the movement of droplets in a vertical electrical field was examined; likewise the quantum properties of the photoelectric effect were proven. The effect of fog formation

following the condensation of supersaturated steam on gaseous ions served as a basis for the creation of one of the most important devices in modern physics - i. e., the WILSON cloud chamber. The method of smoke trails is widely used in experimental hydrodynamics for studying flow patterns in tests on models.

Among nearly all the afore-mentioned phenomena, as well as processes and methods of research, a particularly important part is presented by the movement of aerosol particles influenced by various internal forces and molecular collisions. A rainfall or snowfall necessitates that the particles in the clouds come in contact and coagulate, but that the resulting drops must be large enough to reach the ground before evaporating. The concentration and dispersion of particles of various dimensions in the atmosphere are determined (regardless of the velocity of their entry into the atmosphere) by the velocity of their descent on one hand, and by the magnitude of the accompanying atmospheric turbulent changes on the other. Considering the important process of aerosolic precipitations, it is essential that under all circumstances the ascending particles reach some kind of macroscopic surfaces ("walls") and attach themselves to the latter. Another more important process that transpires within aerosols - coagulation - follows as a result of particles coming in contact with each other due to actions of thermal (BROWNIAN movement) currents or dissimilar external influences. The absorption of sound waves by aerosols is explained by a relative movement of particles and gaseous agents. The completeness of combustion of pulverized fuels is determined, apart from the speed of combustion, also by the trajectories of burning particles, etc.

The study of the motion of aerosol particles and their precipitation and coagulation constitutes the topic of a highly important chapter of science about aero-dispersion systems, which can be named the mechanics of aerosols.¹ It would be advantageous if we refer here to the question which is closely related to the problems of precipitation and coagulation among the phenomena which transpire after aerosolic particles have made contact with each other, as well as with macroscopic bodies. Furthermore, we should also refer here to an extremely important problem, although usually it is little known, i. e., about the inverse processes of particles being separated from "walls" and about the transformation of powdery bodies into an aerosolic condition.

1. This term appears for the first time in literature.

One must note that among the very incomplete book and monographic references pertaining to the systems of aero-dispersions, the theory of mechanics of aerosols is given comparatively little consideration in spite of its considerable practical importance. Even pertinent journal articles, scattered throughout periodical publications and dedicated to very diversified branches of science and technology, usually offer scant relevant features and only in rare instances contain data which acknowledge an interest in the theory. Unfortunately, a majority of experimental researches in aerosols was conducted with immoderate polydispersible systems and at these instances the variations of particle dimensions were either not studied at all, or were very roughly determined. It is usually difficult to utilize such findings for testing theoretical deductions and for finding new rules.

The primary mission of this book is to compile and to review with comments the entire theoretical and experimental material pertaining to the mechanics of aerosols. Some chapters on the mechanics of aerosols (e.g., the theory of rectilinear uniform motion of particles of various dimensions and the theory of thermal coagulation of aerosols) have been quite thoroughly examined (this is also reflected in the contents of the respective chapters in this book). On the other hand, such important problems, as ... movement, precipitation and coagulation of aerosols in a turbulent current, as well ... as suspending and disintegration of particles, appear as kind of "blank spots" in the mechanics of aerosols; therefore, the pertinent chapters in this book may cause the reader to feel disappointment.

Many theoretically disputable matters of the mechanics of aerosols present considerable mathematical problems; often their solution can only be obtained by complicated, ill-matched series, the practical application of which requires immense calculative work. Because of this, in some instances, especially in the problems of diffusion emanating from currents, it was only reasonable to renounce strict solutions and to adopt well known suggestions, simplifying the problem to obtain at least a rough presentation of the analyzed phenomena.

In all chapters of the book the author made an attempt to quote all the more-or-less reliable experimental data of analyzed problems; yet, if we take under consideration the type of this book, it would be ill-conceived to include in it the descriptions of mensuration techniques and experimental details. On the other hand we have included in this book many tables and graphs, which may be of use to persons, who in their work encounter many problems in the field of the mechanics of aerosols.

We must, however, emphasize the great importance which the Soviet science attaches to the research in aero-dispersion systems and particularly so in the mechanics of aerosols. We must acknowledge the classical work of N. ZHUKOVSKIY and S. CHAPLIGIN, relevant to the theory of snow drifts; then, the work of M. AGANIN, S. GORBACHEV, B. DERYAGIN, and P. PROKHOROV, about the phenomena resulting from collisions of water droplets, subsequently, the theoretical and experimental researches of I. PETRYANOV, L. RADUSHKEVICH, N. TUNITSKIY, N. SHISHKIN, I. ARTEMOV, and N. FUKS, relevant to coagulations of aerosols; also, the work of S. SYRKIN and P. KOUZOV, relevant to the employment of models in researches in cyclones; likewise the research of A. KOLMOGOROV and M. LEONTOVICH in a theory of BROWNIAN movement and diffusion of particles; and finally, the theoretical work of L. LEVIN, pertinent to precipitations of aerosols from currents, etc.

The author considers it a pleasant obligation to express his gratitude to the academician M. DUBININ and to the associate correspondents of the Academy of Sciences of the U. S. S. R., B. DERYAGIN and I. PETRYANOV, for their contributions to this book, as well as to L. LEVIN, G. NATANSON, and P. PROKHOROV for their examination of the manuscript and for their many valuable comments.

Chapter I

Classification of Aerosols. Dimensions and Shape of Particles in Aerosols

§ 1. Classification of Aerosols

Dispersible systems, which remain within gaseous surroundings and maintain their solid or liquid dispersible aspects, are named aerosols, or aero-dispersion systems. Up to the present time there was no singular classification of aerosols commonly accepted and no unique system designating various types of aerosols; in connection with this one can note a complete arbitrariness in the literature. It is obvious to us that a logical classification of aero-dispersion systems must be based upon the distinction existing between the dispersible and condensable aerosols on the one hand, and between the systems with solid and liquid dispersible aspects on the other hand. In conjunction with the above, the designation of individual types of aerosols must coincide, as far as possible, with the names which are used in everyday non-technical language (road dust, natural fog, furnace smoke, etc.).

Dispersible aerosols are formed upon dispersion (pulverization, atomization) of solid and liquid bodies and upon a transition of powdery substances into a suspended state due to influences of air currents, concussions, etc. Condensable aerosols are formed upon a voluminous condensation of supersaturated vapors and as a result of gaseous reaction, which influences the formation of non-volatile substances, e.g., soot. The distinction between the two categories of aerosolic systems (in addition to their mode of origin) is that dispersible aerosols in most instances are considerably more coarse than condensable aerosols. They also possess a greater polydispersion and even if they are of a solid dispersible phase, they usually consist of individual or loosely adhering particles of a quite irregular shape ("fragments"). Now considering condensable aerosols, their solid particles represent quite frequently friable components mostly of the original particles which are of a true crystalline or spheroidal shape.

The difference between aerosols with a liquid phase and with a solid dispersible phase is that the former have particles of a true spheroidal shape which fuse together during coagulation and thus produce again individual spheroidal particles. However, the solid particles may have a quite different shape and during coagulation likewise form more-or-less friable components of dissimilar shape. The apparent density of these components may be many times lower than that of the substance of which they are formed.

Considering the afore-mentioned statements, we have adopted in this book the subsequent designations of various types of aerosols.

Thus, we shall name the condensable and dispersible aerosols with liquid particles (regardless of their degree of dispersion) fogs; they are known in the Russian language under the same name (a natural fog, i. e., condensable fog or one which is formed following the atomization of droplets, etc). In the given case the difference between the condensable and dispersible systems is not very great.

We shall name the dispersible aerosols with solid particles (also without regard to their degree of dispersion) dusts. The existing opinion that only coarse dispersion systems should be named dusts, is erroneous, because due to an artificial separation or that occurring naturally in the atmosphere, dust with a high dispersion degree can also be formed.

Finally, we shall name the condensable aerosols with a solid dispersion phase smokes. To this classification we can even refer the systems of condensable origin, which contain solid and liquid particles, and the most important agents being smokes, which form upon the incomplete combustion of fuel; then we can also include smokes from hygroscopic substances (e. g., those of ammonium chloride), whose particles may be solid, semi-liquid, or liquid, depending upon the moisture content of the environment; and, subsequently, smokes from organic and slightly under-cooled substances, within which a progressive conversion of liquid particles into a crystallized state takes place, etc. If we assume such a separation of smokes and condensable fogs, then a strict adherence to a proposed terminology is at times rather difficult; thus such a delineation is in all respects still better than combining the two types of aerosols into one (smoke), as English authors do.

Furthermore, it is quite often necessary to deal in practice with aerosols, which contain particles of a dispersible and condensable origin. Thus, in a furnace smoke there is always a larger or smaller amount of ashes, which are mechanically carried off from the fire grate; the so-called "atmospheric nuclei of condensation" consist partly of evaporated spray of sea water and partly of droplets of sulphuric acid, which is formed through oxidation of sulphurous anhydride in furnace gases. In the air around industrial centers there is a considerable amount of such components as soot, ashes, and products of dry distillation of carbonaceous matter combined with atmospheric moisture, which measures from tenths of a micron to tenths of

a millimeter. These aerosols can neither be referred to any type, nor to any of the existing classifications; therefore a special name was proposed for them: "smog" (smoke + fog).

All the afore-mentioned types of aerosols may possess very dissimilar dispersions and this would have a great influence over almost all characteristics of dispersion systems; therefore, it would be expedient to divide aerosols into highly dispersible and coarsely dispersible groups (see page 12).

The term "cloud", used by some foreign (1) and Soviet (2) authors, is used to designate all condensable aerosols with particles the diameter of which is larger than 10^{-5} cm. In the Russian language this term has entirely different meaning, i. e., it implies a mobile aero-dispersion system including any type (rain cloud, dust cloud, gun-smoke cloud, etc) of definite dimensions and shape. In that sense we shall use the term "cloud" in this book.

§ 2. Dimensions of Particles in Aerosols

We shall now review the problem of the lower range of mensurations of aerosol particles. It must be considered that the determination of dimensions of very small particles ($\sim 10^{-7}$ cm) is only possible by two ways:

1. By mensuration of the particle's mobility in an electric field (see § 27) with the aid of an electrometer;
2. By mensuration of the particle's diffusion coefficient, which is usually carried out also by electrometric methods. Thus in both instances, only charged particles can be measured.

As experiments show, there are in gases two kinds of charged particles, small (gaseous, light) ions and large (heavy, slow) ions. The mobility of the first ones is proportional numerically and that of the second ones is proportional to $10^{-3} - 10^{-4}$ cm² B⁻¹ sec⁻¹. It has been recently determined that gaseous ions are molecular components, which are formed by a charged central molecule (strictly speaking, by an ion) and attached to it (by means of electrostatic and molecular forces) sheaths of neutral molecules of gas.

The heavy ions, unlike light ones, develop only in gases containing solid or liquid suspended particles; i. e., they represent the charged portion of highly dispersible aerosols. The presence of "medium" ions, i. e., the particles with the mobility of $10^{-3} - 10^{-1}$ cm² B⁻¹ sec⁻¹, have also been discovered. Thus, the products of combustion of illuminating-gas sodium flame even contain particles with a mobility of 0.2 cm² B⁻¹ sec⁻¹ (3, 4). The gaseous ions in vapors of certain organic substances (4), e. g., amyl alcohol, possess a similar mobility. Thus, it is impossible to distinguish, according

to mobility, the gaseous ions from the charged particles of aerosols and due to this, one can profit by the diverse behavior during coagulation. During coagulation (recombination) of gaseous ions, the complex development of neutral molecules disappears instantly, i. e., the ions are destroyed. Yet, during the coagulation of particles in aerosols, whose existence is not connected with the presence of an electric charge, larger particles are being formed. Actually the mobility of the afore-mentioned ions, which are formed in the flame, drops several hundred times per time sequence of 1 sec (3, 4). Since the probability of the presence of multiple charges in particles drops rapidly with the decrease of their dimensions (see page 141) it can be assumed that the ions possess only one basic charge. In this case a mobility of $0.2 \text{ cm}^2 \text{ B}^{-1} \text{ sec}^{-1}$ is equal to the radius of $1.5 \cdot 10^{-7} \text{ cm}$ (see page 46). In view of the fact that the content of charged particles in aerosols also rapidly decreases along with a reduction of particle dimensions, it is quite probable that there are still much smaller particles, which we cannot discover, or rather measure.¹ It is curious that the smallest sizes of aerosol particles are obtained by examination with an electron microscope, as long as the sizes conform approximately with the limitations of the allowable capacity of the electron microscope. However the abundance of particles with a radius of $r = 1.5 \cdot 10^{-7} \text{ cm}$ (e. g., in smokes of silver iodide /5/) compels us to think that there are still smaller particles of silver iodide. We noticed that the ultra-microscopy enables us to discover only considerably larger particles of aerosols.

So much for the experimental side of the problem. Yet, from the theoretical standpoint, it is entirely possible that the substances with a solid crystalline structure may produce aerosols with particles of dimensions of 2-3 molecular diameters. Unquestionably due to the high diffusion velocity of these particles, they usually settle rapidly on larger particles (see § 49), or on the walls, etc.

Now as we turn to the problem of the upper range of dimensions of particles in aero-dispersion systems, we notice that, in the systems with a stationary medium, the particles with a radius of up to several hundred microns settle so rapidly that they can hardly be detected in a suspended condition. On the other hand, in sharply rising or in turbulent aerial currents, e. g., in clouds during thunderstorm showers, in the course of friable matter being vacuum-lifted, in the fluidization of catalytic agents, during sand and snow storms, etc. - particles with dimensions of several millimeters are detected in suspension. Because of the existence of the afore-mentioned problems in the mechanics of aerosols, these particles should be taken under consideration.

-
1. Particles of the order 10^{-7} cm can probably be discovered by measuring devices for the nuclei of condensations, but their dimensions will, at the same time, remain unknown.

Thus, the objectives of aerosol studies are the systems lying in this enormous extent of dispersions - from 10^{-7} to 10^{-1} cm. No wonder the transition from the lower range to the upper range entails not only numerous changes in nearly all physical aspects of aerosols, but also changes in the essence of laws which interpret these changes. This reveals itself most typically in the example of the resistance law of the gaseous medium toward the movement of particles. Taking into account the very small particles ($r < 10^{-6}$ cm), the resistance is proportional to the velocity and to the square of the radius of the particles. In the interval of 10^{-6} - 10^{-4} a progressive transition to the STOKES' law takes place; the resistance remains proportional to the velocity, but the quadratic dependence upon radius does change into a linear one. With a further enlargement of the radius, the deviations from the STOKES' law occur again. If we take into account not-extremely-low speeds, the proportionality of the resistance and velocity transgresses and at the sufficiently high speeds, where large sizes of particles are involved, the resistance becomes at first approximation proportional to the square of the radius and to the square of velocity (see page 50).

The changes in the essence of laws, which rule some of the most important aspects of aerosols, are shown on figure 1: here, in all instances,

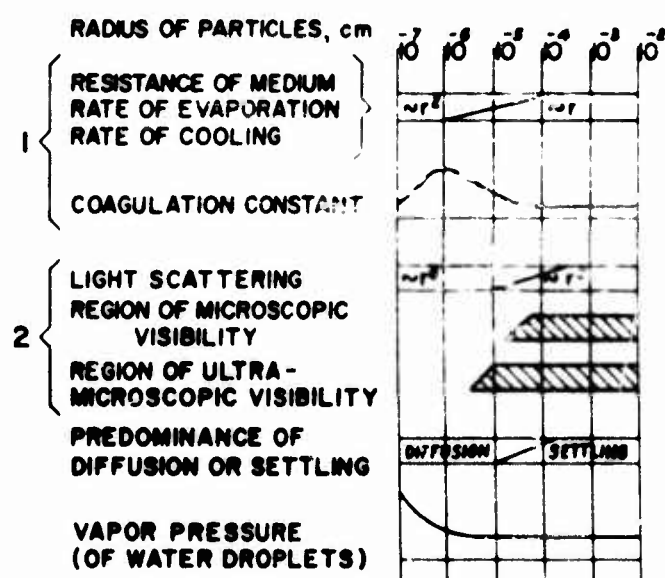


FIG. 1. DISPERSION AND BASIC CHARACTERISTICS OF AEROSOLS

the transitional region, generally speaking, is located in the interval from $0.5 \cdot 10^{-5}$ to 10^{-4} cm. Therefore, these attributes are included in groups

1 and 2 on figure 1 because they are dependent upon the relationship of particle radius to the length of gaseous molecular free path (which is formed in the air in conjunction with the atmospheric pressure of approximately 10^{-5} cm) or to the medium wave length of a visible light ($\lambda = 0.55 \cdot 10^{-4}$ cm). Pertinent to the remaining attributes, this coincidence is of an incidental nature. The factors stated previously enable us to define a natural classification of aerosols according to their dispersions.

A group of highly dispersible aerosols with particle radius below, let's say: $0.5 - 1 \cdot 10^{-5}$ cm, is characterized as follows: that the resistance to the movement, as well as the rate of evaporation and cooling of particles, is proportional to r^2 ; that the light dispersion by particles is proportional to r^6 ; and, that the coagulation constant depends upon r . The particles which are invisible under the usual microscope, except under the most favorable conditions, can be detected with the aid of an ultramicroscope. The vapor pressure of the dispersible phase of these aerosols surpasses considerably the normal vapor pressure of the substance; consequently, in these aerosols, a rapid "killing" of smaller particles by larger ones may be in progress. Finally, the BROWNIAN movement of particles becomes more important than the settling influenced by gravity.

In coarsely dispersed aerosols with the radius of particles above 10^{-4} cm, one can determine with the aid of a microscope the dimensions as well as the form of particles; the coagulation constant does not depend upon r ; the settling prevails considerably over BROWNIAN movement and all the afore-mentioned basic characteristics transgress into others, as shown on figure 1.

Finally, it would be expedient to separate into another aerosol group (with an average dispersion and with transitional attributes) the systems, the particle radii of which range from $0.5 - 1 \cdot 10^{-5}$ to 10^{-4} cm. It should be noted that this group plays a very important part in the exploration of aerosols, because the indicated dimensions of particles are particularly suitable for the ultramicroscope, which is one of the basic methods of studying the aerosols. Besides, in the process of formation of condensable aerosols out of substances possessing a small vapor tension, the systems usually obtained, as a rule, are those which belong to that group.

§ 3. Distribution of Particle Dimensions in Aerosols

Most of the naturally and artificially formed aerosols possess a rather extensive polydispersion.¹ In view of the afore-mentioned strong dependency of the physical aspects of aerosols upon their dispersion degree, the "medium" size particles in most instances are unsatisfactory for rating purposes of the aero-dispersible systems; therefore, it is necessary to find out the distribution of particle sizes. Prior to the invention of the electron microscope, only the ordinary microscope served this purpose in the mensuration of particles of coarsely dispersible aerosols ($r > 3 - 5 \cdot 10^{-5}$ cm), or of the corresponding group of higher dispersible aerosols. Among the latter was determined either the general number of particles without mensuration of their sizes, merely in a small group, or even the group as such was generally omitted. At the present time the distribution of particle sizes can be obtained among the aerosols, the particle radii of which exceeds that of $1 - 2 \cdot 10^{-7}$ cm.

The distribution of sizes can be expressed in several ways. One can assume that df is a quota of the number of particles, the radii of which are on the order ($r, r + dr$):

$$df = f(r)dr \quad (3.1)$$

providing that

$$\int_0^{\infty} f(r)dr = 1. \quad (3.2)$$

The curve expressed by the function $f(r)$ is named a curve of the density of distribution, i.e., either a differential curve of the distribution of particle sizes (figure 2), or, more precisely, a curve of a numerical

-
1. Partially monodispersible aerosols are obtainable by LAMER'S generator (6) and in Nature they include pollen and spores of some plants. The radii of particles of clover pollen are of the order of $24.8 - 26.9\mu$ (7).

distribution, in contrast to the curve of weight distribution, determinable by the gravimetric quota dg of the particles with a radius $(r, r + dr)$:

$$dg = g(r)dr \quad (3.3)$$

if

$$\int_0^{\infty} g(r)dr = 1. \quad (3.4)$$

Let us assume, that the area limited by the differential curve of distribution, also by the axis of abscissas and by two verticals at the points of r_1 and r_2 , expresses the quota (calculating or gravimetric) of particles, the radii of which are included between r_1 and r_2 .

According to terms of the function $g(r)$ one can write down:

$$g(r) = \beta m_r f(r),$$

where m_r is the mass of particles with a radius r ;

where β is the proportionality factor, readily determinable by way of the integration:

$$\int_0^{\infty} g(r)dr = 1 = \beta \int_0^{\infty} m_r f(r)dr = \beta \bar{m}$$

where \bar{m} is the mean (arithmetical) mass of the aerosol particles.

Thus the functions $f(r)$ and $g(r)$ are combined by the simple equation:

$$g(r) = \frac{m_r}{\bar{m}} f(r) \quad (3.5)$$

Inasmuch as $\bar{m} = \gamma \bar{v}$ (where γ is the density), while \bar{v} denotes a mean volume of particles, thus, with a constant γ , i. e., in the case of a homogeneous composition of the aerosol and in the absence of aggregates in it, the gravimetric distribution of $g(r)$ identical with a volume distribution is:

$v(r) = \frac{v_r}{\bar{v}} f(r)$. Now considering a heterogeneous composition of the aerosol

(e.g., atmospheric dust), or in the case of aggregated aerosols, the particles which possess an apparent dissimilar density (see page 34), one can obtain from microscopic measurements a practical volume distribution only, which in a given case can differ considerably from the gravimetric distribution.

The calculated and gravimetric functions of distributions of particle sizes are most commonly used. However, as will be shown later, in some cases it is necessary to use other functions of distribution with a common formula:

$$f_v(r) = r^v f(r) / r^v;$$

where v is the positive or the negative whole quantity. Particularly important is the quadratic distribution ($v = 2$).

In some problems connected with aerosols, it is expedient to express distribution by a function not that of a radius, but of a mass (or volume) of particles.

The function of the distribution of the masses of the particles shows, whether the calculated function $f'(m)dm$ or the gravimetric function $g'(m)dm$ controls the quota of particles, where mass is included within the range $(m, m + dm)$. If there are spherical particles, the functions $f(r)$ and $f'(m)$, as well as $g(r)$ and $g'(m)$, are combined in the formula:
 $4\pi r^2 f(m) = f(r)$.

The differential curves of distribution possess a greater exemplification. However, in processing the results of measurements of aerosol particles and in solving some technical problems, it is more convenient to apply the integral ("cumulative") distribution curves indicating which quotas of particles (the calculated or gravimetric one) have a larger or smaller radius than the given value r . The corresponding distribution functions to be used for a calculated distribution are obtained by integration of the functions $f(r)$ from r to ∞ in the first instance (a) and from 0 to r in the second instance (b). Thus,

$$F_a(r) = \int_r^{\infty} f(r) dr, \quad F_b(r) = \int_0^r f(r) dr \quad (3.6)$$

and analogically on behalf of the gravimetric distribution

$$G_a(r) = \int_r^{\infty} g(r)dr, \quad G_b(r) = \int_0^r g(r)dr. \quad (3.7)$$

The function $G_a(r)$ is used notably often in techniques of the research in various industrial dusts. The integral curve of the gravimetric distribution being determined by this function is named a "characteristic curve" of a given dust, as well as a "curve of sedimentation" because the latter is determined according to the weight of dust remaining on a given sieve, or in an air centrifuge, if we have a certain air velocity. The $G_b(r)$ curve is named a "transition curve." Let us assume that

$$F_a(r) + F_b(r) = G_a(r) + G_b(r) = 1. \quad (3.8)$$

Thus we shall explain the above by an example of distribution of the sizes of droplets in one stratum of a cloud (8), as it was determined with the aid of a microscope. Let us assume that, unlike the systems with a liquid medium for which (with the aid of sedimentometry) one can obtain immediately continuous curves of distribution in aerosols, there is determined usually during a test, a quota of particles, the radii of which remain within the order of ultimate ranges, i.e., step "histograms" are obtained instead of continuous curves.

In the present considered case, during measurements of 100 droplets, we obtained results which are submitted in table 1.

Table 1
Distribution of Droplets Sizes in a Cloud Stratum

Intervals of radii of droplets, $\mu \dots$ Number of droplets	2.5-4	4-5.5	5.5-7	7-8.5	8.5-10	10-11.5
	4	6	15	24	24	12
Intervals of radii of droplets, $\mu \dots$ Number of droplets	11.5-13	13-14.5	14.5-16	16-17.5	17.5-19	
	4	4	4	1	2	

The histogram illustrated on figure 2 was prepared according to the afore-mentioned data. It can be used directly for computation of various mean values (see page 26), but in most instances it is desirable to convert the histogram into a continuous curve, rectifying at the same time certain irregularities caused by insufficient number of measurements (e.g., at the right edge of the histogram the ascent is scarcely probable from the standpoint of physics).

The rectification of the results obtained by experiments is justified by the circumstance that the amount of particles used in the measurements was by necessity limited; therefore the statistical fluctuations are rather noticeable. It would be inexpedient to correct the histogram directly. It would be better by using experimental points (marked by little crosses on figure 3) to begin with a preparation of a smooth integral curve $F_p(r)$. With this it would be comparatively easy to correct incidental mistakes in measurements and fluctuations pertinent to the number of particles of each group. Thereupon a differential curve $f(r)$ /see figure 2/ should be prepared according to the integral curve, using known methods of graphic differentiation.

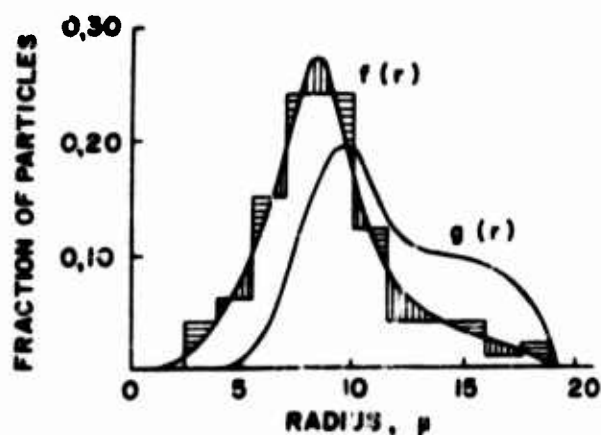


FIG. 2. DIFFERENTIAL CURVES OF PARTICLE SIZE DISTRIBUTION

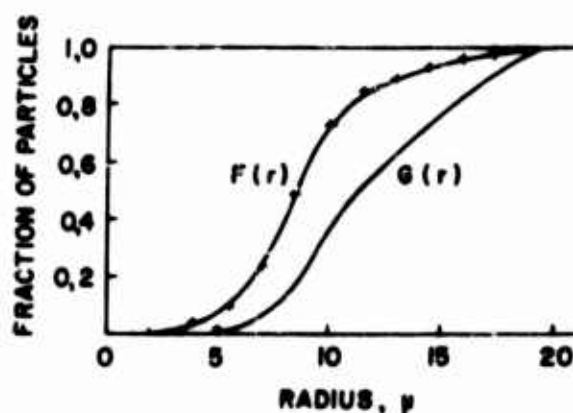


FIG. 3. INTEGRAL CURVES OF PARTICLE SIZE DISTRIBUTION

In order to proceed with the curves of a gravimetric distribution, one could begin with a preparation of a "gravimetric histogram" directly from the experimental data; however, in such a case the afore-mentioned fluctuations might emphasize themselves particularly strongly. Therefore it would be better to proceed with the curve $f(r)$ using the rectified experimental data. Having divided the axis r into sufficiently narrow intervals Δr , we compute the (conformable with the latter) mean values of the mass of particles, $m_r = \frac{4}{3} \pi r^3$; then with the aid of the curve $f(r)$

we determine the mass $m_r f(r) \Delta r$ of a dispersible phase in each interval and the average mass \bar{m} , from which, according to the formula (3.5), we find the unknown function of the gravimetric distribution. As a result, we arrive at the integral curve $G_b(r)$ /see figure 3/.

If a sieving or sedimentation analysis of dust is considered, the $G(r)$ function is determined directly from the experiment. A reverse transition from the latter to a calculated distribution is effected by the same method. The curves of quadratic or other distribution of sizes are prepared in a similar way.

The selection of one or another way of expressing distribution of the sizes of particles in aerosols depends upon the factor: what aspects of the latter are to be characterized. Thus, when computing the rate of a thermal coagulation of aerosols, it is necessary to know the accountable distribution of particle sizes $f(r)$ /page 341/. The rate of evaporation of a coarsely dispersible aerosol at any given time is determined by a linear distribution of sizes of the particles $rf(r)$, because the rate of evaporation of particles is proportional to the radii of the latter. The optical density of coarsely dispersible fogs is determined by a quadratic distribution of the sizes $r^2 f(r)$, because the reflection and diffusion of the light by larger droplets is proportional to the square of their radii. The completeness of precipitations of aerosols, influenced by the forces of gravitation and the forces of inertia, are determined by the afore-mentioned distribution.

In the above described examples we are concerned with differential curves of distribution. The integral curves are considered useful above all to compute the completeness of the separation of the dispersible phase of aerosols from a gaseous medium with the aid of various instruments provided for this purpose and also to express the distribution of sizes by means of empirical equations (see page 20). We still wish to add, that the characteristics of industrial powdery materials, e. g., of the insecticide powders, usually show the weight percentage of the group which settled on a sieve of a given size mesh after passing through a sieve with a mesh of another size, i. e., the afore-mentioned procedure offers the value of the $G(r)$ function with two determined meanings of the r .

It is necessary to add a few words about the distribution curves (figure 4), frequently encountered in the literature, as they intersect the axis of ordinates at an ultimate distance from the beginning of co-ordinates. Curves of this type thus offering a completely false presentation of the actual state of distribution of the particle sizes are obtained according to intervals of final dimensions by which the particle sizes are divided during their measurements. Let us assume in actuality that the curves on figure 5 represent the actual

distribution of sizes. If we consider sufficiently small intervals ($\Delta r = 0.1\mu$), e.g., during the measurements of particles with the aid of an electron microscope, we should obtain the histogram shown on figure 5, a. An effected "smoothing out" of the latter would produce a curve very close to that of the real distribution curve. However during the measurements of particles with the aid of the usual microscope, we would rather use the

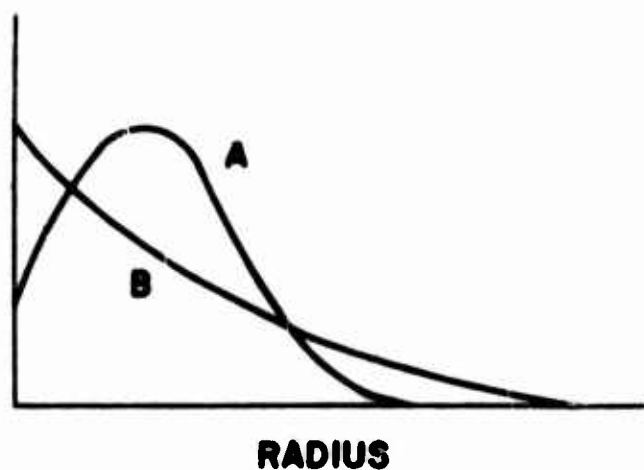


FIG. 4. FALSE DISTRIBUTION CURVES

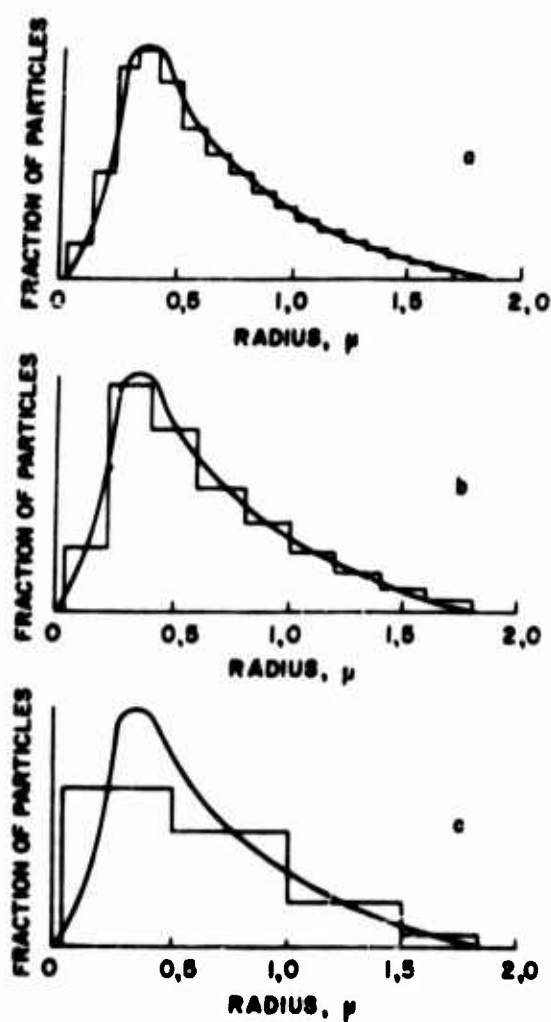


FIG. 5 CONVENTIONAL PRESENTATION OF FALSE DISTRIBUTION CURVES

$\Delta r = 0.2\mu$ and thereby obtain the histogram shown on figure 5, b and the type A curve shown on figure 4. Finally by using the intervals $\Delta r = 0.5\mu$, adopted in usual hygienic work, we would obtain the histogram shown on figure 5, c and the type B curve shown on figure 4.

Usually such a dissemblance of a true distribution takes place when a considerable part of the distribution curve is positioned in the region of the particle magnitude, where the applied method of determination of sizes is already ineffective due to the smallness of particles, and in another instance, when the interval of particle sizes is extended over several categories of magnitudes. Actually we assume that the particle radii of some aerosols are of the order of 0.1 - 200 μ and that the entire length of the graph along the axis of abscissas equals 100 mm. Thus, considering a part of the dissemination curve which corresponds to the range of 0.1 to 1 μ , the imparted interval amounts to only 0.5 mm and this makes it impossible to render accurately the distribution on such a graph.

It would seem that in such instances one could use a logarithmic scale along the axis of abscissas. Actually in this case the unequal position of very minute particles is eliminated because to every order of magnitude on the graph there is an equal space allotted. However a new difficulty arises here. If, having adopted a logarithmic scale to the radii we subsequently draw a distribution curve plotting it straight along the ordinates' axis and with the value of the $f(r)$ function, then the area delineated by the curve, by the axis of abscissas, and by the verticals at the points of r_1 and r_2 will be equal to:

$$\int_{r_1}^{r_2} f(r) d \lg r = \int_{r_1}^{r_2} \frac{1}{r} f(r) dr,$$

i. e., the area will no longer be proportional to the fraction of particles with radii from r_1 to r_2 and the curve will lose its descriptive value. In order to retain the indicated magnitude of this area it is necessary to plot $rf(r)$ along the axis of ordinates instead of $f(r)$, notwithstanding the fact that in highly polydispersible aerosols the $rf(r)$ curve practically coincides with the axis of abscissas in the region of small r 's. So we have again no chance to represent graphically the distribution of sizes by means of a curve. In researches with aerosols a tendency developed recently to reject the above discussed methods of the graphic representation of distribution of sizes and to substitute for it such systems of co-ordinates in which the distribution would be shown in a straight line. This problem is closely connected with another one, which we intend to discuss now.

It is very inconvenient to use distribution curves in order to describe industrial aerosols and to solve various theoretical and relevant problems of aerosols. It would be expedient to prepare these curves using

an equation with a minimum number of coefficients, the values of which would describe a certain distribution. Naturally, in conjunction with this it would be desirable if such an equation was applied, if possible, to a greater number of aerosolic systems, i. e., in passing from one system to another only the values of coefficients would be changed. Having at disposal a sufficiently great number of coefficients it would be possible to describe all distributions as they actually occur, with the aid of one unique equation. However, the selection of coefficients would each time require a substantial amount of work and furthermore, it would be difficult to ascribe any physical significance to these coefficients; thus multi-coefficient equations thus attained would have no practical acceptance. As a rule, only the equations with two coefficients are considered and while in this example the number of coefficients is already at a minimum, the first coefficient thus describes the average size of particles and the second one indicates the polydispersion degree in aerosols.

In spite of a greater complexity and insufficient knowledge about the processes of the formation of both, the condensable and dispersible aerosols, the distribution formulas from theoretical deductions as yet do not exist (with one exception - see below), but there are series of empirical formulas applicable primarily to aerosols formed by a mechanical atomization of solid and liquid bodies. Among the best known are:

1. ROLLER'S equation (9), which according to the aforementioned specifications appears in the form as follows¹

$$G_b(r) = ar^{1/2} \exp(-s/r) \quad (3.9)$$

and is applicable to a greater number of industrial powdery materials with a very diversified dispersion degree.

2. ROSIN-RAMMLER'S equation (10)

$$G_a(r) = \exp(-ar^b) \quad (3.10)$$

applicable equally to coarsely dispersible dusts and to fogs obtained from a mechanical atomization.

1. With $r \rightarrow \infty$ $G_b(r)$ there is also $\rightarrow \infty$ used in this formula. Therefore it is necessary here to separate the integral of the distribution curve if such r_1 are present, so that $G_b(r_1) = 1$.

A more ideal equation for such fogs was prepared by HYKIAMA and TANASAVA (11)

$$f(r) = ar^2 \exp(-br^s), \quad (3.11)$$

in which a and b remain independent and are defined by a function s and limited to medium size droplets. These functions are computed and quoted by authors in tabular form.

The (3.9) equation may be presented in the form

$$\lg[G_b(r)/r^{1/2}] = \lg a - 0.434 s/r. \quad (3.12)$$

If we plot according to the axis of abscissas $1/r$ and according to the axis of ordinates $\lg(G_b/r^{1/2})$, then in the event of applicability of this equation, the experimental points must be arranged in such a way that it would be easy to determine a and s .

Analogically we obtain from the equation (3.10)

$$\lg G_a(r) = -0.434 ar^s. \quad (3.13)$$

In this case it is necessary to select such an s value, by which the experimental points at the selection time would be arranged straight according to the co-ordinates r^s and $\lg G_a$. In a similar way follows the processing of experimental data according to (3.11), which assumes this form

$$\lg[f(r)/r^2] = \lg a - 0.434 br^s. \quad (3.14)$$

When equations are brought to such a state in which the dispersion of sizes is expressed rectilinearly, then this often simplifies the problem of the selection of coefficients in the equations and it disinvolves the experimental data.

In a very few aerosols, e.g., among those formed by spores of plants (12), the distribution curves assume a symmetrical form, which closely resembles the form of GAUSS curve, conforming with the "normal" distribution:

$$f(r) = \frac{1}{\beta\sqrt{2\pi}} \exp\left[-(r-\bar{r})^2/2\beta^2\right] \quad (3.15)$$

where \bar{r} is the average radius of particles;

where $\beta^2 = \overline{(r-\bar{r})^2}$ is the mean quadratic deviation (degree of dispersion) value of the radius from \bar{r} .

If we introduce an auxiliary variable, thus

$$\xi = (r - \bar{r}) / \beta \sqrt{2}. \quad (3.16)$$

The fraction of particles with a radius $\leq r_1$ equals

$$\int_0^{r_1} f(r) dr = \frac{1}{\beta \sqrt{2\pi}} \int_0^{r_1} e^{-(r - \bar{r})^2 / 2\beta^2} dr = \frac{1}{\sqrt{\pi}} \int_{\frac{\bar{r}}{\beta\sqrt{2}}}^{\frac{r_1 - \bar{r}}{\beta\sqrt{2}}} e^{-\xi^2} d\xi. \quad (3.17)$$

Since, according to the meaning of the function $f(r)$ the latter differs from 0 only $r \geq 0$, then one can apply $-\infty$ in intervals of a lower range.

$$\int_0^{r_1} f(r) dr = \frac{1}{\sqrt{\pi}} \int_{-\infty}^{\frac{r_1 - \bar{r}}{\beta\sqrt{2}}} e^{-\xi^2} d\xi = \frac{1}{2} \left[1 + \operatorname{Erf} \left(\frac{r_1 - \bar{r}}{\beta\sqrt{2}} \right) \right] = \frac{1}{2} (1 + \operatorname{Erf} \xi_1), \quad (3.18)$$

where

$$\operatorname{Erf} \xi_1 = \frac{2}{\sqrt{\pi}} \int_0^{\xi_1} e^{-\xi^2} d\xi \quad (\text{KRAMP'S function}), \quad (3.19)$$

and ξ_1 is the ξ value, which corresponds to r_1 .

Assuming that we plot ξ within an arbitrary scale according to the axis of ordinates (figure 6) and we mark on the latter the corresponding values $0.5 [1 + \operatorname{Erf}(\xi)]$, i. e., the fraction of particles under consideration within a normal distribution, for which $r < \bar{r} + \beta\sqrt{2}\xi$. We plot r as before, according to the axis of abscissas. If within this "presumable" system of co-ordinates we prepare an integral curve $F_b(r)$, which expresses the fraction of particles with a radius of less than r , then in case of a normal distribution of sizes, according to the equation (3.16), one should obtain a straight line intersecting the axis of abscissas at the point $r = \bar{r}$. The tangent of the inclination angle of the straight line to the axis of abscissas equals $1/\beta\sqrt{2}$.

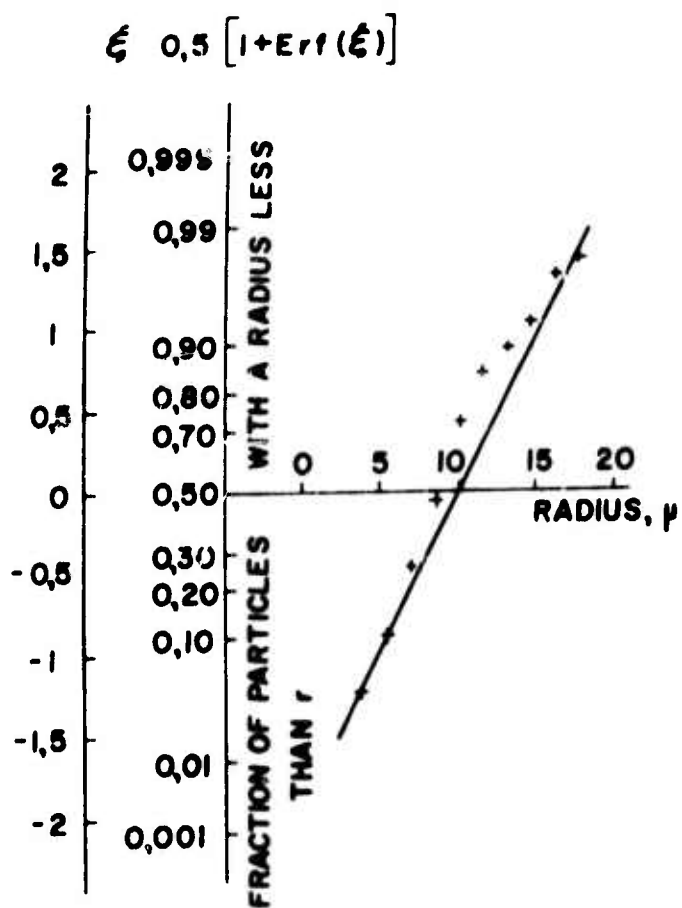


FIG. 6. DISTRIBUTION CURVE WITHIN AN ARBITRARY SCALE

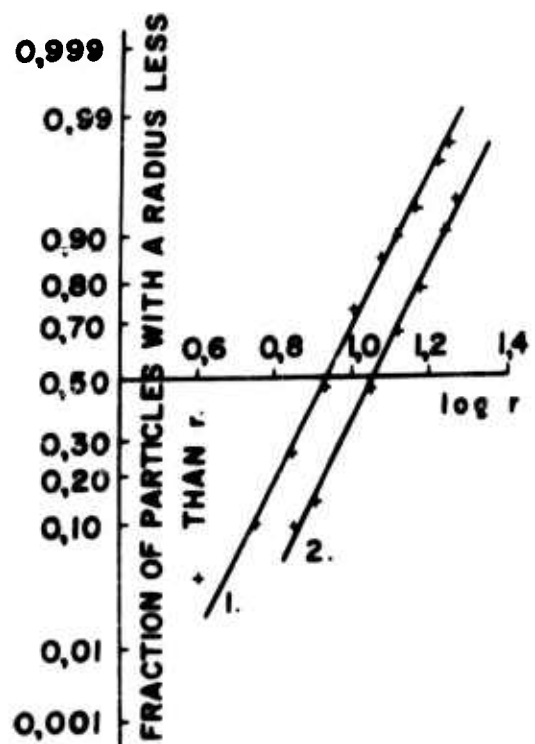


FIG. 7. DISTRIBUTION CURVE WITH A LOGARITHMIC SCALE

The data from table 1, pertinent to aqueous fogs, offer no rectilinear graphs within a presumable grid, as is shown on figure 6, where the distribution of the sizes of droplets in the fog is plotted with little crosses on account of the asymmetry of the differential curve of distribution in the considered fog (see figure 2). It should be noted that, in the overwhelming majority of cases among the condensable and dispersible aerosols, the distribution curves possess the asymmetrical form with a more abrupt inclination toward the small r 's. Apparently this is connected with the aforementioned inequality among small particles at the time of the selection of particle size intervals, which are to serve as the abscissas in distribution curves. If we take the logarithm of a radius for abscissa, the distribution curves assume a more symmetrical form and they resemble quite often GAUSS'S curves. In such a case the distribution can be expressed by this equation (of a normal logarithmic distribution).

$$f(r)dr = \frac{1}{\lg \beta_g \sqrt{2\pi}} \exp \left[- \frac{(\lg r - \lg r_g)^2}{2(\lg \beta_g)^2} \right] d \lg r. \quad (3.20)$$

Here $\lg r_g = \overline{\lg r}$, therefore r_g is a mean geometric of particles

radii. $(\lg \beta_g)^2 = \overline{(\lg r - \lg r_g)^2}$, i. e., it represents as such a mean quadratic slope of the logarithm of radii. In a foreign literature β_g is usually named a "standard geometric slope." As figure 7 shows, fog (a cloud stratus) used by us as an example renders a rectilinear graph 1 within a presumable logarithmic grid.¹ A normal logarithmic distribution of droplet sizes in natural clouds was determined by L. LEVIN (13) in a vast amount of material, compiled by him on the ELBRUS (TN: mountain in N. CAUCASUS). This distribution was also discovered recently in other aerosols of dispersible and condensable origin: in lithoidal (14) and uranic (15) dusts, formed by mechanical pulverization; in a haze produced by disc saws (16); in aerosols of $\text{NH}_4 \text{Cl}$ and $\text{H}_2 \text{SO}_4$ formed out of combined gaseous components (17), etc. Unlike other afore-mentioned distributions, a normal logarithmic distribution undoubtedly possesses a theoretical value (18) too. If we consider simple hypotheses, especially as to the type of processes in breaking down solid particles, thus - as KOLMOGOROV (19) pointed out - one can prove, that the distribution of particles according to an asymptotic method has a tendency to progress to the pattern course of pulverization which is logarithmically normal (20).

1. When straight lines are drawn across the experimental points within presumable grids, it is necessary to pay attention that the points distant from the axis are considered as of small statistical importance, because they represent a small number of particles.

value. Nevertheless, the practical value of these equations is certain, because, since they allow that all aspects of aerosols can be defined according to their dispersions by two parameters, they compare the aerosols with one another, etc. The effort expended on the selection of a suitable equation and on determination of the values of coefficients is usually much smaller than that required for mensurations of sufficiently large amounts of particles. Therefore for the utmost development of the knowledge of aerosols and especially on behalf of the theory of evolution of aerosols, it would be desirable that the indicated processing of the results of mensurations be conducted upon a greater number of the aero-dispersible systems, if possible.

The knowledge of distribution of particle sizes is usually of great importance during research in aerosols, because almost all aspects of the latter depend to a very large degree upon their dispersion. Therefore the experimental research in aerosols should be conducted in the field of iso-dispersible systems, because as long as their production still remains an unsolvable problem, we have to work on the polydispersible aerosols. In this case more or less reliable conclusions from the results of tests can be obtained only when the distribution of the sizes of particles is known.

§ 4. "Average" Sizes of Aerosol Particles

A complete characteristic of aerosols requires that the distribution of particle sizes be known. Yet in practice one becomes frequently limited by specifications of the "average" sizes in all such instances, when for some reason a research in distribution of particle sizes was not conducted and instead some other aspect of an aerosol was analyzed, which depends upon the aerosol dispersion, e. g., the coefficient of diffusion, the expansion of lines in a roentgenogram taken of the precipitated particles, the diameter of the diffracted corona, etc. The mensurations of aerosol dispersions are very often conducted according to a calculated gravimetric method, i. e., according to a gravimetric concentration (the mass of a dispersible phase in a unit of volume) and the calculated concentration (the number of particles in a volume unit)¹ of the aerosol; hence, the average mass of particles appears and, if the particles density is known, the average size of particles becomes known too.

-
1. In the Soviet literature there is a frequently used term, a "partial" concentration, which indicates the number of particles in a volume unit of aerosols. Due to its ambiguity ("partial" is a contrast to "complete"), we have adopted the term, a "calculated" concentration, following the example of G. ROMASHOV (22).

It would be very interesting to clarify under what conditions one can obtain such a distribution in processes of a condensable type.

Let us still assume that in case of a normal logarithmical calculated distribution of sizes (formula /3.20/), the gravimetric and other derived distributions will also be normal logarithmical within the same magnitude β_g , i. e., all derived distribution are expressed by parallel straight lines (21).

Actually in case of a distribution, which equals to a ν -th degree of a radius (a - a normalizing multiplier containing just constant values)

$$\begin{aligned} a \exp(2.302\nu \lg r) \frac{1}{\lg \beta_g \sqrt{2\pi}} \exp \left[- \frac{(\lg r - \lg r_g)^2}{2 \lg^2 \beta_g} \right] &= \\ = \frac{a}{\lg \beta_g \sqrt{2\pi}} \exp \left[- \frac{(\lg r - \lg r_g)^2 - 2.302\nu \lg r \cdot 2 \lg^2 \beta_g}{2 \lg^2 \beta_g} \right] &= \\ = \frac{1}{\lg \beta_g \sqrt{2\pi}} \exp \left\{ - \frac{[\lg r - (\lg r_g + 2.302\nu \lg^2 \beta_g)]^2}{2 \lg^2 \beta_g} \right\}. \end{aligned}$$

The straight line 1 on figure 7 represents fog with a calculated distribution; the gravimetric distribution of droplet sizes is expressed by a parallel straight line 2.

All distribution equations examined in this paragraph have one common characteristic, i. e., the points situated close to one edge or another of the graph deviate more or less from the straight line. This, however, has no great practical value for the characteristics of aerosols, because within the integral curves of distribution just a small fraction of particles responds to the marginal points. Some authors (9) are inclined to regard the equations submitted as correct within their full extent and then they explain the deviations by errors made during the tests, or by a premature settling of particles, etc. One must disagree with this, because, as we already explained, no theoretical value whatsoever should be ascribed to these equations (with the exception /3.20/). They are more or less opportune and purely empirical approximations to the actual distribution. Furthermore, due to the fact that every equation was successfully applied to one or another group of aerosols, it is to be expected that none of them represents a general

It is necessary to consider, that the "average" sizes of particles being determined by various methods may differ noticeably from one another. Like the calculated, gravimetric, etc., distribution of particle sizes also various mean values of particles exist, such as:

1. The arithmetical mean radius

$$r_1 = \bar{r} = \int_0^{\infty} r f(r) dr \approx \sum_v r_v N_v / N, \quad (4.1)$$

where N_v is the number of particles in the v -th interval;

where r_v is the middle of the interval;

where N is the total number of particles;

2. The mean quadratic (mean according to the surface) radius

$$r_2 = \sqrt{r^2} = \left[\int_0^{\infty} r^2 f(r) dr \right]^{1/2} \approx \left[\sum_v r_v^2 N_v / N \right]^{1/2}; \quad (4.2)$$

3. The mean cubic (mean according to volume or mean gravimetric) radius

$$r_3 = \sqrt[3]{r^3} = \left[\int_0^{\infty} r^3 f(r) dr \right]^{1/3} \approx \left[\sum_v r_v^3 N_v / N \right]^{1/3}, \quad (4.3)$$

etc.

Within these means, derived from a calculated distribution of sizes, large and small particles are equal. For practical purposes the weight mean possesses a greater value than that which is derived from a gravimetric distribution $g(r)$, e. g.,

$$r'_1 = \int_0^{\infty} r g(r) dr \approx \sum_v r_v g_v / G, \quad (4.4)$$

where g_v is the weight of particles in the v -th interval;

where G is the total weight of particles.

In addition to the above, there are frequently used:

4. The mean geometric radius r_g , which is determined by the equation

$$\lg r_g = \overline{\lg r} = \int_0^{\infty} \lg r \cdot f(r) dr \approx \sum_v N_v \lg r_v / N; \quad (4.5)$$

5. The calculated median radius r_m , which is determined under the conditions $F_a(r_m) = F_b(r_m) = 0.5$. This indicates that one half of the particles possess the radius $>r_m$ and one half $<r_m$;

6. The mass median radius $r_{m'}$, which is determined under analogous conditions $G_a(r_{m'}) = G_b(r_{m'}) = 0.5$, which means that a mass of particles with a radius $>r_{m'}$ constitutes one half of the entire mass of aerosol.

Let us assume that during a normal distribution $r_m = \bar{r}$ and during a normal logarithmic distribution $r_m = r_g$.

To illustrate this, let us compute various mean sizes of particles in the above described fog. In this case it would be expedient to proceed directly from the test data (see table 1), without "smoothing out" the latter and to conduct the computation according to the formula

$$r_1 = \sum_v r_v N_v / N, \quad (4.6)$$

In this way we arrive at: $r_1 = 8.9\mu$; $r_2 = 9.4\mu$; $r_3 = 9.9\mu$. According to the curve for F_b and G_b on figure 3 we obtain next that $r_m = 8.5\mu$; $r_{m'} = 11.1\mu$; according to curves 1 and 2 on figure 7 we should obtain the values $r_m = 8.6\mu$ and $r_{m'} = 11.5\mu$.

Within the experimental determination of average sizes of particles one can obtain any average, depending upon the method of mensuration. Thus, according to the computed gravimetric method it is obvious that r_3 is determined by the "corona" method (from diameters of diffraction rings) — r_1 , etc.

The logical selection of a mean to describe dispersions of aerosols, as well as to select a distribution curve, is determined by the characteristics of aerosols intended to be described. Thus, in order to describe the optical density of coarse aerosols and the rate of their precipitations within the field of gravity or forces of inertia, one should use a mean

quadratic radius r_2 ; to describe the rate of evaporation of aerosols one should use r_1 , etc. In certain unique instances one has to prepare more complicated averages. Thus, a specific area of aerosol, i. e., the magnitude of the area, which comes from a unit of mass or from a unit of volume within a dispersible phase will be estimated with the aid of particles of such a specific area, as those present in the entire aerosol. It is obvious that radii of these particles r_s are determined from the equation

$$\int_0^{\infty} 4\pi r^2 f(r) dr / \int_0^{\infty} \frac{4}{3}\pi r^3 f(r) dr = 4\pi r_2^2 / \frac{4}{3}\pi r_3^3 = 4\pi r_s^2 / \frac{4}{3}\pi r_s^3 \quad (4.7)$$

or

$$r_s = r_3^{3/2} / r_2.$$

In the fog being described the $r_s = 11.0\mu$. This value is obtained by studying the problem of light absorption by a unit of volume of the substance, from which a coarse aerosol is composed.

As we see, the various averages in the present case do not differ very much from each other. The more monodispersible an aerosol is, the smaller of course is the difference between the various averages. With regard to aerosols, the particle sizes of which extend over several orders of magnitude, the conception of a mean radius generally loses every physical meaning.

We shall return a little later to the problem of average radii and to the distribution of sizes in aerosols whose particles are of irregular shape.

§ 5. Shape and Formation of Aerosol Particles

The most simple aero-dispersible systems are fogs, the particles of which, as a rule, have a spherical shape and as they combine together during the coagulation, they form anew spheroidal droplets. It is substantially true, that in fogs formed of very viscous liquids (e. g., "Apiezon" oil) the process of conversion of a twin drop into a single, spheroidal drop may

become delayed and in such instances one can sometimes observe droplets of an irregular shape (23). More complicated phenomena can be observed in mercury fogs. In numerous tests designed to determine the electron charge by mensuration of velocity of aerosol-particle movement in a vertical electrical field (see page 79), the following phenomenon was discovered: at the time when the particles in oil fogs possessed a normal density equal to that of oil from which they were produced, the particles in mercury fogs frequently possessed a considerably smaller density than that of the mercury (24-26). At the same time the following important observation was made: the sizes of particles with a normal density diminished in the course of time following the evaporation of mercury, while the particles with an abnormal density did not evaporate (25). The normally evaporating particles were obtained from a very pure mercury by mechanical atomization (24) or upon evaporation at a temperature not very high, i. e., under the conditions detrimental to the oxidation of mercury. On the contrary, in fogs obtained by electrical discharges (25,27) or from mercury polluted with lead (28), as a rule, the particles did not evaporate. Hence, one can deduce, that the non-evaporating particles were covered with a more-or-less thick film of oxides which obstructs the evaporation of mercury. Since the density of the oxides is considerably lower than the density of the metallic mercury, such circumstance can not only lower the density of particles noticeably, but in addition still another phenomenon takes place here: the mercury droplets covered with a film of oxides do not fuse upon contacting each other, but they produce units similar to those of solid particles. The apparent density of these units, determined by mensurations in a vertical electrical field, is sometimes ten times smaller than the density of mercury. Such friable units are typical in aerosols with solid particles, and oxidized mercury fogs, which according to their characteristics, are entirely analogous to smokes.

One should distinguish in aerosols with solid particles the shape of primary particles and that of the units formed out of the latter. In smokes the original particles formed by direct conversion of vapor to crystals usually have a regular crystalline shape; if, however, the formation of smokes proceeds condensation of vapor to a kind of liquid droplet and then by subsequent solidification, the particles of smoke may have a crystalline shape as well as that of small spheres. The primary particles of smoke are frequently so small that even on electronic microphotographs it is neither possible to determine their shape nor their size; however, sometimes, the primary particles are well distinguishable even under the usual microscope.

The electronic microphotographs, shown on figures 8 (29) and 73 (page 364), present some diversified shapes and sizes of the primary particles in smokes. Usually the particles of dust have an irregular shape peculiar to the fragments of solid substances. Otherwise, the crystalline nature of the substance manifests itself also among the following: in some dusts even the

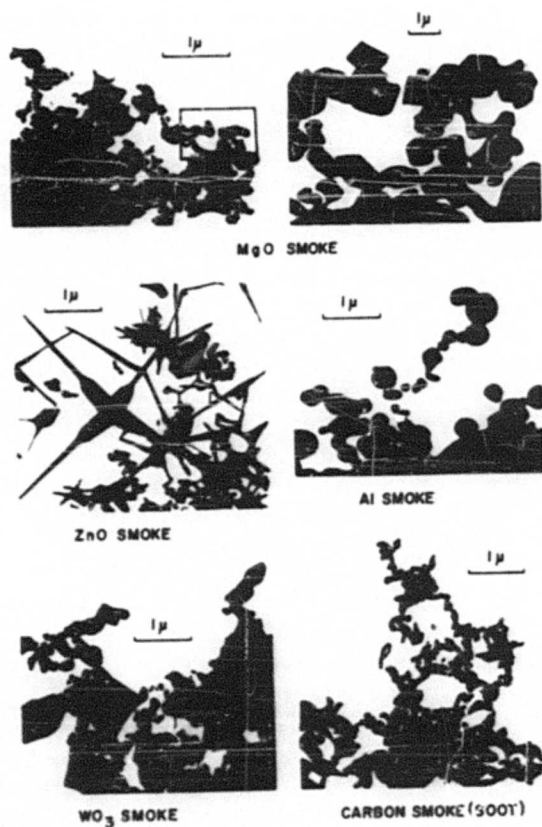


FIG. 8 ELECTRON MICROSCOPE PHOTOGRAPHS OF AEROSOL PARTICLES

smallest particles preserve the lamination peculiar to a given substance (e.g., in micaceous, slate-like and graphitic dusts), or to a fibrous shape (e.g., in asbestos and textile dusts).

It is expedient to divide into three categories and three measurements the various forms of aerosol particles according to their respective dimensions, as follows:

1. The isometric particles in which all three dimensions are approximately of equal magnitude. We refer here to the particles of a spherical shape, or to those of a regular polyhedron shape, as well as to the irregularly shaped particles, which more or less resemble the two categories.

2. The particles, which in two dimensions possess a considerably greater extent than in a third dimension, such as laminas, thin leaves, scales, etc.

3. The particles with a greater extent in one dimension, such as prisms, aciculae, fibers, etc.

The aggregates in aerosols can be formed during the coagulation of individual smoke or dust particles, also as a result of an incomplete disaggregation of powdery substances at the time of their transformation into the aerosol state (see § 58).

The number of individual particles included in the aggregates may frequently vary within a wide range from many millions to two particles. The rate of a thermal coagulation of aerosols increases rapidly at a certain gravimetric concentration as the sizes of particles diminish; at the same time the solidity of aggregates also increases, as well as their capabilities to withstand the dispersive influence of turbulence, etc. (see § 58). Consequently, the more minute the primary particles are, the stronger is the aggregation in aerosols emphasized. As a rule, the systems with highly dispersible primary particles are composed of aggregates and they comprise individual particles only as a peculiarity.

During the microscopic examination of aerosols, the individual particles and aggregates can be identified by this characteristic, i. e., at the same rate of settling the particles have a greater BROWNIAN movement than the aggregates (27). However, it is very difficult to distinguish the two types of particles under the ultramicroscope due to their very minute sizes and this is regarded as one reason for the formation of the hypothesis about a "subelectron" (see page 77).

The aggregates, according to their shape, belong to one of the two types: a more or less isometric, or linear (thread-like). The linear aggregates as such represent little chains of primary particles (see page 364).

The aggregates are quite frequently formed of such little chains. The possibility by which aggregates are allotted to one or another group, depends upon the nature of the dispersible phase and upon the gaseous medium (30), rather than upon the presence of the electrical field, etc. The subject about the formation of linear aggregates is discussed in detail in Chapter VII.

As we already pointed out the apparent density of aggregates may be considerably smaller than the actual density of the substance. The research of WHYTLAW-GREY (31) conducted specifically in conformance with the method of a vertical electrical field (see page 79) produced the following values revealing the density of particles in certain smokes (table 2):

Table 2
Density of Particles in Smokes

Substance	Density		Method of a smoke formation
	Actual	Apparent	
Au	19.3	0.2-8.0	Vaporization in an electric arc
Ag	10.5	0.64-4.22	Vaporization in an electric arc
Hg	13.6	0.07-10.8	Heating in a small open vessel
MgO	3.6	0.24-3.48	Burning metallic magnesium
HgCl ₂	5.4	0.62-4.3	Heating in a small open vessel
CdO	6.5	0.17-2.7	Vaporization in an electric arc

Taking into consideration that a divergence from a spherical shape of particles leads also to lower values of density (see page 79), one must assume that the upper range of particle density in table 2 pertains to individual particles. The very small values of apparent density (0.07 for Hg; 0.2 for Au) no doubt pertain to the aggregates of a thread-like shape and they are therefore very low. The factual proportion of apparent and actual densities of particles in smokes apparently varies in relation to the type of packing of the primary particles in the approximate range of 0.1 - 0.7, which is similar to the proportion of the "heaping" and actual densities of various powders.

It is necessary to mention here some opinions expressed by several authors (32,33), that the apparently small density of aerosol particles is influenced by the presence of an immobile gaseous coating on the particles surfaces. In order to explain the observed deviations from the

actual density of particles, it was necessary to ascribe to the coating the width of several tenths of a micron. This false opinion has neither theoretical nor experimental basis. It was frequently applied in the history of the development of aerosol physics in order to assist in the explanation of incomprehensible facts about the hypothetical coating. We shall refer back to this question later.

In solving some problems it is desirable to have a numerical expression for a "degree of irregularity" of particles. Inasmuch as all rules which determine the characteristics of aerosols with regard to particles of a spherical shape are expressed with a remarkable simplicity, the deviations from a spherical shape are usually accepted as a "degree of irregularity". In all respects it is a simple matter to accept as a "coefficient of sphericity" (34) the proportion of a sphere surface with a volume, which is equal to a volume of a given particle and to its surface. The coefficient of sphericity α_s equals 1 for spherical particles and with regard to any other shape of particles it is: $\alpha_s < 1$. The α_s equals to approximately 1 in isometric particles; thus, the α_s equals to 0.846 for an octahedron, 0.806 for a cube and 0.670 for a tetrahedron. The α_s is much less than 1 in particles considerably elongated in one or two dimensions than in crystalline shells (e.g., snow flakes) and so on.

The aerosols with a non-spherical shape of particles present greater difficulties to the problem of defining the degree of aerosol dispersions. Even among particles with a shape of regular polyhedrons, such as the tetrahedrons are, the problem of how to compute their volumes is not readily solved. Still greater arbitrariness is possible when the "sizes" of elongated particles are determined. It is even more complicated to define the dimensions of particles with the aid of two or three numbers. One must use some neutralized value, in which capacity either an "equivalent" or a "sedimentation" (STOKES') radius is employed most often. The equivalent radius of a particle r_e is the term for a radius of a sphere with a volume equal to that of a given particle and the sedimentation radius of a particle r_s is the term for a radius of a sphere with the same density and rate of sedimentation. Within the spherical particles $r_e = r_s$. Generally speaking these values vary and at the same time the difference increases in proportion to the decrease in a coefficient of sphericity of particles. The matter about the r_s value for particles of various shape and about the dependency between the r_s and r_e is discussed in § 12. The methods of determination of sizes of aerosol particles according to the rate of their sedimentation obviously offer the r_s values and the atmospheric centrifugal forces separate powdery substances into fractions also according to the r_s values. It is obvious that, during determination of sizes of particles by a calculated gravimetric method, the mean value of the equivalent radius r_e is produced; the latter can also be determined by the

method of "suspension" of particles in a vertical electrical field (page 74) and by mensurations of particles with the aid of an optical or electron microscope.

The determination of particle sizes in three dimensions under a microscope in case of coarsely dispersible aerosols is indirectly possible by setting a microscope on the upper and lower surfaces of particles, or by applying the stereo-microscopical method of YU. RANKO (35); however these methods are not applicable to particles with smaller sizes than $2-3\mu$. The mensuration of thickness is not essential in the case of isometric and

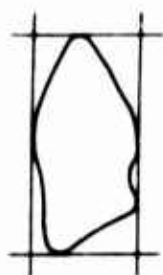


FIG. 9 DETERMINATION OF AN AVERAGE SIZE OF PARTICLES OF AN IRREGULAR SHAPE

cylindrical particles, because it coincides with the width of particles. The greatest difficulties occur in mensurations of the thickness of flaky particles, which are usually arranged in dispositions with their broad sides perpendicularly to the axis of a microscope. In general, the determination of equivalent radii under a microscope is very troublesome and sometimes, as we observed, it is an infeasible problem; therefore, it is very seldom solved in practice. Usually the efforts are limited to the determination of an

average size of particles projected within a visual field of a microscope, for which particle mensurations are effected in two mutually perpendicular directions (36), preferably toward a maximum and a minimum range of the projection (figure 9), by taking an arithmetical mean and considering it as a value of a doubled mean radius of a particle. Of course, the above "mean" radius may vary considerably from the r_e .

The basic industrial method of defining the sizes of solid particles and of the fractionation of powders is the screening analysis. A "screen" radius, which is determined by one half of the width of openings in sieves for spherical particles, coincides with the r_s and r_e and approximates same in case of isometric particles. Considering the flaky, scaly and such types of particles, the screen radius is determined by the width of flakes and therefore it surpasses the r_s and r_e ; considering the needle-shaped, prismatic and such types of particles, the screen radius being determined by the thickness of needles is smaller than the r_s and r_e . Due to this, the screen and sedimentation measurement methods of the analysis of powders with an irregular shape of particles (e. g., coal dust) frequently afford quite diversified results.

Chapter II

Rectilinear, Uniform Motion of Aerosol Particles

§ 6. Resistance of a Gaseous Medium to Motion of Very Small Particles

The mechanics of aerosols are characterized by this peculiarity, that three categories of forces influence the particles - the external forces (gravity, electrostatic, etc.) of resistance to the medium¹ and the forces of interaction between the particles. The latter in most instances are considerably more ineffectual than the rest and may be disregarded, i. e., the movements of particles may be considered as independent of each other. Thus, research in the mechanics of aerosols may be reduced to a theoretical and experimental study of the individual particle movement within a resisting medium while under the influence of various external forces; in case of necessity a correction is made to affect the interaction between particles. A certain similarity also exists relative to some other aspects of aerosols, e. g., those associated with the diffusion of light and the rapidity of evaporation, wherein one can also compute to a first approximation that every particle evaporates or scatters light in such a way, as though it were an individual particle and after this a pertinent correction is made affecting the secondary dispersion, etc. This method of research is widely used in the theory of aerosols.

It is expedient to begin the consideration of aerosol dynamics with the most simple occurrence, i. e., with a uniform motion of particles influenced by a constant force. The most studied in a theoretical as well as in an experimental way is the motion of spherical particles, which we shall analyze as the first topic.

As we already mentioned (page 12), the form of equations which express some aspects of aerosols and in this case also the resistance of a gaseous medium to a movement of particles, depends upon the value of the magnitude of the particle's radius and upon the mean length l of the free path of the gaseous molecule. With $r \ll l$, i. e., in highly dispersible aerosols or in the presence of low pressures of gas, respectively, the particle movement

1. The forces, which actuate a particle from the direction of a quiescent or a moving medium, will not be quoted here as "external" forces.

assumes a molecular character: the movement does not disturb MAXWELL'S distribution law of the molecular velocities in the medium either in value, or in direction and does not create any currents in the gas. The gas resistance in this case, depends upon the following factor: a greater number of molecules collide at the frontal surfaces of moving particles and with a greater velocity than at the rear. In this case the resistance value should be proportional to the surface, i. e., to a square of the radius of a particle. If the volume of a particle m is considerably greater than the volume of the gaseous molecules m_g , i. e., when $r = 0.5 \cdot 10^{-7}$ cm, the resistance of the medium within the examined "molecular" region of the particle movement is expressed by the formula

$$F_M = -\frac{4}{3} \pi a n_g m_g G_g r^2 V, \quad (6.1)$$

where n_g is the number of gaseous molecules in 1 cm^3 ; where G_g is the median velocity; where V is the velocity of the particles; where a is the coefficient, the value of which depends upon the mechanism of repulsion of the molecules of the gas from the surface of particles (P. EPSTEIN /37/).

In a mirror-like repulsion $a = a_1 = 1$; in a diffuse repulsion with the preservation of the absolute velocity by the colliding molecules $a = a_2 = 13/9 = 1.442$; in a diffuse repulsion, following the pickup by gaseous molecules of the velocity distribution, which corresponds to a temperature of the particle surface, i. e., in a total equilibrium, $a = a_3 = 1 + \frac{\pi}{8} = 1.393$. All other mechanisms of molecular repulsion, adopted by some authors, differ from the principles of statistical mechanics.

With the aid of the familiar term pertinent to the viscosity of a gas

$$\eta = 0.3502 n_g m_g G_g l, \quad (6.2)$$

one can express the resistance of the medium in a following manner (38):

$$F_M = -\frac{4/3 \pi a r^2 \eta V}{0.3502 l} = -\frac{6 \pi a r^2 \eta V}{0.3502 \cdot 4.5 l} = -\frac{6 \pi \eta r^2 V}{(A + Q) l}. \quad (6.3)$$

Here, according to the considerations stated below, the value of $0.3502 \cdot 4.5/a$ is designated by: $A + Q$. In the three discussed mechanisms of repulsion $A + Q$ assumes accordingly these values: $(A + Q)_1 = 1.175$; $(A + Q)_2 = 1.091$; $(A + Q)_3 = 1.131$. The movement of oil droplets was the most

carefully studied (by MILLIKAN) experimentally; with it the value of 1.154 was obtained (39) for $A + Q$. The results of tests with larger droplets (page 44) lead to a conclusion that, in the case under consideration, a diffuse repulsion of gaseous molecules from the surface of the droplets takes place in accordance with a small persistency in velocities, i. e., with a tendency toward the preservation of the component of tangential velocity of the molecules. According to mathematics, the above is tantamount to a condition in which a definite fraction of molecules (in the case of oil droplets - about 10%) are repulsed mirror-like and the remaining ones - diffuse-like. In this supposition the theoretical value of the coefficient $A + Q$ happens to be equal to 1.125 with the preservation of the velocities of gaseous molecules and to 1.164 - in the total equilibrium. Upon comparing the experimental value of $A + Q = 1.154$, it follows that the diffuse repulsion is apparently accompanying the total equilibrium of the molecules.

Concerning the range of applicability of the equations (6.1) or (6.3), see page 38.

§ 7. STOKES' Law Equation

In case $r \gg l$ and additional conditions, discussed below, prevail, the resistance of the medium to movement of spherical particles is expressed by the familiar STOKES' law equation, as follows:

$$F_M = - 6\pi\eta rV. \quad (7.1)$$

Thus, the resistance is proportional to the first power of the radius.

In this case the movement of particles has hydrodynamic features: it disturbs the isotropism of the distribution of the molecular velocities within the medium and it develops in the latter a hydrodynamic current. The resistance of the medium is caused here by hydrodynamic forces.

A more important instance of the applicability of the STOKES' law is the settling of aerosol particles under the influence of gravity. In this case the force activating a particle is equal to

$$F = \frac{4}{3} \pi r^3 g (\gamma - \gamma_g) \approx \frac{4}{3} \pi r^3 g \gamma. \quad (7.2)$$

where g is the acceleration of gravity; where γ and γ_g are the densities of the particles and of the medium, respectively. In view of its smallness, the latter may be disregarded. From (7.1) and (7.2) we obtain for a constant velocity of settling of particles

$$V_s = \frac{2}{9} \frac{r^2 g \gamma}{\eta} = g \tau, \quad (7.3)$$

where $\tau = \frac{2}{9} \frac{r^2 \gamma}{\eta}$ - is the value with a time dimension, which, as we shall see later, plays an important part in the mechanics of aerosols.

According to the conclusions of STOKES' law and derivations from the basic equations of the dynamics of viscous liquids, it is assumed that the following conditions prevail (40):

1. The incondensability of the medium;
2. The infinite expansion of the medium;
3. The infinitely small velocity of the movement;
4. The constancy of the velocity of the movement;
5. The rigidity of the particle;
6. The non-sliding condition on its surface.

1. As we know, the condensability of the medium in hydrodynamics begins to manifest itself only in flow velocities comparable with the velocity of the propagation of mechanical impulses within the medium, i. e., with the velocity of sound. Thus, with the exception of the phenomena, such as the movement of aerosols resulting from an explosion, etc., the gaseous medium may be regarded in the mechanics of aerosols as incondensable.

2. The condition of an infinite expansion of the medium in all directions is never fulfilled in practice: at a greater or smaller distance from the particles of an aerosol there are some macroscopic bodies (e. g., vascular walls) as well as other particles present everywhere. The problem of the influence of walls upon the movement of fine particles in the region of applicability of STOKES' law was examined quite in detail from the theoretical standpoint as well as in an experimental way, the latter included systems with a liquid medium; in conjunction with the above a high conformity of the

theory with experiments was obtained (41). The influence of walls leads to an increase of the medium's resistance by a multiplier $1 + b \frac{r}{x}$, in which x denotes the distance of a particle center from a wall and b denotes the coefficient dependent upon the shape and the spacing of the walls. In conjunction with the above it is assumed that r/x is sufficiently small (not over 0.1). Since in a particle movement parallel to a flat wall b equals $9/16$ to a first approximation, so in a movement perpendicular to a wall $b = 9/8$ and in a movement lengthwise to the axis of an infinitely long cylinder $b = 2.1$. Thus a correction of the influence of the walls amounts to a noticeable value only at a distance x of the $10r$ order. However, in view of a comparatively greater rapidity of aerosol particle displacement at the expense of Brownian movement, convection, and sedimentation, the particles cannot remain for any length of time at such a close distance away from a wall without settling on it. Therefore in most instances one can exclude from the mechanics of aerosols the influence of walls affecting the resistance of the medium. We shall discuss later a more complicated problem about the reciprocal influence of aerosol particles affecting their movement (see § 13).

3. According to derivations of STOKES' law the inertia terms are omitted in equations of the movement of viscous liquids; this is permissible only during infinitely small velocities of the movement. Thus STOKES' law as such represents the first approximation. The second approximation of the inertia forces at the expense of particles as obtained by OSEEN (42) appears as follows:

$$F_M = -6\pi\eta rV \left(1 + \frac{3}{8} \frac{r\gamma_g V}{\eta}\right) = -6\pi\eta rV \left(1 + \frac{3}{16} Re\right), \quad (7.4)$$

where γ_g is the density of the medium and

$$Re = 2r\gamma_g V / \eta, \quad (7.5)$$

which refers to a particle movement, is a REYNOLDS number. Hence, it is obvious, that STOKES' law can only be used with small Re 's. We shall explain later (see page 50), that the error which is admissible here is almost proportional to Re and it comprises approximately 1.7%, if $Re = 0.1$.

4. The influence over the inconstancy of the particles velocity, which also affects the resistance, is discussed in Chapter III.

5. According to the conclusions of STOKES' law it is assumed that a particle as such represents a solid substance. Proceeding to fluid droplets, two new factors appear:

a. A droplet can be deformed by the action of medium's resistance (this effect assuming noticeable magnitudes only among very large droplets is discussed below /page 66/).

b. A circulation of the fluid, developing in a moving droplet and directed at the droplet surface counter to its movement, reduces the friction between the droplet and the medium, hence, the resistance too. The resistance of the medium to the movement of spherical particles is expressed in the given case by the following equation (43, 44):

$$F_M = - 6\pi\eta rV \frac{1 + (2\eta/3\eta_p)}{1 + (\eta/\eta_p)}, \quad (7.6)$$

where η is the viscosity of the medium; where η_p is the viscosity of liquid from which the droplet was formed.

Due to the fact that the viscosity of gases is considerably lower than that of liquids, the correction in STOKES' law is insignificant. It amounts to 0.7% in water fogs in the atmosphere and to hundredths or a few thousandths of one percent in oil fogs.

6. According to deductions from STOKES' law it is assumed, that near the surface of a particle no drop in velocities occurs, i. e., an infinitely thin layer of medium, adjacent to the surface, is immobile in relationship to the particle. If such a drop of velocities, or a "slipping" of the medium on a surface of a particle is present, naturally the resistance of the medium must be reduced. If we take into consideration that the tangential forces actuating a particle are proportional to such a drop of velocities and if we denote by η_e the factor of proportionality, named "a coefficient of an external friction," the resistance will be expressed by this equation (45)

$$F_M = - 6\pi\eta rV \frac{2\eta + r\eta_e}{3\eta + r\eta_e} \quad (7.7)$$

Hence, an infinitely larger η_e results from STOKES' law.

When denoting by β the proportion of η/η_e , which is named "a coefficient of slipping," we obtain for small values β/r

$$F_M = -6\pi\eta rV \frac{1 + (2\beta/r)}{1 + (3\beta/r)} \approx -6\pi\eta rV / \left(1 + \frac{\beta}{r}\right). \quad (7.8)$$

The experiment indicates that in case of a liquid medium the slipping on the surface of a moving particle does not take place and the discussed correction is not necessary. However, there is another questionable point in a gaseous medium. Here the phenomenon of slipping, associated in a small degree with the action of filling up the volume of substances in gases, plays a more important role.

§ 8. Resistance of the Medium in a Transitional Region

In all processes of transfer, which is discussed in the theory of gas kinetics, such as those of heat conductivity (transfer of thermal energy), viscosity (impulse transfer), and diffusion (transfer of matter), there is a rapid change in a pertinent parameter (of temperature, velocity, concentration) at the surface of a solid substance from which the specified transfer emanates. The magnitude of the change, roughly speaking, is equal to the product of the parameter gradient at the surface, by the average length of the molecular gas path l . Therefore the effect produced by the rapid change attains a noticeable magnitude in comparison with the dimension of the gaseous volume either with a greater value of l , or during a greater gradient value at the surface and particularly so at the surface of small particles. In the latter case the gradient value in all processes of transfer is proportional to y/r ; where y is the difference in temperature, in velocity, or in the vapor pressure of a particle and also the pressure of the surrounding medium (at an infinitely greater distance from a particle).¹ Thus, the decrease of the parameter is equal to Ayl/r ; where A is the numerical coefficient, which depends upon the nature of repulsion of gaseous molecules from the particle surface and the effective difference of parameters (of temperature, velocity or vapor pressure) becomes reduced due to the decrease from y to $y(1 - \frac{Al}{r})$. As a result of the above, the change of velocity in the process of transfer due to the decrease is expressed by the correction multiplier: $1 - A\frac{l}{r} \approx 1 / (1 + A\frac{l}{r})$.

1. In principle the gradient of tangential velocity at the surface of a moving particle, with small Re 's is equal to $3/2V\sin\theta/r$; where θ is the angle between a radius-vector at a given point of the surface and the direction of the movement; V denotes a particle velocity.

UNCLASSIFIED

AD

2271876

**FOR
MICRO-CARD
CONTROL ONLY**

2 OF 9

Reproduced by

Armed Services Technical Information Agency

ARLINGTON HALL STATION; ARLINGTON 12 VIRGINIA

UNCLASSIFIED

"NOTICE: When Government or other drawings, specifications or other data are used for any purpose other than in connection with a definitely related Government procurement operation, the U.S. Government thereby incurs no responsibility, nor any obligation whatsoever; and the fact that the Government may have formulated, furnished, or in any way supplied the said drawings, specifications or other data is not to be regarded by implication or otherwise as in any manner licensing the holder or any other person or corporation, or conveying any rights or permission to manufacture, use or sell any patented invention that may in any way be related thereto.

As the accurate analysis of the decrease of the tangential velocity at the surface of particles indicates (P. EPSTEIN /37/), the coefficient of slipping β in the equation (7. 8) is equal to

$$\beta = 0.7004 \left(\frac{2}{f} - 1 \right), \quad (8.1)$$

where f stands for a fraction of gaseous molecules being reflected from the surface diffusively and $1-f$ stands for those being reflected mirror-like. Hence, we obtain for resistance of the medium the expression

$$F_M = - 6\pi\eta rV / \left(1 + A \frac{1}{r} \right), \quad (8.2)$$

where

$$A = \beta / 1 = 0.7004 \left(\frac{2}{f} - 1 \right), \quad (8.3)$$

and for velocity of the particles settling:

$$V_s = \frac{2}{9} \frac{r^2 \gamma g}{\eta} \left(1 + A \frac{1}{r} \right) = \frac{mg}{6\pi\eta r} \left(1 + A \frac{1}{r} \right). \quad (8.4)$$

Since (7. 8) reveals for small values $\beta/r = A \frac{1}{r}$ and the value of A is of a unit order, thus equation (8. 2) submitted at first by CUNNINGHAM (46) is true only when $1/r$ is small

MILLIKAN (38) ascertained that the A value for oil droplets in the atmosphere is equal to 0.864 and this, according to (8. 3), corresponds to $f = 0.895$. Thus, approximately 10% of molecules are reflected from the surface mirror-like and the remaining ones - diffusively.

Unquestionably the 10% represents the degree of persistency of the tangential velocity of molecules during their repulsion (see page 38). The coefficient of air-slipping upon an oil surface was also determined by means of KUETT'S¹ viscosimeter, coated with a layer of oil (47). Thus, the very close value of $A = 0.870$ was obtained. For droplets of oil, of mercury, and of water solutions $BaHgI_4$ many authors obtained A values within a range

1. KUETT'S viscosimeter consists of two coaxial cylinders, one of which is rotary. A measured movement of rotation is transferable by a friction to the other cylinder.

of 0.820 - 0.900 (see /48/); the latter indicates comparatively small changes in the nature of a molecular repulsion: from 8 to 12% of the molecules are reflected mirror-like. Similar results were also obtained for solid spherical particles of selenium. Considerably greater variations of the slipping coefficient were observed among other solid substances (47). Thus, $\beta = 0.82 \cdot 10^{-5}$ was found for small vitreous balls; $0.66 \cdot 10^{-5}$ for sharp, cylindrical brass fragments; $0.97 \cdot 10^{-5}$ for cylindrical fragments covered with a shellac and $0.68 \cdot 10^{-5}$ for similar fragments, but with a layer of aged shellac. If in equation (8.3) we substitute $l = 0.94 \cdot 10^{-5}$, it follows that the indicated values of β correlate with the following values for f : 0.92; 1.00; 0.81 and 0.99. This supports the fact, that on a recently fused and extremely smooth surface of an amorphous substance the repulsion assumes almost such a character, as on the surface of a liquid. However, a mechanically processed, or an aged and cracked surface, is rough only to the extent that the repulsion of molecules upon it is entirely diffusive. From a practical standpoint one can assume that $A = 0.86$ in liquid droplets and in very smooth, small solid spheres, while in small rough spheres $A = 0.70$. According to (8.3), the $A = 0.70$ is the smallest possible value. Actually owing to unique efforts during which smaller values of A were discovered, it was easy to detect errors in the procedures.

We have examined the problem of resistance of the gaseous medium in two instances, under the molecular ($r \ll l$) and the hydrodynamic ($r \gg l$) conditions of particle movement. There is an abandoned problem to be discussed, that of the resistance of a medium in the transition region, with the identical order of r and l values, which is concerned with the range of applicability of the afore-mentioned limitation laws. This task appeared to be too difficult for a theoretical review; it was necessary to confine oneself to the introduction of an equation satisfactorily conforming with the experiment, i.e., the empirical equation (39, 49)

$$F_M = - 6\pi\eta rV / \left(1 + A\frac{1}{r} + Q\frac{1}{r}e^{-br/l}\right), \quad (8.5)$$

which being readily convincing, is developed asymptotically in (8.2) with $r \gg l$ and in (6.3) with $r \ll l$. It was found (39) that, for oil droplets in the atmosphere, $A = 0.864$, $Q = 0.29$, and $b = 1.25$. Considering water solutions of BaHgI_4 droplets in the atmosphere (50), $A = 0.879$, $Q = 0.23$, and $b = 2.61$. Taking into account vitreous small spheres in the air¹, $A = 0.77$; $Q = 0.40$;

1. KNUDSEN'S and WEBER'S article (49) contains somewhat higher values of A and Q , because in the term (6.2) for gaseous viscosity authors have adopted the coefficient of 0.310.

Table 3

Mobility of Oil Droplets in the Air at 23° and 760 mm of Mercury

lg r	lg B	Δ	lg u ¹	lg r	lg B	Δ	lg u ¹
8.3	12.898	200	1.102	6.9	7.893	156	4.097
8.4	12.698	200	0.902	5.0	7.737	148	5.941
8.5	12.498	200	0.702	5.1	7.589	141	5.793
8.6	12.298	200	0.502	5.2	7.448	135	5.652
8.7	12.098	199	0.302	5.3	7.313	129	5.517
8.8	11.899	199	0.113	5.4	7.184	122	5.388
8.9	11.700	199	1.904	5.5	7.062	118	5.266
7.0	11.501	200	1.705	5.6	6.944	115	5.148
7.1	11.301	199	1.505	5.7	6.829	113	5.033
7.2	11.102	199	1.306	5.8	6.716	111	6.920
7.3	10.903	200	1.107	5.9	6.605	109	6.809
7.4	10.703	199	2.907	4.0	6.496	107	6.700
7.5	10.504	198	2.708	4.1	6.389	106	6.593
7.6	10.306	197	2.510	4.2	6.283	105	6.487
7.7	10.109	196	2.313	4.3	6.178	103	6.382
7.8	9.913	195	2.117	4.4	6.075	103	6.279
7.9	9.718	194	3.922	4.5	5.972	102	6.176
6.0	9.524	193	3.728	4.6	5.870	101	6.074
6.1	9.331	192	3.535	4.7	5.786	100	7.972
6.2	9.139	190	3.343	4.8	5.667	101	7.871
6.3	8.949	187	3.153	4.9	5.567	101	7.771
6.4	8.762	183	4.966	3.0	5.466	101	7.670
6.5	8.579	180	4.783	3.1	5.365	101	7.569
6.6	8.399	175	4.603	3.2	5.264	100	7.468
6.7	8.224	169	4.428	3.3	5.164	100	7.368
6.8	8.055	162	4.259	3.4	5.064		7.268

1. u - electric mobility (see page 140).

$b = 1.62$ It must be considered that the accuracy in the experimental determination of Q and b is much smaller than that in the determination of A .

We wish to emphasize that in the equations (8.2), (8.4), and (8.5), l does not denote the actual mean length of the free path of gaseous molecules but a conditional value of the length, which is calculated according to equation (6.2), also a component value of $0.942 \cdot 10^{-5}$ cm for the air at 23° and 760 mm of mercury. In the succeeding definition of the coefficient within equation (6.2), as a result of the adaptation of the theory of collisions between the gaseous molecules, MILLIKAN retained the value of l and hence, the values of the parameters A , Q , and b as well, as they are

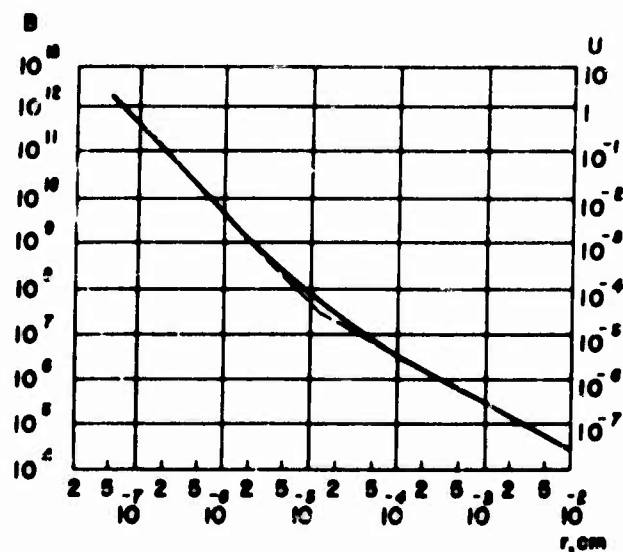


FIG. 10 RELATION OF THE MOBILITY OF AEROSOL PARTICLES TO THEIR SIZES

introduced in the equations in computing the resistance. The effected (between 1935 and 1938) correction of the coefficient of the viscosity of air (increasing it by approximately 0.5%) also did not change the values of the parameters.

The ratio between the particle velocity V and the force F actuating it, is named the particle mobility B . According to (8.5)

$$B = \left(1 + A \frac{1}{r} + Q \frac{1}{r} e^{-br/l} \right) / 6\pi\eta r. \quad (8.6)$$

Conforming with the above equation there are in table 3 $\lg B$ values as a function of $\lg r$ for oil droplets in the air at 23° and 760 mm of

mercury. The value of $18.3 \cdot 10^{-5}$ poise has been accepted for the viscosity of air. The same relation is represented on figure 10. We assume that with the given magnitude of the scale, the curves for particles of various substances practically coincide.

As the calculations obtained with the aid of equation (8.6) indicate, the error in the application of the molecular-kinetic equation (6.3) amounts to 1% at $r = 2 \cdot 10^{-7}$ cm and 10% at $r = 2 \cdot 10^{-6}$ cm. The error in the application of CUNNINGHAM'S equation (8.2) amounts to 1% at $r = 1.8 \cdot 10^{-5}$ cm and 10% at $r = 5 \cdot 10^{-6}$ cm. Finally, STOKES' law (7.1) gives an error to the amount of 1% at $r = 8 \cdot 10^{-4}$ cm and 10% at $r = 0.8 \cdot 10^{-4}$ cm.

Depending upon a safe degree of exactness, we have prepared a table of the range of applicability of these equations (table 4). Shown in the table are

Table 4

Range of Applicability of Various Formulae for Resistance of the Medium

Formula	Admissible Error	
	1%	10%
STOKES' (7.1)	$8 \cdot 10^{-4} < r < 15 \cdot 10^{-4}$ cm	$0.8 \cdot 10^{-4} < r < 35 \cdot 10^{-4}$ cm
CUNNINGHAM (8.2)	$1.8 \cdot 10^{-5} < r < 8 \cdot 10^{-4}$ cm	$5 \cdot 10^{-6} < r < 8 \cdot 10^{-5}$ cm
Molecular - kinetic (6.3)	$1 \cdot 10^{-7} < r < 2 \cdot 10^{-7}$ cm	$5 \cdot 10^{-8} < r < 2 \cdot 10^{-6}$ cm

compiled recognized deviations from STOKES' law, which are developed by inertia forces (see equation /7.4/) and there is an upper range of the adaptability of the equation (7.3) for particles with a density 1, which settle freely in the air under the influence of gravity. There are also deviations (possessing a magnitude of order m_g/m) obtained from the equation (6.3) for particles of molecular sizes with a density 1 in the atmosphere.

§ 9. Experimental Proof of STOKES' Law and Its Exactness

The mode of experimental testing of STOKES' law by measuring the velocity of solid particles settling is especially favorable in so far as a liquid

medium is involved. By using liquids of high viscosity one can connect the settling of small spheres with large size spheres, which have a slow rate of settling, i. e., one can attain a higher degree of exactness in the measurements with respect to sufficiently low REYNOLD'S numbers. The only difficulty in working with spheres of a larger size is the necessity of using a rather large correction for the influence of the walls. Tests conducted with a liquid medium revealed that in a measured rate of settling of small spheres the deviations from the rate computed according to STOKES' law do not exceed the errors in the measurements (52). Hence, by applying the principle of hydrodynamics to similarity one can draw a conclusion about the applicability of STOKES' law even with gaseous mediums; however, it is also necessary to confirm this deduction with a direct experiment.

These experiments are by far more difficult than those with liquids, because the condition for a satisfactory smallness of Re can only be fulfilled by using very small spheres ($r < 10\mu$) with which the deviations due to slipping already begin to appear. Furthermore, it is extremely difficult to obtain strictly spherical solid particles of that size and as for liquid droplets, it is difficult to determine exactly their size under the microscope. Thus direct tests enabled us to determine only the approximate accuracy of STOKES' law for a gaseous medium (12). The degree of exactness of the formula was determined by the following indirect way: the value of an electron charge, as defined by MILLIKAN (53) (page 75), based on the principle of STOKES' law (with correction for slipping) at $4.77 \cdot 10^{-10}$ ES units, appeared very close to the value of $4.80 \cdot 10^{-10}$ ES units, which was computed from the sizes of elemental nuclei in crystals, the latter determined by a roentgenographic method. Then, after we clarified the reason for the small (0.6%) difference in results evolved from using incorrect values of the air viscosity (54), new and more precise viscosity measurements were performed and the difference was reduced to 0.1%. Yet, with a unanimous opinion of all physicists working in this field, the remaining difference was nevertheless explained by insufficient accuracy of the viscosity measurements (51). Thus, STOKES' law expresses one of the more accurate laws of physics pertaining to a liquid as well as to a gaseous medium.

The importance of STOKES' law in the theory of aerosols is extremely great. Although, as we explained above, the range of aerosol dispersion within which the formula is more or less exactly followed is very narrow, yet, by means of proper corrections, or by limiting its greater exactness, one can succeed in expanding the formula into a rather wide range ($10^{-5} \text{ cm} < r < 5 \cdot 10^{-3} \text{ cm}$), which encompasses a greater share of a practical value to aerosols. As we shall explain later, almost all mechanics of aerosol-dispersible systems and particularly so the theory of the motion and

precipitation of particles in suspension in various industrial devices are based on STOKES' law.

§ 10. Resistance of the Medium Within Ultra-STOKES' Region

As we mentioned above, due to the increasing influence of inertial forces with the increase of the Re number, the resistance of the medium computed according to STOKES' law lags behind the actual resistance and even at $Re = 0.5$ the deviation surpasses 5%. The OSEEN equation (7.4) and the somewhat more exact equation of GOLDSTEIN (55),

$$F_M = -6\pi\eta rV \left(1 + \frac{3}{16} Re - \frac{19}{1280} Re^2 + \dots\right), \quad (10.1)$$

both derived with a particular accounting for the inertial forces, offer to some extent a better approximation and at the same time the computed resistance, in this case, is closer to the actual one. Yet, the prevalent opinion, that OSEEN'S equation offers a considerably better approximation than STOKES' law, is in some measure exaggerated. This opinion is primarily based on SCHMIEDEL'S (56) experiments, which are considered as very exact within the region of small Re's. Meanwhile the experimental values of resistance obtained by SCHMIEDEL with very small Re's are undoubtedly too high, because they obviously surpass even the values computed according to OSEEN'S method and this is in contradiction with data of all other researchers. Apparently this is explained by errors, amounting 1% - 2% in the measurements of the viscosity of liquids, on which SCHMIEDEL conducted his experiments. As a result, the experimental points came closer to OSEEN'S curve and they receded from the curve of STOKES. In the more recent measurements of MOLLER (57) which must be considered as more exact, the following results were obtained: STOKES' law at $Re = 0.1$ offers a departure of -1.5%; OSEEN'S equation +0.4%, at $Re = 0.2$ the departure comprises -3% and +0.8%; and at $Re = 0.5$, -6.5% and +1.5%. Thus, OSEEN'S equation offers approximately a four times better approximation than STOKES' law. According to equation (10.1) one can still obtain a somewhat better approximation, which, however, does not atone for its perplexity. The application of these equations has generally no specific significance in practice, inasmuch as it is easier to use experimental data and this we shall discuss later.

The proportionality is not disturbed by the difference between molecular and viscous regions of flow, where the resistance is exactly proportional to the particles velocity, i. e., in the region of greater Re values, where one must not disregard the forces of inertia. Thus, the

resistance changes proportionally to V_g and at the same time V_g increases continuously. Therefore the conception of the particles mobility, as being independent of the velocity, loses its significance: one must determine the functional dependence of resistance not from only one, but from two variables, i.e., from the size and from the velocity of the particle. However, if a hydrodynamic principle of similarity is applied, the complicated problem may be considerably simplified: the non-dimensional value of

$$\psi = F_M / \frac{\gamma_g V^2}{2} \cdot \pi r^2, \quad (10.2)$$

which is named the coefficient of a frontal resistance of a sphere, must be a well-defined unique function with a non-dimensional value, i.e., a Re number.

Particularly so in the realm of applicability of STOKES' law as one can convince himself, this function aims at

$$\psi = 24 / \text{Re}, \quad (10.3)$$

while regarding OSSEN'S equation, this function is correlated with

$$\psi = 24 / \text{Re} + 4.5. \quad (10.4)$$

The functional dependence between ψ and Re was defined in many experimental problems (58), during which either the velocity of solid small spheres' settling in liquids was measured, or the force, which influences an immobile sphere present in a flowing liquid or in a gas. If we digress from the influence of walls, the force of interaction between the sphere and the medium depends only upon their relative velocities and it has an equal value when a substance is moving within a quiescent medium, or when the case is reversed.

The results of these examinations are presented in table 5. In compiling it we used MÖLLER'S (57) data in the realm of $\text{Re} < 0.4$ and for $\text{Re} > 0.4$ DAVIES' (59) data obtained by striking a balance among the results of some of the more reliable works. The probable error in ψ values submitted on table 5 amounts to approximately 1% for $\text{Re} < 0.5$ and as it progressively increases with the increase of Re, it amounts to 3% - 4% at $\text{Re} = 500$.

Various authors submitted a rather great number of empirical equations connecting ψ with Re. However, the most successful equation among them, for simplicity and degree of approximation, is the one

submitted by L. KLYACHKO (60)

$$\psi = \frac{24}{Re} + \frac{4}{\sqrt[3]{Re}}, \quad (10.5)$$

which, in the range of $3 < Re < 400$, offers variations not exceeding 2% above the values quoted on table 5.

In order to compute, according to table 5, the settling velocity of particles with a radius of $>10^{-3}$ cm (it is simpler and more accurate to use the equation /8.4/ for very small particles) one proceeds in the following way. From (7.5) and (10.2) one can derive the following equation:

$$Re^2 \psi = \frac{8F_M \gamma g}{\pi \eta^2} \quad (10.6)$$

or by comparing F_M with the gravitation force on a particle

$$Re^2 \psi = \frac{32}{3} \frac{r^3 \gamma \gamma g}{\eta^2}. \quad (10.7)$$

If we know particle radius and all the remaining values included in the (10.7), we compute the $Re^2 \psi$; next, we find, according to table 5, the corresponding value of Re ; and finally, according to (7.5), we determine the velocity of settling V_g . A similar procedure follows during computation of any other external force actuating a particle.

In a reversed problem, that of finding the size of particles according to the velocity of their settling, we proceed from the equation

$$Re/\psi = \frac{3V_g^3 \gamma^2}{4\gamma g \eta}. \quad (10.8)$$

Figure 11 shows a graph prepared according to this method; it pertains to the velocity of settling of spherical particles with a density of 1, 2, and 4 in the atmosphere at 20° and 760 mm. The broken curves are plotted according to STOKES' law.

Table 5

Coefficient Values of a Frontal Resistance ψ and of the Functions $Re^2 \psi$ and ψ/Re for Spherical Substances in the Realm of Re 0.01 - 1000

$lg Re$	$lg \psi$	Δ	$lg Re^2 \psi$	$lg (\psi/Re)$	$lg Re$	$lg \psi$	Δ	$lg Re^2 \psi$	$lg (\psi/Re)$
$\bar{2}.0$	3.380		$\bar{1}.380$	5.380	0.6	0.928		2.128	0.328
$\bar{2}.1$	3.281	99	$\bar{1}.481$	5.181	0.7	0.852	76	2.252	0.152
$\bar{2}.2$	3.181	100	$\bar{1}.581$	4.981	0.8	0.778	74	2.378	$\bar{1}.978$
$\bar{2}.3$	3.082	99	$\bar{1}.682$	4.782	0.9	0.706	72	2.506	$\bar{1}.806$
$\bar{2}.4$	2.982	100	$\bar{1}.782$	4.582	1.0	0.636	70	2.636	$\bar{1}.636$
$\bar{2}.5$	2.883	99	$\bar{1}.883$	4.383	1.1	0.568	68	2.768	$\bar{1}.468$
$\bar{2}.6$	2.783	100	$\bar{1}.983$	4.183	1.2	0.502	66	2.902	$\bar{1}.302$
$\bar{2}.7$	2.684	99	0.084	3.984	1.3	0.438	64	3.038	$\bar{1}.138$
$\bar{2}.8$	2.585	99	0.185	3.785	1.4	0.375	63	3.175	$\bar{2}.975$
$\bar{2}.9$	2.486	99	0.286	3.586	1.5	0.314	61	3.314	$\bar{2}.814$
$\bar{1}.0$	2.387	99	0.387	3.387	1.6	0.255	59	3.455	$\bar{2}.655$
$\bar{1}.1$	2.289	98	0.487	3.189	1.7	0.198	57	3.598	$\bar{2}.498$
$\bar{1}.2$	2.191	98	0.591	2.991	1.8	0.143	55	3.743	$\bar{2}.343$
$\bar{1}.3$	2.093	98	0.693	2.793	1.9	0.090	53	3.890	$\bar{2}.190$
$\bar{1}.4$	1.995	98	0.795	2.595	2.0	0.039	51	4.039	$\bar{2}.039$
$\bar{1}.5$	1.898	97	0.898	2.398	2.1	$\bar{1}.991$	48	4.191	$\bar{3}.891$
$\bar{1}.6$	1.802	96	1.002	2.202	2.2	$\bar{1}.945$	46	4.345	$\bar{3}.745$
$\bar{1}.7$	1.707	95	1.107	2.007	2.3	$\bar{1}.902$	43	4.502	$\bar{3}.602$
$\bar{1}.8$	1.613	94	1.213	1.813	2.4	$\bar{1}.861$	41	4.661	$\bar{3}.461$
$\bar{1}.9$	1.521	92	1.321	1.621	2.5	$\bar{1}.823$	38	4.823	$\bar{3}.323$
0.0	1.430	91	1.430	1.430	2.6	$\bar{1}.787$	36	4.987	$\bar{3}.187$
0.1	1.341	89	1.541	1.241	2.7	$\bar{1}.754$	33	5.154	$\bar{3}.054$
0.2	1.254	87	1.654	1.054	2.8	$\bar{1}.723$	31	5.323	$\bar{4}.923$
0.3	1.169	85	1.769	0.869	2.9	$\bar{1}.695$	28	5.495	$\bar{4}.795$
0.4	1.086	83	1.886	0.686	3.0	$\bar{1}.671$	24	5.671	$\bar{4}.671$
0.5	1.006	80	2.006	0.506	3.1	$\bar{1}.650$	21	5.850	$\bar{4}.550$
		78							

It must be emphasized, that the afore-cited equations and tables can be used directly only in relatively rare instances to compute the velocity of settling and of other well regulated movements of aerosol

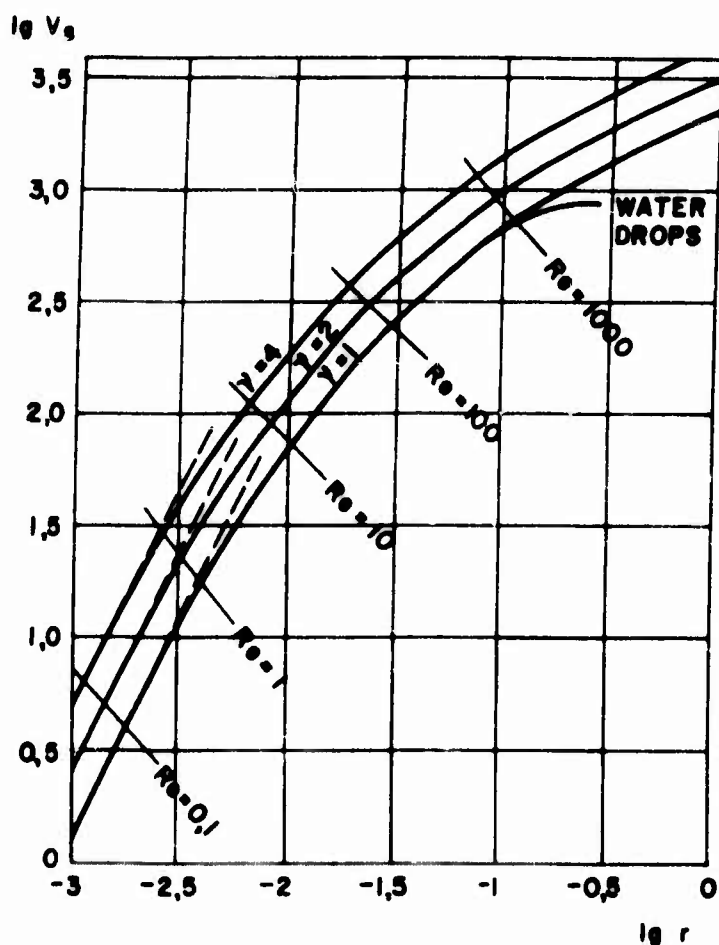


FIG. II VELOCITY OF SETTLING OF AEROSOL PARTICLES
IN THE ATMOSPHERE

particles found in nature and in manufacturing processes, because the presence of turbulence and of convective currents changes the nature of settling entirely (see Chapter VI).

§ 11. General Properties of Motion of Non-Spherical Particles

Up to this point we discussed the motion of spherical particles only, because this topic is studied the most from the theoretical standpoint, as well as in an experimental way. Meanwhile, it is known that solid particles of aerosols are usually of a non-spherical shape. The theoretical

problem about the resistance of a medium to the movement of non-spherical particles has, up to this time, been solved only with regard to ellipsoids and among them with respect to infinitely thin ellipsoidal flakes (a limiting ellipsoidal example) and with regard to cylinders with an infinitely large ratio of their length to their diameter. As to experimental studies of this problem, we must iterate here, what has been said about the experimental test of STOKES' law, that it is far easier to perform it in a liquid than in a gaseous medium. Actually, almost all experimental data, pertinent to this problem, were obtained by testing with a liquid medium. This data supported by the principle of similarity can also be applied to the mechanics of aerosols.

Phenomena occur during the movement of non-spherical particles in a resistant medium, which are absent when particles of a strictly spherical shape are involved. If during motion low velocities prevail and are identified with a purely viscous condition of flow, particles can orientate themselves in any manner depending upon the direction of their movement (61, 62) and, depending upon their size either maintain their originally assumed path, or, due to Brownian spinning, take all possible paths. The above fact firmly established experimentally is in full agreement with inferences of hydrodynamics, according to which the spinning moment actuating a particle of an irregular shape is equal to zero (63) within a purely viscous range of the movement.

The characteristic peculiarity of the movement of non-spherical particles is confined to this, that the directions of the particles movements and of the medium's resistance do not depend upon a single straight line, but they form a certain angle α . The exception is in movement parallel to the axis of a particle symmetry. GANS (63) computed α angle at a small Re with the aid of equations (12.2) to (12.5), for spinning particles having an ellipsoid shape (see page 57). The α value results from inclination angle θ of the axis of a spinning ellipsoid to the direction of the movement and it attains its maximum value at $\theta = 40 - 45^\circ$ for oblated ellipsoids and at $\theta = 45 - 55^\circ$ for elongated ellipsoids. The α angle increases with an increased ratio of a larger to a smaller ellipsoid axis β . In case of oblated ellipsoids the maximum value of α equals 4.6° at $\beta = 2$ and 9.4° at $\beta = 10$; in case of elongated ellipsoids it is 3.9° at $\beta = 2$ and 10.4° at $\beta = 10$.

Upon reaching a certain critical value of Re of the order $0.05 - 0.1$, the character of the particle movement begins to change. The elongated particles tend to assume a position, at which the resistance to the motion would be at its maximum: as to plates, needles, etc., the position would be such, at which their better developed faces and much elongated ridges would be situated perpendicularly to the direction of the motion (62, 64). The

particles shaped like regular polyhedrons, cubes and tetrahedrons tends to arrange one of their faces also perpendicularly to this direction (61). Thus- wise the orientated action is extended in proportion to the increase of Re and upon attaining an Re value, which is approximately equal to several tenths, the orientation is completed. The particles mobility, naturally, decreases in relation to the increased rate of orientation. Also this phenomenon fully coincides with the theory: within an ideal range of flow, coinciding with larger values of Re , a couple actuates moving non-spherical particles and tends to turn them around, as we explained above (65).

The α angle increases in relation to the increase of Re ; the trajectory of freely settling particles deviates from the vertical line the larger the particles are. This was determined by experiments with particles of coal ashes in the absence of air currents (66). The average deviation from the vertical line considering a fall from a height of 100 cm amounted to 0.45 cm with particle radius $r = 0.04$ mm and to 1.4 cm at $r = 0.15$ mm. In the presence of sufficiently large Re the rectilinear motion of the particles changes into a spiral or a zigzag line (61, 66). This phenomenon is particularly marked among elongated particles, needle-shaped, flaky, etc. During the above described orientation of these particles their mobility due to the external force, which actuates the particles, is considerably smaller in a perpendicular direction and thus at the time of settling the particles slip to the side, "wander" (67), which is easy to notice while observing a movement of dust particles in sun rays. The degree of "wandering" i. e., the ratio between a horizontal and a vertical velocity of a movement is determined by the shape of the particles, as well as by their size, upon which the Re value depends and, consequently, the degree of orientation too. This phenomenon is not observable when $Re < 0.1$, i. e., when $r < 10$, during settling of particles actuated by gravity, but it may occur at higher movement velocities, e. g., in a cyclone, during explosions, etc.

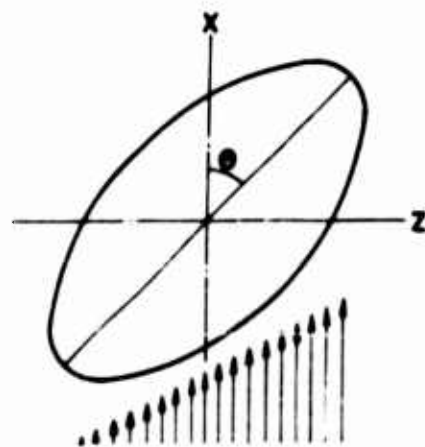


FIG. 12 ORIENTATION OF AN ELLIPSOID IN A CURRENT

In conclusion we shall examine during flow the orientation effect of elongated particles in the presence of a velocity gradient perpendicular to the direction of flow (figure 12). If in a rectilinear laminar current, directed along the axis x with a gradient ∇ directed along the axis z , there is

an elongated spinning ellipsoid which at the same time has its larger axis situated within a plane xz , it is very obvious, that with a progressive movement of the ellipsoid, the latter must spin around its smaller axis toward the axis y . As the theory (68, 69) indicates, the velocity of the spinning is equal to

$$\frac{d\theta}{dt} = \Gamma \cdot \frac{a^2 \cos^2 \theta + c^2 \sin^2 \theta}{a^2 + c^2}, \quad (11.1)$$

where a is the small semiaxis of the ellipsoid;

where c is the larger semiaxis of the ellipsoid;

where θ is the angle between the larger axis and the axis x .

Because $c > a$, the spinning velocity is at its minimum, when $\theta = 0$, i. e., when the position of the larger axis is directed toward the current; it is at its maximum, when $\theta = \frac{\pi}{2}$. Thus the larger axis of the ellipsoid, during most of the time, will be getting closer to the direction of flow. If, however, the axis is situated within the plane xy , it is obvious that no orientation will take place. Finally, in intervening instances, when the larger axis is more or less inclined to the plane xy , the ellipsoid will be orientated all the more completely the larger the inclination angle is. Such is the orientation picture of particles elongated in one dimension. The theory of this phenomenon was verified by way of model tests conducted with viscous liquids (70).

Particles elongated in two dimensions (flakes, lamellae) are similarly orientated with their wide sides toward the current. Since in laminar flow there is virtually some gradient of velocity, the phenomenon of orientation of elongated particles in a current is almost a universal characteristic. It is well known in colloidal solutions and in a suspension, yet it has not even been described for aerosols, although it can be easily detected and quantitatively examined according to changes occurring in the visual characteristics of an aerosol, i. e., the changes in the optical density and in polarization of light diffused by an aerosol.

The Brownian spinning of particles counteracts the orienting action of the current. From the results of interaction between these two factors one can obtain a definite statistical distribution of the direction of the particles axes. It can be computed (68), yet the derived equations are so cumbersome, that we have omitted them.

§ 12. Resistance of a Medium to Motion of Non-Spherical Particles

At first we shall discuss a case of a purely viscous movement (small Re). As experiments indicate, the resistance of a medium, even among particles of non-spherical shape, is expressed by STOKES' law; however, it can be expressed by other numerical coefficients which depend upon the shape of the particles. A theoretical expression for these coefficients has been obtained only for the ellipsoidal particles and then the integrals developed in this expression for spinning ellipsoids are simplified to elemental functions. If we denote an equatorial semiaxis of a spinning ellipsoid by a and the ratio of the larger to the smaller axis by β , then the resistance of the medium (71) is expressed by this equation:

$$F_M = -6\pi\eta V a \alpha', \quad (12.1)$$

and subsequently the coefficient α' is expressed by one of the following equations during the movement of an elongated ellipsoid along a polar axis:

$$\alpha'_c = \frac{4}{3} (\beta^2 - 1) / \left\{ \frac{2\beta^2 - 1}{\sqrt{\beta^2 - 1}} \ln (\beta + \sqrt{\beta^2 - 1}) - \beta \right\}; \quad (12.2)$$

and during the movement of an elongated ellipsoid across a polar axis:

$$\alpha'_a = \frac{8}{3} (\beta^2 - 1) / \left\{ \frac{2\beta^2 - 3}{\sqrt{\beta^2 - 1}} \ln (\beta + \sqrt{\beta^2 - 1}) + \beta \right\}; \quad (12.3)$$

during the movement of an oblated ellipsoid along a polar axis:

$$\alpha'_c = \frac{4}{3} (\beta^2 - 1) / \left\{ \frac{\beta(\beta^2 - 2)}{\sqrt{\beta^2 - 1}} \operatorname{arctg} \sqrt{\beta^2 - 1} + \beta \right\}; \quad (12.4)$$

and during the movement of an oblated ellipsoid across a polar axis:

$$\alpha'_a = \frac{8}{3} (\beta^2 - 1) / \left\{ \frac{\beta(3\beta^2 - 2)}{\sqrt{\beta^2 - 1}} \operatorname{arctg} \sqrt{\beta^2 - 1} - \beta \right\}. \quad (12.5)$$

Listed in table 6 are α' values computed according to these equations. If the polar axis of a particle forms a θ angle with a direction of a movement,

Table 6

Coefficient Value of α' Shape Factor for Ellipsoidal Particles

Ratio of β axis	Elongated Ellipsoids in Movement			Oblated Ellipsoids in Movement		
	Along a polar axis	Across a polar axis	Statistical mean	Along a polar axis	Across a polar axis	Statistical mean
2	1.20	1.38	1.32	0.90	0.79	0.82
3	1.40	1.73	1.62	0.88	0.72	0.77
4	1.60	2.06	1.91	0.87	0.68	0.74
6	1.97	2.68	2.44	0.86	0.64	0.72
8	2.31	3.26	2.94	0.85	0.62	0.70
10	2.65	3.81	3.42	0.85	0.61	0.69
20	4.16	6.38	5.64	0.85	0.59	0.68
∞	—	—	—	(infinitely thin round flake)		
				$\frac{8}{3} \pi \approx 0.850$	$\frac{16}{9} \pi \approx 0.566$	0.66

then by applying the linearity of equation (12.1), the particle movement can be divided into one, which is parallel and the other, which is perpendicular to the polar axis. The correlated component resistances of the medium are equal to $-6\pi\eta Va\alpha'_c \cos \theta$ and $-6\pi\eta Va\alpha'_a \sin \theta$ and their resultant generally deviates from the direction of the movement, as we have shown above. The projection of the resultant to the direction of the particle movement is equal to:

$$F_M = -6\pi\eta Va \left(\alpha'_c \cos^2 \theta + \alpha'_a \sin^2 \theta \right). \quad (12.6)$$

Due to Brownian spinning the orientation of particles changes constantly. By neutralizing the resistance of the medium in all directions of the polar axis, we obtain for F_M the expression:

$$F_M = -6\pi\eta Va \left(\frac{1}{3} \alpha'_c + \frac{2}{3} \alpha'_a \right). \quad (12.7)$$

i. e. , such a resistance as though the polar axis was orientated 1/3 of time along a particle movement and 2/3 of time perpendicularly to the movement. In conformity with the above, we submitted in the table the statistical means of resistance values.

If we assume in equations (12. 4) and (12.5) that $\beta \rightarrow \infty$, we obtain the following expressions for resistance of the medium to a movement of an infinitely thin round flake with a radius a :

$$F_M = - 16\eta aV \quad (12. 8)$$

when the flake is positioned perpendicularly to the direction of the movement, and likewise

$$F_M = - \frac{32}{3} \eta aV \quad (12. 9)$$

for a parallel position. Equation (12. 8) in which OSEEN'S correction has been entered

$$F_M = - 16\eta aV \left(1 + \frac{Re}{2\pi}\right), \quad (12. 10)$$

offers an excellent conformity with the test¹ data (72).

Likewise one can obtain from the (12. 2) and (12. 3) equations, the following expressions for the medium's resistance to the movement of an "ellipsoidal needle" with a length of $2L$:

$$F_M = - \frac{4\pi\eta VL}{\ln 2\beta} \quad (12. 11)$$

in a movement of the needle along its axis, and

$$F_M = - \frac{8\pi\eta VL}{\ln 2\beta} \quad (12. 12)$$

-
1. In a recently published work of AOI (561) there is an accurate computed resistance of the medium to the movement of ellipsoids with various values β at $Re \leq 4$.

in a movement of the needle across its axis (β is the ratio of the length of the needle to its width).

Let us assume that a cylindrical needle, having a much greater ratio of its length to its radius (R), follows a movement across its axis; thus, the resistance of the medium per unit of the cylindrical length is expressed according to LAMB'S equation (73):

$$F_M = - \frac{4\pi\eta V}{2.002 - \ln Re} \left(Re = \frac{2RVYg}{\eta} \right), \quad (12.13)$$

which is well conformable with the test (74) for $Re \leq 0.5$. Thus in this case the resistance is no longer proportional to the velocity of the movement.

In the afore-cited equations the resistance is directed to the smallest (or largest) diameter of an ellipsoidal particle. The other method of expressing the dependence of the medium's resistance upon the shape of a particle has a greater theoretical importance. We shall designate a "dynamic coefficient of shape" of a particle \mathfrak{K} , the ratio of the medium's resistance to the movement of a particle, which has the same volume as a spherical particle. Its radius, named an "equivalent radius" r_e , is obviously equal to $a\beta^{1/3}$ with regard to an elongated ellipsoid and to $a\beta^{-1/3}$ in case of an oblated ellipsoid (" a " denotes an equatorial semiaxis). Thus

$$\mathfrak{K} = \frac{6\pi\eta Va \mathfrak{K}'}{6\pi\eta Vr_e} = \mathfrak{K}' \beta^{1/3}, \quad (12.14)$$

whereupon the numerator pertains to elongated and the denominator to oblated ellipsoids. If the densities of both particles are also equal, then the coefficient \mathfrak{K} is equal to the ratio of the velocity of settling (under the influence of gravity) of a spherical particle to the particle in question. The velocity of settling of non-spherical particles is thus expressed by the equation

$$V_s = \frac{2r_e^2 \gamma g}{9\eta \mathfrak{K}}. \quad (12.15)$$

It follows from the calculation of the sedimentation radius (see page 35).

$$V_s = \frac{2r_s^2 \gamma g}{9\eta} \quad (12.16)$$

and, consequently,

$$\alpha = r_e^2 / r_s^2, \quad (12.17)$$

i.e., the dynamic coefficient of shape is equal to a square of the ratio of equivalent and sedimentation radii.

The values α for ellipsoidal particles are given in table 7.

Table 7

Values of a Dynamic Coefficient of α Shape Factor for Ellipsoidal Particles

Ratio of β axis	Elongated Ellipsoids in Movement			Oblated Ellipsoids in Movement		
	Along a polar axis	Across a polar axis	Statistical mean	Along a polar axis	Across a polar axis	Statistical mean
1.1	0.994	1.005	1.001	--	--	--
1.3	0.970	1.027	1.008	--	--	--
1.5	0.940	1.044	1.010	1.072	0.958	0.996
2	0.95	1.09	1.05	1.14	0.99	1.04
3	0.97	1.20	1.12	1.26	1.04	1.11
4	1.01	1.30	1.20	1.38	1.08	1.18
6	1.08	1.47	1.34	1.56	1.17	1.30
8	1.15	1.62	1.47	1.71	1.25	1.40
10	1.22	1.76	1.58	1.83	1.32	1.49
20	1.54	2.34	2.08	2.31	1.59	1.83

Particles of a regular ellipsoidal shape are found very seldom. Consequently of greater importance are the recently published results of measurements, carried out in the study of the velocity with which models of various shape fall in viscous liquids at small Re (62, 75). These tests were conducted with spinning ellipsoids and with round cylinders, as well as with right-angled, parallelepiped bodies having a square profile and finally, with substances formed of two cones with their bases set together (table 8).

Table 8

Dynamic Coefficient of Shape Factor

Ratio of Height to Diameter (or to a Profile Side, or Proportion of Axes)	Cylinders ¹		Parallelepiped with a Square Profile ¹		Spinning Ellipsoids ²		Substances Formed of Two Cones With Their Bases Set Together ²	
	Axis Position		Position of a Mean to a Profile		Elon-gated	Oblated		
					Position of Long Axis		Axis Position	
	Hori-zontal	Ver-tical	Hori-zontal	Ver-tical	Hori-zontal	Ver-tical	Hori-zontal	Ver-tical
0.25	1.09	1.31 (1.34)	1.15	1.39 (1.40)	--	--	--	1.48
0.50	1.04	1.16	1.07	1.18	--	--	--	--
1.00	1.06	1.04 (1.00)	1.08	1.08 (1.04)	--	--	--	1.07
2.00	1.14	1.02	1.16	1.04	--	--	--	--
3.00	1.24	1.04	1.22	1.03	--	--	--	--
4.00	1.32 (1.30)	1.07	1.31 (1.29)	1.09	1.28	1.36	1.27	--

1. HEISS tests (75), in parentheses experiments of McNOWN and MALAIKA (62).

2. Experiments of McNOWN and MALAIKA (62).

Let us note, first of all, that there is a rather satisfactory agreement of the experimental values η for ellipsoids (1.28 and 1.36) with the theoretical values (1.30 and 1.38). These data reveal, that the η values remain very close to one another for elongated bodies of a dissimilar shape, which, however, maintain an equal ratio of their axes. Hence it follows that in computing mobilities of rod-shaped and similar particles one can mistake them for elongated ellipsoids and the flaky particles -- for oblated ellipsoids; thus the allowable error in this would be on the order of a few percent.

The η value was also determined with the aid of models with regard to regular polyhedrons (61), whereupon the following η values were obtained: 1.06 for octahedrons, 1.07 for cubes, and 1.18 for tetrahedrons.

At $Re < 0.05$, the η value is almost non-dependent upon orientation of polyhedrons.

Finally, the measurements of η at small Re were also done with models of aggregates, agglutinated from vitreous spheres (64). The aggregates shaped like little chains or flakes were positioned perpendicularly while falling. For little chains formed of two particles the experimental value was $\eta = 1.16$; for those formed of three particles - 1.31; of four particles - 1.70; of eight particles - 2.14; for flat aggregates of three particles - 1.26; of seven particles - 1.70; and for octahedrons of six particles - 1.31. These results clearly indicate why the apparent density of particles, determined according to the velocity of motion, is particularly low in the case of linear aggregates (see page 34). One important conclusion emanates from the above statement. As table 7 indicates, during a movement of ellipsoidal particles directed toward their larger axes the η can assume values somewhat smaller than 1. It is possible that profiles exist, which during a favorable orientation offer still smaller values of η . However, due to Brownian movement or to hydrodynamic forces, such orientation is precarious. Considering larger particles, which orientate themselves with their elongated axes perpendicularly to the direction of a movement, the η is always larger than 1. With regard to small particles, the statistical mean value of η , as the table shows, does not descend practically below 1. Therefore one can express a general view that the particles shaped like spheres possess a greater mobility than the particles of any other shape, although they represent the same volume. In other words, the radius of sedimentation of non-spherical particles is always smaller than the equivalent radius of particles (see equations /12, 17/). This explains why, in the determination of an apparent density of particles in smokes (see table 2), even the maximal values of density, which undoubtedly pertain to individual particles, are noticeably smaller than those of the actual density.

The problem pertinent to the magnitude of η at greater Re numbers has been studied very little. Some critical Re values of η stated below are more or less constant and then they begin to increase rapidly (61, 62). The increase associated with air currents flowing around protruding edges begins to take effect rapidly, depending on the sharpness of the edges. Hence, the critical Re value equals approximately 100 when considering cubes and octahedrons, and 10 in case of tetrahedrons, as well as flakes, which fall in a horizontal position.

Thus, one can draw the following practical conclusions: in computing the dynamics of particles of non-spherical shape, one is required, above all, to determine a probable mean value of η for particles of a certain

shape by using the above-quoted data; in regard to larger particles, which in their movement orientate themselves within a definite position, it is sufficient to know the κ which conforms with this position. Now, considering smaller particles, which change their orientation because of Brownian spinning, one must use a mean statistical value of κ . Subsequently, in the case of small particles one applies STOKES' law in the following form:

$$F_M = -6\pi\eta V r_e \kappa; \quad (12.18)$$

and, in the case of Re values, to which STOKES' law is no longer applicable, the method of computation is the one described in § 10, which changes ψ into $\psi\kappa$ and considers in all equations for r the equivalent radius of r_e . As we pointed out, apparently one can use κ values in regard to rounded particles and those of cubic shape, or octahedron shape, up to $Re = 100$ and up to $Re = 10$ in regard to particles having much sharper angles and edges.

The theory of a uniform motion of aerosol particles manifests its importance of applicability in connection with aerial fractionation of powdered substances. As we know, the fractionation of powders by sieves is applicable only to particles of $>60\mu$ in diameter and for particles of smaller sizes one has to resort either to elutriation or to winnowing (aerial separation). A sketch of the apparatus (elutriator), used in analysis of dispersed powders by winnowing, is shown in figure 13

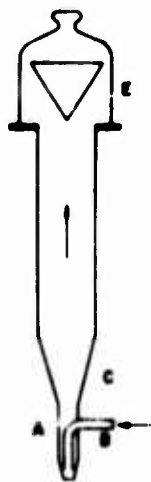


FIG. 13 ELUTRIATOR

(76, 77). A quantity of powder is placed into the narrow lower part A of the apparatus. Air conveyed through a tube B atomizes the powder and carries it upwards. The purpose of the conical part (diffuser) C is to equalize the aerial current. The cap E serves as a trap. The air velocity in the separator must be so, to induce a laminar character on the flow, i. e., the number $Re_f = 2 R \bar{U} \gamma g / \eta$ (\bar{U} denotes a mean air velocity and R the separator's radius) should not exceed a critical value (about 2000).

The air velocity in the cylindrical part of the apparatus conforms with a definite size of particle. If this velocity were constant at all points of the separator's cross section, then all particles whose $V_s < U$ would be carried out of it

and only the particles with $V_g > U$ would remain. However, the air velocity near the separator's axis U_1 is higher than that near the walls. For that reason the particles with V_g close to U_1 are carried out only if they fall into the separator's center and then their removal proceeds rather slowly. Upon completion of winnowing at a certain velocity, whereby the percentage of the exhausted powder is determined, the same operation is repeated at a higher rate of air velocity, i.e., suitable to particles of a larger size, etc. The results of fractionation depend within a known degree upon the duration of winnowing; this was substantiated by the tests of G. ROMASHOV (76).

Another factor influencing the kinetics of the separator's effectiveness is the solidity of the aggregates of small particles. In order to atomize the aggregates completely, a prolonged winnowing is sometimes necessary. However, among powders such as kaolin, a complete disaggregation in an air current is generally not attained and small aggregates are carried out of the separator instead of individual particles.

Furthermore, according to the statement quoted above, the aerial separator fractionates particles according to the magnitude of their sedimentation radius and in case, e.g., of flaky particles, the results of fractionation either by sieves or by air must differ considerably. Actually, a microscopic analysis of nominally identical groups of coal dusts, obtained by both methods, revealed that in an aerial separation particles are encountered which have 2-3 times larger sizes than among corresponding sieve-processed groups (78). These particles, as should be expected, represent comparatively thin lamellae of coal.

In conclusion we shall comment upon the resistance of a gaseous medium to the movement of very large drops. This problem is of great importance in the theory of rain clouds. Tests indicate, that when drops of a large size fall, they become noticeably deformed (flattened), (figure 14 /579/) and this causes an increase of resistance.

Recent experimental data pertinent to the terminal velocity of water drops falling through the air (79, 80) are submitted in table 9 and figure 11. The table data and the figure 11 prove, that a noticeable deviation of the velocity of falling drops, as compared with the velocity of equidimensional solid spheres as they fall, begins approximately at $r_e = 0.4$ mm. With $r_e > 2$ mm, the subsequent

increase of velocity of falling drops is almost discontinued, because the increase of the drops weight is compensated for by a proportionally increased deformation.

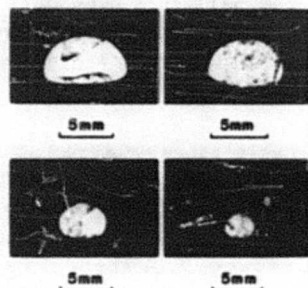


FIG. 14 SHAPE OF FALLING WATER DROPS



FIG. 15 BURSTING OF FALLING DROPS

Table 9

Terminal Velocity of Water Drops Falling Through the
Air at 20° and 760 mm of Mercury

r_e , cm	0.005		0.01	0.015	0.02	0.025	0.03	0.035	0.04	0.045	0.05	
V_s , cm/sec	27		72	117	162	206	247	287	327	367	403	
r_e , cm	0.06	0.07	0.08	0.09	0.10	0.11	0.12	0.13	0.14	0.15	0.16	0.17
V_s , cm/sec	464	517	565	609	649	690	727	757	782	806	826	844
r_e , cm	0.18	0.19	0.20	0.21	0.22	0.23	0.24	0.25	0.26	0.27	0.28	0.29
V_s , cm/sec	860	872	883	892	898	903	907	909	912	914	916	917

When a drop reaches an equivalent magnitude in radius of 2.5-3 mm, deformation of a falling drop becomes so great, that the drop

bursts. For this reason larger rain drops are not seen. However, during tests conducted in an aerodynamic tube provided with an anabatic air current it was possible to suspend drops of a radius up to 4.5-5 mm (81). In conjunction with the above, the degree of the current turbulence is apparently of great importance: if a hand is passed under a drop suspended in the current, the drop bursts immediately. The same effect follows upon a sudden small increase in current's velocity. The mechanism of bursting, shown on figure 15, was obtained by way of photographing the suspended drop.

§ 13. Settling of Clouds

Up to now we discussed only the movement of isolated particles of aerosols. It is necessary to consider along with the mechanics of particle systems the hydrodynamic interaction between the particles (see page 123). At this point it is expedient to analyze separately two essentially different instances of particle motion: in a free cloud, which is unrestricted by walls ... and in an aerosol, which fills a space limited by walls.

Now, we shall consider the first incident. Suppose we imagine that some constant force actuates a particle of a cloud, e.g., gravity: mg . Particles which move under influence of the force entrain to a certain degree the medium surrounding them and, consequently, the resistance of the medium to the movement of particles becomes reduced. A theoretical calculation pertinent to this reduction of resistance was derived only for the systems formed of twin spherical particles (82, 83). In this case the velocity of both particles under the influence of force F is equal to

$$v = \left(F / 6\pi\eta r \right) \left[1 + \frac{3}{4} \left(1 + \cos^2\theta \right) \frac{r}{2p} + \dots \right], \quad (13.1)$$

where $2p$ is the distance between the centers of particles; where θ is the angle between a center line of particles and a direction of motion.

The discarded term of the series includes a third and even higher degree of r/p . The comparison (13.1) with the expression (34.4) for the velocity of the flow around liquid spheres at small Re_f indicates that the additional velocity gained by every particle is merely equal to the velocity of a current generated by another particle at the center point which is occupied by the first particle¹.

1. In the presence of not very small Re 's the symmetry of this effect is disrupted with regard to both particles; therefore, the effect upon a rear particle is by far a greater one than that upon a frontal particle (see the beginning of page 374).

BURGERS' (83) interpretation with regard to multiple particles is that additional velocity gained by a certain particle accumulates with the remaining ones according to equation (13.1). The computation of the resultant velocity of the particles in this suggestion showed in respect to the relation of a spherical cloud the following results: the particles and the surrounding medium move with the same velocity, i. e., the medium is completely entrained by the dispersed phase; the cloud moves as a whole according to laws governing the movement of liquid spheres in a medium possessing the same viscosity. In this case the cloud center moves with a velocity

$$V = \frac{4}{3} \pi R^3 n F / 5 \pi \eta R. \quad (13.2)$$

The numerator denotes a composite force actuating all particles of the cloud (R is the radius of the cloud, n is the number of particles in 1 cm^3); the denominator denotes the resistance of the medium at $V = 1$ according to the equation (7.6) in which it is assumed that $\eta_p = \eta$. At the same time in a progressive movement of the cloud a circulation develops, which supports the shape and the size of the cloud (see figure 63, page 267).

According to BURGERS' conclusions, this type of cloud movement is developed in any aerosol concentration, also in a cloud of any size, yet it is impossible to agree with this statement. In order to simplify the evaluation of the problem, let us assume that the cloud particles are stationary in space and that the medium moves past them with a velocity U . Furthermore, the force with which a medium actuates every particle is expressed in STOKES' law without any corrections. Usually such a correction is very small in aerosols (see page 72). Then the entire force active on the cloud would be equal to

$$F_1 = 6 \pi \eta U \cdot n v = 6 \pi \eta U \cdot \frac{4}{3} \pi R^3 n, \quad (13.3)$$

where v is the cloud volume. This force, as such, represents a frontal resistance of the cloud at the time of being air-swept. If, however, the medium flows around the cloud, the resistance would be equal to

$$F_2 = \psi \pi R^2 \cdot \gamma_g U^2 / 2. \quad (13.4)$$

If $F_1 \gg F_2$, a cloud is not air-swept and the medium flows around it completely. In a freely moving cloud, cloud particles entrain the medium completely and they remain immobile with regard to the medium (occurrence

examined by BURGERS). If $F_1 \ll F_2$, a cloud is air-swept by the medium; this implies that in a freely moving cloud the entrainment of the medium by particles is slight and the velocity of particles in relation to the medium is expressed by STOKES' law without any corrections. If F_1 and F_2 are single order values, a cloud is partially air-swept and partially by-passed by the medium and thus the dispersed phase moves in relation to the medium with a lower velocity than that indicated by STOKES' law.

Inasmuch as the U velocities in equations (13.3) and (13.4) are not given since they are determined by an external force acting on a cloud, it is convenient - instead of F_1 and F_2 forces - to compare the velocities of a cloud at various phases of the motion while the particles remain under influences of a certain external force. With a greater difference between velocities, a phase of motion eventuates, which conforms with a higher velocity; with a smaller difference, an intermediate phase of motion occurs. Thus, during a cloud settling under the influence of gravity, the velocity corresponding to the air sweeping through is equal to

$$V_{s1} = \frac{2r^2\gamma g}{9\eta}. \quad (13.5)$$

A velocity corresponding to that of the by-passed air can be obtained by comparing the entire dispersed phase of a cloud $\frac{4}{3}\pi R^3 n$: $\frac{4}{3}\pi r^3 \gamma g$ with a resistance of the medium (see equation /13.4/)

$$V_{s2} = \sqrt{\frac{32Rn\pi r^3 \gamma g}{9\psi \gamma_g}}. \quad (13.6)$$

The type of motion is determined by its ratio

$$\mathfrak{K} = V_{s2}/V_{s1} = \sqrt{\frac{72\pi Rn\eta^2}{\psi \gamma_g \gamma r g}}. \quad (13.7)$$

The by-passing of the air takes place at $\mathfrak{K} \gg 1$ and the phase of air-sweeping through at $\mathfrak{K} \ll 1$. If to the motion of the entire cloud we apply STOKES' law for a liquid sphere (13.2), thus

$$V_{s2} = \frac{4R_n^2}{15\eta} \cdot \frac{4}{3} \pi r^3 \gamma g, \quad (13.8)$$

$$\alpha = V_{s2}/V_{s1} = 1.6\pi R_n^2 r n. \quad (13.9)$$

This occurrence was examined by SMOLUCHOWSKI (82).

It should be noted that in a majority of the clouds seen in nature, in industry, and in everyday life, $\alpha \gg 1$ at least during the first period of their existence and that they move around as a whole. However, during the dispersion of a cloud by air currents and by diffusion, the $R^3 n$ term, which is proportional to the total number of particles in the cloud, remains constant and therefore the Rn and $R^2 n$ terms included in the equations (13.7) and (13.9), become reduced upon the increase of the cloud volume and with them α also becomes reduced, so that in the end the cloud becomes air-swept.

It is necessary to remember also the condition, that practically in all clouds of condensable origin, as well as in those produced from volatile substances by dispersion, the gaseous medium inside and outside the cloud possesses a somewhat diversified composition and temperature and, consequently, a dissimilar density too. The difference in densities usually exceeds by far the difference dependent upon the influence of a dispersed phase. Thus, in natural clouds the contents of liquid water is on the order of $1\text{g}/\text{m}^3$. The disparity among densities, which is equal to the afore-mentioned value, is attained when the difference in temperatures inside and outside a cloud is on the order of 0.2° , or when the difference of absolute humidity is on the order of 1 mm of mercury. Consequently, the influence of the dispersed phase in vertical movements of natural clouds assumes a secondary role and, basically, such a movement is determined by a difference in temperature and humidity of the air inside and outside the cloud. A similar condition also exists in clouds formed during explosions and from combustion of fuel in furnaces, fire boxes and internal combustion engines; they are also produced with the aid of special smoke generators, which are engaged for camouflage and insecticide clouds and likewise from smoke pots, etc. At first, due to the high temperature, the clouds rise. If they had time to cool off prior to being dispersed in the atmosphere, they would begin to settle to the ground, because they contain CO_2 or a high concentration of a dispersed phase. In all such instances, regardless of size and aerosol concentration, a cloud moves as a whole, because its continuous mass of gas ("a gaseous cloud") is not air-swept but is only superficially diluted by diffusion and hydrodynamic currents.

Lack of these considerations sometimes brings erroneous conclusions. Thus, in order to explain the outline of the trajectory of tobacco smoke, which was let horizontally into a smoke chamber by PROSAD (84) (who maintains a supposition that smoke particles settle individually), we were compelled to assume for the mean radius a very absurd value of 24μ . Yet, actually the trajectory-like outline is undoubtedly determined by the jet's rapidity in settling as a whole, because its density exceeded that of air due to the carbonic acid present in the smoke. As a striking example of rapid settling of a cloud we consider "a flame cloud", which with an enormous speed was projected down the Mount Pelee volcano and reduced to ashes the town of Saint-Pierre in 1902. Evidently the concentration of the dispersed phase (volcanic ashes, etc.) was so great, that the density of the cloud, regardless of its high temperature, was many times higher than the air density.

The picture of movements of cumulus rain clouds, which contain drops of all sizes: from $r = 10\mu$ to $r = 2-3$ mm, is very complicated. Let us consider, as discussed previously, how under the influence of a very high temperature of the cloud (in comparison with the atmosphere surrounding it), a sharp rise of velocity up to $10 \text{ m} \cdot \text{sec}^{-1}$ takes place in the entire cloud simultaneously with the settling of droplets with a velocity from 0.01 to $8-9 \text{ m} \cdot \text{sec}^{-1}$. Thus, the resultant velocity of some droplets is projected downward and that of other droplets, upward. These phenomena plays an essential role in processes of rain clouds (see page 375).

§ 14. Motion of Aerosols in a Confined Space

In considering aerosols within a limited space the movement of particles also includes a joint movement with the medium, induced by convectional currents, artificial agitation, etc., and the movements with relation to the medium. At the present time we are only interested in the latter and we shall discuss it by exemplifying the settling of particles actuated by force of gravitation. As particles of an aerosol, which fill a space limited by walls, settle with a rapidity V , the medium moves reversely with an average velocity of ϕV ; where ϕ is usually a small volumetric share of a dispersed phase. Since the medium near the particles becomes entrained by the latter, the velocity of a counterflow beyond the particles (i. e., at a distance comparatively greater than the radius of particles) is greater than ϕV . Thus in the above case, unlike in the movement of a loose cloud, the velocity of the particle settling is smaller by the factor $1 + K\phi$ (where $K > 1$) than the velocity of isolated particles contained in a vast volume.

According to CUNNINGHAM (46), still another condition should be taken under consideration: following the conclusions of STOKES' law, one of

the approximate conditions suggested is that the velocity of the medium equals zero at an infinitely great distance from a particle. When systems of particles settle within a limited space, it should be assumed (disregarding a counterflow of the medium) that the velocity of the medium equals zero at a distance ρ from the center of a particle, where $2\rho \approx n^{-1/3}$, i.e., at an average distance between the adjacent particles. Consequently, every particle is affected by such a resistance, as the one to which it would be exposed if found in the center of a closed spherical vessel, whose radius equals ρ . According to CUNNINGHAM'S computations, the resistance according to STOKES' approximation is equal to $6\pi rV\eta (1 + 1.25 \frac{\lambda}{\rho})$.

According to OSEEN, the experimental correction is smaller and it gets smaller as the REYNOLDS number $V\rho\gamma/\eta$ becomes larger. All other authors, studying the problem, arrived by rather complicated although not exact considerations to a factor of $1 + K\phi$, whose K values are equal to 5.5 (85), to 7.0 (83), and to 4.5 (86). It seems, that an accurate solution of the problem is extremely difficult.

The difference between the correction factors, such as $1 + K\phi(I)$ and $1 + K\frac{r}{\rho} \approx 1 + K\phi^{1/3}(II)$ is, of course, extremely factual, because in the presence of ordinary ϕ values in aerosols the factor I is practically equal to 1, while the factor II may be some percent larger than 1. For experimental purposes this problem being of interest to us for small values of ϕ was examined only by KERMAK (85) by measuring the velocity of settling of extremely monodispersed suspensions of various animal erythrocytes, with radii 2.4, 3.0, 3.7, and 4.4 μ in water. It was proven that at $\phi \leq 0.04 - 0.08$ the results of the tests conform well with the correction factor $1 + K\phi$, wherein the K contains values suitable for various erythrocytes within 4.8 - 6.9. It is regrettable that the velocity of settling of isolated particles was not measured in this test, but determined by extrapolation.

Thus, from the rather scant data available we can only state that, during settling of aerosols within a limited space, the resistance of the medium at small ϕ is probably equal to $6\pi rV\eta(1 + K\phi)$ and, subsequently, K is close to 5-6. Recently the question of the velocity of settling of concentrated dispersed systems assumed importance in conjunction with a research in fluidization of powders (see page 413). In order to measure this velocity systems of identical spheres or of differently shaped substances are fluidized, i.e., they are converted into a suspended condition in an anabatic liquid current. The concentration of globules is determined automatically, when the velocity of settling is equal to the current's velocity. The results of these tests can be expressed by the equation:

$$V'_s = V_s (1 - \phi)^a, \quad (14.1)$$

where V'_g is the velocity of a system of particles settling; where V_g is the velocity of isolated particles settling. LEWIS and BOWERMAN (87), also RICHARDSON and ZAKI (88), obtained a concurrent value of 4.65 for a coefficient α with regard to a system of globules. An approximate theoretical estimation of the settling of a system of spheres was also carried out by RICHARDSON and ZAKI. Using two models to show the positions of globules in the space, authors obtained two curves (V'_g , ϕ), one of which runs approximately 40% higher and the other 20% lower than the experimental curve.

In conclusion we shall refer to a phenomenon, which is known to everybody who works on aerosols: in the settling of concentrated aerosols the upper border of the dispersed phase is usually flat and horizontal. This phenomenon can be studied in laboratories and in natural fogs. The cause of the phenomenon is found in that when the density of an aerosol exceeds the density of the medium in contact with the aerosol, the hydrostatic forces resist the dislocation of the horizontal upper border of the aerosol under the influence of convection. In this instance aerosols behave like liquids. Naturally, the stabilization of the upper border will be observed in such a case only if the dispersed phase moves as a whole with the medium, i. e., during a sufficiently great concentration of aerosol (see the preceding paragraph). For this reason the surface of aerosols is particularly stable when weighted with chlorine gas, carbon dioxide, etc. (89).

§ 15. Vertical and Horizontal Electrical Field Methods and Their Application

The movement of aerosol particles in an electrical field does not differ in principle from a movement within a field of terrestrial gravity. The force, actuating a particle in an electrical field, is equal to qE , where q is a particle charge and where E is a field potential. If equation (8.2) is applied, the velocity of a particle is equal to

$$V_E = qEB = qE \left(1 + A \frac{1}{F} \right) / 6\pi r \eta. \quad (15.1)$$

The research in aerosol particles movement in a vertical field is extremely interesting for its practical application, i. e., the superimposition of an electrical field upon a field of terrestrial gravity. MILLIKAN'S (90) and EHRENHAFT'S (91) exploitation of the laws of a vertical electrical field is one of the very fruitful methods of studying aerosolic systems, which play an extremely important role in the development of our sciences concerning this domain. The method is based on this, that aerosol particles are let into a vessel, which is formed of two horizontally positioned condenser plates and side walls made of insulating material and provided with

little windows for observation, illumination, and charging the particles. The observation is effected by means of a horizontal microscope with an ocular grid. The field intensity is $E = \pi/h$; where π is a potential difference and where h is a distance between plates of the condenser. The magnitude and intensity of the electrical field can be changed as desired. The rapidity of particles settling is determined as V_s when the electrical field is disconnected; whereupon the velocity of the identical particle's motion under the simultaneous influence of electrical and gravitational fields is $V_s + V_E$, or $V_s - V_E$, depending upon the direction of the electrical field. Hence we obtain V_E . Besides this, the field intensity E_B is determined, which equalizes accurately the gravitational force acting upon the particle. Thus:

$$E_B = mg/q = \frac{4}{3} \pi r^3 \gamma g / q. \quad (15.2)$$

In vessels of a certain construction an opportunity is provided for changing within wide range the internal pressure in relation to the atmospheric pressure. The procedure of the experiment, according to the vertical field method, is well explained in the literature (53, 92, 93) and it enables us to solve the subsequent series of problems.

A. Determination of the Value of the Elemental Electrical Charge and Finding of the Resistance Law of a Gaseous Medium to the Movement of Small Particles.

In order to solve these important problems, we applied (53) for the first time the method of a vertical electrical field. We write the following expression for V_s :

$$V_s = mgB = mg \left(1 + A \frac{1}{r} \right) / 6 \pi r \eta \quad (15.3)$$

or

$$V_s = \frac{2r^2 g \gamma}{9\eta} \left(1 + A \frac{1}{r} \right). \quad (15.4)$$

If we extract a square root from (15.4) and multiply it by (15.1), we produce the equation

$$q = \left[\frac{18 \pi V_E \left(\frac{\eta^3 V_s}{2 \gamma g} \right)^{1/2}}{E} \right] \left(1 + A \frac{1}{r} \right)^{-\frac{3}{2}} = q_{st} \left(1 + A \frac{1}{r} \right)^{-\frac{3}{2}}. \quad (15.5)$$

We designate by q_{st} the expression quoted in brackets, i. e., the value of a particle charge as defined from the test proposing a hypothesis as to the adaptability of STOKES' law. With regard to liquid (oil) droplets, all values included in this expression, such as: viscosity of air, density of particles, intensity of a field and of velocity, V_E and V_s , can be determined from the test. When a particle is charged by Roentgen rays or by γ -rays, the modification of its charge Δq is equal to a small integer of a positive or a negative quantity of the elemental charge \mathcal{E} .

$$\Delta q = (\nu_1 - \nu_2) \mathcal{E}, \quad (15.6)$$

where $\nu_1 - \nu_2$ is usually equal to ± 1 and hardly ever to ± 2 , etc. Similarly $\Delta q_{st} = (\nu_1 - \nu_2) \mathcal{E}_{st}$. Consequently, if we apply the largest common denominator of some Δq_{st} , it is easy to determine \mathcal{E}_{st} .

Inasmuch as it follows from the equation (15.5), that

$$\mathcal{E} = \mathcal{E}_{st} / \left(1 + A \frac{1}{r}\right)^{3/2}, \quad (15.7)$$

thus

$$\mathcal{E}_{st}^{2/3} = \left(1 + A \frac{1}{r}\right)^{2/3} \mathcal{E}^{2/3} = \mathcal{E}^{2/3} + A \mathcal{E}^{2/3} \cdot \frac{1}{r}. \quad (15.8)$$

If in the function $1/r$ we set aside $\mathcal{E}_{st}^{2/3}$ values, which were found for various droplets, then with regard to applicability of CUNNINGHAM'S equation the points must, in agreement with (15.8), align themselves in a straight line. The point of intersection of the straight line with the axis of ordinates offers the value of $\mathcal{E}^{2/3}$ and the tangent of the inclination angle to the axis of abscissae offers the value of $A \mathcal{E}^{2/3}$. Actually from the experiment the true value of the radius r is not directly determined, but

$$r_{st} = \left(\frac{9V_s \eta}{2\gamma g}\right)^{1/2}, \quad (15.9)$$

i. e. , the computed value of the radius which presumes the correctness of STOKES' law. However, in view of the small values of the Al/r corrective term, the r_{st} hardly differs from r ; therefore if we change r into r_{st} in the equation (15.8), the change will scarcely reflect itself in the results and particularly so in the experimental points, which so well align themselves in a straight line. In this way the first accurate determination of the value of the elemental electrical charge was carried out and the applicability of CUNNINGHAM'S law was substantiated by small l/r values. In order to obtain correct results in determination of ϵ one should exclude, as far as possible, the influence of Brownian movement, i. e. , one should work with comparatively large droplets ($r = 2-5\mu$).

In order to find the medium's resistance law with large values of l/r , small droplets are not used for this purpose, but measurements are carried out with low pressures, i. e. , with larger l . In such tests (39) the pressure in a small vessel was brought to 0.5 mm Hg, and we succeeded in measuring the medium's resistance down to the value of $l/r = 134$. As a result, the empirical equation (8.5) was prepared. The most ideal method of studying the law of resistance with regard to minute particles includes the measurements of velocities of movement of the same particle at various pressures (94, 95, 28).

We take cognizance of the fact that the initial tests according to the method of a vertical electrical field were conducted not with individual droplets, but with a water fog obtained from a vapor condensed on gaseous ions. In this case each droplet in the fog possessed one elemental charge. V_s and V_E were determined according to the movement of the upper border of the cloud, whereupon the value obtained for ϵ was approximately 30% lower than the actual one (96). No wonder! - inasmuch as the velocity of the movement of the upper border is always determined by slowest particles (by smallest particles, when measuring V_s and by the largest ones, when measuring V_E). Thus, according to (15.1), a lower value of the particle charge is obtained.

All afore-quoted statements refer to spherical, individual particles. When proceeding to particles of non-spherical shape and aggregates, it should be taken under consideration that γ indicates the apparent density of aggregated particles. Thus, if we substitute in (15.5) a true density for γ , then for q , and consequently for ϵ , we can obtain values several times smaller than the actual ones. Hence, the hypothesis about a "subelectron" (97) revealed itself. Furthermore, if a particle shows a non-spherical shape, then in (15.4) r_e^2/κ should be substituted for r^2 (see 12.15) and in (15.1) $r_e \kappa$ for r (see 12.18). As a result, a multiplier $\kappa^{3/2}$ appears in denominator of the expression for q (see formula 15.5). Since in non-spherical particles $\kappa > 1$

(see page 64) and if we disregard this condition, we obtain again a lowered value for an elemental electrical charge.

When the value of \mathcal{E} and the medium's resistance law are known, the following problems can be solved according to the method of a vertical field.

B. Measurements of Charge and Mobility of a Particle.

As measurements of velocity of a particle motion are repeated in a vertical electrical field and as they sometimes go up, sometimes down, the arithmetical mean of both velocities $V_E - V_g$ and $V_E + V_g$ is taken, which is equal to V_E and is proportional to the number of elemental charges in a particle ν . When the latter is charged several times, we arrive at ν , as is shown above, and at the value of a particle charge $q = \nu \mathcal{E}$. If V_E and q are known, the mobility of a particle B is determined according to equation (15.1).

The mobility of a particle B can also be determined by its velocity of fall in the absence of V_g field (see equation /15.3/) and with the aid of a value of an equilibrated field E_B , which characterizes a particle's mass (15.2). The shape and the density of the particle are eliminated in both variants of the method.

It is very essential that the mobility of a particle in an electrical field - when determined by the first variant, and the mobility in the gravitational field, when determined by the second variant, - be able (considering a particle of an irregular shape) to vary between one another due to the orienting action of the electrical field, which tends to turn the particles with an elongated axis toward the direction of the field (see § 43). This circumstance, which for some reason or other is in no way considered among the researchers working in this field, explains many instances of differences between the theory and experiment in the research of aerosol particle motion in a vertical electrical field.

C. Determination of Particle Sizes.

Two difficulties are encountered during determination of the sizes of aerosol particles by the velocity of their settling under the influence of the force of gravity (i. e., according to the equation /15.4/):

1. What has been frequently pointed out in regard to aggregated particles is that the apparent density which is used in (15.4) is not known beforehand;

2. In case of small particles ($r < 10^{-4}$ cm) the Brownian movement leads to rather considerable fluctuations in the results of the measurements. The above difficulties are in a great measure eliminated, if the

following variant method (98) is applied. If, as shown above, we determine V_E and q , according to (15.1) we find the r , or in case of non-spherical particles, the r_e . With this, the density of particles is eliminated. Here the influence of Brownian movement is accordingly diminished because the V_E velocity (unlike V_s) can be sufficiently increased by increasing the intensity of E-field.

If the density is unknown, the size of particles can also be found by measuring the velocity of the particles falling at various pressures (90). Inasmuch as the length of gaseous molecular free path is inversely proportional to the pressure of the gas, equation (15.4) can be written down in this way:

$$V_s = \frac{2\gamma r^2 g}{9\eta} \left(1 + \frac{A'}{pr} \right). \quad (15.10)$$

Here $A' = A p_l = A p_0 l_0$; where l_0 is the length of the molecular free path at atmospheric pressure of p_0 . Hence, if V_{s1} and V_{s2} are the velocities of falling at p_1 and p_2 pressures, then

$$\frac{V_{s1}}{1 + (A'/p_1 r)} = \frac{V_{s2}}{1 + (A'/p_2 r)}, \quad (15.11)$$

whereupon

$$r = \frac{V_{s2} p_2 - V_{s1} p_1}{V_{s1} - V_{s2}} \cdot \frac{A'}{p_1 p_2} \quad (15.12)$$

Since according to the above equation r is proportional to differences of rather close values, the method cannot offer accurate results. Furthermore, the theory of movement of small particles in a gaseous medium and in a transitional region (§ 8) was exploited only with regard to particles of spherical shape; relative to other shapes it is still not known which coefficient of shape should be entered into the corrective factor of $1 + A/r$.

D. Determination of Apparent Density and Determination of a Dynamic Coefficient of Particle Shape.

When a particle radius is determined, as shown above, and subsequently a particle mass according to a value of an equilibrated field, we find γ , which in case of aggregated particles is the apparent density. In this way

WHYTLAW-GREY (31) obtained (quoted on page 34) values of particle density in certain smokes. However, the correct results can only be obtained for particles of a spherical shape. For particles of other shapes in (15.1), a coefficient α must be introduced, otherwise an oversized value will be obtained for the equivalent radius r_e and an undersized value will be obtained for an apparent density.

For non-spherical individual particles, whose density is known beforehand, one can determine, according to (15.2), their equivalent radius r_e by the particle charge and by the magnitude of an equilibrated field. Furthermore, through the velocity V_E one can find the α value in connection with the movement in an electrical field, while through the velocity V_g the same value is obtained in connection with a movement actuated by forces of gravity. As we already pointed out, in view of the particles orientation in an electrical field, the values thus found may be dissimilar in the two instances.

A determination of the particle density may be carried out with the aid of the method submitted by PLACZEK (24) which pertained to the original modification of a vertical field, i. e., the method which suggested the use of an irregular electrical field having diverging lines of forces. As the theory indicates, the force actuating a non-charged particle in a field F is equal to

$$F_E = \alpha_E v \text{grad } E^2, \quad (15.13)$$

where v is the particle volume and α_E is a coefficient, which is dependent upon a shape and the dielectric constant of ϵ_k particle and is equal to $\frac{3}{8\pi} \frac{\epsilon_k - 1}{\epsilon_k + 2}$ with regard to a non-conducting sphere and to $\frac{3}{8\pi}$ considering a conducting sphere. It is very important that in the latter case α_E possesses the same value for solid individual particles as for aggregates, as long as electrical contact is maintained among the primary particles of which the aggregates are formed. If particles possess a vertical direction at the junction of E and $\text{grad } E$, the force actuating a particle will be equal to

$$F_E = 2 \alpha_E v E dE / dz. \quad (15.14)$$

If a gradient is directed upward under the condition of $F_E = mg$, then

$$E dE / dz = \frac{mg}{2 \alpha_E v} = \frac{\gamma g}{2 \alpha_E} \quad (15.15)$$

and a particle will be equilibrated in the air. As is obvious from (15.15), all non-charged spherical particles possessing an identical density and a dielectric constant, regardless of their sizes, equalize themselves in the presence of the same value of EdE/dz . This conclusion was proved in tests with oil and individual mercury droplets. In order to create an irregular field, the upper plate of the condenser was appropriately shaped. Thus it became apparent that the EdE/dz is proportional to a square of the voltage on the plate of the condenser.

The following important fact was revealed in these tests: the comparison of EdE/dz values, corresponding to the equilibration of oil and mercury droplets, points out that the coefficient α_E has almost identical value for both. Thus, oil droplets in a constant electrical field, practically speaking, produce polarization as conductors of electricity, because apparently they contain ionized contamination. Since mineral oils belong to a group of very poor conductors of electricity, a similar phenomenon probably occurs among particles of most other substances, too. Consequently, to simplify further discussions we shall consider that aerosol particles behave like conductors in an electrical field.

According to (15.5) and with the aid of observations made upon individual droplets, one can measure accurately the magnitude of EdE/dz at various points of the electrical field formed by a condenser. Hence, as we pointed out above, the apparent density of these particles was determined by similar observations conducted upon aggregated particles of metallic aerosols. In this case the particles were put in equilibrium at various magnitudes of EdE/dz because they possessed a dissimilar apparent density. Thus it was determined that in mercury fogs obtained by mechanical atomization at a low atmospheric pressure droplets possessed a normal density and in fogs obtained by atomization at higher pressures, or by sublimation, droplets possessed 5-10 times smaller density (see page 30).

The vertical field method was also used in researches in the following fields: kinetics of droplet evaporation; irradiation of particles; Brownian movement; movements in a temperature gradient field, and in many other aerosol problems.

The movement of aerosol particles in the field of terrestrial gravity, with a horizontal electrical field superimposed over the latter, can also be used to determine ϵ , as well as some other problems discussed before. In the case under consideration the movement of particles is proportional to the slope of a straight line; it is described by the same equations (15.1) and (15.3), but the only difference is, that V_g denotes here a vertical and V_E a horizontal component of a particle's velocity. The equation (15.5) and all other conclusions also are operative here. Both

component velocities are measured by an intermittent photographic exposure (100), which offers an opportunity for working with much larger droplets (up to $r = 10\mu$) than is possible in the method of a vertical field, also this is to be preferred for a precise determination of ϵ . On the other hand a repeated charging of droplets during the test is excluded here; inasmuch as the method applied here was used only for making the value of elemental charge more precise, while the approximate estimate of the latter was assumed to be known, so the number of elemental charges on droplets could be directly determined from the test (see page 136 about the other variant method).

§ 16. Radiometric Forces in Aerosols (Thermophoresis)

The phenomenon of aerosol particles being repelled by heated bodies was well known even in the last century during the Eighties, although it obtained its proper interpretation comparatively recently. This phenomenon is readily discovered, when aerosols in contact with a heated body are subjected to a lateral irradiation; the body is surrounded by a "black" layer devoid of particles and whose thickness increases with a rise of temperature of the body.

The phenomenon is produced by the so-called radiometric forces, which because of the gaseous medium act upon non-uniformly heated particles present in the medium, in this case the aerosol particles. The mechanism of radiometric forces, as in other instances of interaction between particles and gas, depends essentially upon a magnitude of the proportion of the particle radius and the mean length of the gaseous molecular free path. When $r \ll 1$, the radiometric force is developed due to the fact that gaseous molecules are repulsed from the hotter side of a particle with a greater velocity than from the cooler side. That is why particles transmit impulses directed toward a lower temperature. The magnitude of this force, as molecular-kinetic computation (101) indicates, is equal to

$$F_M = \frac{\pi \alpha p r^3 \Gamma_i}{3T}, \quad (16.1)$$

Γ_i denotes a temperature gradient inside a particle; α denotes a coefficient of accommodation of gaseous molecules on a particle surface.

Thus in this case the radiometric force is proportional to the gas pressure and to the cube of the radius of the particle.

If $r \gg 1$, the mechanism of radiometric forces is somewhat more complicated (102). Let us discuss a not-uniformly heated wall, which comes in contact with gas. An almost similar tangential temperature gradient sets

itself in a gas stratum adjacent to the wall. If the gradient leads to the left, then gaseous molecules colliding from the left of the surface element ds possess on the average a greater velocity than those colliding from the right. As a result, the wall receives an impulse directed to the right, i. e., opposite the gradient, while an equal and directed impulse to the left is transmitted toward the gas. This impulse compels the gas to slip upon the surface to the side of the increased temperature with velocity as follows:

$$U = \frac{3\eta\Gamma_1}{4\gamma_g T}. \quad (16.2)$$

The nature of a radiometric circuitous flow of a substance not uniformly gas-heated differs essentially from the usual viscous flow, which is discussed in § 34. In the latter case the tangential velocity of the gas equals zero on the surface of the substance and then it increases in proportion to its distance from the surface. That is why the friction force acting on the substance is directed toward the flow. However, during a radiometric circumfluence a gas velocity attains its maximum value (16.2) at a distance l from the surface of the substance and it decreases in proportion to the distance from the latter. For this reason in the given case the force actuating a substance is directed oppositely to the current, i. e., toward the temperature drop. As the hydrodynamic computation (103) indicates, the force in question which pertains to a sphere is equal to:

$$F_M = - \frac{3\pi\eta^2 r R_g \Gamma_1}{pM}, \quad (16.3)$$

where R_g is the gas constant;

where M is the molecular weight of the gas.

Consequently in this case the radiometric force is inversely proportional to the gas pressure (if the latter is not too small, so that viscosity of the gas may be considered as constant) and is proportional to the radius of the particle.

HETTNER (103) submitted the following empirical interpolated equation for a transitional region (l is comparable with r):

$$F_M = - \frac{\pi r^2 \eta \sqrt{\frac{\alpha R_g}{MT}} \Gamma_i}{\frac{p}{p_0} + \frac{p_0}{p}}, \quad (16.4)$$

where

$$p_0 = \frac{3\eta}{r} \sqrt{\frac{R_g T}{Ma}}. \quad (16.5)$$

One can readily see that equation (16.4) is converted into (16.1) when $l \gg r$, and into (16.3) when $l \ll r$. As the analysis of equation (16.4) indicates, the absolute value of the force F_M reaches its maximum at $p = p_0$. Then

$$p_0 \approx 1.5 \cdot 10^{-5} / r \text{ aTM}. \quad (16.6)$$

in the air at ordinary temperatures and at $\alpha = 1$.

The dependency of a radiometric force upon pressure, as expressed by equation (16.4), was quantitatively confirmed in tests by photophoresis of selenium particles (104). The fact that some authors have not discovered the influence of pressure upon velocity of photophoresis is explained as follows: they worked with pressures close to p_0 , i.e., in a region of maximal values of a radiometric force, within which the force is comparatively little changed with pressure.

The basic difficulty in a theoretical calculation of a radiometric force actuating a particle lies in the determination of a temperature gradient value in the particle itself. There is a comparatively simple solution of the problem if a gradient is conditioned by a temperature variation of the medium itself. In the absence of convectional currents (i.e., when a temperature gradient of the medium is directed upward), if the emission of the particles heat by radiation is to be disregarded, the gradient inside a spherical particle is expressed (in case $r \gg l$) by the following equation (105):

$$\Gamma_i = \frac{3\chi_a \Gamma_a}{3\chi_a + \chi_i}, \quad (16.7)$$

where Γ_a is the temperature gradient of the medium;

where χ_i is the heat conductivity of the (particle) substance;

where χ_a is the heat conductivity of gas.

Thus a radiometric force in this case is equal to:

$$F_M = - \frac{9\pi\chi_a}{2\chi_a + \chi_i} \frac{\eta^2 r R_g \Gamma_a}{pM} = - \frac{9\pi\chi_a}{2\chi_a + \chi_i} \frac{\eta^2 r \Gamma_a}{\gamma_g T}. \quad (16.8)$$

This equation, prepared by EPSTEIN (105), was tested in an experimental way, according to a vertical electrical field method by ROSENBLATT and LAMER (106) on droplets of tricresyl phosphates with radii 0.4-1.6 μ . For this purpose the temperature of the upper plate of the condenser was maintained at a much higher level than the temperature of the lower plate and, thereby, the convection in the condenser was eliminated. Thus after the velocity of a vertical movement of a particle was measured with a temperature gradient present and without the latter,

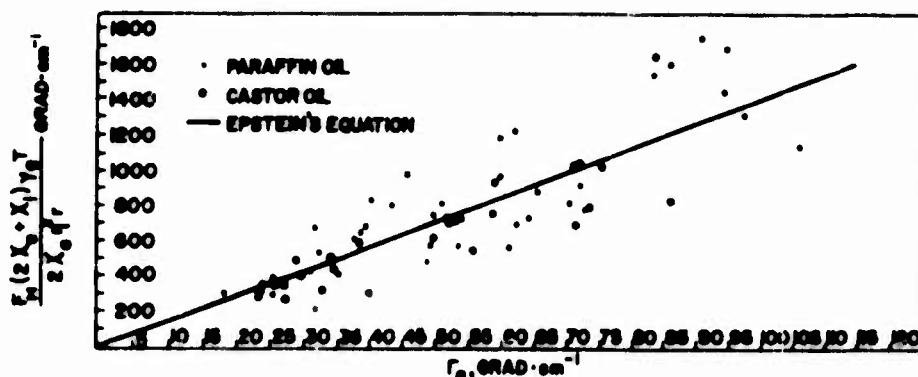


FIG. 16 RADIOMETRIC FORCE ACTING ON A PARTICLE

the velocity of a particle movement, as influenced by a radiometric force, was determined according to the difference obtained and, hence, the magnitude of the radiometric force was determined according to equation (8.2). The force appeared to be exactly proportional to the temperature gradient. Furthermore the tests conducted with the same particle at various pressures revealed, that along with a greater magnitude of r/l the radiometric force increased linearly with $1/p$ in accordance with equation (16.8). However as the l approximates r , the graph begins to diverge from the straight line downward, which is to be expected according to equation (16.4). At a greater pressure (760 mm Hg), the radiometric force is proportional to the particle radius in accordance

with equation (16.8), i. e., F_M/r is not dependent upon r ; however, at lower pressures F_M/r became somewhat enlarged in proportion to a decrease of r , which is contradictory to equation (16.4). The absolute magnitude of the force proved to be 50% higher than the theoretical value, evidently because an unreliable valuation of the tricresyl phosphates heat conductivity was used during the computations.

SAXTON and RANZ (107) - in their more recent work conformable to the same method and conducted on paraffin and castor oils' droplets (with $r = 0.5-2\mu$), at atmospheric pressure and a temperature gradient of $18-140 \text{ grad. cm}^{-1}$ - obtained the results, which are depicted on figure 16; there a straight line is plotted according to the equation (16.8). If we discount the noticeable experimental errors, which are inevitable in such measurements and which lead to a considerable dispersion of the experimental points on the graph, the formula may be assumed to be confirmed by the test.

One can observe in everyday life precipitation of aerosol particles in a field of a temperature gradient. Due to this phenomenon, thick deposits of dust¹ settle on heating systems; smoke in a flame of a kerosene lamp rapidly covers its glass with a layer of soot; a similar settling of soot and ashes also takes place on walls of smoke-stacks, the temperature of which is below that of flue gases. If we let an aerosol flow through a tube², where a wire heated by an electric current is installed along the tube's axis, the aerosol will settle on the tube's wall. Such a method of settling (thermal precipitation) has found a wide acceptance in aerosol research (110, 111). The method has a greater preference due to the circumstance that, according to equation (16.3) and (16.4), the velocity of the movement of particles (in an order of magnitude 0.1μ and higher) in a thermal precipitator is only slightly dependent upon particles sizes, whereas the velocity of a movement, influenced by gravity and inertia forces rapidly decreases in proportion to the particle size decrease. Another reason that a thermal precipitation is preferable to an inertial precipitation is that aggregates do not disintegrate and that precipitating particles are not blown off.

1. Because air in a room with steam-heating, or with a hot-water heating system gets warmer than walls, after some time the walls become covered with a uniform coat of dust (108).
2. For instance through a CLAUSIUS tube, where gases are distributed by a thermodiffusion (109).

The thickness of the "black" layer, which contains no particles and which surrounds the heated bodies (to simplify the matter we shall regard the latter as spinning bodies), is determined by a trajectory of these particles, which at a distance from the body travel according to the latter's elongated spinning axis (figure 17). Thus, in turn, this trajectory is determined by the arrangement of the velocities of a convection current, which flows around the body and actuates a particle by radiometric forces, as is explained in § 30. According to experimental data, the thickness of the "black" layer is approximately proportional to the square root of the difference between the temperature of the body and that of the medium (112).

Of special significance to researchers is the movement of aerosol particles during a one-sided illumination (photophoresis), which is the occurrence peculiar to a thermal cataphoresis. The phenomena observed here are of more complex nature than a movement of particles in a non-uniformly heated medium, because the distribution of temperature in an illuminated particle may be very dissimilar in so far as it is influenced by the particle's shape, size, transparency and a coefficient of refraction. Particularly so among transparent particles, the back side of which may be more heated by rays refracted in a particle than the latter's front (facing the source of light) side. In such a case a particle will converge toward the light (a negative photophoresis).

Particles of certain substances (e.g., selenium) manifest a negative photophoresis until their size becomes smaller than the one determined by a critical dimension; if particles of a larger size are present, the manifestation of a photophoresis is changed inversely (101). This phenomenon is explained as follows: that in ratio to a particle's enlargement the weakening of light passing through it increases and consequently, the heating of particle's rear side decreases.

This was presented very descriptively in tests with a monochromatic illumination of naphthalene colored smokes (113): at a time of

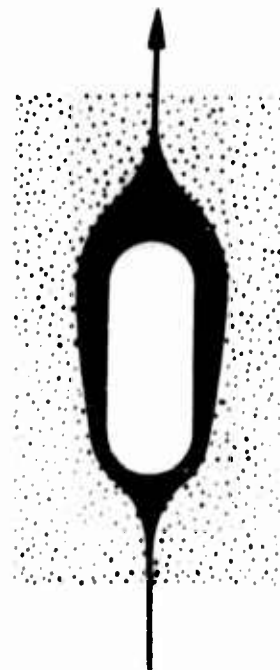


FIG. 17 "BLACK" LAYER SURROUNDING A HEATED BODY

illumination with light rays, which were strongly absorbed by the particles, a positive photophoresis was observed, while during illumination with light rays which were slightly absorbed, a negative photophoresis was produced. In the latter case when the concentration of coloring matter was sufficiently increased, a negative photophoresis was changed into a positive one.

The computation of a temperature gradient in an illuminated particle presents a very complex problem. In order to find a magnitude (if only roughly approximated) of a photophoresis force in a most simple case of an absolutely black spherical particle with $r \gg l$ and also to simplify the problem, it should be established, what constitutes a constant (according to magnitude and direction) gradient ∇_1 in an illuminated particle and what is to be omitted for the particle's heat emissivity by radiation. A natural component of the medium's temperature gradient at a particle's surface with an established distribution of temperature is equal to:

$$\frac{dT}{d\rho}_{\rho=r} = -\Delta T/r \quad (16.9)$$

/see a similar problem on page 232 equation (38.35)/. Hence it follows, that the quantity of heat emitted in 1 sec. by the particle's surface element dS is equal to:

$$d\Omega = \frac{\chi_a \Delta T dS}{r} \quad (16.10)$$

The amount of luminous energy absorbed by a particle in 1 sec. is equal to:

$$\Omega = \pi r^2 I, \quad (16.11)$$

where I is the density of the luminous energy flux ($\text{erg} \cdot \text{cm}^{-2} \cdot \text{sec}^{-1}$).

In accordance with the above-quoted term, the following is the expression for temperature of the surface element dS :

$$T = T_0 + \int_1 r \cos \theta, \quad (16.12)$$

where T_0 is the temperature on the equatorial surface of a particle;

where θ is the angle formed between a radius vector to the element of the surface and the direction of luminous rays.

A thermal equilibrium for a frontal half of a particle is expressed by the equation:

$$\pi r^2 I - \frac{\chi_a}{r} \int_{\pi r^2} \Delta T dS - \pi r^2 \chi_i \Gamma_i = 0, \quad (16.13)$$

where the integral is taken according to the surface of the frontal half of a particle. The first term of the equation expresses an inflow of luminous energy to a particle, the second term indicates emissivity of heat to the gas and the third term denotes emissivity of heat to the rear side of a particle. On behalf of the rear side of a particle we have an analogous term:

$$- \frac{\chi_a}{r} \int_3 \Delta T dS - \pi r^2 \chi_i \Gamma_i = 0. \quad (16.14)$$

If we express T by (16.12), then after integration and subtraction of (16.14) from (16.13) is carried out, we obtain:

$$\Gamma_i = \frac{I}{2(\chi_i + \chi_a)}. \quad (16.15)$$

Thus a radiometric force is equal in this case

$$F_M = - \frac{3\pi\eta^2 r R_g I}{2pM(\chi_a + \chi_i)}. \quad (16.16)$$

If a particle is non-transparent, but it is not absolutely black, then instead of I one must take I_a , where a is the coefficient of light absorption.

EPSTEIN (105) developed a similar formula for particles shaped like flattened spinning ellipsoids, when the proportion of the polar semi-axis c to the equatorial semi-axis a was small, and when the polar axis was set parallel to the luminous rays. It follows:

$$F_M = - \frac{3\pi\eta^2 a R_g I}{2pM\left(\frac{\pi}{4}\chi_a + \frac{a}{4c}\chi_i\right)}. \quad (16.17)$$

A dispute developed, which contradicted the afore-mentioned explanation of a negative photophoresis, that a temperature gradient set lengthwise to luminous rays inside a particle cannot be established at all due to Brownian movement of a particle (114). Of course, the dispute refers not only to a negative photophoresis, but also to all other instances of radiometric effects in aerosols.

In order to explain the influence of Brownian spinning upon photophoresis, we evaluate the length of time of the particle's temperature relaxation τ , i. e., the time necessary to establish a steady temperature gradient (16.15). For this purpose we use the already discussed simplified system of temperature distribution in an illuminated particle.

Suppose that at a movement of $t = 0$ a particle possesses in every volume a temperature T_0 , determined according to the equation for thermal equilibrium

$$\pi r^2 l = 4\pi \Delta T_0 \chi_a r, \quad (16.18)$$

from which

$$\Delta T_0 = \frac{rl}{4\chi_a}. \quad (16.19)$$

If we consider that the difference in temperatures of the frontal and rear part of a particle, with a steady gradient, is small in comparison with $c\Delta T_0$, we can omit the difference in heat emission of both halves of the particle. This would be equivalent to abandoning the χ_a in the equation (16.15) and this is permissible, because the heat conductivity of solid and liquid substances is usually considerably greater than that of gaseous substances. According to this hypothesis, one half of the luminous energy absorbed by a particle is given off to the gas by the frontal portion of the particle, while the other half of the energy is transmitted by the rear half of the particle. In the presence of the gradient of Γ_i , the heat contents of the frontal half of the particle is:

$$\Omega = \gamma c_p \int T dv = \gamma c_p \int_0^r (T_0 + \Gamma_i x) \pi y^2 dx = \gamma c_p \left(\frac{1}{2} \pi T_0 r^3 + \frac{\pi}{4} \Gamma_i r^4 \right), \quad (16.20)$$

where γ is the density;

where c_p is the heat capacity of the particle.

The thermal equilibrium in the frontal half of the particle is expressed by the equation:

$$\frac{d\Omega}{dt} = \frac{\pi}{4} \gamma_{cp} r^4 \frac{d\Gamma_i}{dt} = \frac{\pi}{2} r^2 I - \pi r^2 \chi_i \Gamma_i, \quad (16.21)$$

the solution of which becomes zero, if $t = 0$; thus,

$$\Gamma_i = \frac{I}{2\chi_i} \left[1 - \exp\left(-\frac{4\chi_i t}{\gamma_{cp} r^2}\right) \right]. \quad (16.22)$$

Consequently, the period of thermal relaxation of an illuminated particle is equal to:

$$\tau = \frac{\gamma_{cp} r^2}{4\chi_i}. \quad (16.23)$$

Inasmuch as heat conductivity χ_i/γ_{cp} among most of the solid and liquid substances is on the order of magnitude of 10^{-3} or above¹, hence it follows that $\tau < 2.5 \cdot 10^{-6}$ sec. when $r = 1\mu$, and $\tau < 2.5 \cdot 10^{-8}$ sec. when $r = 0.1\mu$.

The average square of the deflection angle of a spherical particle during a period of τ (see § 43), is equal to:

$$\overline{\theta^2} = \frac{kT\tau}{4\pi\eta r^3}. \quad (16.24)$$

Hence, considering the air at room temperature and at atmospheric pressure, it follows: $\sqrt{\overline{\theta^2}} < 0.4^\circ$ with $r = 1\mu$ and $\sqrt{\overline{\theta^2}} < 1.1^\circ$ with $r = 0.1\mu$. Thus, for a period of thermal relaxation a particle is able to turn around through a very small angle and consequently the influence of Brownian spinning remains insignificant upon photophoresis of aerosol particles of the magnitude of 10^{-4} to

1. Heat conductivity of water is equal to $1.5 \cdot 10^{-3}$, that of mineral oils - $0.7 \cdot 10^{-3}$, and that of the medium - $3 \cdot 10^{-3}$.

10^{-5} cm. As a result it is not difficult to become convinced that the aforementioned deduction remains true also on behalf of transparent particles.

Considering, that the pressure of light upon a particle is equal (in case of non-transparent, absolutely black particles) to $\pi r^2 I/c$ - where c is the velocity of light - thus, the measure does not play any essential role in the phenomena of photophoresis, because it is considerably lower than the radiometric force.

The afore-discussed most simple type of photophoresis is that of homogeneous spherical particles. This phenomenon is more complicated, if we consider a non-spherical shape or a heterogeneity of particles. Thus, the temperature on a particle surface, or on projecting edges and corners, or within a reduced light absorption region of the surface, is lower than that on the flat facets or in strongly absorbent regions. The direction of the resultant radiometric force will, in general, no longer coincide with the direction of rays of light and the resultant moment of these forces will not be equal to zero. Consequently, the movement of illuminated particles acquires a rather complicated nature (562).

Complicated movements are also observed during simultaneous actions of radiometric and other forces upon a particle (electrophoresis, magnetophoresis, gravitophoresis, etc.). The magnetophoresis is known best of all. Solid particles found in a uniformly magnetic field and affected by illumination, travel via spiral course, the axis of which leads toward the vector of field intensity. The component of the particle's velocity in direction of the vector V_H increases at first with a rising field intensity H , then it attains a maximal (during a certain illumination) value and finally remains constant. The theory of magnetophoresis was developed by ROHATSCHEK (563). The magnetic field orientates a particle in a certain way. Radiometric forces compel a particle to move at a determined angle toward the field and also cause a spinning effect around the particle's axis and parallel to the field. Due to the spinning, the direction of the resultant radiometric force changes constantly and the particle depicts a spiral movement. Inasmuch as the Brownian movement interferes with the particles' orientation, the degree of orientation and consequently V_H as well, both increase along with intensification of H , so long as a full orientation is not reached. The relation between V_H and H , as derived by ROHATSCHEK, coincides satisfactorily with the results of measurements.

Chapter III

Rectilinear Irregular Motion of Aerosol Particles

§ 17. Nonuniform Motion of Particles With Small Re Numbers

The motion of aerosol particles at a constant velocity, as discussed in the preceding chapter, represents as such a well known idealization. Actually the particle velocity always changes according to rate and direction: it is sufficient to recall convectional and turbulent currents in a gaseous medium, which, for practical purposes, are eliminated only artificially at laboratories and even so in only a very small measure.

The nonuniform motion of aerosol particles is, of course, far more complicated and diverse than the motion at constant velocity. Differential equations of the motion can generally be solved in comparatively few instances and the others must be handled by numerical approximation methods. Thus, we are in a position to examine only a few of the more important examples of nonuniform motion and in order to simplify the matter, we shall consider that the particles are of a spherical shape. Furthermore, we shall confine ourselves mostly to the region of small Re , where the medium's resistance is proportional to the particles' velocity.

We shall begin with a rectilinear nonuniform motion of the particles. A general differential equation of a mono-uniform motion of particles within a resistant medium at small Re appears as follows (115, 116):

$$m \frac{dV}{dt} = F(t) - \frac{2}{3} \pi \gamma_g r^3 \frac{dV}{dt} - 6 \pi \eta r V - 6 r^2 \sqrt{\pi \eta \gamma_g} \int_0^t \frac{dV}{dx} \frac{dx}{\sqrt{t-x}}. \quad (17.1)$$

The first term at the right side of the equation represents an external force¹ actuating a particle; generally, the force is dependent upon time. The third term obviously expresses the medium's resistance during motion at a constant velocity, which is equal to the value of the velocity at a given moment.

1. We shall not consider the "external" forces with the forces actuating a particle from the side of a quiescent or a moving medium.

Finally, the second term and the one following express a part of the resistance, which results from the expenditure of energy to set the medium in motion. However, the influence of the second term, which expresses resistance of an ideal liquid to the nonuniform motion of a spherical body leads to an apparent augmentation of the body's mass displaced by one half of the medium's² mass. Therefore in view of the small density of the gaseous medium, as compared with the density of particles, the term may be disregarded. Speaking of the integral term, up to now it has been omitted in all publications pertinent to work on aerosols, without any reason offered for permitting such a simplification.

Before we start reviewing this problem, as we abandon the integral term, we present an equation of motion of a particle, quiescent at the moment of $t = 0$ and settling under the influence of the force of gravity. If, conforming with the afore-mentioned, we likewise disregard the second term in the (17.1), then we arrive at the equation:

$$\frac{dV}{dt} + \frac{V}{\tau} - g = 0, \quad (17.2)$$

where

$$\tau = m/6\pi\eta r = \frac{2r^2\gamma}{9\eta}. \quad (17.3)$$

The solution of the equation (17.2), which becomes zero at $t = 0$, is the following:

$$V = V_s \left(1 - e^{-t/\tau}\right), \quad (17.4)$$

where $V_s = \tau g$ is the terminal (fixed) velocity of a precipitating particle. The path traced by the particle is

$$x = V_s t - V_s \tau \left(1 - e^{-t/\tau}\right), \quad (17.5)$$

-
2. We wish to remind, that resistance to a sphere of an ideal liquid, moving with a constant velocity, amounts to zero.

and the acceleration is

$$\frac{dV}{dt} = g e^{-t/\tau} = \frac{V_g}{\tau} e^{-t/\tau}. \quad (17.6)$$

If a particle travels under the influence of some other constant force F , it is necessary to substitute F/m for g in the equations.

Thus the equivalent mathematical instantaneous case of particle motion with an initial velocity of V_0 , can be shown in the absence of external forces (as can readily be seen) to be the following equations:

$$V = V_0 e^{-t/\tau}, \quad (17.7)$$

$$x = V_0 \tau (1 - e^{-t/\tau}). \quad (17.8)$$

We use again the expression (17.6) for acceleration, but with a reverse sign.

The equations for a nonuniform motion of the particles acquire a much simpler form, if we assume a τ value for a time unit. In accordance with the equations (17.4) and (17.7), when the time interval is $t = \tau$, the velocity of a particle constitutes a $1/e$ part of the initial velocity in the case of (17.7), or it just differs by $1/e$ part from the terminal velocity in case of (17.4). Thus, the τ can be named a "relaxation period" of a moving particle. As we shall explain later, τ defines a type of a nonuniform motion and in all instances of similar motion as such, it represents a basic characteristic value in the mechanics of aerosols.

Suppose we designate a time by t' and a particle's velocity in terms of V' . It is obvious, that $t' = t/\tau$, $V' = V\tau$, and $dV'/dt' = \tau^2 dV/dt$. Thus the equations (17.4) and (17.6) imply that

$$V' = V'_g (1 - e^{-t'}), \quad (17.9)$$

$$dV'/dt' = V'_g e^{-t'}, \quad (17.10)$$

and if the second term in the right part of the (17.1) is abandoned, the latter will be converted into:

$$\frac{1}{\tau^2} \frac{dV'}{dt'} + \frac{1}{\tau^2} V' - \frac{F'}{m\tau^2} + \frac{6r^2\sqrt{\pi\eta\gamma g}}{m} \int_0^t \tau^{-3/2} \frac{dV'}{dx'} \frac{dx'}{\sqrt{t'-x'}} = 0, \quad (17.11)$$

where $x' = x/\tau$ and $F' = \tau^2 F$ is the value of an external force in new terms.

If we replace m by $\frac{4}{3}\pi r^3\gamma$ and τ by the expression (17.3), we obtain after abbreviation:

$$\frac{dV'}{dt'} + V' - \frac{F'}{m} + \frac{3\sqrt{\gamma g}}{\sqrt{2\pi\gamma}} \int_0^{t'} \frac{dV'}{dx'} \frac{dx'}{\sqrt{t'-x'}} = 0. \quad (17.12)$$

The solution of the equation (17.12) applicable to a force, which begins to actuate a quiescent particle at a moment of $t = 0$, was prepared by BOGGIO (117, 118) in the following form:

$$V'(t') = \frac{1}{\lambda_1 - \lambda_2} \int_0^{t'} \Phi(x) \left[e^{\lambda_1(t'-x)} - e^{\lambda_2(t'-x)} \right] dx + C'_1 e^{\lambda_1 t'} + C'_2 e^{\lambda_2 t'}, \quad (17.13)$$

where $C'_1 = -C'_2 = g'(0) (\lambda_1 - \lambda_2)$; $g' = F'/m$; λ_1 and λ_2 are radicals of the characteristic equation $\lambda^2 + (2 - \alpha^2)\lambda + 1 = 0$;

$$\Phi(x) = g'(x) + \frac{dg'(x)}{dx} - \frac{\alpha}{\sqrt{\pi}} \frac{d}{dx} \int_0^x \frac{g'(z)dz}{\sqrt{x-z}}; \quad \alpha = \sqrt{\frac{9\gamma g}{2\gamma}}.$$

The equation (17.13) offers a general solution of the problem of a nonuniform motion of a particle, quiescent at the moment of $t = 0$. In the event a force actuating a particle is constant $g' = \text{const.}$, $\Phi(x) = g' \left(1 - \frac{\alpha}{\sqrt{\pi x}} \right)$ and (17.13) is converted into

$$V'(t') = g' + \frac{g'}{\lambda_1 - \lambda_2} \left\{ e^{\lambda_1 t'} \left(\frac{1}{\lambda_1} + 1 \right) - e^{\lambda_2 t'} \left(\frac{1}{\lambda_2} + 1 \right) - \frac{\alpha}{\sqrt{\pi}} \int_0^{t'} \frac{e^{\lambda_1(t'-x)} - e^{\lambda_2(t'-x)}}{\sqrt{x}} dx \right\}. \quad (17.14)$$

Considering the smallness of a to radicals λ_1 and λ_2 , one can adopt the approximate expressions like $\lambda_1 = -1 + ia$; $\lambda_2 = -1 - ia$ and then $\frac{1}{\lambda_1} + 1 = \frac{a^2}{2} - ia$; $\frac{1}{\lambda_2} + 1 = \frac{a^2}{2} + ia$.

If we introduce these expressions in (17.14) and substitute by g' the constant velocity of particle's motion V'_0 in the adopted system of coordinates, we finally obtain:

$$V'(t') = V'_0 \left\{ 1 - e^{-t'} \left[\cos(at') - \frac{a}{2} \sin(at') + \frac{1}{\sqrt{\pi}} \sin(at') \int_0^{t'} \frac{e^x \cos(ax)}{\sqrt{x}} dx - \frac{1}{\sqrt{\pi}} \cos(at') \int_0^{t'} \frac{e^x \sin(ax)}{\sqrt{x}} dx \right] \right\} \quad (17.15)$$

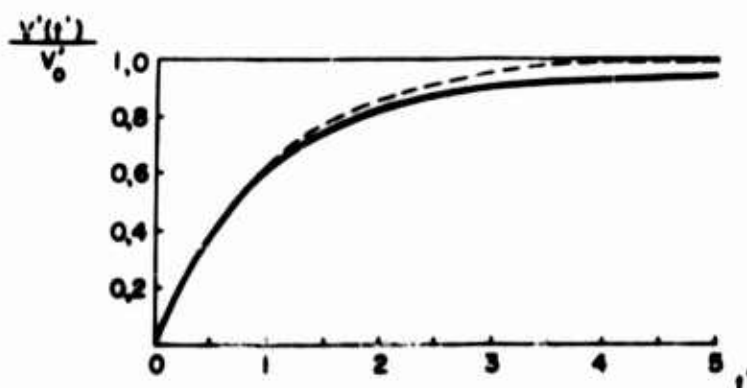


FIG. 18 MOTION OF PARTICLES ACTUATED BY A CONSTANT FORCE

Thus, for particles with a density equal to unity in air $a = 0.0736$ at 20° and 760 mm of mercury. Figure 18 delineates by a solid line the function $V'(t')$ computed by means of a graphic integration. In the absence of an integral term in the equation (17.12) we would obtain

$$V'(t') = V'_0 (1 - e^{-t'}). \quad (17.16)$$

The equation (17.16) is represented on the above drawing by a dotted line.

Thus, the presence of an integral term brings about a small reduction of the particles acceleration, during which the magnitude of the

effect depends neither upon size of particles, nor upon viscosity of medium, but exclusively upon the magnitude of α , i. e. upon the ratio of the density of a particle and a medium. Because of this reason the effect remains large among liquids, but it is insignificant among gases. Considering a path negotiated by a particle within a specific time, the maximal value of the integral term's correction does not exceed 4%, if a particle's density is equal to unity and 2%, if the density is equal to 4, etc.

Thus, considering the discussed example of a motion, the omission of an integral term does not lead to a noticeable error regardless of the particles' size and the resistance may be practically considered as a "non-inertial", i. e., as corresponding to a resistance at a constant velocity equal to velocity value at a given moment. An analogous condition also exists during oscillatory movements of particles in a gaseous medium.

We shall proceed now to a retarded movement of particles, the initial velocity of which is V_0 in the absence of external forces. Here, instead of the (17.12), the basic equation of the movement appears as follows:

$$\frac{dV'}{dt} + V' + \frac{3\sqrt{\gamma g}}{\sqrt{2\pi\gamma}} \int_0^{t'} \frac{dV'}{dx'} \frac{dx'}{\sqrt{t' - x}} = 0 \quad (17.17)$$

with the initial condition of $V'(0) = V'_0$. If we introduce the function $V^*(t) = V'_0 - V'(t)$, we obtain the equation equivalent to (17.12) with F'/m being substituted by V'_0 and the initial condition $V^*(0) = 0$. Thus, considering $V^*(t)$, the solution (17.15) is correct and, if we turn the figure 18 around by 180° , we shall obtain an accurate curve and an approximate curve of $V'(t)$ for a given case. However, in the discussed case, a correction conditioned by the integral term (as we shall see it now), is more important than in an accelerated motion of the particles.

Assuming in (17.8) that $t = \infty$, we find that a maximal distance l_1 traced by a particle is equal to

$$l_1 = V_0 \tau = \frac{2V_0 r^2 \gamma}{9\eta} \quad (17.18)$$

The l_1 value, which we shall name an "inertial run" of a particle with initial velocity V_0 , plays, as we shall see later, a greater role during the motion of particles in trajectory. It is evident from figure 18, that the l_1 value is expressed by the area situated above the solid-line curve V_t , i. e., during calculation of the integral term it noticeably exceeds the value of $V_0 \tau$.

which corresponds to the area situated above the approximate dotted-line curve. At this it must be noted that the velocity of a slowly moving particle, due to a specific make-up of the integral term, continues for some time to remain different from zero by a small, yet a definite value (as is obvious from figure 18). This phenomenon depends on the factor, that the current - developed by a particle travelling in a surrounding and infinitely expanded medium (to which all equations of this paragraph are referable) - attenuates much slower than the motion of the particle itself in relation to the medium. Yet, in the first place, since STOKES' law for a spherical particle (surrounded by a viscous liquid) is correct only in the immediate proximity of the particle and, in the second place, since the particle motion in all practical instances is effected within a space limited by walls or by other particles, the latter stage of attenuation of the particle motion proceeds actually not according to the curve on the figure 18, but considerably faster. For this reason we shall ultimately use a simple expression (17.18) for l_i .

The equation (17.5) enables us to draw the following conclusion: if a particle movement is examined for a time interval longer than T , one can disregard the second term in the right part of the equation (17.5), i.e., to assume that the particle from the very beginning travels at a fixed velocity V_s . As we shall explain below, this conclusion can be theorized in the following manner: during the examination of the movements, whose duration is large when compared with T , it may be assumed that the particles remain immobile in relation to a medium, if they are not actuated by external forces, or if they travel at a velocity of $V(t) = BF(t)$; where $F(t)$ is the momentary value of an external force. Such a movement of particles we shall name a quasi-fixed.

BERKOWITCH (119) conducted an experimental research in non-uniform, rectilinear motion. In his work a charged particle of selenium was put in equilibrium in an M condenser shunted with a large resistance R_E , where in, due to this resistance, an M_2 condenser, with a capacity C_E and with the initial potential difference π_0 was discharged. The change of voltage in the M_1 condenser assumed in time a rather complicated nature due to the onset of electrical oscillations. Yet, the period of these oscillations is considerably shorter than the relaxation period of the examined particles ($r \approx 10^{-4}$ cm; $\gamma = 4.4$; $T \approx 2 \cdot 10^{-4}$ sec.), therefore the oscillations practically do not check the motion of the particles. In order to disregard these oscillations, the kinetics of the M_2 condenser's discharges are expressed by the differential equation:

$$-C_E \frac{d\pi}{dt} = \frac{\pi}{R_E}, \quad (17.19)$$

from which it follows, that

$$\pi = \pi_0 e^{-t/C_E R_E} \quad (17.20)$$

In these experiments $C_E = 5.74 \cdot 10^{-9}$ farads, $R_E = 1.5 \cdot 10^6$ ohms, and $\pi_0 = 2500$ volts. Thus the relaxation period of the condenser $C_E R_E = 8.6 \cdot 10^{-3}$ sec. is considerably longer than τ and the motion of particles may be considered as quasi-fixed. The velocity of particles is expressed by the equation

$$\frac{dx}{dt} = \frac{\pi_0 q B}{h} e^{-t/C_E R_E}, \quad (17.21)$$

where h is the distance between the condenser's plates M_1 ; where q is the particle charge, while for the path traced by the particle we obtain

$$x_\infty = \frac{\pi_0 q B}{h} \int_0^\infty e^{-t/C_E R_E} dt = \frac{\pi_0 q B C_E R_E}{h}. \quad (17.22)$$

The above expression is the result of a more exact conclusion with the computed electrical oscillations within a condenser's shape and with the computed inertia of the particles (still without computing any integral term). The maximal velocity of particles in these tests did not exceed 20 cm/sec., which conforms with $Re \ll 0.03$, i. e., with the region of applicability of the equation (17.1).

The values x_∞ measured by BERKOWITCH conformed very well with the equation (17.22); they were in exact proportion with each of the following values: π_0/h , C_E , R_E , and B ; deviations did not exceed $\pm 1 - 1.5\%$. The particle mobility B was determined according to the velocity of the falling particles and according to the balancing force of the field (see § 15, B). Also the absolute magnitude x_∞ differed by no more than $\pm 3\%$ from the theoretical value, at the same time the deviations had a total random nature and undoubtedly were caused by the Brownian movement of the particles. It is important to note that particles of selenium had a spherical shape in these tests, therefore the phenomenon of the particles' orientation in the field could not occur. The correction in the integral term, disregarded by BERKOWITCH, must, in the given case, remain insignificant due to high density of selenium.

Furthermore, in the first stage of the condenser's discharges a particle travels with an acceleration, while in the second one - with a deceleration, so the corrections in the integral term in both stages compensate themselves to a well known degree.

§ 18. - Nonuniform Motion of Particles at Greater Re Numbers

A nonuniform, rectilinear motion at much higher Re numbers, occurring in the mechanics of aerosols (approximately up to $Re = 1000$) was not examined theoretically, therefore the experimental data in question are insufficient and contradictory. The velocity of air-borne small balloons filled with hydrogen, with a radius of 8 and 26 cm ($Re = 5,000$ to $35,000$), was measured by SCHMIDT (120) in tests by a photographic method (also in all other researches mentioned in this paragraph). Experimental data when processed revealed that the air resistance at every moment exceeded noticeably the resistance of a specific constant velocity of the motion. Furthermore, the velocity of the small balloons did not increase uniformly with time, but at a certain moment it decreased noticeably and then it increased again. Identical results were obtained by testing water-borne small waxen balls, with $r = 1.0 - 1.5$ cm, ($Re = 500 - 1,500$), during which the study of currents (by colored streams) near the small balls led the author to the conclusion that the indicated complex dependence of velocity upon time is influenced by the emergence, growth and breaking away by whirl pools from little balls.

LUNNON (121) measured the velocity of falling small solid balls of various substances, with $r = 1 - 10$ mm, in a deep shaft and he also discovered that medium's resistance to an accelerated movement is considerably greater than at a constant velocity: thus, at $Re = 10,000$ and at acceleration of $5 \text{ m} \cdot \text{sec}^{-2}$, the ψ is greater by 15%, while at acceleration of $8 \text{ m} \cdot \text{sec}^{-2}$, it is higher by 35% than during a constant velocity; at $Re = 35,000$ it corresponds to 25 and 100%.

G. KHUDYAKOV and Z. TCHUKHANOV (122, 123) studied the motion of small grains of sand, with $r = 35, 100$ and 420μ , in a vertical tube, through which air was blown from the top down with a velocity of $10-25 \text{ m} \cdot \text{sec}^{-1}$. Grains of sand were led into the tube without any noticeable initial velocity, therefore their movement in the first stage was decelerated as regards to air. At $Re = 20 - 600$, the medium's resistance, on the average, appeared approximately twice as small, than at a constant velocity. However, due to strong turbulence in these tests and "twisting" of the current, particles were not falling vertically, but they centrifuged in a zigzag way toward the walls of the tube, therefore the ψ values obtained are not completely reliable.

On the other hand the experimental data of LAWS (124), who measured the rapidity of water droplets (with $r = 0.6 - 3$ mm) falling through the air at various distances from the initial point, are well responsive to

UNCLASSIFIED

AD

2271876

FOR
MICRO-CARD
CONTROL ONLY

3

OF

9

Reproduced by

Armed Services Technical Information Agency

ARLINGTON HALL STATION; ARLINGTON 12 VIRGINIA

UNCLASSIFIED

"NOTICE: When Government or other drawings, specifications or other data are used for any purpose other than in connection with a definitely related Government procurement operation, the U.S. Government thereby incurs no responsibility, nor any obligation whatsoever; and the fact that the Government may have formulated, furnished, or in any way supplied the said drawings, specifications or other data is not to be regarded by implication or otherwise in any manner licensing the holder or any other person or corporation, or conveying any rights or permission to manufacture, use or sell any patented invention that may in any way be related thereto.

theoretical curves (125), plotted according to ψ values for a constant velocity of similar falling droplets ($Re \leq 1500$). In this calculation a certain error was introduced, in view of the fact that with the increasing ψ the deformation of droplets depends upon their velocity and the value of ψ is known only in connection with one velocity, i.e., a constant velocity of falling droplets. LAWS' data for droplets with $r = 0.6$ mm ($Re \leq 200$), among which the flattening effect is small, were processed by the author of the book, wherein the discovered ψ values appeared lower by 5-10% than those submitted in table 5. Thus, considering Re numbers not exceeding the range of several hundred, one can apparently assume without committing a great error, as this usually occurs in technical calculations, that medium's resistance does not depend upon acceleration.

In this case the motion of an aerosol particle in the absence of external forces may be calculated in the following manner. Since in the equation (7.5) $V = Re \eta / 2r\gamma_g$, it follows that

$$\frac{dV}{dt} = \frac{\eta}{2r\gamma_g} \cdot \frac{dRe}{dt} \quad (18.1)$$

If we introduce into the equation of a particle motion in the absence of external forces

$$m \frac{dV}{dt} = -F_M \quad (18.2)$$

the expressions for F_M (10.2), V and $\frac{dV}{dt}$, we obtain (126) after abbreviations

$$\frac{dRe}{\psi Re^2} = - \frac{\pi \eta r dt}{4m} \quad (18.3)$$

from which

$$\int_{Re_1}^{Re_2} \frac{dRe}{\psi Re^2} = - \frac{\pi \eta r (t_2 - t_1)}{4m} = - \frac{3\eta (t_2 - t_1)}{16r^2\gamma} \quad (18.4)$$

The integral in (18.4) may be computed graphically according to the afore-cited (page 53) values of the function ψRe^2 . Thus, one can find the variation of Re and subsequently the variation of a particle velocity as a time function. In a similar manner the following equation is developed:

$$\int_{Re_1}^{Re_2} \frac{dRe}{\psi Re^2} = - \frac{\pi r^2 \gamma_g (x_2 - x_1)}{2m} = - \frac{3\gamma_g (x_2 - x_1)}{8r\gamma}, \quad (18.5)$$

which provides the dependence between the distance travelled by a particle and the velocity.

In the essence of the example in regard to the applicability of these equations we find a magnitude of the inertial run l_i with such dimensions and velocity of particles, to which equation (17.18) is no longer applicable. For this reason in the equation (18.5) one must assume $Re = 2rV_o\gamma_g/\eta$; where V_o is the initial velocity of a particle and $Re_2 = 0$. Then, $x_2 - x_1$ will be equal to l_i .

By using a graphic integration the value of the integral $\int \frac{dRe}{\psi Re^2}$ was determined and likewise the curve was obtained, submitted on figure 19, which gives the value $\frac{3\gamma_g l_i}{8r\gamma}$ in the function of $\frac{2rV_o\gamma_g}{\eta} = Re_o$. The broken line on the chart

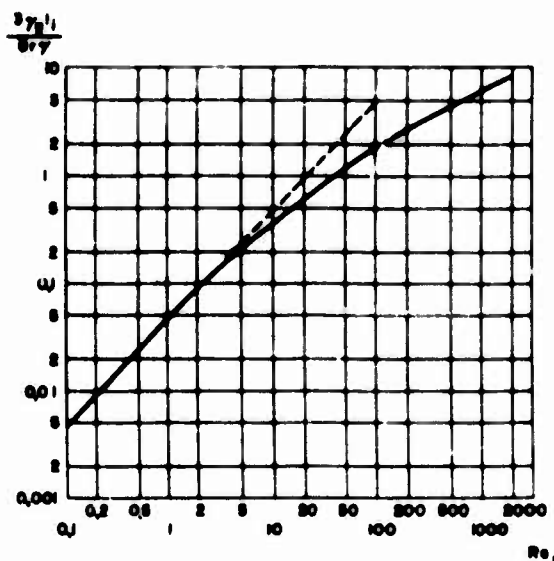


FIG. 19 THE INERTIAL RUN OF PARTICLES IN THE ULTRA-STOKES RANGE

was plotted according to the formula (17.18), i. e., with the supposition of the adaptability of STOKES' law. We shall also compute with the aid of equation (18.4) the time of relaxation τ for particles with a radius of 1 mm and with the density 1 at the initial velocity of $30 \text{ cm} \cdot \text{sec}^{-1}$. We find this computation in § 45. Assuming that $Re_1 = 2 \cdot 0.1 \cdot 30/0.17$ and $Re_2 = Re_1/e$, we find by a graphic integration that $\tau = 6.3 \text{ sec.}$ (instead of 12 sec. according to STOKES).

In a similar way one can solve the problem of a nonuniform movement of particles actuated by a constant force, e.g., by a gravitational force. In this case the equation of motion is

$$m \frac{dV}{dt} = -F_M + mg \quad (18.6)$$

and instead of (18.4) we obtain

$$\int_{Re_1}^{Re_2} \frac{dRe}{a - \psi Re^2} = - \frac{3\eta(t_2 - t_1)}{16r^2\gamma}, \quad (18.7)$$

where $a = 32\gamma\gamma_g r^3 / 3\eta^2$.

Instead of (18.5) we obtain

$$\int_{Re_1}^{Re_2} \frac{Re d Re}{a - \psi Re^2} = - \frac{3\gamma_g(x_2 - x_1)}{8r\gamma}. \quad (18.8)$$

Also here by using a graphic integration one can find the dependence between the particle velocity on the one hand and either the time, or the path travelled, on the other.

§ 19. Oscillations of Aerosol Particles Actuated by a Periodic External Force

STOKES prepared (an accurate, assumed, small Re) equation (127) for oscillations of spherical particles in a resistant medium under the influence of a periodic variable external force F. It follows:

$$m \frac{dV}{dt} = F - \frac{9}{4} m' \omega \beta (1 + \beta) V - \left(\frac{1}{2} + \frac{9}{4} \beta \right) m' \frac{dV}{dt}, \quad (19.1)$$

where m is the particle mass;

m' is the mass of the medium displaced by the particle mass;

where ω is the angular frequency of oscillations (equal to number of oscillations

per sec. multiplied by 2π); $\beta = \frac{1}{r} \sqrt{\frac{2\eta}{\omega \gamma g}}$. Let us assume that β is of the order of magnitude $1/r\sqrt{\omega}$ and in air at usual conditions $\beta = 0.55/r\sqrt{\omega}$.

Since $m \gg m'$, we shall replace it, as before, by the term $\frac{1}{2} m' \frac{dV}{dt}$ and we shall bring the equation (19.1) to this form:

$$m \frac{dV}{dt} + \frac{9}{4} m' \beta \frac{dV}{dt} + \frac{9}{4} m' \omega \beta V + \frac{9}{4} m' \omega \beta^2 V - F = 0. \quad (19.2)$$

When $\omega \rightarrow 0$, the second term of the equation can have trends towards infinity. Yet, in oscillatory movements, to which (19.2) is referable, $V = V_0 \sin \omega t$ and $dV/dt = \omega V_0 \cos \omega t$. Thus, all the terms (19.2), except the last two, trend toward zero at $\omega \rightarrow 0$. The penultimate term, as can easily be proved, is equal to $6\pi\eta r V$, i. e., as such it represents the resistance of the medium at a constant velocity V . Thus, when $\omega \rightarrow 0$, the equation (19.2) changes into the usual STOKES' equation.

If we designate a "reduced mass" of a particle $m + \frac{9}{4} m' \beta$ by m_r and $\frac{9}{4} m' \omega \beta (1 + \beta) = \frac{9}{4} m' \omega \beta + 6\pi\eta r$ by $1/B_r$ (B_r denotes a "reduced mobility"), thus equation (19.2) is brought to this form:

$$m_r \frac{dV}{dt} + \frac{V}{B_r} - F = 0. \quad (19.3)$$

If F changes sinusoidally with the time, i. e., $F = F_0 \sin \omega t$, the solution (19.3), which at $t = 0$ reverses to 0, assumes this form:

$$V = \frac{F_0 B_r \sin(\omega t - \varphi)}{\sqrt{1 + B_r^2 \omega^2 m_r^2}} + \frac{F_0 B_r e^{-t/B_r m_r} \sin \varphi}{\sqrt{1 + B_r^2 \omega^2 m_r^2}} \quad (19.4)$$

whereupon

$$\operatorname{tg} \varphi = B_r \omega m_r. \quad (19.5)$$

The second term in (19.4), which corresponds to the initial, irregular stage of oscillations, rapidly trends toward zero and, at a stationary condition of the particles' oscillation, occurs according to the equation

$$V = V_0 \sin(\omega t - \varphi) \quad (19.6)$$

with a velocity range

$$V_0 = \frac{F_0 B_r}{\sqrt{1 + B_r^2 \omega^2 m_r^2}}. \quad (19.7)$$

If we replace m_r and B_r by their expressions, we obtain

$$V_0 = \frac{F_0 f}{\omega m \sqrt{f^2 + 3\beta f + \frac{9}{2}\beta^2 + \frac{9}{2}\beta^3 + \frac{9}{4}\beta^4}}, \quad (19.8)$$

$$\operatorname{tg} \varphi = \left(\frac{2}{3}f + \beta \right) / \beta (1 + \beta), \quad (19.9)$$

where

$$f = \frac{2m}{3m'} = \frac{2\gamma}{3\gamma_g}. \quad (19.10)$$

The equations indicate that the types of oscillations are determined by relationship of the density of a particle and of the medium as well as by the parameter β , i. e., for the medium in question by the product $r\sqrt{\omega}$.

If we omit in equation (19.2) the second term and the third term, which express the inertial part of medium's resistance and are equivalent to the integral term in the equation (17.1), then m_r is converted into m and B_r into B ; we also obtain, instead of (19.8) and (19.9), much simpler equations, such as:

$$V_0 = \frac{F_0 B}{\sqrt{1 + \omega^2 \tau^2}} = \frac{F_0 B}{\sqrt{1 + (2\pi\tau/t_p)^2}} = F_0 B \cos \varphi, \quad (19.11)$$

$$\operatorname{tg} \varphi = \tau \omega = 2\pi\tau/t_p, \quad (19.12)$$

where $t_p = 2\pi/\omega$ is the oscillation period. Hence, for the amplitude of oscillations this expression follows:

$$a = F_0 B / \omega \sqrt{1 + \omega^2 \tau^2}. \quad (19.13)$$

In order to estimate the allowable error in this simplification, we determine the magnitude of the ratio of the amplitude of the particle's oscillation velocity in a gaseous medium V_0 , to that in a vacuum V_0^0 . The latter may be obtained by a differential equation of the oscillations in a vacuum

$$m \frac{dV}{dt} = F_0 \sin \omega t, \quad (19.14)$$

whose solution will be as follows:

$$V^0(t) = V_0^0 \sin \left(\omega t - \frac{\pi}{2} \right) = \frac{F_0}{\omega m} \sin \left(\omega t - \frac{\pi}{2} \right). \quad (19.15)$$

According to the exact equation (19.8)

$$V_0/V_0^0 = f / \sqrt{f^2 + 3\beta f + \frac{9}{2}\beta^2 + \frac{9}{2}\beta^3 + \frac{9}{4}\beta^4}. \quad (19.16)$$

According to the simplified equation (19.11)

$$V_0/V_0^0 = \frac{B\omega m}{\sqrt{1 + \omega^2 \tau^2}} = \frac{\omega \tau}{\sqrt{1 + \omega^2 \tau^2}}. \quad (19.17)$$

The dependence expressed by the equation (19.17) is illustrated on figure 20 (dotted line 2). The solid line represents the dependence of $\gamma = 1$ upon (19.16) in the air under usual conditions. We see, that in determination of the

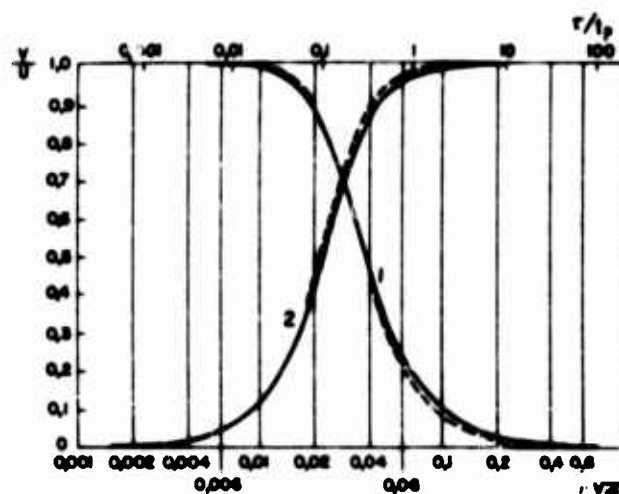


FIG. 20 OSCILLATIONS OF AEROSOL PARTICLES

amplitude of the particles oscillations, the error, which occurs when the initial terms in the basic equation (19.2) are abandoned, is small, therefore it may nearly always be disregarded for practical purposes. One can readily see that with the increase of the particles density the error still decreases, as is the case explained in § 17.

As is obvious from the equations (19.11) and (19.12), the type of particle oscillation is determined by the magnitude of the ratio of a particle's relaxation time τ to the magnitude of the oscillation period t_p . If the magnitude of such a ratio is very substantial (large particles, high frequencies), $\tan \varphi \rightarrow \infty$, $\varphi \rightarrow \frac{\pi}{2}$, $V_0 \rightarrow F_0/\omega m$, we arrive at the equation of oscillations in a vacuum. Thus, at larger τ/t_p one can disregard the medium's resistance (inertial region of oscillations).

At very small values τ/t_p $\tan \varphi \rightarrow 0$, $\varphi \rightarrow 0$, $V_0 \rightarrow F_0 B$, the equation of the particle's oscillation assumes a form:

$$V = F_0 B \sin \omega t = FB. \quad (19.18)$$

Thus, in the discussed case, the movement is of a quasi-fixed type: the inertia of the particles drops out from the equation of oscillations and a particle travels at every moment with a velocity, which is equal to the value of a variable force at a given moment (viscous region of oscillations).

We conclude from figure 20, that the transition from a viscous to an inertial region of oscillations is effected during the interval of τ/t_p values of approximately 0.002-1. In a viscous region the oscillations of the particles are in phase with the forces; the oscillations of a particle begin to lag with the increase of τ/t_p and in the inertial stage the lagging amounts to 1/4 of the time period

Of more importance is the example of aerosol particle oscillations, actuated by external forces, i. e., oscillations of charged particles in an alternating electrical field. Here $F = Eq$; where E is the field intensity and where q is the particle charge. The most elaborate experimental research on the above mentioned oscillations is the one conducted by YU-CHEN-YANG (128). In his experiments a charged particle was put in equilibrium in a stationary vertical electrical field and then, above the latter, an alternating vertical field with a frequency of 50 hertz was superimposed. The particle's radius was of the order 10^{-4} cm. Thus, τ was of the order 10^{-5} sec. and the oscillations could be considered as purely viscous. Re did not exceed 0.03 in these experiments.

The oscillating particles, under these conditions, appeared like vertical lines, the length of which was equal to that of oscillations of a double amplitude. It appeared that the amplitude was exactly proportional to the field intensity and to the charge of particle, i. e., to the force actuating it and conforming with the equation (19.18). Yet, the absolute measure of the amplitude was greater than that computed according to the (19.18) and at the

time the variations reached 7% in individual tests. Likewise, the mobility of a particle influenced by a constant force was determined according to the velocity of settling in the absence of an electrical field and according to the magnitude of the balanced field (§ 15, B). Thus, during the computation of mobility it was not necessary to introduce any corrections for the shape and density of particles. The author attributed the reason for the afore-mentioned divergence to the imperfection of the sinusoidal condition of the alternating field, but in this case the variations probably were constant instead of fluctuating from test to test. Apparently the diversity is explained by this, that the work was conducted with particles obtained with electric sparks passing between metal electrodes and, therefore, undoubtedly, appeared as aggregates. Since aggregates of elongated shape orientate themselves with their lengthy axes parallel to the electrical field (see § 43), they therefore while moving through the field retain a greater mobility than at the time of settling in a nonexistent field.

The measurements of particle oscillations in an alternating electrical field look like a very convenient method for determination of particle charges (see page 135). Oscillations of particles in an electrical field could be used for artificial coagulation of aerosols, although more effective in this respect are the oscillations in a sonic field (see § 20). A peculiar phenomenon is that of a "scintillating" smoke, coming out of a locomotive smokestack, passing under the electric wires of an electrified railroad, which, undoubtedly, is explained by the oscillations of charged particles of smoke in an electrical field between the wires and the smokestack (129).

§ 20. Oscillations of Aerosol Particles Actuated by Sonic Waves

A particle present in an oscillating medium induces oscillations by itself. Let us denote the particle's velocity by V and the medium's velocity by U . The force actuating a spherical particle in an ideal liquid moving with an acceleration dU/dt is equal to

$$F_M = m' \frac{dU}{dt} - \frac{m'}{2} \left(\frac{dV}{dt} - \frac{dU}{dt} \right), \quad (20.1)$$

where m' is the mass of liquid displaced by the particle.

In order to comprehend the physical meaning of the equation, let us suppose that densities of the particle and of the medium are equal. Furthermore, it is obvious that the particle will be moving as a whole with the medium, so in this case $V = U$. Inasmuch as the only force actuating the particle is the influence of the medium F_M and in this case the latter is equal to the sum of the particle mass at its acceleration, so:

$$F_M = m' \frac{dV}{dt} = m' \frac{dU}{dt}. \quad (20.2)$$

By this the first term in the right side of (20.1) expresses the influence of the medium upon the particle moving along with the medium. The term $-\frac{m'}{2}\left(\frac{dV}{dt} - \frac{dU}{dt}\right)$ expresses the share of the medium's influence, which depends upon acceleration of the particle with regard to the medium. In case of an ideal liquid this influence amounts to an apparent expansion of the particle mass by one half of the medium's mass displaced by it. Thus, the equation of a particle movement in an ideal liquid assumes this form:

$$m \frac{dV}{dt} = m' \frac{dU}{dt} - \frac{m'}{2} \left(\frac{dV}{dt} - \frac{dU}{dt} \right) = \frac{3}{2} m' \frac{dU}{dt} - \frac{m'}{2} \frac{dV}{dt}. \quad (20.3)$$

In a tangible medium the terms on the right side, which are dependent upon viscosity, must be combined. Moreover, V in (19.1) denotes a relative velocity of the particle and of the medium, which in the present discussed case are equal to $V - U$. Finally, we arrive at the equation for the particle movement in the oscillating viscous medium:

$$m \frac{dV}{dt} = \frac{3}{2} m' \frac{dU}{dt} - \frac{1}{2} m' \frac{dV}{dt} - \frac{9}{4} m' \omega \beta (1 + \beta) (V - U) - \frac{9}{4} m' \beta \left(\frac{dV}{dt} - \frac{dU}{dt} \right) \quad (20.4)$$

or, as previously, by abandoning the term $-\frac{m'}{2} \frac{dV}{dt}$ and by using the symbols of the preceding paragraph, we obtain:

$$m_r \frac{dV}{dt} + \frac{V}{B_r} = \frac{9}{4} m' \omega \beta (1 + \beta) U + \left(\frac{9}{4} m' \beta + \frac{3}{2} m' \right) \frac{dU}{dt}. \quad (20.5)$$

If oscillations of the medium are conveyed by the expression

$$U = U_0 \sin \omega t, \quad (20.6)$$

then equation (20.5) assumes a form:

$$m_r \frac{dV}{dt} + \frac{V}{B_r} = \frac{3}{2} m' \omega U_0 \sqrt{1 + 3\beta + \frac{9}{2}\beta^2 + \frac{9}{2}\beta^3 + \frac{9}{4}\beta^4} \sin(\omega t + \theta), \quad (20.7)$$

where

$$\operatorname{tg} \theta = \left(\frac{2}{3} + \beta \right) / \beta (1 + \beta), \quad (20.8)$$

is in agreement with the equation of the particle oscillation actuated by an external force (19.3). The following will be a firm solution for (20.7)

$$V = U_0 \mu \sin(\omega t + \theta - \varphi) \quad (20.9)$$

where

$$\mu = \frac{V_0}{U_0} = \sqrt{\frac{1 + 3\beta + \frac{9}{2}\beta^2 + \frac{9}{2}\beta^3 + \frac{9}{4}\beta^4}{f^2 + 3f\beta + \frac{9}{2}\beta^2 + \frac{9}{2}\beta^3 + \frac{9}{4}\beta^4}} \quad (20.10)$$

$$\operatorname{tg}(\varphi - \theta) = \frac{\frac{3}{2}(f - 1)\beta(1 + \beta)}{f(1 + \frac{3}{2}\beta) + \frac{3}{2}\beta + \frac{9}{2}\beta^2 + \frac{9}{2}\beta^3 + \frac{9}{4}\beta^4} \quad (20.11)$$

The equations (20.10) and (20.11), developed for the first time by KÖNIG (130), pertain to the relationship of the amplitude of oscillations¹ on behalf of the particle and the medium $\mu = V_0/U_0$, with a pertinent displacement of the oscillation phase $\varphi - \theta$. His rather complicated deduction was superseded by us with a more simple one. We still have to find the magnitude of the amplitude relative to oscillatory movement of the particle and the medium $V_R = V - U$. To do this, we remove the first two very small terms from the right side of (20.4) and having subtracted from both parts $m \frac{dU}{dt}$ we convert the equation in the following manner:

$$m_r \frac{dV_R}{dt} + \frac{V_R}{B_R} = -m \frac{dU}{dt} \quad (20.12)$$

If we substitute $U = U_0 \sin \omega t$ and solve the obtained equation, we acquire (as above):

$$V_R = - \frac{U_0 f \sin(\omega t + \frac{\pi}{2} - \varphi)}{\sqrt{f^2 + 3f\beta + \frac{9}{2}\beta^2 + \frac{9}{2}\beta^3 + \frac{9}{4}\beta^4}} \quad (20.13)$$

1. The ratios of the amplitude of oscillations, also the amplitude of velocities of oscillations of a particle and of medium, are equal to each other in case of simple harmonic oscillations.

Comparison with the equation (19.16) disclosed that the ratio of the amplitudes of the relative oscillations of the particle and the medium to the oscillations of the medium itself is equal to the proportion of the amplitudes of the oscillations of the particle which has been actuated by a periodic external force in a gaseous medium and in a vacuum (figure 20, curve 2). Therefore for computing the amplitudes of comparative oscillations of the particle and the medium, one can use the simplified equation (19.17), instead of the exact equation (19.16). Thus:

$$\frac{V_{R_0}}{U_0} = \frac{\omega \tau}{\sqrt{1 + \omega^2 \tau^2}}, \quad (20.14)$$

$$V_R = -V_{R_0} \sin(\omega t + \frac{\pi}{2} - \varphi), \quad (20.15)$$

$$\operatorname{tg} \varphi = \omega \tau \quad (20.16)$$

If in the right part of the (20.4) we drop all terms, except

$$\frac{9}{4} m' \omega \beta^2 (V - U) = 6\pi \eta r (V - U),$$

i. e., if we compute the medium's resistance as non-inertial, then instead of (20.7) we shall obtain the equation

$$m \frac{dV}{dt} + \frac{V}{B} = \frac{U}{B} = \frac{U_0 \sin \omega t}{B}. \quad (20.17)$$

Instead of (20.10), the following expression is obtainable for the ratio of the amplitude of a particle and the oscillation of a medium:

$$\mu = \frac{V_0}{U_0} = \frac{1}{\sqrt{1 + \omega^2 \tau^2}} = \frac{1}{\sqrt{1 + (2\pi\tau/t_p)^2}} \quad (20.18)$$

and instead of (20.11) the following is the expression for phase displacements:

$$\operatorname{tg}(\varphi - \theta) = \omega \tau - 2\pi\tau/t_p. \quad (20.19)$$

On figure 20 the curves 1 illustrate this dependence (20.18) i.e., the dotted-line curve and the (20.10) solid-line curve; the latter pertains to $\gamma = 1$ in the air under usual conditions. The difference between both curves is so small, that in practice one can certainly use the simplified equation (20.18).

An important equation results from (20.14) and (20.18):

$$v_{R_0}^2 = U_0^2 - v_0^2. \quad (20.20)$$

In this manner also the type of aerosol particle oscillations, actuated by sonic waves, is determined by the magnitude of the ratio τ/t_p . In the presence of very small values $\tau/t_p \rightarrow 0$, $\mu \rightarrow 1$, a particle oscillates with the same amplitude and in the same phase, as the medium, i.e., it moves as a whole with the latter. In the presence of very large values τ/t_p , $\mu \rightarrow 0$ a particle remains practically immobile¹. The transition from a full stimulation to immobility of particles takes place approximately in the intervals of values τ/t_p 0.02 - 20. The type of oscillations of particles under the influence of sonic waves manifests, as we shall see below, a decisive influence upon all processes of interactions of aerosols with sonic waves.

The above-quoted equations are inapplicable to very large particles at high sonic frequencies due to a greater Re value, nevertheless in such a case, as we pointed out, particles remain practically immobile.

During experimental testing of the theory of aerosol particle oscillations in a sonic field, the main difficulty presented was the exact measurement of the medium's oscillation amplitude at a place where a particle is detected. We succeeded in overcoming the difficulty by applying V. ZERNOV'S (132) method and creating a uniformly oscillating mass of air. At a shank of a tuning fork a closed cylindrical vessel is fastened, which is provided with little windows for illumination and observation; the size of the vessel must be considerably smaller than the length of waves produced by the tuning fork. In this case the air inside the vessel fluctuates with the vessel as a whole; thus the amplitude of oscillations of the vessel itself and that of particles suspended inside the latter can be conveniently measured. The measurements of WAGENSCHNEIN (133) with spores of lycopodium ($r = 16\mu$, $t_p = 0.012$ sec.) carried out according to this method, afforded a satisfactory

1. These conclusions are also confirmed by ultramicroscopic photographs of large and small particles found in an ultrasonic field (131).

conformity with the theory. Yet the exactness of these tests is rather limited and, furthermore, the spores of lycopodium are not very suitable for such measurements because they have rather marked ribs on their surfaces.

The following method of determination of particles' sizes in aerosols (134) is based upon a relationship of the type of particle oscillations to the ratio of τ/t_p . At first, the amplitude of the particles' oscillations is determined photographically at $t_p \gg \tau$, equal to the amplitude of medium's oscillations and subsequently, at t_p comparable with τ ; hence, according to equation (20.18), we find τ , and then r .

As the experiment indicates - in the presence of particles of larger sizes, and also at higher frequencies and amplitudes of sonic waves, i. e., at higher Re numbers - the particles or aggregates of a flat shape orientate themselves perpendicularly to the direction of oscillations (135) in accordance with the explanation submitted in § 11.

An important conclusion pertinent to the mechanics of aerosols follows as explained in § 17, 19 and 20: during non-uniform movements of particles, in the region of applicability of STOKES' formula, one may regard - without any substantial error - the resistance as being non-inertial, i. e., assuming it equals $6\pi\eta r V_R$; where V_R is the momentary value of the particles velocity in relation to the medium. This circumstance, of course, facilitates immensely a theoretical research in particles movement.

§ 21. Sonic Pressure Upon Aerosol Particles

The influence of sonic waves upon suspended particles is not confined to the forces previously discussed, which are variable in their directions and are linked with the viscosity of the medium. A particle is also actuated by a constant (in its direction) hydrodynamic "sonic pressure", which is not dependent upon viscosity, but upon density of the medium. If a particle radius is smaller in comparison with the length of a sonic wave λ , then - in the event of moving waves - an immovable spherical particle is actuated by the force expressed below (KING/136/):

$$F_M = 2.4\pi U_0^2 \gamma_g r^6 \left(\frac{2\pi}{\lambda}\right)^4, \quad (21.1)$$

which is directed toward the expansion of the waves. Of considerably greater magnitude is the sonic pressure in standing waves and specifically:

$$F_M = \frac{5}{3\lambda} \pi^2 \gamma_g r^3 U_0^2 \sin(4\pi x/\lambda), \quad (21.2)$$

where x is the distance of a particle from the nearest wave node. The quoted force leads to the next antinode. At $x = (1/8)\lambda$, $(3/8)\lambda$, $(5/8)\lambda$, and $(7/8)\lambda$, i. e., halfway between the antinodes and the nodes, the force assumes its maximal value. In antinodes and in nodes $F_M = 0$, with which, if we consider the former, a particle is in a stable equilibrium and, considering the latter, in an unstable equilibrium. KING'S formula was confirmed in tests involving little cork balls ($r = 1$ mm), which were suspended on threads in standing waves of a frequency 400 - 2,800 hertz (137). Notwithstanding the above, WESTERVELT (138) pointed out, that the effects of viscous losses of energy in a gas stratum bordering near the surface of the particles were not taken into consideration and, likewise (emanating from OSEEN'S theory) the asymmetry of the field of flow at both sides of particles. As the first effect yields a force proportional to the first degree of particles radius, the second one yields a force proportional to the square of the radius and subsequently these forces can exceed by entire order the force computed by KING. A comparative magnitude of the indicated forces increases with a decrease of particle size; probably, as a result of this, they were not mentioned in the reported tests. Therefore it is highly desirable to conduct measurements of sonic wave pressure upon small particles.

A sonic pressure may surpass the gravity force in sufficiently intensive ultrasonic waves; it may also put particles in equilibrium in a vertical tube, where standing waves were developed.

Apparently the sonic pressure is the main cause of the formation of KUNDT'S "powder patterns" from dust intermittently precipitated in horizontal tubes, where standing waves were developed. These precipitations appear like narrow combs positioned perpendicularly to the tube axis at a short distance from each other. The combs, that assume their maximal size close to antinodes, disappear close to nodes. The mechanism of their formation probably follows this course. Standing sonic waves in tubes are accompanied by a gas circulation; the latter is developed as a result of a gas-induced friction against the walls of the tube. The circulation resembles the one shown on figure 21 (139). Dust becomes turbulent due to gaseous flow combined with the circulatory movement and then it acquires - due to influence of sonic pressure - a component velocity directed toward the antinodes. Following this, the dust drops out of the circulatory flow and precipitates on walls of the tube at the antinode level.

The development of not one, but of several combs within a half-wave amplitude is explained by the presence of overtones inside the tube, i. e., by the waves with a frequency equal to a whole multiple of the basic frequency. As the equation (21.2) indicates, the sonic pressure increases rapidly with the increase of particle sizes. Consequently it is necessary that dust particles become turbulent in order to form powder patterns. This phenomenon is particularly well feasible with coarse, yet light dusts, e. g., with cork dust.

It is presumed in equations (21.1) and (21.2) that particles in a sonic field remain immobile. Otherwise one would have to consider U_0 as the amplitude of relative oscillations of the particles and a medium. In proportion to the increase in the particles entrainment by the oscillating medium, the sonic pressure declines accordingly and in the presence of a total entrainment it becomes equal to zero.

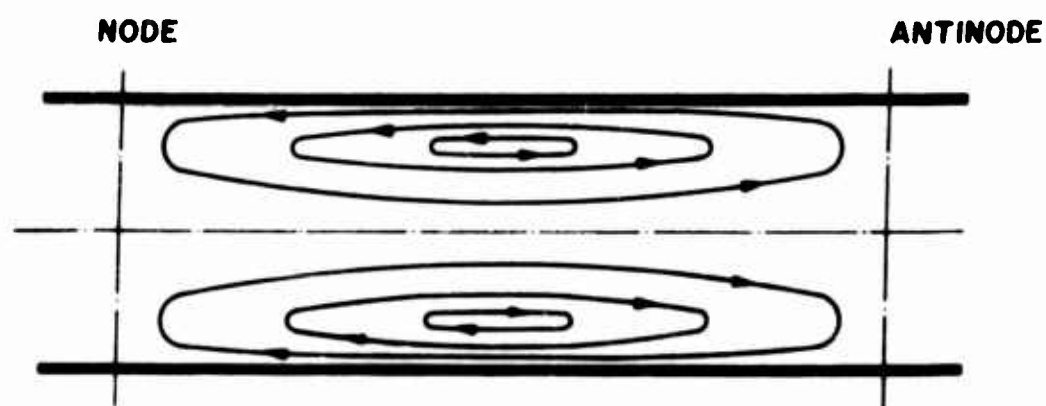


FIG. 21 CIRCULATION OF AIR IN A SONIC FIELD

The sonic pressure is apparently of greater importance in conjunction with coagulations of aerosols by ultrasonic waves (see § 53).

§ 22. Dispersion and Absorption of Sonic Waves by Aerosols

Sonic or electromagnetic waves passing through aerosols are accompanied by phenomena, such as: reflection, dispersion, absorption, diffraction, etc. In case of sonic waves these phenomena manifest themselves comparatively to a minor extent and we shall confine ourselves to a very brief presentation of the problem.

The theory of the dispersion of waves becomes notably simple, when particles are present in their path and if the immobile particles are of a spherical shape and small, as compared with a length wave λ . We shall designate by U_0 the range of oscillation velocity and by ω the angular frequency of the system of horizontal sonic waves, which react upon a spherical particle. The energy flow carried by the waves in 1 sec. per cm^2 of a wave's front is equal to:

$$I = \frac{U_0^2 \gamma c_s}{2}, \quad (22.1)$$

where c_s is the sonic velocity. The energy carried per second by waves being dispersed by particles is, according to the theory (140), equal to:

$$\Omega = \frac{7\pi\gamma_g U_o^2 \omega^4 r^6}{18c_s^3} \quad (22.2)$$

Hence, when sonic waves penetrate a stratum of aerosols of the dx thickness and the aerosol contains n quantity of similar particles per cm^3 , the relation of energy of dispersible and incident waves is equal to:

$$a_d dx = \frac{7\pi\omega^4 r^6 n}{9c_s^4} dx = \frac{7\pi(2\pi)^4 r^6 n}{9\lambda^4} dx. \quad (22.3)$$

Hence, the energy of the waves which passed through a stratum of an aerosol of x thickness is equal to:

$$I = I_0 e^{-a_d x}, \quad (22.4)$$

where I_0 is the initial energy of the waves and

$$a_d = \frac{7\pi(2\pi)^4 r^6 n}{9\lambda^4} \quad (22.5)$$

is the coefficient of dispersion of sonic waves by aerosols. If particles in a sonic field do not remain immobile and become to a greater or a smaller extent entrained by the medium's oscillations, the coefficient of dispersion becomes reduced accordingly.

With the usual sonic waves ($\lambda \approx 1$ m) passing through natural clouds or fogs ($r \approx 10^{-3}$ cm, $n \approx 10^3$) a_d there is an insignificantly small value of the order 10^{-20} . The a_d still remains very small even in ultrasonic waves and in the most dense aerosols encountered in the nature or in industry, therefore one can practically always disregard the dispersion of sound by aerosols.

As we proceed to the absorption of sound by aerosols, induced by viscosity of gas, we quote the elementary conclusion of the basic equation

assuming, that the resistance is expressed according to STOKES' law. With a particle movement in a viscous medium the entire operation of the resistance forces

$$\Omega = \int_0^x F_M dx = \int_0^x \frac{V}{B} dx \quad (22.6)$$

is in the presence of small Re converted into heat. If the medium moves also with velocity U, then V in the equation (22.6) must be substituted by a relative velocity $V_R = V - U$ and the appropriate differential dx for the path must be substituted by $V_R dt$. The result is:

$$\Omega = \frac{1}{B} \int_0^t V_R^2 dt. \quad (22.7)$$

In the case being discussed a particle's movement in an oscillating medium is expressed by the equation (20.15). Thus

$$\Omega = \frac{V_{R_0}^2}{B} \int_0^t \sin^2\left(\omega t + \frac{\pi}{2} - \varphi\right) dt. \quad (22.8)$$

In the presence of a sufficiently longer $t \rightarrow V_{R_0}^2 t / 2B$, i.e., a particle absorbs on the average per time unit the amount of energy, which is equal to $V_{R_0}^2 / 2B$. Hence, as previously, it follows that, with a sonic wave passing through a stratum of an aerosol of dx thickness, the ratio of the absorbed energy to the supplied energy is equal to:

$$\alpha_a dx = \frac{V_{R_0}^2 ndx}{U_0^2 B \gamma_g c_s} = \frac{V_{R_0}^2 6\pi\eta r ndx}{U_0^2 \gamma_g c_s}, \quad (22.9)$$

and we arrive at the equation

$$I = I_0 e^{-\alpha_a x}, \quad (22.10)$$

in which the coefficient of the absorption of sonic waves by aerosol is equal (see formula /20.14/) to:

$$\alpha_a = \frac{\omega^2 \tau^2}{1 + \omega^2 \tau^2} \frac{6\pi\eta rn}{\gamma_g c_s} \quad (22.11)$$

A more exact conclusion is brought forward by SEWELL (141) in the expression:

$$\alpha_a = \frac{\omega^2 \tau^2}{1 + \omega^2 \tau^2} \frac{6\pi\eta rn}{\gamma_g c_s} \left(1 + \sqrt{\frac{r^2 \omega \gamma_g}{2\eta}} \right) \quad (22.12)$$

The expression obtained by RYTOV, VLADIMIRSKIY and GALANIN (142) is somewhat more complicated. If we introduce in (22.12) the values η , γ_g and c_s for air at the usual pressure and temperature, we obtain

$$\alpha_a \approx 8.3 \cdot 10^{-5} \cdot rn \left(1 + r \sqrt{\frac{\omega}{0.3}} \right) \frac{\omega^2 \tau^2}{1 + \omega^2 \tau^2} \quad (22.13)$$

As is obvious from this, the absorption of sound by aerosols depends in a large measure upon a degree of the particles entrainment by sonic waves.

In the afore-mentioned discussions particles are regarded as absolutely solid small spheres. The work of EPSTEIN and CARHART (143) includes the effect of particles deformation and particularly that of liquid droplets, although the effect is insignificant. The second and a more important factor included in this work is dispersion of energy due to heat conductivity, which increases the coefficient of absorption for aqueous fogs by approximately 40% (see table 10).

First measurements of the absorption in ultrasound waves by aerosols (tobacco smoke) were conducted by V. ALTBURG and M. HOLTZMAN (144). It is regrettable that the particles' sizes were not determined in these tests and, furthermore, that tobacco smoke contains large amounts of carbonic acid, which intensely absorbs sonic waves with which the measurements were conducted. Therefore it is difficult to compare the results obtained with the theory.

In tests conducted by LAIDLER and RICHARDSON (145) an aerosol of *Lycopodium* spores ($r = 2.5\mu$) was used, which contained $1.5 \cdot 10^6$ particles per cm^3 . With the high sonic frequencies employed, the $\omega\tau$ reached an order of magnitude of several decades, whereby the particles remained practically motionless. The following values of the coefficient of absorption were obtained: at a frequency of 42,000 hertz $\alpha_a = 0.029$ and at 98,000 hertz $\alpha_a = 0.031$. The theoretical values of α_a are accordingly equal to 0.038 and 0.042¹.

The rapidity of the damping of sonic vibrations in a resonant chamber filled with an aerosol was measured in the work of KNUDSEN, WILSON and ANDERSON (146). It specified the presence of aerosol particles and it expressed in $\text{decibel} \cdot \text{sec}^{-1}$ a composite coefficient of sound damping β combined with α_a in the equation:

$$\beta = 10 \lg e \cdot \alpha_a c_s. \quad (22.14)$$

If we convert equation (22.13), we can obtain the following expression for β :

$$\beta = \frac{2.94\phi}{r^2} \left(1 + r \sqrt{\frac{\omega}{0.3}} \right) \frac{\omega^2 \tau^2}{1 + \omega^2 \tau^2}, \quad (22.15)$$

where ϕ is the volume of a dispersed phase contained in 1 cm^3 of aerosol.

It is regrettable that the work of the authors was conducted with highly polydispersed aqueous and oil fogs, obtained by mechanical atomization. The following results (table 10) were obtained with the aqueous fog with $\phi = 2 \cdot 10^{-6}$ and $\tau = 6.25\mu$:

1. Theoretical values of α_a computed by authors of this work are incorrect.

Table 10

Absorption of Sonic Vibrations in Aqueous Fog

Frequency of vibrations, hertz	Coefficient of damping β , decibel \cdot sec ⁻¹		
	Experimental	Theoretical	
		According to KNUDSEN	According to EPSTEIN
500	5	10.1	5.0
1000	7	13.8	5.7
2000	9.4	16.0	6.3
4000	10.1	17.1	6.9
6000	12.0	18.2	7.5
8000	13.2	18.8	7.7

While comparing empirical and theoretical values β one should, above all, consider the influence of the polydispersion of an aerosol upon results of theoretical calculations. To simplify the matter, if we actually consider only the main multiplier $6\pi\eta rn/\gamma_g c_s$ in the equation (22.12), thus the coefficient of absorption must be proportional to $\sum n_i r_i = \bar{n} \bar{r}$. Furthermore, $\phi = \frac{4}{3}\pi \sum n_i r_i^3 = \frac{4}{3}\pi n \bar{r}_3^3$; where $\bar{r}_3 = \sqrt[3]{\frac{\sum r_i^3}{n}}$... see page 28.

Since n is proportional to ϕ/\bar{r}_3^3 , therefore $1/\bar{r}^2$ in equation (22.15) should also be substituted by \bar{r}/\bar{r}_3^3 .

Inasmuch as in polydispersed aerosols $\bar{r}_3 > \bar{r}$, then calculating according to equation (22.15) one obtains the value of β which increases as the degree of polydispersion increases. KNUDSEN and others did not consider this circumstance and relying in equation (22.15) on $r = \bar{r}$, they obtained considerably larger values of β as submitted in table 10. EPSTEIN and CARHART (143), taking advantage of the fact that the fractional composition of the fog - to which the data in table 10 refer - was known, calculated β according to each fraction. Although they did consider the effect of heat conductivity in their calculations,

yet all their computed values of β - except at the frequency of 500 hertz - are considerably lower than the experimental ones. Evidently, during the sound absorption the effect of evaporation and condensation of steam on droplets assumed a prominent role (see blow). Otherwise, the exact proof of the theory of sound absorption by aerosols is apparently possible only by the use of isodispersed aerosols.

As we proceed to the absorption of sound by atmospheric fogs, one can assume that $r = 5\mu$ and $n = 2000$ are as typical mean value, consequently

$$\alpha_a \approx 8 \cdot 10^{-5} \frac{10^{-7} \omega^2}{1 + 10^{-7} \omega^2} \approx \frac{0.34}{\lambda^2 + 4200} \quad (22.16)$$

where λ is the sonic wave length. Thus, in this case, the coefficient of sound absorption depends comparatively little upon a wave length and in regard to metric waves, it is only three times smaller than with regard to centimetric waves. At the same time the coefficient of sound absorption in gases is in the first approximation proportional to $1/\lambda^2$. With $\lambda = 5$ cm, the coefficient of sound absorption in the air is equal to $0.8 - 1.6 \cdot 10^{-4}$, i. e., in this case the gaseous medium and the dispersible phase weaken the sound to an equal degree. For longer waves, the sound absorption effected by water droplets exceeds the one effected by a medium. Thus, according to theoretical calculations, dense atmospheric fogs /contrary to the belief (148) established at the time of TYNDAL'S (147) tests/ should considerably weaken the sound: the energy of sonic waves, with a frequency of 500 hertz, in the fog examined by us, should, according to equation (22.16), be weakened at a distance of 100 m by approximately 1.5 times. According to observations of SIEG (149, 150), a sound of such a frequency is weakened in a fog at the indicated distance by 1.3 times. It is regrettable that the concentration and the size of droplets were not measured.

In addition to the above discussed hydrodynamic absorption of sound by aerosols, a sound absorption also takes place in fogs composed of volatile substances, due to periodically occurring processes of evaporation and condensation of steam on droplets, resulting from temperature variations in a sonic field (151). The evaporation and condensation, lagging according to the phase of temperature variations, represent as such thermodynamic, irreversible processes, which cause the transition of the mechanical energy of sonic waves into heat energy. The sound absorption is insignificant at very low frequencies, because in the case in point an equilibrium between droplets and steam has a chance to establish itself; this is also the case at very high

frequencies, when very small amounts of liquid evaporate. The theory of the phenomenon indicates, that one should expect the highest absorption of sound in aqueous fogs at frequencies closer to the lower boundaries of sonic audibility (~ 16 hertz) and this conclusion (146) was obviously verified by observations.

The experimental research in sound absorption by natural fogs encounters greater difficulties, therefore all experiences in this direction were, up to now, of barely qualitative nature. The difficulties are created due to weakening of sound, following the extension of the distance from the point of the sound origin, because of the expansion of the waves' front and then also due to heterogeneities in the atmosphere. The first factor becomes eliminated, when a source of sound and a receiver (or an observer) are positioned at permanent points and the measurements are conducted in the presence as well as in the absence of fog between these two points. Naturally, it is impossible to eliminate atmospheric heterogeneities of density and humidity, which cause reflection, refraction, and dispersion of sonic waves. Meanwhile, the phenomena in question weaken the force of sound far more than the absorption of sound by air and by fog (152) discussed by us. From this point of view may be explained the numerous and frequently contradictory observations referred to here. Although the gaseous medium of the clouds of fog usually have a somewhat different temperature and humidity than the air surrounding it, they, at the same time, are also "acoustic" clouds and if several such clouds are between a point of sound origin and an observer, a complete damping of sound frequently takes place. On the other hand, continuous and heavy masses of fog frequently possess a homogeneity; in such a case, if the entire area between the point of sound origin and the observer is filled with fog, the weakening of sound may even be smaller than in the absence of fog, notwithstanding the presence of heterogeneities. Hence, an opinion was formed, that atmospheric fogs do not absorb sounds. This problem requires a further and more exact study.

§ 23. Hydrodynamic Interaction Between Aerosol Particles

A particle in movement in relation to a medium develops in the latter a current, which in its course actuates other particles. Thus, the forces of a hydrodynamic interaction between particles in motion are developed. These forces within aerosols may appear mainly at the time of a parallel and identically directed motion of the particles. We shall confine ourselves to discuss such cases.

The magnitude and the direction of forces of a hydrodynamic interaction depend in a greater measure upon the type of current developed by the

motion of particles. In a current within a viscous region, i. e., at small Re numbers, the interaction between two identical particles, moving with a constant velocity toward the same direction, contributes to a diminution of the medium's resistance, according to equation (13.1), as we explained in § 13. When a larger number of particles is present, the forces of interaction integrate and consequently an aerosolic cloud is capable of moving considerably faster than isolated particles.

In considering a component of the hydrodynamic interaction attempting to change a distance between particles, the resultant equals zero in a purely viscous region of motion, i. e., at very small Re numbers. Neither attraction nor repulsion takes place between particles. OSEEN'S theory including a partial calculation of inertial forces indicates (153) that, along the line of particles centers, the first particle is actuated by the force

$$F_{M1} = - \frac{9\pi\eta^2 r^2}{\gamma_g \rho^2} \left\{ 1 - \left(1 + \frac{\gamma_g V \rho}{2\eta} \right) \exp \left[- \frac{\gamma_g V}{2\eta} \left(\rho + x_1 - x_2 \right) \right] \right\}, \quad (23.1)$$

and the second particle by the force

$$F_{M2} = \frac{9\pi\eta^2 r^2}{\gamma_g \rho^2} \left\{ 1 - \left(1 + \frac{\gamma_g V \rho}{2\eta} \right) \exp \left[- \frac{\gamma_g V}{2\eta} \left(\rho + x_2 - x_1 \right) \right] \right\}, \quad (23.2)$$

where x_1 and x_2 are the coordinates of the first and the second particle axes, respectively, directed toward the motion of the particles. Moreover, the direction of the force from the first to the second particle is considered to be positive. Analysis of the equations (23.1) and (23.2) indicates, that when particles move in a single front ($x_1 = x_2$), they repel one another and in a movement of particles one behind the other, the particle in the front is repulsed and the one in the back is attracted. The problem of a hydrodynamic interaction at small Re numbers was not examined. Let us assume that a particle in a movement parallel to a wall and at a small Re number is repulsed via the wall with a force (154)

$$F_M = \frac{9}{16} \pi \gamma_g r^2 V^2, \quad (23.3)$$

not dependent upon distance x of the particle center from the wall. Such an equation is true only in so far as a small magnitude of the proportion x/r is involved.

A quite different picture is observed at larger Re numbers. The theory of a hydrodynamic interaction at larger Re was prepared by KIRCHHOFF on behalf of an ideal liquid, i. e., not accounting for eddies (155) developed during motion. According to the theory, a spherical particle with a radius r_1 actuates another particle with a radius r_2 (figure 22) by a force which is not dependent upon the movement of the second particle. If the distance between particles' centers ρ considerably exceeds their radii, the component of the force which is lengthwise to the lines of centers is equal to:

$$F_{\rho} = \frac{3\pi\gamma g r_1^3 r_2^3 v^2}{\rho^4} \left(\frac{3}{2} \cos 2\theta + \frac{1}{2} \right), \quad (23.4)$$

and that which is perpendicular to the lines of centers equals

$$F_{\tau} = \frac{3\pi\gamma g r_1^3 r_2^3 v^2}{\rho^4} \sin 2\theta, \quad (23.5)$$

where θ is the angle between the line of centers and the direction of the motion. Figure 23 shows (created by a moving particle) a field of force of a hydrodynamic interaction. The field coincides with that developed by the forces of interaction between two identically directed electric dipoles (see § 52), but the direction of forces is reversed.

The equation (23.4) implies that with $\cos 2\theta < -1/3$ $F_{\rho} < 0$, attraction occurs, while with $\cos 2\theta > -1/3$, repulsion occurs. Maximal attraction values are reached at $\theta = \frac{\pi}{2}$, namely:

$$F_{\rho} = - \frac{3\pi\gamma g r_1^3 r_2^3 v^2}{\rho^4}. \quad (23.6)$$

A maximal repulsion value (at θ equal 0, or π) is twice as large

Only in the two instances is $F_{\tau} = 0$, i. e., when the force of interaction is directed lengthwise to the line of particle centers. As we already pointed out, the force with which the first particle actuates the second one depends only upon the movement of the first particle in relation to the medium and it does not depend upon the movement of the second particle. Therefore, generally speaking, the action and the counteraction here are not equal to each other, except when the velocities of both particles are equal according to

their rate and when they are identically directed. Such forces also actuate immobile small spheres, occurring in a uniformly flowing medium with a velocity V .

A particle moving parallel to a wall attracts the latter at larger Re numbers with a force

$$F = - \frac{3\pi\gamma_g r^6 V^2}{16x^4}, \quad (23.7)$$

where x is the distance from the particle center to the wall (156).

How the above-quoted equations should be changed, when eddies forming in a tangible medium are to be computed, was not examined. Since eddies form only behind small spheres in motion and since the flow in its remaining volume differs little from a potential flow of an ideal

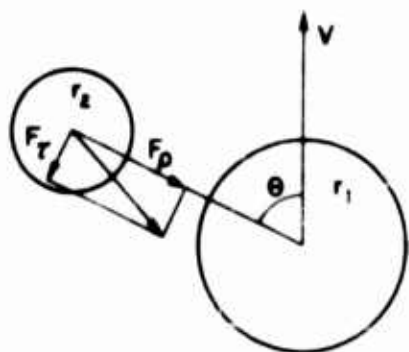


FIG. 22 HYDRODYNAMIC FORCES BETWEEN PARTICLES

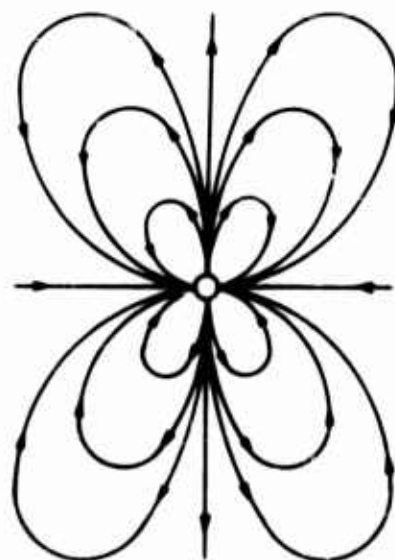


FIG. 23 HYDRODYNAMIC FIELD DEVELOPED BY A MOVING PARTICLE

liquid, thus in the most important case of aerosol physics (such as the attraction between particles is presumed to be) the specific equations are probably correct even with regard to a tangible medium.

Another important problem also remains unexplained: at which Re values does the attraction or repulsion between particles appear according to the equations (23.4) and (23.1).¹ In experimental tests of the

1. We wish to remind, that attractions between particles occur at $\theta = \pi/2$ and with larger Re numbers, while repulsions occur with small Re numbers.

theory of hydrodynamic interaction between substances moving forward we usually confined ourselves to the establishment of the very fact of attraction or repulsion, but the measurements of the magnitude of the forces interaction were not carried out. Tests were performed in liquids with fairly large drops, i.e., at larger Re numbers. C. GORBACHEV and A. SEVERNYI (157) discovered a hydrodynamic attraction (at $\theta = \pi/2$) and repulsion (at $\theta = 0$) between drops of liquid with a 25μ radius suspended on thin threads in a gaseous current moving with a velocity of $15 \text{ cm} \cdot \text{sec}^{-1}$, i.e., at $\text{Re} = 0.5$. The discussed problem requires additional experimental research.

Some authors attached a greater importance to the hydrodynamic interaction between particle settlings under the influence of the force of gravity, as being the main cause of coagulation in precipitations of aerosols and specifically of coagulation of atmospheric clouds and their precipitations. Yet this opinion is undoubtedly erroneous (see § 54). A hydrodynamic interaction is of greatest importance during oscillations of aerosol particles and particularly so in a sonic field. The forces which are effective between two particles oscillating with identical amplitude and in the same phase are expressed according to BJERKNES (158) by the same equations (23.4) and (23.5), but V^2 in this case is equal to mean quadratic velocity of particles $\overline{V_R^2}$ in relation to the medium. Thus

$$F_{\rho} = \frac{3\pi\gamma_g r_1^3 r_2^3 V_{Ro}^2}{2\rho^4} \left(\frac{3}{2} \cos 2\theta + \frac{1}{2} \right), \quad (23.8)$$

$$F_{\tau} = \frac{3\pi\gamma_g r_1^3 r_2^3 V_{Ro}^2}{2\rho^4} \sin 2\theta, \quad (23.9)$$

where V_{Ro} is the amplitude of the relative oscillation of a particle and a medium, equal to $\sqrt{2\overline{V_R^2}}$.

If particles oscillate in an opposite phase (e.g., particles with a positive and a negative charge in an alternating electrical field), then the minus sign should be entered in equations (23.8) and (23.9) in their right hand side. During interactions between an oscillating and an immobile particle, the first one attracts the second one from any position, yet the force in this case is considerably less effective than that when both particles oscillate. Thus, if oscillations proceed lengthwise to center lines, the force of attraction is equal to

$$F_{\rho} = - \frac{3\pi\gamma_g r_1^6 r_2^3 V_{Ro}^2}{\rho^7}. \quad (23.10)$$

The problem of how the viscosity of a medium influences a hydrodynamic interaction has not been explained also with regard to oscillations of particles. As the theory of oscillations in a viscous liquid (159) indicates, the influence of viscosity upon a wave developing during oscillation of spherical substance becomes insignificant at such a distance from the center of a liquid

drop ρ , at which $\rho \sqrt{\frac{\omega \gamma g}{2\eta}} \gg 1$, i. e., in the air at $\rho \gg \sqrt{\frac{0.3}{\omega}}$. Hence it affects the ($r \leq 10^{-4}$ cm) size of particles, to which a hydrodynamic attraction in a sonic field has a specific relation in connection with the appearance of ultrasonic coagulation (see § 51) and in regard to the frequency of 10 hertz, the ρ/r should be $\gg 22$. Yet, according to equation (23.8), the force of interaction at such a distance is immeasurably small. Therefore, the theory exposed above, apparently lacks essential corrections in the matter of influence of viscosity

The experimental research of a hydrodynamic interaction between particles suspended in a sonic field is usually conducted with solid or liquid small spheres, suspended on thin threads in a tube in which standing sonic waves were produced (160, 161, 162). The magnitude of the attraction or repulsion is measured according to deviations of threads from their vertical positions. A qualitative conformity with the theory was obtained, i. e., small spheres positioned lengthwise in the tube repulsed one another and those positioned across the tube, attracted one another.¹ Air circulation in the tube should have strongly influenced the results of the measurements (see page 115).

For this reason such tests are of little use in relation to a qualitative verification of theory. Measurements conducted by THOMAS (163), according to the method of ZERNOV (see page 113) were more exact; they produced a full conformity with the theory tested by way of small spheres (radius 3–7 mm) oscillating at a frequency of 60 hertz lengthwise to the axis in a closed cylindrical vessel. The force of interaction proved to be exactly proportional to the square of the amplitude of the oscillations at any distances between centers of the small balls. The relation of the force with distance proved to be in a full conformity with the theory, i. e., in case of attraction even at small distances and also in case of repulsion (that is with small spheres positioned lengthwise in the cylinder) - at a distance over 4 r . At a closer distance the force of repulsion was smaller than that indicated in the theory,

-
1. It should be noted that in tests with small spheres positioned across the tube, whenever they approached to a sufficiently close distance (of the order 1/10 diameter), their attraction under certain conditions was converted into repulsion, which increased with a further approach (564) of the small spheres.

probably due to development of eddies. Also the derived relation of the force to the frequency of oscillations was correct. As to small spheres with a radius of 3-4 mm, the absolute magnitude of the force coincided with the theoretical value. The afore-mentioned condition, as concerns the influence of viscosity, leads in the given case to an inequality of $\rho/r \gg 0.07$, but it still may be regarded as practicable. Inasmuch as the amplitude of oscillations in these tests was of the order 0.1 cm, i. e., $Re = 70-150$, the problem related to the magnitude of hydrodynamic forces between oscillating particles of aerosols at small Re numbers is still considered open.

§ 24. Electrostatic Dispersion of Aerosols

In conclusion we shall review the phenomenon of electrostatic dispersions of aerosols (164, 165), which occur when an algebraic sum of charges of aerosol particles is other than zero. We shall analyze at first the most simple case of isodispersed aerosols, all whose particles have a positive charge q identical in magnitude. Thus, the density of electricity σ in aerosol equals to nq . According to the basic equation of electrostatics

$$\text{Div } E = 4\pi\sigma = 4\pi nq, \quad (24.1)$$

where E is the vector of the field intensity. Since it is linked with a vector of the velocity of positive particles by way of the equation

$$V = BEq, \quad (24.2)$$

thus

$$\text{Div } V = 4\pi nq^2 B. \quad (24.3)$$

According to properties of velocity divergence we have

$$\text{Div } V = - \frac{1}{n} \frac{dn}{dt}, \quad (24.4)$$

consequently

$$- \frac{1}{n} \frac{dn}{dt} = 4\pi nq^2 B, \quad (24.5)$$

from which

$$\frac{1}{n} - \frac{1}{n_0} = 4\pi q^2 Bt, \quad (24.6)$$

where n_0 is the initial concentration of particles.

The same equations are obtained also when particles are negatively charged.

It follows from these equations, that unipolarly charged aerosols disperse uniformly under the influence of their space charge.¹ The velocity of dispersion, i.e., the decrease in concentration of aerosol is the same in all its parts and it depends neither upon a size, nor upon a shape of the occupied by aerosol space, thus it is an "inner" property of aerosol. If we deal with a cloud, it increases uniformly in volume retaining its shape and at the same time the rapidity of relative increase of volume is evidently equal to the rapidity of relative decrease of concentration $-\frac{1}{n} \frac{dn}{dt}$, which is expressed in the right part of the equation (24.5). If an aerosol is restricted by walls, particles settle upon them, wherein the same magnitude $-\frac{1}{n} \frac{dn}{dt}$ indicates what share of the particles available at a given time does precipitate per time unit. The above-quoted equations may be regarded as correct even with regard to the current aerosol, if we assume that the constancy of concentration in the entire space of aerosol is maintained during its electrostatic dispersion in the medium's movement and then if we disregard the inertia effect, which has no influence whatsoever upon dispersion.

Let us suppose now, that 1 cm^3 of aerosol contains n_+ of positive and n_- of negative particles, which have the same absolute magnitude of the charge q , with which $n_+ > n_-$, as long as the density of electricity is equal to $(n_+ - n_-)q$. If we repeat the afore-cited reasoning, we find that dispersion of positive particles is expressed by the following equation equivalent to (24.5):

$$-\frac{1}{n_+} \frac{dn_+}{dt} = 4\pi q^2 B(n_+ - n_-). \quad (24.7)$$

We obtain for negative particles

$$\frac{1}{n_-} \frac{dn_-}{dt} = 4\pi q^2 B(n_+ - n_-). \quad (24.8)$$

1. The phenomenon discussed here is known in foreign literature by the name of "electric diffusion" (165), but since we deal here with a well regulated movement of particles, such designation can hardly be acknowledged as being correct.

This indicates that negative particles (i.e., particles which have such a sign of charge and their concentration is smaller) are drawn together in the center of aerosol and their concentration increases there. The density of electricity $(n_+ - n_-)q$ in the "central core" of aerosol asymptotically declines, until the core, practically speaking, becomes neutral and, consequently, stable. At the same time, a dispersion of the outer, purely unipolar part of aerosol continues outside the core.

The quoted equations may be readily applied to polydispersed aerosols and to particles of diverse magnitude of charges.

Experimental tests on the electrostatic dispersion phenomenon were conducted by WOLDDKIEWITCH (165), also by N. FUKS and I. PETRYANOV (166). The former worked with highly dispersed amicronic aerosols ($r \approx 10^{-6}$ cm), obtained by heating magnesium oxide to 1000-1200°. A well ascertained fraction of the particles which were formed at the same time were charged and a greater number of charged particles probably had one elemental charge each (see page 140). The mobility of α particles was determined by passing the aerosol through a condenser connected with an electrometer (see § 27). While passing the aerosol through a charged sieve, which intercepted particles with an opposite sign, it was possible to obtain strictly unipolar aerosols by using sieves of a sufficiently high power. The rapidity of dispersion of aerosols was determined according to a decrease in their space charge and it could also be measured by the condenser. Thus a satisfactory conformity was obtained of the test data with the theory.

N. FUKS and I. PETRYANOV examined dispersion of an oil fog ($\bar{r} = 0.55\mu$), which was charged by a corona discharge. In this, from 70 to 100% of particles were charged negatively and the rest were without a charge, yet the charges of particles differed rather widely as to absolute magnitude and likewise the degree of polydispersion of the fog increased considerably during charging. Measurements of the rapidity of dispersion were conducted by the method of computing particles. In accordance with the equation (24.6) it was found that, as the relation of the reciprocal of the magnitude of particles concentration to time was expressed by straight lines, the slope of lines increased among particles with average charges (containing from 0 to 48 elemental charges); yet, according to absolute magnitude, the rapidity of dispersion was several times smaller than the theory indicated. The reason for the discrepancy could not be explained.

Likewise, it was possible to reproduce in a test (167) a formation of a "central core" in aerosols having a partial unipolarity in their charges.

In an electrostatic dispersion the characteristic feature is this, that unlike the usual settling actuated by gravity, particles precipitate with a rapidity almost uniform, not only at the bottom of a chamber occupied by aerosols, but also at its upper and side walls. This circumstance could be utilized in disinfection and disinfestation of rooms by aerosols, if sufficiently simple, portable equipment for a unipolar charging were developed. Since usual insecticide aerosols obtained by smoke pots, cartridges, and special generators¹ settle for the most part on the ground, they are, therefore, very little effective; also the unipolar charged aerosols would make it possible to reach the ceiling and staircase, including their cracks. Similar considerations pertain to inhalation of medicinal aerosols: by a unipolar charge their settling in respiratory tracts would be more extensive (see page 263). Nevertheless, the opinion disseminated by DESSAYER (168) and A. CHIZHEVSKII (169) about curative properties of aerosols unipolarly charged did not establish itself in the science of medicine.

-
1. Naturally, we don't imply here any mechanical sprayers, Freon bombs nor other devices of such kind, which produce a jet-flow of a heavy fog or dust that settle on walls due to inertia forces.

Chapter IV

Curvilinear Motion of Aerosol Particles

§ 25. General Theory of a Curvilinear Motion of Particles. Precipitation of Aerosols in an Alternating Horizontal Electrical Field

The theory of a curvilinear motion of aerosol particles is comparatively simple within the region of the proportionality of the medium's resistance and velocity of particles. If we assume (practically speaking) that a non-inertial type of a medium's resistance is maintained (as we have indicated before) during rectilinear motion of the particles with a curvilinear trajectory, which is continuous, we arrive at the following equation of the particles motion in a vectorial form:

$$m \frac{dV}{dt} = - 6\pi\eta r(V - U) + F, \quad (25.1)$$

where V and U are the vectors of the particle's velocity and medium's velocity, respectively; F is a vector of external force.

The equation (25.1) in a coordinated form is resolved into the following:

$$m \frac{dV_x}{dt} = - 6\pi\eta r(V_x - U_x) + F_x; \quad m \frac{dV_y}{dt} = - 6\pi\eta r(V_y - U_y) + F_y, \quad (25.2)$$

where V_x is the component of the particle velocity along the axis x , etc.

As equation (25.2) indicates, the component of the axially undetermined motion conforms with the same equation, as that of the rectilinear motion and at the same time the motions, which are axially diverse, are independent of each other. Naturally, this circumstance extremely simplifies the analysis of the curvilinear motion of the particles.

The circumstance of larger Re numbers poses another condition. In such a case it is considered that

$$Re = \frac{2\gamma g r \cdot / (V - U) /}{\eta}, \quad (25.3)$$

and we obtain the following vectorial equation of the particles motion:

$$m \frac{dV}{dt} = - \psi \left(\frac{2\gamma_g r \cdot / (V - U) /}{\eta} \right) \gamma_g \frac{\pi r^2}{2} (V - U) \cdot / (V - U) / + F, \quad (25.4)$$

where $/ (V - U) /$ is the length of the vector $V - U$.

If we resolve equation (25.4) axially according to coordinates, we obtain

$$m \frac{dV_x}{dt} = - \psi \left(\frac{2\gamma_g r / (V - U) /}{\eta} \right) \gamma_g \frac{\pi r^2}{2} (V_x - U_x) / (V - U) / + F_x, \text{ etc.} \quad (25.5)$$

The first term on the right side of this equation depends upon both, the component of the relative axial velocity x and the absolute rate of this velocity. Thus, the different axial motions are independent. In general, the system of equations (25.5) is not solvable and the analogous research of a curvilinear motion of the particles at larger Re numbers is possible only in some instances.

The matter of curvilinear motion of aerosol particles break down into two groups: the movement in an immobile and in a mobile medium. Considering the first group, we shall only discuss the fall of particles which oscillate simultaneously in a horizontal direction under the influence of an external force, such as an electrical field. This is one of a few examples of experimentally examined curvilinear motion of aerosol particles. If we consider the above-mentioned case, we obtain the following equations for a steady movement of such a type.

$$V_z = mgB = \tau g, \quad (25.6)$$

$$m \frac{dV_x}{dt} = F - 6\pi\eta r V_x, \quad (25.7)$$

where x is the horizontal axis;

where z is the vertical downward axis.

If force F changes sinusoidally with time, $F = F_0 \sin \omega t$, then the horizontal velocity of a particle is expressed by the equations (19.6) and (19.11) and the horizontal displacement by the following equation.

$$x = - \frac{FB \cos (\omega t - \varphi)}{\omega \sqrt{1 + \omega^2 \tau^2}}, \quad (25.8)$$

wherein

$$\operatorname{tg} \varphi = \tau \omega = V_z \omega / g. \quad (25.9)$$

Furthermore, the vertical displacement of a particle per time unit t is equal to

$$z = \tau g t. \quad (25.10)$$

Thus, the trajectory of a particle as such represents a sinusoid

$$x = - \frac{F_0 B \cos \left(\frac{\omega z}{\tau g} - \varphi \right)}{\omega \sqrt{1 + \omega^2 \tau^2}}. \quad (25.11)$$

ABBOTT (170) conducted an experimental test relevant to these conclusions by photographing water droplets with a radius of $30-40\mu$ falling with a frequency of 60 hertz through a sinusoidal, horizontal electrical field. The trajectories of the particles proved to be exact sinusoids. With the aid of a special adjustment, photographs recorded moments of time corresponding to values of $F = 0$ and in this way the phase displacement of oscillations φ was determined. The obtained values φ were satisfactorily conformable to the equation (25.9).

The apparent small discrepancies ($1-2^\circ$) are explained by deviations from STOKES' law for the horizontal and vertical components of a droplet movement.

Naturally, this method may be used for a simultaneous determination of the size and the charge of aerosol particles. Yet, in connection with this, it was found that it is more convenient to work not in a sinusoidal field, but in a field which is constant in regard to magnitude and alternating in regard to direction. In such case one can obtain zigzag lines, made up of parts of a straight line. The vertical displacement of a particle during one cycle of oscillation is determined by distances between the zigzags, hence, according to (25.10), by τ and then by the particle radius. The horizontal velocity of a particle is equal to $V_x = BEq$ (E denotes field intensity and q particle's charge). Thus the tangent of the angle of inclination of segments of the trajectory to the

horizontal is equal to $V_z/V_x = gm/Eq$; hence, if the radius of a particle is known, one can determine its charge. This "oscillatory" method, developed by N. FUKS and I. PETRYANOV (171), proved to be quite convenient in a research of distribution of charges among fog droplets with a radius of $> 0.5\mu$. However, in examining smokes it is necessary to consider that the apparent density of particles may be considerably lower than the actual. The oscillatory method was first introduced by WELLS and GERKE (172); however, these authors did not allow the particles being measured to settle, but conducted an aerosol slowly through a small vessel and only measured the amplitude of the particles oscillations and then assuming that each particle possessed one elemental charge, they computed their radii. Yet, the particles to which we shall apply the oscillatory method ($r > 0.5\mu$), carry, on the average, considerably more than one elemental charge (see page 143); thus the method of WELLS and GERKE can only be applied in exceptional instances, for instance, to aerosols obtained by an "embryonic" method by ammicronic nuclei (173).

For examining the charges in a coarsely dispersible aerosol, the following variant method developed by N. ROZENBLUM (174) proved to be successful in industrial conditions: particles are allowed to fall in a horizontal sinusoidal field, obtained with the aid of industrial alternating current. Simultaneously the particles assume a form of luminous horizontal lines, the length of which is equal to a doubling of the oscillation's amplitude. The rapidity of settling and the length of the afore-mentioned lines are determined simultaneously by an ocular grid and a timing device. The computations are conducted as is explained in § 19.

§ 26. Precipitation of Aerosols During Laminar Flow Under the Influence of Gravity

The movement of particles in a gaseous current forms an important part of the mechanics of aerosols. This chapter is dedicated to the motion of particles in laminar flow. A considerably more complicated problem concerning movements in a turbulent flow is discussed in chapter VI.

At first, we shall examine the precipitation of particles of an aerosol flowing laminae-like through a horizontal tube of such a small cross section, that vertical convective currents are absent in the tube, or at least they have a small velocity in comparison to the rapidity of the particles settling. Thus the computations quoted below are adaptable to aerosols precipitated at laboratories with the aid of instruments, baffled tubes, etc., but not by industrial precipitation chambers. We shall confine ourselves to such details as a flat tube, having a much greater proportion of its width to its height and circumference.

A vertical movement of particles in relation to the medium is expressed by equation (see /17.4/):

$$V = V_s \left(1 - e^{-t/\tau} \right). \quad (26.1)$$

The term $e^{-t/\tau}$ may be disregarded, if the average time of the particles presence in the tube is comparatively longer than the relaxation time τ . In such case the vertical velocity of particles may be regarded as constant and equal to V_s , while the horizontal velocity of particles may be regarded as coinciding with velocity of the medium at the same point. As is evident from the values of τ and V_s , relevant to particles of diverse sizes quoted in table 13 (see page 206), these conditions are fulfilled with usual problems in conjunction with aerosols.

Since velocity of the flow at the entrance to the tube remains constant along the entire cross section of the tube, therefore, at a distance - of the order $0.1R \cdot Re_f$ - from the entrance (175) (where R is the radius or one half of the tube's height and where Re_f is a Reynold's number pertaining to the flow in the tube) a stationary distribution of velocities is set up, which in case of a flat tube is expressed by the equation

$$U_x = \left(\frac{3z}{h} - \frac{3z^2}{2h^2} \right) \bar{U}, \quad (26.2)$$

where h is one half of the tube's height;

where \bar{U} is an average velocity;

where z is a distance from the bottom of the tube.

Thus the lines of the flow in the intermediate section of the tube are inclined toward the horizontal.

The components of velocity of laminar flow at any point of a flat tube may be expressed by the flow's function ψ :

$$U_x = \partial\psi/\partial z; \quad U_z = - \partial\psi/\partial x. \quad (26.3)$$

The component velocities of particles are, according to the afore-quoted statement, equal to

$$\frac{dx}{dt} = U_x = \frac{\partial\psi}{\partial z}; \quad \frac{dz}{dt} = U_z - V_s = - \frac{\partial\psi}{\partial x} - V_s. \quad (26.4)$$

If we eliminate dt from these equations, we can obtain a differential equation of the particles trajectories

$$-\frac{dx}{\partial\psi/\partial z} = \frac{dz}{(\partial\psi/\partial x) + V_s} \quad (26.5)$$

or, in another form,

$$-V_s dx = \frac{\partial\psi}{\partial x} dx + \frac{\partial\psi}{\partial z} dz = d\psi \quad (26.6)$$

If we integrate along the entire length of tube L , we shall obtain

$$V_s L = \psi_0 - \psi_L, \quad (26.7)$$

where ψ_0 and ψ_L are values of the flow's function at points occupied by the particles at the entrance to the tube and at its exit. The function of the flow expresses a volume of gas passing per time unit between the bottom of the tube and a given line (surface) of the flow per cm of the tube's width. Supposing that $\psi_L = 0$, we find a trajectory adjacent to a dividing trajectory of particles precipitating and not precipitating in the tube. Because of the dividing trajectory at the entrance to the tube $\psi = \psi_0 = V_s L$; consequently, the entire flow of gas in the tube is equal to ψ and the fraction of an aerosol precipitated in the tube, or the "effectiveness of precipitation" \mathfrak{Z} is equal to:¹

$$\mathfrak{Z} = \psi_0 / \psi = V_s L / \psi. \quad (26.8)$$

Inasmuch as

$$\psi = 2h\bar{U}, \quad \text{thus } \mathfrak{Z} = \frac{V_s L}{2h\bar{U}}. \quad (26.9)$$

The above reasoning leads to an important conclusion, that the effectiveness of precipitation does not depend upon distribution of velocities in the tube. The length of a tube necessary for a total precipitation is equal to

$$L_{kp} = \frac{2h\bar{U}}{V_s}. \quad (26.10)$$

1. This conclusion was reported by its author G. NATANSON.

The computations become very difficult if we deal with a round tube. Here, the distribution of velocities is expressed by the equation:

$$U = 2\bar{U}\left(1 - \frac{\rho^2}{R^2}\right), \quad (26.11)$$

where ρ is the distance from the tube's axis. Since the distribution is set up at the very entrance to the tube, in order to simplify the matter, we also compute the length of the tube L_{kp} , which is required for a complete precipitation of an aerosol. To accomplish this, it is necessary to find the trajectory of the particles, which enter the tube at an upper point of the cross section and move along a vertical plane, which passes through the axis of the tube. The distribution of velocities within this plane is provided in the expression: $U = 2\bar{U}\left(1 - \frac{z^2}{R^2}\right)$; where z is the vertical distance from the axis.

Like above, we find a differential equation of the trajectory of particles

$$\frac{dx}{2\bar{U}\left(1 - \frac{z^2}{R^2}\right)} = - \frac{dz}{V_s}. \quad (26.12)$$

By integrating along z from $-R$ to R , we find

$$L_{kp} = \frac{8R\bar{U}}{3V_s}. \quad (26.13)$$

CHISTOV (176) developed this equation for computing precipitation of aerosols at industrial installations, however, as we already mentioned, in this case it is necessary to compute the effect of convection. G. NATANSON derived the following equation for the effectiveness of precipitation in a round tube:

$$\beta = \frac{2}{\pi} \left(2\mu \sqrt{1 - \mu^{2/3}} + \arcsin \mu^{1/3} - \mu^{1/3} \sqrt{1 - \mu^{2/3}} \right), \quad (26.14)$$

$$\text{where } \mu = \frac{3V_s L}{8R\bar{U}}.$$

With $\mu = 1$, i. e., $L = 8R\bar{U}/3V_g$, equation (26.14) gives $\beta = 1$ in accordance with equation (26.13).

§ 27. Precipitation of Aerosols During Laminar Flow Under the Influence of an Electrical Field

We shall examine in a flat condenser precipitation of charged particles from laminar gaseous flow. We confine ourselves to the incidence of small particles disregarding their inertia, i. e., we shall, as in the preceding paragraph, consider their motion as quasi-fixed (see page 99). The particles' motion, directed perpendicularly to the condenser's plane, is expressed by the equation:

$$V_z = \frac{\Pi q B}{h}, \quad (27.1)$$

where Π is the condenser's plates voltage;

where h is the distance between the plates;

where q is the particle's charge;

where B is the particle's mobility.

According to the theory of gaseous ions, the velocity of ions in a field intensity $1 \text{ B} = \text{cm}^{-1}$ is named the mobility of ions. This designation is also applicable to heavy ions, i. e., to aerosol particles which are charged and are very small. Thus the "electrical mobility" u is combined with a "mechanical mobility" B according to the equation:

$$u = q B / 300 \quad (27.2)$$

(The coefficient 300 expresses the proportion of the electrostatic unit of potential to a volt). As we mentioned in § 2, the research in highly dispersible aerosols is conducted mainly by electrometric measurements of aerosol mobility u ; the latter is the main characteristic of heavy ions. The relation between the radius of particles and their mobility u , when they possess one elemental charge $e = 4.802 \cdot 10^{-10}$ E. S. Units each, is quoted in table 3 and by figure 10.

Here we have to pause briefly at the problem of magnitudes of the charges on aerosol particles. The charges may be of diverse origin: thus,

at a time of pulverization of dust, the particles obtain triboelectric charges; during atomization of liquids, the droplets are charged by way of fluctuations of concentrations of ions in liquid; among aerosols, which are formed at high temperatures, charges are produced by thermoionic emission; finally, a quite important and a common source of the charges is the settling of gaseous ions and electrons upon particles of aerosols.

Notwithstanding the initial distribution of charges in particles of an aerosol, the distribution gradually approaches a definite stationary condition due to continued settling of the ions, which are constantly developed in a gaseous medium. The theoretical and experimental researches, conducted at laboratories of the Physical-Chemical Institute dedicated to L. YA. KARPOV (177, 178), have shown that a stationary distribution of charges during a symmetrical bipolar ionization of a gaseous medium are expressed in first approximation by the following BOLTZMANN'S equation: the fraction of particles with elemental charges ν (ν is either positive or negative integer) is equal to:

$$f(\nu) = \frac{1}{\Sigma} e^{-\frac{(\nu e)^2}{2rkT}}, \quad (27.3)$$

where

$$\Sigma = \sum_{-\infty}^{+\infty} e^{-\frac{(\nu e)^2}{2rkT}}$$

Thus, a stationary distribution of charges does not depend upon a magnitude of gas ionization; yet, the stronger the ionization is, the shorter the time is needed to determine the distribution.

Most of the amicronic particles existing in the atmosphere, which are named "nuclei of condensation" and "heavy ions", have radii, the magnitude of which is of the order $1 - 5 \cdot 10^{-6}$ cm. Inasmuch as the distribution of charges in atmospheric aerosols is perhaps almost stationary, then according to equation (27.3) we obtain the following (table 11) distribution of charges, where n_0 denotes a percentage of uncharged particles and n_1 denotes particles with one elemental charge, etc.

Since the percentage of particles with few elemental charges is small, then with the aid of table 3 and without falling into a great error, one

Table 11
Distribution of Charges of Particles in Highly Dispersed
Atmospheric Aerosols

$r \cdot 10^6 \text{ cm}$	n_0	n_1	n_2	n_3
1	90	10	--	--
3	55	43	2	--
5	43	48	8.6	0.4

can determine the size of these particles according to their mobility u . Submitted below is a classification (as accepted in atmospheric physics) of atmospheric aerosol particles, according to their mobility (179) and with indication of their sizes (table 12):

Table 12
Classification of Atmospheric Aerosol Particles According
to their Mobility u

Particles	u	$r \cdot 10^6 \text{ cm}$
Ultraheavy ions	$< 2.5 \cdot 10^{-4}$	> 5
Heavy (LANGEVIN ions)	$2.5 - 10 \cdot 10^{-4}$	$2.5 - 5$
Large "average" ions	$10^{-3} - 10^{-2}$	$0.7 - 2.5$
Small "average" ions	$> 10^{-2}$	< 0.7

In order to express the potential in volts we convert equation (27.1) into:

$$V_z = \frac{dz}{dt} = \pi u/h. \tag{27.4}$$

If a particle movement is directed parallel to a condenser's plates, it is expressed by the equation:

$$\frac{dx}{dt} = U(z), \quad (27.5)$$

where U is the velocity of gaseous flow. It follows from the above equations that if a particle enters a condenser near the plate whose charge is of the same sign, then the particle reaches the second plate at a distance of x_0 (figure 24), which is equal to:

$$x_0 = \frac{h}{\pi u} \int_0^h \bar{U}(z) dz = \frac{\bar{U} h^2}{\pi u}. \quad (27.6)$$

As in equation (26.10), the above equation is correct in so far as any distribution of flow velocities in a condenser is concerned.

Thus, a path passed by a particle lengthwise within a condenser is inversely proportional to the particle's mobility u . The method developed by CHAPMAN (180) and based on the above statement, deserves greater consideration, although up to now it was not used to determine particle mobilities in highly dispersed aerosols. Aerosols are admitted by a slit-shaped nose B into a square tube (figure 25) and the latter is filled with pure air blown through it. As the aerosol currents assume direction parallel to the walls of the tube, their velocity is small in comparison with the air velocity in the tube. Naturally, the current in the tube is laminar. The A_1 and A_2 walls of the tube act like plates of a condenser. Particles, the charges of which are similar to the A_1 wall, move exactly as we explained above and then, having passed the condenser's path x_0 lengthwise, they settle on the A_2 wall (see /27.6/). Yet, it is better to release the stream of aerosol particles exactly midway between the walls with a velocity equal to that of air within the plane ($1.5\bar{U}$). In such case the distance x_0 will be twice as small as the previous one.

Two methods may be used to determine x_0 : a microscopic examination of the settled particles, or measuring the amount of electricity yielded by the precipitating particles.

In the first instance we place on the A_2 wall a copper screen coated with a thin layer of collodion, upon which particles precipitate. After completion of the test, the sediments are examined with the aid of an electronic microscope.

The distribution of mobilities u among aerosol particles (analogous to distribution of their sizes) is, as a rule, expressed by a

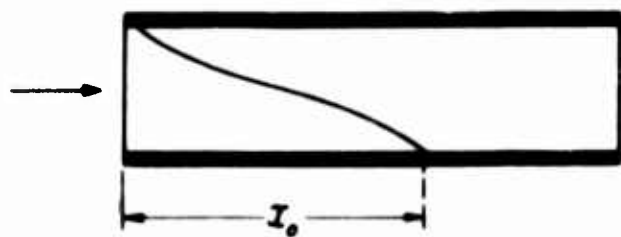


FIG. 24 PRECIPITATION OF AEROSOL PARTICLES IN A CONDENSER

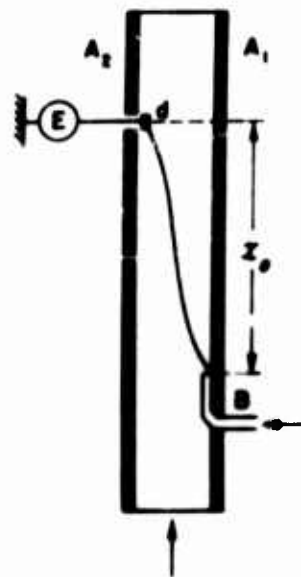


FIG. 25 DIFFERENTIAL METHOD FOR COMPUTING MOBILITIES

continuous curve (which nevertheless may have few peaks). The number of particles with a mobility within a range of u and $u + du$, is equal to

$$dN = f(u)du. \quad (27.7)$$

Consequently the same tendency will also manifest itself in a spatial distribution of particles among the obtained sediments, as we explained above. Hence, the number of particles in a radius bounded by the coordinates x and $x + dx$ will be expressed by the equation

$$dN = \phi(x)dx. \quad (27.8)$$

Now let us compare the expressions (27.7) and (27.8). Since it ensues from (27.6) that du is proportional to dx/x^2 , thus $f(u)$ is proportional to $x^2 \phi(x)$. Therefore, having determined the experimental $\phi(x)$, one can

find the distribution of the particle mobilities $f(u)$. Then, having measured, with the aid of the experimental microphotograms, the magnitude of the particles and having computed with the aid of table 3 the u mobilities, which the particles with one elemental charge are supposed to have, one can determine the actual number of charges of the particles. Such a research, which as yet has never been conducted by anybody, would finally enable one to solve the problem about the number of elemental charges on very small particles.

In testing the second method, a narrow electrode d (figure 25) is inserted into the condenser; the electrode is insulated from the wall A_2 , although it is positioned at a very close distance to it. The electrode being connected with an electrometer can be shifted lengthwise in relation to the condenser. A charge obtained by the electrode is, of course, equal to the number of particles settling upon the electrode; the number is multiplied by the the particles' average charge \bar{q} and the latter is equal to $\bar{q}\phi(x)\Delta x$, according to (27.8); where Δx is the electrode's width. Thus, the method does not offer

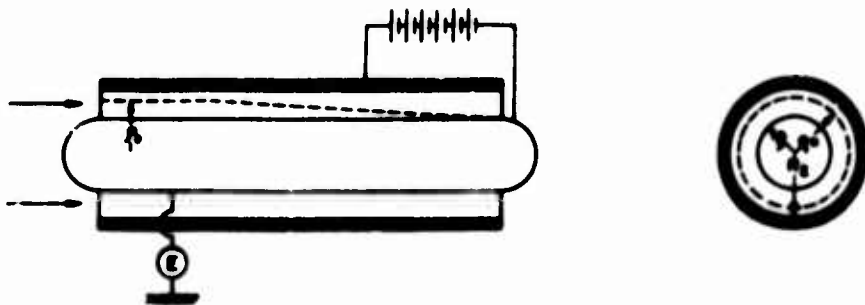


FIG. 26 ORDINARY METHOD FOR DETERMINING MOBILITIES

any distribution of velocities $f(u)$, but a function $\bar{q}(u)f(u)$; where $\bar{q}(u)$ is the average charge of the particles with a mobility u . The method lends itself to a finding of a distribution $f(u)$ only in such instances, when the magnitude of $\bar{q}(u)$ can be computed theoretically, or when very small sizes of particles suggest that they may possess one elemental charge each.

The discussed "differential" method of determination of the particles mobility in aerosols has in principle a greater advantage than the generally used "integral" method, because it offers directly a percentage of particles with mobilities prevailing in a certain narrow range. On the other hand the potential of a current flowing through the electrode is according to this method so small, that its measurement is rather difficult.

The usual (integral) method of determination of the particles mobility is as follows: an aerosol with a constant velocity is let in through a condenser, one of whose plates is connected with an electrometer and then the

measurements are carried out of strength of the current I flowing over the plate at dissimilar magnitudes of the potential π within the condenser, i. e., data are taken of π and I which are plotted on a curve of characteristics. A distribution of $\bar{q}(u)f(u)$ can thus be determined according to these characteristics (181, 182). Virtually any shape condenser may be used, but a preference is usually given to cylindrical condensers.

When a laminar gaseous current flows through such a condenser (figure 26), the current velocity of the particles directed parallel to the condenser's axis $V_x(\rho)$, is a function of the distance ρ from the axis. A field intensity in a cylindrical condenser is equal to:

$$E = \pi / \rho \ln \left(\frac{R_2}{R_1} \right), \quad (27.9)$$

where R_2 is the radius of the outer plate;

where R_1 is the radius of the inner plate.

Consequently, a radial velocity of particles in a condenser is equal to:

$$V_\rho = \pi u / \rho \ln \left(\frac{R_2}{R_1} \right). \quad (27.10)$$

Supposing the outer plate is charged positively. If a positively charged particle is in a motion toward the inner plate which is connected with an electrometer, then within a time dt it will pass in a radial direction the distance:

$$d\rho = - \pi u dt / \rho \ln \left(\frac{R_2}{R_1} \right).$$

At the same time, the particle will pass lengthwise to the condenser's axis the distance of:

$$dx = U(\rho) dt.$$

By eliminating dt from these equations we arrive at:

$$dx = - U(\rho) \rho \ln \left(\frac{R_2}{R_1} \right) d\rho / \pi u. \quad (27.11)$$

If a particle, while entering the condenser, was at a distance of ρ_1 from the axis, it will reach the inner plate at a coordinated point

$$x = - \frac{\ln(R_2/R_1)}{\pi u} \int_{\rho_1}^{R_1} U(\rho) \rho d\rho = \frac{\ln(R_2/R_1)}{\pi u} \int_{R_2}^{\rho_1} U(\rho) \rho d\rho. \quad (27.12)$$

Let us assume that all particles possess an identical mobility u . If the condenser's length equals L , then the inner plate will be reached by such particles, whose $x \leq L$. Among such particles $\rho_1 \leq \rho_0$, where ρ_0 is determined from the equation:

$$\frac{\ln(R_2/R_1)}{\pi u} \int_{R_1}^{\rho_0} U(\rho) \rho d\rho = L. \quad (27.13)$$

Thus, such particles precipitate at a certain potential Π in a condenser, when they enter it at a distance from the axis less, than ρ_0 . If 1 cm^3 of aerosol contains n positively charged particles with a charge q , then the following volume of particles will pass per time unit through a ring-shaped section (delimited within peripheries of R_1 and ρ_0 radii /figure 26/) of the condenser and will precipitate on its inner plate

$$N = \int_{R_1}^{\rho_0} n U(\rho) 2\pi \rho d\rho. \quad (27.14)$$

At the same time the strength of the current flowing over the inner plate will be equal to

$$I = qN = 2\pi qn \int_{R_1}^{\rho_0} U(\rho) \rho d\rho \quad (27.15)$$

or, according to the equation (27.13)

$$I = 2\pi qnuL\pi / \ln\left(\frac{R_2}{R_1}\right). \quad (27.16)$$

Thus, the strength of the current is proportional to the potential on condenser's plates. At the same time, as the potential reaches a magnitude of

$$\pi_s = \frac{\ln(R_2/R_1)}{uL} \int_{R_1}^{R_2} U(\rho) \rho d\rho, \quad (27.17)$$

i.e., as ρ_0 reaches R_2 , all positive particles entering the condenser will precipitate inside and then, upon a further magnification of the potential, the strength of the current I_s will remain constant (saturation current, figure 27, a).

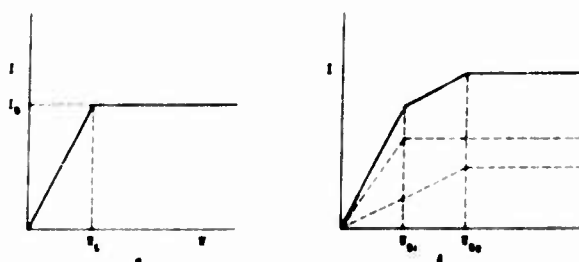


FIG. 27. CHARACTERISTICS OF AEROSOLS WITH SINGLE AND DOUBLE VALUES OF MOBILITIES

Since

$$\int_{R_1}^{R_2} 2\pi \rho U(\rho) d\rho = \Phi, \quad (27.18)$$

where Φ is the volumetric velocity of aerosol in the condenser, it follows from the equation (27.17), that

$$u = \frac{\ln(R_2/R_1) \Phi}{2\pi L \pi_s}. \quad (27.19)$$

Hence, one can determine the mobility of particles from the point of the break in characteristics. All the afore-quoted equations, like the preceding examples, are correct in so far as any distribution of streamline velocities in a condenser is concerned, if the streamlines are straight and parallel. It is distinctly clear that the strength of the saturation current is

$$I_s = qn\Phi, \quad (27.20)$$

and according to the latter one can determine the sum of the charges among positive particles contained in 1 cm^3 of aerosol. Of course, the above statements also pertain to particles charged negatively, if the condenser's plate is connected with an electrometer, which is positively charged.

If an aerosol has two groups of particles, the mobilities of which are: u_1 and u_2 , charges: q_1 and q_2 and concentrations: n_1 and n_2 , then equations (27.16) and (27.17) will be applicable to each group. Figure 27, b shows with dotted lines the characteristics of each group of particles, while solid lines express overall characteristics determined experimentally. Thus, the mobilities of both groups of particles are defined according to the points of break in their overall characteristics.

Deviations between the sides of the curves characteristics become more or less rounded for a number of reasons. This circumstance is of no specific importance if only two groups of characteristics exist, but where a larger number of groups prevails, then, instead of a dotted line, a continuous curve is obtained. On the other hand, as incidental errors in measurements occur in a continuous curve and the latter must be obtained with a continuous spectrum of particle mobilities, they may easily lead to a wrong conclusion about the presence of breaks in their characteristics, i. e., about the existence of discrete groups of mobilities. There is no doubt whatsoever that authors became victims of a self-deception in many researches, which included highly dispersed aerosols of diverse origin, among which discrete groups of mobilities were detected.

The defining of the distribution of mobilities in a smooth flow of continuous characteristics is effected in the following way. At first, let us assume that all particles have one elemental charge each. Then, let us agree that in the presence of a potential π_L all particles with a mobility of $>u_L$ precipitate in a condenser. The dependence between π_L and u_L expresses itself in the equation

$$u_L = \frac{\ln(R_2/R_1)\Phi}{2\pi L\pi_L} \quad (27.21)$$

The strength of the current transmitted by the particles, according to (27.20), is equal to

$$I_1 = \Phi \epsilon n \int_{u_L}^{\infty} f(u) du. \quad (27.22)$$

Particles with a mobility of $< u_L$, on their part, transmit, according to (27.16), the following strength of current.

$$I_2 = \frac{2\pi\epsilon L\pi_L n}{\ln(R_2/R_1)} \int_0^{u_L} uf(u) du. \quad (27.23)$$

Thus, the full strength of the current is equal to:

$$I = I_1 + I_2 = \Phi\epsilon n \int_{u_L}^{\infty} f(u) du + \frac{2\pi\epsilon L\pi_L n}{\ln(R_2/R_1)} \int_0^{u_L} uf(u) du. \quad (27.24)$$

We differentiate (27.24) again by π_L :

$$\begin{aligned} \frac{dI}{d\pi_L} = & -\Phi\epsilon n f(u_L) \frac{du_L}{d\pi_L} + \frac{2\pi\epsilon L\pi_L n u_L f(u_L)}{\ln(R_2/R_1)} \frac{du_L}{d\pi_L} + \\ & + \frac{2\pi\epsilon L n}{\ln(R_2/R_1)} \int_0^{u_L} uf(u) du. \end{aligned} \quad (27.25)$$

According to (27.21), the first two terms in the right part of this equation can be reduced and thus we obtain

$$\frac{dI}{d\pi_L} = \frac{2\pi\epsilon L n}{\ln(R_2/R_1)} \int_0^{u_L} uf(u) du. \quad (27.26)$$

Hence it follows, that

$$I - \pi_L \frac{dI}{d\pi_L} = h = \Phi\epsilon n \int_{u_L}^{\infty} f(u) du, \quad (27.27)$$

where h is the section, the length of which is cut off tangentially by characteristics at a point u_L on the axis of the ordinates (figure 28). The above section

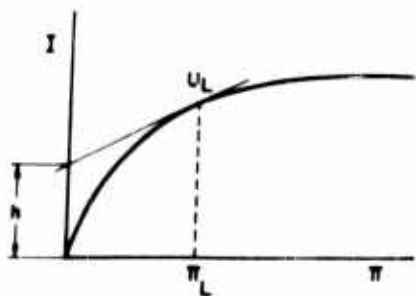


FIG. 28 CHARACTERISTICS OF AN AEROSOL WITH A CONTINUOUS DISTRIBUTION OF MOBILITIES

is proportional to the number of particles, the mobilities of which are within a range of u_L and ∞ , hence u_L is determined according to the pertinent potential Π_L and according to equation (27. 21). In this way we determine the spectrum of particles mobilities, or, if the charges of particles are not identical, we determine the function $q(u)f(u)$. The discussed method has a disadvantage in that small errors occurring in defining I leads to sizeable errors in magnitudes of the segments on the axis of ordinates and consequently to errors in the values of the function of distribution.

The above described method may lead to incorrect results in examination of the spectrum of particle mobilities in the atmosphere, due to the usual changes in the course of time, which affect the average content of aerosol particles in the atmosphere. In such a case it is expedient to use two condensers (181): the air is let in, at first, with the potential Π_1 through the first condenser, where the strength of the current (not measurable, I_1) is expressed by equation (27. 24) and then the air passes thru the second capacitor with such potential, that practically all the particles precipitate in it. The strength of current in the second capacitor I_2 , measured with an electrometer, obviously is equal to $\Phi en - I_1$. If the potential in the first condenser equals zero, then the current will flow through the second condenser with a strength $\Phi en = I_0$, i. e., proportional to the general contents of charged particles in the air. The measurements are conducted in the following way: having determined the strength of current I_2 , which is appropriate to a given potential Π , the I_0 is measured and the magnitude of the proportion is computed $(I_0 - I_2)/I_0 = I_1/I_0$; then, as Π becomes somewhat increased, the corresponding strength of current I_2 is determined, the I_0 is measured again, etc. In this way the "normalization" of I_1 is carried out toward a constant, total volume of charged particles in the air. Although the principle of the method stresses the assumption that the distribution of the particle's mobility in the atmosphere does not depend upon their concentration, nevertheless the method can only be correct in specific cases and the two-condenser method still offers more reliable results than the one-condenser method. It is desirable in both methods to remove gaseous ions from the air beforehand; this is attained by passing the air with a small pressure sufficient to eliminate all gaseous ions with their high mobilities of the first

order through an auxiliary condenser. Meanwhile, the number of aerosol particles intercepted by this condenser would be insignificant.

We emphasize that everything aforesaid is correct only in so far as it pertains to a laminar flow of gas through a condenser. The trend of the phenomena changes considerably with a turbulent flow and the strength of current flowing through a condenser at a certain potential becomes noticeably smaller than equation (27. 24) indicates (181). See page 299.

As we already mentioned, the electrometric determination of particle mobility is the basic method of research in highly dispersed aerosols and specifically so when a highly dispersed component of atmospheric aerosols is involved, because in such case particles are much too small for ultra-microscopic research. On the other hand, the exactness of the electrometric method diminishes with the increased size of particles; therefore, according to the quoted equations, one must either increase the field of force in a condenser or reduce the velocity of flow of an aerosol. However, very strong fields develop leakage factors and also local atmospheric conditions cause other complications, while convectional currents in a condenser also create serious difficulties at small velocities of flow. The r value of approximately 10^{-5} cm may be regarded as the highest point in applicability of the electrometric method; this value somewhat exceeds a lower point of applicability of ultra-microscopy in aerosol research. Thus, the two methods supplement one another and facilitate practical research in aerosols within any degree of dispersion.

It should be stated that prior to an electrometric examination of highly dispersed aerosols it is necessary that the latter be charged by means of a radioactive compound (183), etc. From a practical standpoint the following observation (184) would be of value: while conducting atmospheric air through a rubber tubing it was noted that a considerable loss of charged nuclei of condensation occurred in the tube, whereas only a very small number of non-charged nuclei lagged behind. The effect was intensified in bends of the tube and it was disapproved after the tube had been coated with conducting liquids. Evidently in bends of the tube, at their concave and convex sides, charges of an opposite sign were generated and an electrical field was developed inside the tube.

COCHET (185) studied the sedimentation of noncharged droplets in motionless air upon a charged and infinitely long, horizontal cylinder (e.g., upon electrical transmission wires), which included a simultaneous effect of gravitational and induction forces. Disregarding the inertia of the particles and assuming that resistance of the air in the first degree is proportional to

the velocity of the droplets, COCHET found the following expression for the coefficient of droplet settling (see page 174):

$$\mathfrak{Z} = \left(\frac{9\lambda E_0^2}{8\gamma g R} \right)^{1/3}, \quad (27.28)$$

where $\lambda = (\epsilon_k - 1)/(\epsilon_k + 2)$;

where ϵ_k is the dielectric constant of droplets;

where R is the radius of cylinder;

where E_0 is the field potential on the surface of a cylinder, which is connected with the cylinder's length by the equation: $E_0 = 2q/R$.

The equation (27.28) is applicable only with $E_0 > \sqrt{4\pi\gamma g R/3\lambda}$; in the opposite case \mathfrak{Z} can only be determined by a numerical method. \mathfrak{Z} does not depend upon a size of particles, because gravitation and induction forces are proportional to the volume of particles.

The experimental determination of \mathfrak{Z} by way of photographing trajectories of droplets falling upon a charged cylinder has indicated that, with $R = 0.6$ cm, $E_0 = 47$ or 88 E. S. Units and $r < 25\mu$, the coincidence between the theory and the experiment is very high, i. e., the inertia of particles can actually be disregarded. With $r = 40\mu$ and $E_0 = 88$ E. S. Units the experimental value of \mathfrak{Z} was estimated to be 14% higher according to equation (27.28) due to the inertia effect.

The precipitation of particles in an electrical field is widely used in technology for purification of gases from dust, mists, etc. In the COTTRELL precipitator, which is used for that purpose, a negatively charged inner plate of the condenser has a very small radius (on the order of 1 mm); a corona discharge over the plate passes and develops in a COTTRELL precipitator a high concentration of negative gaseous ions and electrons, which impart charges to the particles. Thus, two processes take place simultaneously in the precipitator: the charging of particles and their precipitation.¹ Furthermore, due to a strong ionic wind, entrained by a corona charge, the flow of gas in the precipitator has random tendencies, therefore the precipitation of the particles must be calculated as is explained in § 44.

1. There also takes place in the precipitator a "directed" coagulation of particles, which is effected by the field.

However, in recent times precipitators have been developed, in which the two afore-mentioned processes are spatially separated: basically, only the charging of particles takes place in the first part of the precipitator, while in the second part only precipitation occurs (186). With such an arrangement it is possible to use a positive corona electrode, which yields far less harmful oxidation products (nitric oxides, etc.), than a negative electrode. Therefore this method of dust precipitation is of great importance in air conditioning.

§ 28. Precipitation of Aerosols in a Field of Centrifugal Force. Aerosolic Centrifuge

We shall examine the motion (in a medium) of aerosol particles, as they spin around an immobile axis with a velocity $U(\rho)$, which is a function of the distance from the axis. Now, if we consider a quasi-fixed motion of a particle, i. e., if we imagine that its tangential velocity coincides with that of the medium, we obtain for the radial velocity of the particle the following expression:

$$V_{\rho} = \frac{U^2(\rho)mB}{\rho} - \frac{U^2(\rho)\tau}{\rho}. \quad (28.1)$$

We encounter the most simple case of such movements in an aerosolic (bacterial) centrifuge, which is used in studying the bacterial microflora in the air (187). A vessel A (figure 29) spinning around on its axis is coated inside with a thin layer of an agar culture. The air to be examined is conveyed through a stationary tube B, which reaches almost to the bottom of the vessel. At a certain distance from the bottom of the vessel the air practically achieves the same angular velocity ω , with which the vessel rotates. Particles in the air being influenced by the centrifugal force precipitate on walls of the vessel. After a specific volume of air has passed through the apparatus, the vessel is placed under thermostatic control and the number of grown bacterial colonies is counted.

In the given case $U(\rho) = \omega\rho$ and the radial velocity of a particle is

$$V_{\rho} = \frac{d\rho}{dt} = \omega^2\rho\tau. \quad (28.2)$$

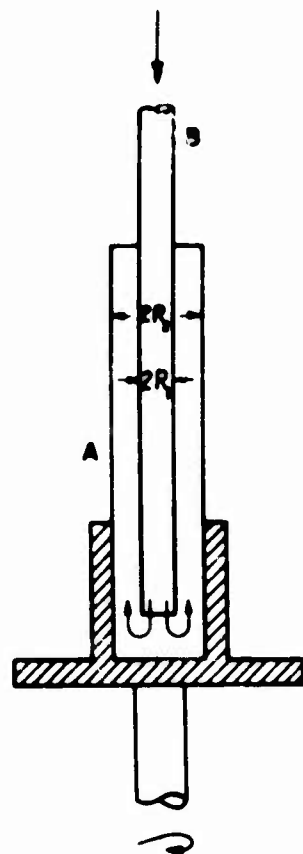


FIG. 29 AEROSOLIC CENTRIFUGE

The distribution of velocities of gas flowing lengthwise in the vessel is expressed by the equation (188)

$$U_{\rho} = \frac{2\bar{U} \left\{ R_1^2 \ln(R_2/\rho) - R_2^2 \ln(R_1/\rho) - \rho^2 \ln(R_2/R_1) \right\}}{(R_1^2 + R_2^2) \ln(R_2/R_1) + R_1^2 - R_2^2}, \quad (28.3)$$

where \bar{U} is the average velocity of the flow;

where R_2 is the inner radius of the vessel;

where R_1 is the outer radius of the tube B.

Assuming, that the velocity of a particle parallel to the axis of the vessel coincides with the velocity of the air, i.e., that

$$\frac{dx}{dt} = U(\rho), \quad (28.4)$$

then, having excluded dt from this equation, as well as from (28.2), we obtain a differential equation of the particle's trajectory in a plane passing through the vessel's axis, which rotates with the latter. Thus:

$$dx = \frac{U(\rho)d\rho}{\omega^2 \tau \rho}. \quad (28.5)$$

Hence, we obtain the following expression for the vessel's height, which is essential to the precipitation of all particles of a certain size:

$$L = \frac{1}{\omega^2 \tau} \int_{R_1}^{R_2} \frac{U(\rho)}{\rho} d\rho = \frac{2\bar{U} \frac{1}{2} \ln(R_2/R_1) \left\{ (R_1^2 + R_2^2) \ln(R_2/R_1) + R_1^2 - R_2^2 \right\}}{\omega^2 \tau \left\{ (R_1^2 + R_2^2) \ln(R_2/R_1) + R_1^2 - R_2^2 \right\}} = \frac{\bar{U} \ln(R_2/R_1)}{\omega^2 \tau} \quad (28.6)$$

which is the expression that would be obtained, if the air velocity remained constant in the entire cross section of the vessel. A. SHAFIR (189) quotes the

following data, which pertain to the centrifuge and are applicable when: $\omega = 2\pi \cdot 50$, $L = 17$ cm, $R_2 = 2$ cm, $R_1 \approx R_2/3$, $\bar{U} = 36$ cm \cdot sec $^{-1}$. Assuming that a density of bacterial particles is equal to one unit, hence, according to the equations (28.6) and (17.3), we see, that only such particles, whose radius is $\geq 1.4 \cdot 10^{-4}$ cm 1 must precipitate completely in the centrifuge, i. e., when the radius exceeds several times the average sizes of bacteria. If we consider that the rapidity of particles precipitation in the centrifuge is proportional to a square of their radius, one should expect that the percentage of bacteria unassociated and able to settle in the centrifuge should be small. The fact that in A. SHAFIR's tests from 83 to 89% of bacteria were entrapped in the centrifuge is explained by the incidence that the bacteria do not remain in the air in a loose stage, but they are included in much larger particles, which are formed of various organic substrata. If we consider that the air current in the above example corresponds to an Re number of approximately 300-400, then the hypothesis about a laminar trend of the current justifies itself.

Hence, such centrifuges, which rotate with the usual standard speeds are suitable only for precipitation of particles, the magnitude of which is of the order of 1-2 μ . We would need a supercentrifuge capable of making several hundred revolutions per second in order to precipitate particles, the sizes of which are of the order of magnitude of tenths of a micron.

More interesting, anyway, is a "conifuge" /figure 30/, which was recently introduced (190) to analyze the dispersion of coarse aerosols. The rotor of the apparatus consists of two firmly interconnected coaxial cones A and A' with parallel surfaces of generation. As the rotor turns, an air current develops in the air space between the cones and it assumes a circulatory trend because of the presence of a covering C. An aerosol to be examined is introduced via tube B into the apparatus. Particles, which move by centrifugal force from the inner to the outer cone, precipitate on the latter. The smaller the particles, the greater is their travel within the space prior to precipitation. A narrow strip of glass, which is inserted lengthwise to the surface of the outer cone, is positioned flush with the cone's surface; the glass slide is removed upon completion of test and the precipitation formed upon it is examined under a microscope. The separation of particles according to their size (in case of particles of irregular shape - according to the magnitude of their sedimentation radius), progresses quite thoroughly; hence it is easy to determine a distribution

1. Actually the radius is still greater, because we did not consider the circumstance that the air does not assume a rotary velocity of $\omega\rho$ immediately.

of particle sizes from the obtained arrays. A highly advantageous feature of the apparatus is, that the centrifugal force increases in proportion to the distance from the top of the cone, while the velocity of the air current decreases.

A rather difficult mathematical calculation leads to the following equation of the trajectory of aerosol particles in the apparatus (at the same time it is assumed that the air is completely entrained by the rotor, i.e., that it has the same rotary speed):

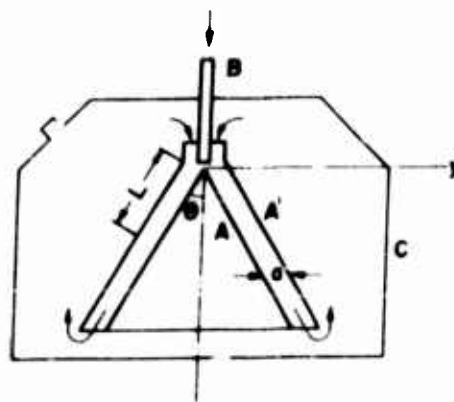


FIG. 30 CONIFUGE

$$y = \pi^{1/2} \operatorname{tg} \theta \exp \left[A^2 (x + a)^2 \right] \left\{ \operatorname{Erf} A (x + a) - \operatorname{Erf} A a \right\} / 2A, \quad (28.7)$$

(TN: Translator assumes that in (28.7) and in (28.8) the 0 symbol should be substituted by θ)

where

$$A = (\pi a \omega^2 V_s \operatorname{tg} \theta / \dot{\phi} g)^{1/2};$$

$$a = \frac{1}{2} a \operatorname{ctg} \theta;$$

$\dot{\phi}$ denotes a volumetric velocity of the circulating air.

The values of other letters are self-explanatory from the above figure. Since the surface of the outer cone is expressed by the equation

$$y = a + x \operatorname{tg} \theta, \quad (28.8)$$

then from the two equations one can determine the space l , upon which particles of a certain magnitude will precipitate. The experiments with the conifuge were conducted while taking into account that $\theta = 30^\circ$, $\dot{\phi} = 11.6 \text{ cm}^3 \cdot \text{sec}^{-1}$, $\omega = 2\pi \cdot 50$, $a = 0.56 \text{ cm}$ and also included particles, the radii of which ranged from 0.3 to 10μ . At the same time it was discovered that experimental values l exceeded the theoretical calculations by 0.4 cm for particles of all sizes. This divergence is explained in the first instance by the fact that the rotating air lags behind the rotor.

§ 29. Cyclones (191, 192)

Of far greater practical importance are cyclones, the centrifugal dust extractors, which function according to another principle: the apparatus as such remains immobile, while a circulation of gas around the cyclone's axis is followed by a change in the direction of the alternating motion. Gas enters the cylindrical part of the cyclone through an entrance tube A which has a rectangular cross section (figure 31); here the gas acquires a spiral motion and

then descending by an outer spiral (figure 32), it subsequently ascends by an inner spiral and then escapes via an exit tube C (figure 31). Particles influenced by centrifugal force precipitate on the cyclone's walls, wherein they slide downward and then flow out through the opening E into a container.

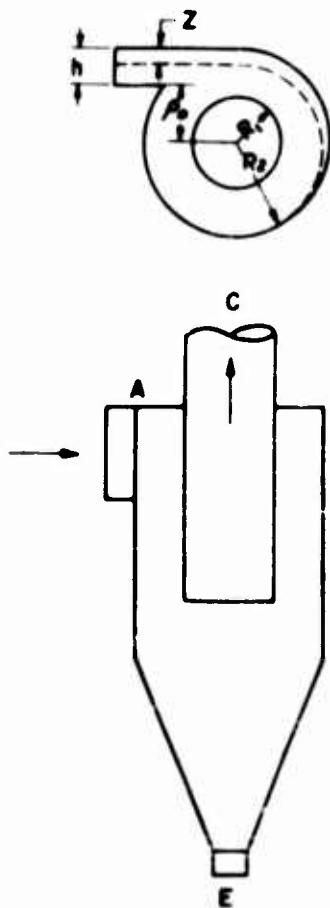


FIG. 31 CYCLONE SEPARATOR



FIG. 32 MOTION OF GAS IN A CYCLONE SEPARATOR

Considering the inexpensiveness, simplicity of construction and maintenance (due to the absence of movable parts with filtering surfaces, which require periodic cleaning) and also the comparatively small resistance and high output, all of which are the attributes of the apparatus in question, - cyclones are incomparable apparatuses to purify gases from suspended particles. However, they entrap coarse aerosols only. Therefore the basic region of their usage is in the purification of large volumes of gas from dust (involving mainly large particles), whenever a small residue of dust in the gas does not matter and also

for the purpose of preliminary purification prior to filtering through highly effective apparatuses (e.g., COTTRELL precipitators). Cyclones gained their greatest importance in purification of smoky gases from ashes and unburned particles of coal, particularly so during consumption of dust-like fuel.

The flow of gas in cyclones has a very complicated pattern and its study has, so far, been insufficient. Since the theory of its operation is still incomplete, we are not able to design cyclones. Particularly the question of the most advantageous forms of cyclones up to now has been solved exclusively by empirical methods.

The universally adopted theory of cyclones (193-197) contains a number of simple hypotheses. It is assumed that the flow along the outer spiral is laminar (which is absolutely incorrect when currents of greater velocities prevail in cyclones) and that a tangential velocity of the gas may be expressed by the formula $U(\rho) = b/\rho^s$, in which various authors assume values, which range from -1 to +1 for the exponent s . Furthermore, they usually disregard the flow of gas from the periphery toward the cyclone's axis (effluence); also they do not admit the feasibility of the retrogression of the particles, which precipitated under the flow of gas and likewise they do not consider any precipitation in the conical part of the cyclone nor the ejection of particles from the inner spiral to the outer spiral, as well as many other phenomena occurring in cyclones. Finally, they consider the movement of the particles to be quasi-fixed. The latter is justified in that the estimation of cyclones is always made according to minute and difficult precipitating fractions, on behalf of which a specified simplification is permissible.

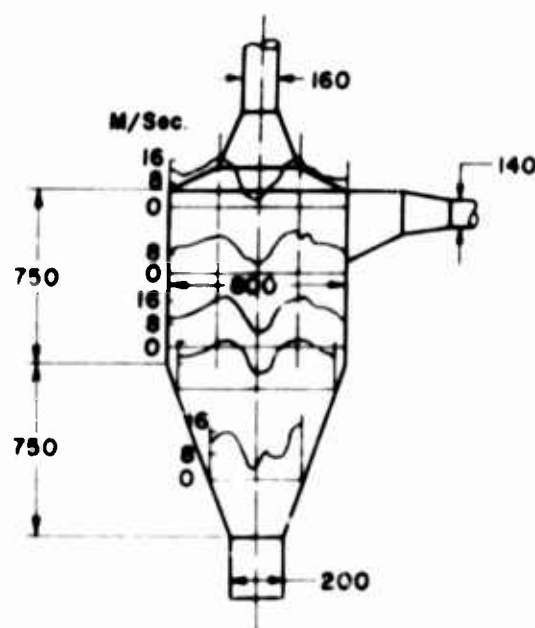


FIG 33 DISTRIBUTION OF VELOCITIES IN A CYCLONE SEPARATOR

The experimental study of gaseous flow in a cyclone is considered very difficult due to the strong turbulence of the current. Besides, it is rather difficult to determine the diameter of the inner spiral, which, generally speaking, is equal to the diameter of the exit tube. Figure 33 illustrates the distribution of the average tangential velocities of gas in a cyclone (198). The diagram shows, that velocity, which increases at first from the periphery to the cyclone's axis, reaches its maximum limit and then it diminishes rapidly to

UNCLASSIFIED

AD

227 876

FOR
MICRO-CARD
CONTROL ONLY

4

OF

9

Reproduced by

Armed Services Technical Information Agency

ARLINGTON HALL STATION; ARLINGTON 12 VIRGINIA

UNCLASSIFIED

"NOTICE: When Government or other drawings, specifications or other data are used for any purpose other than in connection with a definitely related Government procurement operation, the U.S. Government thereby incurs no responsibility, nor any obligation whatsoever; and the fact that the Government may have formulated, furnished, or in any way supplied the said drawings, specifications or other data is not to be regarded by implication or otherwise as in any manner licensing the holder or any other person or corporation, or conveying any rights or permission to manufacture, use or sell any patented invention that may in any way be related thereto.

zero. A string-like eddy is formed at the cyclone's axis and it spins like a solid body. It happens frequently, that when the width of the inlet tube h (see figure 31) is equal to the width of the ring-shaped space between the exit tube and the cyclone's walls $R_2 - R_1$, then the distribution of tangential velocities below the exit tube in the outer spiral may be expressed quite accurately by this formula (197):

$$U(\rho) = \frac{U_0}{2} \sqrt{\frac{R_2}{\rho}}, \quad (29.1)$$

where U_0 is the gas velocity in an inlet tube;

where R_2 is the radius of cyclone's cylindrical part;

where ρ is the distance to the axis.

Let us assume that for an ideal liquid the distribution of velocities would be expressed by the formula $U(\rho) = b/\rho$. Hence it follows, that a potential (laminar) flow of ideal liquid like in an inlet tube should be also the same inside a cyclone and that the distribution of velocities during laminar circulation of a liquid has the above indicated tendencies. Actually some equalization of velocities takes place as a result of turbulent agitation in a cyclone and this influences the reduction of exponent in $1/\rho$ from 1 to 0.5.

In the ring-shaped space between the exit tube and the walls of a cyclone, when comparing its width with the width of an inlet tube h , the distribution of tangential velocities roughly speaking, may be represented in this form (197):

$$U(\rho) = \frac{U_0 \rho}{1.2 R_2}. \quad (29.2)$$

If, however, the ratio of $h/(R_2 - R_1)$ is not equal to 1, then the expressions (29.1) and (29.2) should be multiplied by the value of this ratio.

Let us consider the movement of particles in a cyclone, proceeding from the distribution as in (29.1). Thus we obtain for a radial velocity of particles the following equation:

$$\frac{d\rho}{dt} = \frac{U^2(\rho)mB}{\rho} = \frac{U_0^2 R_2 \tau}{4\rho^2}, \quad (29.3)$$

from which

$$dt = \frac{4\rho^2 d\rho}{U_0^2 R_2 \tau} \quad (29.4)$$

Then, we denote by $\rho_0 = R_2 - h$ the minimum distance from the axis of the cyclone to particles entering the latter (see page 37). In this case according to (29.4) all particles of a certain size will reach the walls within a time

$$t = \frac{4}{U_0^2 R_2 \tau} \int_{\rho_0}^{R_2} \rho^2 d\rho = \frac{4(R_2^3 - \rho_0^3)}{3U_0^2 R_2 \tau} \quad (29.5)$$

However, considering the time during which particles remain in a cylindrical part of the cyclone, we can write down:¹

$$t = \frac{2\pi\rho_m}{U(\rho_m)} = \frac{4\pi s \sqrt{\rho_m^3}}{U_0 \sqrt{R_2}} \quad (29.6)$$

where s is the number of turns of an outer spiral in the cyclone's cylindrical part; where ρ_m is a certain average of the value ρ ($\rho_0 < \rho_m < R_2$). If we substitute τ by its value $\frac{2r^2\gamma}{9\eta}$, we obtain the following expression for the smallest radius of the particles, which fully precipitate in a cyclone:

$$r_{min} = \sqrt{\frac{3\eta(R_2^3 - \rho_0^3)}{2\pi\gamma s U_0 \sqrt{R_2 \rho_m^3}}} \quad (29.7)$$

In order to simplify the equation we write down

$$R_2^3 - \rho_0^3 = (R_2 - \rho_0)(R_2^2 + R_2\rho_0 + \rho_0^2) = h(R_2^2 + R_2\rho_0 + \rho_0^2) \quad (29.8)$$

1. We omitted here the difference between the length of a spiral coil and its projection upon a plane perpendicular to the cyclone's axis.

and then we substitute in the fractions $h(R_2^2 + R_2\rho_0 + \rho_0^2)/\sqrt{\rho_m^3\rho_0}$ the term R_2 for ρ_0 and ρ_m . At the same time both the numerator and the denominator become somewhat larger and the value of the fractions changes slightly. In addition to this, the equation (29.7) will be changed into

$$r_{\min} = 3 \sqrt{\frac{\eta h}{2\pi U_0 \gamma s}}. \quad (29.9)$$

Following the distribution in (29.2) one can, by a quite similar manner, arrive at the equation

$$r_{\min} = 3 \sqrt{\frac{0.3 \ln(R_2/R_1) \eta R_2}{\pi U_0 \gamma s}} \quad (29.10)$$

Practically, both equations offer identical values of r_{\min} . Usually in designing cyclones the h is obtained from $R_2/3$ up to $R_2/2$. When $h = R_2/2$, equation (29.9) is converted into

$$r_{\min} = \frac{3}{2} \sqrt{\frac{\eta R_2}{\pi U_0 \gamma s}}, \quad (29.11)$$

and equation (29.10) into

$$r_{\min} = 3 \sqrt{0.3 \ln 2} \cdot \sqrt{\frac{\eta R_2}{\pi U_0 \gamma s}}. \quad (29.12)$$

The numerical coefficients in (29.11) and (29.12) are equal to 1.5 and 1.37. The insignificance of the difference is obvious, if one considers that the number of spiral turns s in a cyclone is not known exactly and that it is assumed to be between 1 and 3. As to particles of irregular shape and aggregates, r denotes a sedimentation radius and γ the apparent density of particles.

The equation (29. 9) can also be used to determine cyclone's effectiveness on behalf of particles of a certain size, i. e., to compute the percentage of intercepted particles. To do this, it is necessary to substitute h in the equation by z , i. e., the distance where the particles enter the cyclone up to the latter's cylindrical wall (see figure 31) and to find for z a solution in the given equation. Consequently one obtains from (29. 9):

$$z = \frac{2\pi U_0 \gamma s r^2}{9\eta} = \pi U_0 s \tau. \quad (29. 13)$$

The thus determined z represents as such the maximum initial distance from the wall, i. e., the distance at which particles with a radius r precipitate in a cyclone. If we assume that aerosol particles are uniformly distributed in the inlet tube, then the cyclone's effectiveness as to particles of a certain size is obviously equal to z/h . Hence,

$$\mathfrak{Z} = z/h = \pi U_0 s \tau / h = \pi s l_1 / h. \quad (29. 14)$$

All particles in polydispersed aerosols, in a stratum depth dz , positioned at a distance z from the cyclone's wall, which precipitate, have a radius larger, than r_{min} , which is determined according to equation (29. 9) or (29. 10). The mass of these particles is equal to $bG_a(r_{min})dz$; where b is the constant of proportionality; $G_a(r)$ is the integral function of the gravimetric distribution of the particle sizes (see page 16) and it indicates, which gravimetric fraction of particles possess a radius $> r$. Thus the aggregate mass of intercepted particles in a cyclone is equal to

$$M = \int_0^h bG_a(r_{min})dz, \quad (29. 15)$$

and the aggregate mass of particles carried through the cyclone is

$$M_0 = \int_0^h b dz = bh. \quad (29. 16)$$

Hence, the effectiveness of a cyclone, considering a polydispersed aerosol, is equal to

$$\mathfrak{Z} = M/M_0 = \frac{1}{h} \int_0^h G_a(r_{min})dz = \frac{1}{h} \int_0^h G_a\left(\sqrt{\frac{9\eta^2 z}{2\pi U_0 \gamma s}}\right)dz \quad (29. 17)$$

In the above we substitute in the integral r_{\min} by $(9\eta z/2\pi U_0 \gamma s)^{1/2}$ according to equation (29.13).

The effectiveness of cyclones computed in this manner is, as a rule, considerably higher than in the actual one and this is explained, in the first place, by the turbulence¹, which causes particles approaching the wall to be repulsed toward the cyclone's axis. Apparently of essential significance is the action, whereby the particles which precipitated on walls² are pulled away, as well as the action of gas flowing toward the cyclone's axis and, finally, the circumstance, that particles of an elongated or a flaky shape orient themselves in cyclone with their elongated axes parallel to the direction of the current (see § 11) and thus the radial velocity of the particles becomes reduced. The influence of turbulence and possibly that of particles being pulled away point out the dependency of the cyclone's effectiveness upon the velocity of gaseous flow U_0 . With the increase of U_0 , turbulent fluctuations and the pulling away from walls must also increase. Actually, as experiment indicates, the cyclone's effectiveness at first increases considerably in proportion to the increase of U_0 , (according to the above theory) ... then less and finally, it begins to diminish (193). Technical improvements in cyclones, as well as in any other apparatus used for purification of gases probably should include greater effectiveness with the least hydraulic resistance, which is determined by the energy expended on passing a gas through a cyclone. Inasmuch as such resistance is proportional to U_0^2 , it is expedient to work with velocities somewhat smaller than with a velocity suitable for a maximum effectiveness. Usually, the U_0 is on the order of 10-20 m · sec⁻¹. Of extreme importance is the experimentally determined fact, that in cyclones dissimilar in dimensions, yet similar geometrically, the resistance at the same velocity U_0 is approximately identical (194). The influence of turbulence is also noticeable with a cyclone performing properly as a result of its inner "smoothness": any protuberances, partitions, etc., found inside a cyclone noticeably reduce its effectiveness and increase the resistance.

At first glance it appears from equations (29.9) and (29.17) that the effectiveness of a cyclone does not depend upon its diameter, but solely upon the width of the inlet tube h , yet in practice the matter seems to be different. At a constant U_0 the contraction of the inlet tube leads (as we indicated above) to a decline of the gas velocity inside the cyclone and thus, as is known from practical experience, this does not produce any important effect. Furthermore,

1. The influence of turbulence upon the effectiveness of cyclones is discussed in § 46.
2. This is indicated by a noticeable increase of cyclone's effectiveness as its walls become moistened (192).

the operating efficiency of a cyclone is obviously reduced at the same time. Hence, following the experimental facts, as cyclones are constructed, the width of the inlet tube is usually $1/3$ to $1/2$ of the cyclone's radius. Thus, in solving the given problem one must use equations (29.11) and (29.12), from which it is directly obvious that effectiveness of a cyclone increases with a decrease of the cyclone's diameter. Actually, this increase is still greater than the quoted equations indicated and this, above all, is explained by a lower turbulence in small cyclones. The reason for this is obviously in the greater magnitude of pressure gradients and gas density from the axis to the periphery of small cyclones and this gradient is proportional to U_0^2/ρ . In the meantime, a density gradient being similar to a temperature inversion point in the atmosphere, undoubtedly counteracts the turbulent agitation in a cyclone. Small cyclones of 5 - 15 cm proved to be considerably more effective than larger apparatuses of several meters in diameter used earlier, and when connected parallel into a battery, they met with a wide acceptance in technology under the name of "multicyclones" (196). According to theoretical data they can produce effectiveness of up to 99% with particles of $r \approx 3\mu$.

In the above exposed and generally accepted theory of cyclones no consideration was given to the effect of reversing the particles' movement along the axis of a cyclone near the end of its conical part, i.e., at a point of transition from the outer to the inner spiral (199). The fact that particles in here fly out from the gaseous flow with a greater velocity is proved by the following observation. small cyclones function very well when in a turned-over position (196) and dust particles (but not gas) fly out simultaneously upwards from the exit. It is difficult to say what comparative importance this factor is in an overall effectiveness of a cyclone.

Usually in the mechanics of aerosols the phenomena of a cyclone are important, such as an increasing effectiveness and a diminishing resistance are, when the concentration of an aerosol which passes through, becomes increased. Thus, in one instance, when a concentration of kaolin dust was increased in the air from 0.1 to 100 grams \cdot m $^{-3}$, the effectiveness of a cyclone improved from 70 to 90% (193). This phenomenon was undoubtedly caused by a kinetic coagulation of the aerosol (see § 54) in a cyclone, i.e., due to entrapment of small particles by much larger and faster moving particles.

The influence of dust concentration upon resistance in a cyclone may be explained by the following figures. In a cyclone of 22 cm diameter, with a highly polydispersed dust having particles of average radius of $\sim 8\mu$ and of a specific dust gravity 2.8, the ratio of the resistance Δ_p to the concentration of dust C (g \cdot m $^{-3}$) is expressed, according to BRIGGS (200), by the formula $1 - \Delta_p/\Delta_{p_0} = 0.013C$; where Δ_{p_0} is the resistance for pure air. M. ZAITSEV and A. SHAKHOV noticed an approximately 2.5 - 3 times stronger

effect, in which case, at a certain gravimetric concentration, the effect increased with the size of particles.

Among specialists in the field of gas purification there is a widely spread impression that the main cause of the above indicated decrease in the cyclone's resistance is the specific gravity increase and, consequently, a larger quantity of flowing gas and dust enters the cyclone, if we compare it with pure gas moving with the same velocity. Yet, at the same time, one forgets that the excess of the moving bulk dissipates itself in precipitation of particles on walls of the cyclone and is not transmitted to the gaseous medium.

In connection with the above it is necessary to note one fact, that in passing gas with dust through a VENTURI tube, i. e., in a case where the precipitation of particles on walls does not take place, but the particles are carried away by current, the resistance in the tube does not decrease but increases with the increase of dust concentration. According to FARBAR'S (201) experiments likewise conducted with highly polydispersed dust ($r = 1 - 100\mu$) of 2.45 specific gravity, the proportion noted is:

$$\Delta_p / \Delta_{p_0} - 1 = kc, \quad (29.18)$$

where c is the dust concentration expressed in g of dust per g of air; where k is a coefficient ≈ 0.3 . Theoretical examination of aerosolic flow through a VENTURI tube, based on BERNOULLI'S theorem, also refers to the same equation (29.18) but with a coefficient of 1. Thus in this case the resistance is lower than should be expected. We shall return in § 45 to the problem of the influence of gas with dust upon the resistance.

In conclusion we shall mention a fruitful idea realized in recent years, which involves gases previously enriched with dust and the way of passing them through cyclones. The enrichment is effected in a jalousie-like dust interceptor (202) with the aid of a system of sloping slots, between which a greater part of the gas passes through, while the dust is deflected by the slots and then escapes from the apparatus as a concentrated and gas-dust laden mixture, which is thus routed into a cyclone (figure 34, a). Gas entering the tubular apparatus (203) assumes a spinning motion (as in a cyclone), which

centrifuges dust to the tube's periphery (figure 34, b). In this way one obtains a reduction of the gas volume, which passes through a cyclone; likewise, an increase in dust concentration is effected. The two circumstances increase

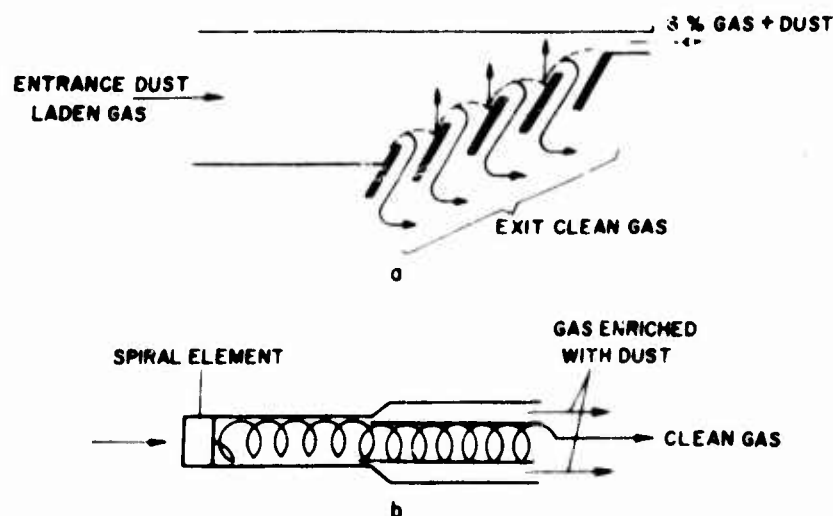


FIG 34 INERTIAL ENRICHMENT OF AEROSOLS

considerably the output and the effectiveness of the purification method by cyclones.

§ 30. Determination of Trajectories of Aerosol Particles in Curvilinear Flow

Smallest aerosol particles follow strictly the lines of flow of a medium, hence, the use of aerosols in experimental hydrodynamics is based upon the afore-mentioned factor. In order to examine the flow of a gas, fine striae of smoke are let into the gas and they follow the lines of flow. The width of the striae, at the same time, indicates the velocity of flow at a given point, in so far as the transfer of velocity to the cross section of the striae remains constant. In this way the distribution of gas velocities is completely determined.

Yet, larger particles emerge from the lines of flow and displace themselves due to their inertia to a larger or smaller extent in relation to the lines in question, wherein the order of magnitude of such displacements, as we shall see in the following paragraphs, is indicated by an inertial path of the particles l_i . The displacement leads to "inertial precipitation" of particles on the walls following a change of direction of the flow, e.g., at the bends of tubes and passages, at points of passing around various obstacles, etc. The inertial precipitation of aerosols is commonly employed in various apparatuses, which are used for separation of aerosols in a dispersible phase

from gases. Inertial precipitation is even the cause of ice formation on various objects as they move through supercooled clouds and fogs; they likewise play an important role in collisions between large particles of an aerosol (see § 54), and therefore they are of great importance in meteorology.

We examined in § 28 and 29 a few examples of inertial precipitations of aerosols in a spinning medium. One could assume from these examples that particles are completely entrained by a medium in the direction of its movement and since they are influenced by a centrifugal force, they move in a perpendicular direction in relation to the medium. Generally speaking, such simplification is admissible provided that characteristic dimensions of a certain system, such as the width of striae or the radius of curvilinear current, etc., are large enough when compared with the l_1 . However, in the precipitation of aerosols upon various obstacles and mountings in places where the current changes its direction rapidly, etc., wherever the indicated condition does not prevail, such simplification is not admissible and it may lead, as we shall explain below (page 185), to fundamental mistakes. In such a case it is necessary to take into consideration not only a normal but also a tangential component of the inertial force as well, i.e., to compute the trajectory of a particle according to differential equations of its motion. These equations, at small Re numbers, take this form:

$$\frac{dV_x}{dt} = \frac{1}{\tau} (U_x - V_x) + \frac{F_x}{m}; \quad \frac{dV_y}{dt} = \frac{1}{\tau} (U_y - V_y) + \frac{F_y}{m}, \quad (30.1)$$

where U_x and F_x are assigned components of the velocity of the medium and of the external force along the axis x . We omitted here analogous equations for coordinates z .

Generally, a solution of such a system of equations presents rather extensive difficulties; it has turned out well only in comparatively few problems. Usually in computing trajectories of particles one has to resort to a method of approximation. Thus one proceeds in the following manner /204, 205, 206/ - (we shall confine ourselves to a fixed flow of a medium). Not disturbing a general principle of the problem, one can assume that $F = 0$, because it is equivalent to a change of the assigned field of flow $U(x, y, z)$ by the field $U + (\tau/m)F$. Let us break up the time into equal, small intervals and the particle's trajectory into corresponding sections, also assuming that for i interval there is approximately

$$\frac{dV_x}{dt} = \frac{1}{\tau} (U_{x_i} - V_x), \quad (30.2)$$

where U_{x1} is a value U_x in the beginning, or, still better, in the center of the interval. If we integrate and assume that in the beginning of the interval $t = 0$ and $V_x = V_{x1}$, we find

$$V_x = U_{x1} + (V_{x1} - U_{x1})e^{-t/\tau} = V_{x1} + (U_{x1} - V_{x1})(1 - e^{-t/\tau}). \quad (30.3)$$

Hence, upon repeated integration we find the coordinates of a particle

$$x = x_1 + U_{x1}t + \tau(V_{x1} - U_{x1})(1 - e^{-t/\tau}), \quad (30.4)$$

where x_1 is the particle's coordinate in the beginning of the interval. The same equations are obtained for the remaining coordinates.

The calculation of a trajectory begins at a point where the velocity of the particle is known. Usually in problems of that kind within a determined range of space, e.g., at a sufficiently large distance from an obstacle or a bend, the movement of the medium may be regarded as rectilinear and uniform and the velocities of a particle and of a medium as identical, if external forces are absent. The velocity of the flow should be known at all points, where the trajectories of particles (in which we are interested) pass through: that is the velocity which is stipulated in theoretical and hydrodynamic equations, or the measured velocity. Beginning with a point, where $V_x = U_x$, we compute subsequently for all coordinates the position and velocity of particles according to equations (30.3) and (30.4) at the beginning of the intervals: 1st, 2nd, 3rd, etc. The exactness of computations increase with a reduction of intervals, yet, simultaneously, the loss of time on calculating increases. Therefore it is expedient to do this work with the aid of computers. In order to estimate the required amount of intervals, we assume that particle velocity increases per Δt time according to (30.2) by $\Delta V_x \approx (U_{x1} - V_{x1}) \frac{\Delta t}{\tau}$ and according to (30.3) by

$$\Delta V_x = (U_{x1} - V_{x1})(1 - e^{-\Delta t/\tau}) = (U_{x1} - V_{x1})\left(\frac{\Delta t}{\tau} - \frac{1}{2}\left(\frac{\Delta t}{\tau}\right)^2 + \dots\right)$$

Inasmuch as both expressions must give close values of ΔV , we arrive at the requirement that $\Delta t \ll \tau$, hence it follows that without impairing practical exactness of the computations one can use instead of (30.3) a more simple equation:

$$V_x = V_{x1} + (U_{x1} - V_{x1}) \frac{\Delta t}{\tau}, \quad (30.5)$$

and instead of (30.4), this equation:

$$x = x_i + V_{xi}t + \left(U_{xi} - V_{xi} \right) \frac{t^2}{2\tau} \approx x_i + V_{xi}t, \quad (30.6)$$

Otherwise at a sufficiently great distance from an obstacle or a bend one can use much larger intervals to shorten the work. Since, in this case $U_x - V_x$ is very small, then, at the same time, the absolute error in computing V_x and x is also very small.

A graphic plotting of particle trajectories is also possible and is especially convenient in case when a velocity of flow is determined in an experimental way, although the graphic method is considerably less exact than the computation method.

§ 31. Theory of Similarity in the Mechanics of Aerosols (207 - 209)

The method described in the preceding paragraph and relevant to an approximate computation of trajectories of aerosol particles enables us to work out a problem within a fixed range of the system, as well as within the range of velocity of flow and it includes even particles with a certain time of relaxation. If we had to do this computation over again on behalf of other values of such dimensions, the method, practically speaking, would be useless; yet, thanks to the theory of similarity the results obtained in this manner assume general values. The theory of similarity also plays an important role in development and application of results of experimental research in the field of motion and precipitation of aerosol particles with regard to modulation of various apparatuses used for separation of the dispersed phase of aerosols, etc., and not only in instances of inertial precipitation, but also in diffused, electrostatic and other precipitations. Thus, the importance of the theory of similarity in the mechanics of aerosols is extremely great.

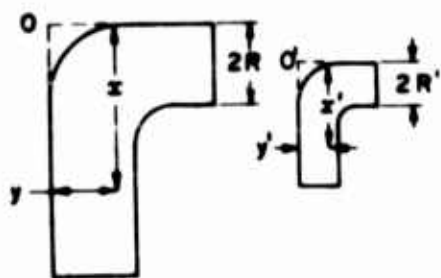


FIG. 35 GEOMETRICAL SIMILARITY

In order to make the motion of two aerosolic systems similar, it is necessary to have:

1. A geometrical similarity of the area of separation (by walls, etc.) regions, where the motions take place (figure 35);
2. A similarity of the medium's motion within the systems;
3. A similarity of the movements of every particle.

A geometrical similarity of both systems is expressed by equation

$$x/x' = y/y' = R/R' = C_1, \quad (31.1)$$

where x and y are coordinates of any point within the first system;

where x' and y' are coordinates of pertinent points within the second system;

where R and R' are values of specific linear dimensions of both systems, such as tube's radius, half-diameter of streamlined body, etc.

For purposes of similarity of the medium's motion within both systems it is above all necessary to maintain kinematic conditions:

$$U_x/U_{x'} = U_y/U_{y'} = U_0/U_0' = C_u, \quad (31.2)$$

where U_x , U_y and $U_{x'}$, $U_{y'}$ are components of velocity at pertinent points of both systems;

where U_0 and U_0' are constant characteristic velocities of a flow within the systems, e.g., a mean velocity of flow in a tube, or a velocity at an infinitely great distance from a streamlined body.

Analogous equation resulting from the similarity of particles motion within both systems is as follows:

$$V_x/V_{x'} = V_y/V_{y'} = C_v. \quad (31.3)$$

In parts of the systems, where a medium moves uniformly in a straight line, while the external forces equal zero, velocities of the medium and particles coincide, i.e., $V_x/V_{x'} = U_x/U_{x'}$; it follows hence, that $C_v = C_u$.

Furthermore, the pertinent moments of time in both systems are combined by way of the equation

$$t/t' = C_t, \quad (31.4)$$

and then, since $U_x = dx/dt$, the following correlation occurs:

$$C_u = C_l/C_t. \quad (31.5)$$

Similarly we have for pertinent accelerations

$$\frac{dV_x}{dt} \bigg/ \frac{dV_{x'}}{dt'} = \frac{dV_y}{dt} \bigg/ \frac{dV_{y'}}{dt'} = C_a, \quad (31.6)$$

upon which

$$C_a = C_u / C_t. \quad (31.7)$$

As is known from hydrodynamics, a dynamic condition of similarity in movements of a medium within two geometrically alike systems appears in the equation

$$U_o / U'_o = C_u = \frac{\eta / R \gamma_g}{\eta' / R' \gamma'_g} \quad (31.8)$$

or even in

$$\frac{2U_o R \gamma_g}{\eta} = \frac{2U'_o R' \gamma'_g}{\eta'} = Re_f = \text{const.} \quad (31.9)$$

Naturally, all the afore-said does not depend upon the law of a medium's resistance.. If the resistance is proportional to velocity, then differential equations of the particles motion assume this form (30.1). If the discussed equations are referred to the first system, then, to find pertinent motion in the second system, we must substitute in these equations all variable values by their expressions resultant from the equations (31.2) and (31.6).

If we designate by "a" the acceleration influenced by external forces F/m , we obtain

$$C_a \frac{dV'_{x'}}{dt'} = \frac{C_u}{\tau} (U'_x - V'_{x'}) + C_a a'_x \quad (31.10)$$

or

$$\frac{dV'_{x'}}{dt'} = \frac{C_u}{C_a \tau} (U'_x - V'_{x'}) + a'_x. \quad (31.11)$$

Inasmuch as a differential equation of the particle motion in the second system must assume a form of

$$\frac{dV'_{x'}}{dt'} = \frac{1}{\tau'} (U'_x - V'_{x'}) + a'_x, \quad (31.12)$$

then, in so far as similarity of the particle motion within both systems is involved, it is necessary, that the particles' relaxation time in the second system τ' becomes combined with τ by the equation

$$\tau' = \frac{C_a}{C_u} \tau = \tau/C_t, \quad (31.13)$$

since this follows directly from the (31.4) anyhow. If we take under consideration that $C_t = C_l/C_u = RU'_0/R'U_0$, we can write equation (31.13) in the following way:

$$\frac{\tau U_0}{2R} = \frac{\tau' U'_0}{2R'} = \text{const} = \text{Stk} \quad (31.14)$$

or

$$\frac{l_i}{2R} = \frac{l'_i}{2R'} = \text{Stk}. \quad (31.15)$$

A non-dimensional ratio of an inertial path of the particles and the system including characteristic dimensions is known as a "STOKES' number" (Stk). If according to conditions of a problem $a = a'$ (e.g., if F is a gravitational force and $a = g$), then $C_a = C_u^2/C_l = 1$, $U_0^2/R = U'_0{}^2/R'$, which can be written down in the form of

$$\frac{U_0^2 g}{2R} = \frac{U'_0{}^2 g}{2R'} = \text{const} = \text{Fr (FROUDE'S number)}. \quad (31.16)$$

If an Re number characterizing a pertinent movement of a particle and a medium is large and the medium's resistance is not proportional to the velocity, then the application of the theory of similarity is complicated and it becomes unsuitable, except in case when a medium's flow is rectilinear and uniform (see § 18).

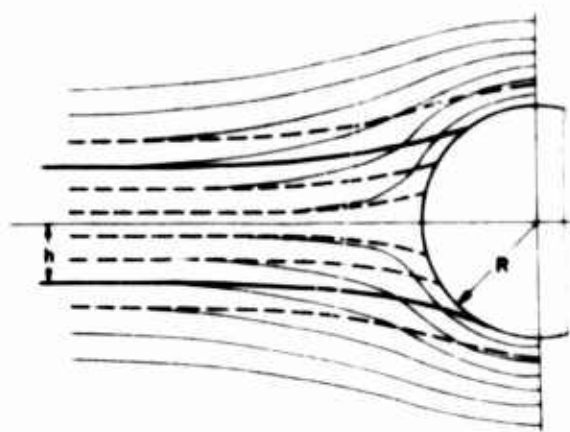


FIG. 36 INERTIAL PRECIPITATION OF PARTICLES AND THE COEFFICIENT OF PRECIPITATION

Thus, it appears that a condition of similarity for the motion of two aerosolic systems is the equality of two non-dimensional values, i.e., that of REYNOLD'S number and STOKES' number and, if gravitational forces are included, also FROUDE'S number in both systems.

If there is laminar flow through tubes, passages, etc., the similarity of the medium's motion in geometrically alike systems is fulfilled automatically regardless of the Re_f value involved in the flow, provided that the Re_f value is

below its critical point. The similarity of the medium's motion is also attained when a sphere is circumflowed at small Re_f numbers and likewise, when a sphere and a cylinder are circumflowed at large Re_f numbers, if the existence of bordering stratum could be disregarded (see § 34).

The most important problem in the mechanics of aerosols is how to detect the conditions among particles precipitating¹ upon walls, streamlined bodies, etc. A proportion of the number of particles precipitating upon a body, as compared with the number of particles, the centers of which would pass through a body if they were in a straight forward movement at all times, we shall name a "coefficient of precipitation" (Φ) of particles upon a streamlined body resulting from a rectilinear flow (figure 36). In order to find Φ , one must determine the outer trajectories of particles, where the centers of particles still come in contact with a body. If we denote by h the distance from the boundary trajectories to the central lines of flow (directed toward the center of a sphere, toward the axis of a cylinder, etc.) at an infinitely great distance from a body, then in a case of a cylinder $\Phi = h/R$ and in case of a sphere $\Phi = (h/R)^2$. Thus, according to the afore-said, Φ depends solely upon Stk number in case of inertial precipitation.

Yet, it follows from the appearance of the streamlines in an ideal and viscous flow around bodies (see figure 45 on page 191), that in the first instance at the same Stk value the coefficient of precipitation must be larger than in the second instance, because in an ideal flow the streamlines curve around the body at a much closer distance and they buckle more sharply than in viscous flow. It is not difficult to become convinced that the presence of the boundary line's laminar stratum on the surface of a streamlined body causes a decrease of Φ ; inasmuch as with a decrease of velocity of flow the distance between the streamlines increases, then as a result of a comparatively low velocity of flow in a boundary stratum the streamlines are drawn away from the surface of a body. As far as the reduction Re_f and along with the latter an increase in depth of a boundary stratum is concerned, the coefficient of precipitation appropriate to a certain value of Stk is continuously reduced, until it reaches a circumfluent value appropriate to a viscous region (the problem is discussed in more detail in § 34).

-
1. We shall name a movement of particles influenced by a constant external force and particularly by a gravitation force - settling and deposition of particles upon the surface of various bodies - precipitation.

In a case, where it is impossible to disregard the influence of a gravitational force, one should also take into account the condition of (31.16). If we combine the latter with the condition for (31.15), we obtain

$$\frac{4Stk}{9Fr} = \frac{2\gamma r^2 g}{9\eta U_0} = V_s/U_0 = \text{const.} \quad (31.17)$$

If particle inertia can be disregarded, the only remaining condition (31.17), to which a fraction of particles would accordingly precipitate in a system of a certain geometrical form depends solely upon the proportion of the rapidity of the particles settling as compared with the velocity of flow. We found a specific instance in § 26, i.e., the effectiveness of precipitation in a horizontal tube is a function of $LV_s/2h\bar{U}$; where L is a length, and $2h$ is the height or a diameter of the tube. Thus, the efficiency of precipitation in geometrically alike tubes depends only upon the ratio of V_s/\bar{U} .

Having computed (as shown above) or determined experimentally a value of Φ in the Stk function involving a predominant value of inertia, or in the function of V_s/\bar{U} involving a predominant force of gravity, we may be in a position to find a value of the precipitation coefficient for particles of any aerosol at any velocity of flow including bodies of a specific shape under one condition only: that of similarity of flow.

If in contrast to cases just examined a distribution of velocities in a current depends also upon an Re_f number, then one can only differentiate between the systems with identical Re_f , e.g., with the same ratio of depth of boundary stratum to diameter of body. At the same time the opportunity for adapting the theory of similarity becomes considerably reduced. Consequently, if only the particles' inertia is considered, the combination of conditions in (31.9) and (31.15) offers $Re/18 Stk = R^4 \gamma_g / r^2 \gamma = \text{const.}$, or, when an identical composition of a medium and dispersible phase in the systems are compared, then it follows:

$$r/R = \text{const.} \quad (31.18)$$

Hence, the movements of aerosol particles will be similar only if the magnitude of the particles is proportional to the linear dimensions of the system and the efficiency of precipitation in such a case becomes a function of two ratios: $l_i/2R$ and r/R .

It seems strange that this condition (31.18) was brought about while calculating the influence of geometrical sizes (not that of a mass!) of particles upon a value of Φ . Up to this moment we assumed that a particle precipitates at such a point, where a trajectory of its center meets the surface of a body.

In actuality, however, this occurs when the particle center approaches a surface at a distance equal to the particle radius (a "contact" effect). This effect considerably increases the Φ during precipitation of aerosol particles upon very thin cylindrical bodies (fibers) or upon other aerosol particles. One can imagine without any effort that in order to maintain similarity in precipitation of particles, while taking into account a "contact effect", it is necessary to maintain the condition of (31.18).

Without regard to geometrical form of the system and the region of flow, the effectiveness of inertial precipitation Φ_i increases with $l_1/2R = \tau U_0/2R$, while the effectiveness of precipitation under the influence of gravitational force Φ_g increases with $V_g/U_0 = \tau g/U_0$. Thus in both instances the dependency of Φ is affected identically by properties (size and density) of every particle and of the viscosity of the medium, since both are included in the expression for τ . However, the matter of dependency of Φ differs with the linear dimensions of the R system and with the velocity of flow U_0 . Φ_i expands with the increase of U_0 and with a decrease in R (while geometrical similarity of the system is maintained); Φ_g does not depend upon R and it decreases while U_0 increases. These rules, which will be explained by a few examples, are very important in everyday life and in technical procedures as well.

It is a known fact that in supercooled aqueous fogs narrow objects, as thin twigs, conductors, etc., become very strongly ice-coated (figure 37 shows a schematic illustration of the cross section of ice-coated blades of grass at a tree trunk). The ice formation becomes intensified with the increase of droplets sizes and wind velocity, since it attains a particularly great magnitude on frontal edges of wings and screw propellers of aeroplanes. If we consider dust settling on horizontal surfaces (i.e., under the influence of a gravitational force), this phenomenon assumes an inverse procedure in areas where the velocity of air movement is slow.

Coarse dust inhaled along with dusty air settles in the upper respiratory tracts and fine dust which enters the lungs is particularly dangerous.

During sandstorms minute particles of sand easily pass through cracks in windows and doors, therefore it is impossible to seek shelter from dust even at home.

Rain to a certain degree purifies the atmosphere from coarse dust, but it has little effect upon very minute particles filling the air (heavy ions).

In conclusion, we shall mention a problem important from a practical standpoint, i.e., that of adjustment of cyclones, which was explored mostly by Soviet authors in two ways. S. SYRKIN (207) and P. VOLKOV (210) became influenced by these considerations: that if constancy of Re_f number is maintained during adjustment one can decrease the velocity of flow and the dimensions of a cyclone as well by merely excluding the gaseous medium and changing over to water, in which case η/γ_g is 15 times smaller than in the air and therefore the $U_0 R$ could be decreased that many times. Consequently the authors worked on a cyclone principled by water adjustment.

P. KOUZOV (192) progressed with the assumption of similarity of gaseous flow in cyclones. When Re_f values are very high (characteristic in cyclones), the movement of a medium becomes more or less "self-modeling", i.e., independent of Re_f . According to KOUZOV'S non-

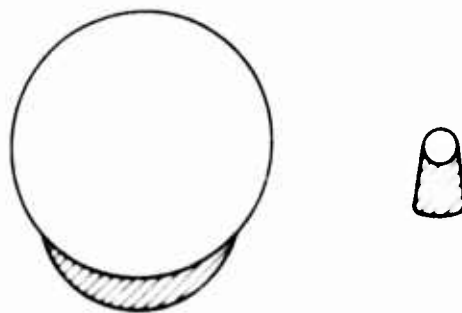


FIG 37 ICE COATING DUE TO INERTIAL PRECIPITATION

dimensional characteristics obtained for cyclones of the tested type, i.e., according to values of the cyclone's effectiveness in functions of Stk and Fr numbers, one can theoretically calculate the effectiveness with the aid of a certain size of cyclone, then by velocity of flow and by characteristics of aerosol. It is regrettable that in KOUZOV'S tests just the overall effectiveness of precipitation was determined and not the effectiveness of individual parts of dust. A mean radius of highly polydispersed dust was used for a radius of particles with the Stk number expression. For this reason it is difficult to use these data to compare the theory of a cyclone by test. Generally speaking, there are not in existence any essential and reliable data in literature, because they would require that experiments be conducted with more or less monodispersed dusts, which is a rather difficult thing to accomplish due to the large quantities of dust needed for work on cyclones.

§ 32. Theory of Procurement of Aerosol Specimens

Every research in aerosols begins with obtaining samples with one or another type of apparatus such as filters, condensers, TYNDALL'S meter, ultramicroscopic cell, etc. To obtain accurate results, it is essential that the difference in concentration and distribution of particles sizes in the original aerosol and in the sample be as small as possible. The difference in question is caused partly by precipitations of aerosols in the sampling apparatus, partly in the tube through which aerosol enters the apparatus, and

partly by phenomena occurring at the intake opening to the apparatus (beginning of the intake tube). The precipitation of aerosol particles in the intake tube, as well as other parts of instruments, is discussed in §§ 26, 39 and 46; however, we shall pause only at the first stage of sample taking, which occurs at the entrance to the apparatus.

In taking samples of a flowing aerosol it is necessary to fulfill the following conditions. If intake tube is positioned at an angle to the current's direction (figure 38, a and 39, d), some particles, due to inertia, will precipitate on the inner wall of the tube and the concentration of aerosol in a

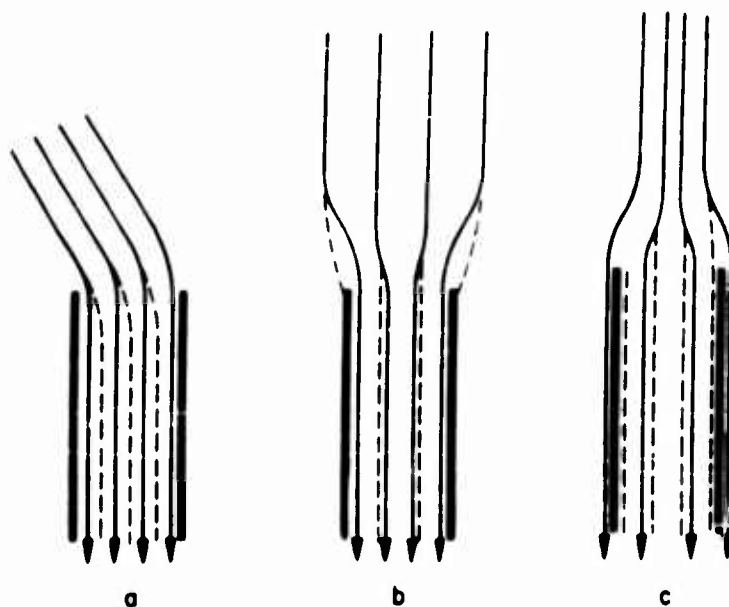


FIG. 38 VARIOUS METHODS OF AEROSOL SAMPLING

specimen will be lower than the actual one. If an intake tube is positioned in a parallel line with a current, but velocity of flow in the tube is either higher (figure 38, b, and 39, c) or lower (figure 38, c, and 39, b) than in the main current, then, in the first instance, no particles will get in from the outer streamlines of the current entering the tube and in the second instance, the particles getting in will be those from the closest outer streamlines of current passing the tube. Consequently, in the first instance the concentration of aerosol in a specimen will be lower and in the second case, it will be higher. In an accurate ("isokinetic") probe sampling (figure 39, a) the velocities of flow in the tube and in the main current must be equal. Furthermore, the tube's walls at the inlet opening must be sufficiently thin in order to bar precipitation of particles at the face of the tube.

In the theory of taking probe samples of an aerosol precipitating under the influence of a constant force (e. g., gravitational force) the following

practical procedures (211) are correct when the particles' inertia can be disregarded, i. e., according to the afore-mentioned (page 175) statement at a low velocity of flow at the time of probe sampling:

1. No current in a cloud of sedimenting non-inertial particles with a uniform initial concentration can change this concentration¹ (at a sufficient distance from cloud's boundary lines). This situation becomes obvious considering non-sedimenting particles, because they behave like molecules of the

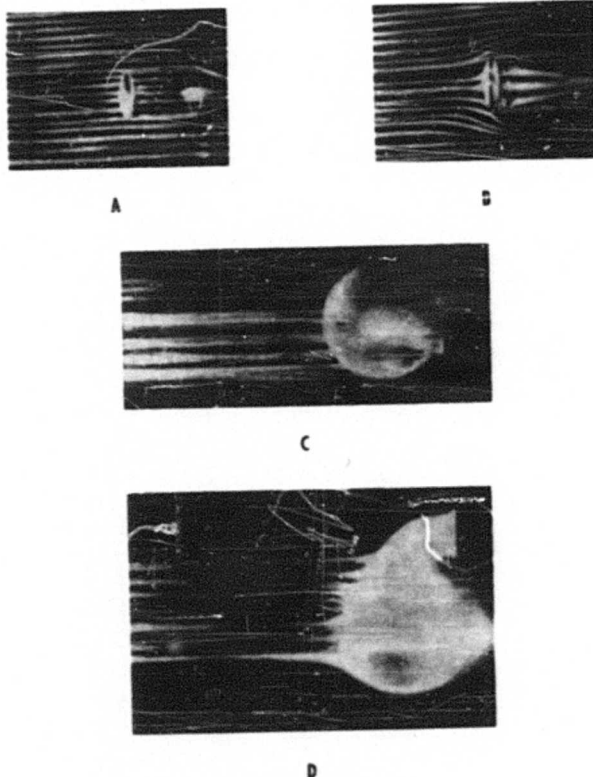


FIG. 29 PHOTOGRAPHS OF FLOW LINES DURING PROBE SAMPLING

medium. Settling of particles with a velocity V_s is equivalent to a settling of the entire cloud with the same velocity, because its inside concentration does not change. Settling in a polydispersed cloud disturbs the uniformity of concentration only at the upper and lower boundary lines of the cloud.

1. Naturally, if inertia is involved, this situation is incorrect. Thus, the particles' concentration in an eddy tube will be reduced.

2. In a sedimenting noninertial cloud the number of particles passing in 1 sec. through a certain immobile place, whose horizontal projection takes up an area S , is equal to the number of particles which would pass through the place in the absence of settling, plus the number of particles which would pass the place in the absence of the medium's movement, i. e., at $V_g S$. The above situation results when the entire velocity of particles in a cloud of that type is equal to the vectorial sum of the medium's velocity combined with rapidity of settling in an immobile medium.

Here especially the effect is such, that in taking aerosol samples with the aid of a small horizontal tube from cells, rooms, etc., if the particles' inertia could be disregarded, accurate results must be obtained. But in taking samples with the aid of a small vertical tube set upwards, the concentration of aerosol in a sample will be larger than the actual one by $1 + (V_g/\bar{U})$ times; where \bar{U} is a mean velocity of flow in the tube.

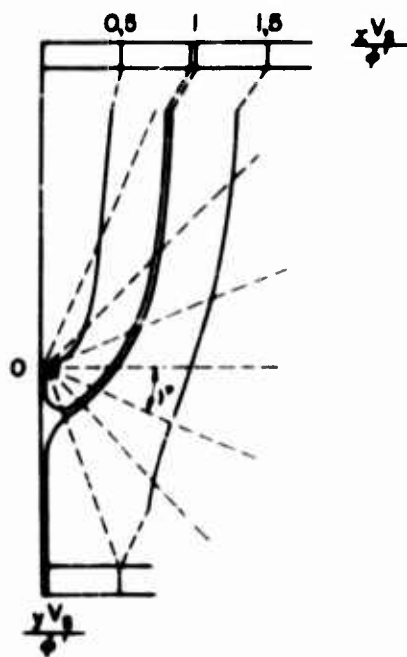


FIG. 40 SAMPLE TAKING IN AN INFINITELY NARROW HORIZONTAL SLIT

The conclusion concerning aerosols sucked-in horizontally would be beneficial if subjected to a test on a concrete example, such as suction through an infinitely long horizontal slot in an infinitely narrow vertical wall¹. In this case it is possible to assume the lines of flow as straight lines (figure 40) and the velocity of flow as equal to $\Phi'/\pi\rho$; where Φ' is a gas volume, sucked in one sec. per cm of the length of slot and where ρ is a distance from the slot. If the particles' inertia could be disregarded here, the components of their velocities would be equal to

$$V_x = -\frac{\Phi'x}{2}, \quad V_y = -\frac{\Phi'y}{2} + V_s. \quad (32.1)$$

1. A similar task is in suction of aerosol through a perforated opening, as discussed by DAVIES (212).

Hence, for the particles' trajectories one can calculate this equation:

$$(x_0 - x) V_s / \phi' = \varphi / \pi, \quad (34.2)$$

where the value of φ angle is shown on figure 40; x_0 denotes initial coordinate of a particle (at $y = -\infty$). At $x_0 V_s / \phi' < 1$ particles are sucked in and at $x_0 V_s / \phi' > 1$, they fall out by the slit. Thus, particles falling into the slit are primarily those found in a stratum adjacent to the wall; the stratum's depth is $\Delta = \phi' / V_s$. At $y = -\infty$ across a horizontal strip 1 cm wide, directed along the axis x , pass, per one sec. $N = n V_s \Delta$ sedimenting particles, which belong to the afore-mentioned stratum (n is the aerosol's concentration). Of course, the concentration in a sample is equal to $N / \phi' = n$, i. e., to the initial concentration.

Figure 40 shows, that in the presence of inertia, particles, which move near the boundary trajectory to the latter's left, will tend to escape from non-inertial trajectories and will not get into the slit, but will either settle on a wall near the slit, or drop below. Thus, a total effect of sedimentation and inertia leads to a decrease of concentration in a sample, while separately neither sedimentation nor inertia will cause such a decrease.

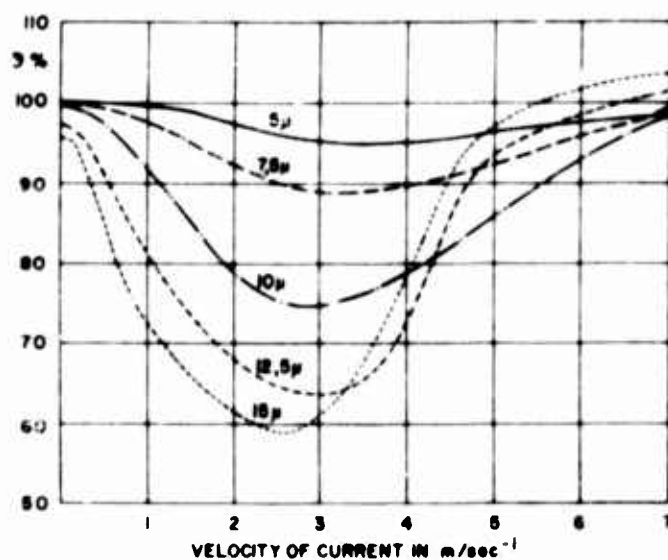


FIG 41 EFFICIENCY OF SAMPLING AEROSOLS FROM A CURRENT

Naturally, the effect discussed here decreases as we pass to a slit with $2h$ as its final width. One can get a rough idea about the magnitude of the effect in the following way. As particles move upward, they displace themselves downward from the noninertial trajectories to the extent of \bar{V} ; where \bar{V} is the mean velocity of the particles moving upward and being on the order of

magnitude: V_g . Thus the comparative amount of particles lost is $\approx V_g T/2h = gT^2/2h$, which is in agreement with the effectiveness of the sampling.

$$\beta \approx 1 - \frac{gT^2}{2h} \quad (32.3)$$

Considering the aerosol in question, i.e., with a given T , the error will be inversely proportional to the height of the entrance. It is important in correct sampling to consider the efflux of particles, especially those which enter near the edges of the opening at noninertial trajectories and therefore the greater the ratio of the area of opening to its perimeter, i.e., the larger the opening, the smaller the error will be.

The problem of interdependence between the effectiveness of samples taken from a current and the velocity of the latter at a constant suction velocity was examined in detail in an experimental way. Figure 41 shows the results of MAY'S (213) tests: fogs having variable dispersions were conducted with different velocities through a horizontal aerodynamic tube and then through a 6 mm round opening which was positioned at an angle of 45° to the horizontal, they then were sucked in with a velocity of $6 \text{ m} \cdot \text{sec}^{-1}$ (see figure 39, d). Illustrations showing the suction of aerosols through a tube set up facing a current (214) have the same appearance. Figure 41 shows that in taking samples in a calm air, practically a 100% efficiency is obtained. As the current velocity increases, the efficiency at first declines, then it increases and again attains its 100% under isokinetic conditions. This can be explained by the factor that while samples are taken from motionless air the streamlines are rectilinear or slightly convex toward the axis of flow, consequently no inertial losses occur. If samples are taken from a current, the lines of flow at a certain distance from the intake opening assume a concavity toward the axis, wherein their curvatures increase at first as the velocity of flow becomes accelerated and then the losses of particles also increase. With a continued increase of flow velocity concavities in the flow lines begin to decrease and thus they reach zero at the time of isokinetic sample taking.

The fact that particles of various sizes according to the value of β are not arranged in the same order on figure 41 can probably be explained by inaccurate measurements. A 100% efficiency is on the average attained with a current velocity exceeding the velocity of suction; this is explained by the retarded action of the current near the instrument into which the sample is sucked in. The exact concurrence of these velocities can be controlled with a 100% effectiveness only while using a long and narrow sampling tube with very thin walls.

§ 33. Slit Instruments

During research in aerosols and especially work in hygienics, slit instruments are widely used for precipitation of particles (215). An aerosol is allowed to enter these instruments with a velocity on the order of $100-200 \text{ m} \cdot \text{sec}^{-1}$ and then it passes through a flat slit or a round opening, behind which a glass plate is set up perpendicularly to the current. As the flowing aerosol leaves the slit, it collides with the plate, spreading over it. Due to inertia particles come out of lines of flow and precipitate upon the plate. A deposit left in a form of straight line or a round spot is examined under a microscope. In order to improve the stickiness of solid particles to the plate, the latter is coated either with glycerin, or with a combination of colophony and castor oil, polyisobutylene, etc., or high humidity is developed in the instrument's chamber by using wet paper; with adiabatic expansion of gas escaping from the slit, moisture condenses on particles and promotes their sticking. If a glass plate is substituted by a slowly spinning PETRI dish, coated with a nutrient agar, a convenient instrument is obtained for purposes of determining the number of aerosol particles in 1 cm^3 of air containing various types of microorganisms (216).

At the time of impingement a precipitation takes place at the bottom of a test tube containing water. An aerosol is conducted through a tube having a drawn-out end, which reaches to several mm from the bottom of the test tube. As

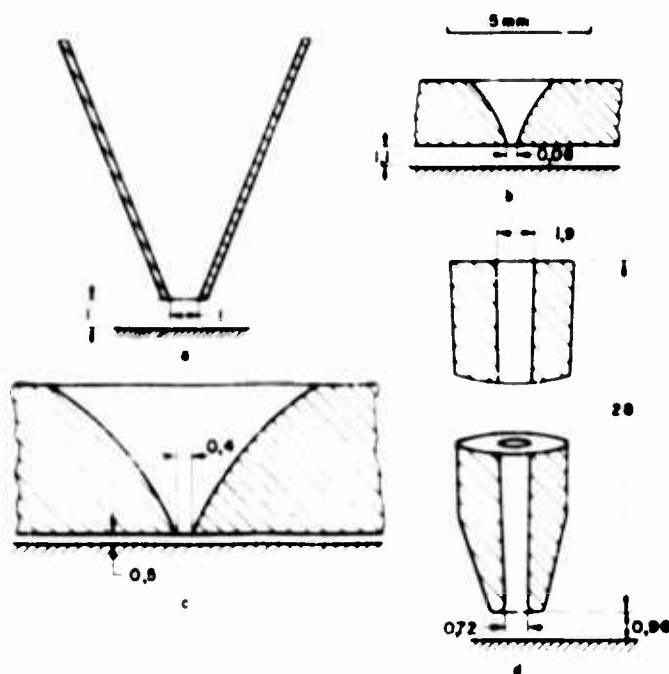


FIG 42 DESIGNS OF VARIOUS SLIT INSTRUMENTS

the aerosol passes through, gas forces water out and the bottom of the test tube becomes exposed, whereupon particles colliding with a moistened glass surface are wetted. Particles which don't precipitate after colliding against the bottom of the test tube probably get entrapped anyhow during the time the gas bubbles pass

through a layer of water. The examination of particles is in this case with a suspension obtained as described.

The walls of the slits are made either flat (figure 42, a), as e.g., in MAY'S (217) impactor, or rounded, as e.g., in OWEN'S (218) instrument (figure 42, b), or BAUSCH and LOMB instrument (figure 42, c). If the opening is round, the walls are made conical as e.g., in KOTZE'S instrument (figure 42, d). As we shall see below, the design of the slit in some instances shows a substantial influence in the work the instrument performs. The proportion of slit's plate distance to the slit's width is in various instruments equal to 1.0 - 2.0, which, according to data of many authors, does not influence noticeably the effectiveness of precipitation.

The only attempt at exact calculation of the particle movement in slit instruments is attributed to DAVIES (219). In this he assumed that the length of a slot is infinitely great in comparison to its width of $2h$, that the flow everywhere is ideal, and that inside the slit and above the plate, at a sufficiently large distance from the slit, the current is rectilinear and is parallel to the walls when at all cross sections of the flow a constant velocity prevails (i.e., when a boundary stratum is non-existent). Subsequently a field of flow was determined and the following dependence between the proportions was particularly established: $\beta = d/2h$ and $a = h/\Delta$; where d is a distance from the slit to the plate; Δ is a depth of flow at an infinitely greater distance from the slit (figure 43):

$$2\beta = \frac{(a^2 + 1) \ln(a + 1)}{\pi a^2 (a - 1)} + \frac{1}{a} \quad (33.1)$$

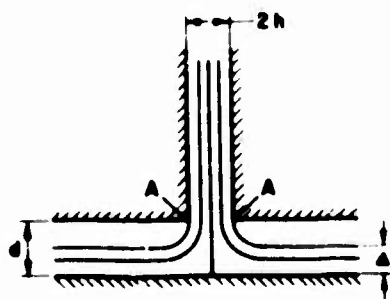


FIG. 43 FIELD OF FLOW IN A SLIT INSTRUMENT

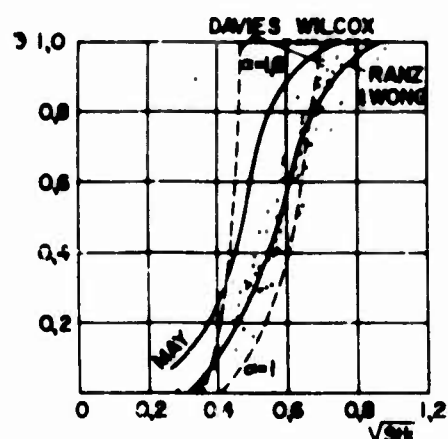


FIG. 44 EFFECTIVENESS OF SLIT INSTRUMENTS

Furthermore, according to the approximate computations' method, discussed in § 31, trajectories of particles and effectiveness of precipitation

were calculated with the function of $Stk = l_1/2h$ for $\alpha = 1.0; 1.6; 2.5$ and 5.0 . Figure 44 shows curves for $\alpha = 1.0$ ($\beta = \infty$) and $\alpha = 1.6$ ($\beta = 0.8$), as well as data obtained in other theoretical and experimental researches, which we discuss below. On the axis of abscissae a value $\sqrt{Stk} = \sqrt{l_1/2h}$ is plotted, which is proportional to particles' radius. As DAVIES' curves indicate, there are critical values of STOKES number (Stk_{cr}), below which a precipitation in a slit instrument equals zero. Thus, for $\alpha = 1$, the $Stk_{cr} = 0.16$ and for $\alpha = 1.6$, the $Stk_{cr} = 0.12$. These Stk_{cr} values approximate the ones obtained in an experimental way (see below). Yet, while computing particle movement along the central (passing through the axis of the slot) line of current, DAVIES encountered the value of $Stk_{cr} = 0.32$, which coincides with L. LEVIN'S (220) value of $1/\pi$, obtained by an analytical method (see page 195), although it differs sharply from the experimental value. A similar divergence is also found with critical points for other α . The reason for the discrepancy is rather difficult to explain.

We shall attempt to calculate the effectiveness of particle precipitation in a slit instrument by the following primitive method: let's assume that $\Delta = h$, next that velocity of current U_0 is constant along the cross section of the flow in its entire extent, and that the streamlines of the current on curves form arched circles the centers of which are at points AA (see figure 43). Therein we assume that the tangential velocities of a particle and a medium coincide. The particle velocity is considered normal with the velocity of the streamlines of the current being $V_\rho = U_0^2 \tau / \rho$; where ρ is the curvature of radius of the streamlines of the current, which, within dt -time period, becomes displaced proportionally to the medium at the distance $d\rho = V_\rho dt$ toward ρ , or at the distance $dz = V_\rho \sin \varphi dt$ toward the plate. Considering that the entire displacement of particle proportionally to the medium within a time period of the movement over the curvature is small, i.e., when ρ is constant, we shall obtain the following value¹ for a component of the displacement toward the plate.

$$\Delta z = \int \frac{U_0^2 \tau \sin \varphi}{\rho} dt = U_0 \tau \int_0^{\pi/2} \sin \varphi d\varphi = U_0 \tau = l_1. \quad (33.2)$$

Thus, for the effectiveness of precipitation the following simple expression is used:

$$\mathfrak{Z} = l_1/h = 2 Stk. \quad (33.3)$$

1. In WILCOX' (221) work there is erroneous expression $\frac{\pi}{2} l_1$ derived for Δz

Although in case of larger Φ the equation (33.3) conforms more or less with the experimental data, yet it has a large principal drawback: according to the equation, critical STOKES' numbers do not exist and this fact is inconsistent with the afore-mentioned exact conclusion, as well as with the experimental data (see below). It is not difficult to find the reason for this error: at small Φ and Stk values, the precipitation proceeds only from current's streamlines nearest to the slot's axis, i.e., the streamlines which pass close to the stagnation point, where the current's velocity is considerably reduced and the inertial displacement of the particles outside the streamlines of the current is insignificant. Speaking of the current's reduced field, the velocity of the current along such lines and the inertial displacement are rather great. Thus, if the current's streamlines are distant from the slit's axis, the reduced field of the current approximates the actual one and our primitive computation thereby becomes more or less exact.

As we proceed to experimental data about the effectiveness of slit instruments, it is necessary to remember that in order to compare such data with the theory one can only use the results of tests in precipitation of fogs, because many complications arise in tests with solid particles and this we shall discuss later. Apparently the most exact tests are those of RANZ and WONG (222) with rather monodispersed glycerine fogs, whose particles' radii varied in different tests from 0.17 to 0.69 μ . The width of the flat slits equalled 0.2-0.7 mm, that of the round openings - 1.0 to 1.9 mm and the velocity of current in the slit was 10-180 $m \cdot sec^{-1}$. The magnitude of the ratio of $d/2h$ varied within a range of 1-3 and did not influence the results noticeably. Figure 44 illustrates the results of tests with flat slits (experimental points and the curve plotted over the latter). The value of ~ 0.11 was obtained for Stk_{cr} . If abscissae of all points on the curve were reduced 1.5 times for a flat slit, one could obtain a rather exact curve for a round opening, which thus offers a greater effectiveness than a flat slit with the same width.

MAY'S (217) tests were conducted with the aid of a cascade-type impactor, having four slots which gradually decreased in width, through which the aerosol passes from one slot after the other and as the current's velocity increases, all the finer fractions are intercepted. Figure 44 shows the results obtained in the third cascade of 1 mm wide slit, at a current's velocity of 50 $m \cdot sec^{-1}$. One can visualize from the curve of the effectiveness of the precipitation, as submitted in MAY'S article, that the Stk_{cr} should come close to 0.06 in each cascade as a function of the sizes of droplets which approximate this magnitude (see figure 44). Yet, MAY himself does not refer to it and traces his curve (Φ , Stk) arbitrarily over the original coordinates.

In most of the tests performed on slit instruments only the smallest sizes of particles were determined, i. e., particles which at a certain velocity of the current (the smallest values of Stk for $\Phi = 1$) fully precipitate in the instrument. The results of lengthy tests of WILCOX (221) conducted on variously constructed instruments with 0.25-6 mm wide slots and provided with a current velocity of 2.2-174 $m \cdot sec^{-1}$, offer, as is evident from figure 44, a wider scope and at the same time they disclose some existent dependence among Stk values, since they conform with complete precipitation within the region of the instrument's work, which is a rather difficult one.

Furthermore, it follows from figure 44, that the concurrence is rather poor between the theoretical and experimental curves concerning the effectiveness of slit instruments as well as between the test data of various authors. At present it is difficult to indicate the basic reason for these deviations. A characteristic distinction between the theoretical and experimental curves lies in that the latter noticeably bend to the right at greater values of Φ , which means that particles in movement along current's streamlines farthest from the axis of the slot precipitate the least; therefore the afore-quoted theoretical computations are inapplicable on their behalf. In all probability this is explained by eddies, which inevitably develop at the open surface of the flow and at the latter's exit from the slot, causing erosions on the surface.

The effectiveness of slit instruments employing solid particles of aerosols may be considerably reduced, as precipitated particles are blown off the slides. Since the working conditions of these instruments allow the large particles to be blown away easier than the small ones, there exists in addition to a lower also an upper range of sizes of particles entrapped in the instrument. Thus, according to observations of TS. PIK and SHURCHILOV (223), the maximal radius of particles of Carborundum dust intercepted in OWEN'S instrument is equal to 1.8μ without any moistening process and to 3.7μ with a moistening process. According to JORDAN'S (224) tests, conducted with the instrument shown on figure 42, a, quartz particles with $r = 2\mu$ and 1μ are the first ones visibly blown off a dry glass slide at an air velocity in the slot of 60 to 150 $m \cdot sec^{-1}$. The blowing-off effect produced in instruments with a round opening has a curious appearance: around a thick center of sedimentation in the diameter on the order of 1 mm, which forms opposite the very opening, one can frequently see an eroded ring of 5-10 mm in diameter formed of particles blown off the center of sedimentation and deposited at the place where current's velocity has sufficiently decelerated (225).

The blowing-off effect of particles in OWEN'S instrument is particularly substantial (see figure 42, b), because the air velocity in the

latter is rather high ($300 \text{ m} \cdot \text{sec}^{-1}$); even particles with $r = 0.5 \mu$ are visibly blown off. The blowing-off effect is considerably reduced (218) in the instrument of BAUSCH and LOMB (see figure 42, c) at the air velocity of approximately $150 \text{ m} \cdot \text{sec}^{-1}$.

Apparently the best way of combatting the blowing-off effect is by coating a plate with a sufficiently viscous and sticky composition. In this way one can practically eliminate any blowing-off effect of particles of coal dust with a radius up to 4μ at a current velocity in the slot between $200 - 300 \text{ m} \cdot \text{sec}^{-1}$. Without coating, particles with $r = 4 \mu$ under similar conditions are completely blown off. The method of moistening the air provides considerably worse results than does the coating, not only with regard to coal, but also pertinently to hydrophilic quartz dust (218).

Another feature of slit instruments is the secondary phenomenon of breakup of particles, as they impact on the plate's surface. This phenomenon is observed among particles of $5 - 10 \mu$ in diameter and of such solid and friable substances as quartz and orthoclase (226). It is interesting that much softer and flaky particles, such as spores of plants, remain intact at the same time.

In processing dusts containing aggregated particles one can notice that they are split by air current prior to their collision with a plate. The evidence that aggregates actually are fractured before they collide with the plate, was substantiated by DAVIES in the following way (216). As coal dust was let through a 0.4 mm slot without a plate, a calculated concentration of dust was determined (by means of a thermoprecipitator), as well as the distribution of particles sizes up to and past the slot. Dust remained unchanged at a velocity of $50 \text{ m} \cdot \text{sec}^{-1}$ and at $170 \text{ m} \cdot \text{sec}^{-1}$ the number of small particles increased considerably, while that of large ones - decreased. During a dust intake into a slit instrument equipped with a well coated plate, the number of particles with the radius of 1μ did not change, with the radius above 1μ - became somewhat reduced, and below the radius of 1μ - was increased several times. The described effect declines in moist air, because humidity makes the aggregates much stronger. The effect is likewise strongly influenced by the slot's profile: in slits with a rounded profile it is far greater than in the slits with a conical profile. The reason for splitting of the aggregates lies, according to DAVIES theory, in the enormous relative velocity of the particles motion and that of the medium at the entrance to the slit, as a result of the particles inertia. Thus, in the slit illustrated on figure 42, b the relative velocity reaches, as computed, $150 \text{ m} \cdot \text{sec}^{-1}$ for particles with a radius of 10μ . It is obvious that with regard to a conical profile, i.e., with a uniformly accelerated current, the relative velocity

should be lower than that in a rounded profile. Likewise an important factor in disaggregation of particles by air current appears to be the nonuniformity of the current and the presence of higher gradients of the current's velocity at the entrance to the slit (see page 423).

According to DAVIES, in slits with a rounded profile the inertial precipitation of particles also takes place on walls of the slit itself. This phenomenon grows larger with the increase of linear velocity of air in the slit, therefore it emphasizes itself much better in OWEN'S instrument.

Some industrial apparatuses for the elimination of dust from gases are based on the very principle of collisions of aerosolic flow with a surface (227): gas, allowed to pass through a great number of openings of 2-5 mm in diameter, reaches a metallic plate and then collides with another plate positioned parallel to the first one at a distance of 2-3 mm from the latter. It is regrettable that no data as to the effectiveness of the apparatuses in question pertinent to the particles of a definite magnitude are available, since no comparison with a theory can be made.

§ 34. Inertial Precipitation of Aerosols Upon Substances of Ordinary Shape

Notwithstanding the great practical importance of inertial precipitations of aerosol particles from a current upon substances of dissimilar shape, very limited material concerning experimental tests has been published on this subject. Somehow many more theoretical computations were accomplished with regard to the coefficients of precipitations (see page 174) of particles upon substances of an ordinary shape. These computations were realized according to the method discussed in § 30; they concern precipitations for flow around a sphere, an infinitely long cylinder and a flat strip, all positioned perpendicularly to the current. The following hydrodynamic equations were used (written in nondimensional coordinates) in principle for the computed circumstances

1. Passing of an ideal liquid around an infinitely long round cylinder (an ideal flow) /228/ 1

$$U_x = 1 - \frac{\cos 2\theta}{\rho^2}, \quad U_y = - \frac{\sin 2\theta}{\rho^2}. \quad (34.1)$$

1. See (232) for an ideal passing around an infinitely long strip.

2. Passing of a viscous liquid around an infinitely long circular cylinder, at small Re_f (229)¹

$$U_x = \frac{\ln \rho - 0.5 \left(1 - \frac{1}{\rho^2}\right) \cos 2\theta}{2.002 - \ln Re_f}, \quad U_y = - \frac{0.5 \left(1 - \frac{1}{\rho^2}\right) \sin 2\theta}{2.002 - \ln Re_f} \quad (34.2)$$

3. Passing of an ideal liquid around a sphere (230)

$$U_x = 1 + \frac{1 - 3 \cos^2 \theta}{2\rho^3}, \quad U_y = - \frac{3}{4} \frac{\sin 2\theta}{\rho^3} \quad (34.3)$$

4. Passing of a viscous liquid around a sphere at small Re_f (231)

$$U_x = 1 - \frac{3}{4\rho} (1 + \cos^2 \theta) - \frac{1}{4} \frac{1}{\rho^3} (1 - 3 \cos^2 \theta),$$

$$U_y = - \frac{3}{8} \frac{\sin 2\theta}{\rho} \left(1 - \frac{1}{\rho^2}\right). \quad (34.4)$$

U_x and U_y are in these equations the components of the current's velocity, at the same time the current's velocity at an infinitely great distance from the substance U_0 (directed toward the positive side of the axis x) is accepted as a unit. ρ denotes the distance from sphere's or cylinder's center and their radius is accepted as a unit. θ denotes the angle between the

1. We included this equation for the sake of its completeness although the computations of precipitation coefficients for this specific case were, as yet, not published

radius-vector and the axis x . The fields of current, in instances 3 and 4, are illustrated on figures 45, a and b.

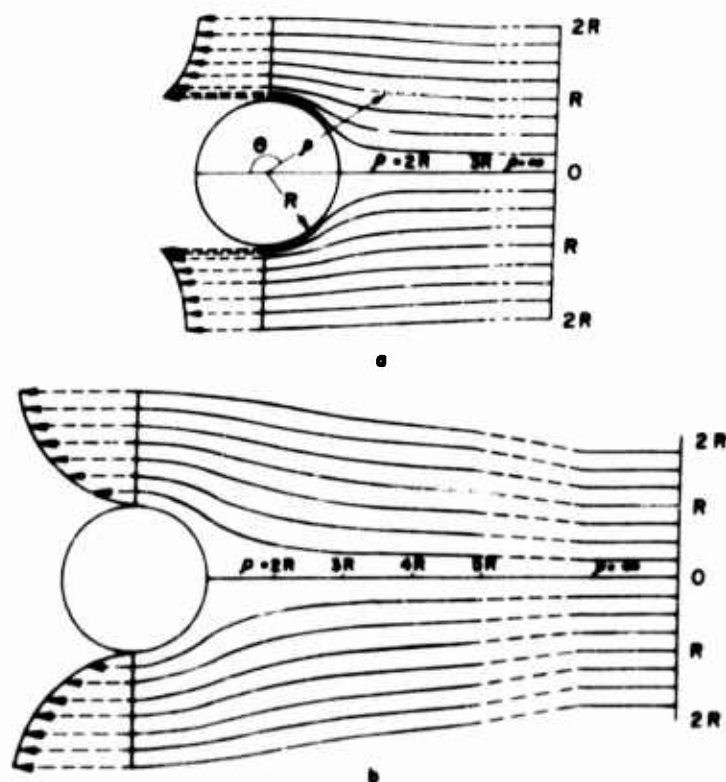


FIG. 45 FLOW LINES AROUND A SPHERE (a) POTENTIAL FLOW
(b) VISCOUS FLOW

In connection with the afore-mentioned equations we note the following. The (34.2) and (34.4) equations describe exactly the movement of a medium near a cylinder or a sphere, but they are very inaccurate as the cylinder or the sphere recede from the medium. Since in computing the coefficients of the particles precipitation from a current the particle movement is of primary importance as the substance is by-passed around, the computations based on such equations are probably closer to reality. It is a known fact that OSEEN'S equations (for a viscous liquid flowing around a sphere) convey better than the STOKES' equations (34.4) /233/ do the medium's motion which takes place far from the sphere, while becoming worse, if the movement happens to be close to the sphere. Therefore, in this case, it is expedient to use the latter equations.

As Re_f increases, a thick jacket of the medium, which surrounds the substance and which is slowed down by the substance during viscous flow, becomes gradually thinner and is finally transformed into a border stratum.

In addition to this, the nature of the current behind the substance changes suddenly, eddies develop and at much stronger Re_f the current becomes turbulent. In contrast with the above, a laminar type of current is maintained in the forepart of the substance even at very high Re_f (if the current is not turbulent of its own accord); therefore equations (34.1) and (34.3) are accurate up to the point, where the substance adjoins the border stratum and where the increase of the current's velocity develops from zero to the magnitude expressed by the equations. The thickness of the border stratum constantly decreases as the Re_f increases. Inasmuch as the inertial precipitation, as computed in the afore-quoted equations, becomes in its windward course exposed to the wind, i. e., faces the side of the substance meeting the current, then the eddies and the turbulence behind the substance do not influence the precipitation. On the other hand the eddies, at times, cause a precipitation of particles at a lee side of the substance (see page 307).

As we proceed to give an account of the results published about the estimated coefficients of precipitation upon substances of an ordinary shape, we wish to emphasize that in these computations we considered: 1) neither the effect of capture (see page 175), i. e., the computations include only in a small measure the ratio of the particle sizes and of the substance being by-passed, 2) nor the influence of the border stratum, i. e., the computations are applicable only with very high Re_f . We shall discuss a little later the question of the extent of errors caused by these simplifications.

LANGMUIR'S and BLODGETT'S (234, 235), as well as MAZIN'S (206) data of computations, being very close to each other, seem to be the most dependable with regard to an ideal flow around an infinitely long cylinder (figure 46). LANGMUIR and BLODGETT obtained for Stk_{cr} in particular the 0.0625 value, which coincides exactly with that of L. LEVIN determined in an analytical way, which confirms the reliability of the computations in question. The results of the much earlier works of SELL (204) and ALBRECHT (205) in this and in other instances reviewed below, are visibly erroneous in some places; therefore they are not quoted here.

LANDAHL (236) preparing a (very roughly) computation for by-passing a cylinder at $Re_f = 10$ used the distribution of current's velocities computed theoretically for this specific case by THOM (236) and he arrived at the following empirical equation:

$$\beta = \frac{(Stk)^3}{(Stk)^3 + 0.77(Stk)^2 + 0.22} \quad (34.5)$$

We see from figure 46, that at higher Stk values the curves for a coefficient of precipitation at $Re_f = 10$ and at very high Re_f are close to each other; at small Stk the coefficient of precipitation increases considerably along with the Re_f .

DAVIES (565) prepared a computation for a case of $Re_f = 0.2$. His curve is shown on figure 46.

LANGMUIR and BLODGETT plotted a curve for an ideal flow around an infinitely long strip without interrupting the current at the edges of the strip (238); also this curve is shown on figure 46.

According to LANGMUIR and BLODGETT (239, 240), the coefficient of precipitation at an ideal flow around a sphere is expressed in the range of $Stk \geq 0.1$ by the following empirical equation (figure 47)

$$\eta = \frac{(Stk)^2}{(Stk + 0.125)^2}. \quad (34.6)$$

The value of 0.0417 was obtained for Stk_{cr} in full accordance with the theoretical value of $1/24$ derived by L. LEVIN.

For a viscous flow around a sphere LANGMUIR and BLODGETT (239, 241) plotted a curve, which is expressed by the following equation:

$$\eta = \left[1 + \frac{0.75 \ln(4Stk)}{2Stk - 1.214} \right]^{-2} \quad (34.7)$$

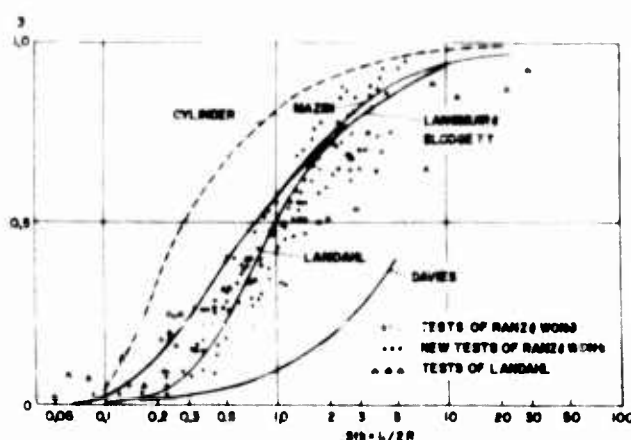


FIG 46 EFFECTIVENESS OF INERTIAL PRECIPITATION UPON A CYLINDER

As was to be expected, the coefficient of precipitation is considerably smaller here than for ideal flow and it even equals zero at $Stk = 0.607$.

For an intermediate hydrodynamic range LANGMUIR proposed to compute β on a sphere by interpolation values found for an ideal and viscous flow (242); yet, the interpolation method suggested by LANGMUIR is not sufficiently proved, therefore the results obtained being extremely unreliable are not quoted here.

It is not needless to mention, that although β decreases with the increase of the size of a by-passed substance, the general amount of the settling upon a substance grows with the latter's size. This is obviously due to the fact that the curves (β, Stk) including usual coordinates are always bent in toward the axis of abscissae; therefore β/Stk and consequently βR as well decrease with the growth of Stk , i. e., with the decrease of R .

L. LEVIN (220) made a large step forward in the theory of inertial precipitation of particles by introducing a general analytical method for determination of Stk_{cr} at an ideal by-passing of substances of various shapes. Thus, near the point of stagnation the current's velocity of the central stream-line of the current which passes through that point can be expressed approximately by the following equation:

$$U_x = -ax, \quad (34.8)$$

if the principle of coordinates is placed at the point of stagnation. Thus, e. g., the current's velocity in flowing around a cylinder along the central stream-line of the current ($\theta = -\pi/2$) is, according to (34.1), equal to $1 - (1/\rho^2)$, or with a new system of coordinates at small x it is equal to:

$$U_x = 1 - \frac{1}{(1-x)^2} \approx -2x, \quad (34.9)$$

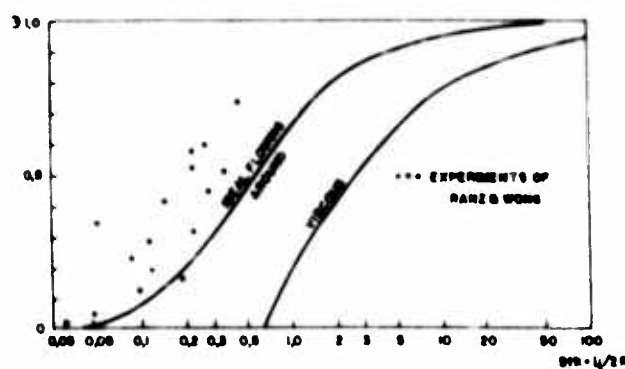


FIG 47 EFFECTIVENESS OF INERTIAL PRECIPITATION UPON A SPHERE

i. e., $a = 2$. A differential equation of the particle movement along a central streamline of the current assumes the form (see /30.2/):

$$\tau \frac{d^2x}{dt^2} + \frac{dx}{dt} - \bar{U}_x \equiv \tau \frac{d^2x}{dt^2} + \frac{dx}{dt} + ax = 0. \quad (34.10)$$

The radicals of a pertinent characteristic equation $\tau\lambda^2 + \lambda + a = 0$, at $1 - 4\tau a < 1$, will remain complex; $\lambda = \alpha \pm i\beta$ and the solution of the equation (34.10) will assume the following general form:

$$x = A \cos \alpha t + B \sin \beta t. \quad (34.11)$$

Since the equation $A \cos \alpha t + B \sin \beta t = 0$ has the ultimate radicals with any final values of A and B (points of intersection of sinusoids $A \cos \alpha t$ and $B \sin \beta t$), then in case $1 - 4\tau a < 0$ or $\tau > 1/4a$ the particles should reach the stagnation point at a final time. In case $\tau < 1/4a$, as L. LEVIN pointed out, the particles can reach the stagnation point only at $t = \infty$. If we assume that in a non-dimensional system of coordinates $Stk \equiv \tau U_0/2R = \tau/2$, we obtain

$$Stk_{cr} = 1/8a. \quad (34.12)$$

According to computations of LANGMUIR and BLODGETT, $Stk_{cr} = 1/16$, especially for a cylinder. We shall bring forward some Stk_{cr} values, found in this way by L. LEVIN for an ideal flowing around of certain substances with an ordinary shape.

In flowing around:

an infinitely long strip of $2R$ in width, without interruption: $1/6$;
with interruption: $2/(\pi + 4)$;

an elliptical cylinder, with a proportion of large and small axes equal to χ : $1/8(1 + \chi)$;

a circular cylinder: $1/16$;

a sphere: $1/24$;

a circular disc: $\pi/32$

at an impact of a flat stream with a surface at a right angle, with $d/2h = \infty$ (see figure 43): $1/\pi$.

Let us assume that in case of a viscous flowing around the Stk_{cr} cannot be determined by the afore-mentioned method, because in such a case the velocity of the currents at the point of stagnation cannot be expressed by the equation (34.3).

The influence of the capture effect upon a coefficient of precipitation at a small value of the proportion $\kappa = r/R$ may be evaluated in the following manner (243). We calculate how much the β would be increased as a result of capture in the following two extreme cases:

1) at $Stk = \infty$, i. e., when the particle's inertia is so big that the particle moves straight-forward at all times, and 2) at $Stk = 0$, i. e., when a particle has no inertia and moves according to the streamlines of the current. In the first case the increase of β is equal to

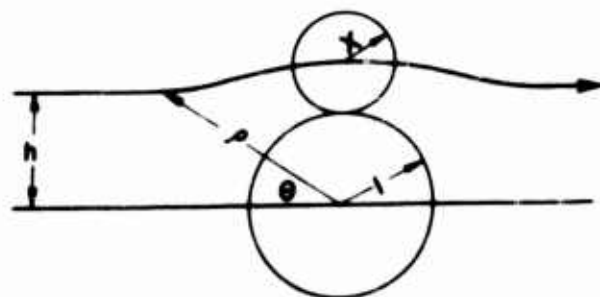


FIG. 48 INFLUENCE OF IMPACTION

$$\Delta\beta = \frac{r+R}{R} - 1 = \frac{r}{R} = \kappa \quad (34.13)$$

for a cylinder, and to

$$\Delta\beta = \left(\frac{r+R}{R}\right)^2 - 1 = \kappa^2 + 2\kappa \approx 2\kappa \quad (34.14)$$

for a sphere. In case a cylinder with a radius l is flowed-around, the equation of current's lines assumes a form: $\psi = \left[\rho - 1/\rho\right] \sin\theta = C$ (figure 48). At $\rho \rightarrow \infty$ $C = \rho \sin\theta$. Thus, the constant C is the distance h from the corresponding line of current to the axis at an infinitely great distance from the cylinder. At $\theta = \pi/2$, i. e., in the equatorial section, $C = \rho - 1/\rho$. In the illustration on figure 48 in the particle's position $C = l + \kappa = 1/(1 + \kappa)$ and, inasmuch as for a noninertial particle without the capture effect $\beta = 0$, consequently

$$\Delta\beta = 1 + \kappa - \frac{1}{1 + \kappa} \approx 2\kappa. \quad (34.15)$$

In behalf of an ideal flowing around a sphere

$$\psi = \left[\rho^2 - (1/\rho)\right] \sin^2\theta = C^2$$

$$\Delta\beta = (1 + \kappa)^2 - \frac{1}{1 + \kappa} \approx 3\kappa. \quad (34.16)$$

In behalf of a viscous flowing around a sphere $\psi = \left[\rho^2 - 1.5\rho + \left(1/2\rho\right) \right] \sin^2\theta = C^2$

$$\Delta\mathfrak{P} = (1 + \mathfrak{x})^2 - \frac{3}{2}(1 + \mathfrak{x}) + \frac{1}{2(1 + \mathfrak{x})} \approx \frac{3}{2}\mathfrak{x}^2. \quad (34.17)$$

In behalf of a viscous flowing around a cylinder, it follows from the equations (34.2) that

$$\Delta\mathfrak{P} = \left[(1 + \mathfrak{x}) \ln(1 + \mathfrak{x}) - \frac{\mathfrak{x}(2 + \mathfrak{x})}{2(1 + \mathfrak{x})} \right] / (2.002 - \ln \text{Re}_f). \quad (34.18)$$

Thus, at an ideal flowing around a cylinder $\Delta\mathfrak{P}$ lies between \mathfrak{x} and $2\mathfrak{x}$ and at an ideal flowing around a sphere, between $2\mathfrak{x}$ and $3\mathfrak{x}$. This method of evaluation of the capture effect is ineffective with regard to viscous flowing around.

One can find in practice some instances in which the size of particles is in the same order of magnitude as a cross-section dimension of the substance being flowed-around. For example, in studying atmospheric aerosols the latter are allowed to precipitate on very fine threads (0.1 μ thick) stretched perpendicularly to the wind. Either the threads made from solutions of high polymers (244) are stretched, or cowebs produced by certain spiders are used (245). If the particle's size exceeds the diameter of a thread, one can disregard the deviation of the particles' trajectory from the rectilinearity, i.e., the coefficient of precipitation will practically be equal to $1 + (r/R)$ /see equation (34.13)/.

The influence of the border stratum upon the value of a precipitation coefficient includes this feature: that the current's streamlines nearest to the substance are somewhat drawn back from the latter. We shall assume that "the thickness of displacement" (246) δ is a measure of the thickness of the border stratum, i.e., we shall consider that inside the stratum the velocity of the current equals zero and that the velocity outside the stratum is expressed by the hydrodynamic equations (34.1) or (34.3)¹. In such a case the streamline of the current nearest to the substance is drawn back from the latter at a

-
1. We limit ourselves to the instance of laminability of the border stratum up to the breaking-away point ($\text{Re}_f < 10^5$).

distance δ . One can consider very roughly that the trajectories of particles by which the value of \mathfrak{Z} is determined are also drawn away from the substance to the same distance, i.e., the trajectories of particles most remotely drawn away from the axis, but still precipitating upon the substance. In this hypothesis the influence of the border stratum is the same as that of the effect of capture for particles with a radius $r = \delta$, although symbolically it is in contrast.

The thickness of displacement increases somewhat from the point of stagnation toward the equatorial cross section, near which breaking-away of the border stratum from the body takes place. The ratio of $\delta Re_f^{1/2}/R$ for a cylinder is equal to 0.44 at the point of stagnation ($\theta = 0^\circ$), then it equals 0.57 at $\theta = 60^\circ$ and 0.80 at $\theta = 90^\circ$ (247). The value of δ for a sphere is almost the same. Inasmuch as the particles of interest to us precipitate approximately at $\theta = 60-80^\circ$, we shall assume that $\delta Re_f^{1/2}/R = 0.7$. Thus, on behalf of cylinders the decrease of \mathfrak{Z} , due to the border stratum, is located, roughly speaking, between $0.7 Re_f^{-1/2}$ and $1.4 Re_f^{-1/2}$ and as for the spheres, between $1.4 Re_f^{-1/2}$ and $2.1 Re_f^{-1/2}$. It would be highly desirable to make a computation of the particles trajectories and of the effectiveness of precipitation including the border stratum and the capture effect. In such case one must determine \mathfrak{Z} as the function of two parameters, Stk and Re_f , or (what amounts to the same) of Stk and r/R .

DAVIES effected such computation for a cylinder at $Re = 0.2$. He expressed the results of the computation by the following empirical equation:

$$\mathfrak{Z} = 0.16 \left[\mathfrak{X} + (0.5 + 0.8 \mathfrak{X}) Stk - 0.1052 \mathfrak{X} Stk^2 \right]. \quad (34.19)$$

The equation was not verified during experimental tests.

We proceed now to the experimental studies of inertial precipitations of aerosols upon bodies of ordinary shape. By setting vertically and perpendicularly to wind some cylinders of 0.1 to 9 mm in diameter, LANDAHL (236) was able to determine the amount of mist precipitated upon the cylinders; the mist was obtained by the mechanical atomization of butylphthalate. The average radius of droplets varied between 1.6 and 13μ and the wind velocity was between 0.5 and $4 \text{ m} \cdot \text{sec}^{-1}$, so the Re_f was equal to from 2.5 to 2500. Some data of LANDAHL are shown on figure 46. They show a greater dispersion, therefore it is impossible to clarify what influence the Re_f has upon the shape of the curve (\mathfrak{Z} , Stk). It should be noted in general that highly polydispersed fogs, obtained by mechanical atomization, represents as such an unusual unsuccessful objective for this type of studies.

It is difficult to utilize the tests of YEOMANS (248), who investigated precipitations of fog upon circular discs set up perpendicularly to wind. The tests were conducted at very small Stk and β values.

RANZ and WONG (222) conducted their tests with more or less isodispersed sulphuric-acid fogs, containing droplets of average radii $0.18-0.65\mu$; the air velocity in the aerodynamic tube during the tests ranged between 12 and $97\text{ m} \cdot \text{sec}^{-1}$. The precipitations were effected upon fine wires of 77μ in diameter and upon little balls 0.9 mm in diameter. Thus, in the first instance, the Re_f equaled $55-450$ and in the second instance from 650 to 5000 . It was impossible to obtain much higher Re_f , because the liquid was drawn off the surface at higher current velocities. As figure 46 shows, the test data of RANZ and WONG pertinent to a cylinder coincide with the theoretical curve of LANDAHL at small Stk and they are somewhat smaller than the theoretical values at larger Stk . Figure 46 also shows the results of more recent measurements conducted by the authors (566) on fine wires of $29-106\mu$ in diameter at $Re_f = 13-330$.

Taking into account the difficulty of obtaining exact and reproducible results in such tests one must consider with satisfaction the concurrence between the theory and the test in the given case. On the contrary, in the case of precipitation upon a sphere (see figure 47), the experimental values of β are several times larger than the theoretical values. The reason for the discrepancy evidently lies in some error in the arrangement of tests with a sphere.

M. KHIMACH and N. SHISHKIN (249) studied with the aid of a microscope the development of water droplets of 0.1 mm radius, which were suspended on glass thread in aerodynamic tube, through which a condensed water fog (containing droplets of $3-12\mu$ in diameter) was blown with a velocity from 0.3 to several $\text{m} \cdot \text{sec}^{-1}$. The magnitude of Re_f number in these tests was on the order of 10 . The authors assumed that the passing of air around immobile droplets was STOKES'-like and they adopted for the computation of precipitation coefficient the following empirical equation:

$$\beta = \left(1 - \frac{0.607}{Stk}\right)^2, \quad (34.20)$$

which provides values for β rather close to those computed according to equation (34.7), but it is more suitable for integration. Having found by microphotographs the distribution of droplet sizes in the fog, authors did not take advantage of the distribution directly, but determined accordingly the r_m radius, corresponding to the maximum on the distribution curve. Then,

having adopted M. SMOLUCHOWSKI'S (49. 36) asymptotic distribution for calculations, they computed a theoretical rate of growth of the droplets at the expense of the inertial precipitation, assuming that every contact between droplets leads to their merging. The proportion of computed and measured rate of growth of the droplets varied in individual tests very strongly, but on the average the proportion (0. 97) of the value of all tests came very close to one unit. Analogous results were obtained in GUNN'S tests (see page 373).

The values found by BOUCHER (250) on behalf of the coefficients of droplet precipitation upon a plate 0. 5 cm wide differed considerably from the values computed and at the same time deviations appeared in both directions, which, according to all probability, was the result of imperfections in experimental techniques. It should be generally acknowledged that experimental studies of inertial precipitations still remain in a very inadequate stage.

COCHET (185) having a practical interest in ice formations on high-tension wires examined the problem of nonchargeable aqueous fog, precipitating upon a charged and infinitely long horizontal cylinder; the settling of droplets under the influence of gravity was also considered. Assuming that the by-passing of a cylinder by air is ideal, that the movement of droplets conform with STOKES' law, and that the droplets are conductive, i. e., that the induction factor $(\epsilon_k - 1)/(\epsilon_k + 2) = 1$, and disregarding the inertia of the droplets, COCHET computed β for a set of values for E_0^2/R from 0 to 15, 400 and for U_0/r^2 from 0 to $1.6 \cdot 10^8 \text{ cm}^{-1} \text{ sec}^{-1}$; where E_0 is the potential of an electrical field (in E. S. Units) at the surface of cylinder; where R is the radius of the latter (in cm); where U_0 is the velocity of the current at a distance from the cylinder (in $\text{cm} \cdot \text{sec}^{-1}$). In this case $R = 0.65 \text{ cm}$, $r = 10^{-3} \text{ cm}$, $E_0 = 100$ and the curve β in the function of U_0 is also computed with the inertia of the droplets considered.

Chapter V

Brownian Movement and Diffusion in Aerosols

§ 35. Brownian Movement in Aerosols

The theory of the Brownian movement is sufficiently clarified in the literature (251, 252, 253), therefore we shall pause only at some problems directly connected with the physics of aerosols.

The thermal movement of particles suspended in a resistant medium is expressed by EINSTEIN (254) in the following derived equations:

$$\overline{x^2} = 2 Dt, \quad (35.1)$$

$$D = kTB, \quad (35.2)$$

where $\overline{x^2}$ is the average square of a particle displacement along each coordinate axis per time unit t and

where D (the value characterizing the intensity of the Brownian movement) is the coefficient of diffusion of a particle combined with its mobility in the equation (35.2).

In drawing conclusions from these equations it is necessary to make the following hypotheses:

1. Particles in a dispersible system move independently of each other;
2. The average energy of the progressive movement of a particle along each coordinate axis is equal to $\frac{1}{2} kT$, in accordance with the general rule of statistical mechanics;
3. Movements of a particle during consecutive intervals, $0-t$, $t-2t$, $2t-3t$, etc., are independent.

We shall review these hypotheses individually. The first hypothesis amounts to a condition of the absence of interaction between aerosol particles. This interaction leads to hydrodynamic (§ 23), molecular and, in

case of charged particles, to electrostatic forces. As a result of rapid and irregular changes in the Brownian movement of particles, the time average of hydrodynamic forces should be equalized here to zero. The molecular forces between particles may appear only when the distance between them is small in comparison with the particles' sizes, while the electrostatic forces act at distances which exceed several times the size of particles.

In this case, if the distance between particles is so small that the forces of interaction are of an outstanding magnitude, equation (5.1) is already inapplicable and it should be substituted by a more complex equation in which a well ordered movement under the influence of these forces is taken into account (see § 51).

The fact that the average energy of a progressive thermal movement of the particles along each coordinate axis is equal to $\frac{1}{2}kT$ cannot

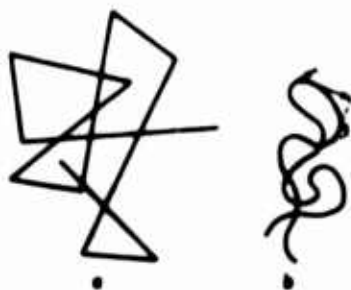


FIG. 49 TRAJECTORIES OF GASEOUS MOLECULES (a)
AND OF BROWNIAN PARTICLES (b)

produce, of course, any doubts in the absence of a well ordered movement of the particles under the influence of external forces. In order to explain the results of some tests, according to which a horizontal Brownian displacement of aerosol particles differs from a vertical one, F. FRANK (255) expressed the opinion that with the average energy of a vertical Brownian movement there should also be included the energy of settling $mV_g^2/2$. In this case it would remain less

than $\frac{1}{2}kT$ of the amount of energy per quota of the thermal movement and accordingly the vertical Brownian displacement of particles should be reduced. It is not difficult to note that this point of view contradicts the principles of the statistical mechanics.

The hypothesis about the independence of the magnitude of the particle movements during consecutive intervals of t may still be expressed in the following manner (253): The consecutive position of a particle at the moments of $0, t, 2t, \dots$ form a "discrete circuit of MARKOV"; i.e., the position of a particle at a moment $(n+1)t$ depends only upon the position of the latter at the prior nt moment, but it does not depend upon a position at the moment $(n-1)t$ and upon a position at other earlier moments. It is easy to become convinced that the time t cannot be so permissively small. Consequently we shall review the molecular-kinetic mechanism of the Brownian movement. Figure 49 shows sketches of movements of a nitrogen

molecule (fig. 49-a) schematically presented to scale of $3 \cdot 10^5:1$, as projected upon a surface and also the sketched movement of an aerosol particle of a radius 1μ (fig. 49-b) and of density ρ in the air at the usual pressure and temperature.

The trajectory of a gaseous molecule consists of parts of a straight line. Each part corresponds to a molecular path between two collisions. At each collision the direction and velocity of the molecule motion change abruptly: if the persistency of velocity at the collisions were disregarded, one could consider that for a molecule upon collision all directions are equally probable on the average. If G_g is a velocity, l is the average length of the free path of a molecule and $T = G_g/l$ is the average time of traversing the path, then, in order that the velocities of a gaseous molecule motion be independent during the subsequent intervals of t , it is essential that $t \gg T$.

In actuality, even during collisions of gaseous molecules, as is known, the persistency of velocity does exist, i. e., a molecule upon collision retains on the average a certain component of velocity of the prior direction. As to aerosol particles, the persistency of velocity is shown to be immeasurably greater: due to the greater mass of the particles, as compared with the mass of a gaseous molecule, the velocity of a particle changes very little upon a collision with molecules. A noticeable change of direction and of velocity of a particle movement can occur only as a result of a great number of such collisions. For this reason the trajectory of a particle has, practically speaking, the shape of a smooth curve. A part of the average length of the free path becomes the "path of average apparent length" (256) of a particle l_B , i. e., the distance a particle travels until it fully changes the direction of its motion. The l_B can be determined as an average length of a tangent to the particle's trajectory, up to the point of intersection with the nearest tangents running perpendicularly to the others (see figure 49-b). A more exact l_B value can be obtained by means of the following reasoning. A particle possesses at all times a progressive velocity, whose average square is equal to $\overline{G^2} = 3kT/m$. The surrounding medium constantly delays the progressive movement of a particle in accordance with the general equation (see 17.7):

$$G = G_0 e^{-t/T} \quad (35.3)$$

At the same time, as a result of fluctuations in the magnitude of the impulses, which a particle obtains from gaseous molecules bombarding it, the particle develops its velocity in a direction perpendicular to the primary direction. Consequently, in spite of the afore-mentioned delaying action, the

average absolute velocity of a particle does not change. The path traveled by a particle in the primary direction equals, according to the equation (17.18):

$$l_B = \bar{G}\tau, \quad (35.4)$$

where τ is the particle's relaxation time and where \bar{G} is an average velocity of its thermal movement. Thus, the direction of the motion of a particle changes essentially per time of the τ order and, in order that positions of a particle at the moments $0, t, 2t, \dots$ are able to form the MARKOV'S circle, it is necessary, that $t \gg \tau$.

This reasoning can be defined more accurately (257, 258) and the following expression can be obtained for an average square of displacement of a particle along the x axis:

$$\overline{x^2} = 2\bar{G}_x^2\tau \left[t - \tau(1 - e^{-t/\tau}) \right], \quad (35.5)$$

where \bar{G}_x^2 is the average square of the velocity of a particle in the direction of the x axis. Since $\bar{G}_x^2\tau = \frac{kT\tau}{m} = kTB = D$, then the equation (35.5) can be rewritten in the following form:

$$\overline{x^2} = 2D \left[t - \tau(1 - e^{-t/\tau}) \right]. \quad (35.6)$$

With $t \gg \tau$, the (35.6) changes into the basic equation (35.1). With $t \ll \tau$, upon arranging into a series of $e^{-t/\tau}$ in the equation (35.5), we shall obtain:

$$\overline{x^2} = \bar{G}_x^2 t^2, \quad (35.7)$$

i.e., the equation of the movement of a particle with a constant velocity \bar{G}_x . Hence, it becomes clear, that the condition of adaptability of the basic equation (35.1) is the requirement that $t \gg \tau$.

According to opinions of some authors (259) the persistency of the Brownian movement in a vertical direction (due to the particles' settling) is greater than that in a horizontal direction, therefore a Brownian displacement should also be greater than it is according to the equation (35.1). We shall not

discuss this complex problem, but we shall merely indicate that this opinion is in contradiction with the results of exact measurements of the Brownian movement in a gaseous medium (see § 36).

The important circumstance (that a particle's mobility included in the equation (35.2) coincides with the mobility influenced by a constant force) did create individual doubts among some authors in view of the Brownian movement's specific character. The unsubstantiality of these doubts follows from EINSTEIN'S deduction of the discussed equation. We shall examine an isodispersed system, which is in a balanced stage in a field of gravity and in which the particles of the system do not coagulate and do not stick to walls of a container. The concentration of particles at the height z is expressed by the following BOLTZMANN'S equation:

$$n = n_0 e^{\frac{-mgz}{kT}} \quad (35.8)$$

Through a horizontal area of one cm^2 , at a height z , there will pass downward, per time unit, as a result of sedimentation

$$I_1 = nV_s \quad (35.9)$$

particles. At the same time, due to diffusion, there will pass in the opposite direction¹

$$I_2 = -D \frac{dn}{dz} = \frac{nDmg}{kT} \quad (35.10)$$

particles. Since the system remains in an equilibrium, $I_1 = I_2$, i.e.,

$\frac{D}{kT} = \frac{V_s}{mg} = B$, from which the equation (35.2) follows. It is apparent from the derivation, that B denotes mobility in the presence of influences of a constant force and there is no specific need to substantiate this by way of a lengthy research in the mechanism of the Brownian movement (260).

Table 13 contains comparison of values characteristic to Brownian and other movements of aerosol particles; it includes: coefficients of diffusion

¹ - See § 37 concerning the applicability of diffusion equations to Brownian particles.

D, values of average velocity $\bar{c} = \sqrt{\frac{8G^2}{3\pi}}$, values of relaxation time τ , values of the apparent average length of path l_B , values of average displacement in a determined direction $\bar{\Delta x}_B = \sqrt{\frac{4Dt}{\pi}}$ (see page 220) for one sec and for comparison with Δx_g the distance which spherical particles of various sizes with a density 1 pass per one sec under the influence of gravity in air at atmospheric pressure and 23°C. At the same time the derived expression (8.6) pertains to the mobility of particles. Finally, the bottom row of the table shows by which degree of γ one must multiply the values introduced in the table for particles of other density.

Table 13

Characteristic Values in the Mechanics of Aerosols

r, cm	D, cm ² ·sec ⁻¹	G, cm·sec ⁻¹	τ , sec	l_B , cm	$\bar{\Delta x}_B$, cm	Δx_g , cm
10 ⁻⁷	1.28·10 ⁻²	4965	1.33·10 ⁻⁹	6.59·10 ⁻⁶	1.28·10 ⁻¹	1.31·10 ⁻⁶
2·10 ⁻⁷	3.23·10 ⁻³	1760	2.67·10 ⁻⁹	4.68·10 ⁻⁶	6.40·10 ⁻²	2.62·10 ⁻⁶
5·10 ⁻⁷	5.24·10 ⁻⁴	444	6.76·10 ⁻⁹	3.00·10 ⁻⁶	2.58·10 ⁻²	6.63·10 ⁻⁶
10 ⁻⁶	1.35·10 ⁻⁴	157	1.40·10 ⁻⁸	2.20·10 ⁻⁶	1.31·10 ⁻²	1.37·10 ⁻⁵
2·10 ⁻⁶	3.59·10 ⁻⁵	55.5	2.97·10 ⁻⁸	1.64·10 ⁻⁶	6.75·10 ⁻³	2.91·10 ⁻⁵
5·10 ⁻⁶	6.82·10 ⁻⁶	14.0	8.81·10 ⁻⁸	1.24·10 ⁻⁶	2.95·10 ⁻³	8.64·10 ⁻⁵
10 ⁻⁵	2.21·10 ⁻⁶	4.96	2.28·10 ⁻⁷	1.13·10 ⁻⁶	1.68·10 ⁻³	2.24·10 ⁻⁴
2·10 ⁻⁵	8.32·10 ⁻⁶	1.76	6.87·10 ⁻⁷	1.21·10 ⁻⁶	1.03·10 ⁻³	6.73·10 ⁻⁴
5·10 ⁻⁵	2.74·10 ⁻⁷	0.444	3.54·10 ⁻⁶	1.53·10 ⁻⁶	5.90·10 ⁻⁴	3.47·10 ⁻³
10 ⁻⁴	1.27·10 ⁻⁷	0.157	1.31·10 ⁻⁵	2.06·10 ⁻⁶	4.02·10 ⁻⁴	1.28·10 ⁻²
2·10 ⁻⁴	6.10·10 ⁻⁸	5.55·10 ⁻²	5.03·10 ⁻⁵	2.80·10 ⁻⁶	2.78·10 ⁻⁴	4.93·10 ⁻²
5·10 ⁻⁴	2.38·10 ⁻⁸	1.40·10 ⁻²	3.08·10 ⁻⁴	4.32·10 ⁻⁶	1.74·10 ⁻⁴	3.02·10 ⁻¹
10 ⁻³	1.38·10 ⁻⁸	4.96·10 ⁻³	1.23·10 ⁻³	6.08·10 ⁻⁶	1.23·10 ⁻⁴	1.21
	γ^0	$\gamma^{-1/2}$	γ	$\gamma^{1/2}$	γ^0	γ

As the table indicates, all values shown here change very extensively in relation to the size of particles, with the exception of the average apparent length of the particles path l_B , which retains the order of its magnitude down to molecular dimensions (for gaseous molecules $l \approx 10^{-5}$ cm). The next inference, which follows from the table, is that of the practical impossibility of observing actual trajectories of particles by using contemporary technical means; to effect this, for example in case of particles with a radius 10^{-4} cm, one would have to make no less than 10^6 photographs per sec., thus increasing magnitude to the order of 10^5 . We also see that the limitations imposed by the theory of the Brownian movement upon the magnitude of the interval of observations ($t \gg \tau$) have no practical significance, because the minimum value t , allowable by the theory, cannot be attained experimentally anyhow. Furthermore, we usually notice a sharp increase of the ratio $\overline{\Delta x_B} / \Delta x_g$ at the transition of the value r from 10^{-4} to 10^{-5} cm. This circumstance allows, in a certain test, a visual (not measured) estimation of the particle sizes during important intervals of dispersion in accordance with the type of the particles movement. Finally, the table shows that the Re number for a thermal movement of particles is very small and thus the medium's resistance is proportional to the velocity of particles, as can be assumed from the conclusion of the basic equation (35. 2).

§ 36. Experimental Study of the Brownian Movement in Aerosols

The theory of the Brownian movement obtained its first experimental verification by means of systems in liquid mediums. One could frequently observe, in work with aerosols, some existing deviations from the theory; particularly, the average quadratic displacements in a horizontal direction appear smaller in some tests and larger in other tests than the displacements in a vertical direction (259, 261). Especially noticeable deviations are obtained while working with a reduced pressure, during which large particles produce too great displacements and small particles, too small (262). As we already pointed out, in order to explain these observations we even offered special hypotheses. It is very difficult to find in every individual problem a reason for the deviations from the theory. No doubt one of the reasons was the insufficient number of observations taken with the same particle. At any rate, as we shall see below, in the few instances where the number of observations was sufficiently great and all possible systematic errors in observations were eliminated, an excellent concurrence with the theory was obtained.

Generally speaking, the measurement of the Brownian movement in gases is more difficult than those in liquids, due to the greater intensity of convection in the medium and the more rapid settling of particles. On the other

hand, unlike a system with a liquid medium, one can determine the mobility of the particles with a greater accuracy by using the method of a vertical electrical field in aerosols (see § 15) and, in addition to that, can observe particles in a current for a very long time, i. e., to effect a greater number of measurements with the same particle.

The study of the Brownian movement in aerosols is possible along a horizontal, as well as a vertical, displacement of particles. In the first instance one measures the time interval of the passage between two vertical lines in the eyepiece of a horizontal microscope by the particle's image. The test is repeated a considerable number of times. If t_v is the time of v -th test and h is the actual distance corresponding to the distance between the lines of the eyepiece, then the coefficient of a particle diffusion will be expressed by the following formula (see page 225):

$$D = \frac{1}{2} h^2 \lim_{v \rightarrow \infty} \frac{1}{v} \sum \frac{1}{t_v} = \frac{1}{2} h^2 \left(\frac{1}{\bar{t}} \right). \quad (36.1)$$

The average relative error in determination of D at v observations is equal (263) to:

$$\left| \frac{\Delta D}{D} \right| = \sqrt{\frac{2}{v}}. \quad (36.2)$$

For various reasons it is convenient to measure in aerosols a vertical component of the Brownian movement. Hence, we determine the time interval of the passage between two vertical lines in the eyepiece of a horizontal microscope by the image of a particle settling under the influence of gravity force, whereupon the particle is lifted by electrical field, then it is allowed to fall again, and so on. In order to prevent the particle from drifting off the visual field in a horizontal direction, one of the condenser's covers is made of two parts, the outer and the inner, insulated from each other (264). Inasmuch as the difference in potential of the proper sign, which is set up between these parts, is reversed by a particle escaping from the center part of the condenser, the observations can go on a countless number of times. In this manner we succeeded in carrying-out the number of observations of the same particle to 6000.

The magnitude of t_g , obtained by way of neutralization of found t_v values, determines the rapidity of a particle settling $V_g = h/t_g$. According to the above, one can determine on behalf of a nonaggregated spherical particle

its radius and mobility B . There are two methods for determining coefficient of diffusion according to the t_v values obtained. In the first one (see page 225) we use the equation (263), which is analogous to (36.1)

$$D = \frac{1}{2} h^2 \lim_{v \rightarrow \infty} \left[\frac{1}{v} \sum \frac{1}{t_v} - \frac{1}{\frac{1}{v} \sum t_v} \right] = \frac{1}{2} h^2 \left[\left(\frac{1}{\bar{t}} \right) - \frac{1}{\bar{t}} \right]. \quad (36.3)$$

The average relative error is determined by equation (36.2).

In accordance with the other method (265), all experimental values of t_v are grouped as larger and smaller than t_s . Assuming that the average value of the first ones is equal to t_+ and of the second ones to t_- and

$t_d = \frac{t_+ - t_-}{2}$, then the coefficient of diffusion can be determined according to the equation:

$$\frac{1}{D} = \frac{4t_s^3}{\pi h^2 t_d^2} \left[1 - \frac{(\pi - 2) D t_s}{\pi h^2} \right]^2, \quad (36.4)$$

and at the same time the relative error would again be approximately equal to $\sqrt{2/v}$ (266). If we consider that, following the conditions of tests in measuring the Brownian movement in gases, the second term in the quadratic brackets of the equation (36.4) is usually of the order of magnitude of 0.01, then the term in question may be disregarded.

For checking the theory of the Brownian movement, the D values obtained by any method are compared with those computed according to the equation (35.2). In table 14 are submitted for illustration the results of FLETCHER'S (264) measurements carried out with oil droplets in the air at

pressures of 120-200 mm. The table shows the radius of a droplet, the number of observations of v carried out, the ratio of observed (D_E) and

Table 14

Coefficient of Diffusion of Oil Droplets Taken from
Measurements of the Brownian Movement

$r \cdot 10^5$, cm ...	3.12	3.21	3.39	3.41	3.99	3.68	3.31	4.11	3.64	2.79	3.93	4.04
v ...	617	1713	1079	907	1854	1768	1354	1377	5950	380	557	1281
D_E / D_C	1.023	1.002	1.030	1.038	1.023	1.012	0.973	0.967	1.003	0.940	1.015	0.987
β_E ...	0.023	0.002	0.030	0.038	0.023	0.012	0.027	0.033	0.003	0.060	0.015	0.013
β_T ...	0.056	0.035	0.043	0.047	0.031	0.033	0.038	0.038	0.018	0.072	0.059	0.039

computed according to (35.2) (D_C) values of the coefficient of diffusion¹, the relative error $(D_E - D_C) / D_C = \beta_E$ and the average theoretical relative error according to (36.2), β_T .

Since the average weighted valued D_E / D_C out of 18837 observations is 1.003, then the average relative error is 0.003 and the average theoretical error is 0.010. Thus, the relative errors in these tests became systematically smaller than the theoretical values. It is presumed that the author rejected some series of observations which produced greater variations than those of average value.

SCHMID (267) working on selenium particles in an atmosphere of nitrogen found on the average that out of 9000 observations $D_E / D_C = 1.015$, $\beta_E = 0.015$ and $\beta_T = 0.015$.

As these problems were completed with a great accuracy, they verify the unconditional applicability of the basic equations (35.1) and (35.2) to the Brownian movement in aerosols.

1. FLETCHER in his computations used the equation (36.4) with another coefficient in the second term. However, as we indicated above, this circumstance is of no great importance.

The Brownian movement can be used for measuring the size of particles in aerosols, although this method is less exact and suitable than the methods described in the preceding chapters, which are based upon the measurements of velocities of particle motion influenced by a constant force. Actually, we suppose, that a particle's size is first of all measured according to the average time t_g of passing a definite vertical distance h and then according to deviations from this average (as we showed above), with which all v observations were made. In the second instance, the average relative error in determination of D and B is expressed by the equation (36.2). In the first approximation the error in determination of r will also be of the same magnitude. It is obvious that the error in determination of t_g at v observations will be the same as that of a single measurement of the time of a particle passing a vertical distance vh . During this time a particle experiences the average vertical Brownian displacement $\sqrt{2Dvt_g}$ and then the relative error in determination of the velocity of settling amounts to $\sqrt{2Dvt_g}/hv$. Since the V_g in the first approximation is proportional to r^2 , the relative error in the determination of r will be twice as small.

Let's compile the ratio of β in both errors. We find, that

$$\beta = \sqrt{2Dvt_g}/2hv : \sqrt{2/v} = \frac{1}{2} \sqrt{\frac{Dvt_g}{h^2}} = \frac{1}{2} \sqrt{\frac{D}{hV_g}}. \quad (36.5)$$

As table 14 shows, for particles with a radius 0.3μ , $D/V_g = 3.6 \cdot 10^{-4}$. In view of the fact that it is inconvenient to take less than 10^{-2} cm for a distance of h , then a value of ≤ 0.1 is obtained for β , i.e., the error in determination of the size of particles by the indicated value according to the Brownian movement is 10 times greater than is anticipated according to the rapidity of settling. The difference becomes still greater if we measure the velocity of the particle movement in a sufficiently strong electrical field (see page 79). Only for particles with $r \leq 10^{-5}$ cm, i.e., near the point of ultramicroscopic visibility, can the measurement of the Brownian displacement offer more exact results than the measurement of the velocity of a well ordered movement.

In order to determine the size of aerosol particles according to the Brownian movement, it is expedient to use a photographic method, which permits us to measure a great number of particles at the same time. Very promising at first sight is the method of photographing particles moving steadily in a horizontal direction, with the aid of motion picture film which, with intermittent illumination, facilitates the time reading of the exposure (268).

Over wavy dotted lines obtained photographically, straight lines are drawn to allow the most satisfactory approximation with the wavy lines; the straight lines are used in determination of the velocity of the particles settling, and deviations from these lines are regarded as Brownian displacements. Authors of the work regarded as satisfactory for the determination of a particle size the photographing of 100 dots with 20 intermittent exposures per second; they also measured photographically a particle's displacement from dot to dot. At the same time, it was found that the radii of the particles, computed according to the velocity of settling, systematically and considerably exceeded the radii found according to Brownian displacements. The authors' opinion was that this occurred as a result of downward convection currents in the center of the receptacle. However, this method meets with serious objections: according to (36.2), a particle's radius is determined with an average of 15% error per 100 displacements. Furthermore, among the particles with radii of $0.2 - 0.6 \mu$, on which tests were conducted, the average displacement from dot to dot, i.e., per 0.05 sec. , constituted $1 - 2 \mu$, which could only be measured very roughly. Finally, if we consider particles with a radius of 0.2μ , the average Brownian displacement and settling, per time $0.05 \times 100 = 5 \text{ sec.}$, are the values of a digital order and thus, in determination of the velocity of settling, by way of photographs, possible errors range within 100%. Actually the authors found that among some particles of known magnitude, the velocity of settling equaled zero. We specifically paused at this work, because it clearly shows what results Brownian-movement tests can come to, if their arrangement is insufficiently critical. It is obvious that one could obtain more reliable results, which are also sufficiently exact for practical purposes, if a motion picture film was in vertical motion for the purpose of measuring the horizontal displacement of particles and increasing the number of exposures several times.

§ 37. Probabilities of Transition. Occurrence and Arrival at a Boundary of Particles

I. Certain probable functions play basic roles in the theory of Brownian movement of aerosol particles. At first, we shall review the act of projecting a particle movement over the axis x . With this in mind, let us suppose that, in addition to the Brownian movement, a particle also has a well-ordered movement under influences of an external force, or those of the medium's movement. Let's assume that at the moment of $t = 0$, a particle's coordinate equals x_0 . We shall designate by $w(x_0, x, t)dx$ the probability of a situation, that within the time period t a particle will find itself in the interval of $(x, x + dx)$. The function of $w(x_0, x, t)$ satisfies the integral equation (269)

$$w(x_0, x, t + t') = \int w(x_0, x', t)w(x', x, t')dx, \quad (37.1)$$

where the integration is effected within the region of x' values, quite accessible to a particle. The physical meaning of the equation (37.1) is as follows: the transition from the situation of x_0 into the situation of x within the period of $t + t'$ can be effected, first, by way of the transition from x_0 into any accessible x' within a period of t , and then, from x' to x , within a period of t' . The probability of two such transitions under conditions of their independence is equal to a product of probabilities of both, i.e., $w(x_0, x', t) \times w(x', x, t')$, while the unknown probability of $w(x_0, x, t + t')$ is obtained by summing up the probabilities of all possible double transitions which lead from x_0 to x . The condition of the correctness of (37.1) is the independence of $w(x_0, x', t)$ and $w(x', x, t')$, or, in accordance with the statement in § 35, the requirement of $t \gg \tau$.

In a strictly mathematical way, one can derive from the equation (37.1) the so-called EINSTEIN-FOKKER'S equation¹, which on behalf of a homogeneous medium assumes this form:

$$\frac{\partial w}{\partial t} = - \frac{\partial (V_x w)}{\partial x} + D \frac{\partial^2 w}{\partial x^2}, \quad (37.2)$$

where D is the coefficient of diffusion of a particle; where V_x is a projection of the velocity of its well ordered movement upon the axis x . Inasmuch as the probability of transition to any accessible point equals 1, regardless of (37.2), the w must also be satisfied in the equation

$$\int w dx = 1, \quad (37.3)$$

as well as the original conditions of

$$\begin{aligned} w(x_0, x_0, 0) &= 1, \\ w(x_0, x, 0) &= 0 \text{ with } x \neq x_0, \end{aligned} \quad (37.4)$$

whose significance is obvious.

-
1. A. KOLMOGOROV'S (270) conclusion offers the most general form of EINSTEIN-FOKKER'S equation and a profound analysis of mathematical problems to which we refer here. M. LEONTOVICH quotes this conclusion in an abbreviated form.

In the absence of external forces or the medium's movements, the $V_x = 0$ and the (37.2) changes to

$$\frac{\partial w}{\partial t} = D \frac{\partial^2 w}{\partial x^2}. \quad (37.5)$$

The (37.2) and (37.5) are familiar equations for thermal conductivity and for diffusion in a mobile (37.2) and motionless (37.5) medium. We notice, however, that, if adapted to Brownian movement, these equations should be written in a form of finite increments, whereupon Δt should conform with the afore-mentioned $\gg \tau$. But, considering the smallness of τ , this circumstance can have its practical value only in connection with certain specific problems (in theory of coagulation, see § 49).

In view of the isotropism of a gaseous medium and the independence of the diffusion coefficient of spherical particles during their path, similar equations are also obtained for other coordinates. The probability $w(x_0, x; y_0, y; z_0, z; t) \times dx dy dz$ of a particle transition from a point x_0, y_0, z_0 into an element of space $(x, x + dx; y, y + dy; z, z + dz)$ is obviously equal to a product of¹ $w_x dx \cdot w_y dy \times w_z dz$. Since w_x does not depend upon y, z , etc., it follows hence, that

$$\frac{\partial w}{\partial t} = w_y w_z \frac{\partial w_x}{\partial t} + w_x w_z \frac{\partial w_y}{\partial t} + w_x w_y \frac{\partial w_z}{\partial t}, \quad (37.6)$$

$$\text{div}(Vw) = w_y w_z \frac{\partial(V_x w_x)}{\partial x} + w_x w_z \frac{\partial(V_y w_y)}{\partial y} + w_x w_y \frac{\partial(V_z w_z)}{\partial z}, \quad (37.7)$$

$$\begin{aligned} -D\Delta w &= -D \left(\frac{\partial^2 w}{\partial x^2} + \frac{\partial^2 w}{\partial y^2} + \frac{\partial^2 w}{\partial z^2} \right) = \\ &= -D \left[w_y w_z \frac{\partial^2 w_x}{\partial x^2} + w_x w_z \frac{\partial^2 w_y}{\partial y^2} + w_x w_y \frac{\partial^2 w_z}{\partial z^2} \right], \end{aligned} \quad (37.8)$$

1. - $w_x = w(x_0, x, t)$ and so on.

where V is a velocity vector of the defined movement of a particle; Δ is LAPLACE'S operator. In summing up these equations, according to (37.2) and analogous equations for other coordinates, we obtain:

$$\frac{\partial w}{\partial t} = - \operatorname{div}(Vw) + D\Delta w, \quad (37.9)$$

i. e., a well-known equation for diffusion, or for thermal conductivity in three dimensions. With $V = 0$, this changes into

$$\frac{\partial w}{\partial t} = D\Delta w. \quad (37.10)$$

The condition of normalization, as well as for the original conditions, are expressed here by the equations

$$\int w dv = 1, \quad (37.11)$$

where the integral is spread over the entire volume accessible to a particle and

$$w(x_0, x_0; y_0, y_0; z_0, z_0; 0) = 1,$$

$$w(x_0, x; y_0, y; z_0, z; 0) = 0, \text{ if the points } (x, y, z)$$

$$\text{and } (x_0, y_0, z_0) \text{ do not coincide.} \quad (37.12)$$

11. We denote by $W(x, t)dx$ a probability of a particle appearing in the interval $(x, x-dx)$ at a moment t , if at a moment $t = 0$ the probability is expressed by the function $W(x, 0)dx$. The probability of occurrence, of course, satisfies the equation

$$W(x, t) = \int W(x_0, 0)w(x_0, x, t)dx_0. \quad (37.13)$$

Then, we find to what the function is equal:

$$\Phi(x, t) = \frac{\partial W}{\partial t} + \frac{\partial(V_x W)}{\partial x} - D \frac{\partial^2 W}{\partial x^2}. \quad (37.14)$$

Having effected in (37.13) a differentiation under the integral's symbol, we shall obtain in accordance with (37.2)

$$\Phi(x, t) = \int W(x_0, 0) \left[\frac{\partial w}{\partial t} + \frac{\partial(V_x w)}{\partial x} - D \frac{\partial^2 w}{\partial x^2} \right] dx_0 = 0. \quad (37.15)$$

Thus, W is satisfied by the same equation (37.2) as is w , also to the same condition of normalization (37.3), although the original conditions, in this case, are assigned to the function $W(x, 0)$. Similarly, the spatial probability of occurrence $W(x, y, z, t)$ is satisfied in the equations (37.9) or (37.10) and (37.11).

If we refer the quoted equations to a system containing a great number of particles n_0 , then $n(x, t) = n_0 W(x, t)$ would denote, of course, a calculated concentration of particles in the interval $(x, x + dx)$ at the moment t . Thus, the equations (37.5) and (37.2) will be converted to general equations of mono-dimensional diffusion in an immobile medium

$$\frac{\partial n}{\partial t} = D \frac{\partial^2 n}{\partial x^2} \quad (37.16)$$

or in a current

$$\frac{\partial n}{\partial t} = - \frac{\partial(V_x n)}{\partial x} + D \frac{\partial^2 n}{\partial x^2}. \quad (37.17)$$

Now, the (37.10) and (37.9) equations will be converted to spatial diffusion equations

$$\frac{\partial n}{\partial t} = D \Delta n \quad (37.18)$$

or

$$\frac{\partial n}{\partial t} = - \operatorname{div}(Vn) + D \Delta n. \quad (37.19)$$

Thus, these equations are also applicable to the Brownian movement of the individual particle and to the diffusion system of particles, as is observed with the microscope.

III. Among certain problems concerning aerosols the function of probability of arrival at a boundary is of great importance; it was introduced to the theory of Brownian movement by A. KOLMOGOROV and M. LEONTOVICH (271). Let's assume, that a particle's coordinate equals x . We shall denote by $W^*(x, t)$ the probability that within a time period t a particle will attain a certain limiting. It is much simpler to regard x as a distance from that point. We shall denote by $w^*(x, x', t)dx'$ a probability that our particle, at a moment t , will find itself at a distance $(x', x' + dx')$ from a boundary without being in contact with it even once during that interval; it is obvious that $w^*(x, x', t) \leq w(x, x', t)$.

The functions of W^* and w^* are interconnected by way of the equation

$$W^*(x, t) + \int_0^\infty w^*(x, x', t)dx' = 1. \quad (37.20)$$

The first term in the left part of the equation denotes a probability that, within a time period t a particle will arrive at a boundary, while the other term denotes that a particle will not arrive at a boundary. Then comes the equation

$$W^*(x, t + t') = W^*(x, t) + \int_0^\infty w^*(x, x', t)W^*(x', t')dx', \quad (37.21)$$

whose meaning is as follows. A particle can arrive at a boundary within a time period $t + t'$ in two mutual excluding instances: 1 if a particle has already attained a limitation within a time period t ; 2 if a particle has not attained a boundary within a time period t , but will attain it during a time interval $(t, t + t')$. The first and the second term on the equation's right side express, respectively, the probabilities of both instances.

One can derive from the equation (37.20) and (37.21) the following differential equation

$$\frac{\partial W^*}{\partial t} = V_x \frac{\partial W^*}{\partial x} + D \frac{\partial^2 W^*}{\partial x^2}. \quad (37.22)$$

Furthermore, the $W^*(x, t)$ must, of course, satisfy the original conditions:

$$W^*(x, 0) = 0 \quad \text{with } x \neq 0, \quad W^*(x, 0) = 1 \quad \text{with } x = 0 \quad (37.23)$$

UNCLASSIFIED
AD

2271876

**FOR
MICRO-CARD
CONTROL ONLY**

5

OF

9

Reproduced by

Armed Services Technical Information Agency

ARLINGTON HALL STATION; ARLINGTON 12 VIRGINIA

UNCLASSIFIED

"NOTICE: When Government or other drawings, specifications or other data are used for any purpose other than in connection with a definitely related Government procurement operation, the U.S. Government thereby incurs no responsibility, nor any obligation whatsoever; and the fact that the Government may have formulated, furnished, or in any way supplied the said drawings, specifications or other data is not to be regarded by implication or otherwise as in any manner licensing the holder or any other person or corporation, or conveying any rights or permission to manufacture, use or sell any patented invention that may in any way be related thereto.

and for a boundary condition

$$W^*(0, t) = 1 \text{ with } t \geq 0. \quad (37.24)$$

We notice that the equation (37.22) coincides with EINSTEIN-FOKKER'S equation (37.2) only in the case where V_x is not dependent upon x . If there is a large number of identical particles n_0 , then $n_0 W^*$, of course, specifies the number of particles which occur at the moment $t = 0$ and at a point x ; also, that they have arrived at a boundary within a time period t .

A similar probability $W^*(x, y, z, t)$, of a particle with coordinates x, y, z , reaching a surface which delimits a certain space, or, in general, any surface within a time period t , is satisfied in the equation

$$\frac{\partial W^*}{\partial t} = V \text{ grad } W^* + D \Delta W^* \quad (37.25)$$

or, in case $V = 0$,

$$\frac{\partial W^*}{\partial t} = D \Delta W^*, \quad (37.26)$$

and with the conditions of

$$W^*(x, y, z, 0) = 0 \text{ for points not positioned on the surface,} \quad (37.27)$$

$$W^*(x, y, z, 0) = 1 \text{ for points positioned on the surface.} \quad (37.28)$$

Finally, we still need the function of $W^{**} = \partial W^* / \partial t$, which, it is obvious, expresses a probability that a particle will reach a boundary within a time interval $(t, t + dt)$. Differentiating the equation (37.25) by t , one can see that when V is independent of time, the function W^{**} also satisfies this equation.

With the aid of the afore-discussed functions of probabilities, one can solve many important problems of the Brownian movement in aerosols. From the standpoint of mathematics, the question boils down to the integration of EINSTEIN-FOKKER'S differential equation with various original and limiting conditions, for which one can use the theory of heat conductivity which is so well described with the aid of mathematical methods.

As to the probability of transition of $w(x_0, x, t)$ in the absence of a well-defined particle's movement, the following expression (272) is obtained:

$$w(x_0, x, t) dx = \frac{1}{\sqrt{4\pi Dt}} e^{-\frac{(x-x_0)^2}{4Dt}} dx, \quad (37.29)$$

and in the presence of a well-ordered movement, with constant velocity V_x included, this expression follows:

$$w(x_0, x, t) dx = \frac{1}{\sqrt{4\pi Dt}} e^{-\frac{(x-x_0-V_x t)^2}{4Dt}} dx. \quad (37.30)$$

For a probability of transition in space, in case $V = 0$, we have:

$$\begin{aligned} w(x_0, x; y_0, y; z_0, z; t) dx dy dz = \\ = \frac{1}{\sqrt{(4\pi Dt)^3}} e^{-\frac{[(x-x_0)^2 + (y-y_0)^2 + (z-z_0)^2]}{4Dt}} dx dy dz = \frac{1}{\sqrt{(4\pi Dt)^3}} e^{-\frac{\rho^2}{4Dt}} dv, \end{aligned} \quad (37.31)$$

where ρ is the distance between points x, y, z and x_0, y_0, z_0 ; and where dv is an element of volume.

If we use equation (37.29), it is easy to determine the magnitude of the average quadratic displacement of a particle $\overline{(x-x_0)^2}$ within a time period t . By substituting $(x-x_0)/\sqrt{4Dt} = \xi$, we obtain:

$$\overline{(x-x_0)^2} = \frac{1}{\sqrt{4\pi Dt}} \int_{-\infty}^{\infty} (x-x_0)^2 e^{-\frac{(x-x_0)^2}{4Dt}} dx = \frac{4Dt}{\sqrt{\pi}} \int_{-\infty}^{\infty} \xi^2 e^{-\xi^2} d\xi = 2Dt, \quad (37.32)$$

i.e., the basic equation (35.1). Similarly, with (37.31) one can determine the magnitude of the average quadratic displacement in space $\overline{\rho^2}$, although it is simpler to find it by taking into account that $\overline{(x-x_0)^2} = \overline{(y-y_0)^2} = \overline{(z-z_0)^2} = 2Dt$, consequently

$$\begin{aligned} \overline{\rho^2} &= \overline{(x-x_0)^2 + (y-y_0)^2 + (z-z_0)^2} = \\ &= \overline{(x-x_0)^2} + \overline{(y-y_0)^2} + \overline{(z-z_0)^2} = 6Dt. \end{aligned} \quad (37.33)$$

If a particle possesses a constant and well-defined velocity V_x , then by using the equation (37.30) and by substituting $(x-x_0 - V_x t) / \sqrt{4Dt} = \xi$, one can obtain (273):

$$\begin{aligned} \overline{(x-x_0)^2} &= \frac{1}{\sqrt{4\pi Dt}} \int_{-\infty}^{\infty} (x-x_0)^2 e^{-(x-x_0 - V_x t)^2 / 4Dt} dx = \\ &= \frac{1}{\sqrt{\pi}} \int_{-\infty}^{\infty} (V_x t + \xi \sqrt{4Dt})^2 e^{-\xi^2} d\xi = \\ &= \frac{1}{\sqrt{\pi}} \left(V_x^2 t^2 \sqrt{\pi} + 4Dt \frac{\sqrt{\pi}}{2} \right) = V_x^2 t^2 + 2Dt. \end{aligned} \quad (37.34)$$

Thus, in this case the average quadratic displacement is merely equal to the sum of squares of a "well-ordered" displacement with a Brownian displacement, as the latter would appear in the absence of a well-ordered movement.

As to an average, absolute magnitude of Brownian displacement at $V_x = 0$, the following analogous expression is obtained:

$$\overline{|x-x_0|} = \frac{1}{\sqrt{4\pi Dt}} \int_{-\infty}^{\infty} |x-x_0| e^{-(x-x_0)^2 / 4Dt} dx = \sqrt{\frac{4Dt}{\pi}}. \quad (37.35)$$

§ 38. Diffusible Precipitation of Aerosol in an Immobile Medium

Of greater practical importance is the problem resulting from Brownian movement, which is followed by precipitation of aerosols on "walls", i.e., on a surface with which solid or liquid substances of aerosols come in contact. According to the ideas exposed in §56 one may assume that as the particles come in contact with the walls they tend to stick and, in the absence of strong vibrations or air currents, such particles do not return to a suspended state. Thus, a determination of the rapidity of the particle precipitation on walls boils down to an estimate of the probability of the particles attaining the well known boundary conditions in a definite manner,

and this may be effected with the aid of the function W^* , referred to in the preceding paragraph. Yet, in most instances, it is convenient to use a more suggestive method of research by examining the precipitation process of a large number of identical particles and viewing it as a diffusion system, which uses an "absorbing" wall. Inasmuch as particles coming in contact with a wall are instantly removed from the gaseous space, the particles' concentration near the wall should be assumed to equal zero. In all cases examined below, except those specifically stipulated, it is assumed that no particles retain any well-defined movement.

I. We shall examine a simpler case of a flat wall, coming in contact with an infinitely great volume of aerosol and possessing everywhere an identical original concentration n_0 (a vertical wall). We shall include the axis x , set perpendicularly to the wall, establishing basic coordinates upon the latter. The concentration of particles $n(x, t)$ should, as we are informed, be satisfactory in the equation

$$\frac{\partial n}{\partial t} = D \frac{\partial^2 n}{\partial x^2} \quad (38.1)$$

and also in the original condition

$$n(x, 0) = n_0 \text{ with } x > 0 \quad (38.2)$$

and in the boundary condition

$$n(0, t) = 0 \text{ with } t > 0. \quad (38.3)$$

The solution of the problem is offered in the expression (274):

$$n(x, t) = \frac{2n_0}{\sqrt{4\pi Dt}} \int_0^x e^{-\xi^2/4Dt} d\xi = \frac{2n_0}{\sqrt{\pi}} \int_0^{x/\sqrt{4Dt}} e^{-\xi^2} d\xi = n_0 \operatorname{Erf} \left(\frac{x}{\sqrt{4Dt}} \right), \quad (38.4)$$

where Erf is an interval of probabilities (KRAMP'S function). The distribution of the particle concentration, as expressed in equation (38.4), is shown on figure 50.

It follows from equation (38.4) that the concentration gradient at the wall is equal to $\partial n / \partial x_{x=0} = n_0 / \sqrt{\pi Dt}$ and the number of particles precipitated within the time period $(t, t + dt)$ upon 1 cm^2 of wall is equal to:

$$I dt = D \frac{\partial n}{\partial x_x = 0} dt = n_0 \sqrt{\frac{D}{\pi}} dt. \quad (38.5)$$

Hence, for the number of particles precipitating within a time period t , the following expression is obtained:

$$N(t) = \int_0^t I dt = 2n_0 \sqrt{\frac{Dt}{\pi}}. \quad (38.6)$$

The following simplified method of procedure for the determination of the number of particles precipitated on a wall due to diffusion is frequently

used in working with aerosols. Taking into account that one half of the particles is, at every moment, in movement toward the wall and the other half, away from the wall, one can assume that within a time period t , one half of all particles will precipitate, which forms a layer $\bar{\Delta x}$ deep, adjacent to the wall; where $\bar{\Delta x}$ is the average absolute displacement of the particles within a time period t , as is expressed in equation (37.35). At the same time, it is apparent that the obtainable number will be twice as small, as the one in agreement with equation (38.6). Thus, in adapting this method of computation, one must consider that all the particles which do precipitate are included in the afore-mentioned layer. The reason for the difference will become clear, if we examine the question of how many particles would

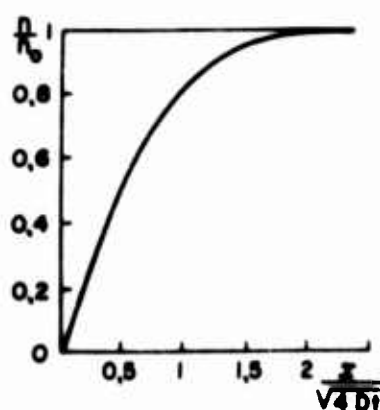


FIG. 50 DISTRIBUTION OF AEROSOL CONCENTRATION NEAR A FLAT WALL

depart from an aerosol within a time period t by way of a wall freely penetrable by particles, as, e.g., through an opening in a wall of a container.

In such case, of course, to the previous basic condition of $n(x, 0) = n_0$, with $x > 0$, one must add the condition of $n(x, 0) = 0$, with $x < 0$, which means that at the initial moment, no particles existed behind the wall. Now the boundary condition (38.3) drops off, because particles do not depart from a gaseous space. The solution of the problem is offered in the equation (272):

$$n(x, t) = \frac{n_0}{2} \left[1 + \operatorname{Erf} \left(\frac{x}{\sqrt{4Dt}} \right) \right] \quad (38.7)$$

i. e., in the given case, a permanent concentration of particles is established near the wall; the concentration is equal to $n_0/2$ (figure 51), and the concentration gradient and also the velocity of diffusion at the wall will be twice as small as at an absorbent wall. From the standpoint of Brownian movement involving an individual particle, the difference can be so explained that, on behalf of a particle which passes through a penetrable wall, there is an identical probability of returning or not returning to the space from which the departure took place. This is impossible in the presence of an absorbent wall. Thus, in the second case, the decrease of particles in an aerosol progresses twice as fast.

The third possible case, that of a "repulsive" wall, is not discussed here, because it does not occur within aerosols, at least for that degree of dispersion at which Brownian movement and diffusion, generally speaking, have any significance.

II. We shall find a condition of probability whereby a particle placed at a distance h from a flat wall while in a well-ordered movement toward the wall with a constant velocity V_0 , will reach the wall for the first time within the time interval $(t, t + dt)$. We have indicated this probability above by

$W * dt$ and could have determined it by solving the equation (37.22) with suitable basic and limiting conditions. Yet, it is simpler to solve the following equivalent problem. At a moment $t = 0$, at a distance h from an absorbent wall, there is a large number N of identical particles possessing the well-ordered velocity V_0 , directed toward a wall. What share of the particles will reach the wall within the time interval $(t, t + dt)$? Here, of course, it is necessary to solve the equation (37.17) with the previous boundary condition (38.3) and with the initial conditions of:

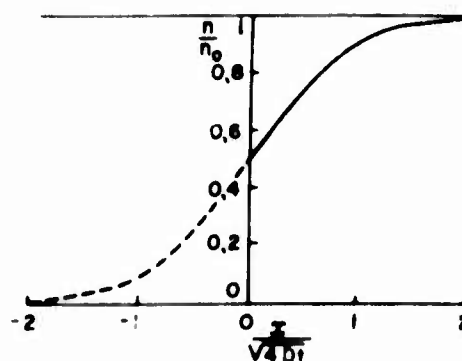


FIG 51 DISTRIBUTION OF AEROSOL CONCENTRATION NEAR AN OPENING

$$n(x, 0) = 0 \text{ with } x \neq h; \int_{h-\Delta}^{h+\Delta} n(x, 0) dx = N, \quad (38.8)$$

whereupon the integration is carried out according to an infinitely small interval 2Δ containing the point h . The solution of the problem is offered in the expression (275):

$$n(x, t) = \frac{N}{\sqrt{4\pi Dt}} \exp\left[-\frac{2V_0(x-h) + V_0^2 t}{4D}\right] \left\{ \exp\left[-\frac{(x-h)^2}{4Dt}\right] - \exp\left[-\frac{(x+h)^2}{4Dt}\right] \right\} \quad (38.9)$$

It is easy to see that the solution actually satisfies the equation (37.17) and the afore-mentioned conditions. Hence, on behalf of the probability that a particle will come in contact with a wall within a time interval $(t, t + dt)$, we obtain:

$$W^{**}(x, t)dt = \frac{D}{N} \frac{\partial n}{\partial x}_{x=0} dt = \frac{h}{\sqrt{4\pi Dt^3}} \exp\left[-\frac{(h-V_0 t)^2}{4Dt}\right] dt \quad (38.10)$$

It follows from the equation (38.10) that the average time of the particle in reaching the wall is equal¹ to:

$$\bar{t} = \int_0^{\infty} t W^{**} dt = \frac{h}{\sqrt{4\pi D}} \int_0^{\infty} t^{-1/2} e^{-(h-V_0 t)^2/4Dt} dt = h/V_0, \quad (38.11)$$

i.e., the same as in the absence of Brownian movement. As to the average magnitude of the inverse time involved, it is equal¹ to:

$$\left(\frac{1}{t}\right) = \int_0^{\infty} \frac{1}{t} W^{**} dt = \frac{h}{\sqrt{4\pi D}} \int_0^{\infty} t^{-3/2} e^{-(h-V_0 t)^2/4Dt} dt = \frac{2D}{h^2} + \frac{V_0}{h}. \quad (38.12)$$

1. By substituting $t = ht'/V$ the intervals assume the forms of

$$\int_0^{\infty} t^{-1/2} e^{-\frac{t^2+1}{qt}} dt \quad \text{and} \quad \int_0^{\infty} t^{-3/2} e^{-\frac{t^2+1}{qt}} dt, \quad \text{whose values are}$$

quoted in reference books

The following important equation emerges from (38.11) and (38.12):

$$D = \frac{h^2}{2} \left[\left(\frac{1}{t} \right) - \frac{1}{t} \right]. \quad (38.13)$$

During the experiments referred to in §36, the time of progress was measured with the aid of the particle's image, as it intersects at the moment

$t = 0$, one horizontal line with another mark in microscope's eyepiece. It is apparent that equation (38.13) is also applicable to these experiments.

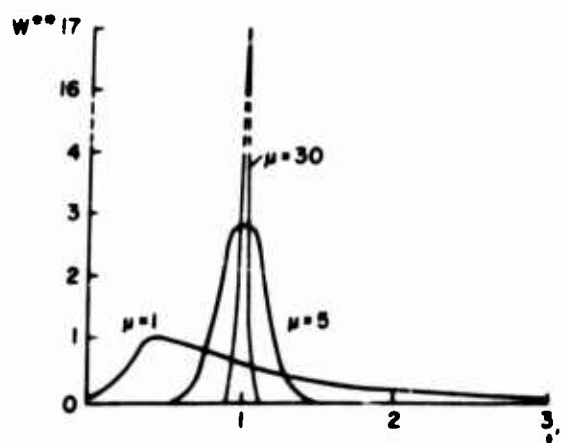


FIG. 52 SETTLING OF BROWNIAN PARTICLES

In the presence of $V_0 = 0$, instead of (38.10), a more simple equation is obtained, such as:

$$W^{**}dt = \frac{h}{\sqrt{4\pi Dt^3}} e^{-h^2/4Dt} dt, \quad (38.14)$$

and the $\left(\frac{1}{t} \right)$ in this case is equal to:

$$\left(\frac{1}{t} \right) = \frac{2D}{h^2}. \quad (38.15)$$

The above equation is applicable in examining a horizontal Brownian movement (see page 207).

We shall impart a nondimensional feature to (38.10), for which we adapt the average time of reaching the wall, $\bar{t} = h/V_0$ as a time unit, i.e., we assume $t' = t/\bar{t}$. Indicating the nondimensional value $\sqrt{V_0 h/4D}$ by μ , we can bring (38.10) to this form:

$$W^{**}dt' = \frac{\mu}{\sqrt{\pi t'^3}} e^{-\mu^2(1-t'^2)/t'} dt'. \quad (38.16)$$

Figure 52 shows curves traced according to the latter equation for $\mu = 1, 5$ and 30 , which, with $h = 0.4$ cm, match the particles' radius values of $0.1, 0.3$ and 1μ , respectively. The figure shows distinctly how some relative functions of precipitation and Brownian movement change sharply at the indicated interval of dispersion.

III. In order to explain the calculation of the particle precipitation under the influence of gravity, we shall examine on a horizontal wall the precipitation of an infinitely extended aerosol having a uniform particles' concentration n_0 . We can use for the purpose the expression (38.10), again integrating it on behalf of h from 0 to ∞ . At the same time, for the number of particles which precipitated within the time period $(t, t + dt)$ on 1 cm^2 of the wall, we can use the equation:

$$I(t) dt = n_0 \left\{ \sqrt{\frac{D}{\pi t}} e^{-V_0^2 t / 4D} + \frac{V_0}{2} \left(1 + \text{Erf} \sqrt{\frac{V_0^2 t}{4D}} \right) \right\} dt. \quad (38.17)$$

This equation, at $t \gg \frac{4D}{V_0^2}$, changes into $I(t) = n_0 V_0$, which means that the Brownian movement no longer influences the rapidity of precipitation and the latter is merely determined by the velocity of settling. If $t \ll \frac{4D}{V_0^2}$, (38.17) changes into $I(t) = n_0 \left(\sqrt{\frac{D}{\pi t}} + \frac{V_0}{2} \right)$.

Thus, in this case, the precipitation consists of a diffused precipitation in the absence of settling /see (38.5)/ and also of half of the sedimentation precipitation in the absence of diffusion. The above example shows clearly that, while computing the rapidity of aerosols settling on walls with a simultaneous action of the Brownian movement and of external or inertial forces, a simple summation of both effects may lead to serious errors. It is regrettable that, due to considerable mathematical difficulties, one must frequently confine oneself to such summations.

We must note that the afore-quoted equations are correct only in the presence of an immobile medium which, practically speaking, can only occur in a small volume of gas. Even in smoke chambers, not to mention the open atmosphere, the convection changes the entire situation very sharply.

IV. The following problem may be of interest as to practical purposes for ultramicroscopic calculations of particles: what would be the probability

that a particle, present somewhere between two parallel vertical walls, will precipitate on the latter, due to diffusion and within the time period t . If we place initial coordinates on one of the walls, the problem boils down to a solution of the equation (37.16) under the following initial conditions:

$$n(x, 0) = n_0 \text{ at } 0 < x < h; \quad n(x, 0) = 0 \text{ at } x < 0 \text{ and } x > h, \quad (38.18)$$

where h is the distance between walls under these limiting conditions:

$$n(0, t) = 0; \quad n(h, t) = 0 \text{ at } t > 0. \quad (38.19)$$

The solution of the problem affords an endless series (276) of

$$n(x, t) = \frac{4n_0}{\pi} \sum_{\nu=1}^{\infty} \frac{1}{2\nu-1} \sin\left[(2\nu-1)\frac{\pi x}{h}\right] \exp\left[-\frac{(2\nu-1)^2 \pi^2 Dt}{h^2}\right]. \quad (38.20)$$

Thus, within the time period $(t, t + dt)$, there will precipitate

$$Idt = 2D \frac{\partial n}{\partial x_{x=0}} dt = \frac{8Dn_0}{h} \sum_{\nu=1}^{\infty} \exp\left[-\frac{(2\nu-1)^2 \pi^2 Dt}{h^2}\right] dt \quad (38.21)$$

particles, while within the time period t there will precipitate

$$N(t) = \int_0^t Idt = \frac{8n_0 h}{\pi^2} \sum_{\nu=1}^{\infty} \frac{1}{(2\nu-1)^2} \left\{ 1 - \exp\left[-\frac{(2\nu-1)^2 \pi^2 Dt}{h^2}\right] \right\} =$$

$$n_0 h \left\{ 1 - \frac{8}{\pi^2} \sum_{\nu=1}^{\infty} \frac{1}{(2\nu-1)^2} \exp\left[-\frac{(2\nu-1)^2 \pi^2 Dt}{h^2}\right] \right\} \quad (38.22)$$

particles¹. If we divide this expression by the initial number of particles existing between the walls on 1 cm^2 of their area, i.e., on $n_0 h$, we can find the unknown probability of

1. Here we used the equation: $\sum_{\nu=1}^{\infty} \frac{1}{(2\nu-1)^2} = \frac{\pi^2}{8}$.

$$W^*(t) = 1 - \frac{8}{\pi^2} \sum_{v=1}^{\infty} \frac{1}{(2v-1)^2} \exp\left[-\frac{(2v-1)^2 \pi^2 D t}{h^2}\right]. \quad (38.23)$$

For the average time a particle will remain between the walls, the following expression¹ is obtained according to (38.21):

$$\bar{t} = \frac{1}{n_0 h} \int_0^{\infty} t dt = \frac{8D}{h^2} \int_0^{\infty} t \sum_{v=1}^{\infty} \exp\left[-\frac{(2v-1)^2 \pi^2 D t}{h^2}\right] dt = \frac{h^2}{12D}. \quad (38.24)$$

In ultramicroscopic chambers designed with a mechanical control to obtain a calculated volume, we compute the particles present in a layer 0.1 mm thick between two parallel glass plates². It is presumed that in this method of computation, some particles, due to Brownian movement, will precipitate on the walls as long as the counting is continued. Let us assume that, in order to estimate particles after a standstill condition in an aerosol, we need a time period of the order 0.1 sec. Thus, for particles with a radius 0.1 μ , which corresponds approximately to the lower limitation of applicability of ultramicroscopy to aerosols, we can obtain, according to the equation (38.23), $W^* = 0.11$, while $r = 0.3 \mu$ - $W^* = 0.05$, which means that the specified error will be comparatively small. The corresponding values of \bar{t} will be 3.8 and 16.7 sec, respectively. Hence, it is apparent that the examinations which require much longer observations, as, e.g., measurements of Brownian displacements, are impossible in such small vessels. For this reason, the use of cardioid and other optical condensers in working with aerosols is decreasing.

1. Here we used the equation: $\sum_{v=1}^{\infty} \frac{1}{(2v-1)^4} = \frac{\pi^4}{96}$.

2. It is necessary to indicate that the discussed method is somewhat antiquated at the present time. More precise is the "continuous" method of particles computation, as prepared by B. DERYAGIN and G. VLASENKO (277).

L. RADUSHKEVICH (278) examined the rapidity of settling of stearic-acid particles on walls of a plane-parallel vessel, with 1 mm opening, in order to determine by ultramicroscopic calculations the concentration of particles remaining in the vessel. The average size of particles was determined by a weight-computing method. Some satisfactory results of tests in agreement with the equation (38.23) were obtained, and they involved relatively isodispersed and newly formed smokes, but on behalf of coagulated and more polydispersed smokes, the rapidity of settling proved to be closer to that computed theoretically. Thus, L. RADUSHKEVICH explains correctly the difference as follows: the average cubic radius of particles

$\sqrt[3]{\overline{r^3}}$, determined by a weight-

computing method, is in the case of a polydispersed smoke, larger than the

average magnitude of r' determined by the equation $(1 + A\frac{1}{r'})/r' = (1 + A\frac{1}{r})/r$, upon which the velocity of diffusion of a polydispersed aerosol depends.

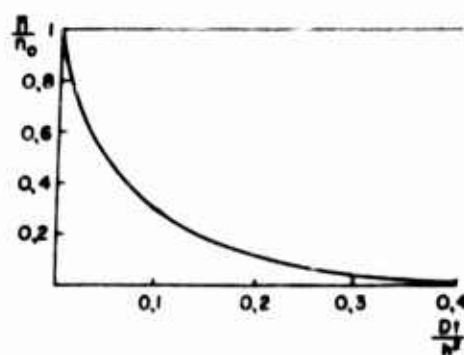


FIG. 53 DISTRIBUTION OF AEROSOL CONCENTRATION IN A VERTICAL PLANE-PARALLEL SLIT

Figure 53 shows a change in the number of particles in a layer in course of time, i.e., the function $1 - W^*$. The time is expressed in non-dimensional units of Dt/h^2 .

Likewise, of well known significance is the layer of aerosol enclosed between parallel horizontal walls (279). If we introduce the non-dimensional variables $x' = x/h$, $t' = t/t_0$ (where $t_0 = h/V_g$) and designate, as above, $\sqrt{V_g h/4D}$ by μ , then we obtain the following expression for the distribution of the aerosol concentration:

$$n = n_0 \sum_{v=1}^{\infty} \frac{2}{\pi v} \frac{1 - (-1)^v e^{-2\mu^2}}{1 + \frac{4\mu^4}{\pi^2 v^2}} \sin \pi v x' \exp \left\{ \frac{2x' - \left(1 + \frac{\pi^2 v^2}{4\mu^2}\right)t'}{\mu^2} \right\} \quad (38.25)$$

Figure 54 shows such distributions including values $\mu = 0$ (in the absence of settling), 1, 2 and 5. The figure shows that at small μ , i.e., in

highly dispersed aerosols, a distinct top limitation cannot be attained even under ideal conditions, i. e., in the absence of convection and in a fully isodispersed system.

V. If an aerosol with an initial concentration n_0 is in a spherical container of R radius, then the average concentration per time t will drop to the magnitude (276) of:

$$\bar{n} = n_0 \frac{6}{\pi^2} \sum_{\nu=1}^{\infty} \frac{1}{\nu^2} e^{-D\pi^2\nu^2 t/R^2}. \quad (38.26)$$

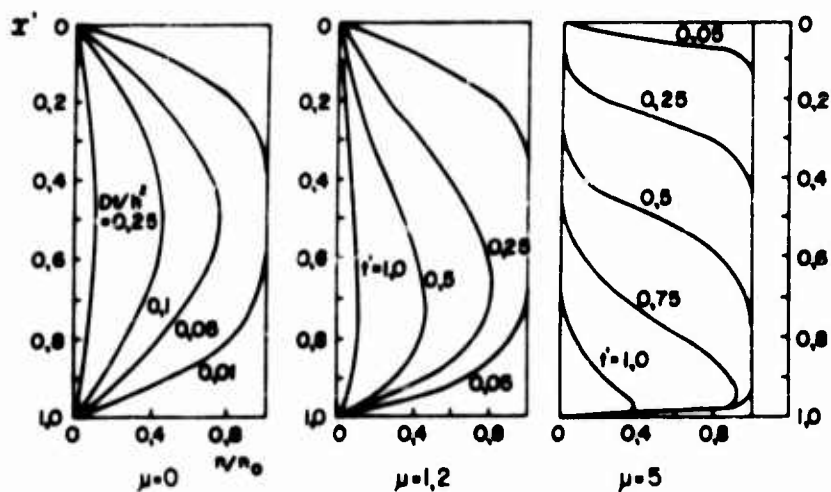


FIG. 54 DISTRIBUTION OF AEROSOL CONCENTRATIONS IN A HORIZONTAL, PLANE-PARALLEL SLIT

It is obvious that the number of particles which precipitated on the walls within this time would be equal to $\frac{4}{3} \pi R^3 (n_0 - \bar{n})$. Figure 55 shows the dependence between \bar{n}/n_0 and the nondimensional value of Dt/R^2 .

VI. A similar problem concerning aerosols in infinitely long cylindrical vessels, whose radius is R , leads to the following expression of average concentration of particles at a moment t (276):

$$\bar{n} = 4n_0 \sum_{\nu=1}^{\infty} \frac{1}{\beta_{\nu}^2} e^{-D\beta_{\nu}^2 t/R^2} \quad (38.27)$$

The $\beta_1^2, \beta_2^2 \dots$ symbols found here are squares of zeros of BESSEL'S function of the zero order of the first kind, $I_0(x)$; they represent the following values: $\beta_1^2 = 5.784$; $\beta_2^2 = 30.47$; $\beta_3^2 = 74.89$; $\beta_4^2 = 132.8$; $\beta_5^2 = 222.9$.

Figure 56 shows the dependence between \bar{n}/n_0 and Dt/R^2 . If we had to compute \bar{n} according to the already discussed simplified method, assuming that within the time period t all particles (which at the moment $t = 0$ happen to be at a shorter distance from the wall than $2\sqrt{\frac{Dt}{\pi}}$) will precipitate on the walls, then we should obtain a dotted curve which fits approximately $Dt/R^2 = 0.1$.

Of very great importance to the physics of aerosols is the problem of diffusion towards the surface of a sphere in an aerosol of an infinitely great volume with an initial concentration of n_0 . The basic condition of the problem is $n(\rho, 0) = n_0$ at $\rho > R$; the boundary condition is $n(R, t) = 0$ at $t > 0$. In the presence of polar coordinates and due to the diffusion-coefficient value being not dependent upon direction, the equation (37.18) becomes converted into:

$$\frac{\partial(n\rho)}{\partial t} = D \frac{\partial^2(n\rho)}{\partial \rho^2}. \quad (38.28)$$

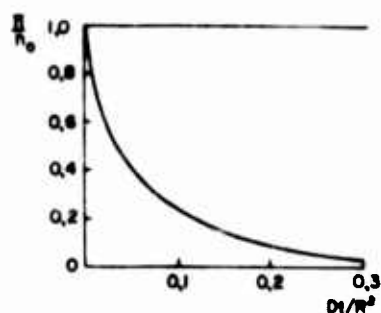


FIG 55 CHANGES OF AEROSOL CONCENTRATION IN A SPHERICAL VESSEL

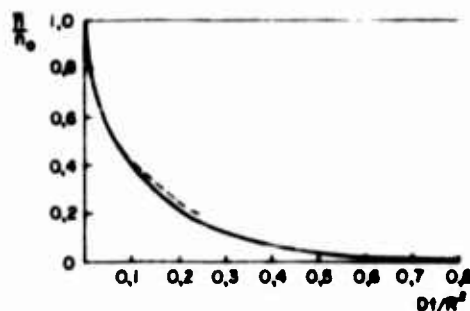


FIG 56 CHANGES OF AEROSOL CONCENTRATION IN A CYLINDRICAL VESSEL

Thus, the function $\rho n(\rho, t)$ satisfies the equation (38.28), as well as the conditions:

$$\rho n(\rho, 0) = \rho n_0 \text{ at } \rho > R, \quad (38.29)$$

$$Rn(R, t) = 0 \quad \text{at} \quad t > 0. \quad (38.30)$$

The solution of the problem is offered in the expression (280):

$$n = n_0 \left[1 - \frac{R}{\rho} + \frac{2R}{\rho \sqrt{\pi}} \int_0^{\frac{\rho - R}{2\sqrt{Dt}}} e^{-\xi^2} d\xi \right]. \quad (38.31)$$

It follows, hence, that within the time period $(t, t + dt)$ there will precipitate on a sphere

$$\Phi dt = 4\pi R^2 D \frac{\partial n}{\partial \rho}_{\rho=R} dt = 4\pi D R n_0 \left(1 + \frac{R}{\sqrt{\pi Dt}} \right) dt \quad (38.32)$$

particles, while within the time period t there will precipitate

$$N = \int_0^t \Phi dt = 4\pi D R n_0 \left(t + \frac{2R\sqrt{t}}{\sqrt{\pi D}} \right) \quad (38.33)$$

particles. With $Dt/R^2 \ll 1$, the precipitation upon a sphere progresses (from the narrow layer of aerosol adjacent to the sphere's surface) with the same rapidity as upon a flat wall (see equation (39.6)). Now, with $Dt/R^2 \gg 1$, practically speaking, a uniform distribution of the particle concentration is established around the sphere; this may be expressed in the equation

$$n = n_0 \left(1 - \frac{R}{\rho} \right) \quad (38.34)$$

Thus, the concentration gradient near the sphere's surface is equal to:

$$\frac{\partial n}{\partial \rho}_{\rho=R} = - \frac{n_0}{R}, \quad (38.35)$$

and the rapidity of precipitation (i.e., the number of particles precipitating per 1 sec) upon the sphere also becomes uniform and is equal to:

$$\Phi = 4\pi D R n_0. \quad (38.36)$$

VIII. More complicated is the solution of problems of a diffusible precipitation of aerosols upon an outer surface of an infinitely long cylinder (281) In the following table, we shall confine ourselves to quoting the $\Phi'/\pi R^2 n_0$ values (Φ' is a number of particles which precipitated upon the cylinder's unit of length, per time period t) as a function of Dt/R^2 .

Table 15
Diffusible Precipitation of Aerosol Upon an
Infinitely Long Round Cylinder

$Dt/R^2 \dots\dots\dots$	0.001	0.005	0.01	0.02	0.05	0.1	0.2	0.4
$\Phi'/\pi R^2 n_0 \dots$	0.072	0.164	0.235	0.337	0.550	0.805	1.190	1.632
$Dt/R^2 \dots\dots\dots$	0.6	0.8	1.0	1.5	2.0	2.5	3.0	3.5
$\Phi'/\pi R^2 n_0 \dots$	2.279	2.721	3.125	4.04	4.87	5.67	6.38	7.10

It is necessary to make a correction in inferences of this paragraph as to the "proper" size of particles (see page 176). This can be effected very simply by using the case as follows: an "absorbent" surface is set up at a distance r (equal to particles radius) from the surface being examined, parallel to the latter. Inasmuch as upon contact with the affected surface of particle, its center touches the absorbent surface, particles can be examined as points and all afore-mentioned inferences can be adopted to this system.

§ 39. Diffusion of Aerosols in Laminar Flow

Only in very few instances was the much more difficult problem of aerosol diffusion in a laminar flow solved accurately.

I. The problem of diffusion (or transmission of heat) against the walls of a round tube from a liquid flowing in it laminae-like was solved at various times by certain authors who did not know the work of their predecessors (282-285). At the same time, a supposition was introduced into the principle conclusion, that the velocity of convective transmission of a substance was considerably greater than that of its diffusible transmission. In other words, if the axis x is leaning parallel to the lines of flow, then in the basic equation (37. 17) the term $D\partial^2 n/\partial x^2$ is very small when compared with $\partial(V_x n)/\partial x \approx U\partial n/\partial x$ (U is the rate of flow) and as such can be disregarded.

Let us assume that n_0 is the initial concentration of particles in an aerosol; that \bar{n} is the average concentration in an aerosol which passed through a tube whose radius is R and the length is x ; that \bar{U} is the average velocity of flow in the tube. Thus, for \bar{n}/n_0 we obtain the expression:

$$\bar{n}/n_0 = 0.82 e^{-3.66\mu} + 0.097 e^{-22.2\mu} + 0.0135 e^{-53\mu} \quad (39.1)$$

in which μ is a nondimensional value equal to:

$$\mu = Dx/R^2\bar{U}. \quad (39.2)$$

We used here some practical and some equivalent values of coefficients found by NUSSELT (283) GORMLEY and KENNEDY (285). TOWNSEND (284) discovered the 0.78 value for the first coefficient. In derivations of equation (39.1) it is presumed that concentration constantly decreases along the axis and from the axis toward circumference, and this corresponds to the established region of diffusion toward walls. In actuality, however, in the presence of small μ such a region has not as yet been successfully established, that is, $n = n_0$ along the entire cross section except in a layer near the wall and therefore equation (39.1) is not applicable. Actually, in the presence of $\mu = 0$, the equation yields $\bar{n}/n_0 = 0.93$ instead of 1. In this case, one can use a simplified method of computation assuming that within a time period t there will precipitate on the walls of the tube all particles available there at the moment of $t = 0$, i.e., while entering the tube at a smaller distance than

$$\delta = 2\sqrt{\frac{Dt}{\pi}} \quad (39.3)$$

from the walls. The distribution of velocities near the walls in the presence of established laminar flow (see equation (20.11)) can be approximately described in the form of:

$$U = 2\bar{U} \left(\frac{R^2 - \rho^2}{R^2} \right) = 2\bar{U} \left(\frac{R + \rho}{R} \right) \left(\frac{R - \rho}{R} \right) \approx 4\bar{U} \frac{\delta}{R}, \quad (39.4)$$

where δ is a distance from the wall. The average velocity in a layer of δ depth near the wall is thus equal to $2\bar{U}\delta/R$ and a particle present in the layer

will, within a time period t , pass along the axis of the tube at an average distance of

$$x = 2\bar{U}\delta t/R. \quad (39.5)$$

If we exclude t from (39.3) and (39.5) we shall obtain:

$$\delta = \left(\frac{2DxR}{\pi\bar{U}} \right)^{1/3}. \quad (39.6)$$

Thus, the number of particles passing per sec through a cross section of a tube, at a distance x from the entrance is equal to:

$$\Phi = \int_0^{R-\delta} n_0 2\bar{U} \left(\frac{R^2 - \rho^2}{R^2} \right) 2\pi\rho d\rho \approx (R^2 - 4\delta^2) \pi n_0 \bar{U} = \frac{R^2 - 4\delta^2}{R^2} \Phi_0, \quad (39.7)$$

where Φ_0 is a corresponding number at the entrance to the tube. Since the proportion of $\bar{n}/n_0 = \Phi/\Phi_0$, then

$$\frac{\bar{n}}{n_0} = 1 - \frac{4\delta^2}{R^2} = 1 - 2.96\mu^{2/3}. \quad (39.8)$$

The conclusion of LEVEQUE (286) and V. LEVICH (287) is more exact and is quoted in the equation:

$$\frac{\bar{n}}{n_0} = 1 - 2.57\mu^{2/3}. \quad (39.9)$$

Figure 57 shows curves which respond to the equations (39.1)

(curve 1) and (39.9) (curve 2).

They should be used accordingly in the presence of $\mu > 0.03$ and $\mu < 0.03$. In practice one can use a graph with a continuous line, as traced on Figure 57.

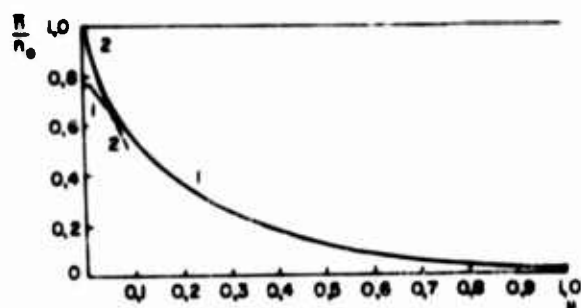


FIG. 57 DROP IN A CONCENTRATION OF AEROSOL AS IT FLOWS THROUGH A CYLINDRICAL CAPILLARY

In drawing a conclusion from the above indicated equations, it is assumed that POISEUILLE'S flow is established at the very entrance

to the tube. Actually this occurs only at the approximate distance of $0.1R \text{ Re}_f$

from the entrance and this exemplification is necessary because the location of the entrance reflects itself in the exactness of the indicated equations. For this reason we shall evaluate which part of α of the aerosol precipitates upon the walls of the tube's entrance. In view of the fact that the greater the speed of flow near the walls, the smaller will be the share of the aerosol's precipitation due to diffusion and inasmuch as, beginning with the entrance to the tube and up to the end of the entrance, the flow velocity is constantly reduced, we shall use the upper limitation for α , assuming that POISEUILLE'S flow did set itself at the very entrance, i. e., $\alpha = 2.57\mu^{2/3}$. Supposing that $x = 0.1R \operatorname{Re}_f$, we shall obtain $\alpha = 2.57(0.2D/\nu)^{2/3}$; where ν is the kinematic viscosity of the medium. In regard to air, $\nu = 0.15$ and $\alpha \approx 3D^{2/3}$. Table 13 shows that, if we consider particles even with $r = 10^{-6}$ cm, $\alpha < 0.01$. Thus, equation (39.9) lacks essential corrections only on behalf of aerosols with particles of the order of magnitude 10^{-7} cm.

L. RADUSHKEVICH (288) used equation (39.1) for the determination of the average sizes of particles in fumes of ammonium chloride. He conducted the fumes, with an average velocity of $1.84 \text{ cm} \cdot \text{sec}^{-1}$, through a system of vertical capillary tubes, 20 cm long and 0.012 cm in radius, and thus he determined, with the aid of ultramicroscopic computation, the concentration of the fumes prior to and during their passage. In these tests, μ was of the order 0.5. From the \bar{n}/n_0 values thus obtained, he calculated the average magnitude of radius of the particles, which proved to be 20-30% above the radius determined by the weight-computing method. The difference can probably be explained by the fact that particles of ammonium chloride fumes, as such, represent more or less porous aggregates and their actual size is larger than that determined by the weight-computing method.

II. An analogous problem pertaining to a plane-parallel conduit, with h the distance between the surfaces (289), leads to the equation¹

$$\left(\mu = Dx/h^2 \bar{U} \right).$$

$$\bar{n}/n_0 = 1.066 e^{-7.34\mu} + 0.0065 e^{-88.8\mu}. \quad (39.10)$$

NOLAN and GUERRINI (289) conducted atmospheric air through a system of vertical plane-parallel conduits and, with the aid of an AITKEN

1. The more exact equation (578) is $\bar{n}/n_0 = 0.910 e^{-7.54\mu} + 0.053 e^{-86\mu} + \dots$

recorder, they determined the percentage of atmospheric nuclei of condensation precipitated upon the walls of the conduits. Having found μ according to equation (39.10), the authors obtained the magnitude of $2.85 \cdot 10^{-6}$ cm for the radius of nuclei of condensation. Moreover, with the conduits in a horizontal position, they repeated their test and, seeing that the difference between the results of both tests corresponded with the number of nuclei which precipitated due to sedimentation, they computed the average velocity of their settling, and from this, their mass and density. The absurd great value of density (1.7) they obtained points out to the inadmissibility of such simplified method of computation.

III. The problem of diffusion from a flow against a surface of a sphere was examined theoretically and experimentally on behalf of condensation of vapor on a surface of droplets (or their evaporation). The velocity of diffusion against a sphere, expressed in the case of an immobile medium by equation (38.36), was increased in a flow by the factor: $1 + 0.27 \text{Re}^{1/2} \text{Sc}^{1/3}$; where $\text{Sc} = \nu/D$ is the SCHMIDT'S number (290). Yet in an aerosol, D is several orders of magnitude smaller than in vapor; the Sc number in vapor is of the order of a unit, while in aerosols it is very large ($\sim 10^5$ at $r = 10^{-5}$ cm, $\sim 10^3$ at $r = 10^{-6}$ cm). Due to this reason, it is inadmissible to transfer experimental data pertaining to diffusion of vapors to aerosols. The Sc number may be used as a rating of the ratio of the velocity of convective to diffusible transfer of a substance (at a constant Re) with regard to the type of problems discussed here. At $\text{Sc} \approx 1$, the depth of the diffusible and hydrodynamic layers of friction surrounding a circumfluent body are of identical order of magnitude. At $\text{Sc} \gg 1$, a diffusible transfer is equal to the convective one only at a very small distance from the surface of a body, i.e., a diffusible layer is very thin in comparison with the friction layer¹. Therefore the velocities of diffusion in these two instances should have a different mathematical expression. Inasmuch as the Sc during diffusion in solutions is also very large, we can profit by results of the work of V. LEVICH (293), who found for the velocity of diffusion against a sphere, in connection with a STOKES' circulative flow, the following expression.

$$\Phi = 7.9 n_0 D^{2/3} U^{1/3} R^{4/3} \quad (39.11)$$

It was assumed in accordance with the afore-said from the conclusion drawn from this equation that the depth of a diffusible layer is very

1. D. FRANK-KAMENETSKIY (291) and V. LEVICH (292) analyzed in detail the problem of types of diffusion against a surface of by-passed bodies in relationship to the order of magnitude of the Sc .

small in comparison with a radius of the sphere. Since with a decrease of U the depth of the diffusible layer increases, then at a very low velocity of flow, equation (39.11) is inapplicable.

IV. In conclusion we shall review the open diffusion of an aerosol upon its release from a narrow opening ("point-source") or from an infinitely long, flat slot ("line-source"), positioned perpendicularly to the direction of flow in a medium, which moves rectilinearly with a velocity U , which is everywhere identical. At the same time, we shall omit the particles' precipitation. We shall set the axis x parallel to the flow and place the initial coordinates at the source and in the case of a line-source, we shall superpose the y axis over the latter.

The most simple solution is that of a momentary source (294), because in the system of coordinates, moving together with the flow, the solution in the case of a point-source becomes somewhat different from the equation (37.31)

$$n(x, y, z, t) = \frac{N}{\sqrt{(4\pi Dt)^3}} e^{-\left(x^2 + y^2 + z^2\right)/4Dt}, \quad (39.12)$$

where N is the number of particles released from a source at a moment $t = 0$. The (39.12) will change with an immobile system of coordinates into:

$$n(x, y, z, t) = \frac{N}{\sqrt{(4\pi Dt)^3}} e^{-\left[(x - Ut)^2 + y^2 + z^2\right]/4Dt} \quad (39.13)$$

In the case of an infinitely long line-source we have the analogous equation:

$$n(x, y, z, t) = \frac{N'}{4\pi Dt} e^{-\left[(x - Ut)^2 + z^2\right]/4Dt} \quad (39.14)$$

where N' is the number of particles released from a source 1 cm long.

V. In the case of a continuous source, one should set up a fixed distribution of aerosol concentrations in a space. Its exact computation

is too difficult. Yet taking into consideration the afore-mentioned comparative magnitude of the convective and diffusible transfer of particles, i. e., by

discarding the term $D \frac{\partial^2 n}{\partial x^2}$ in the equation (37. 19) and by calculating in it $\frac{\partial n}{\partial t} = 0$, we can bring it, in case of a line-source, to this form:

$$\frac{\partial n(z, x)}{\partial x} = \frac{D}{U} \frac{\partial^2 n(z, x)}{\partial z^2} \quad (39. 15)$$

along with the limiting condition

$$n(z, 0) = 0 \text{ with } z \neq 0 \quad (39. 16)$$

and the condition of normalization

$$U \int_{-\infty}^{\infty} n(z, x) dz = \Phi'. \quad (39. 17)$$

This indicates that any surface perpendicular to axis x intersects in 1 sec the number of particles (equal to Φ' per 1 cm length of source) which a source releases. The solution of the equation (39. 15), which from the standpoint of mathematics is equivalent to the equation (37. 16), is offered in the equation obtained from the (37. 29) upon changing t by x and $x - x_0$ by z , then D by D/U , and upon multiplying by Φ'/U .

$$n = \frac{\Phi'}{\sqrt{4\pi D U x}} e^{-\frac{U z^2}{4 D x}} \quad (\text{line - source}), \quad (39. 18)$$

and for a constant point-source the following equation is obtained:

$$n = \frac{\Phi}{4\pi D x} e^{-\frac{U(y^2 + z^2)}{4 D x}} \quad (39. 19)$$

§ 40. Cloth and Fibrous Filters

We shall discuss two important types of mechanical filters for aerosols: 1) cloth (netted) and, 2) fibrous filters. The most important examples of the latter are filter papers and pulpboard made of cellulose, glass, asbestos and other fibers.

Cloth filters are used to intercept rather coarse aerosols. In conjunction with this, the inertial precipitation of particles upon filaments (discussed in § 34) is the basic feature of the filters. If the ratio of the pores between $2h$ filaments to their $2R$ diameters is greater than 1 (coarse fabric), the gas flowing through cloth differs little from gas flowing around segregated filaments, and in this case the effectiveness of a filter is very insignificant at low velocities of flow.

However, with a decrease of h/R , lines of flow come closer to the surfaces of the filaments and thereby the effectiveness of precipitation should be increased considerably. It is regrettable that distributions of velocities of gas flowing through a dense cloth ($h/R < 1$) are unknown, because at the present time we are compelled to omit theoretical reviews of filtration processes of aerosols through filters made of a dense fabric. Tests indicate (295) that the intercepting capabilities of fabrics actually show a sharp increase along with the increase of their thickness (much faster than the relative number of filaments per cm^2 in a fabric).

Experiments with multi-layer fabric filters show (296, 297) that a concentration n of aerosol, which passed through v layers, may be approximately expressed by the equation:

$$n_v = n_0 e^{-va} \quad (40.1)$$

or

$$\lg(n_v/n_0) = -0.43va, \quad (40.2)$$

where n_0 is the initial concentration

Thus, the concentration passing, i.e., the logarithm n_v/n_0 , depends linearly upon the number of layers. This correlation is accurate only if every layer passes the same percentage e^{-a} of particles as they

enter, e. g., while filtering isodispersed aerosols. With regard to polydispersed aerosols, α has different magnitudes for various groups. Considering particles with a radius exceeding 0.1μ , the α becomes larger with an increase of r and, consequently, much larger particles are intercepted more often in the frontal layers of a filter. At the same time the aerosol's dispersion increases, as α declines and the curve $\lg(n_v/n_0)$ as a function of v becomes more or less convex toward the v axis in relation to the aerosol's degree of polydispersion. Inasmuch as large particles rapidly clog the frontal layers of a filter, it is suggested that the latter be changed from time to time. This, of course, pertains to multi-layer filters made of either fabric or network as well as to those made of filter paper (296, 297).

The effectiveness of fabric filters increases considerably as they intercept dusts (298-300). As a layer of filtered dust is formed, pores between particles of the layer get noticeably smaller than between the filaments of fabrics, thereby the effectiveness of the layer increases. Particularly effective is asbestos dust (300, 301). It is expedient to deposit this dust on a filter fabric prior to using the latter. As fabric filters are periodically shaken up, it is recommended that some part of dust be left upon them (301). But then some references include even opposite instructions (302) according to which the increase in dust passing takes place as filters (made of wool fibers) become clogged. The reason for this inconsistency is not clear.

Thick and fleecy fabrics, particularly woolen fabrics, are considerably more effective than thin and smooth paper fabrics and, unlike the latter, they give good results even without a prior deposition of dust (298). Besides, the increase in their resistance with relation to becoming dust-clogged progresses far slower than with thin and smooth fabrics (300), i. e., owing to their higher performance volume, they possess a considerably greater dust capacity.

Dust settling on filters provided with metal networks is blown off almost completely due to the gas currents; therefore it is necessary to coat these networks with a viscous liquid (303). Such networks are most often used for filtering air entering internal combustion engines (automobile engines), in which only comparatively coarse dust particles present a risk.

As we proceed to fibrous filters (filter paper and pulpboard)¹ we note that, due to their comparatively higher hydraulic resistance, they are

1. Fibrous filters made of cotton, wool, down, etc., are now obsolete and as such they are used only in specific instances.

used in most instances with low velocities of flow, where their resistance is proportional to the first degree velocity. This points to a laminar type of flow. The Re_f in capillary passages through fibrous filters is of the order of magnitude 0.001 - 0.1. Thus, attempts to compute the magnitude of inertial precipitation of aerosols in fiber filters, as based (in § 34) on data concerning precipitations of particles on cylinders during ideal circuitous flow, cannot lead to any correct results.

The gas flow in fiber filters is of a very complicated type in so far as the flow changes its direction constantly while confusedly encircling the positions of the fibers. In order to obtain if only a notion about a magnitude of aerosol precipitation in fibrous filters, it is necessary to proceed from an idealized filter model. For example, the one shown on figure 58 represents in diametrical profile a system of identical parallel cylinders (fibers), positioned in a checkered order at $2h$ distance from each other (304). Inasmuch as the porosity (contents of pores in 1 cm^3 of material) in fiber papers and pulpboards varies approximately between 0.70 to 0.98, then the proportion of h/R is confined approximately within a range of 0.6 to 5.0.

The estimation of a field of flow presents rather great difficulties even in this very simple model of filter. Yet, more difficult, of course, is the computation of a filter's effectiveness. Therefore the computations quoted below should not even be regarded as roughly quantitative; they may only be of use in initial orientation, where the problem of the mechanism of a fibrous filter's operation is involved.

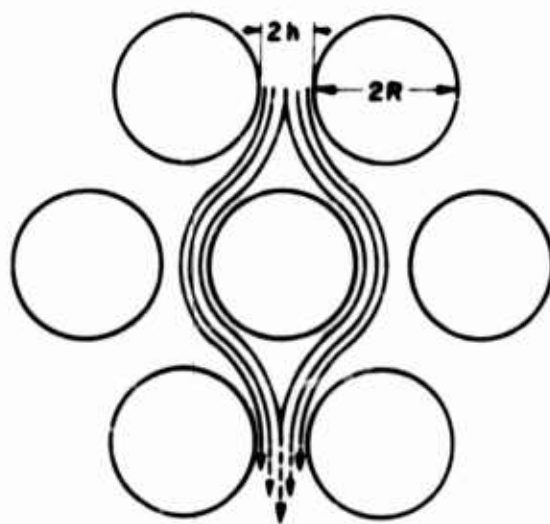


FIG. 58 MODEL OF A FIBROUS FILTER

In computing the magnitude of the particles precipitation in filters one may proceed (having considered the smallness of Re_f) from the equations for a cylinder involved in viscous flow (34. 2). This method is particularly suitable (we shall return to this topic later) with regard to filters with high porosity, i. e., with a large ratio of h/R , and thus the fibers can be examined as segregated cylinders. Some authors have selected an opposite way, which is correct with small h/R values, i. e., considering very dense filters, they assumed that, in curvilinear capillaries formed by spaces between fibers, flow assumes a POISEUILLE'S nature (figure 58 illustrates a few flow tubes

within a current). Subsequently the flow becomes retarded, at times from one and then from another side. In view of the smallness of Re_f , it may be assumed that POISEUILLE'S flow takes place in every part of the capillaries

In so far as we digress from the effects of electrostatic forces, four mechanisms are in operation during the precipitation of aerosols in fibrous filters: effect of inertia, capture effect, sedimentation, and diffusion of particles. Effects of inertia can be examined as, e.g., with the aid of slit instruments (see page 186), assuming that lines of flow do not run at 90° , but approximately at $30-45^\circ$. Thus we obtain, for a coefficient of precipitation upon one cylinder (fiber) and, consequently, upon one set of fibers, the equation (33, 3), whose numerical coefficient is approximately twice as small:

$$\mathfrak{P}_1 = l_1/2h = \tau \bar{U}/2h, \quad (40.3)$$

where for \bar{U} we adopt an average rate of flow in spaces between fibers. It is obvious, that

$$\bar{U} = \left(1 + \frac{R}{h}\right) U_0, \quad (40.4)$$

where U_0 is the velocity of gas at the entrance to a filter. A layer of Δx depth, parallel to the filter's surface, contains $\Delta x/\sqrt{3}(R+h)$ sets of fibers (precisely their axes). As an aerosol with n concentration passes through this layer, the concentration decreases by the magnitude of

$$\Delta n = \frac{l_1 n \Delta x}{2\sqrt{3}h(R+h)}. \quad (40.5)$$

It follows hence, that an aerosol leaving a filter of H depth will have a concentration equal to:

$$n = n_0 e^{-a_1}, \quad (40.6)$$

where n_0 is a basic concentration. The magnitude of

$$a_1 = \frac{\tau U_0 H (1 + R/h)}{2\sqrt{3}h(R+h)} = \frac{\tau U_0 H}{2\sqrt{3}h^2} \quad (40.7)$$

will be termed the aerosol's coefficient of inertial absorption in a filter¹. The effectiveness of a filter (fraction of intercepted particles) is equal to:¹

$$\mathfrak{Z}_1 = 1 - e^{-a_1}. \quad (40.8)$$

In computing capture effects, it is necessary to proceed from the velocity of flow at the very surface of fibers. Assuming that distribution of flow velocities in spaces between fibers is the same as in a plane-parallel capillary of $2h$ depth/sec (26.2)/, we shall obtain, for the flow velocity at a distance x from the fiber's surface, the following approximate expression

$$U = 3x\bar{U}/h \quad (40.9)$$

The flow of gas per sec in a near-wall layer of x depth per fiber's length unit is equal to:

$$\int_0^x U dx = 3x^2\bar{U}/2h. \quad (40.10)$$

Thus, due to the capture effect, $3r^2n\bar{U}/2h$ particles will precipitate upon the fiber's unit of length per sec and from each side. Inasmuch as the full flow of particles in a space between fibers per sec is equal to $2hn\bar{U}$, the precipitation coefficient on behalf of one set of fibers will be expressed by the equation:

$$\mathfrak{Z}_h = 2 \cdot 3r^2n\bar{U}/2h : 2hn\bar{U} = \frac{3r^2}{2h^2}, \quad (40.11)$$

and the aerosol's absorption coefficient, due to the capture effect, will be equal to:

$$a_h = \frac{3r^2H}{2\sqrt{3}h^2(R+h)} \quad (40.12)$$

In the theory of fibrous filters, the sedimentation of particles is usually omitted. We shall examine sedimentation effects in our model of a

1. Here, unlike in § 22 and 42, the coefficients a do not refer to a layer of absorptive medium one cm deep, but to a specific filter.

filter. On a unit of length of a horizontal cylinder being flowed-around by aerosol, $nV_s : 2R$ particles will precipitate per time unit to the first approximation. At the same time, the aerosol flows through the filter invariably either horizontally or vertically. Since the volume of gas flowing around a fiber's length unit per sec is equal to $2U_0(h + R)$, then on behalf of of one set of fibers

$$\mathfrak{Z}_s = V_s R / U_0 (h + R) = gT / U_0 (1 + h/R); \quad (40.13)$$

also the coefficient of an aerosol's sedimentation absorption by way of a filter will be equal to:

$$\alpha_s = \frac{gTH}{\sqrt{3}U_0 R(1 + h/R)^2} \quad (40.14)$$

Thus, α_1 is proportional and α_s is inversely proportional to the velocity of flow. Both effects become equal only at very low velocities of flow of the order of tenths of $\text{cm} \cdot \text{sec}^{-1}$ and sedimentation effect in practical circumstances is actually of secondary importance.

As we proceed to the diffusible precipitation of aerosols in filters, we note that our filter model reminds us very much of a tubulated cooler and thus it appears inviting to utilize data about heat transmission within such coolers. Yet, as we mentioned on page 237, such comparison is inadmissible and we again take advantage of the simplified computation method, as discussed in § 39 I. By using equation (40.13) and referring back to considerations of § 39 I we arrive at the following expression instead of (39.6) for the depth of a layer being "absorbed" by fibers:

$$\delta = \left(\frac{8LhD}{3\pi\bar{U}} \right)^{1/3} \quad (40.15)$$

We take one half of a fiber's circumference, i.e. πR , considering it to be a path L , passed over by a diffusible particle along the fiber's surface. Thus,

$$\delta = \left(\frac{8hDR}{3\bar{U}} \right)^{1/3} \quad (40.16)$$

Proceeding identically as in the computation of a capture effect, we find

$$\mathfrak{D} = 3x_0^2/2h^2, \quad (40.17)$$

$$\alpha_D = \frac{2HD^{2/3}}{3^{1/6}U_0^{2/3}Rh^{2/3}\left(1 + h/R\right)^{5/3}}. \quad (40.18)$$

It follows from equation (40.7), (40.12), (40.14) and (40.18) that the inertial precipitation is sin-bathic with the size and density of particles, as well as with the velocity of flow; sedimentation precipitation is sin-bathic with the size and density of particles and it is anti-bathic with the velocity of flow; precipitation influenced by the capture effect increases with the size of particles and it is dependent neither upon their density nor upon velocity of flow. A diffusible precipitation is anti-bathic with regard to sizes of particles as well as velocity of flow and it does not depend upon the density of particles. All types of precipitations increase rapidly with a decrease in distances between fibers. The dependence of precipitation upon the width of fibers, i.e., in the presence of an invariable magnitude of distances between fibers, is of a more complicated type. Precipitation rapidly increases in the presence of an invariable porosity in a filter as the fibers' widths decrease. All the above inference derive their origin neither from the filter's model adopted here, nor from the suppositions about the types of flow, and as such they are of general significance. Since, with a greater packing (decrease of porosity) in an up-to-now sufficiently dense filter, the h decreases rapidly, then a filter's effectiveness should simultaneously increase rather sharply, which is known practically. It is quite another matter, when speaking of porous filters and this we shall discuss later.

The following table of a filter's effectiveness is prepared for illustration purposes. The effectiveness influenced by various mechanisms is computed according to the afore-quoted equations for a filter whose depth is 0.2 cm, whose fibers' radii = 10μ and which has two velocities of flow in the proportion of $h/R = 0.7$.

Table 16
Effectiveness of a Model Filter

r, cm	$U_0 = 1 \text{ cm} \cdot \text{sec}^{-1}$				$U_0 = 20 \text{ cm} \cdot \text{sec}^{-1}$			
	\mathfrak{Z}_i	\mathfrak{Z}_h	\mathfrak{Z}_s	\mathfrak{Z}_D	\mathfrak{Z}_i	\mathfrak{Z}_h	\mathfrak{Z}_s	\mathfrak{Z}_D
10^{-6}	0	0	0	1	0	0	0	1
$3 \cdot 10^{-6}$	0	0	0	1	0.10	0	0	0.30
10^{-5}	0.03	0.02	0.01	0.95	0.43	0.02	0	0.33
$3 \cdot 10^{-5}$	0.17	0.16	0.06	0.67	0.97	0.16	0	0.14
10^{-4}	0.80	0.86	0.41	0.35	1	0.86	0.03	0.06
$3 \cdot 10^{-4}$	1	1	1	0.17	1	1	0.20	0.03

Speaking summarily about the magnitude of effectiveness, it can only be stated that it is greater in individual components, yet it is lower than their arithmetical sum. Hence, from all the afore-said, it follows that at very high and very low values of the particles radii, the effectiveness of filters should come closer to a unit. Consequently, the curve \mathfrak{Z} as a function of r should include a minimum with some $r = r_{\min}$, whereas r_{\min} decreases with the increase of velocity of flow (see page 252).

Inasmuch as, with very low and very high flow velocities, the effectiveness of filters also comes closer to unity, then the curve of \mathfrak{Z} as a function of U should also include a minimum with some $U = U_{\min}$, whereas U_{\min} should depend upon r and upon the filter's structure, as was shown from the experiments (see figure 59).

Thus, a decrease in spaces between fibers, i. e., filter packing, or a change to much thinner fibers, leads to the increase of the filters' effectiveness, although at the same time their resistance also increases. The quality of a filter is determined by its effectiveness at a certain resistance. A theoretical estimate of the dependence of the filter's quality, considering its

depth and the positions of fibers, is very difficult to make. Yet, experimental data indicate that the effectiveness of filters improves with a decrease in the fibers' thicknesses (305, 308 - 310), although a filter's quality may, at the same time, be either improved or deteriorated, depending upon the circumstances of filtrations.

DAVIES (565), LANGMUIR, and CHEN (567) used another method in computing the effectiveness of fibrous filters. Proceeding from equations for flow around a cylinder at small Re_f , they computed at first the coefficients of the particles' precipitation involving a separate fiber, and they acknowledged various mechanisms influencing the coefficients. Thereupon, they introduced theoretical or empirical corrections as to the influence of adjoining fibers. The range of applicability of this method obviously includes filters with high porosity.

For a coefficient of inertial precipitation upon a cylindrical fiber, DAVIES adopted values computed by himself, which are plotted on figure 46 (all computations of DAVIES refer to the instance of $Re = 0.2$). According to LANGMUIR, inertial precipitations may be disregarded as a rule in filtering highly dispersed aerosols. Among American authors the equation (34.18) is adopted for precipitation coefficient involving capture effect, while DAVIES, with his computation charts which provide (at $\alpha = 0.75 - 1.5$) magnitudes of η and which concur approximately with those computed according to the equation (34.18), although with $\alpha < 0.7$ they offer much higher values. DAVIES actually used the equation (34.19) for a general precipitation coefficient involving inertia and capture effect. LANGMUIR used, for the computation of diffusible precipitation, the coefficient in equation (34.18) in which he substituted $\alpha = r/R$ by δ/R ; where δ is the depth of a layer surrounding a cylinder from which all particles were able to diffuse forward to the surface of the cylinder within the circuitous flow period. LANGMUIR defined δ according to the following roughly approximate equation:

$$\delta/R = \left[1.12(2.0 - \ln Re_f) D / \bar{U} R \right]^{1/3} \quad (40.19)$$

where \bar{U} is the average air velocity in a filter. DAVIES introduced a non-dimensional parameter $D / \bar{U} R$, characterizing the intensity of diffusible precipitation; he summed up the parameter with the Stk number in the equation (34.19) without quoting any reasons for his method of computation.

In order to compute the influence of adjoining fibers upon the magnitude of η , DAVIES used a field of flow of a liquid passing through a two-dimensional network at small Re_f , computed by KOVASZNAY (568) and

obtained, for a precipitation coefficient β involving the capture effect, the following expression:

$$\beta_h = \alpha(0.16 + 10.9\phi - 17\phi^2) \quad (40.20)$$

Upon combining the latter equation with (34.19), DAVIES developed the following expression for a general coefficient of precipitation:

$$\beta = \left[\alpha + (0.5 + 0.8\alpha) \text{Stk} - 0.105\alpha \text{Stk}^2 \right] (0.16 + 10.9\phi^2 - 17\phi^2), \quad (40.21)$$

in which in the Stk number, the diffusible parameter, is again included. At the same time it follows from the expression $\alpha = r/R$ (according to DAVIES) that one should interpret by R the "effective" radius of fibers, which differs from their actual average radius because erratic and nonuniform location of fibers, and the presence of aggregates and so on. $R_{\beta\phi}$ may be defined according to the filter's resistance (see below).

From the coefficient of the particles' precipitation upon a single fiber, one may proceed to a coefficient of aerosol absorption by a filter, using the equation:

$$a = \frac{2\phi\beta H}{\pi(1-\phi)R}, \quad (40.22)$$

which is easy to develop, if one assumes, that upon a fiber's unit length there will precipitate $2R\beta n\bar{U}$ particles per second and that $\bar{U} = U_0/(1-\phi)$; where U_0 is the air velocity above the filter. Then, we can conclude that the overall length of the fibers contained in one cm^3 of the filter is equal to $\phi/\pi R^2$. The above conclusion implies that all fibers are positioned uniformly and perpendicularly to the flow.

A large number of theoretical and empirical equations was proposed on behalf of the hydraulic resistance of fibrous filters. The well-known formula of KOZEN and KARMAN is widely used in defining specific surfaces of powders according to their penetrability for liquids and gases, which proved applicable only in very dense filters, but not in filters with a high porosity. Using various fibers having different degrees of density ($\phi = 0.006 - 0.3$), DAVIES expressed the results of processing a large amount of data about a filters' resistance in the following equation:

$$\Delta_p = \frac{16\eta U_0 H}{R_{3\phi}^2} \phi^{1.5} \left(1 + 56 \phi^3\right). \quad (40.23)$$

Here $R_{3\phi}$ is the "effective" radius of fibers, which coincides with the actual average radius at small ϕ and surpasses it at greater ϕ . Nevertheless, in computing the effectiveness of a filter, one should introduce in equation (40.21), according to DAVIES, another "effective" radius $R'_{3\phi}$, which is defined from the equation:

$$\Delta_p = \frac{17.5\eta U_0 H}{R_{3\phi}'^2} \phi^{1.5} \left(1 + 52 \phi^{1.5}\right). \quad (40.24)$$

$R'_{3\phi} = R_{3\phi}$ only at $\phi < 0.2$ and at greater ϕ $R'_{3\phi} > R_{3\phi}$. According to experiments of BLASEWITZ and JUDSON (569), the resistance of filters made of glass fibers varies with the increase of their density within the range $\phi = 0.004 - 0.04$ and proportional to $\phi^{1.5}$, which is in accordance with equation (40.23); therefore, in this case, the term with ϕ^3 may be disregarded. SILVERMAN and FIRST (570) discovered that the resistance in various filters is proportional to $\phi^{1.4}$.

CHEN (567), in his computations of filter resistance, proceeded from a force affecting a single fiber by the flow around it. This force, being similar to the force discussed in § 14 and influencing a system of particles precipitating in a limited space, depends upon the distance between fibers, i.e., upon the magnitude of ϕ . We denote here, by $F(\phi)$, the force influencing a unit length of a fiber positioned perpendicularly to the flow. Using WHITE'S (571) empirical equation for resistance as applied to a cylinder moving in a viscous medium within a space limited by walls, CHEN found the following expression for $F(\phi)$:

$$F(\phi) = -A\eta\bar{U}/(B + \lg \phi), \quad (40.25)$$

where A and B are constants.

Assuming that the general length of the fibers in 1 cm^3 of a filter is equal to $\phi/\pi R^2$, we obtain from the equation (40.25) the following expression for the filter's resistance:

$$\Delta_p = \frac{\phi H F(\phi)}{\pi R^2} = - \frac{\phi H \eta U_0 A}{(1 - \phi) \pi R^2 (B + \lg \phi)} \quad (40.26)$$

CHEN'S experiments with filters made of glass fibers $0.5 - 14 \mu$ in diameter, at $\phi \leq 0.1$, have shown that, in accordance with the equations (40.25) and (40.26), Δ_p is proportional to the velocity of flow up to a maximal applied velocity equal to $Re = 6$. Furthermore, identically the same material with a dissimilar degree of density $1/F(\phi)$ depends linearly upon $\lg \phi$, although the values of the constants A and B for filters, which are distinctive as to the fibers' thicknesses and methods of manufacture, offer rather great deviations from the average values of $A = 5.3$ and $B = 0.388$. It is difficult to find from CHEN'S data any dependence between the magnitude of these constants and the fibers' diameter. Evidently the position of the fibers in a filter is of great importance.

It is obvious from equation (40.25) that $F(\phi)$ decreases with a decrease of ϕ . Within the defined value of ϕ , which is dependent upon an Re_f number, $F(\phi)$ reaches a magnitude which corresponds to the resistance of a fiber tested in the absence of adjoining fibers, as is expressed in LAMB'S equation (12.13), whereas resistance ceases to be proportional to velocity of flow. This happens: when $Re_f = 1$ e.g., at $\phi = 6 \cdot 10^{-2}$; when $Re_f = 0.1$ e.g., at $\phi = 6 \cdot 10^{-3}$; when $Re_f = 0.01$ e.g., at $\phi = 7 \cdot 10^{-4}$ and when $Re_f = 0.001$ e.g., at $\phi = 7 \cdot 10^{-5}$. These computations are confirmed by WONG'S tests.

Hence, it follows from the proportionality of the resistance and velocity of flow that the flow in filters is self-patterned, i.e., a field of flow does not depend upon Re_f . Therefore, it must be assumed that the equations (34.18) and (40.19), which basically imply that a field of flow in filters depends upon Re_f , cannot be used for computation of the filters' effectiveness.

In the experimental research of a glass-fiber filter effectiveness in so far as being dependent upon a certain degree of fiber density, CHEN arrived at the following empirical equation for a coefficient of precipitation upon a single fiber. The equation which follows, is exact only when

$$\phi < 0.1;$$

$$\eta = \eta_0(1 + 4.5\phi). \quad (40.27)$$

A comparison of the (40.27) and (40.21) equations indicates that the latter implies a much larger influence of the thickness of a filter upon its effectiveness. It should be pointed out that, according to experiments of SILVERMAN and FIRST (570), a contraction of very porous filters made of glass fibers, leading to an increase of ϕ from 0.0007 to 0.003, does not change the filters' effectiveness. WONG (567) came to the same conclusion upon contracting filters from $\phi = 0.045$ to 0.1. We shall emphasize again that, upon increased contraction of dense filters, the matter assumes other aspects.

Upon comparing the equations (40.27) and (40.26), or (40.23) it follows that resistance of porous filters increases upon their contraction more rapidly than the coefficient of precipitation. For this reason the position of LANGMUIR (567) in acknowledging the proportionality of the two magnitudes is incorrect in his computations of filters effectiveness.

CHEN passed aerosols dissimilar in their degree of dispersion ($r = 0.07 - 0.4\mu$) through filters made of glass fibers 2.5μ in diameter with the value of $\phi = 0.02 - 0.08$. His tests have shown, that the effectiveness of filters seldom improves with the increase of particle sizes at a flow velocity of 47 cm/sec, that the effectiveness is almost unaffected by changes, when $U_0 = 5.2$ cm/sec, and that it becomes somewhat reduced when $U_0 = 1.7$ cm/sec. An increase in the flow velocity results in a sharp decline in the effectiveness as to the particles with a radius of 0.075μ , yet it involves a very slight decrease, when $r = 0.36\mu$. Thus, CHEN was able to discover only at $U_0 < 4$ cm·sec⁻¹ the existence of a particle size with which the effectiveness of filters is brought to a minimum.

While filtering aerosols through a filter paper with a velocity of 3.28 cm·sec⁻¹, LAMER (567) discovered that the effectiveness unvaryingly declines with a decrease of particle size up to the very small size examined: $r = 0.02\mu$.

GREEN and THOMAS (572), using aerosols' particles up to $r = 0.1\mu$, while experimenting with filters made of wood-pulp paper, did not discover any minimum of effectiveness at a flow velocity of $24 \text{ cm} \cdot \text{sec}^{-1}$. At $U_0 = 6 \text{ cm} \cdot \text{sec}^{-1}$, the $r_{\min} = 0.03 - 0.05\mu$. As to asbestos-cellulose filters, $r_{\min} = 0.15\mu$ at $U_0 = 2.5 \text{ cm} \cdot \text{sec}^{-1}$ (307). Some references contain specifications such as $r = 0.20\mu$ (305) or 0.17μ (306), which are correct only under the particular conditions of the filters' use.

RAMSKILL and ANDERSON (310), experimenting with fogs of H_2SO_4 and dioctylphthalate of a rather high degree of monodispersion, published detailed data about the effectiveness of fibrous filters. Table 17 contains some data about the filters used in their work.

The results of the tests are shown on figure 59¹. Figures 59a and 59b illustrate the dependence of the effectiveness upon particles' radii, which is shown with the aid of curves. We see that 3, at least as to the J filter,

Table 17

Characteristics of Filters Used in RAMSKILL'S and ANDERSON'S Work

Filters	Material	Average diameter of fibers, μ	Fiber's depth, cm	Filter's resistance, mm H_2O at $U = 14 \text{ cm/sec}$	Resistance per 1 cm filter's depth	Method of manufacture
A	Viscose	17	0.110	7	64	Wet process, without calendering
B	Glass	3	0.05	10	200	The same
C	"	3	0.028	10	350	Dry process, without calendering
D	Esparto	15	0.06	67	1100	Wet process, with average calendering
E	Wood pulp	15	0.015	219	15000	Wet process, with strong calendering
F	Viscose	12	0.15	21	140	Wet process, without calendering
G	Cotton	16	0.075	4	53	The same
H	Viscose	17	0.22	14	64	" "
I	Glass	3	0.08	14	175	" "
J	"	2	0.07	40	570	" "
K	"	1	0.045	100	2200	" "

1. The charts prepared according to the axis of ordinates do not plot the effectiveness of filters 3, but the fraction penetrating, i. e., $1 - 3$.

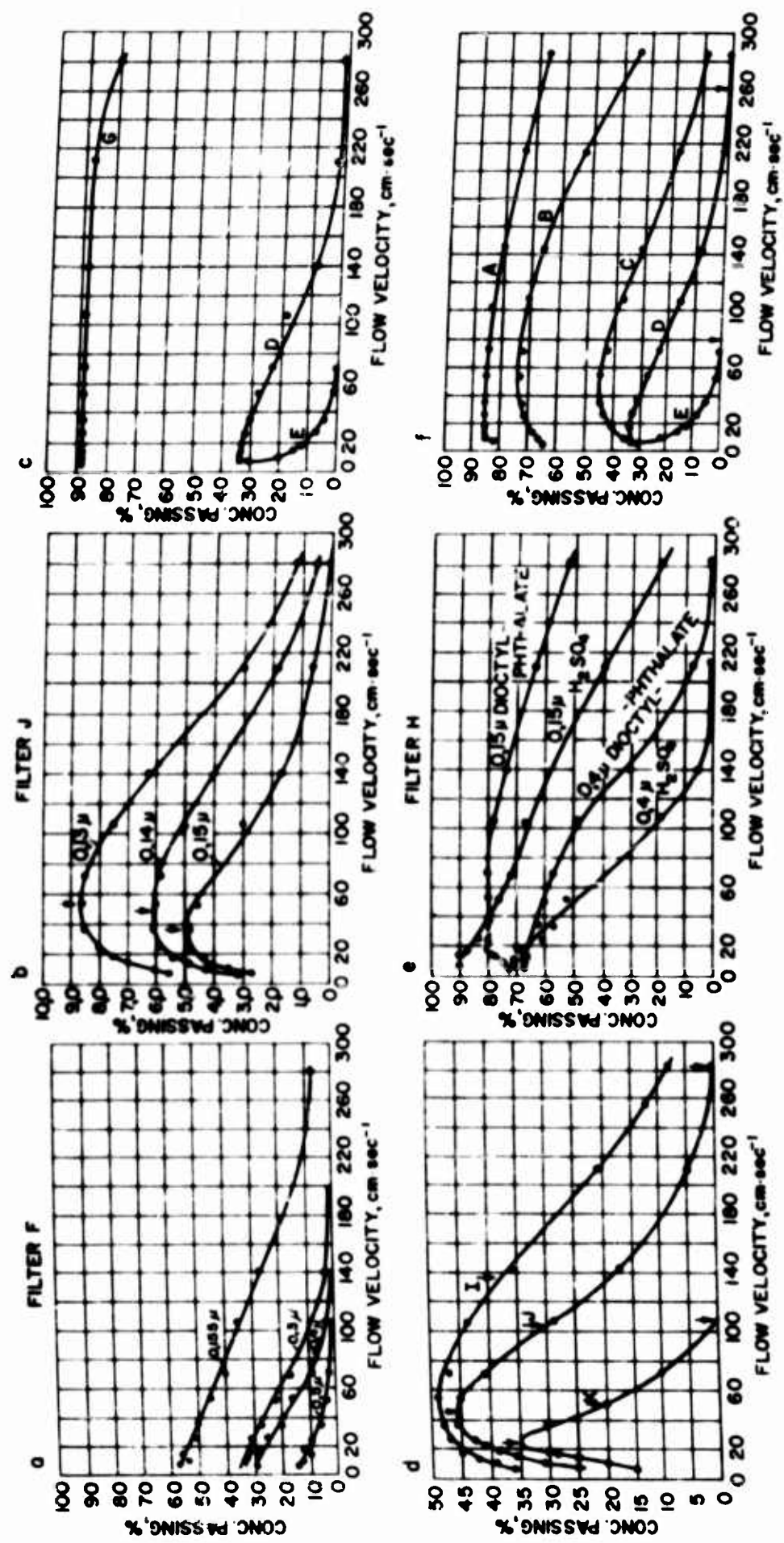


FIG. 59-EFFECTIVENESS OF FIBER FILTERS

decreases considerably during transition from $r = 0.15\mu$ to $r = 1.3\mu$ in the entire range of examined velocities. Figure 59c shows the influence of compression (calendering) upon the effectiveness of filters G, D and E, which are made of fibers of almost identical thicknesses. Nevertheless, as is apparent from Table 17, the increase of β upon compression of the filter is followed by an enormous increase of resistance. Figure 59f (fogs of dioctylphthalate, $r = 0.15\mu$) shows how a filter's effectiveness declines upon decrease in the fibers' diameter. Yet, it is apparent from comparison of Table 17 data that the quality of a glass filter improves upon decrease in the fibers' diameter only at higher flow velocities, and it decreases at lower velocities. Figure 59d shows how much β does increase upon the increase of the particles density, which is characteristic in considering inertial precipitation.

Curves (β , U) for filters made of thin fibers (B, C, I, J, K) contain clearly expressed minimums, if we consider that with regard to thick fibers, the minimums are either expressed feebly, or not at all, because they are out of place along with very low flow velocities, with which no measurements were conducted. This fact can be explained by the following example. It is apparent from the equations (40.7) and (40.18), that the diffusible precipitation increases rapidly upon reduction in the fibers' thicknesses, whereas inertial precipitation is not directly dependent upon R. Therefore at small R, diffusible precipitations prevail over inertial precipitations (and consequently β is anti-bathic to U) up to much higher flow velocities than if we compare large R.

The first smoke filters were made of a layer of cotton or similar materials, which possessed sufficient intercepting capacities only if the layer was of rather considerable depth. Such filters possess a rather high resistance. The introduction of filters with pleated surfaces (figure 60), made of filtering pulpboard (311), was considered a better progress. These filters, due to their enlarged surfaces ($\sim 1000 \text{ cm}^2$), operate under normal conditions at a low velocity of flow (in gas masks $\sim 1 \text{ cm} \cdot \text{sec}^{-1}$); therefore they possess a very low resistance (less than 20 mm of H_2O with 30 l. of air passing per minute). Meanwhile, as filters are used in gas masks and respirators, their resistance is of decisive importance because a constrained respiration feeling already appears with a higher resistance of 20 - 25 mm of H_2O .

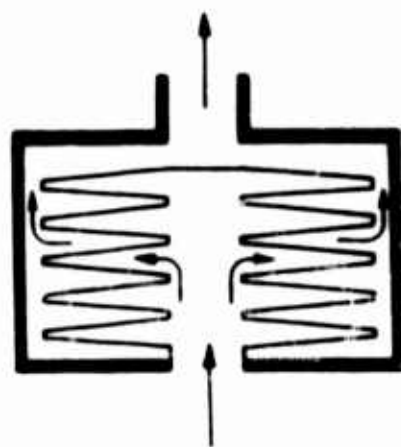


FIG.60 FILTER WITH PLEATED SURFACE

It seems that among modern filters, the best are those made of asbestos-cellulose filtering papers and pulpboard (300, 307, 312). Cellulose

fibers $\sim 15\mu$ thick serve in these filters as a support on which rest very thin asbestos filters with thicknesses of the order of a micron. With a resistance equal approximately to U cm of H_2O (where U is flow velocity in $cm \cdot sec^{-1}$), they offer, at an U order of some $cm \cdot sec^{-1}$, the effectiveness of about 0.999 as regards aerosols with $r = 0.15\mu$ possessing a high penetrating capacity. The effectiveness of asbestos-cellulose and other fibrous filters increases (simultaneously with resistance) as smokes and dusts pass through them. If aerosols contain comparatively coarse particles which rapidly clog the filter's front layer, it is necessary to set up a fore-filter and to change it as it becomes clogged.

Filters made of glass fibers $\sim 1\mu$ in diameter (308) surrender some of their superiority to asbestos-cellulose filters, as the former are coated with a special composition probably to improve sticking effect of hard particles to a smooth surface of glass (305).

Of very high quality are "electrostatic" filters which are made on carding (combing) machines from a mixture of wool and powdery dielectrics (300, 305, 307).

The effectiveness of these filters is undoubtedly induced by electrical charges of triboelectric origin which develop on particles of tar and on the fibers, especially during their combing process. When tars with high insulating properties are used, the tar-particles' charges discharge very slowly, yet with their prolonged storage the effectiveness of these filters gradually declines (313). This factor limits somewhat the field of usefulness of these filters although, if properly manufactured, they are more effective (along with a comparable resistance) than the asbestos-cellulose filters, especially at higher flow velocities. The effectiveness of electrostatic filters declines considerably with the passage of strongly ionized gases and upon exposure to Roentgen rays, i.e., upon elimination of charges inside the filter. This effect follows upon the passage of oil or aqueous vapors which, as droplets of liquids which precipitate and spread upon the surface of fibers and tar, impart a noticeable electrical conductivity to the surface. The electrostatic filters, which lost their charges, may be regenerated by way of a repeated combing. Particularly harmful to these filters are oil vapors which are likely to dissolve the tar. The effectiveness of usual cellulose filters is generally strongly increased upon their impregnation with polystyrene latex, i.e., they become converted to electrostatic filters (314). Filters made with electrets, which are dielectrics with a permanent polarization, similar to permanent magnets, are highly effective (311).

Still, it is necessary to note that electric forces probably play a substantial part also in usual fibrous filters. The fact is that effectiveness

of all filters declines considerably upon the passage of humid gas (315, 305, 300). Inasmuch as fibers of glass, asbestos, etc., are not noticeably thickened by humidity, then the influence of moisture in all probability boils down to a sharp increase in the electrical surface-conductivity of the fibers and also to the charges' discharge. The theory that the effectiveness of fibrous filters noticeably improves with a passage of solid particles of the aerosols (316) through filters is apparently brought about not only by clogging of the capillary passages, but also by triboelectric charges, as is the case with electrostatic filters. This circumstance is pointed out by the microscopic examination of dust, which settled in filters and, namely, a large amount of aggregates which apparently are formed owing to the attraction of the particles by the dust particles which settled there and were charged beforehand. We shall also point to the fact that dry fumes of NH_4Cl are better intercepted by filters than moist fumes (317).

The natural charges of the particles are also of certain importance during filtration; thus, in case of non-charged fogs of dioctylphthalate, with $r = 0.2\mu$, the effectiveness of a military type filter, which was (at $U = 2.5 \text{ cm} \cdot \text{sec}^{-1}$) 0.8, was stepped up to 0.85 upon an average charging of the particles with ~ 60 elemental charges (318).

In conclusion, we shall mention a few words about interception of aerosols by granular materials. One can observe here the same regularity as in fibrous filters, such as the increase of effectiveness with a decrease in the granules' sizes. Thus, in filtering fumes (obtained by sublimation of Sudan G dye, with the particles' radius of the order of several tenths of μ and with the velocity of $2 \text{ m} \cdot \text{sec}^{-1}$), through a No 2 porous glass filter, with an average radius of the glass granules 23μ $\eta = 0.15$ and in a No 3 filter, with granules' radius 8.6μ $\eta = 0.5$ (295). It is strange that effectiveness of glass filters improves when they are saturated with a mordant of hydrofluoric acid. It is obvious that on any etched glass surface, the particles are better intercepted than on a smooth surface. In allowing "heavy ions" of a kerosene-lamp flame ($r = 0.8 - 2.6 \cdot 10^{-6} \text{ cm}$) to pass through a layer of activated carbon 1 cm deep with a velocity of $15 \text{ cm} \cdot \text{sec}^{-1}$, the effectiveness of absorption was equal to 0.18 in the presence of carbon-granules with a radius of 0.125 - 0.275 cm; next, to 0.50 with a radius of 0.05 - 0.125 cm and, finally, to 0.86 with a radius 0.01 - 0.05 cm (179). At the same time, the inner structure of the carbon was unaffected by the results, which clearly shows that particles did not infiltrate into the pores of the granules, but settled on the outer surfaces of the latter.

Analogous observations were also made with the aid of towers, provided with a bed made of coke moistened with sulfuric acid to serve as an

absorbent for the sulfuric acid fumes. Thus, the smaller the elements of the bed, the higher the absorption was observed to be (319). It is necessary to note that granular filters possess considerably lower effectiveness than fibrous filters with the same resistance.

§ 41. Precipitation of Aerosols in Respiratory Tracts

The problem of precipitation of aerosols in respiratory tracts is of extremely great importance with regard to industrial hygiene. Thus, in addition to general amounts of specific sizes of particles precipitating at certain velocity and at certain depth of breathing, the distribution of these deposits over various parts of the respiratory system is also of great importance. Dust precipitated in the upper respiratory tracts, such as the naso-pharynx, trachea and bronchi, do comparatively little harm; it is eliminated with the aid of ciliophora, rhythmic contractions of mucous membrane, expectorations, etc.¹ Much more harmful is the dust which gets into the pulmonary alveoli, because it can only be eliminated from there with much greater difficulty. Thus, one can often recognize a man's occupation from the appearance of his lungs (e g., lungs of a coal miner). Particularly harmful to lungs is silicate dust which causes a dangerous occupational illness: silicosis. On the other hand, in so far as treatments of some illnesses with the aid of medicinal aerosols, it is important that the latter do precipitate in lungs, if possible, fully and entirely.

We shall approach this problem with the explanation of some experimental data. There are three basic methods used in examination of aerosol precipitation in the respiratory tracts. The first one is based on the microscopic studies of particles coming from the lungs, bronchi and so on; it is particularly advantageous to use, at the same time, fluorescent (e. g., willemite) dust during observations made under ultraviolet exposure (320). It has been determined in this manner that the number and size of the precipitated particles decreases steadily in proportion to the far deeper parts of the respiratory system; also that very many particles settle in bifurcations and winding paths of respiratory tracts. This indicates that inertial precipitation plays a greater role under the circumstances. There are many aggregates among the sediments and thus some narrow bronchioles as well as alveolar ducts become clogged completely with dust.

1. Some aerosols cause strong irritations in upper respiratory tracts (naso-pharynx). Thus, some people are affected by floral pollen which produces so-called "hay fever".

For quantitative determination, the best method seems to be that of radioactive indicators, i. e., the utilization of aerosols which possess a known radioactivity. In tests performed on animals, individual parts of the respiratory system are cut out from the animals' corpses and the amount of precipitated radioactive aerosol is determined in the usual way. In tests performed on humans, the amount of aerosol precipitated in the lower respiratory tracts is determined by a GEIGER counter set against the human chest (321).

Generally, the effectiveness of precipitation in respiratory tracts can also be determined by the ratio of the particle concentrations found in inhaled and exhaled air (aerosol). In order to find the distribution of the sediments in various parts of the respiratory system, measurement of the aerosol concentration is taken of separate samples of air as it is exhaled (322); the first unit contains air from the upper respiratory tracts and the last unit includes air from alveoli.

Two methods, both rather inadequate, are used especially in examining precipitations in nasal tracts. According to one of them, an individual inhales aerosol through his nose and immediately exhales it through his mouth; by this means, it is assumed, the precipitation in far deeper parts of the respiratory system may be disregarded, i. e., the precipitation takes place only in the nasal cavity (323). In tests performed on animals, the trachea of a killed animal is cut across, then the upper section of the trachea is connected to a pump and the aerosol is sucked in through the nose (324).

In reviewing the experimental data on the precipitation of aerosols in the respiratory tracts, there are noticeable personal differences in results of tests performed on humans as well as on animals. According to observations of E. VIGDORCHIK (2), this is particularly attributable to the precipitation of coarse aerosols while breathing through the nose. The effectiveness of precipitation may differ multifold among various individuals under identical test conditions, due to the great differences found in shapes and widths of the nasal tracts (324). If, in breathing through the mouth, ultra-highly dispersed aerosols are involved, the differences are not so great. Furthermore, precipitation of aerosols in a nasal cavity increases with an intensified respiration rate and consequently inertial precipitation plays here a basic part (323). Submitted in table 18 are average results of tests pertaining to oil fumes of dissimilar degree of dispersion and their precipitation in a nasal cavity (323). Radii of floral pollen, which produces hay fever, are of the order 10 - 20 μ (325) pollen precipitates fully in a nasal cavity.

On the other hand, in breathing through the mouth, a full precipitation of aerosols in the respiratory tracts decreases proportionally to the increased rate of breathing (see figure 61, where N denotes a number of inhalations per minute).

Table 18

Effectiveness of Precipitation of Oil Fumes in Man's Nasal Cavity

\bar{r}, μ	η at a breathing rate		\bar{r}, μ	η at a breathing rate	
	10 l·min ⁻¹	29 l·min ⁻¹		10 l·min ⁻¹	29 l·min ⁻¹
6	0.87	0.99	1.1	0.14	0.25
3.7	0.42	0.71	0.9	0.06	0.19

Utilized in this work are effective, isodispersed glycerine fumes which contain radioactive Na²⁴Cl (321).

Table 18 and figure 61 also illustrate that the precipitation of aerosols in respiratory tracts increases with the sizes of particles, as is indicated by the entire range of sizes examined, i. e., from 0.2 μ . In view of the above and considering bi-logarithmic coordinates, the dependence between η and r (if values of η are not very large) is expressed by a straight line. The dotted line on figure 61, reflecting breathing through the nose, indicates that, in breathing through the nose, the increase of η upon the increase of particles size proceeds much faster than in breathing through mouth. The decrease of η with an increased breathing rate through the mouth, and with a decrease of particle size, indicates that sedimentation precipitation plays a basic role at $r > 0.2\mu$. At the same time a considerable part of the aerosol precipitates during the arrest of breathing, between inhalation and exhalation. As the duration of the arrests increases, i. e., when breathing becomes suspended upon an inhalation, the effectiveness of precipitation increases considerably (326) and such suspension is recommended in treatments of pulmonary illnesses by means of aerosols.

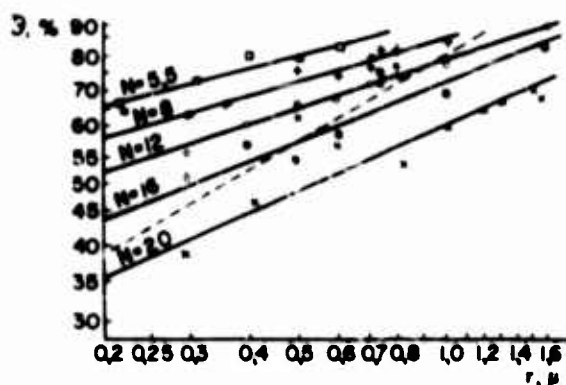


FIG. 61 SETTling OF AEROSOLS IN RESPIRATORY TRACTS

The following data are available pertinent to precipitations of aerosols in various parts of the respiratory system. In tests with rabbits, it was discovered (327) that, of all particles of an inhaled aerosol (with $\bar{r} = 0.5\mu$), 29% precipitated in the naso-pharynx, 13-19% in the trachea, and 51-58% in the lower respiratory tract. The percentage of precipitation in the naso-pharynx at $\bar{r} = 2\mu$ increased to 65% and, at $\bar{r} = 4\mu$, to 98%. In tests with mice (328) involving a distribution of sedimentation of oil fumes between a- bronchi, b- bronchioles and alveolar ducts, as well as c- alveoli, the following percentages were discovered: at $r = 0.2 - 0.62\mu$, 26, 32 and 42%; at $r = 0.62 - 1.05\mu$, 33, 33 and 34%; at $r = 1.05 - 1.46\mu$, 35, 37 and 28%; at $r = 1.46 - 1.88\mu$, 48, 37 and 15%; at $r = 1.88 - 2.28\mu$, 46, 40 and 14%; at $r = 2.28 - 2.71\mu$, 53, 37 and 10%; at $r = 2.71 - 3.13\mu$, 62, 34 and 4%; at $r = 3.13 - 3.55\mu$, 67, 33 and 0%; at $r > 3.55\mu$, 90, 10 and 0%.

Thus, proportional to the increase of particle sizes, the general effectiveness of precipitation in a respiratory system increases, but primarily at the expense of sedimentation in the upper respiratory tracts. Of utmost interest to industrial hygiene is the magnitude of precipitation in the lower respiratory tract, naturally, proportional to the passage of particles through the

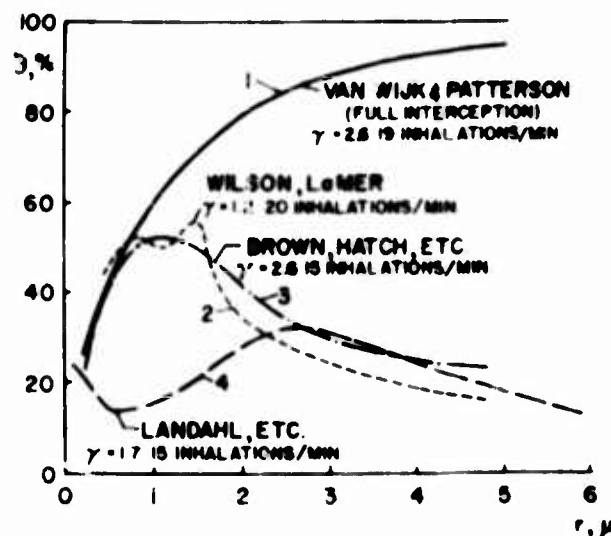


FIG 62 SETTLING OF AEROSOLS IN RESPIRATORY TRACTS

upper respiratory tracts, as well as proportional to the effectiveness of precipitation of particles infiltrated into the lower respiratory tracts. As the particle size increases, the indicated penetration decreases to zero and the effectiveness of precipitation in the lower respiratory tracts decreases from 1 (for very large particles) to a comparatively small magnitude (with r of the order 0.1μ). In connection with this, the curve indicating precipitation in the lower respiratory tracts, as a function of the particles radius, should present a

maximum, as this is also evident in the tests. Figure 62 shows such curves plotted by several authors. Only curve 1, prepared by VAN WIJK and PATTERSON (329) for aerosol with $\gamma = 2.6$, at 19 respirations per minute, pertains to precipitation in the entire respiratory system. The No. 2 curve was prepared by WILSON and LAMER (321) for glycerine fumes, with $\gamma = 1.2$, at 20 respirations per minute; curve No. 3 was prepared by BROWN and HATCH (330) for dust, with $\gamma = 2.6$, at 15 respirations per minute; curve No. 4 was prepared by LANDAHL (322) for triphenylphosphate fumes, with $\gamma = 1.17$, at 15 respirations per minute. Since, at small r , precipitation in the upper respiratory tracts may be disregarded, the curves 1-3 coincide rather well with each other. The considerable difference of curve No. 4 can probably be explained by systematic errors in the determination of the droplet sizes (331). Thus, the particles with r of the order of 1μ precipitate mostly in the lower respiratory tract and these particles constitute the greatest danger to an organism. One must remember that, together with a size of particles which are suitable for a maximum precipitation in the lungs, there is (the same as in precipitations in filters) a size, which is proper for a minimal precipitation and which has not been discovered in tests, whose results are shown on figure 62. According to DAVIES (331), $r_{\min} = 0.12 - 0.15\mu$, which is close to the proper magnitude for fibrous filters.

We shall still refer to one circumstance, mentioned in tests of I. LIFSHITS, E. LYKHIN and G. ERENBURG (332), that the percentage of charged particles precipitating in the respiratory tract is considerably greater than that of noncharged particles. Thus, from aluminum dust containing 69% of small particles ($r < 0.5\mu$) and 27% of large particles ($0.5\mu < r < 1.5\mu$), there was precipitated during respirations 34% of noncharged and 66% of charged particles. It appears that the cause of this effect is induction (reflex) forces, which attract charged particles to the walls of the respiratory tracts.

An interesting theoretical study of the problem discussed in this paragraph is by FINDEISEN (333), who proceeds from a very simplified model of a respiratory system. He described respiratory tracts as straight tubes, whose length, width and location agree approximately with anatomic data and subsequently he described lungs' alveoli as hollow little spheres. He assumed that an inhalation and exhalation takes place with an identical constant rate ($200 \text{ cm}^3 \cdot \text{sec}^{-1}$) and that they last 2 sec each without stops in between. Then he took into account sedimentation and diffusion in the respiratory tracts, as well as inertial precipitation in bifurcations, and he also considered precipitation during the inflow as well as during the outflow. Thus FINDEISEN computed the percentage of a certain size of particles which precipitate in every part of the respiratory system. In assuming the flow velocity of air as being constant at all cross sections of the tubes, he inevitably obtained greater values of β .

Table 19, computed by FINDEISEN, quotes values of η in various parts of a respiratory system, influenced by all the afore-mentioned factors as to the range of r values. The left part of the table contains data referring to numbers of v , length L , radius R and a general transverse cross section S of respiratory tracts, velocity of air flow U , and that of time t during which particles pass through a certain part of the respiratory system. In computing sedimentation precipitation, the average inclination angle of the respiratory tracts to the horizontal is assumed to equal 50° . Numbers placed between the names of the respiratory tract pertain to inertial precipitation in appropriate bifurcations. The value of 90° was used for the deflection angles at bifurcations in a transition from alveolar bronchioles to alveolar ducts, and 30° for all of the remaining transitions.

If we compare data included in table 19 and in figure 61, it becomes obvious that the results computed by FINDEISEN differ rather extensively with the test. This can be explained by the primitiveness of his computation method and by the necessary idealization of the entire process of precipitation in respiratory tracts. Yet, all these results introduce an undeniable interest: they offer a picture (correct in general patterns) of precipitation of aerosols in various parts of the respiratory system. FINDEISEN'S computations were defined in part more accurately by LANDAHL (334).

As we pointed out in § 24, one of the methods of intensification of the precipitability of aerosols in respiratory tracts appears to be unipolar charging of aerosols (335). In unipolar-charged, highly dispersed smokes of MgO , used by DESSAYER (168) for therapeutic purposes, the concentration of particles was of the order 10^7 per cm^3 and the mobility u was equal to $0.002 - 0.007$. Assuming that on the average the particles possessed one elemental charge each, and considering that $u = Bq/300$, we find, according to the equation (24.6), that during an aerosol's interval of stay in the respiratory tract (~ 2 sec), and owing to electrostatic dispersion, some 10 - 30% of particles would precipitate, whereas DESSAYER's measurements imply that full precipitation comprised 70 - 80%. Yet, with this, one must consider that the interval of an aerosol's stay in the lungs (according to table 19) is considerably greater than in the upper respiratory tract, i.e., that during an electrostatic dispersion, precipitations take place mainly in the lungs.

As we mentioned already, the therapeutic value of unipolarly charged smokes of MgO is uncertain. If unipolar charging in medicinal (e.g., penicillin) aerosols (for purposes of increasing their precipitability in lungs) is to produce an appreciable effect, then, according to the

equation (24.6), a high concentration of particles and a greater magnitude of charges among them are essential. Furthermore, particles should be sufficiently small, so as not to precipitate measurably in the upper respiratory tracts. It is very difficult to obtain aerosols with a calculated high concentration by way of mechanical diffusion (336). Thus, a practical realization of the idea is apparently possible only with the aid of combinations which withstand the heating process essential to convert them to aerosol condition by thermal means.

In conclusion, we shall compute to whatever extent a bipolar charging of particles may influence the precipitability of aerosols in respiratory tracts. In conjunction with this, we shall confine ourselves to the examination of precipitation in the alveoli, representing the latter as hollow little spheres with a radius $R = 0.015$ cm. A particle found at a distance x from the alveolar surface and possessing a charge q (which is small in comparison with R), is attracted to the surface by way of a reflex force which is equal to $q^2/4x^2$ and is moving to the surface with a velocity

$$v = - \frac{dx}{dt} = \frac{q^2 B}{4x^2} \quad (41.1)$$

It follows, hence, that a particle found at a moment $t = 0$ at a distance x_0 from the alveola's surface will reach the latter within the time of

$$t = \frac{4x_0^3}{3Bq^2} \quad (41.2)$$

During the interval (of the order 1 sec) that the particles remain in one alveola, surfaces of the latter will come in contact with particles found at a distance smaller than x_0 , whereupon

$$x_0 = \left(\frac{3}{4} Bq^2 \right)^{1/3}, \quad (41.3)$$

and collectively there will precipitate, due to reflex forces

$$\Phi_1 = \frac{4}{3} \pi R^2 x_0 n = \frac{4}{3} \pi R^2 n \left(\frac{3}{4} Bq^2 \right)^{1/3} \quad (41.4)$$

Table 19

Effectiveness of Precipitation of Aerosols in Various Parts of Human Respiratory Tracts

Parts of respiratory tracts	v	R, cm	L, cm	S, cm ²	U, cm·sec ⁻¹	t, sec	Effectiveness of precipitation (%) with particles' radius, μ						
							0.03	0.1	0.3	1	3	10	30
Trachea	1	0.65	11	1.3	150	0.07	0.16	0.08	0.03	0.10	0.8	7.6	67
Main bronchi	2	0.37	6.5	1.1	180	0.04	0.21	0.10	0.05	0.16	1.2	11.0	33
Bronchi of the 1st order	12	0.20	3.0	1.5	130	0.02	--	--	0.03	0.11	0.7	6.2	--
Bronchi of the 2nd order	100	0.10	1.5	3.1	65	0.02	0.28	0.13	0.07	0.27	2.5	20.0	--
Bronchi of the 3rd order	770	0.075	0.5	14	14	0.04	0.55	0.26	0.04	0.07	0.4	2.5	--
Bronchioles, terminal	$5.4 \cdot 10^4$	0.030	0.3	150	1.3	0.22	1.03	0.51	0.02	0.52	3.8	20.3	--
Bronchioles, alveolar	$1.1 \cdot 10^5$	0.025	0.15	220	0.9	0.17	6.1	3.1	0.29	0.35	2.7	5.0	--
Alveolar ducts	$2.6 \cdot 10^7$	0.010	0.02	8200	0.025	0.82	--	--	0.02	0.84	2.0	5.3	--
Alveoli	$5.2 \cdot 10^7$	0.015*	--	$1.47 \cdot 10^5$ **	0	1.2	37.2	19.1	2.0	4.0	25.4	10.2	--
							--	--	--	0.79	1.5	--	--
							--	--	2.0	3.7	16.0	--	--
							--	--	15.8	1.8	2.5	--	--
							--	--	--	40.3	36.6	--	--
							14.1	8.6	12.7	1.1	--	--	--
							66	35.0	34.2	41.6	--	--	--
Total	--	--	--	--	--	--	66	35.0	34.2	97.4	100	100	100

* Sphere's radius

** Total surface

particles. Furthermore, within this time, there will precipitate under the influence of gravity

$$\Phi_2 = \pi R^2 n V_g = \pi R^2 n B m g \quad (41.5)$$

particles. Speaking of aluminum particles with a radius $\sim 0.5\mu$, on which I. LIFSHITS, E. LYKHIN and G. ERENBURG worked, one may assume, according to data of N. TUNITSKIY, M. TIKHOMIROV and I. PETRYANOV (337), that the average magnitude of the particle charges which emerge during diffusion is equal to approximately 50 elemental charges per particle¹. It follows hence, according to the equations (41.4) and (41.5), that

$\Phi_1/\Phi_2 = 0.67$, i.e., the reflex forces considerably increase the precipitation of charged particles. Let us assume that such high charges can emerge only due to triboelectric effect. So, in the course of a "natural" bipolar charging of particles in an ionized atmosphere (see page 141), the influence of charges upon the precipitability of aerosols in respiratory tracts would be insignificant.

§ 42. Absorption of Aerosols During Bubbling

The absorption of aerosols as they pass through liquids under usual circumstances is comparatively small, thus it is only of limited technical importance. Yet, in the history of development of our knowledge about aerosols, this problem played a fairly important part: one of the first observations about properties of aerosols was precisely their poor absorption (in comparison with gases) during passage through water. Later, we ran into this phenomenon while developing a contact method for obtaining sulfuric acid. A great many experimental tests were devoted to absorption of aerosols during bubbling through water and aqueous solutions and a considerable share of the tests belongs to REMY. Unfortunately, these efforts are of highly empirical nature and their authors did not even attempt to offer any explanations about their observations. Furthermore, the sizes of particles (of hygroscopic fogs) on which most of the tests were performed were not determined precisely; therefore, it is difficult to interpret the results of these tests. Still, one can draw from this work some conclusions about the mechanism of aerosol absorption during bubbling.

1. At the same time $x_0 = 1.45 \cdot 10^{-3}$ cm and the condition of $x_0/R \ll 1$ is retained.

The type of movement of gaseous bubbles through water, as well as through aqueous solutions, depends in a greater measure upon the size of the bubbles (338, 339). A movement of very small bubbles (approximately up to $R = 5 \cdot 10^{-3}$ cm) is correlated to the numbers of $Re < 1$. At the same time, if water does not contain any surface-active impurities, a circulation develops inside the bubbles (figure 63) during which the velocity of gaseous flow near the bubble's surface is expressed by the equation

$$U_{\tau} = 0.5 V_{\pi} \sin \theta, \quad (42.1)$$

where V_{π} is the bubble's rising velocity; where θ is an angle between the radius vector and the direction of the bubble's movement. At $5 \cdot 10^{-3} < R < 10^{-1}$ cm, a movement of bubbles corresponds to $1 < Re < 700$. Within this region, bubbles retain their spherical shape and, as a liquid flows around them, the effect resembles that of an ideal liquid flowing around a sphere (338); furthermore, the velocity of the circulating gas near the surface of a bubble may be expressed approximately by the equation:

$$U_{\tau} = 1.5 V_{\pi} \sin \theta, \quad (42.2)$$

which means that the velocity is three times greater than in the preceding case.

Finally, if $R > 10^{-1}$ cm, a bubble collapses as pulsations develop in it; likewise the gas circulation assumes a more complicated nature, (whereupon) the velocity of the bubble's rise, being at the same time little dependent upon the bubble's size, reaches $\sim 20 - 30 \text{ cm} \cdot \text{sec}^{-1}$. In practice, one has to deal specifically with this size of bubbles. In order to simplify computations, we shall assume that bubbles are of spherical shape and that the gas circulation velocity is expressed by the equation (42.2).

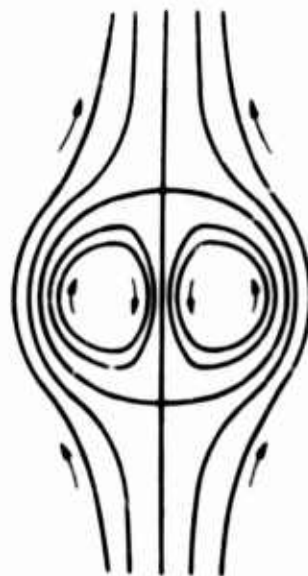


FIG. 63 CIRCULATION IN A SPHERICAL CLOUD AND IN A GASEOUS BUBBLE

The absorption of aerosols during bubbling, as in previously discussed instances, occurs due to inertial precipitation, sedimentation and diffusion. Inasmuch as the sizes of aerosol particles are considerably smaller than the sizes of bubbles, then the capture effect during bubbling may be disregarded. The magnitude of inertial precipitation in a spherical bubble can be

computed according to the equation (28.1), with no effort. We offer the following expression for velocity of the particle's movement, which is influenced by a centrifugal force:

$$V = \frac{U_{\pi}^2 \tau}{R} = \frac{9V_{\pi}^2 \tau \sin^2 \theta}{4R} \quad (42.3)$$

Thus, in one sec there will precipitate in a bubble

$$\phi = \frac{9V_{\pi}^2 \tau n}{4R} \int_0^{\pi} \sin^2 \theta \cdot 2\pi R^2 \sin \theta d\theta = 6\pi V_{\pi}^2 \tau n R \quad (42.4)$$

particles, while within one cm of the bubble's path there will precipitate

$$\phi' = 6\pi V_{\pi} \tau n R \quad (42.5)$$

particles. The proportion of the number of particles precipitated per cm of a path, if compared to the entire number of particles in a bubble or, optionally, a coefficient of inertial absorption during bubbling, α_i , is equal to

$$\alpha_i = \frac{6\pi V_{\pi} \tau n R}{(4/3)\pi R^3 n} = \frac{9V_{\pi} \tau}{2R^2} \quad (42.6)$$

Due to sedimentation in a bubble, within one sec there will precipitate $\pi R^2 n V_s = \pi R^2 n g \tau$ particles and the coefficient of sedimentation absorption during bubbling - α_s - will be equal to:

$$\alpha_s = \frac{3g\tau}{4RV_{\pi}} \quad (42.7)$$

Assuming that $V_{\pi} = 25 \text{ cm} \cdot \text{sec}^{-1}$, we can find for $R = 0.1 - 0.5 \text{ cm}$ that inertial precipitation during bubbling is larger by an order of magnitude than sedimentation precipitation would be.

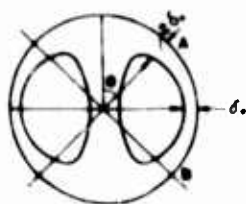


FIG 64 DIFFUSION OF AEROSOL IN A BUBBLE

A more complicated matter is the calculation of a coefficient of diffusible precipitation of aerosols during bubbling; yet, one can find the approximate magnitude of the coefficient in the following

manner. We examine in a bubble the surface delineated by the flow lines, where they pass near the bubble's surface at a distance δ (figure 64). Between both surfaces there flows in one sec a volume of gas which is equal to:

$$\Delta v = 2\pi R \sin\theta \delta U_{\tau} = 3\pi R V_{\pi} \delta \sin^2\theta = 3\pi R V_{\pi} \delta_0, \quad (42.8)$$

where δ_0 is a value of δ in the equatorial plane of the bubble. Inasmuch as velocities of flow in polar areas of the bubble are small, and the lines of flow fall back from the bubble's surface, then the diffusible precipitation here is also small. Consequently, we shall confine ourselves to a computation of precipitation in the equatorial area of the bubble, between latitudes $\pm 45^\circ$, i.e., at $\pi/4 \ll \theta \leq 3\pi/4$. In this area, δ changes from δ_0 to $2\delta_0$, and we shall take the average value $\bar{\delta} = 1.5\delta_0$. The time t during which a particle will pass the path from A to B (figure 64) is equal to:

$$t = \int_{\pi/4}^{3\pi/4} \frac{R d\theta}{U_{\tau}} = \frac{2R}{3V_{\pi}} \int_{\pi/4}^{3\pi/4} \frac{d\theta}{\sin\theta} \approx \frac{1.2R}{V_{\pi}}. \quad (42.9)$$

According to the simplified method of computing a diffusible precipitation, we find:

$$\bar{\delta} = 2\sqrt{\frac{Dt}{\pi}} = 2\sqrt{\frac{1.2DR}{\pi V_{\pi}}} \approx 1.2\sqrt{\frac{DR}{V_{\pi}}}. \quad (42.10)$$

Against the surface of a bubble, such a particle, which is found between the two afore-mentioned surfaces, diffuses and is absorbed by the liquid. Thus, per unit time there will be absorbed

$$\Phi = n\Delta v = 3\pi R V_{\pi} \delta_0 n = 2\pi R V_{\pi} \bar{\delta} n = 2.4\pi n \sqrt{DV_{\pi}} R^3 \quad (42.11)$$

particles.

Hence, for a coefficient of a diffusible absorption of aerosols during bubbling, the following expression is obtained:

$$\alpha_D = 1.8\sqrt{\frac{D}{V_{\pi} R^3}}. \quad (42.12)$$

As is apparent from the afore-quoted equations, the absorption of aerosols during bubbling should be strongly intensified upon decrease in the bubbles' radii. As to influences of particle size, as well as the bubbles' rising velocity affecting individual types of precipitation, we find here the same correlations as in a case of fibrous filters.

We shall proceed to the discussion of testing material used by REMY in ordinary wash bottles and in tall cylinders filled with aqueous solutions. Radii of the bubbles ranged between 0.3 - 0.6 cm. First of all we detected (already mentioned) a considerable increase of absorption with a decrease in the bubbles' sizes (340). A series of tests performed on highly dispersed "dry" aerosols of sulfuric acid and ammonium chloride, consisting of particles with a radius $\leq 10^{-5}$ cm, indicated (341) that these aerosols are absorbed by aqueous solutions in indirect proportion to the vapor pressure of the solution (at a certain temperature). These observations are explainable by the following circumstance. Particles of the indicated size usually absorb moisture from the surrounding medium rapidly, and the higher the pressure of the aqueous vapor in the bubbles, the more these particles grow. Meanwhile, a diffusible precipitation is of basic significance, if particles with a radius $\leq 10^{-5}$ cm are considered. Actually, according to the equations (42.6), (42.7) and (42.12), under typical conditions of the tests in question, with $R = 0.5$ cm, $V_{\pi} = 25$ cm·sec $^{-1}$ and particles' radius of 10^{-5} , we find the following corresponding values for the coefficients of the inertial, sedimentation and diffusible absorptions: $1.0 \cdot 10^{-4}$, $0.14 \cdot 10^{-4}$ and $15 \cdot 10^{-4}$. With the enlargement of particles to $r = 2 \cdot 10^{-5}$ cm, the coefficients of inertial and sedimentation absorptions will be increased proportionally to $3 \cdot 10^{-4}$ and $0.4 \cdot 10^{-4}$, respectively, but the coefficient of diffusible absorption will diminish to $9.3 \cdot 10^{-4}$, i.e., a general absorption will decrease too.

Tests performed on coarse fumes ($r \approx 10^{-4}$ cm) of the same substances produced a contrary picture, namely, an increase in the absorption of aerosols following the increase in vapor pressure of the solution through which the aerosol passed, i.e., with the particles enlarged. This was to be expected because at $r = 10^{-4}$ cm $a_i = 59 \cdot 10^{-4}$, $a_s = 8 \cdot 10^{-4}$ and $a_D = 3.6 \cdot 10^{-4}$; that is, the absorption occurs mainly due to inertia and settling, but it increases with the sizes of particles.

We shall try to compare the absolute values of absorption coefficient (as found by REMY) with theoretical computations. Only one piece of REMY'S (342) work serves our purpose, i.e., that in which he quotes the values of absorption coefficient of the fog which was obtained by blowing air over oleum, aqueous solutions of sulfuric acid. Thus, with $R = 0.5$ cm and $V_{\pi} = 20$ cm·sec $^{-1}$, in a 5% solution of sulfuric acid, the obtained value was

$\alpha = 0.005$. The rapidity of settling of the upper boundary of the fog, up to the start of bubbling, equaled $3.5 \cdot 10^{-3} \text{ cm} \cdot \text{sec}^{-1}$. If we consider the magnitude of 80% of acid concentration in droplets, we find that the radius of droplets up to the start of bubbling amounted to $4 \cdot 10^{-5} \text{ cm}$. At the same time, $\alpha_i = 8.3 \cdot 10^{-4}$, $\alpha_g = 1.7 \cdot 10^{-4}$, $\alpha_D = 6.8 \cdot 10^{-4}$ and, when added up, $\alpha \approx 0.0015$. As the fog became equilibrated with the solution, the acid concentration in the droplets diminished to 5%. At the same time, the droplets' radius increased up to $1.2 \cdot 10^{-4} \text{ cm}$. This size of radius tallies with the values of $\alpha_i = 67 \cdot 10^{-4}$, $\alpha_g = 13 \cdot 10^{-4}$, $\alpha_D = 4 \cdot 10^{-4}$ and, when added up, $\alpha \approx 0.008$. Thus, the effective value of the absorption coefficient should be contained within the interval of 0.0015 - 0.008, which agrees with the order of magnitude of REMY'S data.

During bubbling, as well as in filtering aerosols through fibrous filters, a curve of the effectiveness of absorption as a function of particle size maintains a minimum; therefore, in the course of bubbling of a poly-dispersed aerosol, the latter should become more or less homogeneous and, consequently, the curve of distribution of particle sizes should be drawn somewhat closer to specifications suitable to a maximal passage of particles. This effect, which increases with a repeated bubbling, was used by DAUTREBANDE (326) to obtain some monodispersed aerosols with $\bar{r} \approx 0.2 - 0.3 \mu$ for purposes of physiological research.

The absorption of aerosols is very effective when they are allowed to pass through porous glass filters submerged in water (343). Thus, e.g., the No. 1 filter, which alone intercepted only 50% of sulfuric acid fumes, entrapped approximately 99% of the fog upon submersion. Since the radius of bubbles formed in the course of bubbling through glass filters is equal to $0.025 - 0.10 \text{ cm}$ (depending upon the number of the filter), then the afore-mentioned result is not surprising.

It is interesting that the effectiveness of absorption during bubbling decreases in relation to the increase of water temperature, and thus it practically amounts to zero at a boiling temperature (344). In this case, two factors may be predominant: the enlargement of bubbles at the expense of water vapor (with the approach to boiling temperature, this effect is rather considerable) and the radiometric repelling of particles from the surface of a bubble whose temperature is much higher than that of gas.

In conclusion, it is necessary to pause at the often expressed opinion that some dusts, e.g., that of coal, are poorly intercepted as they pass through water, because "water does not make certain dust particles wet"

(see also page 397). In actuality, this probably can be explained by the apparently small consistency of porous aggregates of dusts, and by particles of scaly form being positioned perpendicularly to inertial forces or to gravity (see § 11). Due to this, the rapidity of their precipitation decreases considerably. The fact that the absorption of dust during bubbling is sometimes increased upon adding surface-active substances to water, can apparently be explained by a decrease in the size of the bubbles.

A noticeable decrease in absorption of aerosols can be observed upon adding gelatin to water (344). In this case, according to all probabilities, the effect is caused by the elimination of circulation.

The description by some authors (345 to 348) of the high absorption of aerosols by foams, notwithstanding the absence of inertial precipitation in this case, can be explained in one way by a small volume of cells in the foams and in another way, by a comparatively longer stopping period of aerosol particles in these cells.

§ 43. Brownian Spinning. Orientation of Aerosol Particles in an Electrical Field

Brownian spinning is determined with the aid of the equation (253)

$$\overline{\theta^2} = 2kTB_{\omega}t, \quad (43.1)$$

where $\overline{\theta^2}$ is an average square of the particle's deflection angle around a given axis per time unit t ; where B_{ω} is a "rotary mobility" of a particle around its axis, i.e., the angular velocity of spinning under the influence of the moment of rotation, which is equal to one unit. In other words

$$d\theta/dt = B_{\omega}P_{\theta}, \quad (43.2)$$

where P_{θ} is a moment of the external forces relative to the axis.

With regard to spherical particles

$$B_{\omega_0} = 1/8\pi\eta r^3. \quad (43.3)$$

Yet, the spinning of spherical particles is of no particular interest in physics of aerosols, because as such it manifests nothing and it does not

reveal itself in characteristics of aerosols. Contrarily, spinning of non-spherical particles manifests itself in a side illumination by glimmering, and for this reason particles of this type can be unmistakably distinguished among spherical particles. Furthermore, particles extended in one or two dimensions orient themselves under the influence of hydrodynamic, electrical and other forces, during which the degree of orientation is determined by a correlation between the magnitude of orienting force and the intensity of Brownian spinning. Finally, the Brownian spinning is of great importance during coagulation of elongated particles.

If we consider spinning of an elongated ellipsoid, provided with a small semiaxis a and with a proportional axis β , the rotary mobility around the small axis will be equal (349) to:

$$B_{\omega} = \frac{3 \left[\frac{2\beta^2 - 1}{\sqrt{\beta^2 - 1}} \ln(\beta + \sqrt{\beta^2 - 1}) - \beta \right]}{16\pi\eta a^3(\beta^4 - 1)} \tag{43.4}$$

Table 20 shows proportional values of rotary mobilities of a sphere with a radius $r(B_{\omega_0})$ and of an ellipsoid with a small semiaxis $r(B_{\omega})$.

With regard to particles shaped like flat discs, with a radius r , the

Table 20
Rotary Mobility of Elongated Ellipsoids Spinning Around
a Small Axis

β	2	3	4	5	6
B_{ω_0}/B_{ω}	3.0	7.0	13.5	23.1	36.4

rotary mobility around one disc's diameter will be equal to:

$$B_{\omega} = 3/32\eta r^3 \tag{43.5}$$

UNCLASSIFIED
AD

227876

FOR
MICRO-CARD
CONTROL ONLY

6

OF

9

Reproduced by

Armed Services Technical Information Agency

ARLINGTON HALL STATION; ARLINGTON 12 VIRGINIA

UNCLASSIFIED

"NOTICE: When Government or other drawings, specifications or other data are used for any purpose other than in connection with a definitely related Government procurement operation, the U.S. Government thereby incurs no responsibility, nor any obligation whatsoever; and the fact that the Government may have formulated, furnished, or in any way supplied the said drawings, specifications or other data is not to be regarded by implication or otherwise in any manner licensing the holder or any other person or corporation, or conveying any rights or permission to manufacture, use or sell any patented invention that may in any way be related thereto.

The following equation (350) can be deduced from (43.1) for a complete deflection angle θ of the long axis of an elongated particle per time unit t :

$$\overline{\sin^2 \theta} = \frac{2}{3} \left(1 - e^{-6kTB_{\omega}t} \right). \quad (43.6)$$

If $t \rightarrow \infty$ $\overline{\sin^2 \theta} = \frac{2}{3}$, this tallies with the probability of being similar with respect to any axial direction.

Of great importance to the physics of aerosols is the orientation of elongated particles in an electrical field, caused by the polarization of particles. If a noncharged particle, having assumed an ellipsoidal form of spinning, is brought into a uniform electrical field by a tension E in such a manner that the polar axis of the ellipsoid forms an angle θ with the direction of the field, then the change caused by the polarized particle in the energy field will be equal (351) to:

$$\Omega = - \frac{vE^2}{2} \left[\frac{\cos^2 \theta}{\frac{1}{\epsilon_k - 1} + \alpha_1} + \frac{\sin^2 \theta}{\frac{1}{\epsilon_k - 1} + \alpha_2} \right], \quad (43.7)$$

where v is a volume; where ϵ_k is the dielectric constant of a particle. The shape coefficients α_1 and α_2 are expressed by proportions of the longer axis, as well as of the shorter axis of the ellipsoid β , in the following manner.

For elongated ellipsoids:

$$\alpha_1 = \frac{1}{\beta^2 - 1} \left[\frac{\beta}{\sqrt{\beta^2 - 1}} \ln \left(\beta + \sqrt{\beta^2 - 1} \right) - 1 \right], \quad (43.8)$$

$$\alpha_2 = \frac{\beta}{2(\beta^2 - 1)} \left[\beta - \frac{1}{\sqrt{\beta^2 - 1}} \ln \left(\beta + \sqrt{\beta^2 - 1} \right) \right]; \quad (43.9)$$

for oblated ellipsoids:

$$\alpha_1 = \frac{\beta^2}{\beta^2 - 1} \left[1 - \frac{1}{\sqrt{\beta^2 - 1}} \arcsin \frac{\sqrt{\beta^2 - 1}}{\beta} \right], \tag{43.10}$$

$$\alpha_2 = \frac{1}{2(\beta^2 - 1)} \left[\frac{\beta^2}{\sqrt{\beta^2 - 1}} \arcsin \frac{\sqrt{\beta^2 - 1}}{\beta} - 1 \right]; \tag{43.11}$$

for conductive particles the (43.7) is converted into:

$$\Omega = - \frac{\nu E^2}{2} \left[\frac{\cos^2 \theta}{\alpha_1} + \frac{\sin^2 \theta}{\alpha_2} \right]. \tag{43.12}$$

Inasmuch as aerosol particles may, for practical purposes, be regarded as conductive (see page 80), in the future we shall only use the equation (43.12).

Table 21 shows values of the coefficients α_1 and α_2 for some β estimations.

Table 21
Values of Coefficients of Particles Shape During Orientation
in Electrical Field Elongated Ellipsoids

Elongated ellipsoids								
β	1	1.1	1.5	2	3	5	10	α
α_1	0.333	0.310	0.233	0.174	0.109	0.056	0.020	0
α_2	0.333	0.345	0.383	0.413	0.446	0.472	0.490	0.5
Oblated ellipsoids								
α_1	0.333	0.347	0.446	0.527	0.635	0.751	0.860	1
α_2	0.333	0.320	0.277	0.236	0.182	0.125	0.070	0

In view of the fact that particles tend to arrange themselves so that the energy of the field would be at a minimum, it follows from the above data that, with regard to a steady position of an elongated ellipsoid, the pertinent value is $\theta = 0$ (a polar one, i. e., lengthwise, where the axis of direction is parallel with the field) and with regard to an oblated ellipsoid, the pertinent value is $\theta = \frac{\pi}{2}$ (a polar one, i. e., short, where the axis of direction is perpendicular with the field). Thus, the orientation of particles in a laminar flow (see page 56) and in an electrical field has an analogous trend. We wish to remind that the orientation of particles involved in a movement concerning a medium at larger Re - is inverse: the (long) axes position themselves perpendicularly to the direction of the movement.

In the absence of Brownian movement, an elongated particle, upon falling into an electrical field, will oscillate around a steady position and will draw nearer to it asymptotically. The orientation of particles in which Brownian movement is accounted is only computed on behalf of elongated ellipsoids. The probability that the angle between the particle's polar axis and the direction of the field is located in the interval $(\theta, \theta + d\theta)$, is, according to BOLTZMANN'S principle, equal to:

$$W(\theta)d\theta = b'e^{-\Omega/kT} \sin\theta d\theta = b'e^{-\frac{\lambda^2 \cos^2\theta}{2kT}} \sin\theta d\theta. \quad (43.13)$$

Here

$$\lambda^2 = \frac{E^2 v \left(\frac{1}{\kappa_1} - \frac{1}{\kappa_2} \right)}{2kT} = \frac{2\pi E^2 \left(\frac{1}{\kappa_1} - \frac{1}{\kappa_2} \right) a^3 \beta}{3kT} \quad (43.14)$$

is the proportion of electrical energy to the energy of Brownian spinning of one particle; where a is a small semiaxis of an ellipsoid; where b' is a constant coefficient whose magnitude is determined by the condition of normalization:

$$1 = \int_0^{\frac{\pi}{2}} W(\theta)d\theta = \frac{b'}{\lambda} \int_0^{\lambda} e^{-x^2} dx. \quad (43.15)$$

Hence, for an average value of $\cos\theta$ the following expression is obtained:

$$\overline{\cos \theta} = \int_0^{\frac{\pi}{2}} b' e^{\lambda^2 \cos^2 \theta} \sin \theta \cos \theta d\theta = \frac{e^{\lambda^2} - 1}{2\lambda \int_0^{\frac{\pi}{2}} e^{x^2} dx} \quad (43.16)$$

Table 22 quotes estimations of $\overline{\cos \theta}$ pertinent to certain values of λ^2 .

Table 22

Orientation of Ellipsoidal Particles in an Electrical Field

λ^2	0.01	0.1	1	2	4	6	9	16
$\overline{\cos \theta}$	0.500	0.508	0.587	0.676	0.817	0.864	0.946	0.993

Let us assume that $\overline{\cos \theta} = 0.5$ denotes the absence of orientation and that $\overline{\cos \theta} = 1$ denotes a complete orientation. Practically speaking, a complete orientation is attained, as we visualize it, when $\lambda^2 \approx 10$.

Thus, for an ellipsoidal particle whose proportion of axes is 3:1 and the magnitude of small semiaxis is $a = 0.1\mu$, a rather strong field is essential, e.g., one of the order $1000 \text{ v} \cdot \text{cm}^{-1}$, while with regard to the magnitude of $a = 1\mu$, a field of $30 \text{ v} \cdot \text{cm}^{-1}$ is already sufficient.

Discrepancies in measurements of the mobility of smoke particles which are influenced by gravity, and of similar particles found in an electrical field (as discussed in §19), can be explained by the particles' orientation phenomenon existent in an electrical field; naturally, in the second instance the mobility of particles oriented toward their movement should be greater than in the first instance, i.e., in the absence of orientation. Furthermore, particles oriented in an electrical field represent, as such, dipoles and this leads to the so-called "directional" coagulation of aerosols in an electrical field (see §52). The variation in intensity of light diffused by aerosols in an electrical field was discovered with the aid of smoke of ammonium chloride (352, 353). Inasmuch as observations directed toward light rays and a field form right angles with one another, the observer sees the light being diffused by lengthy sides of oriented particles. In addition, the intensity of the diffused light increases with stratification of the field. Elongated axes in crystals of ammonium chloride coincide with crystallographic axes; consequently one can also observe in oriented smoke the phenomenon of double

refraction. Still, the orientations of aerosols in an electrical field have so far been little examined.

In view of the fact that relaxation periods during particles' polarizations are extremely brief in comparison with relaxation periods during spinning under the influence of external forces, all the afore-said remains true also with regard to the orientation of particles in an alternating electrical field.

Analogous orientation can be observed in a magnetic field among strokes of ferromagnetic substances (354).

Droplets can also be oriented by strong electrical fields which cause deformation of the droplets due to inductive forces. If we assume that deformed droplets have the shape of elongated spinning ellipsoids (this supposition was confirmed by tests), then we can state (355) that the ellipsoids' shape (the ratio of axes c/a) depends upon the magnitude of rE^2/σ ; where r is the radius of nondeformed droplets; where σ is the effect of the surface tension and dielectric constant affecting the liquid. Due to complexity of the concluded equations, we shall quote the values of c/a as a function of rE^2 , computed in table 23 according to the afore-mentioned equations for water and for dioctylphthalate.

Table 23

Deformation of Droplets in an Electrical Field

rE^2*	0	50	100	150	200
c/a (water)	1	1.07	1.17	1.35	--
c/a (dioctylphthalate)	1	1.06	1.13	1.23	1.34

* E is expressed in $v \cdot cm^{-1}$.

Simultaneously with a deformation of the droplets, there also takes place an orientation of droplets in an electrical field, which was mentioned above.

Chapter VI

Convective and Turbulent Diffusion in Aerosols

§ 44. - Precipitation of Aerosols During Convection and Turbulence

We discussed on preceding pages various instances of aerosol particle movements in an immobile medium and in laminar flow with a known and permanent distribution of velocities. Yet, a complete immobility of the medium, and undisturbed laminar flow, as such, occur relatively seldom in actuality as a result of existent convection, even within the scope of our intelligent observations. It is indicated by experiment (356) that, as gas comes in contact with a vertical wall whose temperature differs by the magnitude ΔT from the gas temperature, a vertical current develops near the wall. Its maximal velocity at the altitude z from the base of the wall is equal to:

$$U = 0.55 \sqrt{gza\Delta T}, \quad (44.1)$$

where a is a coefficient of gas expansion and equal to $1/T$. Thus, in a chamber one m high, even at $\Delta T = 0.01^\circ$, the velocity of a convection current reaches approximately one cm sec^{-1} and this tallies with the velocity of settling of large particles, whose radius is approximately 10μ .¹ Therefore convection currents are, practically speaking, inevitable in smoke chambers; they can be eliminated only with the use of small, massive metallic vessels and by the careful exclusion of thermal radiation from a light source entering the vessel. For this very reason accurate gaseous laminar flow is only possible in narrow tubes and ducts, whereas in wide tubes, by the nature of things, vertical convection currents are superimposed upon the flow. It is true, that convection can be eliminated by the formation of a vertical temperature gradient in a vessel containing the aerosol, yet this method is used in comparatively rare instances.

If one wall of the vessel is maintained at a constant and much higher temperature than other walls (e g., while the glass walls of a smoke chamber are heated by a light beam), convection quite often manifests itself

-
1. Convection currents are less vigorous in liquids than in gases due to the smaller magnitude of the expansion coefficient.

as a well-defined circulation. The distribution of velocities in such case lends itself to a computation; consequently, one can also compute the trajectories of particles. A similar computation is also possible in the presence of free convection near the heated substances of a known shape, as is explained in the theory of heat conductivity. Yet, in practical work on aerosols, the convection usually has an irregular pattern which is beyond the bounds of possibility to compute as one wishes. Thus one must abstain here from the computation of trajectories of individual particles. An analogous condition also prevails during constrained irregular convection caused by artificial turbulence in an aerosol.

In such instances, the only remaining possibility is that of statistical compilation of the movements of a medium and of the particles suspended in the medium. During this, a considerable idealization of the convection phenomenon is essential; it is necessary to consider that a convective transfer of the medium is effected by way of a "conductive diffusion," and that the intensity of convection is determined by the magnitude of a "convective diffusion coefficient." Movements of particles suspended in the medium comprise movements of the medium as such, i. e., they include a well-defined current and a convective diffusion of the medium, as well as the afore-discussed movements of particles in relation to the medium.

We shall review the precipitation of an aerosol in a chamber in the absence, as well as in the presence, of convection. With this we shall assume that the coagulation of the aerosol may be disregarded at a certain concentration of particles. In the absence of convection, but with particles not-too-small in size present (i. e., in the absence of a diffusible "erosion"), as well as with the prevalent monodispersion in the aerosol, the upper border of the aerosol settles with a terminal velocity V_g . Within these limitations of the concentration of the aerosol, the velocity of settling is constant in the aerosol's entire volume and it does not change with time. If the polydispersion in an aerosol is small, the upper border of the aerosol becomes gradually blurred and this, to some extent, remains clearly noticeable for a long time. In actuality, a similar condition can be observed during the settling of more or less monodispersed fogs possessing a high gravimetric concentration, which is conducive to a "hydrostatic stabilization" in the upper confines (see page 73).

If $n(r)dr$ is a concentration of particles with a radius $(r, r + dr)$, then upon one cm^2 area of the bottom of the chamber there will precipitate per sec $V_g(r)n(r)dr$ particles and for a time period t there will precipitate

$$dN = V_g(r)n(r)t dr \quad (44.2)$$

particles.

The above equation is applicable only when $t \leq H/V_s(r)$; where H is the chamber's height. Thus, all particles of an indicated size will precipitate within the time period $H/V_s(r)$. A complete number of particles precipitated per time unit t , can be obtained upon integrating the expression (44. 2) by r .

During very intensive convection (precisely speaking, when the average velocity of the convection currents considerably surpasses V_s), the concentration of aerosol is practically constant in the entire capacity of the chamber, with the exception of the layers near the wall, yet the concentration constantly decreases as time passes. The vertical component of the convection velocity and, consequently, of the coefficient of convective diffusion, is inclined toward zero upon getting close to the chamber's bottom. At a certain close distance δ from the bottom, the magnitudes of convective and molecular diffusions balance themselves so that, in a layer of δ thickness close to the wall, the molecular diffusion becomes predominant. Having examined the precipitation on the chamber's bottom, we can assume that the process resembles a quasi-stationary trend, i. e., that within the time period of a particle passage through a layer close to the wall, the aerosol's concentration at a distance from the bottom n_∞ remains constant. This condition is usually fulfilled when experiments on the precipitation of aerosols in chambers are conducted.

Through a horizontal area of one cm^2 there will pass per sec from above

$$I = V_s n + D_E \frac{dn}{dz} \quad (44. 3)$$

particles.

Here D_E is the effective coefficient of diffusion, which includes both diffusion mechanisms and is dependent upon z . At a distance from the bottom, which surpasses δ considerably, $n = n_\infty$ also

$$I = V_s n_\infty \quad (44. 4)$$

According to the hypothesis about a quasi-stationary process of precipitation, this equation expresses the number of particles which precipitate per sec upon one cm^2 of the bottom area. If we introduce the equation (44. 3) in the form of

$$V_s (n_\infty - n) = D_E \frac{dn}{dz} \quad (44. 5)$$

and solve it for the limiting conditions of $n = n_{\infty}$, with $z = \infty$ and $n = 0$, when $z = 0$, we shall obtain the following expression for the aerosol concentration at a distance z from the chamber's bottom:

$$n = n_{\infty} \left[1 - \exp \left(- V_s \int_0^z \frac{dz}{D_E} \right) \right] \quad (44.6)$$

Thus, a complete flow of particles toward the chamber's bottom consists of the following sedimentation fraction

$$I_1 = V_s n = V_s n_{\infty} \left[1 - \exp \left(- V_s \int_0^z \frac{dz}{D_E} \right) \right] \quad (44.7)$$

and of the following diffusible fraction

$$I_2 = D_E \frac{dn}{dz} = V_s n_{\infty} \exp \left(- V_s \int_0^z \frac{dz}{D_E} \right). \quad (44.8)$$

One can readily convince himself that the latter fraction is noticeable only at a very small distance from the bottom. Thus, diffusion modifies the concentration of particles near the bottom, although it does not influence the rapidity of the precipitation.

According to the afore-said, the rapidity with which particles with a radius $(r, r + dr)$ precipitate upon the chamber's bottom, is equal, as in an immobile medium, to: $V_s(r)n(r)dr$, but $n(r)$ changes with t according to this equation:

$$-Hdn(r) = V_s(r)n(r)dt. \quad (44.9)$$

It follows hence, that

$$n(r) = n_0(r) \exp \left(- \frac{V_s(r)t}{H} \right), \quad (44.10)$$

where n_0 is the initial concentration.

Thus, the concentration of particles of every size decreases exponentially with time, but according to a different rate. Therefore, within the time that the average dispersion of the aerosol prevails in the chamber, it increases constantly. The average concentration of particles at a moment t is equal to:

$$n = \int_0^{\infty} n_0(r) \exp \left(- \frac{V_s(r)t}{H} \right) dr. \quad (44.11)$$

We shall still conclude the expression for the number of mono-dispersed aerosol particles which precipitated upon one cm^2 area on the bottom of the chamber per time unit t :

$$N = \int_0^t V_s n dt = V_s n_0 \int_0^{\infty} \exp \left(- \frac{V_s t}{H} \right) dt = n_0 H \left[1 - \exp \left(- \frac{V_s t}{H} \right) \right]. \quad (44.12)$$

The examination of the intermediate phenomenon for a comparable velocity of settling during convection is very complicated, and we shall not study it. It should be noted, however, that during the settling of aerosols in smoke chambers, the convection appears to be very strong even in the absence of artificial turbulence, and this type of settling usually resembles the second one of the types discussed. Thus, during tests conducted by GILLEPSIE and LANGSTROTH (357), the concentration of NH_4Cl fumes, with particles with radii 0.3 to 2.0μ , appeared constant at all points of the 12 m^3 capacity chamber as long as all these fumes existed. During tests conducted by E. VIGDORCHIK (358) one could detect particles of quartz dust with $r = 12.5\mu$ in 1.2 m high chamber even 3 hours after the intake of dust into the chamber. Such particles should have settled within 12 minutes in calm air.

It follows from equation (44.10) that

$$\ln n(r) = \ln n_0(r) - \frac{V_s(r)t}{H}, \quad (44.13)$$

i. e., in the case of a monodispersed aerosol, a change in the logarithm of concentration according to time is expressed by a straight line, whose angle of inclination toward the axis of abscissae increases with the size of the particles. Unfortunately, almost the entire available experimental material

pertinent to the kinetics of precipitation of aerosols in chambers concerns somewhat polydispersed systems. In due time, the average size of particles in an aerosol decreases; consequently the inclination angle of curves $(\ln n, t)$ also decreases. Then the curves of the polydispersed aerosols assume a shape which is convex to the axis of abscissae, and their curvature increases with the degree of polydispersion. Curves with such shapes are usually observed (358).

It follows from the equation (44.12) that in a convective region of particle precipitation

$$-\frac{H}{V_s} \ln \left(1 - \frac{N}{n_0 H} \right) = t. \quad (44.14)$$

This equation was verified by DAVIES (219) for highly aggregated coal dust. Figure 65 shows curves plotted for various intervals of the particles' radii in individual fractions of the dust. A linear type dependence is maintained for small fractions. The bend seen on the curves for coarse groups is explained by the author as a polydispersion inside the groups.

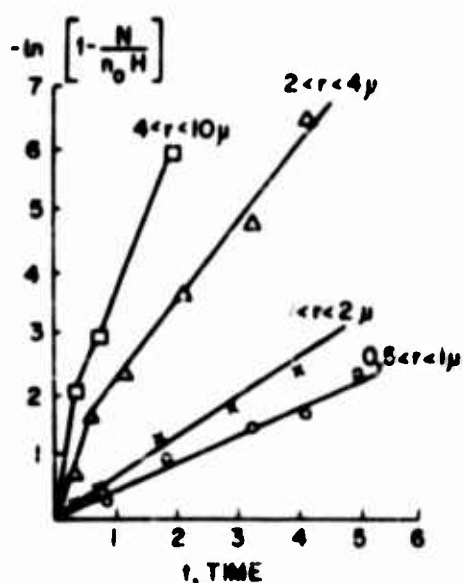


FIG. 65 AEROSOL SETTLING UPON BOTTOM OF CHAMBER

The problem of precipitation of aerosols upon side (vertical) walls of chambers is far more difficult to study. In any mechanism of precipitation, the rapidity of the latter is proportional to the aerosol's concentration n ; it follows, hence, that $dn/dt = -\beta n$. Thus, the kinetics of precipitation on vertical walls are expressed by an analogous (44.13) equation

$$\ln(n_0/n) = \beta t, \quad (44.15)$$

and the problem boils down to the conclusion of a theoretical expression for the coefficient β .

Inertial precipitations of aerosols on flat walls of a chamber should, in the absence of artificial turbulence, be extremely small. Actually, under these conditions, large particles ($r \approx 7\mu$) do not precipitate

on vertical walls at all (248). We deal here with a purely diffusible precipitation, during which particles converge to walls by way of a convective diffusion and precipitate due to molecular diffusion within a thin layer close to the walls (see page 301). Inasmuch as the law of modification of the coefficient of convective diffusion at the approach to the wall is unknown, the problem has to be simplified considerably. One has to consider that within the close-to-the-wall layer of the thickness δ , only molecular diffusion takes place, but beyond this layer convective diffusion is so intense that the aerosol's concentration outside the layer remains constant. In this case, the rapidity of precipitation of the aerosol on a vertical wall is expressed by the equation

$$I = \frac{Dn}{\delta} \text{ particles/cm}^2 \cdot \text{sec}; \quad (44.16)$$

where D is a coefficient of molecular diffusion of particles. If v is the capacity and S is the surface of the chamber's side walls, then

$$-v \frac{dn}{dt} = SI \quad (44.17)$$

Thus, we obtain the following expression for the β coefficient in the equation (44.15):

$$\beta = \frac{SI}{vn} = \frac{SD}{v\delta}. \quad (44.18)$$

One should remember that δ not only depends upon the intensity of convection, but also upon D . Actually, the magnitude of δ is determined by the condition that, at δ distance from the wall, the coefficients of molecular and convective diffusions are rendered equal. The higher the coefficient of molecular diffusion, the greater the δ is. Consequently, there can't be any direct proportionality between the rapidity of settling on the walls and the D ; thus the rapidity of settling should be proportional to D^a , $0 < a < 1$.

One can draw the following conclusion from the afore-said: the higher the aerosol's dispersion, the more particles precipitate on the side walls and the fewer particles precipitate on the bottom.

K. SHIFRIN and his coworkers (359) studied (by measuring the transparency of smoke) the kinetics of precipitation of smoke with $r \approx 0.5\mu$ on walls of a cylindrical chamber 9 m high and 4 m in diameter. They discovered that, in the given case as the equation (44.15) was applied, the concentration decreased twice within 2 to 3 hours. Since the initial

computable concentration of smoke was of the order $10^4/\text{cm}^3$, the decrease in concentration at the expense of coagulation in the aerosol may be disregarded. In conjunction with the indicated dispersion of the aerosol and the height of the chamber, the precipitation on the bottom of the chamber did not play any noticeable part. From curves plotted by SHIFRIN, one can calculate that the ratio of the number of particles precipitated on one cm^2 of the area of the walls per sec, i. e., I , as compared with the particles' concentration, equaled $5 - 7 \cdot 10^{-3} \text{ cm} \cdot \text{sec}^{-1}$. Hence, for the thickness of the layer close to wall, the value $\delta \approx 0.5\mu$ is obtained.

In tests of GILLEPSIE and LANGSTROTH (357), conducted in a 12 m^3 capacity chamber on fumes of NH_4Cl , with the particles' radii ranging between 0.3 and 2.0μ , the number of particles which precipitated on the bottom, on the side walls and on the ceiling of the chamber was defined by way of direct calculations of the laminae, determined in a pertinent manner. It was found that precipitation on the ceiling was insignificant, and also that approximately three times less particles settled within the first 100 minutes on side walls than on the bottom. After 100 minutes, the precipitation on side walls practically stopped. It can be roughly estimated, from the graph prepared by the authors, that the value of I/n in these tests was of the order of magnitude 10^{-4} and that the depth of the layer near the wall $\approx 20\mu$, i. e., it was almost twice as large as the one submitted by SHIFRIN. Therefore, the rapidity of the decrease in aerosol concentration (as observed by SHIFRIN in the chamber, it was quite large in the absence of coagulation) remains as an obvious contradiction with the data of numerous pieces of work dedicated to the research in coagulation of aerosols. The straightforward data about the precipitation of aerosols on the walls are more reliable than the data computed after the decrease in concentration. Thus, apparently, a predilection should be rendered for the values of I/n and δ , computed according to GILLEPSIE and LANGSTROTH and, in that, new data pertinent to this problem should be produced.

The rapidity of the precipitation of aerosols on walls is strongly influenced by charges on the particles. In recent tests conducted by GILLEPSIE (360), the total number of SiO_2 particles, with $r = 0.4\mu$, which precipitated on the walls and on the bottom of a 0.2 m^3 capacity chamber within the first few minutes of the aerosol's duration, was increased 2 to 3 times upon the increase of the average number of elemental charges on particles from 7 to 14 (at the same time the maximal charge was increased from 50 to 100). We assume that charges can hardly exert any noticeable influence upon rapidity with which aerosols precipitate upon the chamber's bottom; yet, during these tests, the increase of precipitation on the side walls actually was even larger. It seems strange that this influence of the

charges gradually decreased and disappeared within several tens of minutes. Inasmuch as the aerosols' charges were bipolar and rather symmetrical, and also the electrostatic dispersion (see § 24) did not play any noticeable part here, then, undoubtedly, the indicated effect was caused by the inductive adhesion of charged particles to walls.

The influence of this effect can be very roughly computed if we assume that the particles which have reached the layer near the wall converge to the wall under the influence of induction forces. The velocity of this movement at the border of the near-wall layer is, according to equation (41.1), equal to $q^2 B / 4 \delta^2$; hence: $I_q = q^2 B n_o / 4 \delta^2$ particles will precipitate upon one cm^2 area of the wall in one sec. The number of particles precipitated due to molecular diffusion is offered in the equation (44.16). Thus, we make up the following proportion:

$$\frac{I_q}{I} = \frac{q^2 B n_o}{4 \delta^2} \frac{\delta}{D n_o} = \frac{q^2}{4 \delta k T} \quad (44.19)$$

Assuming that $q = e v = 4.8 \cdot 10^{-10} v$ (v is a number of elemental charges), $kT = 4 \cdot 10^{-14}$, $\delta = 20 \cdot 10^{-4}$ cm, we obtain

$$I_q / I = 0.7 \cdot 10^{-3} v^2 \quad (44.20)$$

With regard to particles with maximal charges, $v = 100$, $I_q / I = 7$. These particles precipitate by far more rapidly than noncharged particles, whereas the induction effect among particles with a small charge is insignificant. Consequently, upon precipitation of particles with higher charges, the subsequent precipitation follows "in a normal way."

It was determined in a series of experiments that the gravimetric concentration decreases more rapidly during artificial turbulence of an aerosol in a chamber than in the absence of turbulence. This can partly be explained by accelerated coagulation caused by turbulence (see § 55) and, consequently, by the growth of the particles. Yet, undoubtedly, the main cause appears to be inertial precipitation on the chamber's walls. GILLEPSIE and LANGSTROTH (357) proved this directly by measuring the rapidity of precipitation on the chamber's walls and by defining the coagulation constant of NH_4Cl fumes (by the method discussed on page 383) in the presence of dissimilar turbulence velocities of fumes. It was found that I/n increased linearly with the average velocity of air current in the one m^3 capacity chamber and that, with the velocity of $50 \text{ m} \cdot \text{min}^{-1}$, the I/n

was increased 5 times more than in the absence of turbulence; the effect of turbulence upon the magnitude of coagulation constant was insignificant. According to experiments of E. VIGDORCHIK (358), when air in a chamber $1.2 \times 1.2 \times 1.2$ m size is agitated with the aid of a propeller at average velocity of $4 \text{ m} \cdot \text{sec}^{-1}$, the concentration of quartz dust declines 3 to 4 times faster than in the absence of turbulence. The cause of this phenomenon is the declining width of the laminar layer δ (caused by turbulence) near the wall, as well as the inertial precipitation of particles. Actually, if we consider that the shape of the chamber used during experiments of E. VIGDORCHIK was cylindrical, we can compute that during the indicated air velocity, the centrifugal force at the walls $mV^2/R = m400^2/60$ was almost three times greater than the gravitational force: mg .

Actually, it is very difficult to describe the inertial precipitation involving turbulence; it occurs in distinct places, where eddies that have developed with their axes parallel to the wall, reach the wall. If the eddies' diameter is small, inertial forces emerging here may be considerably greater than the force estimated just now. The type of turbulence is also of great importance. Thus, if a turbulence progressively goes on with wide sweeps which reach the chamber's walls (361), then the rapidity of the decrease in the aerosol's concentration (fumes of NH_4Cl with $\bar{F} \approx 0.5$) increases 3 to 4 times even at the average air velocity of $50 \text{ cm} \cdot \text{sec}^{-1}$. This type of turbulence, undoubtedly, is of assistance in that intensive eddies are formed near the walls, with their axes parallel to the walls.

Although it is extremely difficult to compute the rapidity of inertial precipitation on the walls during turbulence, yet the number of particles precipitating in one sec upon one cm^2 area of walls should in any case be proportional to nT and the decrease in the aerosol's concentration with time should be reconciled with the equation

$$v \frac{dn(r)}{dt} = -Sbn(r)T(r),$$

where b is a coefficient dependent upon intensity and type of turbulence. It follows hence, that

$$n(r) = n_0(r) \exp \left[-\frac{Sb}{v} T(r)t \right].$$

Since $V_g = gT$, then the total variation in an aerosol's concentration in accordance with time (if diffusible precipitation is disregarded) will be expressed by the equation

$$n(r) = n_0(r) \exp \left[- \left(\frac{Sb}{v} + \frac{g}{h} \right) \tau(r) t \right], \quad (44.21)$$

which implies the same condition, as if inertial precipitation were non-existent; yet, it includes the substitution of g/h coefficient by $\frac{Sb}{v} + \frac{g}{h}$. Thus, instead of the equation (44.11), we have the following equation:

$$n = \int_0^{\infty} n_0(r) \exp \left[- \left(\frac{Sb}{v} + \frac{g}{h} \right) \tau(r) t \right] dr. \quad (44.22)$$

As we mentioned already, the variation of $\ln n$ with time should, in case of a polydispersed aerosol, be expressed by an upward concave curve. If, however, simultaneously with precipitation, a noticeable coagulation takes place in the aerosol, then the enlargement of particles associated with the coagulation compensates somewhat the decrease in the average size of the particles caused by coagulation. This leads to the curve's $(\ln n, t)$ rectification. Thus, a practical rectilinear graph is often prepared (361)

A change in the gravimetric concentration of a polydispersed aerosol in accordance with time is expressed by the equation:

$$c = \int_0^{\infty} n_0(r) m(r) \exp \left[- \left(\frac{Sb}{v} + \frac{g}{h} \right) \tau(r) t \right] dr, \quad (44.23)$$

where $m(r)$ is the particle's mass with a radius r . If isodispersed aerosols are considered, it is obvious that $d \ln c / dt = d \ln n / dt$, but in polydispersed aerosols $|d \ln c / dt| > |d \ln n / dt|$, i.e., the gravimetric concentration decreases faster than the calculated one.

Actually, we can write down

$$\frac{d \ln c}{dt} = \frac{1}{c} \frac{dc}{dt} = \frac{1}{n \bar{m}} \frac{\bar{m} dn}{dt}, \quad (44.24)$$

where \bar{m} is an average mass of particles maintained in aerosol; where $\bar{\bar{m}}$ is an average mass of precipitating particles. Since $\bar{\bar{m}} > \bar{m}$, then $|d \ln c / dt| > |d \ln n / dt|$, whereupon the difference of $|d \ln c / dt| - |d \ln n / dt|$ increases

with the aerosol's polydispersion and likewise with the absolute magnitude of dn/dt , i. e., with the velocity of turbulence. An experimental test proved these findings (361).

In conclusion, we shall mention one aspect which is caused by the natural phenomena of convection and which exemplifies some interest on behalf of the practical experimenting in chambers with aerosols. If we place a closed vessel with openings in opposite vertical walls into a chamber with an aerosol, then a certain number of particles, even very large ones ($r \sim 7\mu$), will pass through these openings due to horizontal convection ("draft") (248). If there is only one opening, no infiltration will take place. An analogous phenomenon is also observed in the cracks within wooden walls: an aerosol can penetrate open cracks rather deeply, but it can't penetrate blind slits.

§ 45. Movement of Aerosol Particles in Turbulent Flow

Theoretical and experimental studies of the behavior of aerosols in a turbulent current present, naturally, considerably greater difficulties than in the case of laminar flow. Thus, regardless of great progress in studies of turbulence made in recent times, we still have very scanty data about the movement of particles suspended in a turbulent current. Particularly not clarified is the extremely important question about the extent of particles being entrained due to turbulent fluctuations.

According to existent opinion, a turbulent current can be visualized as resulting from a continuous spectrum of fluctuations which are dissimilar in scale and are imposed upon the basic (average) velocity of the current. Fluctuations, initially developed by way of eddies bouncing back off walls, are in a scale which is comparable with the diameter of the tube through which a fluid flows. Thus, velocities which tally with these fluctuations depends upon a certain direction, particularly, the fluctuating velocities which are set parallel to the walls, depend upon direction more than the velocities set perpendicularly.

The energy of large-scaled fluctuations gradually passes over to the still stronger small-scaled fluctuations, whereupon the fluctuations become isotropic in scale, which is small if compared with the tube's diameter. In accordance with A. KOLMOGOROV'S (362) theory, the total energy of these fluctuations, in a scale $\leq \lambda$ is proportional to $\lambda^{2/3}$. This rule remains true as long as the transition of energy to more small-scaled fluctuations is not followed by a noticeable dissipation (transition into heat) of energy, i. e., it pertains to scales by comparison larger than a certain critical magnitude of λ_0 (the inner scale of turbulence). However, within the

realm of $\lambda < \lambda_0$, the decrease of energy during transition to more small-scaled fluctuations progresses considerably faster

The spectrum of fluctuations can be examined experimentally only in an immobile spot, namely, the value of the function $F(\nu)$ that indicates which part of the turbulent energy is shared with a fluctuation with a frequency $> \nu \text{ sec}^{-1}$, which is calculated with the aid of a fixed observer (we shall name it EULER'S frequency of fluctuations). With the transition to a coordinate system and moving with a neutralized velocity U with the current, a "scaled spectrum" of fluctuations is obtained, i.e., the function $\Omega(\lambda)$, which indicates which part of turbulent energy falls to the share of the fluctuations, whose scale is $\ll \lambda$. Yet, the spectrum of the frequency of fluctuations in a moving system (this we shall name LAGRANGE'S frequency) still remains unknown

We shall use data of SIMMONS and SALTER (363), who measured a spectrum of fluctuations in a 120-cm aerodynamic tube behind a grid with 75 mm openings. The degree of turbulence, i.e., the ratio of u/U (where u is a total average quadratic fluctuation velocity), is equal to 0.03 and was almost independent of Re_f . Thus, the turbulent energy comprised approximately 0.0009 of the total current's energy. From results obtained with the velocity of $U = 7.5 \text{ m} \cdot \text{sec}^{-1}$, we made up table 24, in which u denotes a velocity corresponding to fluctuations with the scale $\ll \lambda$.

Table 24

Spectrum of Turbulence in an Aerodynamic Tube With the Velocity
 $U = 7.5 \text{ m} \cdot \text{sec}^{-1}$, $Re_f = 600\,000$

λ , cm	$\Omega(\lambda)$	$u_\lambda/U \cdot 10^2$	u_λ , cm $\cdot \text{sec}^{-1}$	$u_\lambda/\lambda^{1/3}$	λ/u_λ
37	0.74	2.6	19.5	5.9	2.0
19	0.58	2.3	17.3	6.5	1.1
7.5	0.36	1.8	13.5	6.9	0.55
3.7	0.19	1.3	9.8	6.3	0.37
3.0	0.13	1.1	8.3	5.8	0.36
2.0	0.07	0.8	6.0	4.8	0.33
1.5	0.05	0.67	5.0	4.4	0.30
1.0	0.019	0.41	3.1	3.1	0.32
0.75	0.008	0.26	1.9	1.7	0.40
0.50	0.0025	0.14	1.1	0.9	0.45

Data contained in table 24 indicate that the ratio of $u_\lambda / \lambda^{1/3}$, which must be constant in accordance with A. KOLMOGOROV'S rule, begins to decrease sharply, let's say, with $\lambda = 2$ cm. An analogous effect is also obtained when $U = 10.5 \text{ m} \cdot \text{sec}^{-1}$. Thus, the inner scale of fluctuations λ_0 in an aerodynamic tube, at Re of the order 10^6 , has the order of magnitude of one cm. Inasmuch as considerable errors are possible during examinations of the turbulence spectra, it was expedient to test this conclusion on another material. From the equations and experimental data quoted by A. OBUKHOV and A. YAGLOM (364), it was feasible to obtain the following values: $\lambda_0 = 1.1$ cm at $U = 12.2 \text{ m} \cdot \text{sec}^{-1}$; 0.7 cm at $U = 24.4 \text{ m} \cdot \text{sec}^{-1}$ and 0.6 cm at $U = 30.5 \text{ m} \cdot \text{sec}^{-1}$, i.e., the same order of magnitude of λ_0 . According to OBUKHOV (365), $\lambda_0 \approx 0.5$ cm in the atmosphere at the height of 1-15 m. At the height of 2 m, $\lambda_0 = 2$ cm and at the height of 30 m. = 13 cm (according to TAYLOR /366/). Below the inner scale $\Omega(\lambda)$ is proportional to λ^2 , according to OBUKHOV and YAGLOM, or to λ^6 , according to HEISENBERG (367), i.e., it declines rather rapidly with a decrease in scale.

As we mentioned previously, it is impossible to find directly from experimental data the distribution of turbulent energy as a function of LAGRANGE'S frequencies, nor as a function of fluctuation periods. This distribution is necessary to solve the problem regarding the extent of a particle's growth due to turbulent fluctuations. This can be accomplished very roughly in the following way. Let's assume that fluctuations of a λ scale are produced by eddies of λ diameter which are moving with a flow velocity of U and the axes of the eddies are set perpendicularly to the flow. The velocity of circulation at a distance of $\lambda/4$ from axis of the eddies may be accepted as the average fluctuation velocity of u_λ . For the time being LAGRANGE'S period of correlated fluctuations t_L is equal to $0.5\pi\lambda/u_\lambda$ and the EULER'S period is equal to $t_E = 2$. The proportion of $t_E/t_L \approx u/U$, i.e., it is equal to the rate of turbulence of a first approximation. The entire (conditionally 99%) entrainment of particles by way of fluctuation takes place (according to figure 20, page 107) at $T/t_L \leq 0.02$, i.e., according to table 13 at $T \leq 0.01$, or at $r \leq 30\mu$ relevant to particles with a density of 1.

If we use values of T computed in § 18 for ultra-STOKES' particles at a typical average fluctuation, velocity of 30 cm/sec and specifically the values of $T = 0.1$ sec at $r = 0.1$ mm and of $T = 6.3$ sec at $r = 1$ mm, with the density of 1, we find in the first instance a 70% extent of entrainment and in the second instance, that of 2%. Thus, practically speaking, particles in size of 1 mm order are not involved in a medium's fluctuations.

MacCREADY (368) examined a spectrum of atmospheric turbulence at the height of 70 cm above the ground at average wind velocity of $2.3 \text{ m} \cdot \text{sec}^{-1}$.

The average quadratic vertical fluctuation velocity proved to be equal to $27 \text{ cm} \cdot \text{sec}^{-1}$. It can be calculated from data quoted by the author that the vertical fluctuation velocity of a $\ll \lambda$ scale is approximately three times smaller, i. e., LAGRANGE'S period of fluctuations is three times longer, consequently the extent of the particles' coagulation by the fluctuations is still larger than that in an aerodynamic tube under the conditions corresponding to those quoted in table 24.

Naturally, these computations are very approximate, although it seems they offer a correct order of magnitude of the particles which are and are not entrained by fluctuations. The exact solution of the problem involving the extent of entrainment is possible either by examining, with the aid of an instrument, the spectrum of turbulence moving with the velocity of the current, or by way of ultramicroscopic observations within the current which contains some very small, as well as large, particles.

The discussed question is of great importance in the solution of the second basic problem in the mechanics of aerosols, namely, the vertical distribution of particles in a horizontal turbulent current, as studied at first by SCHMIDT (369). If, during a turbulent aerosol passage through a horizontal duct, it occurs that the precipitation being blown off is shifted into a state of suspension (this happens, e. g., during pneumatic transference of powdery materials), then a definite stationary distribution of particles in depth must establish itself in the duct. The number of particles passing per sec under the influence of gravity from above through a horizontal area of one cm^2 is equal to $V_s n$. The number of particles passing through the same area in reverse direction due to turbulent diffusion is equal to $D_t dn/dz$ (where D_t is a coefficient of turbulent diffusion of particles). If we compare these expressions we obtain

$$\frac{dn}{n} = - \frac{V_s}{D_t} dz, \quad (45.1)$$

hence

$$\ln \frac{n}{n_0} = - V_s \int_0^z \frac{dz}{D_t}, \quad (45.2)$$

where n_0 is the concentration at the bottom of the duct; where z is the distance from the bottom. Inasmuch as D_t changes rapidly with z near the bottom,

although at a distance from the latter it is relatively slow, then, in the central area of the duct, the D_t may be regarded as constant and thus the equation (45. 2) assumes this form:

$$\ln \frac{n}{n_0} = - \frac{V_g z}{D_t} \quad (45. 3)$$

We want to emphasize that distributions expressed by these equations may occur only during a stationary condition, i. e. , if particles which are about to precipitate on the bottom of a duct are carried by the current back into a state of suspension. Otherwise, as is easy to calculate, a greater part of the aerosol would be able to precipitate before the distribution in question could establish itself.

The theory exposed here about the vertical distribution of particles suspended in a turbulent current was subjected to criticism by some hydrologists (370), in which the main objection induced (what usually happens) a supposition about the equality of the coefficients of turbulent diffusion of the particles and a medium. As is evident from the afore-said, this supposition is apparently justifiable with regard to aerosol particles with $r \leq 30\mu$. Furthermore, in the general expression for coefficients of diffusion, $D \approx l^2/t$; where l is a length of "spacing"; where t is the time expended in spacing and, in case of turbulent diffusion, l is evidently the scale and t is the period of fluctuations. Thus, during an incomplete entrainment of particles, the ratio of the coefficients of turbulent diffusion of particles and of medium D'_t/D_t is equal to the ratio of the squares of the amplitudes of the particles fluctuations, or to the "extent of entrainment" of the particles and this is computed as is explained above. If an equation for the coefficient D'_t , calculated as above, is introduced in the equation (45. 2), then, of course, it is applicable also in case of an incomplete entrainment.

We must still refer to the work of B. BROUNSTEIN and O. TODES (371). Proceeding from BOLTZMANN'S distribution of concentrations in the field of gravity that $n = n_0 \exp(-mgz/kT)$ and assuming, if comparable with the kinetic theory equation, that $\frac{3}{2}kT = mv^2/2$ (where v^2 is the average square of fluctuating velocity of a particle and where m is the particle's mass), consequently that $n = n_0 \exp(-3gz/v^2)$, the authors also used for the computation of v the following equation (372), which is accurate with regard to the particle's oscillations in an ideal liquid.

$$v = \left[\frac{3\gamma_g}{(\gamma_g + 2\gamma)} \right] u;$$

where u is the fluctuating velocity of the medium. A formal transference of kinetic energy equations to the motion of particles suspended in a turbulent medium is, in the opinion of the author of this book, not

justifiable. A vertical distribution of particles, according to BROUNSTEIN and TODES, is not dependent upon the particles' size and this is inconsistent with experience. Furthermore, in order to prevent a farther drop in aerosol concentration beyond double the 10 cm depth, one needs for these calculations the fluctuating velocity of air of the order $1 \text{ km} \cdot \text{sec}^{-1}$

A more or less reliable experimental study of vertical distribution of particles in a turbulent current was conducted in aqueous suspensions only. In experiments conducted by VANONI (373), D_t was computed from a profile of flow velocities (see the following paragraph). In research conducted by KALINSKE (374), D_t was defined experimentally according to the dispersion of a spray of aqueous solution in a stream. Later, the revealed vertical distribution of sand particles, with a radius of the order of several tens of microns (up to 70μ), coincided somewhat satisfactorily with the equation (45. 2).

M. KALINUSHKIN (375) conducted the only measurements of aerosols when he studied distributions of sawdust and of other powders, in a 2.5 cm circular horizontal tube, at a velocity of $U = 10 - 17 \text{ m} \cdot \text{sec}^{-1}$. If we assume that in circular tubes a turbulent flow is usually accompanied by gas spinning around the tubes' axes and, as a result, a vertical distribution becomes converted into a radial one, then the particles' concentration is maximal at the tubes' circumference and it decreases along the direction of the tubes' axes. In order to obtain a normal vertical distribution in a circular tube, it is necessary to eliminate the spinning with the aid of a screen. Data of M. KALINUSHKIN are well aligned on a rectilinear graph, which coincides with equation (45. 3).

We still wish to quote data of SHERWOOD and WOERTZ (376), who made measurements of D_t in an air current in a duct of rectangular cross section 5.3 cm high, possessing greater width than height. At $Re_f > 10,000$, with the exception of narrow areas adjoining the upper and lower walls, D_t which, practically speaking, appeared constant, was expressed by the following empirical equation:

$$D_t = 0.044\nu Re_f^{0.75} \quad (45.4)$$

where ν is the kinematic viscosity of a gas. For particles with $r = 5\mu$ and with density 1, at $U = 13 \text{ m/sec}$ ($Re_f = 40,000$), the value of V_s/D_t turns out to be equal to 0.016 and the ratio of concentrations at lower and upper walls, in this case, is equal to 1.1, i. e., we have almost uniform distribution in the

entire cross section of the duct. Yet, when $r = 20\mu$, this ratio is equal to 3.7, i. e., the main mass of particles is in motion in the lower part of the duct.

We have discussed the effect of a turbulent current upon particles suspended in it. Of even greater interest is the reverse problem which presents itself, that of the influence of the dispersible phase upon a turbulent current supporting it. It is known from tests that the critical value of the Re_c number is larger in suspensions of clay than in pure water (377, 378). During tests conducted by VANONI (373) on sabulous suspensions in an open duct, a noticeable decrease of the turbulent viscosity coefficient was noted and, hence, that of hydraulic resistance in comparison with pure water; at the same time, of course, the extent of turbulence in the current, as well as the coefficient of turbulent diffusion, also decreased.

These phenomena develop in the following way: every particle of a dispersible phase participates, as we noted, in fluctuations of the medium which, due to gravity, is in a constant motion as regards to the layer of the medium adjoining it. At the same time, a dissipation takes place (conversion into heat) in the mechanical energy, which can only be drawn out of the energy of fluctuations. With this, the extent of turbulence must decrease. Inasmuch as the amount of energy dissipated by a particle per time unit is proportional to the particle's weight, which energizes the rapidity of particle's settling, i. e., it is proportional to the particle's mass in a range of $5/3(m^{5/3})$, then, at the time of constant gravimetric concentration ($c = nm$) the decrease in the degree of turbulence must be accelerated along with the particles' sizes. The observations referred to in § 29, namely, a decrease in a cyclone's resistance upon the increase in concentration of dust, can thus be explained by the decrease of turbulence under the influence of suspended dust, which is what many authors have already assumed (379).¹

The theory of this phenomenon was developed by G. BARENBLATT (381). The magnitude of the effect is determined by the significance of the nondimensional expression, which in the case of aerosols assumes the following form:

-
1. In a memorandum (380) published in 1951, the author of this book attributed the decrease in turbulence to energy dissipation caused by a relative movement of the particles and that of the medium, as a result of incomplete entrainment of particles by fluctuations. It is obvious from the afore-said that this effect must be very small.

$$K = - \frac{gdc/dz}{\gamma_g (dU/dz)^2} (> 0), \quad (45.5)$$

where z is a distance from the bottom; where U is the average current's velocity.

At $K \ll 1$, a dispersible phase does not influence the extent of turbulence, nor the profile of the flow velocities; thus, only in such a case is the equation (45.2) used with relation to vertical distribution of concentrations. When K is comparable unity, the mean square fluctuating velocity u is expressed by the equation: $u = u_0(1 - K)^{1/4}$; where u_0 is a u -value for pure gas. In this case the equation (45.2) is not applicable and computation of concentration distribution becomes complicated.

§ 46. Precipitation of Aerosols in Turbulent Flow

As we proceed to the problem of precipitation of aerosols in a turbulent current, we will notice that almost everything written in §44 about gravitational precipitation during convection and artificial agitation is also correct with regard to a turbulent current. Inasmuch as the mean square fluctuating velocity directed perpendicularly to a current is approximately equal to $0.03 - 0.1 \bar{U}$ (where \bar{U} is the average velocity of flow /363, 382, 376, 383/), then with \bar{U} of the order of several meters per sec, the rapidity of precipitation of particles with a radius $< 10\mu$ in a horizontal tube is considerably smaller than the vertical constituent of the mean fluctuating velocity. Furthermore, such particles are more or less uniformly distributed over the entire cross section of the tube. Thus, upon a unit length of tube with a radius R there will precipitate per second, under the influence of gravity, $2RnV_g = 2RgnT$ particles; where n is the concentration of particles in a current. As a layer of aerosol one cm deep passes over a path dx , i.e., within dx/\bar{U} time period, $2RgnTdx/\bar{U}$ particles will drop out of the layer. Since the capacity of the layer is equal to πR^2 , we can write down:

$$- \frac{dn}{dx} = \frac{2RgnT}{\pi R^2 \bar{U}} = \frac{2nTg}{\pi \bar{U} R}. \quad (46.1)$$

Hence an equation follows, which is analogous to (44.21)

$$n = n_0 \exp \left[- \frac{2Tgx}{\pi \bar{U} R} \right], \quad (46.2)$$

and which discloses how a change takes place as a function of an aerosol, with a concentration of particles of certain size, which passed through an x path. The rapidity of the aerosol precipitation, when proportional to n, declines exponentially with the direction of flow.

These considerations, no doubt, can also be used in the theory of cyclones. Let's assume that a constant turbulent agitation of aerosols also takes place in cyclones. Furthermore, we shall assume, in accordance with the equation (29.1), that the current's velocity at the outer wall of a cyclone is equal to $U_0/2$. Then, a radial velocity of the particles is equal to $U_0^2\tau/4R_2$ and the number of particles precipitating per sec upon one cm^2 of wall is

$$I = \frac{nU_0^2\tau}{4R_2}. \quad (46.3)$$

If we denote by L/s the height of the spiral spacing formed by the current in a cyclone (where L is the cyclone's height, where s is a number of turns), then upon one cm length of the spiral there will precipitate in one sec IL/s particles. At the same time there will pass through the spiral all the particles which entered the cyclone within one sec and were unable to precipitate on their path, namely, $HhnU_0$ particles; where H and h is the height and width of a cyclone's entry. Thus, we can write down:

$$-\frac{1}{n} \frac{dn}{dx} = \frac{nU_0^2\tau L/4R_2s}{nHhU_0} = \frac{U_0\tau L}{4R_2sHh}, \quad (46.4)$$

where dx is a differential of the spiral's length. Since the entire spiral's length $\approx 2\pi R_2s$, then, if we integrate the equation (46.4), we obtain for the ratio of the number of outgoing and incoming particles involved in the cyclone the following equation:

$$\ln \frac{n}{n_0} = - \frac{U_0\tau L \cdot 2\pi R_2s}{4R_2sHh} = \frac{\pi U_0\tau L}{2Hh} \approx \frac{\pi U_0\tau s}{2h}. \quad (46.5)$$

(We assumed the height of the spiral's spacing L/s to be equal to a height of the entry H). Thus, the effectiveness of the cyclone is equal to

$$\eta = \frac{n_0 - n}{n_0} = 1 - \exp \left(- \frac{\pi U_0\tau s}{2h} \right), \quad (46.6)$$

which is considerably less than the effectiveness computed without accounting turbulent agitation (equation /29.14/).

Although the absence of accurate experimental data about the effectiveness of precipitation in cyclones as a function of particle size does not permit any quantitative verification of the equation (46.6), yet, undoubtedly, the latter is closer to actuality than the (29.14) equation. In accordance with the latter equation, particles larger in size than one determined by a threshold value must precipitate completely. It is based on facts that a 100% precipitation in cyclones is not observed, even among comparatively large particles; instead there is a continuous increase of precipitation effectiveness in conjunction with the size of particles (384), as the equation (46.6) implies.

In a similar manner, turbulence also affects the precipitation of highly dispersed aerosols in a condenser (see § 27); at a transition from a laminar to a turbulent region of flow, the electrical current's force at a certain potential becomes considerably smaller than would be the force of electrical current theoretically calculated for laminar flow (181)

As we proceed to diffusible precipitation of aerosols from a turbulent current, we shall quote, first of all, certain essential information pertinent to hydrodynamics of a turbulent current.

During experimental studies involving distribution of mean velocities of turbulent flow in tubes and open ducts, it was determined that the logarithmic profile of velocities, $U = a \ln z + b$, must be followed at the same time; where U is an average velocity at a distance z from the wall. Beginning with the introduction of the "length of mixing path" (a value which, in the theory of turbulent viscosity and diffusion, plays the same part as does the length of the molecular free path in the theory of molecular viscosity and diffusion), PRANDTL (385) developed the following equation:

$$U/U^* = \frac{1}{\kappa} \ln \frac{zU^*}{\nu} + C \quad (z > \delta_L, \text{ see below}), \quad (46.7)$$

in which κ , KARMAN'S constant, combines the length of the mixing path l with a distance from the wall. According to this equation,

$$l = \kappa z, \quad (46.8)$$

where C is a constant which cannot be defined by a theoretical method; where U^* is the dimensions of velocity, named "dynamic velocity" or "drag velocity," which is defined by the equation

$$U^* = \sqrt{\tau/\gamma_g} \quad (46.9)$$

with the shearing stress τ , transmitted in one sec by turbulent fluctuations passing through one cm^2 area parallel to the wall. One could regard τ near the wall as constant (independent of z) and consequently equal to the frictional force between a flowing gas and one cm^2 area of the wall.

Experiments revealed that $\alpha = 0.4$, $C = 5.5$ and thus the equation (46.7) may be written down in the following way:

$$U/U^* = 2.5 \ln \frac{zU^*}{\nu} + 5.5 = 5.75 \lg \frac{zU^*}{\nu} + 5.5 \quad (z > \delta_L) \quad (46.10)$$

We still want to note that U^* has the identical order of magnitude of the average turbulent quadratic fluctuating velocity u .

This equation is not applicable when the distance from the wall is very close, because at $z \rightarrow 0$, it leads to $U \rightarrow -\infty$, whereas the current's velocity at the wall is equal to zero. Therefore it is necessary to assume that, near the wall, a thin laminar layer δ_L deep exists, in which gas moves according to the usual laws governing a flow of viscous liquid, while transmittal of impulses takes place at the expense of molecular viscosity. Thus, $\tau = \eta dU/dz$ at $z < \delta_L$ and, hence, it follows that in the laminar layer

$$U/U^* = \frac{\tau z}{\eta U^*} = \frac{U^{*2} \gamma_g z}{U^* \eta} = \frac{U^* z}{\nu} \quad (z < \delta_L) \quad (46.11)$$

As experiment indicates, the profile of velocities is expressed at $zU^*/\nu < 5$ by the equation (46.11) and at $zU^*/\nu > 20$ by the equation (46.10), while within an intermediate region, it is expressed by a continuous transitional curve (385). Thus, the depth of the laminar layer is of the order of magnitude

$$\delta_L \approx 10\nu/U^* \quad (46.12)$$

Having applied the idea about "turbulent viscosity," one can write down

$$\tau = \eta_t dU/dz \quad (z > \delta_L) \quad (46.13)$$

If we introduce here the expressions for dU/dz from (46.7) and the expression for T from (46.9), we find that $\eta_t = \gamma_g U^* z \alpha$. Hence, for "kinematic turbulent viscosity" $\nu_t = \eta_t / \gamma_g$ we obtain the following equation:

$$\nu_t = \alpha U^* z. \quad (46.14)$$

Inasmuch as the mechanism of the turbulent transference of impulse and mass is one and the same, then the coefficients of turbulent diffusion D_t and viscosity ν_t must, according to their magnitude, be also close. Actually, according to PRANDTL (386), $D_t / \nu_t = 1.4 - 2.0$, and according to experiments of SHERWOOD and WOERTZ (376), $D_t / \nu_t = 1.6$. If we take advantage of this circumstance, we can express the coefficient of turbulent diffusion by the following equation:

$$D_t = 1.5 \div 2.0 U^* z \alpha \approx 0.6 \div 0.8 U^* z \quad (z > \delta_L). \quad (46.15)$$

Of course, this equation is applicable only at $z > \delta_L$, i.e., outside a laminar layer. As to the mechanism of diffusion inside the layer, there are two points of view: according to PRANDTL and TAYLOR (387), turbulent fluctuations are absent inside a laminar layer, i.e., transmittal of substance takes place exclusively by way of molecular diffusion (transmittal of momentum occurs in the same way). According to LANDAY and LEVICH (388), the turbulent fluctuations penetrating the laminar layers fade away only when close to the surface of wall, whereupon D_t is, in this case, no longer proportional to the 1st, but to the 4th power of z , namely

$$D_t \approx U^* z^4 / \delta_L^3 \quad (46.16)$$

There is a "diffusible under-layer," δ_D thick, close to the wall where molecular diffusion prevails over turbulent diffusion. At the same time $\delta_L \gg \delta_D$. Thus, according to PRANDTL and TAYLOR, the boundary line of the diffusible layer, which in their opinion coincides with the boundary line of the laminar layer, is determined by the factor that coefficients of turbulent and molecular viscosity equalize themselves at the first boundary line; according to LANDAY and LEVICH, it is determined by this fact, that at the first boundary line, the coefficients of turbulent and molecular diffusion coincide instead. In instances where $\nu_t / \nu \approx D_t / D$, these boundary lines actually coincide with one another, thus the hypothesis of PRANDTL and TAYLOR appears to be acceptable. If we consider that $\nu_t / D_t \approx 1$, it is

essential that SCHMIDT'S number, $Sc = \nu/D$, be also of the order 1 and this occurs, e.g., during diffusion of gases. However, in aerosols $Sc \gg 1$, i.e., $\nu_t/\nu \ll D_t/D$. Since the intensity of the turbulent fluctuations in the near-wall area and the mixing length path, consequently also ν_t and D_t , decrease in any event in relation to the nearness to wall, while ν and D are constant magnitudes, it follows from the afore-said that D_t/D become equals to one at a considerably smaller distance from wall than ν_t/ν , i.e., with regard to aerosols δ_D must be considerably smaller than δ_L . Furthermore, at a certain condition of current, i.e., at a certain δ_L , the δ_D value cannot remain constant, but must vary symbasically with D .

It follows, especially from LANDAY'S and LEVICH'S definition of δ_D , that $D = D_t \left(z = \delta_D \right) \approx U_* \delta_D^4 / \delta_L^3$, hence

$$\delta_D \approx D^{1/4} U_*^{-1/4} \delta_L^{3/4} \approx \frac{0.57 \delta_L}{Sc^{1/4}} \quad (46.17)$$

In computing rapidity of diffusible precipitation of aerosols on a tube's wall, we shall disregard the change in concentration of the aerosol along the current's direction, i.e., we shall assume that the concentration depends neither upon time, nor upon the coordinate x to be calculated with the current's direction, but solely upon a distance to the wall z . In view of the low rate of diffusible precipitation and the comparatively higher velocities of the current during a turbulent cycle, such simplification is fully admissible. In this case, the same number of particles, I , will pass within one cm^2 per sec through each area parallel to the wall, on which, due to the greater magnitude of the coefficient of turbulent diffusion at points remote from the walls, the concentration of the aerosol may be regarded as constant (n_0) everywhere except in the layer adjacent to the wall. If we denote by D_E the effective coefficient of diffusion, which includes molecular as well as turbulent transfer of a substance, we can write down in a general way

$$I = D_E \frac{dn}{dz} = \text{const.} \quad (46.18)$$

In order to compute I , it is necessary to proceed from a defined hypothesis about the magnitude of D_E as a function of the distance from the wall. The simplest way to effect this computation would be on the basis of the PRANDTL and TAYLOR hypothesis, i.e., if we assume that at $z < \delta_L$ only

molecular diffusion is active, while at $z > \delta_L$ only turbulent diffusion is effective. In a laminar layer

$$I = D \frac{dn}{dz} \quad (z < \delta_L), \quad (46.19)$$

of which $n = Iz/D + C_1$, or because at $z = 0$, $n = 0$,

$$n = Iz/D \quad (z < \delta_L). \quad (46.20)$$

In a turbulent region, D_E is expressed by the equation (46.15); then if we designate the coefficient $0.6 \div 0.8$ by α , we obtain

$$I = \alpha U_* z \frac{dn}{dz} \quad (z > \delta_L), \quad (46.21)$$

hence

$$n = \frac{I}{\alpha U_*} \ln z + C_2 \quad (46.22)$$

If we designate a distance from the wall by h , on which n assumes a constant value n_0 , we obtain

$$n_0 = \frac{I}{\alpha U_*} \ln h + C_2 \quad (46.23)$$

or, if we eliminate C_2 from (46.22) and (46.23),

$$n = n_0 + \frac{I}{\alpha U_*} \ln \frac{z}{h}. \quad (46.24)$$

At $z = \delta_L$, the expressions (46.20) and (46.22) must coincide. If we substitute in these expressions z by δ_L and then compare same, we obtain

$$I = \frac{n_0 D}{\delta_L + \frac{D}{\alpha U_*} \ln \frac{\delta_L}{U_*}} \quad (46.25)$$

or, if we substitute U^* by $10\nu/\delta_L$ in accordance with (46.12)

$$I = \frac{n_o D}{\delta_L + \frac{D\delta_L}{10a\nu} \ln \frac{\delta_L}{n}} = \frac{n_o D}{\delta_L \left(1 + \frac{1}{10aSc} \ln \frac{\delta_L}{h}\right)} \quad (46.26)$$

Inasmuch as in aerosols $Sc \gg 1$, the second term in brackets may be disregarded and we finally obtain

$$I \approx \frac{n_o D}{\delta_L} \quad (46.27)$$

Thus, according to PRANDTL and TAYLOR, the rapidity of diffusible precipitation is proportional to the first degree of the coefficient of thermal diffusion for an aerosol, whereupon, as is obvious from the equation (46.27), the aerosol's concentration may be considered as practically constant down to the laminar layer's boundary line, just as we have shown on page 284. An analogous computation based on the hypothesis of LANDAY and LEVICH is considerably more complicated, and we shall only quote its final result which is expressed by this equation

$$I = \frac{\beta n_o D}{\delta_D} \quad (46.28)$$

where β is a numerical coefficient of the order of unity whose value cannot be determined theoretically. Since, according to (46.17), δ_D is proportional to $D^{1/4}$, then I is proportional to $D^{3/4}$. Such dependence is explained as due to the effect that, upon a decrease in the coefficient of thermal diffusion, turbulent fluctuations carry particles much closer to the wall and in this way they partly compensate the decrease in D .

Although in the description of the diffusible precipitation of aerosols from a turbulent current (as prepared according to the hypothesis of LANDAY and LEVICH), there is undoubtedly a better approach to actuality than in the description by PRANDTL and TAYLOR, the mechanism of this process may finally be explained solely with the aid of an experiment. Thus, it would be expedient to use isodispersed sulfuric acid fumes, which may be obtained by way of LaMER'S (6) generator. Also, it would be very convenient

in this case to determine the amount of precipitation on the walls. By using smokes with various sizes of particles, one could determine the dependence of I upon D and then, accordingly, define the variables, which affect D_t and which follow upon changes in the distance from the wall.

We shall introduce the equations (46. 27) and (46. 28) in a form suitable for practical use. Then, we shall take advantage of experimental data (389) obtained by means of smooth tubes at $Re_f < 10^5$; they imply, that

$$U^* \approx \frac{0.16 U_M}{Re_f^{1/8}} \approx \frac{0.2 \bar{U}}{Re_f^{1/8}}, \quad (46. 29)$$

where U_M is the current's velocity at the tube's axis; where \bar{U} is average velocity. Hence,

$$\delta_L = 10 \nu / U^* \approx 50 \nu Re_f^{1/8} / \bar{U} = 100 R / Re_f^{7/8} \quad (46. 30)$$

(R is the tube's radius) and

$$I = \frac{D n_0}{\delta_L} \approx \frac{D n_0 Re_f^{7/8}}{100 R} \quad (\text{according to PRANDTL and TAYLOR}) \quad (46. 31)$$

Furthermore, according to (46. 17)

$$\delta_D \approx 57 R D^{1/4} / Re_f^{7/8} \nu^{1/4} \quad (46. 32)$$

and

$$I = \frac{\beta n_0 D}{\delta_D} = \frac{\beta D^{3/4} n_0 Re_f^{7/8} \nu^{1/4}}{57 R} \quad (\text{according to LANDAY and LEVICH}) \quad (46. 33)$$

There are no available experimental data pertinent to an aerosol's precipitation from a turbulent current on the tube's walls without inducing any sedimentation. While spraying atomized water over a short horizontal tube's axis, ALEXANDER and COLDREN (390) measured the fog concentration at

different points of the tube and thus they computed the rapidity of the precipitation on the walls. However, in these tests, the drop in concentration from the tube's axis toward the tube's circumference apparently had nothing in common with diffusible precipitation; actually it implied the familiar concentration profile in a free stream.

We proceed now to inertial precipitation of aerosols from a turbulent current. One might imagine that, in view of a full entrainment of particles by turbulent fluctuations, the inertial precipitation in such case must be absent. Yet, computations on page 292 refer to a central portion of the turbulent current. Meanwhile, as observations indicate, the fluctuation velocity increases proportionally to the wall's proximity and begins to decrease only at a very short distance from the wall (382, 391, 392). On the other hand, the length of the mixing path and, consequently, the eddies' diameters, constantly decrease in relation to the nearness to the wall, while very small-scale fluctuations perpendicular to the wall have already been observed with the ultramicroscope at a distance of the order of several microns from the wall (382). Therefore, it is possible that particles near the walls are influenced by rather significant inertial forces which are able to cause precipitation of particles.

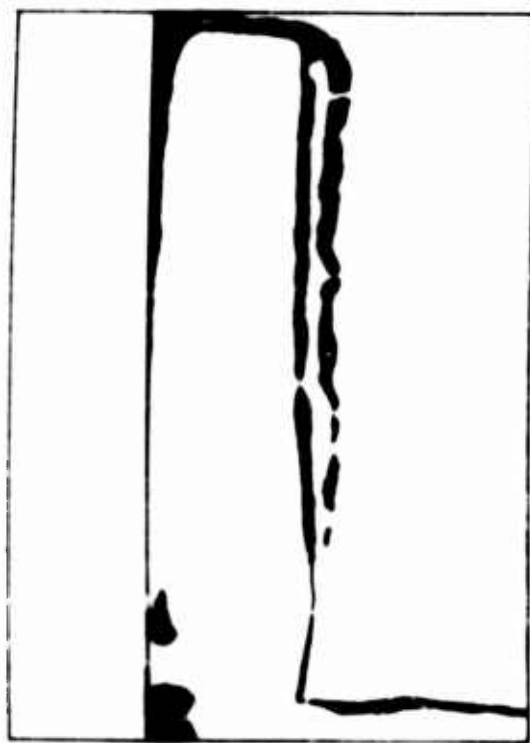


**FIG. 66 EDDY-LIKE SETTLING OF PARTICLES
BEHIND AN OBSTACLE**

Unfortunately, no experimental data pertinent to this question are available. One can frequently observe abundant precipitations of dust on walls of vertical tubes; probably they are caused by inertial precipitation from a turbulent current. It must be implied that, at a greater velocity of current, solid particles may, during precipitation, be blown off by the current; therefore, if sediments are lacking, this cannot serve as an indication of lack of precipitation. In order to solve this question, it is necessary to set up experiments with vapors, or to use a viscous liquid for coating the walls.

On the other hand, one may see on the walls well known sediment which are caused by "constant" local eddies, formed due to various obstacles being by-passed, etc. Figure 66 shows a photograph of the dust sediment formed on a wall of a ventilated room near a telephone line, within a period of one year as a result of a narrow air current escaping from a vertical slot located to the left of the wire. A thick, narrow and sharply contoured sediment of dust was formed in front of the wire, whereas a wide and diffused sediment was behind the wire. In addition, the frontal surface of the wire had inertial sediment of a non-eddy origin. Figure 67 illustrates schematically the eddies being formed during the by-passing of obstacles. A very similar picture was observed by N. ZHUKOVSKIY (393) during theoretical studies of formations of snow drifts near obstacles (fences), although apparently in this case the main role is not assumed by inertial precipitation, but by delayed sedimentation of the snow from a current.

Eddy-like precipitation is also observed under familiar conditions when loosely held bodies are by-passed, whereupon a sediment is formed



FIG 67 EDDIES IN FRONT AND BEHIND AN OBSTACLE

not only toward the windward, i. e., the side facing the current, but also toward the lee of the body. According to experiments of YEOMANS (248), 2.5 times more fog droplets with $r = 5.6\mu$ precipitated on the leeward side than on the windward side at current's velocity $8 \text{ m} \cdot \text{sec}^{-1}$, upon glass discs 7 cm in diameter, positioned perpendicularly to the current. According to LANDAHL (236), at $0.5 \text{ m} \cdot \text{sec}^{-1}$ velocity, more particles precipitated on the leeward side of glass plates 2.5 cm wide, than at $1.5 \text{ m} \cdot \text{sec}^{-1}$ velocity. According to

experiments of ASSET and PURY (394), at $2.3 \text{ m} \cdot \text{sec}^{-1}$ current's velocity, droplets of isodispersed vapor with $r = 6.5\mu$ did not precipitate on the leeward side of glass cylinders 7.5 cm in diameter, nor on the human forearm not covered with hair. However, approximately 4 times less droplets precipitated on the leeward side of the forearm covered with hair than on its windward side. It is possible that, for the occurrence of precipitation on the leeward side, the following definite hydrodynamic conditions are essential: whereas the current's velocity in the eddies must be adequate for inertial precipitation of particles, on the other hand eddies must not depart too rapidly from the body being by-passed.

Still, it is possible to refer here to a formation of thick sediment of dust on walls of diffusers near their exit where the bouncing of eddies off the walls takes place.

§ 47. Spreading of Aerosols in the Atmosphere

The question of aerosol movement in the atmosphere (smoke escaping from factory smokestacks, screening and insecticide smokes escaping from special generators or smoke pots, etc.) is of great practical importance from technical and hygienic standpoints, e.g., with regard to problems of preventing contamination of inhabited places by industrial aerosols. This question may be of specific importance in connection with the production of atomic bombs which, upon explosion, develop a large cloud of radioactive aerosols which spread in the atmosphere and possess concentrations dangerous to man within a distance of several hundred kilometers from the point of explosion. Yet, in spite of a fairly great number of theoretical and experimental achievements the discussed problem still remains insufficiently probed, mainly because of the extremely great complexity and variability of atmospheric currents which cause enormous and unsurmountable fluctuations in measurements reflecting upon mathematical analysis. For these reasons, experimental testing of various theories is highly complicated.

Any movement of aerosols in the atmosphere consists of air movement itself, and of the relative movement of particles together with air and this, with regard to particles not very large in size, boils down to precipitation of particles under the influence of gravity. At the beginning, we shall disregard this precipitation, i.e., we shall examine the spreading of highly dispersed aerosols in the atmosphere. In this case, the laws governing the spreading of aerosols and gaseous impurities are identical. They are described in detail in monographs of SHELEYKHOVSKIY (395), ANDREYEV (396) and SUTTON (397, 398); therefore we shall direct our main attention to the principal side of the matter without elaborating upon various details which are interesting from a practical standpoint. First of all, it is necessary to pause at the mechanism of turbulent dispersion in the atmosphere, because this problem is rather poorly and, at times, even incorrectly explained in books.

The general characteristics of aerosol dispersion in the atmosphere are as follows. A small cloud, or uninterrupted aerosolic streams, emerging from any source move along with the wind and at the same time they become dispersed due to the influence of atmospheric turbulence. A molecular diffusion, practically speaking, plays no part in this process, except with regard to a very thin air layer at the surface of substances coming in contact with the aerosols.

Atmospheric turbulence possesses certain specific features, which of necessity, should be mentioned briefly. In turbulent streams passing

through tubes, passages, rivers, etc., there exists at all points of such current (easy determinable by test, and practically constant as to magnitude and direction) the mean velocity of current U , upon which random turbulent fluctuations superimpose themselves. Variations in U , if they occur in a general manner (e.g., daily or seasonal velocity changes in rivers), have a period larger by several orders of magnitude than would be the period of large-scaled fluctuations as such. Furthermore, U considerably surpasses the mean quadratic fluctuation velocity. Thus, the border line is very abrupt between the current and its fluctuations.

The velocity of atmospheric wind, as measured by weather vanes or otherwise, changes constantly in its magnitude and in its direction, whereas the amplitude of fluctuations invariably increases within the course of time involved in observations. Here we have a continuous spectrum of fluctuations, which commences with a period involving almost imperceptible fluctuations, estimable in hundredths of fractions of a second, and ending with daily and yearly fluctuations of wind velocities. Due to this, it is in no way possible to determine in this case any border line between the average and fluctuating velocities; moreover, an average wind velocity per min., as measured by any meteorological instrument, may in yearly observations be considered as a fluctuating velocity.

We shall examine now the mechanism of diffusion in a turbulent current and this time we shall begin with the example of a more simple current which passes through a tube or through a channel. Let's assume that at a certain point O (figure 68), an aerosol is constantly ejected into the current through an elongated narrow slit, positioned perpendicularly to the current. The mark of O to O' on figure 68 denotes the path of the current of the average

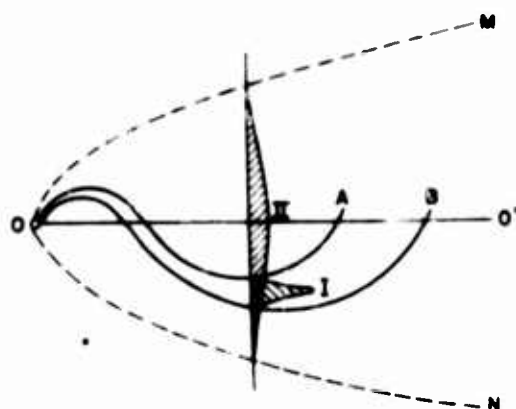


FIG. 68 AEROSOLIC STREAM IN A TURBULENT ATMOSPHERE

stream. The curves OA and OB denote contours of the aerosolic flow, as they are recorded at a determined moment and are so defined as to allow for a condition in which the aerosol's concentration at these contours remains equal, let's say, to 10% of the concentration at the axis of the stream. The mean square of the particle deviations from the immobile axis $O - O'$, registered by an immovable observer (EULER'S diffusion), is expressed by the following general equation

$$\overline{x^2} = 2D_t t. \quad (47.1)$$

(To simplify the matter, it is assumed that D_t , the usual coefficient of turbulent diffusion, is constant in the entire stream of the current.) Hence, on behalf of the distribution of aerosol concentrations in the current (curve II), with a continuously active source included, we obtain the above quoted (page 239) expression

$$n = \frac{\Phi'}{\sqrt{4\pi D_t U x}} e^{-\frac{U z^2}{4 D_t x}} \quad (47.2)$$

whereupon, as follows from the afore-said, the equation yields the average concentration computable according to the usual rules for the time involved.

Another matter of fact is the mutual diffusion of particles in a turbulent current, i.e., their shifting as regards the observer who is moving along with one of the particles (LAGRANGE'S diffusion). Whereas EULER'S diffusion is attained as a result of all fluctuations, in LAGRANGE'S diffusion, participating fluctuations are only of a λ scale and of the same magnitude order or smaller than the distance between particles x . These fluctuations constantly increase the distance between particles, i.e., they tend to expand the stream. Evidently, large-scaled fluctuations with $\lambda \gg x$ cannot change the distance between particles, i.e., the width of stream; however they deflect it and break it up into separate clouds. Naturally, a momentary distribution of concentrations in the stream (curve I) is determined by way of LAGRANGE'S diffusion. As an example, we submit on figure 69 a photograph of smoke escaping from a factory smokestack at dissimilar atmospheric turbulences (399).

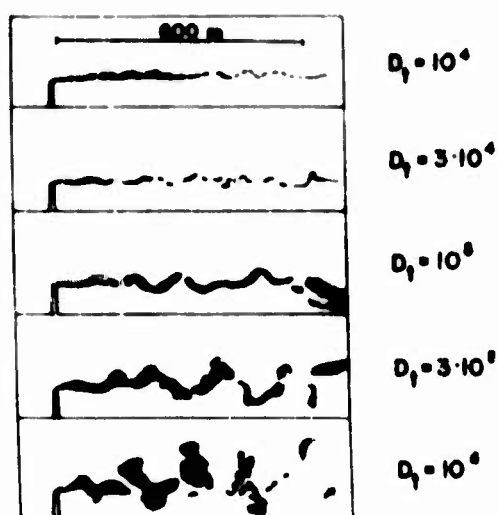


FIG. 69 STREAM OF SMOKE AT DIFFERENT DEGREES OF ATMOSPHERIC TURBULENCE

In relation to the widening of the stream, i.e., the enlargement of x , the increase in fluctuations' scale follows and they are capable of changing the distance. In other words, the coefficient of LAGRANGE'S diffusion D_L constantly increases relatively to the movement and to the expansion of an aerosolic cloud and this constitutes a peculiarity characteristic to turbulent diffusion. We wish to emphasize again that this circumstance is important with regard to the distribution of momentary concentrations, although it does not affect average concentrations according to time. RICHARDSON (400) discovered in an empirical way the following dependence for D_L :

$$D_L \approx 0.2x^{4/3} \quad (47.3)$$

A. OBUKHOV (364) demonstrated that equation (47.3) may be derived in a theoretical way to include the region of scales of fluctuations in which KOLMOGOROV'S theory would be applicable.

One can readily see that, when $x = 0$, actually $D_L = 0$, because particles closely situated side by side cannot become disengaged under the influence of turbulent fluctuations. On the other hand, in some instances, turbulent fluctuations may become independent, e.g., if they are present in a wide river, at two different points with a sufficiently great distance between them. In such a case, equation (47.3) would be inapplicable, since LAGRANGE'S coefficient of diffusion at these points would be equal to the sum of usual (EULER'S) coefficients of diffusion

$$D_L = D_{t_1} + D_{t_2} \quad (47.4)$$

and it would resemble the effect which takes place during molecular diffusion (see page 332). Generally speaking, $D_L \leq D_{t_1} + D_{t_2}$ always; therefore the outline of an average stream MON (see page 82) is always wider than are the contours of an instantaneous stream AOB.¹

As we proceed to diffusions in the atmosphere, it is necessary, above all, to point out a substantial difference between vertical and horizontal fluctuations. Although a small vertical component is usually found in wind velocities, it may be disregarded in the first approximation, and one may assume that the average vertical velocity of the wind equals zero; thus, the question of what should be regarded here as fluctuation velocity and what as the average velocity ceases. The coefficient of vertical turbulent diffusion (EULER'S) D_z , which determines the kinetics of vertical interchange in the atmosphere and thus plays a very important part in meteorology, was the objective of numerous theoretical and experimental studies; consequently its magnitude, which depends upon elevation above the ground, wind velocity and other meteorological conditions, as well as upon terrain features, etc., may be regarded as familiar in the first approximation.

1. Immediately upon completion of this book, its author became familiar with M. YUDIN'S (401) article in which the considerations exposed here, about turbulent dispersion's correlation to an immobile axis and to an axis of a smoke stream are more exactly formulated.

Still more complicated is the matter with regard to horizontal diffusion; here, as we already mentioned, it is impossible to delimit the average and fluctuation velocities; therefore, in the given case, it is necessary to assign a definite time of observation t_{obs} and average (per time t_{obs}) wind velocity U_{obs} ; also, it is necessary to compute per fluctuation the difference between instantaneous values of the wind velocities and the values of U_{obs} . By analogy, the movement of the aerosol must be regarded to include a steady motion with velocity U_{obs} and its dispersion by way of fluctuations. It is quite clear that with the increase of t_{obs} , the average quadratic velocity and the scale of fluctuations will also be increased, because added to these will be changes in wind velocity for the entire greater interval of time; consequently, EULER'S coefficient of diffusion D_{tx} will also be increased. Thus, the longer the t_{obs} is that much more the "aerosol flow averaged according to time" will expand and that much lower will the average concentration of aerosol become in points of the stream, which are at a definite distance from stream's axis, or right at its axis, i.e., the maximal concentration in the stream. Thus, according to experiments of V. RAZANOV (402), the maximal concentration of SO_2 near a point source (factory smoke-stack) comprised at $t_{obs} = 5$ min., 1 diurnal period, 1 month and 1 year, the equivalent of 4.5; 0.94, 0.75 and 0.3 $mg \cdot m^{-3}$. Unfortunately, the law of interchange of the coefficient of horizontal diffusion with time of observation is unknown, and without this, a theoretical computation of concentrations in an aerosol, which is emitted by a point source (or line source, whose length could be compared to a distance from the source) is impossible.

Likewise, nothing is accurately known about the magnitude of LAGRANGE'S coefficients of diffusion in the atmosphere, which are essential in computation of momentary concentrations in a stream, except the equation (47.3), which as such represents a very rough approximation in which even the degree of wind turbulence is not included.

During first attempts to formulate a theory of dispersion of gaseous impurities in the atmosphere (294), usual diffusion equations were used, in which the coefficient of turbulent diffusion and wind velocity were regarded as constant and independent of distance from the ground z . This incident concurs with the problem analyzed in a long run in § 39; consequently a concentration of impurity at a defined point in space is expressed (depending upon a type of source) by the equations (39.13), (39.14), (39.18) or (39.19). Yet, this primitive theory afforded a considerable divergence after testings, in that a concentration actually decreases with distance from a source by far more rapidly than the afore-quoted equations indicate. In the opinion of

SUTTON (403, 398), whose point of view was for a long time regarded with great approval, the cause of the discrepancy lies in the amplification of the effective coefficient of diffusion following the increase of distance from a source. Inasmuch as in tests the average concentrations of impurities (per known time interval) are always measured, SUTTON'S opinion may be accurate only as to horizontal dispersion of a stream from a point source, but not as to the vertical dispersion of the stream, if the latter is emitted by an infinitely long (or, practically speaking, long if compared with distance from a stream) line source.

A differential equation of diffusion in a current coming from a line source and passing through the beginning of coordinates in a perpendicular way to the plane of xz , assumes the form (see /39 15/)¹ as follows:

$$U \frac{\partial n}{\partial x} = \frac{\partial}{\partial z} \left(D_{tz} \frac{\partial n}{\partial z} \right), \quad (47.5)$$

in which U and D_{tz} are functions of height z (the wind is set directionally with the axis z). With this, we omitted (as it frequently happens in conjunction with problems of diffusion in a stream) the diffusion set directionally with the axis x . Border-line conditions of the problem are as follows. $n = 0$ at $x = \infty$,

or $z = \infty$, $n = \infty$ at $x = z = 0$, $\int_{-\infty}^{\infty} U n dz = \Phi$; where Φ is a yield from one cm

of source. The latter condition ensues from the stability of the process and of the law of conservation of matter. Determination of the type of function $D_{tz}(z)$ is effected by the method described on page 301 in accordance with contours of the wind, i.e., according to the function $U(z)$; besides, it is assumed that coefficients of turbulent diffusion and of viscosity remain the same.

Better than any experimental studies were those conducted during a normal (dry adiabatic) temperature gradient in the atmosphere. It was determined that, in this case, the wind's contour is logarithmic, although it differs somewhat from the contour appearing in "smooth" tubes, described on page 299 because under usual meteorological conditions the earth's surface appears "rough" and the stream above it is expressed by the equation

-
1. In this, and in the following paragraph, n may indicate a calculated as well as a gravimetric concentration of aerosol and also a concentration of gaseous impurity.

$$U/U^* = \frac{1}{\kappa} \ln \frac{z - d}{z_0}, \quad (47.6)$$

where z_0 and d are coefficients dependent upon degree of roughness of the earth's surface (height and density of grass level, etc.), upon wind velocity and test findings (404).

Unfortunately, the solution of the equation (47.5) with regard to a logarithmic contour of wind presents insuperable difficulties. They may be by-passed if we approximate the expressions (46.7) and (47.6) with the aid of power functions

$$U = U_1 \left(\frac{z}{z_1} \right)^q, \quad (47.7)$$

or

$$U/U^* = m \left(\frac{z - d}{z_0} \right)^q \quad (47.8)$$

and by selecting q and m coefficients so that, in a defined region of z values, a power function would be as close as possible to a logarithmic region (404).

Proceeding from his own afore-mentioned point of view and from certain aspects of statistical theory of turbulence, SUTTON (403) arrived at a conclusion by a semiempirical method: that the mean square of a relative displacement of particles per time unit t is expressed by the equation

$$\overline{(\Delta z_1 - \Delta z_2)^2} = \frac{1}{2} C^2 (Ut)^s = \frac{1}{2} C^2 x^s, \quad (47.9)$$

in which C is a generalized coefficient of turbulent diffusion and s is combined with the exponent of q in the equations pertinent to the wind's contour (47.7) or (47.8) by the proportion

$$s = 2/(q + 1). \quad (47.10)$$

Assuming for q the value of $1/7$, which according to test data corresponds to a gradient and to a smooth surface, SUTTON obtained $s = 1.75$. The equation (47.9) implies that the coefficient C , with

LAGRANGE'S coefficient of turbulent diffusion D_L (for which the correct formula is $(\Delta z_1 - \Delta z_2)^2 = 2 D_L t$), is combined by the proportion

$$D_L = \frac{C^2}{4} U^{s-1} = \frac{C^2}{4} x^{s-1} U. \quad (47.11)$$

In the solution of the basic differential equation (47.5), SUTTON disregarded the difference between LAGRANGE'S and EULER'S coefficients of turbulent diffusion, as well as the difference between the variation in wind velocity and the coefficients of diffusion with height. Assuming for U the wind velocity at a determined height (2 m), he obtained the equation, in place of (39.18) and (39.19), as follows:

$$n = \frac{\Phi'}{\sqrt{\pi C_z^2 U^2 x^s}} \exp \left(-\frac{z^2}{C_z^2 x^s} \right) \quad (47.12)$$

for a continuous line source, and

$$n = \frac{\Phi}{\pi C_y C_z U x^s} \exp \left[-\frac{1}{x^s} \left(\frac{y^2}{C_y^2} + \frac{z^2}{C_z^2} \right) \right] \quad (47.13)$$

for a point source. Here y is the horizontal distance from the stream's axis; C_y and C_z are C -values in vertical and horizontal diffusions. SUTTON (397) derived expressions for these values from the function of velocity and gusts (i. e., degree of turbulence) of wind. We don't quote these equations (we shall only indicate that C is proportional to U to a degree of $\frac{s}{2} - 1$), because SUTTON (405), in his examples, uses, in the function of the source's height H , other values like C_y and C_z , obtained experimentally under certain conditions (in the presence of an adiabatic gradient and wind velocity of 5 m sec^{-1} , at a height of 2 m above an open plain used as a pasture ground). See table 25.

Table 25

SUTTON'S Coefficients of Diffusion at a Normal Gradient
(In C.G.S. System of Units)

H, m	0	10	25	50	75	100	200
C _y	0.21	0.21	0.12	0.10	0.09	0.07	0.05
C _z	0.12	0.12					

Thus, in order to attain the concurrence with SUTTON'S experiment, one must assume for the coefficient C such values, which decrease with height, whereas the intensity of turbulent diffusion actually increases with a height up to z order of several hundred meters (406). It follows, hence, that the equations (47.12) and (47.13) are virtually empirical and they offer, as we shall explain below, satisfactory concurrence with the experiment at the time of a suitable selection of coefficient values C_y and C_z.

These equations are derived for the case of dispersion in an unlimited volume. Now we have to pause at an important problem pertinent to local conditions near the earth's surface, while working out differential equations of turbulent diffusion. This problem is readily solved in conjunction with the nonabsorption by surface substances (e. g., inert gases), in which case local conditions near nonabsorptive walls happen to be such that the concentration gradient with a normal direction to the wall equals zero, i. e.,

$$\partial n / \partial z = 0 \quad \text{with} \quad z = 0. \quad (47.14)$$

Strictly speaking, it would be proper to assume that $n = 0$ when $z = 0$, in conjunction with aerosols whose particles don't bounce off walls, but adhere to them. Yet, in this case, during the solution of the differential equations of diffusion, we would have to consider, within the near-wall layer, the difference between the effective coefficient of diffusion and the distance from the wall (see page 303), which might lead us to greater mathematical difficulties. Therefore, if we take under consideration that rapidity of aerosol diffusion is very small, i. e., the overwhelming particles' share carried by turbulent fluctuations to this layer does not precipitate on the wall but is carried back, then, in this case, the walls may be considered as "reverberatory to turbulent diffusion" and the condition of (47.14) may be upheld.

If the aerosol's source is at a height H above the ground, then, apparently, z should be substituted by $z-H$ in the equations (47.12) and (47.13). The equations thus obtained are only adaptable to these values of x with which a cloud remains inclined to the ground. In order to obtain a solution satisfactory to the condition of (47.14), the following rule should be applied: a fictitious source with the same yield as the one under consideration is positioned symmetrically with the latter source in relation to the ground surface, i. e., at the point or line with coordinates $z = -H$, $x = 0$. Thus, instead of (47.12) and (47.13), we obtain the equations

$$n = \frac{\Phi'}{\sqrt{\pi C_z^2 U^2 x^s}} \left\{ \exp \left[-\frac{(z-H)^2}{C_z^2 x^s} \right] + \exp \left[-\frac{(z+H)^2}{C_z^2 x^s} \right] \right\} \quad (47.15)$$

for a line source, and

$$n = \frac{\Phi}{\pi C_y C_z U x^s} \exp \left(-\frac{y^2}{C_y^2 x^s} \right) \left\{ \exp \left[-\frac{(z-H)^2}{C_z^2 x^s} \right] + \exp \left[-\frac{(z+H)^2}{C_z^2 x^s} \right] \right\} \quad (47.16)$$

for a point source.

While testing these equations experimentally, SUTTON (405) positioned the aerosol's source close to the ground's surface ($H = 0$). At various distances x from the source but directionally with the wind, the maximal concentration in a cloud was measured with the known x , i. e., at ground level ($z = 0$) in the case of a line source, and at the cloud's axis ($z = y = 0$) in the case of a point source. In the latter instant, as we mentioned above, the maximal concentration tends to decrease with the increase of time t , during which air samples are taken for analysis. Yet, under the conditions of SUTTON'S experiments (a normal gradient), the decrease was hardly noticeable prior to $t > 3$ min. According to the equations (47.15) and (47.16), the maximal concentration is equal to

$$n_{\max} = 2\Phi' / \sqrt{\pi C_z^2 U^2 x^s} \quad (47.17)$$

in the case of a line source, and

$$n_{\max} = 2\Phi / \pi C_y C_z U x^s \quad (47.18)$$

in the case of a point source.

With a nearly normal gradient, which occurred during these experiments (as we already noted), s was equal to 1.75, i.e., in the case of a line source, n_{\max} was proportional to $x^{-0.875}$ and in the case of a point source, to: $x^{-1.75}$. Actually it was found that n_{\max} was proportional to $x^{-0.9}$ in the first instant and to $x^{-1.76}$ in the second instant.

Furthermore, if we take into consideration what was discussed in conjunction with equation (47.15) about the dependence of C upon U , it follows, that $n_{\max} \sim C_z^{-1} U^{-1} \sim U^{-0.875}$. Thus with the ratio of the wind velocities 1:2:3, the corresponding values of n_{\max} must be in the ratio of: $1:2^{-0.875}:3^{-0.875} = 1:1/1.84:1/2.61$. Based on experiments, the ratio found is $1:1/1.84:1/2.77$.

For the absolute value of n_{\max} at $x = 100$ m, $U = 5$ m·sec⁻¹, $\Phi = 1$ g·sec⁻¹, in the case of a point source ($C_y = 0.21$, $C_z = 0.12$), where the $n_{\max} = 1.0$ mg·m⁻³ should have been obtained, it was found to be 2.0 mg·m⁻³. In the case of a line source, with $\Phi' = 1$ g·sec⁻¹·m⁻¹, the theoretical value is $n_{\max} = 33$ mg·m⁻³ and the experimental value is 31 mg·m⁻³.

Assuming that at the "border" of a cloud the concentration is equal to 0.1 of maximal concentration, according to the equation (47.15), in which we suppose $H = 0$, then we can find that the "height" of cloud z_0 produced by a line source is determined by the equation

$$0.1 = \exp \left(-\frac{z_0^2}{C_z^2 x^2} \right), \quad (47.19)$$

i.e., at $x = 100$ m, $z_0 = 10$ m. Thus, it is determined experimentally, that $z_0 = 10$ m.

By analogy, the theoretical value of the "width" of a cloud produced by an on-the-ground point source at a distance of 100 m is equal to 34 m and the experimental value is equal to 35 m.

According to E. TEVEROVSKIY (407), the formula (47.17) with the coefficient $s = 2$ is adaptable in rather wide-range values of a temperature

gradient. E. TEVEROVSKIY found for C_z the average value of 0.027 in the case of a flat locality devoid of vegetation, and the value of 0.086 for a broken terrain covered with tall grasses. At the same time, C_z appeared to be practically independent of wind velocity. It appears, hence, that the data included in table 25 pertain solely to the locality where SUTTON conducted his experiments.

CALDER (408) presented a more satisfactory theory of dispersion of a cloud emitted from an on-the-ground line source at a normal gradient. If we accept the equation (47.6) for the wind's contour, and if we regard coefficients of turbulent diffusion and viscosity as equal in a vertical direction, then, for D_{tz} , according to the rule explained on page 301, we obtain the following expression:

$$D_{tz} = \alpha U^*(z - d). \quad (47.20)$$

Inasmuch as d is usually of the order of magnitude of several centimeters, we can assume that $d = 0$. To illustrate this better, we submit table 26 with DEACON'S (409) experimental data. In this table, h denotes a height of grass above which measurements were conducted; U_1 and U_2 denote velocities of wind at the height of one and two m, according to which the following parameters were computed: d , z_0 and U^* . $\tau_0 = \gamma_g U^{*2}$ is a friction force of wind against one cm^2 of the ground's surface (see page 299). We take notice that basic measurements of τ_0 brought results which are close to those computed according to the (47.6) equation (410) and this attests the reliability of the computations.

Table 26
Wind's Contour and Turbulence Above a Grass-Covered
Locality at a Normal Gradient

$h, \text{ cm}$	$U_1, \text{ cm} \cdot \text{sec}^{-1}$	U_2/U_1	$d, \text{ cm}$	$z_0, \text{ cm}$	$U^*, \text{ cm} \cdot \text{sec}^{-1}$	$\tau_0, \text{ dyn} \cdot \text{cm}^{-2}$	$D_{tz}, \text{ cm}^2 \cdot \text{sec}^{-1}$ at $z = 100 \text{ cm}$
60-70	100	1.45	15	15.9	23.9	0.68	810
	200	1.35	16	8.8	35.5	1.51	1190
	300	1.32	21	5.6	45.4	2.47	1430
	450	1.28	32	3.0	57.8	4.00	1570
1.5	100-800	1.112	0	0.20	6.4-51	0.05-3.2	260-2100
3.0	100-800	1.140	0	0.71	8-65	0.08-5.0	320-2600
4.5	200	1.191	0	2.65	22.0	0.58	880
	450	1.170	0	1.74	44.5	2.38	1780

It is distinctly clear from table 26 that the increase of turbulent diffusion progresses with the force of the wind and with the degree of roughness of the earth's surface.

If, at the time of integrating the equation (47.5), we assume that $U = \text{const.}$, then with D_{tz} proportional to z , we can readily obtain the solution

$$n = \frac{\Phi'}{\kappa U^* x} \exp \left(- \frac{U z}{\kappa U^* x} \right), \quad (47.21)$$

from which

$$n_{\max} = \frac{\Phi'}{\kappa U^* x}. \quad (47.22)$$

The (47.21) and (47.22) equations were tested (408) under the conditions resembling those of SUTTON'S work. The z_0 coefficient equaled 3 cm, wind velocity at 2 m height was $5 \text{ m} \cdot \text{sec}^{-1}$, $d = 0$ and $U^* = 50 \text{ cm} \cdot \text{sec}^{-1}$. With $\Phi' = 1 \text{ g} \cdot \text{m}^{-1} \cdot \text{sec}^{-1}$, the theoretical "height" of the cloud at the distance of 100 m was 10.4 m and the experimental "height" was 10.0 m. The maximal concentration ($z = 0$) was as follows: theoretical, $44 \text{ mg} \cdot \text{m}^{-3}$, and experimental, $36 \text{ mg} \cdot \text{m}^{-3}$. It was further discovered that n_{\max} was proportional to U^{-1} and x^{-1} in accordance with the equation (47.22).

A greater advantage of the equation (47.21) over SUTTON'S equations lies in this; that it is rather accurately derived. The only discrepancy in inferences is the hypothesis about the constancy of U during integration of the equation (47.5). In addition, the equation (47.21) contains only the magnitudes determinable by test, and lacks coefficients whose values have to be selected in order to get a concurrence with a test.

In another work, while approximating logarithmic contours with the aid of power function (47.8), CALDER (404) found D_{tz} (by a method since indicated) as a function of z and thus solved the equation (47.5) without relying upon $U = \text{const.}$, i. e., quite accurately. The equation thus obtained for the distribution of concentrations (which is not submitted here due to its complexity) afforded still better concurrence with the test than equation (47.21).

DEACON (409) developed an analogous conclusion for nonadiabatic gradients, proceeding from the contour

$$U/U^* = \frac{1}{\alpha(1-\beta)} \left[\left(\frac{z}{z_0} \right)^{1-\beta} - 1 \right], \quad (47.23)$$

during which $\beta > 1$ in the case of a superadiabatic gradient, and $\beta < 1$ in the case of an inversion. In both instances, he obtained satisfactory concurrence with the test. FROST (411) prepared a derivation of the $n(x, z)$ equation intended for the contour $U = U_1(z/z_1)^q$. Let's assume that the calculation of D_{tz} , according to the wind's contour, is possible only up to a height at which the magnitude of τ may be regarded as constant and equal to the friction force of the wind against the ground τ_0 , i.e., to a height of the order of several tens of meters. In this way, the equations for concentrations in a cloud are derived with regard to a normal gradient, and they are accurate only up to distances of the order of several hundred meters.

In view of the afore-mentioned peculiarities of horizontal diffusion in the atmosphere, the question of an on-the-ground point source presents much greater difficulties. CALDER (408) derived, by a semiempirical method for a normal gradient, the following equation

$$n = \frac{\Phi U}{2 \alpha^2 \beta U^*{}^2 x^2} \exp \left[- \frac{U}{\alpha U^* x} \left(\frac{y}{\beta} + z \right) \right], \quad (47.24)$$

from which

$$n_{\max} = \frac{\Phi U}{2 \alpha^2 \beta U^*{}^2 x^2}, \quad (47.25)$$

where Φ is the source's yield; where β , the ratio of the average quadratic horizontal and vertical fluctuations velocity, is a magnitude which can be easily determined by experiment. The equation tested under the afore-mentioned (in conjunction with equation /47.21/) meteorological conditions, with $\beta = 2$, brought the following results: the height of the cloud with $x = 100$ m: theoretical, 10.4 m; experimental, 10.0 m (i.e., the same as with regard to a line source); the width of the cloud: theoretical, 41 m; experimental, 35 m; n_{\max} with $\Phi = \text{one g} \cdot \text{sec}^{-1}$: theoretical, $2.5 \text{ mg} \cdot \text{m}^{-3}$; experimental, $2.0 \text{ mg} \cdot \text{m}^{-3}$. The rule of decrease for n_{\max} with x : theoretical n_{\max} is proportional to x^{-1} and experimental n_{\max} is proportional to $x^{-0.8}$. The dependence of n_{\max} upon U : theoretical and experimental n_{\max} is proportional to U^{-1} . However, it is necessary to note that the equation for a point source,

as indicated above, must include, as an essential factor, the time within which a measurement of the concentration at various points was conducted; it must also be considered that in SUTTON'S and CALDER'S experiments the time comprised 3-5 min. The fact that the equations of both authors offer more or less similar results is explained mainly by "padding" SUTTON'S coefficients of C_y and C_z to get the results for the measurements.

The distribution of concentration in an aerosol was studied in a recently published work of CROZIER and SEELY (573). The aerosol was emitted from an on-the-ground point source, along a horizontally directed axis perpendicular to the direction of the wind. Taking of samples was effected from an airplane passing through the aerosolic stream at various altitudes. In this way, practically speaking, a momentary distribution of concentrations was determined. It was found that, up to distances of several tens of kilometers from the source, the concentration of the aerosol was approximately proportional to $\exp(-By^n)$; where y is the distance from the momentary axis of the stream; where B is a constant; $n \approx 1.7$ comes rather close to SUTTON'S exponent 2.0 (see /47.13/).

It appears that, for a continued progress in this field, it is essential.

1. To define more accurately, by theoretical and experimental methods, our knowledge about the magnitude of EULER'S diffusion as a function of height for various meteorological conditions as well as for conditions of roughness of the earth's surface. Recently, Soviet geophysicists attained major successes in this direction (412).

2. To study in a similar manner the coefficient of EULER'S horizontal diffusion as a function of the observation time t_{obs} (see page 312). It is obvious that almost nothing has been done in this direction; therefore the theory of dispersion from a point source, as yet, cannot be founded.

3. Having introduced experimentally determined functions of $U(z)$, $D_{tz}(z)$ and $D_{ty}(z, t)$ into equation (47.5), or into another appropriate equation for a point source, it is essential to solve them exactly with the aid of calculating machines on behalf of numerous specific conditions of weather and locality.

Atmospheric dispersion of smokes, gases and aerosols emitted by factory smokestacks assumes a special interest from the standpoint of communal hygienics. In this case, the concentration of the air contaminants

near the ground's surface is of importance; for such concentration, we obtain from equations (47.15) and (47.16) the following expressions.

$$n_{z=0} = \frac{2\Phi'}{\sqrt{\pi C_z^2 U_x^2 s}} \exp\left(-\frac{H^2}{C_z^2 x s}\right) \quad (47.26)$$

for a line source with a height H , and

$$n_{z=0} = \frac{2\Phi}{\pi C_y C_z U_x s} \exp\left(-\frac{y^2}{C_y^2 x s} - \frac{H^2}{C_z^2 x s}\right) \quad (47.27)$$

for a point source.

At the same time the values quoted in table 25 should be adopted for C_y and C_z .

BOSANQUET and PEARSON (413) obtained other expressions for concentrations near the surface of the ground. In this, they proceeded from the equation for an on-the-ground line source

$$n = \frac{\Phi'}{b_z U_x} e^{-z/b_z x}, \quad (47.28)$$

where b_z is an empirical coefficient.

This equation, which was developed with the assumption that D_{tz} is proportional to z and that $U = \text{const.}$, is analogous to the equation (47.21) and may be converted into the latter if we assume that $b_z = U^*/U$. Furthermore BOSANQUET and PEARSON proved the "theorem of reciprocity" in that the near-the-ground concentration of a cloud, which is emitted from a line source with a height H proportional to z during D_{tz} is equal to the concentration at a height H of a cloud which is released from an on-the-ground line source. Hence we obtain the equation

$$n_{z=0} = \frac{\Phi'}{b_z U_x} e^{-H/b_z x}. \quad (47.29)$$

The authors offer the following semiempirical equation for a point source:

$$n_{z=0} = \frac{\Phi}{\sqrt{2\pi} b_y b_z U x^2} \exp \left(-\frac{H}{b_z x} - \frac{y^2}{2 b_y^2 x^2} \right), \quad (47.30)$$

where b_y is the coefficient analogous to b_z and characteristic for horizontal diffusion.

In the course of experimental determinations pertinent to the contents of atmospheric impurities emitted from factory smokestacks, deviations in the determined results are usually considerable, and data obtained by way of taking the average are very inaccurate. For this reason, it is rather difficult to state which equations (SUTTON'S, or BOSANQUET'S and PEARSON'S) concur better with a test. Owing to numerous experiments, some authors (414, 415) have arrived at the conclusion that, with a proper selection of coefficients, the equations in question offer an approximately identical degree of concurrence with a test.

While applying these equations, one still has to consider that gases escape from a smokestack with a higher vertical velocity, and their temperature is much higher than that of the surrounding medium. The computation of the smoke stream rising above a smokestack (caused by aforementioned factors) was explained at the beginning of this paragraph; therefore it is not offered here.

It follows from the above-quoted equations that the concentration of gases emitted near the surface of the ground from factory smokestacks is insignificant near the smokestack; then it gradually increases in proportion to a recession from the smokestack, and finally it begins to drop. In order to find a maximal concentration, one must find, by the usual method, a maximum of the function $n(x)_{y=z=0}$. In this way, we obtain from the equation (47.27),

$$x_{\max} = H^{2/3} / C_z^{2/3}, \quad (47.31)$$

$$n_{\max} = 2\Phi C_z / \pi C_y U H^2 e, \quad (47.32)$$

and from the equation (47. 30),

$$x_{\max} = H/2b_z, \quad (47. 33)$$

$$n_{\max} = 4b_z \Phi / \sqrt{2\pi} b_y UH^2 e^2. \quad (47. 34)$$

Inasmuch as $2/s$ is close to 1, then, for the two systems of the equations, the following conclusion, important for practical purposes, results: the distance from a smokestack to a place of maximal air pollution is proportional to the smokestack's height and the maximal concentration of impurities is inversely proportional to the square of the smokestack's height and the wind velocity. We recommend to the reader the monographs of P. ANDREYEV (396) and G. SHELEYKHOVSKIY (395) for further details.

In conclusion, we must mention a few words about the outer form of the aerosolic stream escaping from a smokestack (416). With very low values of D_{tz} , which occur during inversion, a formed stream expands very slowly in a vertical direction. The same stream becomes sharply contoured at a very great distance from a smokestack and, practically speaking, becomes confined within two straight lines formed at an angle of several degrees. Yet, the stream is sharply curved in so far as its horizontal plane, which clearly points out the difference between vertical and horizontal diffusions.

In the presence of a normal adiabatic gradient, the angle of the stream's span is considerably larger. With attentive observation, one can note that, among eddies with a horizontal axis, their spinning is in progress as though the eddies were tangential to the underlying layer of air. Actually, in such a case, turbulence is caused by the friction of the wind against the ground. In the presence of a superadiabatic gradient, the stream breaks up into larger clouds of smoke and rapidly moves up and down. In such a case, turbulence is developed mainly by local convection currents rising from the unevenly heated earth's surface. Figure 69 shows photographs of smoke streams at a wind velocity of $10 \text{ m} \cdot \text{sec}^{-1}$ at a level with the tops of smokestacks, and in the presence of dissimilar values (expressed in $\text{cm}^2 \cdot \text{sec}^{-1}$) of EULER'S coefficient of vertical diffusion.

§ 48. Fall-out of Aerosols from the Atmosphere

As we proceed to the question involving movements of aerosols roughly dispersible in the atmosphere and precipitating with a noticeable

rapidity, we shall take notice of the following: the motion of concentrated clouds, which come from any source, is at first defined by the density and size of the clouds moving as a whole with their gases included (see § 13). Particularly, the aerosols formed by thermal means are maintained at much higher temperature than that of the surrounding air, and for this reason they possess at first a considerable vertical velocity. Added to this, if aerosols emitted from vertical smokestacks are considered, is the velocity already acquired by the aerosol in a smokestack. By the time the temperature of the cloud becomes equalized (as a result of turbulent interspersion) with the temperature of surrounding air, the densities of cloud and air, practically speaking, also balance themselves, and then this type of motion expires. By this time, the influence of gravity appears in a form of precipitation of the particles with relation to the medium. Assuming there is dispersed an isodispersed cloud, as discussed above, a uniform precipitation in the cloud superimposes itself with the rapidity of V_g , which conforms with the rapidity of the particle precipitation in motionless air. A polydispersed cloud may be regarded as consisting of several isodispersed clouds which precipitate with different rapidity.

Of great practical significance is the computation of the rapidity of aerosol particle precipitation (the number of particles precipitating per sec upon one cm^2) upon the earth's surface from a cloud or from an aerosolic stream in motion. Unfortunately, this problem presents great difficulties. In case of comparatively small particles and at not too great a distance x from a source ($xV_g/D \ll H$), one could, without committing a big mistake, adopt the distributions deduced in the preceding paragraph for gaseous impurities and then find, accordingly, a concentration of aerosol near the earth's surface $n_z = 0$. The rapidity of precipitation at any point of the surface would be expressed by the equation

$$I = n_z = 0 V_g. \quad (48.1)$$

If V_g is to be compared with the velocity of vertical expansion of an aerosolic stream (e.g., under experimental conditions stated on page 320 at $V_g \approx 0.1U \approx 50 \text{ cm} \cdot \text{sec}^{-1}$, i.e., at $r \approx 0.1 \text{ mm}$), then such a simplified method of computation is no longer acceptable. The case in question is discussed by JOHNSTONE (417) and his coworkers. Inasmuch as aerosol particles are capable of dropping within a time period t to a distance of $V_g t$ with relation to nonprecipitating particles, then in order to find a distribution of the concentrations in an aerosolic stream, JOHNSTONE substituted z by $z + V_g t = z + V_g x/U$ in the expressions derived for gaseous streams. Thus, it is assumed that the distribution of concentrations in a

precipitating and nonprecipitating stream is alike. But this is only possible under the condition of constancy (independence of z) of wind velocity and that of D_{tz} coefficient. Actually, the dispersion of an aerosolic stream will, in relation to the latter's precipitation, differ all the more from the dispersion of a nonprecipitating stream.

Having introduced the afore-mentioned type of changes in the equations (47.15) and (47.16), JOHNSTONE multiplied the second term of the figure in brackets by the "reflection coefficient" of the aerosol from the ground α . With $\alpha = 1$, the obtained equations conform with a smoke stream reflecting from the ground, whereas with $\alpha = 0$, they conform with a stream precipitating in such a manner as though the ground was, in this case, fully penetrable. JOHNSTONE erroneously assumed that $\alpha = 0$ conforms with a stream absorbed by the earth's surface. We discussed the difference between the two circumstances in § 38, 1. If we proceed from the expression which includes α , which is pertinent to the concentration of aerosol near the ground's surface, and also including equation (48.1), we can work out the equation for a physical balance in a precipitating stream. From the afore-mentioned equation, an expression for computing α may be developed according to which $\alpha = 1$ when $x = 0$, and then, proportionally to the source's remoteness, α decreases and hence passes through 0, where it converges to -1 at $x \rightarrow \infty$. Such an outcome clearly indicates that the coefficient α has no physical meaning whatsoever; also that the equations offered by JOHNSTONE are, in their essence, empirical. We paused at length at this work because, outside of BOSANQUET'S (413) equation brought forward without any substantiations, no other paper has as yet appeared in the literature on the subject matter.

In order to solve the problem accurately (in case of a line source), one must proceed from the differential equation (47.5) where the supplementary term essential in the precipitation's calculation is included

$$U \frac{\partial n}{\partial x} - V_s \frac{\partial n}{\partial z} = \frac{\partial}{\partial z} \left(D_{tz} \frac{\partial n}{\partial z} \right). \quad (48.2)$$

and solve the equation by launching into theoretical or experimental expressions for U and D_{tz} , as a function of z , with the marginal condition of (48.1). However, one can probably obtain an approximate solution of the problem, also sufficiently accurate for practical purposes, which can be effected in a much simpler way.

The case in point involves a cloud formed of very large droplets and observed from a height H by DAVIES (418), who is not interested in the locality where the cloud precipitates upon the ground's surface, but in the

distribution of concentrations during settling, i.e., he is interested in LAGRANGE'S diffusion in the cloud. Proceeding from SUTTON'S theory, DAVIES obtained for this distribution the following equation

$$n(x, y) = \frac{Q \cos \theta}{\pi C^2 L^3} \exp \left(- \frac{y^2 \cos^2 \theta - x^2}{C^2 L^3} \right), \quad (48.3)$$

where x, y , are coordinates on the earth's surface originating in the center of precipitation; where Q is the mass of the cloud; where θ is an inclination angle of the precipitating cloud's trajectory toward the vertical plane $\theta = \arctg (U/V_g)$; where L is the trajectory's length; where C is the average SUTTON'S coefficient.

The experiments with aqueous clouds ($r \approx 0.5$ mm) discharged from heights between 300 - 1500 m at a normal gradient provided, according to DAVIES'S statement, good conformity with the equation (48.3). At the same time, C was defined by means of special experiments.

In conclusion, we shall mention a few words about the vertical distribution of aerosol particles in the atmosphere. Numerous observations indicate that the concentration, as well as the particles' average size decrease, is proportional to the remoteness from the earth's surface. A continuous circular motion of aerosol particles takes place in the atmosphere and, with their precipitation, there is in progress a reverse process of particle formation and dispersion in the atmosphere. At this point, only a very rough discussion may take place about some average permanent conditions and, consequently, about the distribution of particles defined according to elevation. This is expressed by the following equation which is quoted from page 293

$$\ln(n/n_0) = - V_g \int_0^z \frac{dz}{D_{tz}}, \quad (48.4)$$

and thus is combined the distribution of particles of a given size (characterized by velocity V_g) with their elevation in the presence of turbulence in the atmosphere.

Chapter VII

Coagulation of Aerosols

§ 49. Thermal (Brownian) Coagulation of Aerosols with Spherical Particles

The term "coagulation of aerosols" implies a process of adhesion or fusion of aerosolic particles upon contact with one another. The approach of particles, leading to their contact, may be effected either solely by Brownian movement (thermal coagulation), or under the condition when a well-directed movement of particles toward each other superimposes itself upon Brownian movement due to influences of hydrodynamic, electrical, gravitational and other forces. The velocity of a well-directed approach of particles may be so high that, practically speaking, it may determine the rapidity of coagulation which, in such a case, becomes nondependent upon Brownian movement of particles. Thermal coagulation may be regarded as self-imposed. The coagulation of aerosols with charged particles should also be referred to this category. A "forced" coagulation may be regarded in the other remaining instances.

In the theory of coagulation of aerosols, one usually proceeds from the assumption that particles do coagulate, i. e., they adhere or fuse together upon every contact. This supposition (at least on behalf of particles not very large) has its firm theoretical and experimental ground. We shall accept it for the time being without any dispute in order to return to it in § 56. At first, we shall examine the theory of thermal coagulation of aerosols with spherical particles, as developed by M. SMOLUCHOWSKI (419), and we shall begin with the most simple case of isodispersed aerosols.

In the first place, we shall assume that one of the particles is stationary and then we shall determine how often (i. e. per average time interval) other particles, which effect the Brownian movement, will come in contact with the stationary particle under the condition that each contact made leads to coagulation. At the same time, in order to simplify the problem, we shall assume that the shape and size of the stationary particle are maintained during coagulation with other particles. We shall show later that this supposition in the initial stage of coagulation does not lead to any noticeable error. Since spherical particles come in contact as the distance between their nuclei becomes equal to the sum of their radii, then the stationary particle may be substituted by the "absorbent sphere" with a radius of $2r$, while other particles may be substituted by their nuclei. In order to solve

this problem, it is much better to use A. KOLMOGOROV'S and M. LEONTOVICH'S method (see § 37, III). We shall denote by $W^*(\rho, t)$ a probability that the nucleus of a particle, which at a moment $t = 0$ remains at a distance ρ from the center of the absorbent sphere, will come in contact with the latter within a time period t . As we explained in § 37, III, the function of W^* satisfies the equation of EINSTEIN-FOKKER which, in the given case, assumes a form (see the equation/38.25/).

$$\frac{\partial(\rho W^*)}{\partial t} = D \frac{\partial^2(\rho W^*)}{\partial \rho^2}, \quad (49.1)$$

while according to the physical meaning of the function W^* , the latter should also satisfy the conditions of

$$W^*(2r, t) = 1 \text{ and } W^*(\rho, 0) = 0 \text{ at } \rho > 2r. \quad (49.2)$$

The solution of this problem is offered in the expression

$$W^*(\rho, t) = \frac{2r}{\rho} \left[1 - \operatorname{Erf} \left(\frac{\rho - 2r}{2\sqrt{Dt}} \right) \right]. \quad (49.3)$$

If an accountable concentration of aerosol equals n , then, within a time period t , on the average, there will come in contact with a stationary particle

$$d\Phi = nW^*(\rho, t) \cdot 4\pi\rho^2 d\rho \quad (49.4)$$

particles, whose nuclei at the moment $t = 0$ were at the distance $(\rho, \rho + d\rho)$ from the nucleus of the stationary particle. Altogether, with the latter particle, there will come in contact within a time period t

$$\Phi = 4\pi n \int_{2r}^{\infty} W^*(\rho, t) \rho^2 d\rho \quad (49.5)$$

particles. Since the function of $W^*(\rho, t)$ very rapidly decreases proportionally to the increase of ρ , then we could use infinity as the upper limit of the integral instead of the radius of a vessel containing the aerosol. Thus, within the time period $(t, t + dt)$, there will come in contact with the stationary particle

$$\frac{d\Phi}{dt} dt = 4\pi n dt \int_{2r}^{\infty} \frac{\partial W^*}{\partial t} \rho^2 d\rho = 8\pi r D n \left(1 + \frac{2r}{\sqrt{\pi D t}} \right) dt \quad (49.6)$$

particles and within the time period (0, t)

$$\Phi = 8\pi r D n \left(t + \frac{4r\sqrt{t}}{\sqrt{\pi D}} \right) \quad (49.7)$$

particles. It follows from the equation (49.6) that, at $2r/\sqrt{\pi D t} \ll 1$, the average time interval between two effected contacts will be equal to $1/8\pi r D n$. Owing to the term $2r/\sqrt{\pi D t}$ at the beginning of the process, these intervals will be somewhat shorter. In order to find the average magnitude of the first interval t_1 (of $t = 0$ up to the first contact), let us assume in equation (49.7) that $\Phi = 1$. Having solved the quadratic equation for \sqrt{t} , we find that

$$t_1 = \frac{1}{8\pi r D n} \left[1 + 64nr^3 - \sqrt{(64nr^3)^2 + 128nr^3} \right] = \frac{1}{8\pi r D n} \left[1 + 15.3\phi + \sqrt{15.3\phi(2 + 15.3\phi)} \right], \quad (49.8)$$

where $\phi = 4/3 r^3 n$ is a volume of the dispersed phase in one cm^3 of aerosol

Thus, having the values of ϕ of the order 10^{-8} to 10^{-5} , with which the quantitative research of thermal coagulation is usually conducted, the magnitude of the first interval of time, practically speaking, no longer differs from $1/8\pi r D n$, and hence it follows that the \sqrt{t} term included in equation (49.7) may be disregarded

The physical meaning of this term is as follows. In the immediate vicinity of a certain particle at a moment $t = 0$, another particle may appear by chance; consequently the first contact may follow very soon, but with a very small ϕ such incident is not very likely. After the nearest particles become coagulated with the given particle or scatter away from it, the rapidity of coagulation assumes a permanent value

We shall abandon presently the supposition about the immobility of an absorbent sphere. We will find the average magnitude of the square of

UNCLASSIFIED
AD

227876

FOR
MICRO-CARD
CONTROL ONLY

7

OF

Reproduced by

9

Armed Services Technical Information Agency

ARLINGTON HALL STATION; ARLINGTON 12 VIRGINIA

UNCLASSIFIED

"NOTICE: When Government or other drawings, specifications or other data are used for any purpose other than in connection with a definitely related Government procurement operation, the U.S. Government thereby incurs no responsibility, nor any obligation whatsoever; and the fact that the Government may have formulated, furnished, or in any way supplied the said drawings, specifications or other data is not to be regarded by implication or otherwise in any manner licensing the holder or any other person or corporation, or conveying any rights or permission to manufacture, use or sell any patented invention that may in any way be related to

comparative displacement of two particles directionally with the axis x . If, within the time period Δt , the first particle becomes displaced by the distance Δx_1 , and the second particle by the distance Δx_2 , then the comparative displacement is equal to $\Delta x_1 - \Delta x_2$, and the average square of the comparative displacement is

$$\overline{(\Delta x_1 - \Delta x_2)^2} = \overline{(\Delta x_1)^2} + \overline{(\Delta x_2)^2} - 2 \overline{\Delta x_1 \Delta x_2}.$$

Because of the nondependence of the displacements Δx_1 and Δx_2 , $\overline{\Delta x_1 \Delta x_2} = 0$. Therefore

$$\overline{(\Delta x_1 - \Delta x_2)^2} = \overline{(\Delta x_1)^2} + \overline{(\Delta x_2)^2} = 2(D_1 + D_2) \Delta t, \quad (49.9)$$

i.e., the coefficient of relative diffusion of the two particles is equal to the sum of diffusion coefficients of both particles, or, in case of their identical size, it is equal to $2D$. Thus, with every particle there will come in contact in one sec, on the average, $16\pi r D n$ other particles, and altogether, within one sec in one cm^3 of aerosol, there will occur $1/2 n 16\pi r D n = 8\pi r D n^2$ contacts. (The multiplier $1/2$ is necessary; otherwise every contact in this calculation would be accounted for twice.) Each contact reduces the number of individual particles by one unit. It follows, hence, that the basic equation of coagulation is

$$\frac{dn}{dt} = -K_0 n^2. \quad (49.10)$$

This equation appears in integrated form as

$$\frac{1}{n} - \frac{1}{n_0} = K_0 t \quad \text{or} \quad n = \frac{n_0}{1 + K_0 n_0 t}, \quad (49.11)$$

where n_0 is the initial concentration of the particles.

At the same time the coagulation constant K_0 is expressed by the following equation

$$K_0 = 8\pi r D. \quad (49.12)$$

Table 27

Coagulation Constants of Isodispersed Aerosols in the Air

$r, \text{ cm}$	10^{-7}	$2 \cdot 10^{-7}$	$5 \cdot 10^{-7}$	10^{-6}	$2 \cdot 10^{-6}$	$5 \cdot 10^{-6}$	10^{-5}	$2 \cdot 10^{-5}$	$5 \cdot 10^{-5}$	10^{-4}	$2 \cdot 10^{-4}$	$5 \cdot 10^{-4}$	10^{-3}
$K_0 \cdot 10^{10}, \text{ cm}^3 \cdot \text{sec}^{-1}$	323	162	65.9	34.0	18.0	8.57	5.56	4.18	3.44	3.19	3.06	2.99	2.93
$K \cdot 10^{10}, \text{ cm}^3 \cdot \text{sec}^{-1}$	4.5	6	9	12	11	7.2	5.2	4.0	3.37	3.14	3.04	2.97	2.97

M. SMOLUCHOWSKI arrived at this equation by the method shown in § 38, VII, i. e., while examining the distribution of concentrations in an aerosol diffusing toward an absorbent medium.

SMOLUCHOWSKI'S reasoning, in due time provoked objections (420), which it seems to us do not affect the afore-mentioned conclusion (253, 421) with the adaptation of the function W^* .

Substituting D by kTE and obtaining the values for B , which are quoted in table 3 (see page 46), one can find the magnitude of an aerosol coagulation constant K_0 as a function of the particle's radius in the air at 23° and with the atmospheric pressure as shown in table 27.

For highly dispersed aerosols, it is necessary to introduce in the afore-quoted theory a correction for the jump in concentration at the surface of the absorbent medium, and an analogous jump in concentration of vapor at the surface of an evaporating droplet, or a droplet growing in a supersaturated vapor, as this was previously explained by the author of this book (421). The jump in question attains a considerable magnitude when the average apparent length of the aerosol particle's free path l_B (see § 35) becomes commensurable with the radius of an absorbent sphere, i. e., according to table 13 (page 206), at $r \leq 10^{-5} \text{ cm}$. The physical meaning of this correction is as follows: as we indicated in § 35, the adaption of diffusion equations to Brownian movement is admissible only when time intervals are comparatively greater than the particle's relaxation time τ , or even when distances are comparatively greater than l_B . Consequently, a diffusion equation is no longer applicable to a particle's movement in a layer of l_B depth

adjacent to the absorbent wall, and this circumstance is (in case of an absorbent sphere commensurable with the l_B magnitude) essentially repulsed by the kinetics of the diffusible precipitation in the sphere.

The exact interpretation of the expression for the correction as indicated presents considerable difficulties, and we shall confine ourselves to a simplified conclusion which offers a roughly approximated corrective measure. For this reason, it is convenient to apply M. SMOLUCHOWSKI'S method and to examine the particle's diffusion in the absorbent sphere in the presence of an established concentration gradient (see § 38, VII). Let's assume that along the average length free path l_B , the particles depart from the surface of the absorbent sphere and that all directions of their initial movement are of equal expectancy (figure 70). The average distance δ' at which the particles, having passed the path l_B , will appear beyond the sphere's surface will depend upon the ratio of $l_B/2r$. One can readily see that at $l_B \gg 2r$ $\delta' = l_B$ and at $l_B \ll 2r$ $\delta' = l_B/2$. Inasmuch as $OA^2 = 4r^2 + l_B^2 + 4rl_B \cos \theta$, thus taking the average of the magnitude of OA , according to all values of θ , we find that

$$\delta' = \frac{1}{6rl_B} \left\{ (2r + l_B)^3 - (4r^2 + l_B^2)^{3/2} \right\} - 2r. \quad (49.13)$$

The appropriate magnitude of a relative movement of two particles δ is approximately equal to $\sqrt{2} \delta'$.

Let's plot a concentric line with the absorbent sphere's spherical surface, whose radius equals $2r + \delta$. One may consider, that in the layer enclosed between the two surfaces, particles are in motion as though in a vacuum, i. e., they move rectilinearly with the average velocity G (see table 13 on page 206). If the particle concentration at the outer surface is equal to n' , and beyond the absorbent sphere it is equal to n_0 , then at a distance ρ from the center of the sphere the concentration will be expressed similarly to equation (38.34) by the equation

$$n = n_0 - (n_0 - n') \frac{(2r + \delta)}{\rho} \quad (49.14)$$

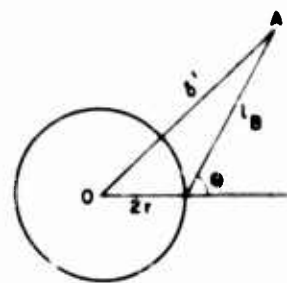


FIG. 70 THEORY OF COAGULATION OF HIGHLY DISPERSED AEROSOLS

Hence

$$\Phi = 4\pi(2r + \delta)^2 2D \frac{dn}{d\rho} \Big|_{\rho = 2r + \delta} = 8\pi D(2r + \delta) (n_0 - n'), \quad (49.15)$$

particles will diffuse per time unit through the outer surface from the outside to the centrum (in the above equation D is already substituted by $2D$). The same number of particles will pass during a stationary cycle of diffusion from this surface toward the absorbent sphere. Generally the same number can also be expressed by the method applicable in the kinetic theory of gases. In case the inner sphere is a droplet of liquid which is in equilibrium with its vapor, then it would evaporate from it per time unit, according to a well known kinetic theory equation and it would also reach the outer sphere, according to the afore-said

$$\Phi_1 = 4\pi(2r)^2 n' \cdot \frac{\sqrt{2}\bar{G}}{4} \quad (49.16)$$

molecules; where n' is a number of molecules in one cm^3 of saturated vapor, where \bar{G} is an average velocity of molecules.

Again as many molecules would pass within the same time from the outer sphere to the centrum. The coefficient $\sqrt{2}$ is used pertinently to the transition from an absolute velocity of particles to a relative one. Thus

$$\Phi = \Phi_1 = 8\pi(2r + \delta) D (n_0 - n') = 4\sqrt{2}\pi r^2 \bar{G} n'. \quad (49.17)$$

Inasmuch as, according to equation (35.4)

$$l_B \bar{G} = \tau \bar{G}^2 = \frac{8kT\tau}{\pi m} = \frac{8kTB}{\pi} = \frac{8}{\pi} D,$$

then the equation (49.17) may be introduced in the form of

$$8\pi(2r + \delta) D (n_0 - n') = 32\sqrt{2}r^2 D n' / l_B$$

Hence, having defined n' as a function of n_0 , and having introduced the resultant expression into equation (49.17), we obtain

$$\Phi = 16\pi r D n_0 \beta, \quad (49.18)$$

where

$$\beta = \frac{1}{\frac{r}{r + \frac{0}{2}} + \frac{\pi l_B}{2\sqrt{2}r}} \approx \frac{1}{\frac{r}{r + \frac{0}{2}} + 1 + \frac{l_B}{r}}, \quad (49.19)$$

or, with $l_B \ll r$,

$$\delta = \sqrt{2} \delta' = \frac{\sqrt{2}}{2} l_B,$$

$$\beta \approx 1 / \left(1 + 0.75 \frac{l_B}{r} \right) \quad (49.20)$$

we obtain the equation, which is analogous to CUNNINGHAM'S equation (see § 8). The actual magnitude of coagulation constant is thus equal to

$$K = K_0 \beta, \quad (49.21)$$

where K_0 is the threshold expression (49.12), which is accurate with regard to large particles. The K values for particles with the density 1, which are quoted in table 17, were computed with the aid of table 13 and with the equations (49.13) and (49.19). We want to emphasize that these figures were obtained as a result of a very simplified conclusion and they don't lay claim to any great exactness. It is obvious from the table that the coagulation constant increases at first in proportion to an intensified aerosol dispersion and, upon attaining its maximal magnitude (approximately with $r = 10^{-6}$), it decreases again. With $l_B \gg r$

$$\beta \approx \frac{1}{\frac{\pi l_B}{2\sqrt{2}r} \left(1 + \frac{4r^2}{\pi l_B^2} \right)} \approx \frac{2\sqrt{2}r}{\pi l_B},$$

and following the substitution of D by $\frac{\pi}{8} l_B \bar{G}$, the equation (49.21) is converted into

$$K = \frac{1}{2} \pi (2r)^2 \sqrt{2} \bar{G} = 2\sqrt{2} \pi r^2 \bar{G}, \quad (49.22)$$

i. e., into the expression for a coagulation constant in connection with the kinetic theory region of procedure, which is calculated in accordance with a well-known equation for the number of molecule collisions in gases. Thus, the correction examined by us expresses a transition from a diffusible to a kinetic theory region of coagulation and as such it resembles (as quoted in § 8) the CUNNINGHAM'S correction, which expresses the transition from the hydrodynamic to the kinetic theory region of particle movement

Now, let's take a glance at how a change would affect the expression for the coagulation constant if we abandon the supposition that every collision between particles leads to their coagulation. We shall denote by α the average effectiveness of collisions, i. e., their share leading to coagulation. The equation (49. 15) will remain unchanged in the reasoning thus brought forward, but the equation (49. 16) will have to be multiplied by the coefficient α . As a result, instead of equation (49. 19), we obtain for β the following expression

$$\beta = 1 / \left(\frac{r}{r + \frac{b}{2}} + 1 + \frac{l_B}{ra} \right). \quad (49. 23)$$

which with $r \gg l_B$ changes into

$$\beta \approx 1 / \left(1 - 0.35 \frac{l_B}{r} + 1.1 \frac{l_B}{ra} \right). \quad (49. 24)$$

With $l_B \gg r$ we obtain for the coagulation constant the following expression

$$K \approx 2\sqrt{2}\pi r^2 G \alpha. \quad (49. 25)$$

It follows hence that the proportionality between the coagulation constant and the effectiveness of collisions is maintained only when $l_B \gg r$, and this is assumed by SMOLUCHOWSKI in his theory of "slow" coagulation (422). Otherwise, K would have comparatively little response to the changes in α . Thus, in the presence of $r = 10^{-4}$ cm during a transition from $\alpha = 1$ (full effectiveness of collisions) to $\alpha = 0.25$, K decreases altogether 5%, which is an approximate measure of exactness in the experimental determination of K . But then, in the presence of $r = 10^{-5}$ cm, the decrease of K by 5% is already reached with $\alpha = 0.60$. Thus, the approximate concurrence of experimentally and theoretically found values of coagulation constants cannot serve as a proof of full effectiveness of collisions among particles.

The physical meaning of the equation (49. 23) comprises this particular; that upon the noneffective collisions, particles go separate ways to a distance of the order δ , but they can immediately and mutually come in contact again. The smaller the proportion of δ/r , the greater is the probability of repeated collisions and, consequently, of coagulations. With ν collisions, the coagulation probability is obviously equal to $1-(1-c)^\nu > a$. Meanwhile, a "multiple" collision is, in SMOLUCHOWSKI'S theory, regarded as a single one and this, in consequence, brings about the incorrect conclusion about the proportionality of K and a .

As we proceed to the coagulation of polydispersed aerosols (423), let us suppose at the beginning that there are two kinds of particles in aerosols: with radii r_1 and r_2 . With one half of the r_1 particles contiguous with r_2 particles, per sec, in one cm^3 of aerosol, and with the concentration of the r_1 and r_2 being equal in one cm^{-3} , $K(r_1, r_2)$ may be named the coagulation constant of r_1 particles with r_2 particles. In this case, the radius of an absorbent sphere is equal to $r_1 + r_2$ and the coefficient of the relative diffusion of particles is equal to $D_1 + D_2$. Thus,¹

$$K(r_1, r_2) = 8\pi \frac{r_1 + r_2}{2} \frac{D_1 + D_2}{2} \beta, \quad (49. 26)$$

where β is the corrective multiplier already referred to. If we repeat the afore-mentioned derivation for the case of two dissimilar particles, we find

$$\beta = 1 / \left(\frac{\bar{r}}{\bar{r} + \frac{\delta_R}{2}} + \frac{4\bar{D}}{G_R \bar{r}} \right) \quad (49. 27)$$

where $\bar{r} = (r_1 + r_2)/2$; $\bar{D} = (D_1 + D_2)/2$; $\delta_R = \sqrt{\delta_1^2 + \delta_2^2}$; $G_R = \sqrt{G_1^2 + G_2^2}$.

The values of $K(r_1 + r_2)$ computed in this way are quoted in table 28.

1. In this case, of course, every collision is calculated only once; therefore it is not necessary to divide the total number of collisions by two. In order to be able to compare the coagulation constants of identical and dissimilar particles while defining $K(r_1, r_2)$, we take here and, later, below, one half of the number of collisions.

Table 28

Coagulation Constants of Particles of Dissimilar Magnitude

$$K(r_1, r_2) \cdot 10^{10}, \text{ cm}^3 \cdot \text{sec}^{-1}$$

r_1, r_2 cm	10^{-7}	$2 \cdot 10^{-7}$	$5 \cdot 10^{-7}$	10^{-6}	$2 \cdot 10^{-6}$	$5 \cdot 10^{-6}$	10^{-5}	$2 \cdot 10^{-5}$	$5 \cdot 10^{-5}$	10^{-4}	$2 \cdot 10^{-4}$	$5 \cdot 10^{-4}$	10^{-3}
10^{-7}	4.5												
$2 \cdot 10^{-7}$	7.5	6											
$5 \cdot 10^{-7}$	30	13	9										
10^{-6}	90	40	15	12									
$2 \cdot 10^{-6}$	300	110	35	17	11								
$5 \cdot 10^{-6}$	1600	550	120	40	15	7.2							
10^{-5}	$5 \cdot 10^3$	1400	270	80	25	8	5	2					
$2 \cdot 10^{-5}$	$13 \cdot 10^3$	4100	600	170	47	11	5	3	4.0				
$5 \cdot 10^{-5}$	$37 \cdot 10^3$	9500	1600	420	115	24	9	4.7	3.4				
10^{-4}	$77 \cdot 10^3$	$20 \cdot 10^3$	3200	840	230	45	16	7.1	3.7	3.2			
$2 \cdot 10^{-4}$	$160 \cdot 10^3$	$40 \cdot 10^3$	6600	1700	450	90	30	12	5	2	3.5	3.0	
$5 \cdot 10^{-4}$	$400 \cdot 10^3$	$100 \cdot 10^3$	$16 \cdot 10^3$	4300	1100	220	72	28	10.3	5.6	3.7	3.0	
10^{-3}	$800 \cdot 10^3$	$200 \cdot 10^3$	$30 \cdot 10^3$	8500	2200	430	140	54	19	9.6	5.5	3	3.0

It is apparent from the table that the coagulation constant rapidly increases proportionally to the increase of the particles' radii. Although during coagulation of large particles with small ones, the size of aggregates obtained, practically speaking, does not differ from the size of the large particles, still, in highly polydispersed aerosols, small particles are rapidly "eaten up" by large ones. Usually, due to this reason, it is impossible to discover in aerosols any particles whose size would be considerably smaller

than the average size, even considering that such particles did exist in the initial stages of an aerosol's life e.g., during the formation of a condensed aerosol out of substances possessing very low vapor pressure. The indicated effects reacts to a well-known degree against the increase of polydispersion of aerosols at the time of coagulation.

Yet, in the initial stages of coagulation of more or less isodispersed aerosols, and especially fogs, the effect of polydispersion is insignificant. Actually, upon fusion of two primary droplets, with radius r , one obtains a "binary" droplet with a radius $r\sqrt[3]{2}$ and upon fusion of three primary droplets, a ternary droplet is obtained with a radius $r\sqrt[3]{3}$, and so on. We shall determine with the aid of equation (49.26) and table 3, what constitutes the coequalities of the coagulation constants of the primary droplets, which include binary, ternary, etc., droplets, assuming that the coagulation constants of the primary particles with one another are equal to 1. (With the sizes of particles indicated in the table, the coefficient β may be regarded as constant.)

Table 29

Comparative Magnitudes of Coagulation Constants of Initial Droplets with Primary (K_{11}), Secondary (K_{12}), etc.

Radius of Initial Droplets, cm	K_{11}	K_{12}	K_{13}	K_{14}	K_{15}
10^{-5}	1	0.96	0.97	0.98	0.99
$3 \cdot 10^{-5}$	1	0.99	1.01	1.03	1.05
10^{-4}	1	1.00	1.02	1.04	1.06

Thus, as shown in table 29, the difference between dispersion constants of fogs, among which research is usually conducted on behalf of kinetics of coagulation, is very insignificant and it does not exceed the experimental error in measurements of the coagulation constants. The origin of the constancy of K lies in this: that among the indicated sizes of particles, a decrease in mobility of one of the droplets is compensated rather accurately by the increase in the absorbent sphere's radius. Such compensation does not occur in highly dispersed aerosols. We also want to mention that the coagulation constants of binary, ternary, etc., particles with one another are already considerably lower than those of the initial particles.

It follows from the above that, in the initial stages of coagulation of isodispersed fogs, when primary droplets still predominate numerically above twins, triplets and so on, the coagulation constant remains practically invariable, just as this was considered in the afore-mentioned conclusion pertinent to the basic equation for coagulation.

As to the coagulation of smokes, the pattern becomes highly complicated. In the first place, it is due to the irregular shapes of primary particles and of aggregates (see § 52). Secondly, it is because we don't have here such direct dependence between the number as well as the size of primary particles in aggregates and between the size of aggregates, as we have in fogs.

Generally, a coagulation constant of the polydispersed aerosols is expressed by the equation

$$K = \int_0^{\infty} \int_0^{\infty} K(r_1, r_2) f(r_1, t) f(r_2, t) dr_1 dr_2, \quad (49.28)$$

where $f(r, t)$ is a function of distribution of particle sizes (see page 13) at time t , and $K(r_1, r_2)$ is the coagulation constant of particles with radii r_1 and r_2 . It is expressed, in the case of coarse aerosols, by the following equation:

$$\begin{aligned} K(r_1, r_2) &= 8\pi \frac{r_1 + r_2}{2} \frac{D_1 + D_2}{2} = \frac{kT}{3\eta} (r_1 + r_2) \left(\frac{1}{r_1} + \frac{1}{r_2} \right) \\ &= \frac{kT}{3\eta} \left(\sqrt{\frac{r_1}{r_2}} + \sqrt{\frac{r_2}{r_1}} \right). \end{aligned} \quad (49.29)$$

If the particles' radii exceed 10^{-5} cm and the particles' mobility is involved, CUNNINGHAM'S equation (8.2) may be applicable; however, as M. TIKHOMIROV, N. TUNITSKIY and I. PETRYANOV (424) pointed out, the knowledge of distribution of aerosol particle sizes is not essential to compute

K if only the average values of \bar{r} , $\left(\frac{1}{\bar{r}}\right)$ and $\left(\frac{1}{\bar{r}^2}\right)$ are known. Actually, in this case

$$K(r_1, r_2) = 8\pi \frac{r_1 + r_2}{2} \frac{D_1 + D_2}{2} = \frac{kT}{3\eta} (r_1 + r_2) \left[\frac{1 + A \frac{1}{r_1}}{r_1} + \frac{1 + A \frac{1}{r_2}}{r_2} \right] \quad (49.30)$$

If we introduce this expression into equation (49.28) and integrate it, we shall obtain

$$K = \frac{2kT}{3\eta} \left[1 + \bar{r} \left(\frac{1}{r} \right) + A \bar{1} \left(\frac{1}{r} \right) + A \bar{r} \left(\frac{1}{r^2} \right) \right] \quad (49.31)$$

The magnitude of

$$\mathcal{Q} = \frac{1 + \bar{r} \left(\frac{1}{r} \right) + A \bar{1} \left(\frac{1}{r} \right) + A \bar{r} \left(\frac{1}{r^2} \right)}{2 \left(1 + A \frac{1}{r} \right)}, \quad (49.32)$$

as such, represents a "polydispersion factor" which is equal to the ratio of the coagulation constant of a polydispersed aerosol with an average particle's radius \bar{r} and also to the ratio of an isodispersed aerosol with the same particle's radius

In working with the basic equation for coagulation of polydispersed systems (49.28) O. TODES (425) arrived at the conclusion that the coagulation constant of coarse fogs (for which one can disregard CUNNINGHAM'S correction in the expression for the diffusion coefficient) asymptotically converges, with $t \gg 1/Kn_0$, or according to equation (49.11), with $n \ll n$ (i.e., in a very highly coagulated aerosol) to the constant which exceeds by approximately 10% the coagulation constant of isodispersed fogs, regardless of the initial distribution of droplet sizes. On behalf of the type of systems which have an initial droplet-mass distribution of $f'(m) = (f'_0/\sigma) \exp(-m/\sigma)$, (σ is a constant), S. PSHENAY-SEVERIN (426) solved the equation (49.28) by the method of consecutive approximations and found that the concentration of droplets in coagulated fogs is 12% lower than if obtained by way of the simplified computation with $K = \text{const}$

As we proceed to compare the theoretical conclusions with the experiment, we take notice, first of all, that such a comparison expediently leads us along the afore-stated (as well as in § 50) reasons to fogs, or to such smokes (e.g., of stearic acid) whose primary particles are of spherical shape and produce round, and to some extent dense, aggregates.

The basic experimental fact established through dozens of experiments is the direct dependence between a reversible concentration of particles and between the time, which coincides with the equation (49.11). That is, the constancy of the coagulation constants in aerosols (also in smokes) is often observed with the particle concentration changing 10 to 30 times in the course of the experiment (see figure 71, obtained from work of B. DERYAGIN and G. VLASENKO /277/). The coagulation constant of aerosols with which experiments are conducted (the initial average magnitude of radius is 0.1 to 0.3 μ), must decrease rather noticeably during the change of the average size of particles by 2 to 3 times (see table 27). Thus the effect of the increase in the average particle's size is apparently compensated for by the simultaneous increase of the polydispersion in a coagulating aerosol. The smaller the initial radius of the particles, the stronger must be the influence of the first effect; thus, actually, in aerosols with a very small gravimetric concentration (1-5 $\text{mg} \cdot \text{m}^{-3}$) and with an average radius of particles 0.5 to 0.7 $\cdot 10^{-5}$ cm, the coagulation constant noticeably decreases proportionally to the progress of the experiment (427).

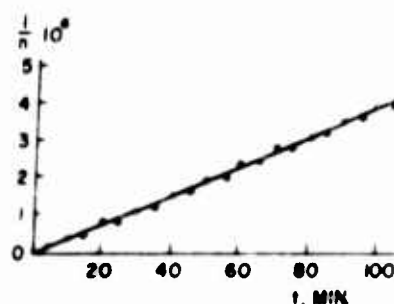


FIG 71 KINETICS OF THERMAL COAGULATION

A careful comparison of experimental and theoretical values of the coagulation constant was effected in the work of M. TIKHOMIROV, N. TUNITSKIY and I. PETRYANOV (424). The experiments were conducted with mineral oil, tricresylphosphate- and sulfuric acid fogs, whose droplets of average radius approximated 0.3 μ . Somewhere near the middle of the experiments, a camera took pictures of the fogs, which were diluted by air in order to discontinue coagulation and thereupon the distribution of particle sizes in the fogs was determined according to the method of the vertical

electrical field. As a result, the magnitudes of \bar{r} , $\left(\frac{1}{\bar{r}}\right)$ and $\left(\frac{1}{\bar{r}^2}\right)$ were

found and, as we mentioned above, the factor of polydispersion was thus computed. In all experiments the value of the factor was found to be higher just by a few per cent (the highest 10%) than one. The theoretical values of coagulation constants, hence computed, were systematically lower by 20 to 30% than the experimental values. For exemplification purposes, we quote below the results of a single experiment with the fog of mineral oil:

$$\bar{r} = 2.63 \cdot 10^{-5} \text{ cm}; \left(\frac{1}{\bar{r}}\right) = 0.378 \cdot 10^5 \text{ cm}^{-1}; \left(\frac{1}{\bar{r}^2}\right) = 0.145 \cdot 10^{10} \text{ cm}^{-2};$$

$$\beta = 1.02; K_{\text{theor}} = 3.95 \cdot 10^{-10} \text{ cm}^3 \cdot \text{sec}^{-1}; K_{\text{exp}} = 4.78 \cdot 10^{-10} \text{ cm}^3 \cdot \text{sec}^{-1}.$$

Although in these experiments, intended to determine the average dimensions, the number of droplets (15-20) estimated by exact measurements is visibly insufficient and, furthermore, there is usually a tendency to select brighter, i.e., larger particles at the time of the visual determination of particle sizes, there is no doubt that all these experimental values exceed the theoretical values.

During the experiments of PATTERSON and CAWOOD (428) with aerosols formed of stearic and oleic acids, and comprising particles of an average initial radius of approximately 15μ , good reproducible value of the coagulation constant was obtained: $5.2 \cdot 10^{-10} \text{ cm}^3 \cdot \text{sec}^{-1}$. Theoretically, and in the absence of a polydispersion effect, approximately $4.6 \cdot 10^{-10}$ should have been obtained at the beginning of the experiments and somewhat less proportionally to the enlargement of particles. This variance can be explained by following the course of theoretical conclusions of O. TODES and PSHENAY-SEVERIN. Another explanation is offered on page 357. It would be highly desirable to conduct measurements of the coagulation constant in extremely homogeneous fogs (6), which can be obtained by way of the seeding method, and when the polydispersion factor is practically equal to 1.

We must still say a few words about LANGSTROTH'S and GILLEPSIE'S (357) work performed on coagulation of aerosols. As defined in their work, the coagulation constant includes a decrease in the calculated concentration of the aerosol, which results from precipitation of particles on the chamber's walls and bottom¹. Inasmuch as the decrease of velocity in the calculated concentration follows at the expense of precipitation and coagulation, which conforms proportionally to n and n^2 , the authors selected at first the coefficients β and K in the equation

$$-\frac{dn}{dt} = \beta n + Kn^2 \quad (49.33)$$

or in the following integrated equation which follows from (49.33)

$$\ln\left(\frac{1}{n} + \frac{K}{\beta}\right) - \ln\left(\frac{1}{n_0} + \frac{K}{\beta}\right) = \beta t \quad (49.34)$$

-
1. Generally speaking, the correction in the particle precipitation is very insignificant if work is conducted in a chamber of several m^3 capacity with particles of the order of tenths of a micron.

whereby, from the two equations, the accurate experimental value for the kinetics of the decrease in n could be found. In this manner, the authors obtained reasonable values for K , although it is obvious that the method is unreliable; it is particularly so (as explained on page 284) considering poly-dispersed aerosols, where the supposition about the linear dependence of $\ln n$ upon t is not realizable. That is why LANGSTROTH and GILLEPSIE subsequently gave up this method and having defined β by way of direct measurements (see page 285), they computed K in accordance with the differences. Yet, K values thus obtained did not remain to any extent constant during the experiment, but they increased or decreased several times and they noticeably exceeded the theoretical values of K , as well as those obtained by other authors. Thus, the data pertinent to coagulation of aerosols as obtained by LANGSTROTH and GILLEPSIE are not very reliable.

In conclusion, we shall briefly pause at the subject of changes in the distribution of particle sizes during coagulation. In conjunction with an initial, isodispersed aerosol, the problem was examined by M. SMOLUCHOWSKI (429) with a supposition that the coagulation constant $K(r_1, r_2)$ maintains the same magnitude among all particles included in a coagulating aerosol. If the initial calculated concentration of an aerosol equals n_0 , then up to the moment in which the average concentration of particles (primary ones and aggregates) attains the magnitude n , the concentration of aggregates (or droplets) formed out of v primary particles will be expressed by the equation

$$n_v = \frac{n^2 (n_0 - n)^{v-1}}{n_0^v} \quad (49.35)$$

Thus, the n_1, n_2, n_3, \dots series, as such, represent a geometrical progression with the denominator $(n_0 - n)/n_0$, whereupon n is expressed as in the equation (49.11). Precisely as M. SMOLUCHOWSKI indicated, with $t \gg 1/Kn_0$, i.e., when an aerosol is very strongly coagulated, the distribution of particle sizes is expressed by the following asymptotic equation (477)

$$n(r) = \frac{25\phi r^2}{4\pi r_m^6} \exp\left(-\frac{5r^3}{3r_m^3}\right), \quad (49.36)$$

where ϕ is a volume of the dispersed phase in one cm^3 of aerosol and

$$r_m = \sqrt[3]{\frac{5K\phi t}{8\pi}} \quad (49.37)$$

is a radius, with which the curve of $r^3 n(r)$ reaches its maximum.

N. TUNITSKIY (430) examined the coagulation of a polydispersed system which included an arbitrary initial distribution of particle sizes. Let's assume that $n(m, t)dm$ is the particle concentration with a mass $(m, m + dm)$ at a time t . The variation of $n(m, t)$ with time will be expressed by the following equation (for simplification purposes we omit t in the right side of the equation)

$$\begin{aligned} \frac{dn(m, t)}{dt} = & \frac{1}{2} \int_0^m K(m, m - m_1) n(m - m_1) dm_1 - \\ & - n(m) \int_0^\infty K(m, m_1) n(m_1) dm_1, \end{aligned} \quad (49.38)$$

where $K(m, m_1)$ is the coagulation constant of particles with a mass m and m_1 . The first term on the right side of the equation expresses an increase in the number of particles with a mass m , since they are formed of much smaller particles; the second term expresses a decrease in the number of aforementioned particles upon their coagulation with other particles. The solution of the equation (49.38) is possible only when K remains constant, i.e., according to the afore-quoted statement, if an aerosol's polydispersion is involved within a small degree. In such a case, the following expression is obtained for the function $n(m, t)$

$$n(m, t) = \frac{1}{2\pi \left(1 + \frac{K}{2} n_0 t\right)^2} \int_0^\infty e^{-im\xi} \frac{\Phi(\xi)}{1 - K\tau\Phi(\xi)} d\xi. \quad (49.39)$$

Here n_0 denotes a general initial concentration of particles and

$$\tau = \frac{t}{2 \left(1 + \frac{K}{2} n_0 t\right)}; \quad \Phi(\xi) = \int_0^\infty e^{im\xi} n(m, 0) dm. \quad (49.40)$$

Thus, knowing the initial distribution of the particle mass $n(m, 0)$, one can find by way of graphic integration the pertinent distribution at any

time, and certainly with avoidance of very extensive efforts. Other methods for the solution of the equation (49.38), with a constant K , are offered by O. TODES and S. PSHENAY-SEVERIN (see pages 342 and 344).

§ 50. Coagulation of Aerosols with Particles of Elongated Shape

As we mentioned already, in order to determine coagulation constants of aerosols with spherical particles, it is necessary to compute the rapidity of the particle diffusion toward an absorbent sphere. In the instance involving nonspherical particles, the absorbent surface assumes another form (431). Precisely as in § 49 the process of diffusion toward an absorbent surface may be regarded as practically stationary at the time when an equation for the coagulation constant is arrived at. At the same time, the equation for general diffusion in space (37.18) is converted to

$$\Delta n = 0 \quad (50.1)$$

(Δ is LAPLACE'S operator), whereupon n must also satisfy the edge conditions: $n = 0$ at absorbent surface and $n = n_0$ at infinitely greater distance from it. The function $\psi = n - n_0$ obviously satisfies the equation $\Delta \psi = 0$, as well as the conditions $\psi = -n_0$ at the absorbent surface and $\psi = 0$ at infinite distance. As follows from the theory of potential, ψ coincides with a field potential formed in the surrounding area by the absorbent surface which possesses conducting properties and is charged up to the potential of n_0 . Thus, the gradient of aerosol concentration near an absorbent surface $(dn/dh)_0$ is equal to the field intensity at the surface and consequently is proportional to the density of electricity σ at the surface, i.e., it depends upon the surface's curvature at a given point. For this reason the concentration gradient, as well as the flow of particles diffusing toward a unit of surface, have maximal values at the poles of elongated ellipsoids and at the equator of oblated spinning ellipsoids.

The full number of particles per unit time in diffusion toward an absorbent surface is equal to

$$\Phi = \int D \left(\frac{dn}{dh} \right)_0 dS, \quad (50.2)$$

where dS is the surface's element; the integral is taken according to the whole surface. Since

$$\left(\frac{dn}{dh} \right)_0 = - \left(\frac{d\psi}{dh} \right)_0 = - 4\pi \sigma,$$

then

$$\Phi = - \int D \cdot 4\pi \sigma dS = 4\pi Dq = 4\pi DC_E n_0, \quad (50.3)$$

where q is the surface's charge with a potential of n_0 .

$C_E = q/n_0$ is the surface's capacity.

Thus, the rapidity of the particle diffusion toward an absorbent surface is proportional to the surface's electrical capacity. We take advantage of the above statement in order to find the coagulation constants of ellipsoidal particles (with a polar semiaxis c and with an equatorial semiaxis a) as well as of spherical particles of the same size. Of course, a particle's radius is equal to $r = \sqrt[3]{a^2 c}$. In this instance, the absorbent surface is a geometrical position of points which is allowed to settle at a distance r from an ellipsoidal particle's surface and which, with the first approximation, can be substituted by an ellipsoid with semiaxes $a + r$ and $c + r$.

The capacity of a spinning ellipsoid is equal (432) to

$$C_E = \sqrt{c^2 - a^2} / \ln \frac{c + \sqrt{c^2 - a^2}}{a}, \quad (50.4)$$

and that of an oblated ellipsoid is equal to

$$C_E = \sqrt{a^2 - c^2} / \arccos \left(\frac{c}{a} \right). \quad (50.5)$$

Using these equations along with the values quoted in table 7 for the dynamic coefficient of shape pertinent to ellipsoidal particles, and then taking the average statistical magnitude of the coefficient for an ellipsoid's dissimilar orientations, one can compute, e.g., that with a 10:1 ratio of axes in ellipsoids, the coagulation constant of elongated particles with spherical particles would be 1.10-times greater than that of spherical particles with each other. In the instance of oblately shaped particles, the ratio is equal to 1.04. We omitted in this conclusion the Brownian spinning of ellipsoidal particles which, it is obvious, would of necessity still magnify the aforementioned ratio. This factor acquires much greater significance if both coagulating particles are elongately shaped. Unfortunately, the theory of coagulation, when taking into account Brownian spinning of particles, presents great mathematical difficulties.

In MUYLLER'S (431) theory of coagulation of particles which are very prominently elongated in one dimension (rod-shaped bacterium), it is assumed that such rods coagulate preeminently by way of their ends (i. e., in

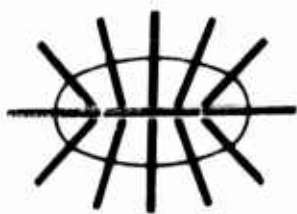


FIG 72 COAGULATION OF ROD-SHAPED PARTICLES

the region of maximal curvature of their absorbent surface), and they move principally lengthwise to their axes, i. e., with the direction of their maximal mobility. In this manner, the diagram of the coagulation was prepared on figure 72. The absorbent surface would, in this case, be a geometric position of the centers of the rods which, with their ends in contact another rod. This surface can be approximately considered as an ellipsoid with its polar axis $4L$ and equatorial axis $2L$; where $2L$ is the length of rod. According to (50.4), the capacity of such an ellipsoid is equal to

$$C_E = \frac{L\sqrt{3}}{\ln(2 + \sqrt{3})} = 1.32 L^1. \quad (50.6)$$

The mobility of the rods, in a direction with their axes, can thus be computed if we consider the rods in question as "ellipsoidal needles," i. e., as very prominently elongated ellipsoids with their axes' ratio equal to β (see equation /12.11/):

$$B = \frac{\ln 2\beta}{4\pi\eta L}. \quad (50.7)$$

In this manner, we obtain the following expression for the coagulation constant of rod-shaped particles

$$K_s = \frac{2\pi \cdot 2 \cdot \ln 2\beta \cdot kT \cdot 1.32L}{4\pi\eta L} = \frac{1.32kT \ln 2\beta}{\eta}, \quad (50.8)$$

and for spherical particles the following expression is obtained

$$K_o = \frac{2\pi 2kT 2r}{6\pi\eta r} = \frac{4kT}{3\eta}. \quad (50.9)$$

1. MUYLLER erroneously indicates $1.49L$.

Consequently, $K_s/K_0 \approx \ln 2\beta$ and with the axes' ratio $\beta = 10$, $K_s/K_0 \approx 3$.

Yet, the diagram of the coagulation of rod-shaped particles, as presented on figure 72, is very far from actuality. In the first place, the mobilities of ellipsoidal needles lengthwise and crosswise to their axes (see equations /12.11/ and /12.12/) differ altogether only twofold¹. In the second place, the values of the concentration gradient at the poles and at the equator of an absorbent ellipsoid, illustrated on figure 72, also differ only twofold. Thus, it is neither possible to talk about considerable predominance of the movement of rods lengthwise to their axes, nor about the rods' coagulation by way of their ends. Actually, particles will come in contact at any of their own points and in truth, with a certain predominance of points positioned closer to the rod ends, i.e., the volume of the absorbent ellipsoid on figure 72 and consequently also the magnitude of the ratio of K_s/K_0 must be reduced. On the other hand, as we already indicated, Brownian spinning must be considered in the theory of coagulation of rod-shaped particles. Therefore, MUYLLER'S conclusions are only of qualitative value.

Experimental data about the coagulation of aerosols with elongated particles are rather scarce. Although considerably elongated, even thread-like aggregates are formed in numerous smokes; yet, generally, this phenomenon is produced by electrical or magnetic forces between particles (see § 52), consequently high values of the coagulation constants in these smokes have no direct connection with the problem presently under discussion.

We shall refer to a strange course of coagulation of aerosols obtained by way of sublimation of dimethylaminoazobenzene (434). In the first place, this fog, which possesses a normal coagulation velocity was formed out of supercooled droplets of the substance. After a while, the droplets began to change into needle-shaped crystals and the coagulation constant increased noticeably.

I. ARTEMOV (30) disclosed in his interesting results that the magnitude of the coagulation constant of ammonium chloride smoke depends to a high degree upon the relative humidity of the gaseous medium: thus,

1. Experimental studies of Brownian movement of rod-shaped bacteria, with the proportion of $\beta = 26$, indicated that Brownian displacement of bacteria lengthwise to the axis is only 30% greater than that crosswise to the axis (433).

with the increase of moisture from 30 to 40%, K decreased from 5 to $3 \cdot 10^{-10} \text{ cm}^3 \cdot \text{sec}^{-1}$. Upon the continued increase of moisture, K began to increase and it attained $6.5 \cdot 10^{-10}$ with 50% humidity and $8 \cdot 10^{-10}$ with 75% humidity.¹

At the same time, microscopic research conducted with precipitating aggregates disclosed that aggregates, in relation to the air humidity, assume a much more rounded shape and compact structure, evidently due to the capillary action of the liquid film which forms on the surface and in the interstices of aggregates. This observation explains the fact of the noticeable scattering of K values (from 4.5 to $9 \cdot 10^{-10} \text{ cm}^3 \cdot \text{sec}^{-1}$) during the experiments of L. RADUSHKEVICH (436). Smokes of NH_4Cl were obtained under quite identical conditions, but the humidity of the air in the chamber was not controlled. At the same time, K values can be well reproduced in stearic acid smokes, where the aggregates preserve rounded shapes, and in carefully set up experiments (428) K values are found within narrow ranges (e.g., 5.0 - $5.3 \cdot 10^{-10} \text{ cm}^3 \cdot \text{sec}^{-1}$).

The decrease of K upon increase in humidity from 30% to 40% is fully explained by the rounding-off effect among ammonium chloride aggregates; yet the subsequent intensification of K upon further increase in humidity is incomprehensible. I. ARTEMOV considered that this phenomenon is caused by the apparent intensification of the sedimentation effect among damp particles, although at a 50% humidity the enlargement of the particles of ammonium chloride cannot be considerable and it should not have caused any increase, but rather a small decrease in the coagulation constant (see table 27).

I ARTEMOV observed a considerable decrease in the coagulation constant in the presence of vapor of the solutions, which favors the formation of round aggregates, and also among smokes of anthraquinone and nitrosodimethylaniline. However, in the presence of ammonia, which favors the formation of thread-like aggregates out of particles of nitrosodimethylaniline, the increase in K was almost 80%. Ammonia also speeds up coagulation of stearic acid smokes, because it simultaneously forms needle-like crystals of ammonium stearate (437).

1 The fact of increased stability in ammonium chloride smokes in the presence of low humidity in the air and the fact of decreased stability in the presence of high humidity were already noted previously by K. SAMOKHVALOV and O. KOZHUKHOVA (435).

§ 51. Thermal Coagulation of Aerosols with Charged Particles.

Influence of Molecular Forces upon Rapidity of Coagulation

We shall find the magnitude of the coagulation constant of spherical particles of identical size, with q_1 and q_2 charges (with identical or with opposite signs /438/. We shall indicate by $F(\rho)$ the electrostatic force acting between particles, where ρ is the distance between their centers. In this instance we have a problem of particle diffusion toward an absorbent sphere in the presence of a directed radial velocity $V = BF$, super-imposed upon Brownian movement. Considering, as we did before, that the diffusion process is stationary, i. e., assuming in the equation (37.19) that $\partial n / \partial t = 0$, we obtain

$$D\Delta n = \text{div}(Vn) = B \text{div}(Fn) \quad (51.1)$$

Due to spherical symmetry, the equation on behalf of polar coordinates assumes the form

$$D \frac{1}{\rho^2} \frac{d}{d\rho} \left(\rho^2 \frac{dn}{d\rho} \right) = B \frac{1}{\rho^2} \frac{d}{d\rho} \left(\rho^2 Fn \right)$$

or

$$\frac{d}{d\rho} \left(D\rho^2 \frac{dn}{d\rho} - B\rho^2 Fn \right) = 0, \quad (51.2)$$

and it follows hence, that

$$4\pi \left(D\rho^2 \frac{dn}{d\rho} - B\rho^2 Fn \right) = \text{const} = \Phi. \quad (51.3)$$

Inasmuch as the first term in the left part of the equation (51.3) is equal to the number of particles which pass, due to diffusion, per unit time, through any spherical surface concentric with an absorbent sphere and, inasmuch as the second term denotes a number of particles which pass through the same surface due to a directed movement, then the sum of both yields the velocity of the particles precipitating upon the absorbent sphere Φ .

The function of $n(\rho)$ must satisfy the threshold condition of $n = n_0$ at $\rho = \infty$ and that of $n = 0$ with $n = 2r$. Following integration of the equation (51.3), when the first of the two conditions is maintained, we obtain

$$n(\rho) = \exp\left(\frac{B}{D} \int_{\infty}^{\rho} F(\rho) d\rho\right) \left[n_0 + \frac{\Phi}{4\pi D} \int_{\infty}^{\rho} \frac{1}{\rho^2} \exp\left(-\frac{B}{D} \int_{\infty}^{\rho} F(\rho) d\rho\right) d\rho \right] \quad (51.4)$$

The result of the second condition is

$$n_0 = \frac{\Phi}{4\pi D} \int_{\infty}^{2r} \frac{1}{\rho^2} \exp\left(-\frac{B}{D} \int_{\infty}^{\rho} F(\rho) d\rho\right) d\rho = 0. \quad (51.5)$$

Having substituted B/D by $1/kT$ and having designated the potential of electrostatic force $\int_{\rho}^{\infty} F(\rho) d\rho$ by $\psi(\rho)$ we obtain

$$\Phi = \frac{4\pi D n_0}{\int_{2r}^{\infty} \frac{1}{\rho^2} \exp\left[\frac{\psi(\rho)}{kT}\right] d\rho} \quad (51.6)$$

For noncharged particles we have

$$\Phi_0 = 8\pi D r n_0. \quad (51.7)$$

If we introduce the new variable $x = 2r/\rho$, we obtain for the ratios of the coagulation constants of charged and noncharged particles $\beta = \Phi/\Phi_0$ the following expression

$$\beta = 1 / \int_0^1 \exp\left[\frac{\psi(2r/x)}{kT}\right] dx. \quad (51.8)$$

At the same time, if $\psi > 0$ (similar charges, repulsion) $\beta < 1$, one obtains a decrease in the coagulation constant and if $\psi < 0$ (opposite charges, attraction), one obtains an increase in the coagulation constant.

If the particles act as conductors of electricity (see page 80), the force $F(\rho)$ is expressed by the series (439)

$$F(\rho) = \left(1 + 15 \frac{r^6}{\rho^6} + \dots\right) \frac{q_1 q_2}{\rho^2} - \left(2 \frac{r^3}{\rho^3} + 3 \frac{r^5}{\rho^5} + 4 \frac{r^7}{\rho^7} + \dots\right) \left(\frac{q_1^2 + q_2^2}{\rho^2}\right). \quad (51.9)$$

The first term of this series ($q_1 q_2 / \rho^2$) represents a force which is effective between free charges, and the remaining series represents an induction force. If we assume that $q_1 = q$ and $q_2 = sq$ ($s/ > 1$; $s > 0$ in the case of repulsion and $s < 0$ in the case of attraction), then we obtain for the potential of ψ the following expression

$$\psi \left(\frac{2r}{x}\right) = \frac{q^2}{2r} \left[s \left(x + \frac{15}{448} x^7 + \dots \right) - (1 + s^2) \left(\frac{x^4}{16} + \frac{x^6}{64} + \frac{x^8}{256} + \dots \right) \right]. \quad (51.10)$$

The relative values of the first term and of the remaining terms of the series depend during computation of the coefficient β upon the magnitude of the ratio $\lambda = q^2 / 2rkT$ of the electrical and kinetic energies of the particles coming in contact with q charges. Since, in the most important case, it would be that of the fixed charging of an aerosol in a bipolar ionic atmosphere (see page 141), the distribution of the particle charges would be expressed, as we previously indicated, by the following BOLTZMAN equation

$$n(q) = \frac{n_0}{\sqrt{2rkT}} \exp \left[- q^2 / 2rkT \right], \quad (51.11)$$

where n_0 is the general concentration of particles; where $n(q)dq$ is the concentration of particles with the charge ($q, q + dq$).

It follows, hence, that the average magnitude $\bar{\lambda} = q^2 / 2rkT$ equals $1/2$. One can compute, with the aid of graphic integration, that in the presence of the earlier value of λ and in the event of equal and analogous charges of particles ($s = 1$), the error (as admitted in repulsion of induction terms in /51.10/ while computing β) would comprise only 1.4%. With $s = 2$, the error equals 4.3%. The error is still smaller in the presence of opposite charges. It follows, hence, that in the discussed case of a bipolar charge, one can, without committing a serious error, confine himself within the range (51.9) of the first (COULOMB'S) term only. At the same time, the following simple equation can be obtained for β

$$\beta = \frac{\lambda_{12}}{e^{\lambda_{12}} - 1} \quad (51.12)$$

in case of repulsion and

$$\beta = \frac{\lambda_{12}}{1 - e^{-\lambda_{12}}} \quad (51.13)$$

in case of attraction. Thus

$$\lambda_{12} = \frac{q_1 q_2}{2rkT}. \quad (51.14)$$

If the bipolar charge is symmetrical, as happens in some measure in the majority of cases, i.e., if every particle with a q_1 charge matches a particle with a $-q_1$ charge, then the change in the coagulation velocity caused by charging may be evaluated in the following manner.

The value of the coefficient β in the coagulation of two particles with q_2 and q_1 charges, and consequently with q_2 and $-q_1$ charges, is given in the equation (51.12) and (51.13). In the event the aerosol is charged in a bipolar ionic atmosphere, and supposing, according to the afore-said, that $\bar{\lambda} = 1/2$, we find the value 1.271 for β in the case of opposite charges and the value 0.770 in the case of identical charges, i.e., the particles with opposite charges coagulate noticeably more rapidly and those with identical charges coagulate noticeably slower than neutral particles. Yet, the average arithmetic value equals here 1.02, i.e., the average effect of charging is very insignificant and it can hardly be discovered by experimental means. Actually, as N. FUKS and I. PETRYANOV (166) have determined by way of TYNDALL'S measurements, it is impossible to discover the difference during the progress of coagulation between charged (by ultraviolet rays) and noncharged oil sprays. WHYTLAW-GRAY and PATTERSON (440) obtained the same results.

GILLEPSIE (360) studied coagulation of SiO_2 dusts possessing relatively higher bipolar charges (see page 286), and discovered that the coagulation constant of such dusts becomes considerably increased with the increase in the average charge of the particles.

As we proceed to the coagulation of unipolar charged aerosols, we note first of all that, due to electrostatic dispersion (see page 129), the velocity of their coagulation cannot be determined according to the decrease in the particle concentration, but exclusively according to the increase in the average size of particles, and for this reason the discussed measurement

is rather complicated. It can be substantiated that the rapidity of decrease in the particle concentration in unipolar charged aerosols always increases (438), i. e., during the joint action of coagulation and electrostatic dispersion. Consequently, no discussion can take place about aerosols being stabilized by way of unipolar charges. As regards the coagulation of particles, generally speaking, the action is retarded in the presence of unipolar charging and it can be practically discontinued with sufficiently high intensity of charging. Yet, as is apparent from the equation (51.10), during a sufficiently high proportion of s charges, the potential of ψ may assume a negative value due to induction forces, i. e., the repulsion may change into attraction even in the presence of identical charges. The influence of induction forces is also stimulated with increased proportion of the particle sizes. Consequently, individual and highly charged particles, or very large particles, may be noticeably coagulated even in unipolar charged aerosols.

At one time a theory was introduced pertinent to stabilization of atmospheric clouds by way of unipolar charges (441). According to this opinion, precipitation comes only from such clouds whose droplets are either slightly charged or possess charges of both signs. The insolvency of the above theory, which identifies the role of electrical forces in dispersible systems as being associated with liquid and gaseous media, follows even from the fact that, in a calculated low concentration of atmospheric clouds (of the order 10^3 to 10^4 cm^{-3}), the rapidity of thermal coagulation in clouds is generally meaninglessly low. Furthermore, as observations indicate, droplets in clouds always possess charges of both signs, although one of them may, to some extent, be prevalent.

The afore-discussed method of computation of the coagulation constant in the presence of forces acting at a distance between particles was introduced by M. TIKHOMIROV, N. TUNITSKIY and I. PETRYANOV (424) in order to clarify the problem of the influence of molecular forces upon the velocity of coagulation in aerosols. Thus, if we take (for the potential of molecular forces which are acting between elemental volumes of substance dv_1 and dv_2 , as the function of the distance between them ρ) the well known equation

$$d\psi = -Q \frac{dv_1 dv_2}{\rho^6}, \quad (51.15)$$

then, for flat parallel flakes positioned at a distance h from each other, the potential (per cm^2) will be expressed by the following equation (442)

$$\psi(h) = -\frac{\pi Q}{12h^2}, \quad (51.16)$$

and for two identical spherical particles with a radius r the following equation will be applicable

$$\psi(\rho) = \frac{\pi^2 Q}{6} \left\{ \frac{2r^2}{\rho^2} + \frac{2r^2}{\rho^2 - 4r^2} + \ln \left(1 - \frac{4r^2}{\rho^2} \right) \right\}. \quad (51.17)$$

If we rationalize the above, we find that the increase in the ratios of the coagulation constant β , caused by molecular forces, is expressed according to the previous equation (51.8), in which the expression obtained for the function ψ is replaced, i.e., by the following equation

$$\beta = 1 / \int_0^1 \exp \left[- \frac{\pi^2 Q f(x)}{6kT} \right] dx, \quad (51.18)$$

where

$$f(x) = \left[\frac{x^2}{2} + \frac{x^2}{2(1 - x^2)} + \ln(1 - x^2) \right]. \quad (51.19)$$

The above equations indicate that the effect of molecular forces is not dependent upon particle size, but merely upon the magnitude of Q/kT . Up to the very last moment, no reliable data were available pertinent to the magnitude of the Q constant. BRADLEY (443) conducted measurements of the cohesive force between quartz globules in a vacuum and obtained the value of $Q = 2 - 5 \cdot 10^{-13}$ erg. From this, with the aid of graphic integration, one can compute that $\beta = 1.35 - 1.5$. M. TIKHOMIROV, N. TUNITSKIY and I. PETRYANOV, using $Q = 6 \cdot 10^{-14}$, for droplets of organic liquids (based on the connection between Q and surface tension) discovered that $\beta = 1.18$. Hence, the authors concluded that the excess of the experimental values of the coagulation constant as compared with the theoretical values (see § 49) is explained by the action of molecular forces.

The magnitude of the effect of molecular forces can be evaluated more reliably if one proceeds from B. DERYAGIN'S and I. ABRIKOSOVA'S (444) direct measurements of molecular forces, which are effective between a quartz lamina and a lens, as the function of distance between the two. It follows from these experiments that, in the equation (51.16), with $h > 5 \cdot 10^{-6}$ cm, the power of the exponent of h should be increased approximately to 3; likewise, hence, it follows that in the expression (51.15)

the exponent of ρ is approximately 7. Because of the exponent of 7, it is rather difficult to derive equations analogous to equations (51.16) and (51.17), so, in order to evaluate the magnitude of the unknown effect, we shall retain the exponent 6, but we will compute Q with dissimilar values of h and according to the equation (51.16), also using the experimental data of B. DERYAGIN and I. ABRIKOSOVA. At the same time, of course, Q will no longer remain a constant magnitude (table 30).

Table 30
Molecular Forces Effective Between Quartz Particles

h , cm	10^{-5}	$2 \cdot 10^{-5}$	$3 \cdot 10^{-5}$
$\psi(h)$, erg·cm ⁻²	$2.7 \cdot 10^{-5}$	$0.6 \cdot 10^{-5}$	$0.2 \cdot 10^{-5}$
Q , erg	$1.1 \cdot 10^{-14}$	$0.9 \cdot 10^{-14}$	$0.7 \cdot 10^{-14}$

Thus, the Q value for quartz is virtually smaller by one order if compared with the value assumed by M. TIKHOMIROV, N. TUNITSKIY and I. PETRYANOV; it is also apparent, that the increase of coagulation constant in aerosols resulting from molecular forces does not exceed 1% to 2%.

The influence of particle charges upon "kinematic" coagulation of aerosols is discussed in §54.

§ 52. Coagulation of Aerosols in an Electrical Field.

"Directed" Coagulation

As we proceed to a forced coagulation of aerosols influenced by external action, we shall begin with coagulation in electrical and sonic fields. Regardless of the dissimilar physical nature of the influences, the two types of coagulation have much in common, owing to the well-known analogy between the properties of electrical and hydrodynamic potentials

The electrical field, with its intensity E , actuates electric dipoles with a momentum $P = Er^3$ among spherical conducting (see page 80) particles, with a radius r , occurring in the field. The interaction force between two such dipoles, whose centers remain at a distance ρ from each other, is expressed, at $\rho \gg r$, by the following equations (23.4) and (23.5) for hydrodynamic forces, but with reverse signs:

$$F_r = - \frac{3E^2 r^6}{\rho^4} \left(\frac{3}{2} \cos 2\theta + \frac{1}{2} \right), \quad (52.1)$$

$$F_T = - \frac{3E^2 r^6}{\rho^4} \sin 2\theta, \quad (52.2)$$

where θ is an angle between the field's direction and the line of the particle centers. Thus, the field of force between polarized particles assumes a form similar to one illustrated on figure 23: particles attract one another, if positioned lengthwise to a field's direction and they repel one another if positioned perpendicularly to a field. The potential of these forces is expressed by the equation

$$\psi(\rho) = - \frac{E^2 r^6}{\rho^3} \left(\frac{3}{2} \cos 2\theta + \frac{1}{2} \right) = - \frac{E^2 r^6}{\rho^3} (2 \cos^2 \theta - \sin^2 \theta) \quad (52.3)$$

which infers that, in contrast to the afore-discussed examples, the potential in question depends not only upon distance between particles, but also upon the direction of the line of particle centers.

Secondary induction forces, not accounted for in these equations, are developed by mutual polarization of particles upon a dipole's approach. Exact expressions for these forces are available in a form of complicated trigonometric series (445). Their utilization in defining the influence of secondary induction forces upon the velocity of coagulation requires such enormous calculation effort that we had to abstain from it. However, an estimation of this influence can be effected by other means (see below). To characterize a magnitude of secondary induction forces we shall only indicate that, upon contact of particles ($\rho = 2r$), the potential of interaction attains the magnitude of

$$\psi(2r) = - E^2 r^3 (0.25 \cos^2 \theta - 0.125 \sin^2 \theta) \quad (52.4)$$

according to the approximated equation (52.3) and

$$\psi(2r) = - E^2 r^3 (1.404 \cos^2 \theta - 0.099 \sin^2 \theta) \quad (52.5)$$

in accordance with the exact equation.

A precise solution of the problem of particle diffusion toward an absorbent sphere within the field of force, which is expressed by the equation (52.3) and which does not retain spherical symmetry, presents great

difficulties. In order to estimate the magnitude of the particle polarization effect by the velocity of coagulation, we omit diffusion and the directed particle movement in a tangential direction, i. e., we will assume that the particles move to an absorbent sphere in a radial direction.

However, we intend to determine, first of all, the velocity of coagulation of a polarized aerosol in the absence of diffusion, i. e., in the absence of the thermal movement of particles. If two particles are in a reciprocal position, suitable to a maximal attraction ($\theta = 0$), they move toward each other with the velocity

$$v = \frac{6E_r^6 B}{\rho^4} \approx \frac{E_r^5}{\pi \eta \rho^4}. \quad (52.6)$$

Thus, a differential equation for the relative movement of particles assumes a form

$$-\frac{d\rho}{dt} = 2v = \frac{2E_r^5}{\pi r \rho^4}. \quad (52.7)$$

If we again integrate the above, we find that particles positioned at a time $t = 0$ and at a distance ρ_0 from each other will come in contact within

$$t_0 = \frac{\pi \eta \rho_0^5}{10 E_r^5} \approx \frac{5 \cdot 10^{-4} \rho_0^5}{E_r^5} \quad (52.8)$$

seconds. Considering that the calculated concentrations are of the order $10^6 - 10^7 \text{ cm}^{-3}$ and as such they facilitate experimental studies of the coagulation course of aerosols, the average distance between particles would equal $0.5 - 1 \cdot 10^{-2} \text{ cm}$ and we presume that $\rho = 0.5 \cdot 10^{-2} \text{ cm}$.

Furthermore, as is explained below, a considerable acceleration of thermal coagulation due to the particle polarization is already attained with $Er^{3/2} = 4 \cdot 10^{-6}$, i. e., it is attained for $r = 10^{-4}$ to 10^{-5} cm in the presence of $Er^{5/2} = 4 \cdot 10^{-10}$ to $4 \cdot 10^{-11}$. The same particles, approaching each other up to a distance of $0.5 \cdot 10^{-3} \text{ cm}$ as a result of the influence of any factor, will come in contact within 0.1 to 10 seconds. Thus, it is clear that the mechanism of coagulation in an electrical field admits the approach of particles under the influence of diffusion at such a distance at which electrical forces attain a noticeable magnitude, whereupon the particle movement assumes a directed tendency. This reasoning also pertains in

equal measure to coagulation of charged particles, as we discussed in the preceding paragraph.

As we return to the problem of radial movement of particles toward an absorbent sphere within a field of force (52.3), we utilize again equation (51.8) for defining the coefficient β , to be equal to the ratio of the velocity of particles precipitation in an absorbent sphere, in the presence as well as in the absence of electrical forces, at which time, in this case, β will also depend upon the angle θ , namely

$$\beta = 1 / \int_0^1 \exp \left[- \frac{E^2 r^3 x^3 \left(\cos^2 \theta - \frac{1}{2} \sin^2 \theta \right)}{4kT} \right] dx = 1 / \int_0^1 e^{-a^3 x^3} dx =$$

$$a / \int_0^a e^{-y^3} dy, \quad (52.9)$$

where

$$a = \left(\frac{E^2 r^3}{4kT} \right)^{1/3} \left(\cos^2 \theta - \frac{1}{2} \sin^2 \theta \right)^{1/3} = a_1^{1/3} \left(\cos^2 \theta - \frac{1}{2} \sin^2 \theta \right)^{1/3}. \quad (52.10)$$

In order to determine the influence of the overall effect of the particle polarization upon the velocity of the particles precipitation in an absorbent sphere, it is necessary to find the average value of β at the sphere's surface

$$\bar{\beta} = \frac{1}{2} \int_0^\pi \beta \sin \theta d\theta = \int_0^1 \beta d \cos \theta. \quad (52.11)$$

We found by way of graphic integration, the following $\bar{\beta}$ values as the function of a nondimensional magnitude of a_1 (table 31).

Table 31
Influence of an Electrical Field upon the Rapidity
of Coagulation in Fogs

α_1	1	2	3	5	10	20	
$\bar{\beta}$	1.0	0.95	1.07	1.7	3.4	6.8	Additional $\bar{\beta} \approx 1/3 \alpha_1$.

Thus, with $\alpha_1 < 3$, the decrease in rapidity of precipitation in the repulsion zone ($\cos^2 \theta - 1/2 \sin^2 \theta < 0$) compensates almost exactly to the increase in the velocity of precipitation in the attraction zone. If $\alpha_1 = 5$, precipitation in the repulsion zone ends completely, but the velocity of precipitation in the attraction zone increases so much that it attains subsequently an overall effect. The value of α_1 corresponds in the air to the value of $Er^{3/2} \approx 4 \cdot 10^{-6}$, i. e., pertinent to particles with a radius 10^{-4} cm and in the presence of field intensity of $1400 \text{ volts} \cdot \text{cm}^{-1}$, whereas for particles with $r = 10^{-5}$ cm, it corresponds to $40,000 \text{ volts} \cdot \text{cm}^{-1}$ of field intensity.

The influence of secondary induction forces upon the effect under discussion can be evaluated in the following manner. Since the potential of the discussed forces is proportional in the first approximation to ρ^{-6} , so we introduce in the equation (52.3) the supplementary term of $\frac{kE^2 r^9}{\rho^6}$ and at the same time we assign to coefficient k such a value that, upon the effected contact of particles ($\rho = 2r$) in the presence of $\theta = 0$ and according to equation (52.5), the potential could assume the correct value of $\psi = -1.404 E^2 r^3$. Thereupon, having arrived at a corrected expression for $\psi(\rho)$, one can obtain β . It was found that the maximal correction to β_1 attainable approximately with $\alpha_1 = 1$ thus computed, comprises about 25%; in proportion to the remoteness of α_1 from 1, the discussed correction rapidly leads to zero. Thus, the correction can be unconditionally disregarded in our rough computations.

It appears from the afore-quoted figures that a noticeable acceleration of coagulation in fogs can only be attained in the presence of a very great force in the field. Actually, no appreciable acceleration of coagulation in oil fogs has been observed in any field of the order of $200 \text{ volts} \cdot \text{cm}^{-1}$ (446). On the other hand, N. FUKS and I. PETRYANOV (166) report that rapid coagulation in an oil fog, which is charged unipolarly in a corona discharge and the formation of giant drops, which consist of several

thousands of primary droplets, is in larger measure produced by intensive polarization of droplets near the corona's conductor, where the field force is very great. Naturally, the same coagulation also takes place in electrical filters and it contributes greatly to their effectiveness. The polarizing coagulation of droplets can also be of great significance in thunderclouds (447), where the intensity in the electrical field attained the magnitude order of $1000 \text{ volts cm}^{-1}$.

Coagulations in aerosols with solid particles assume a unique form in an electrical field. A "twin," resulting from coagulation of two primary particles, directs itself with its lengthwise axis parallel to the field (see §43) and in this position its dipole moment is considerably greater than that among primary particles. The coagulation of a twin with other particles progresses mainly at the twin's ends and thus a twin grows in length. A dipole moment of such a linear aggregate may be computed approximately, if we regard it as an elongated ellipsoid in spinning. As the equation (43.12) (in which $\theta = 0$ should be introduced) and table 21 indicate, a dipole moment of such ellipsoid is approximately proportional to $v\beta$; where v is ellipsoid's volume; where β is the proportion to its axis. Inasmuch as in the given case both v and β are proportional to the number of primary particles in an aggregate n , then the dipole moment of the aggregate is proportional to n^2 and the magnitude of the interaction's potential of two suchlike aggregates is n^4 . Thus, in the given case, the coagulation constant must increase very rapidly in proportion to the course in progress and at the same time the aggregates assume a shape of threads or that of little chains (figure 73, fumes of Fe_2O_3 /448/).

It is a fact well known from experiments that aggregates of the described shape actually do form during coagulation of smokes in any strong electrical field, and that the rapidity of coagulation increases considerably (354, 446, 449). Thus, the rapidity of coagulation of ammonium chloride smoke increases 10^4 times in a field with intensity $5000 \text{ volts cm}^{-1}$; a noticeable effect can already be observed with $E > 200 \text{ volts cm}^{-1}$. This type of coagulation is called "oriented" coagulation. It occurs perhaps with the formation of smokes by way of sublimation of substance in a voltaic arc. Facts point out that almost all smokes obtained in such a way (and particularly the smokes of magnesium oxide) consist mainly of thread-like aggregates (450, 451), while smokes of MgO obtained in burning a ribbon of magnesium contain none (451). I. ARTEMOV (30) noted that directed coagulation of particles in an electrical field can be observed directly by means of an ultramicroscope.

Analogous phenomena are observed during coagulation of ferromagnetic particles (e.g., those of iron smoke obtained from $\text{Fe}(\text{CO})_5$) in a magnetic field (452).

A directed coagulation with a formation of linear aggregates may also occur in the absence of an external electrical or magnetic field if the particles be considered as constant electrical dipoles or magnetic poles (434, 453). In such a case they do not orient themselves in a definite way in space (if we disregard a mild orienting action of the earth's magnetism). As they approach one another, a well-known mutual orientation of dipoles occurs, due to which a positive side of one particle comes in contact with a negative side of another particle. This also leads to the development of line aggregates. Constant electrical dipoles may emerge during the cooling period of crystalline particles of pyroelectric substances in smokes obtained by a thermic method. A smoke of aminobenzene, which possesses highly indicative pyroelectric properties, may serve as a typical example (434). Smokes obtained by sublimation of this substance coagulate 10 to 100 times more rapidly than normal aerosols and, at the same time, thread-like aggregates are formed which grow rapidly in length. The admixture of 10% of paraffin to aminobenzene restrains the pyroelectric properties of the latter; smokes obtained of such mixture coagulate with a normal rapidity and cease to produce line aggregates. Pyroelectric properties may dissipate themselves during sublimation of a substance if the latter is, to a small extent, affected by decomposition. For this reason, directed coagulation is not observed in smokes of certain pyroelectric substances (e. g., of resorcin).

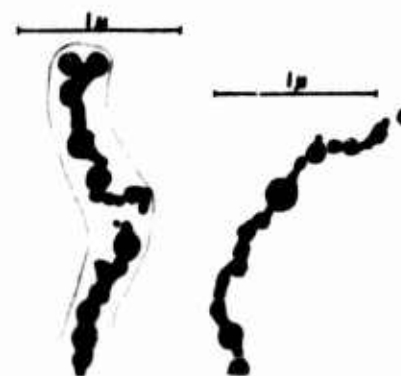


FIG. 73 AGGREGATES IN Fe_2O_3 SMOKE

Smokes of Fe and Ni with particles which possess constant magnetic poles are obtained by heating vapors of carbonyl compounds of the involved metals in the absence of oxygen (453). Below the CURIE point (360° for Ni, 770° for Fe)¹ these smokes do coagulate and form thread-like aggregates; above the CURIE point, they produce rounded aggregates, or very short little chains. Thread-like aggregates orient themselves in a magnetic field and, as the field reverses, they turn by 180° . It is apparent from this that orientation is not caused by induced, but by the constant magnetism of particles. Finally one question remains open: what is the origin of this magnetism? Whereas smokes possessing analogous properties can also be obtained with particles which are composed of crystalline particles of ferric oxide, yet particles composed of amorphous ferric oxide are not ferromagnetic and they do not produce line aggregates in the absence of an outer field.

1. CURIE point is the temperature, at which a substance's ferromagnetic properties become extinct.

A tendency toward the formation of line aggregates is also observed among such smokes whose particles cannot possess any constant electrical nor magnetic moment (see photograph of Al smokes in figure 8). In such instances, the probable reason appears to be a contact polarization of particles, or their free charges (454). According to observation of DALLAVALLE (445), more or less rounded aggregates are formed during coagulation of NH_4Cl smoke possessing neutral particles, whereas, in the case of highly charged particles, line aggregates are formed, although the average number of primary particles in the aggregates and the velocity of coagulation are, in both instances, approximately the same.

§ 53. Coagulation of Aerosols under the Influence of Ultrasonic Oscillations

The phenomenon of aerosol coagulation by means of ultrasonic waves was already described during the early stages of examining the properties of ultrasonics (456). Usually, this phenomenon is studied with the aid of closed glass tubes, filled with an aerosol, in which the standing ultrasonic waves are produced (131, 135). In the presence of a satisfactory frequency and intensity of oscillation, the aerosol coagulates very rapidly (within several minutes, or even seconds). Ring-shaped deposits, formed on the tube's walls, are deposited opposite the antinodes of the waves. Thereupon, as a rule, the aerosol remaining in the tube is of a very low concentration, containing the smallest particles remaining from the initial aerosol; however, the latter coagulates very slowly with the continued action of ultrasonics.

The theory of ultrasonic coagulation was at one time a subject of animated discussion (457). HIEDEMANN (458) considered the basic reason for ultrasonic coagulation is the incident that in all real, i.e., polydispersed aerosols, particles are entrained in a deviative degree by the medium's oscillations (see page 112). Fine particles possessing a greater amplitude of oscillations "sweep" through aerosols also with much larger and almost immobile particles. Both relative movements are caused by sedimentation, turbulence, and so on. The absorbent surface, as such, represents in this case a cylinder whose length is equal to a double amplitude of oscillations of small particles, and whose radius equals the sum of the radii of large and small particles.

The insolvency of the above theory is already apparent from the fact of the rapid coagulation of aerosols effective at such high frequencies of oscillations, in the presence of which, practically speaking, all particles remain immobile (459). Likewise, the above theory cannot explain why the very fine, i.e., the most vigorously oscillating, particles are not involved in coagulation.

According to the opinion of ANDRADE (460), ultrasonic coagulation is caused by the hydrodynamic attraction between particles (see page 126). While computing an aerosol's coagulation velocity in an ultrasonic field, ANDRADE omitted diffusion and made several other mistakes. Therefore, his equation's good concurrence with the experimental data obtained at his laboratory must be regarded as accidental. Precisely so, as we implied in the preceding paragraph, it is inadmissible to disregard diffusion in the presence of forces having a very small radius of action between particles in an electrical or a sonic field (461).

The potential of hydrodynamic forces between identical particles found in a sonic field is expressed by the equation

$$\psi(r) = \frac{\pi \gamma_g V_{R_0}^2 r^6}{3} (\sin^2 \theta - 2 \cos^2 \theta), \quad (53.1)$$

which can be readily compared with the equations (23.4), (52.1) and (52.3). Here V_{R_0} denotes the ratio of the amplitude of the rate of the relative oscillations of the medium and the particle while θ denotes the angle between the direction of oscillations and the lines of centers.

It is uncertain in this case to determine by the method explained in the preceding paragraph the influence of hydrodynamic forces upon rapidity of coagulation, because, according to considerations stated on page 128, equation (53.1) is probably inapplicable. Still, we want to show that the coefficient β , referred to the nondimensional value of

$$\alpha_1 = \left(\frac{\pi \gamma_g V_{R_0}^2 r^3}{8kT} \right)^{1/3} \quad (53.2)$$

is, in this case, somewhat larger than during the coagulation in an electrical field.¹ The effect already attains its noticeable magnitude with $\alpha_1 = 3$.

1. Although the maximal value of attraction in this case is twice as small as that of repulsion, nevertheless the attraction zone is larger than the repulsion zone (in an electrical field it is vice versa).

Experimental data pertaining to the ultrasonic coagulation of aerosols are, in most instances, only slightly suitable for comparison with theoretical findings, because usually they were obtained from rather poly-dispersed aerosols, and also the size and concentration of particles were not precisely determined, etc. We shall compute, for the sake of typical experimental conditions, the values of α_1 , which usually induce a noticeable speeding up of coagulation. In this case, we assume for the frequency of oscillations 10^4 hertz, and for average energy of the sonic field, $100 \text{ erg} \cdot \text{cm}^{-3}$, which corresponds to the maximal amplitude of oscillations of 0.13 mm. If we take under consideration that the average field intensity is $\bar{\Phi} = \frac{1}{4} \gamma_g U_0^2$, we obtain for α_1 the expression

$$\alpha_1 = \left[\frac{\pi (V_{R_0}/U_0)^2 4\bar{\Phi}}{8kT} \right]^{1/3} r. \quad (53.3)$$

If we use figure 20 to establish the ratio of V_{R_0} , we find that, if $r = 0.2, 0.5$ and $1\mu\alpha_1$ respectively, the ratio in question would respectively correspond to 0.6, 4 and 16. In fact, one can observe a considerable acceleration of coagulation effected by ultrasonics under the described conditions (135) even if $r = 0.2\mu$. Yet, one should consider here one essential condition: that an intensive air circulation, having a considerable gradient in flow velocity, occurs in tubes (see page 116) where an ultrasonic field develops, and this is instrumental in drawing particles together more effectively than a molecular diffusion

Thus, the theory of hydrodynamic attraction affords at least a rough evaluation of the conditions essential to the effectiveness of ultrasonic coagulation. The theory also explains the fact why ultrasonics are so little effective among highly dispersed aerosols (462) (the factor $(V_{R_0}/U_0)^{2/3} r$ in equation /53.3/). Also the rapid increase of the ultrasonic coagulation constant is better understood pertinent to the course of the process as such, i.e., in so far as the coagulation of particles is concerned (463). Moreover, the frequently noted noneffectiveness of ultrasonics is better understood with regard to aerosols containing a low calculated concentration (464); if the average distance between particles is great, there is a lesser probability of the particles' mutual approach up to a distance where hydrodynamic forces begin to be effective. Furthermore, the hydrodynamic theory explains why, during ultrasonic coagulation of smokes, flat aggregates which are formed position themselves at a plane perpendicular to the direction of oscillations (135); in the described case, directed coagulation also takes place within this plane ($\theta = \pi/2$). Let's assume that large particles of elongated shape, which do not participate in the oscillations, orient themselves in an ultrasonic field with their long axes perpendicular to the direction

of oscillations (131), as the statement in §11 implies. On the other hand, small particles being fully entrained by the oscillations position themselves with their long axes parallel to the direction of oscillations, which may be due to the orienting effect of the velocity gradient in a circular flow of air.

In the afore-quoted computation, we averaged the energy of sonic oscillations in the entire volume of aerosol. Yet, in actuality, the ultrasonic coagulation takes place near the waves of the antinodes although, due to turbulent agitation occurring with more or less intensive ultrasonic oscillations, all aerosol particles are, on the average, affected by identical conditions.

Although we did not arrange any special experiments to compare the velocities of ultrasonic coagulation in smokes and fogs, nevertheless no great differences apparently exist between the two in this case. Thus, at HIEDEMANN'S laboratories during experiments (465) with oil sprays, whose $\bar{r} = 0.4 \mu$, rapid coagulation was obtained with 10^4 hertz and with $\Omega = 25 \text{ erg} \cdot \text{cm}^{-3}$. During ST. CLAIR'S (135) experiments with NH_4Cl smokes with $\bar{r} = 0.2 \mu$ and an identical frequency, a noticeable acceleration of coagulation was obtained with $\Omega = 50 \text{ erg} \cdot \text{cm}^{-3}$.

There are indications that large aggregates (up to 100μ) are formed only when the intensities of the oscillations are not very great (135). If turbulence does develop in an intensive sonic field, larger aggregates become broken up into particles. Usually the firmness with which the aggregates develop during ultrasonic coagulation is not considerable, and such aggregates frequently disintegrate in precipitation. It appears that the bursting of aggregates into small particles results from the ultrasonic's noneffectiveness, as this is referable to fly-ashes (466). If aqueous or oil vapors are added to the coagulating smokes or dust, this contributes to the aggregate's cementation and also considerably increases the ultrasonic's effectiveness (135, 467).

The following assertions can be made about the frequency of ultrasonics influencing the latter's effectiveness. At a certain stage of the particle's entrainment by the medium's oscillations, i.e., if a certain ratio of V_{R_0}/U_0 is present, the effect depends solely upon the magnitude of U_0^2 (the energy of a sonic field). Thus, the effect at first improves noticeably proportional to the increase in frequency (we should note that the audible sonic waves are entirely ineffective), but having reached the frequencies at which the ratio of V_{R_0}/U_0 comes close to 1, i.e., approaches $\omega^2 r \approx 0.002$, the continued increase in frequency does not provide any appreciable effect in the

energy of the same field; therefore it is practically inept. Experimental data about the influence of frequency of oscillations upon the latter's effectiveness are very scanty. There are indications (461) that the least effective frequency among most aerosols is equal to $4 \cdot 10^3$ hertz, while in the case of tobacco smoke it is equal to $7 \cdot 10^3$ hertz, but this would be difficult to use since the average size of particles in these aerosols is not known.

We should still discuss what influence a sonic pressure has upon particles during an ultrasonic coagulation in an aerosol (see § 21). The following observation is highly significant in this respect (135). In the presence of a definite, but not too high, intensity of oscillations (while turbulent agitation is still indistinct), the concentrated NH_4Cl smoke appears "streaky" up to the beginning of coagulation, because particles tend to concentrate in antinodes of the waves. We shall examine this problem with the aid of the equation (21. 2) as to a sonic wave's standing pressure force affecting particles of aerosol. Thus, we shall estimate the order of magnitude of the time t_0 required by a particle in a wave's node to reach the nearest antinode while under the influence of the afore-described force, i. e., the time needed for a particle to traverse the distance $\lambda/4$. For simplification purposes, we assume that $\sin(4\pi x/\lambda) = 1$, i. e., we presume that the particle moves at all times with the maximal velocity

$$V_{\max} = \frac{F_{\max}}{6\pi\eta r} = \frac{5\pi\gamma_g V_{R_0}^2 r^2}{18\lambda\eta} \quad (53. 4)$$

(in equation (21. 2) we substituted U_0 by V_{R_0} in accordance with the remarks on page 116). Naturally, in this way we obtain for t_0 the lower range:

$$t_0 = \frac{\lambda}{4V_{\max}} = \frac{0.9\lambda^2\eta}{\pi\gamma_g V_{R_0}^2 r^2} \quad (53. 5)$$

On behalf of the above-discussed conditions (frequency 10^4 hertz, $\lambda = 3$ cm and $\Omega = 100 \text{ erg} \cdot \text{cm}^{-3}$) we accordingly find for $r = 0.2, 0.5$ and μ , respectively, that $t_0 = 3 \cdot 10^6, 1.3 \cdot 10^4$ and 400 seconds, respectively. Meanwhile, as aerosols coagulate under these conditions for several decaseconds, so within this time particles would be able to pass an insignificant part of the path toward the antinodes. Nevertheless, it is necessary to consider here the following circumstances. As we explained on page 114 the actual magnitude of the ultrasonic pressure seems, according to the new theoretical procedures, to be much better expressed with equation (21. 2). Furthermore, an ultrasonic field contains rather strong

overtones and the magnitude of the pressure increases up to a well known degree with the frequency of the oscillations. Finally, in relation to the aerosol's coagulation and the growth of particles, the velocity of their movement toward the antinodes is sharply accelerated under the influence of the ultrasonic pressure. Therefore, it is quite possible that the ultrasonic pressure aids considerably the coagulation of aerosols by leading their particles toward the antinodes, where the hydrodynamic forces between particles are particularly strong, and thus high concentrations of particles are developed. Nevertheless, one can hardly ascribe to an ultrasonic pressure a decisive role in coagulation, as ST. CLAIR (468) does. It is particularly difficult to explain from the above standpoint why a calculated concentration of aerosol has such strong influence upon the ultrasonic effect.

It is also impossible to agree with the opinion of P. KUBANSKIY (469) about any substantial role being attributed to collisions between particles caused by an aerosol's circulation in the nodes of an ultrasonic field (see figure 21). The above may be true with regard to very large particles as, e.g., for large aggregates formed due to coagulation, but not with regard to the primary particles of an aerosol.

A practical utilization of ultrasonics, intended to precipitate industrial aerosols, has been delayed for a long time due to lack of sufficiently powerful industrial generators for ultrasonic waves. This problem is presently being solved by means of the production of ultrasonic sirens (462). There are already industrial installations available for precipitation of sulfuric acid smoke and other aerosols by means of ultrasonics; they operate with the efficiency of $1000 \text{ m}^3 \cdot \text{min}^{-1}$. Thus, within 4 seconds, as the smoke moves into an ultrasonic field, up to 90% of these smokes can be coagulated and, as subsequently large droplets form, they precipitate into cyclones. Yet, at the same time, a small part of the highly dispersed smokes still remains in an uncoagulated state and even if the processing continues, it does not bring any substantial effect. Just as we stated before, ultrasonics have little effect with regard to aerosols possessing small calculated concentrations.

§54. Kinematic (Gravitational) Coagulation of Aerosols

A relative movement of particles of dissimilar sizes appears to evolve from dissimilar velocities that the particles acquire under the influence of an external force. This factor leads to collisions between particles and to their coagulation. Of specific importance is the process,

which we shall name a "kinematic coagulation" of aerosols¹; its significance is connected with the precipitation of particles under the influence of gravity ("gravitational coagulation" according to Ya. FRENKEL /470/). This process may also occur in an electrical field under the influence of a centrifugal force, following changes in flow velocity and so on.

The theory of kinematic coagulation is essentially dissimilar considering aerosols which contain large and small particles. In the first instance, the particle diffusion may be disregarded. Let's consider now that a large spherical particle falls freely with a velocity V_s through the aerosol which also contains much smaller particles. If the velocity of fall of the smaller particles is insignificant, then the process will be analogous to the process (discussed in § 34) of by-passing an immobile spherical body which, together with the aerosol, is in motion with a velocity V_s . Thus, if we know the coefficient of precipitation Φ , which in this case could be named the "coefficient of capture," it would be easy to compute the number of small particles captured in one second by a large particle with a radius R , according to the equation:

$$\Phi = \pi \Phi R^2 V_s \quad (54.1)$$

If the sedimentation velocity of small particles cannot be disregarded, then the computation should be conducted according to the comparative velocity of the motion; however, in this case, the distribution of velocities in gas which by-passes a large particle and, consequently, the coefficient of capture, will be somewhat changed. At the same time, this change will be increased when the ratio of the sizes of a large particle to those of small particles approach. It would be very difficult to compute the the magnitude of an appropriate correction, therefore we shall disregard it. It is much more important to take into account accurately the capture coefficient's dependence upon the dimensions of small particles: all methods so far suggested for computation of the discussed coefficient were inaccurate.

As the matter stands, in the first primitive theory of gravitational coagulation offered by FINDEISEN (471), the distortion of the trajectories of the small particles in a current which by-passes a large particle was generally not considered, i.e., the effectiveness of capture was accepted as equal to $\left(\frac{R+r}{R}\right)^2$; where R is the radius of a large particle; where r is the radius of a small particle. Naturally, such a calculation yields oversized values of Φ . While testing his calculations experimentally, FINDEISEN produced by adiabatic expansion of an aqueous fog with particles of radii 5 - 8 μ (472) in a chamber of 60 m³ capacity. Then, while analyzing the changes in distribution

1. In colloidal-chemical reference material, there is an adopted term of "orthokinetic," i.e., "a directed coagulation," which has a wide but less definite meaning, because it refers to coagulations in electrical as well as in sonic fields.

of droplet sizes with the lapse of time, FINDEISEN was able to determine the presence of coagulation, which, due to the fog's small calculated concentration, could only be identified in this case with the discussion about gravitational coagulation. At the same time, since the velocity of coagulation between the droplets did not differ much in its magnitude, it agreed more or less with the computation, but as greater differences in sizes appeared, the velocity of coagulation became considerably smaller than the computed one.

LANGMUIR (239) admitted a different mistake: having computed the trajectories of rounded particles on a calculating machine (see § 34), he determined a capture coefficient as the function of the parameter l_i/R without taking into account the capture effect of small particles, i. e., regarding the latter as points. Naturally, the results thus obtained were considerably undersized and, particularly, what appeared is that small particles ($r < 15\mu$) are, generally speaking, not captured by each other. Moreover, LANGMUIR proceeded in his calculations not from the comparative velocity of fall, but from an absolute falling velocity of the large particles. Finally, as we already indicated, LANGMUIR'S method used for interpolation of Φ values obtained for a viscous and ideal region of by-passing is groundless. The results of computations of the capture coefficient of aqueous drops pertinent to various values of R and r , as published by LANGMUIR, are very unreliable; consequently they are not submitted here (see /473/).

In one of his recent reports, N. SHISHKIN (474) multiplied by $\left(\frac{R+r}{R}\right)^2$ the effectiveness coefficient computed by LANGMUIR, but this does not improve the matter much: the capture coefficient for droplets of $< 15\mu$ radius still equals zero.

Actually, Φ does not equal zero considering particles of any magnitude. If we intelligently assume that the center of a particle which envelops a spherical body moves along the line of flow, and if we disregard the particle's inertness, then we can obtain (table 32) from equations (34. 16) and (34. 17) the threshold (minimal) values of the coefficient Φ for a viscous and ideal flow (243). At the same time, the coefficient Φ will refer to the diameter of a larger particle

Table 32

Threshold (with $l_1 = 0$) Values of the Capture Coefficient Φ
in Aerosols with Spherical Particles

r/R	1	0.8	0.6	0.4	0.2	0.1	0.05	0.025
In a viscous current ...	1.25	0.83	0.48	0.22	0.06	0.014	0.0036	0.001
In an ideal current	3.50	2.69	1.93	1.25	0.62	0.30	0.15	0.075

Actual magnitude of Φ must, in every case be, greater than those quoted in table 32. It is obvious from the table that Φ decreases rapidly, especially in a viscous current, when r/R decreases, and this helps to explain the afore-mentioned observations of FINDEISEN.

In order to compute the full magnitude of the capture coefficient with the inertial displacement of particle taken into account, it is necessary to determine the trajectories of the particles individually, each by a given size; therefore it is impossible to use the principle of similarity, as we already pointed out on page 175. On the other hand, if we consider gravitational coagulation of aerosols, with their particles' maximal radius of 15μ , the inertial displacement would be very small; therefore, for these aerosols (among them, also, natural fogs and clouds whose state of pluviosity has, as yet, not begun), table 32 apparently offers more accurate values of the capture coefficient than the zero value which LANGMUIR accepted. Yet, if we consider the kinematic coagulation of relatively large drops with small droplets in the presence of so much greater Re_f numbers, that the by-passing of larger drops by air can be regarded as ideal, then the Φ values computed by LANGMUIR become more or less accurate and this is confirmed by the subsequently described experiments of GUNN (475). Aqueous drops of 1.6 mm radius were allowed to fall thru a 3 m high tube. The latter was filled with polydispersed aqueous fog which formed droplets of the order of several deca-microns. The weight increase among the larger drops indicated the amounts of water absorbed by them. Having measured the concentration and the distribution of the droplet sizes in the vapor, and knowing the falling velocity of the larger drops at different heights, GUNN computed a theoretical magnitude of the weight increase according to equation (34.6) by means of numerical integration. He obtained a satisfactory concurrence between the experimental magnitude and the computed value. The average magnitude of Re_f in these experiments was of the order of 500.

In a recently published report of TELFORD, THORNDIKE and BOWEN (574), we find that a comparable aqueous fog, with isodispersed droplets

with radii approximating 70μ , obtained with the aid of a disc atomizer, is continuously driven into a vertical tube with a transparent wall. As the air, saturated with aqueous fog, was blown through the tube from below, its velocity slightly exceeded that of the freely falling droplets. The slowly rising droplets in the tube were photographed in brief exposures on a film moving horizontally and the relative velocities of the adjacent droplets, found at approximately one vertical line, were determined by means of the measurement of the angles between the straight lines on a photograph. Thus the average value of the relative velocity $\bar{V}_r = 1.1 \text{ cm} \cdot \text{sec}^{-1}$ was computed. Then, primary droplets were computed from the photographs, as well as those which were formed from the primary droplets colliding and were falling as twin droplets; hence, the concentrations of the primary and of the twin droplets were computed. Inasmuch as \bar{V}_r was known, and also the tube's height, as well as the radii of the primary droplets and the velocity of settling of twin droplets, it was possible to compute the magnitude of the capture coefficient, which was found to be equal to 12.6. Yet, even with the exact rectilinear fall of droplets and the capture effect considered, β ought to be equal to 4.

The authors explained in the following manner the high magnitude of β . Behind a by-passed droplet, the lines of flow are set up at a small angle to the vertical axis, which passes through the droplet's center. Thus a second droplet, found behind the first one and not far from the afore-mentioned axis, will become entrained by the current toward the latter and this will lead toward the increase of β . Inasmuch as the radial velocity of a droplet is not great, its effect may reveal itself only in a sufficiently prolonged radial movement, i. e., at velocities of both droplets being close to one another.

Analogous observations were made by SARTOR (575), employing a measuring apparatus for testing the aqueous drops ($r = 1 - 2 \text{ mm}$) as they were falling through viscous oil. In these tests, Re was of the order of $0.02 - 0.1$. The capture coefficient was found to be 2 - 3 times greater than the one computed according to equation (34.7); it was also clearly visible how an overtaken drop was shifted in a horizontal way into the path of an advancing drop.

From photographs obtained by TELFORD and others which depict colliding droplets, it was also possible to discover the presence of the longitudinal interaction between falling droplets. A frontal droplet retains its constant velocity up to the very moment of collision, while a rear droplet begins to move faster already at an approximate distance of 40 times its diameter to the point of collision, obviously due to the current forming behind the frontal droplet. The Re number equaled 6 during these experiments. We noted in §13 that at small Re , i. e., in the presence of a symmetrical current in front and behind a droplet, the decrease in the medium's resistance is the

same for both droplets; however, if Re is already of the order of several digits, the symmetry is disrupted and the influence of the frontal droplet upon the rear droplet is considerably greater than a reversed influence.

The gravitational coagulation plays a very important role in the process of clouds pluviosity. As fog forms due to condensation, nebulous droplets assume the size of the order of 10μ and their falling velocity is low in comparison with the velocity of vertical currents in the atmosphere. Moreover, such droplets would evaporate before reaching the ground; therefore, they must have a radius of the order of at least 100μ . We have vainly tried for a long time to settle the question about the mechanism of the elements of cloud growth. All proposed mechanisms, such as hydrodynamic attraction between falling drops, thermal, turbulent and kinematic coagulations, then coagulation under the influence of atmospheric electrical field, as well as isothermal sublimation from small to large droplets, all seem not to be sufficiently effective in so far as producing independently a more or less substantial rainfall (473). In 1936 BERZHERON expressed a hypothesis according to which the formation of precipitation begins in the upper parts of the clouds, where a temperature below zero prevails and where supercooled droplets exist. At the time of freezing of some of the droplets, a rapidly developing process of isothermal sublimation from droplets to ice crystals takes place. The enlarged crystals, falling through a cloud, grow still larger by means of kinematic coagulation and they precipitate in a form of rain drops or snow flakes. Apparently BERZHERON'S hypothesis depicts correctly the mechanism of cloud pluviosity in a temperate zone and in a polar climate, but a rainfall in tropics frequently comes from clouds which in their entire extent have a temperature above zero, and in such case the growth may come only by way of coagulation. FINDEISEN (471), LANGMUIR (239), Ya. FRENKEL (476) and N. SHISHKIN (477) developed a theory of growth of nebulous droplets by way of gravitational coagulation. However, with this, the following question presents one main difficulty. According to LANGMUIR'S calculations, if a droplet falling through the entire cloud's depth is to attain the size of a rain drop ($r \approx 1 \text{ mm}$) as a result of coagulation, the droplet must, from the very beginning, be of the magnitude which considerably exceeds the average magnitude of nebulous droplets. Whence, then, do such large drops in a cloud originate? According to LANGMUIR'S opinion, a small initial number of such droplets develops due to the influence of incidental causes. As the droplets grow while falling through a cloud, they reach a critical magnitude at which they become split by air resistance (see page 67). The comparatively large sputter thus obtained is carried upwards by convective currents, whose velocities in cumulus clouds reach several $\text{m} \cdot \text{sec}^{-1}$, whereupon they become enlarged again, then they fall and become split in their turn, ... and so on. Thus, according to LANGMUIR, a cloud's pluviosity assumes a chain-line type of action.

According to calculations of N. SHISHKIN (477), the pluviosity of highly convective clouds is possible as a result of vapor condensing on droplets and then single droplets fall through a cloud; thus LANGMUIR'S hypothesis is not needed here. At the same time N. SHISHKIN accepted, in accordance with LANGMUIR'S calculations, that the growth of droplets resulting from gravitational coagulation is only possible in so far as droplets with a radius $> 15\mu$ are considered. Yet if we consider that the afore-mentioned effects of capture and displacement are horizontally directed, then, of course, the conditions for coagulated rainfall of the clouds will be still more favorable. It will also be necessary to take into account the influence of charges on droplets affecting the course of gravitational coagulation.

In the discussion about kinematic coagulation, the precipitation of an aerosol is based upon atomized water. At the same time, two conditions had to be disequalized:

1. When droplets move through aerosol under the influence of own gravity only, and
2. When droplets are blown into an aerosol with a velocity which exceeds considerably the rapidity of the droplet sedimentation.

First we shall review the first instance. Table 33 shows values of the capture coefficient of aerosol particles of dissimilar magnitude with a density of 2, as they fall with a terminal velocity V_g with aqueous drops of R radii. V_g was determined according to table 9, while T values needed for computation of Stk number were obtained from table 13. The effect of falling and the by-passing of air by drops was considered as ideal and Φ was defined according to the equation (34.6). As r/R is small here, so the capture effect could be disregarded. Each drop, per cm of its path, captures $\pi R^2 \Phi n$ particles; where n is the known concentration of the aerosol. Thus, one cm^3 of atomized water captures $\pi R^2 \Phi n / \frac{4}{3} \pi R^3 = 0.75 \Phi n / R$ particles and the ratio of Φ/R may be calculated as a coefficient of efficiency during precipitation of aerosols by atomized water. We shall assume that Φ values quoted on the left side of the table are oversized, because the by-passing should not be regarded here as ideal; unfortunately, the exact values of Φ are unknown in this transitional region.

As table 33 indicates, the effectiveness of aerosol precipitation by atomized water depends to a very large extent upon the aerosol's dispersion and, at the same time, the precipitation of particles with a density of 2 is possible only if $r > 0.5\mu$, regardless of the sizes of aqueous drops. This conclusion coincides well with experimental data (478, 479), according to which atomized water is effective only for dusts of

Table 33

Effectiveness of Precipitation of Aerosols by Atomized Water

r, μ	$R, \text{ cm}$							
	10^{-3}	$2 \cdot 10^{-3}$	$5 \cdot 10^{-3}$	10^{-2}	$2 \cdot 10^{-2}$	$5 \cdot 10^{-2}$	10^{-1}	
	$(V_g/2R) \cdot 10^{-3}, \text{ sec}^{-1}$							
	0.6	1.2	2.3	3.5	4.0	4.0	3.3	
0.5	Stk	$4.2 \cdot 10^{-3}$	$8.4 \cdot 10^{-3}$	$16 \cdot 10^{-3}$	$24 \cdot 10^{-3}$	$28 \cdot 10^{-3}$	$28 \cdot 10^{-3}$	$23 \cdot 10^{-3}$
	η	0	0	0	0	0	0	0
	η/R	0	0	0	0	0	0	0
0.7	Stk	$0.8 \cdot 10^{-2}$	$1.6 \cdot 10^{-2}$	$3.1 \cdot 10^{-2}$	$4.7 \cdot 10^{-2}$	$5.4 \cdot 10^{-2}$	$5.4 \cdot 10^{-2}$	$4.4 \cdot 10^{-2}$
	η	0	0	0	0.03	0.06	0.06	0.03
	η/R	0	0	0	3	3	1.2	0.3
1	Stk	$1.5 \cdot 10^{-2}$	$3.1 \cdot 10^{-2}$	$6 \cdot 10^{-2}$	$9.1 \cdot 10^{-2}$	$10.4 \cdot 10^{-2}$	$10.4 \cdot 10^{-2}$	$8.5 \cdot 10^{-2}$
	η	0	0	0.07	0.17	0.21	0.21	0.16
	η/R	0	0	14	17	10	4	1.6
2	Stk	0.06	0.12	0.23	0.35	0.40	0.40	0.33
	η	0.07	0.24	0.41	0.54	0.58	0.58	0.53
	η/R	70	120	80	54	29	12	5.3
5	Stk	0.35	0.7	1.4	2.1	2.4	2.4	2.0
	η	0.54	0.7	0.85	0.89	0.90	0.90	0.89
	η/R	540	350	170	89	45	18	9

$r > 0.5 - 1\mu$. We also take notice that the most suitable radius of aqueous drops in this case is approximately equal to 20μ with $r = 2\mu$, also to $50 - 100\mu$ with $r = 1\mu$, and to $100 - 200\mu$ with $r = 0.7\mu$, i. e., it progresses with the increase of aerosol dispersion.

Still another rule, of necessity, must be observed when atomized water is blown into an aerosol with a high velocity, because, with a certain droplet velocity, the effectiveness of capture, and much more so the coefficient of efficiency, of atomized water increases constantly with a decrease in the droplet sizes. The effectiveness of capture, in this case, may even be greater among very small particles. Thus, e. g., the capture coefficient of particles with a density of 2 by the water droplets, whose radius is 50μ , attains 0.4 at a blowing velocity of $16 \text{ m} \cdot \text{sec}^{-1}$ if $r = 0.2\mu$, and then it attains 0.12 if $r = 0.1\mu$. In fact, AVY (480) was able to reduce noticeably the concentration of indigo smoke with $r = 0.1 - 0.15\mu$ by atomizing a 10% solution of sodium chloride directly in a chamber. However, the velocity of droplets blown into the aerosol rapidly decreased with their distance of travel, and thus a high effectiveness of coagulation was only possible close to the atomizer.

A kinematic precipitation of aerosols by atomized water must not be confused with a thermal coagulation of aerosols by means of water fogs. Such coagulation is governed by an entirely different set of rules (see §49) and its rapidity depends mainly upon the calculated concentration of fog. If this concentration is not sufficiently high, no effect whatsoever can be obtained. Thus, in the afore-mentioned experiments, as AVY stopped the atomization of NaCl solution, the further decrease in calculated concentration of indigo smoke progressed with the same rapidity as during a controlled test without fog. Inasmuch as the concentration of fog was of the order of $10^4 \cdot \text{cm}^{-3}$, so the outcome was as expected according to thermal coagulation. In contrast with the above, DAUTREBANDE (482) observed a considerable coagulation effect after he introduced into quartz dust a smoke obtained either from eosin solution, or from sodium chloride, with $r = 0.2 - 0.3\mu$ and with the dispersion of the quartz dust approximately the same. At the same time, large aggregates were obtained which contained both SiO_2 and the solute. DAUTREBANDE emphasized that, in order to obtain a noticeable effect, it is necessary to introduce greater amounts of dispersed water but, unfortunately, he did not disclose any calculated concentration of fog in a chamber. In accordance with the gravimetric concentration and the average size of NaCl particles, it can be concluded that in these experiments the concentration of NaCl aerosol in the chamber comprised $10^6 - 10^7 \cdot \text{cm}^{-3}$, and that the thermal coagulation of SiO_2 particles with NaCl particles must have progressed quite intensely.

It appears that, with the practical precipitation of aerosols by atomized water, the following three processes frequently occur at the same time: a kinematic coagulation (close to the atomizer), then gravitational and thermal coagulations. Coarse fragments of the aerosol precipitate mainly due to the first two processes and the fine fragments precipitate due to the third process.

In recent times, new devices for the removal of dust from gases have found wide acceptance - VENTURI scrubbers, i. e., VENTURI tubes, in whose throats atomized water is sprayed (483). Since water drops cannot assume as high a velocity as that of the gas flowing through the tube's throat, a high relative velocity is developed among the aerosol particles and the droplets, which leads to an intensive kinematic coagulation. According to recent data (484), the capture of particles by droplets takes place not only at the throat, but it extends also some distance from the throat to the diffuser, whose size exceeds the throat's diameter by tenfold. In addition to the coagulation developed from the dissimilar velocities of the particles and droplets, it is obvious that also a "gradient" coagulation takes place in a VENTURI tube and we shall discuss this in the following paragraph. As should be expected, the effectiveness of VENTURI scrubbers improves with the increase in the amount of atomized water; with the velocity of the flowing gas; with the size of the aerosol particles and with a decrease in the size of aqueous drops (485). The effectiveness of scrubbers is very low when considering particles with radii $0.1 - 0.2\mu$ (484, 485). It increases considerably if the gas is saturated with aqueous vapor beforehand. As a decrease in pressure develops following an increase of velocity in the tube's throat, the vapor condenses on aerosol particles and enlarges them. In this way, it was possible to precipitate 99.9% of dioctylphthalate particles with $r = 0.07 - 0.20\mu$ (486). The assertion of BOUCHER (250), that for a maximal effectiveness of VENTURI scrubbers it is necessary that the distribution of sizes of the fog droplets, as well as of the particles of the aerosol being purified, be alike if possible, requires to be checked, which can hardly be done by any theoretical proof.

As we proceed to the kinematic coagulation of such dispersed aerosols, among which it is impossible to disregard the particle diffusion, we shall note that the problem is equivalent to the question of diffusion toward a sphere which is being by-passed by viscous flow. One can use here equation (39.11) with the limitation given on page 237. The approximate solution proposed by MYULLER (487) does not stand up against any serious criticism, therefore it is not quoted here.

We shall explain the region in which diffusion and a relative movement of the precipitating particles are of essential value to coagulation.

Among aerosols with a small degree of polydispersion, the number of particles captured in one sec by one of the larger particles is of the order of magnitude $\pi V_s r^2 n$, because Φ in the given case has the order of magnitude of one (see table 32). The number of particles per sec which came in contact with a certain particle as a result of diffusion is equal to $2 Kn = 16 \pi r D n$. If we assume that the product of $r V_s$ increases rapidly and that of D decreases with the increase of r , then the transition from a thermal coagulation to the region of kinematic coagulation must, in this case, be a quite rapid one. One can readily convince himself from the values of D and V_s , quoted in table 13, that if $r < 0.5 \mu$, gravitational coagulation plays an imperceptible part, while if $r > 2 \mu$, thermal coagulation takes place. Somewhat different is the case among highly polydispersed aerosols: since the rapidity of thermal coagulation of large particles with small ones is high (see §49), and the rapidity of gravitational coagulation among these particles is low, then, in this case, the limits of the transitional region of mixed coagulation are considerably expanded.

Of great interest in the theory of rain clouds is the question of coagulation of fog particles, which fall through the clouds under the influence of gravity of much larger, charged drops. L. LEVIN (488) studied the occurrence in which charged vapor droplets were also involved, whereas between the latter and the larger drops common COULOMB'S forces were active. As long as such a condition prevailed

$$\sigma_1 = \frac{3|Qq|}{4\pi\gamma r^3 R V_s^2} \gg 1, \quad (54.2)$$

where Q and q are charges; where R and r are radii of larger and small drops, respectively; where V_s is the terminal velocity of the larger drops, i. e., if larger charges and small size droplets are involved, the inertial term may be disregarded in a differential equation of the motion of small droplets. But in a viscous (STOKES') region that includes the falling of larger drops, the coefficient of capture (by large drops) of small droplets having the opposite charge is expressed by the equation

$$\Phi = \frac{2|Qq|}{3\pi\eta r(R^2 - r^2)V_s} = \frac{3|Qq|}{\pi\gamma r R^2(R^2 - r^2)g} \quad (54.3)$$

L. LEVIN (488), as well as PAUTHENIER and CHOCHET (489), examined, in connection with induction forces, the capture of neutral droplets by falling charged drops. Thus, if the radius of the falling droplets is

smaller than $10\text{-}15\mu$ and the charge is greater than $4 \cdot 10^{-4}$ E. S. units, then, as we shall show below, one can disregard the inertia of the droplets and the hydrodynamic distortion of the droplet trajectories as they approach, i.e., it may be considered that the medium around falling drops remains immobile. Then, in connection with STOKES' law as to the medium's resistance toward the coefficient of capture, we obtain, according to PAUTHENIER and COCHET, the following expression

$$\mathfrak{C} = \frac{45}{16R^2} \left[\frac{\lambda r^2 Q^2}{\gamma g (R^2 - r^2)} \right]^{2/5}, \quad (54.4)$$

where $\lambda = (\epsilon_K - 1)/(\epsilon_K + 2)$ is the induction factor; $\lambda \approx 1$ pertinent to aqueous droplets. As R increases proportional to the enlargement of a charged drop, equation (54.4) becomes inapplicable, and it is necessary here to take also into account the distortion of the lines of flow close to the droplets, as well as the latter's inertia. Only a numerical solution of the problem is possible in this case. Figure 74 illustrates the curves computed by PAUTHENIER and COCHET; the curves show the dependence of \mathfrak{C} upon R pertinent to aqueous droplets with a charge of $4 \cdot 10^{-4}$ E. S. units and to the series of r values (solid lines). The broken-dotted lines were plotted according to equation (54.4). The broken lines refer to non-charged drops.

L. LEVIN made similar computations taking into account the distortion of the trajectories of the droplets, but disregarding their inertia, which is permissible under the condition:

$$\sigma_2 = \frac{3\lambda Q^2}{2\pi\gamma R^4 V_s^2} \gg 1. \quad (54.5)$$

Thus, L. LEVIN obtained \mathfrak{C} values quoted in table 34 by assuming that the droplet charges in natural clouds are equal to $10^{-3} R$.



FIG 74 COEFFICIENT OF CAPTURE OF NEUTRAL DROPLETS BY CHARGED DROPS

Unfortunately, no reliable data about the dependence between the droplet sizes and their charges in clouds are as yet available; therefore, it is rather difficult to judge at the present time the role that the droplet charges play in the natural pluviosity of clouds. As regards utilization of charged aqueous droplets for the purposes of artificial pluviosity of clouds,

Table 34

Capture of Neutral Droplets by Falling Charged Drops

R, μ	$Q \cdot 10^7$ E. S. units	σ_2	r, μ	β	r, μ	β	r, μ	β
2.5	2.5	1250	1.25	2.32	0.8	1.48	0.5	0.89
3.75	3.75	110	1.87	1.06	1.20	0.69	0.75	0.40
5.00	5.00	20	2.5	0.57	1.6	0.38	1.0	0.22
6.25	6.25	5.1	3.12	0.34	2.0	0.23	1.25	0.13

PAUTHENIER and COCHET estimated that droplets with a 15μ radius and with a charge of $4 \cdot 10^{-4}$ E. S. units are equivalent in their effectiveness to non-charged drops, whose $r = 60\mu$ and whose mass is 64 times greater.

The influence of charges of the drops upon the velocity of gravitational coagulation among aqueous droplets having approximately the same size was examined experimentally in conjunction with the aforementioned work of TELFORD and others (574). When an artificial bipolar charging of the drops was present and the magnitude of the charges was of the order of 10^{-4} E. S. units, the rapidity of coagulation was several times higher than in the presence of a natural charging of the drops during the process of mechanical atomization of water. However, with a unipolar charge present, coagulation was practically discontinued.

In conclusion, we shall mention a few words about the possibility of coagulation of aerosols due to the forces of hydrodynamic interaction between precipitating particles. At one time, there was an important significance ascribed to this effect in so far as the formation of atmospheric precipitation: sizes of droplets in rain and in fogs, defined with untenable accuracy, resulted in distribution curves showing a number of maximums (490). Droplet radii, corresponding to these maximums, were approximately comparable with one another to $1^{1/3}$, $2^{1/3}$, $4^{1/3}$, $8^{1/3}$, and so on, whereas

droplet volumes were comparable to 1, 2, 4, 8, etc. Hence, a hasty conclusion was drawn that primary fogs are isodispersed; next, that droplets falling with identical velocity attract one another and thus become joined together, also that the same action progresses among "twin" droplets and so on. Yet, recent and more exact measurements disclosed that these observations are erroneous, that distribution of droplet sizes appears as is shown on figure 2, and that isodispersed fogs in nature don't exist. As to the principle that the coagulation of falling particles is possible as a result of hydrodynamic interaction, it follows from the statement in § 23, that apparently this is possible only at larger Re numbers, i. e., in so far as large particles are involved. However, if in such case there is even a small difference in size among particles, their relative velocity becomes so high that the effect of the hydrodynamic interaction is not able to develop. A well-known value of hydrodynamic forces can only be found in a "boiling stratum" (see § 58).

§ 55. Coagulation of Aerosols During Agitation and in Turbulent Flow

Experimental studies of coagulation velocity during agitation are very complicated due to the circumstance that agitation considerably accelerates the particle precipitation on the chamber's walls, as we explained on page 288. At the same time, the velocity of precipitation increases with the size of particles; consequently, it is also difficult to judge the progress of coagulation according to the increase in average sizes of particles.

LANGSTROTH and GILLEPSIE (361) tried to solve this problem by the method of selection of the coagulation and precipitation constants. Experiments were conducted with smokes of ammonium chloride ($r = 0.5\mu$, $n = 2 \cdot 10^5 \cdot \text{cm}^{-3}$) in a chamber of one m^3 capacity. Agitation was developed with the aid of wide blades, which extended almost to the chamber walls and revolved pendulum-like around a horizontal axis passing through the center of the chamber. The average air velocity \bar{U} in the chamber was determined by means of a thermoanemometer. The calculated as well as gravimetric concentration of smoke was measured. The latter varied according to the logarithmic law

$$\ln(c/c_0) = -\beta' t, \quad (55.1)$$

whereupon the coefficient β' remained almost constant in the course of the entire experiment, which lasted several hours. The results of the experiments are submitted in table 35.

Table 35

Coagulation of Ammonium Chloride Smoke During Agitation

\bar{U} , cm·sec ⁻¹	0	18	48	67	83
$K \cdot 10^{10}$, cm ³ ·sec ⁻¹	3.7	4.0	5.0	7.5	8.7
$\beta \cdot 10^5$, sec ⁻¹	5.5	9.7	11.0	14.5	16.3
$\beta' \cdot 10^5$, sec ⁻¹	5.5	12.0	13.8	18.3	21.7

The decrease in the gravimetric concentration, which ensues from precipitation and which progresses faster than a decrease in the calculated concentration ($\beta' > \beta$), is explained by the aerosol's polydispersion (see page 289). As we already pointed out, such a method in the determination of the coagulation constant is unreliable when the aerosol's polydispersion is involved. Therefore, one must not consider as definitely conclusive in these experiments the acceleration of coagulation while agitation was applied among aerosols with particles, whose radii are of the order 0.5μ . In a more recent work of these authors (357), β was defined by a direct method (see page 285) and the coagulation constant was defined according to the difference. At the same time, it proved to be that, with the increase in the agitation velocity, K decreases first and then it begins to increase. Undoubtedly, this strange effect appears to be the product of errors in measurements.

RICHARDSON (491) studied by an optical method (by means of the optical density of the aerosol) the influence of agitation upon the rapidity of coagulation and, disregarding completely the particle precipitation, he obtained fantastically large values of the coagulation constant in an agitated and non-agitated aerosol. Inasmuch as the aerosol contained a large group of particles with radii up to 5μ , they settled rapidly on the bottom and walls and so the reason for this absurdity is obvious.

The same author, having obtained an aerosol by atomizing a solution of methylene blue, with the particle radii of the order of $3 - 4\mu$, conducted this aerosol through an aerodynamic tube equipped with a turbulence-generating grid, and determined that the average particle size doubled in growth simultaneously. The flow velocity and aerosol concentration were not indicated.

E. TEVEROVSKIY (407), who measured the calculated concentration in a puff of smoke which was released from the ground, deduced the concentration in question by way of a theoretical computed (in accordance with §47) concentration and, assuming that any difference will depend upon coagulation, he obtained the values of the coagulation constant from

$50 \cdot 10^{10} \text{ cm}^3 \cdot \text{sec}^{-1}$ with a wind velocity of $1.15 \text{ m} \cdot \text{sec}^{-1}$ to $17700 \cdot 10^{10} \text{ cm}^3 \cdot \text{sec}^{-1}$ with a wind velocity of $5.9 \text{ m} \cdot \text{sec}^{-1}$.

Inasmuch as, in measuring this concentration, quite large errors and fluctuations were unavoidable due to pollution in the air, the results, which include atmospheric turbulence that could increase the coagulation constant by several thousand times, must be regarded with a great caution.

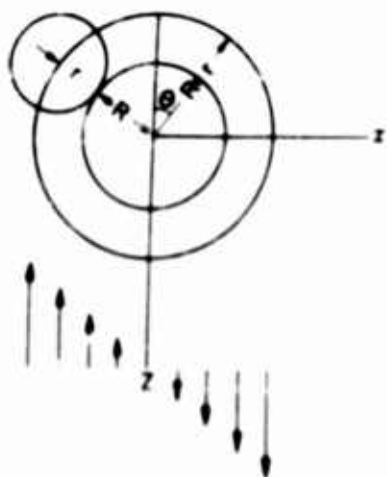


FIG 75 THEORY OF GRADIENT COAGULATION

In view of the above, the coagulation of aerosols during agitation and in a turbulent current has been, up to the present, studied rather badly. As we

proceed to the theory of these phenomena, we shall begin with

M. SMOLUCHOWSKI'S (492) equation for the velocity in the "gradient" coagulation, which occurs if a diametrical gradient of velocity is present in a current. SMOLUCHOWSKI disregarded the diffusion and the distortion of flow lines close to the particles and, with this assumption, the problem can be solved in a simple way. Let's consider that the flow is directed along the axis z and that the gradient of velocity ∇ is along the axis x (figure 75). We take one particle with a radius R in an immobile absorbent sphere, whose radius is $R + r$; where r is the radii of other particles. The current velocity, as regards the selected particle, equals $U = \nabla x = \nabla (R + r) \sin \theta$. The number of particles which in one sec reached the surface of a spherical layer, limited by coordinates x and $x + dx$, is equal to

$$d\dot{\Phi} = nU \cdot 2(R + r) \cos \theta dx = 2n\nabla(R + r)^3 \cos^2 \theta \sin \theta d\theta; \quad (55.2)$$

consequently, the total number of particles which reached the absorbent sphere (from above and from below) is equal to

$$\Phi = 2 \int_{\theta=0}^{\theta=\frac{\pi}{2}} d\Phi = \frac{4}{3} n \Gamma (R + r)^3 \quad (55.3)$$

or, in case of the aerosol's polydispersion, it is equal to

$$\Phi = \frac{32}{3} n \Gamma r^3. \quad (55.4)$$

If we take into account the distortion of lines of flow near the particles and the factor of the relative velocity of the particles which pass each other at a close distance, and also consider their resultant inertial displacement in the given case, both of which are very small, then, according to table 32, it would be expedient to reduce considerably the numerical coefficients in equations (55.3) and (55.4).

Nevertheless, the replicate experiments (493) pertinent to adhesion of vitreous globules, with $r = 60-70\mu$, in a gradient flow of a very viscous liquid (sirupy), whose $\Gamma = 0.4 - 0.8 \text{ sec}^{-1}$, brought a very good concurrence with equation (55.4). It is possible that the rotary motion of the globules in a gradient flow (see page 56) compensates in an estimable amount the effect of the trajectory's distortion.

Thus, the ratio of the velocity of the gradient and of the thermal coagulation is equal to

$$\frac{\Phi}{\Phi_0} = \frac{32n\Gamma r^3}{3 \cdot 16\pi n D r} = \frac{2\Gamma r^2}{3\pi D} \quad (55.5)$$

One can readily see that a gradient coagulation cannot produce the effect which LANGSTROTH and GILLEPSIE described. No doubt during their experiments the gradient reached its maximal magnitude in spaces 10 cm wide between the ends of the blades and the walls of the chamber. Inasmuch as the highest linear velocity of the blades was in the order of $2 \text{ m} \cdot \text{sec}^{-1}$, then the maximal value of the gradient could have amounted to 20 sec^{-1} and the average value was much lower. According to the equation (55.5), at $r = 0.5\mu$ and $\Gamma = 20 \text{ sec}^{-1}$, the $\Phi/\Phi_0 = 0.4 \cdot 10^{-2}$, i.e., the effect of gradient coagulation amounts to zero.

Coarsely dispersed aerosols present a different aspect. Thus, with $r = 10\mu$ and $\bar{\Gamma} = 20 \text{ sec}^{-1}$, the ratio of gradient and thermal coagulation according to equation (55.5) is equal to approximately 16, i. e., with a gradient not very low, the coagulation is noticeably accelerated.

Gradient coagulation can be extremely intense even in a near-wall layer in the presence of turbulent flow, and one may be convinced about it in the following way. The value of a gradient at the wall, $\bar{\Gamma}_0$, may be found with the equation: $\tau_0 = \eta \bar{\Gamma}_0$; where τ_0 is a friction force of the gas against one cm^2 of wall, and it is combined in the equation $U^* = \sqrt{\tau_0 / \gamma_g}$, with U^* denoting a drag velocity. It follows, hence, that $\bar{\Gamma}_0 = U^{*2} / \nu$. According to the experiments of NIKURADZE (389), conducted with tubes, the ratio of \bar{U} / U^* with $\text{Re} = 300 - 100\,000$ was within the range of 14 - 28 and the value of $\bar{\Gamma}_0 / \bar{U}^2 = 0.008 - 0.03$; thus, e. g., with $\bar{U} = 10 \text{ m} \cdot \text{sec}^{-1}$, the value of $\bar{\Gamma}_0 \approx 10^4 \text{ sec}^{-1}$, i. e., a noticeable acceleration of the coagulation may occur in a near-wall layer in the aerosol with particles of radii 0.5μ .

As we proceed to the theory of coagulation of aerosols in a turbulent current, we shall pause at the work of V. LEVICH. In one work (494), he examined the coagulation produced by fluctuations in a scale of the order of the size of the aerosol particles, i. e., considerably lower than was the inner scale of turbulence λ_0 . No authentic experimental data pertinent to the magnitude of these fluctuations are available. Fluctuation velocities, computed according to the theory of HEISENBERG (367), are considerably lower than those computed according to the theory of A. OBUKHOV and A. YAGLOM. Thus, for an average quadratic relative fluctuation velocity of two particles in a turbulent medium (with their velocity directed along the lines of the particle centers), A. OBUKHOV and A. YAGLOM (364) found the following expression

$$u_\lambda = \sqrt{\frac{1}{15} \frac{\epsilon}{\nu}} \lambda, \quad (55.6)$$

which V. LEVICH adopted as a basis for his computations. Here λ denotes the distance between particles; ν is the kinematic viscosity of the medium; ϵ denotes the velocity of the turbulent energy dissipated in one cm^3 of the medium and is connected to λ_0 by the equation

$$\lambda_0 = \left(\frac{\nu^3}{\epsilon} \right)^{1/4}. \quad (55.7)$$

Hence, the following expression is obtained for the coefficient of diffusion for fluctuations of λ scale:

$$D_\lambda \approx \lambda u_\lambda \approx \frac{1}{4} \sqrt{\frac{\epsilon}{\nu}} \lambda^2 = \beta \lambda^2. \quad (55.8)$$

Thus, the velocity of diffusion of two particles toward each other in a turbulent medium decreases proportionally to their approach. Hereupon, for a fixed flow of the particles, diffusing toward an absorbent sphere with a radius of $2r$, the following expression (see equation /38.32/ on page 232) is obtained:

$$\Phi = 4\pi \rho^2 D_\rho \frac{dn}{d\rho} = 4\pi \beta \rho^4 \frac{dn}{d\rho} = \text{const.} \quad (55.9)$$

Considering the limiting conditions for $n = 0$ at $\rho = 2r$ and $n = n_0$ at $\rho = \infty$, we obtain

$$\Phi = 32\pi r^3 \beta n_0 \approx 25 \sqrt{\frac{\epsilon}{\nu}} r^3 n_0. \quad (55.10)$$

The above equation, but with another coefficient, can be obtained by a different method if we consider, according to N. TUNITSKIY (495), that a gradient coagulation of particles takes place in a turbulent current, i.e., the coagulation which is conditioned by the relative fluctuation velocity under given conditions directed toward the line of the particle centers; this velocity according to A. OBUKHOV and A. YAGLOM, can be expressed by equation (55.6) after substitution of the coefficient $1/15$ by $2/15$. Hence, the gradient of the fluctuation velocity is equal to

$$\frac{du_\lambda}{d\lambda} = \sqrt{\frac{2\epsilon}{15\nu}}, \quad (55.11)$$

and so, according to equation (55.4), we obtain the following equation for a flow of particles toward a certain particle as a result of the fluctuations:

$$\Phi = \frac{32}{3} \sqrt{\frac{2\epsilon}{15\nu}} r^3 n_0 \approx 4 \sqrt{\frac{\epsilon}{\nu}} r^3 n_0. \quad (55.12)$$

If we combine the ratio of the coefficients of a turbulent and a thermal coagulation of aerosol, thus

$$\alpha = \frac{\alpha \sqrt{\frac{\epsilon}{\nu}} r^3 n_0}{16\pi D r n_0} = \frac{\alpha}{16\pi} \sqrt{\frac{\epsilon}{\nu}} \frac{r^2}{D}, \quad (55.13)$$

where α equals 4 or 25, depending whether equation (55.10) or (55.12) is used. As to particles with a radius of 1μ , the $r^2/D \approx 0.1$. It follows, hence, that in order to accelerate noticeably the coagulation of such particles by turbulence, it is essential that $\sqrt{\epsilon/\nu}$ be of the order of 100 and λ_0 , according to equation (55.7), be of the order of 0.1 cm. But, as data quoted on page 291 indicate,

this is possible only in a very high flow velocity. As to particles with a radius of 0.1μ , the effect of turbulent coagulation equals zero and it becomes very high with $r = 10\mu$. A greater magnitude of \bar{E} was attained close to the walls, although here there was a sizable gradient of averaged velocity of flow and, apparently, it acted as a primary cause of rapid coagulation of the aerosol during the experiments of RICHARDSON referred to.

It must be noted that the supposition about the possibility of aerosol coagulation by means of small-scale fluctuations was first expressed by E. TEVEROVSKIY; yet his computation of the effect was prepared incorrectly and he obtained visibly exaggerated values for the coefficient of turbulent coagulation of particles with a radius of 0.3μ .

In the work of V. LEVICH (496), there is a discussion of coagulation of aerosols resulting from a dissimilar degree of entrainment of diverse size particles, caused by fluctuations.¹ Thus, V. LEVICH concluded the following expression for an average quadratic velocity of the relative movement of particles and that of the medium.

$$v_R = aT \quad (55.14)$$

where T is the particle's relaxation time, where a is an average quadratic acceleration in turbulent flow. The above equation can be deduced without difficulty, if the fluctuations are represented as harmonic oscillations with an angular frequency ω . In conformance with equation (20.14)

$$v_R = \frac{u\omega T}{\sqrt{1 + \omega^2 T^2}}, \quad (55.15)$$

where u is an average quadratic fluctuation velocity. In the given case, according to indications submitted in §45, that $v_R/u \ll 1$, also

$$v_R = u\omega T \quad (55.16)$$

It follows also from the characteristics of the oscillations that $a = \omega u$; consequently, $v_R = aT$. The relative velocity of two particles whose distance between one another is small, if compared with the scale of fluctuations, obviously equals $v_R' - v_R'' = a(T' - T'')$. Inasmuch as a relative movement of particles and a medium is possible only in the presence of fluctuations with the scale $< \lambda_0$, and, since these periods of fluctuation t_p according to A. OBUKHOV and A. YAGLOM are no longer dependent upon the scale, the following expression is obtained for a maximal acceleration

$$a = \frac{u_{\lambda_0}}{t_p} = \frac{u_{\lambda_0}^2}{\lambda_0} \quad (55.17)$$

1. EAST and MARSHALL suggested another method for the solution of this problem (576)

UNCLASSIFIED
AD

227876

FOR
MICRO-CARD
CONTROL ONLY

8

OF

9

Reproduced by

Armed Services Technical Information Agency

ARLINGTON HALL STATION; ARLINGTON 12 VIRGINIA

UNCLASSIFIED

"NOTICE: When Government or other drawings, specifications or other data are used for any purpose other than in connection with a definitely related Government procurement operation, the U.S. Government thereby incurs no responsibility, nor any obligation whatsoever; and the fact that the Government may have formulated, furnished, or in any way supplied the said drawings, specifications or other data is not to be regarded by implication or otherwise in any manner licensing the holder or any other person or corporation, or conveying any rights or permission to manufacture, use or sell any patented invention that may in any way be related thereto.

or, according to equations (55.6) and (55.7), this expression

$$a \approx \frac{\epsilon^{3/4}}{\nu^{1/4}} \quad (55.18)$$

L. LEVICH, without taking into account a hydrodynamic distortion of trajectories of particles upon their approach, made a computation in which, with regard to particles with $r = 1 - 5\mu$ and whose $\epsilon = 10^3 \text{ erg} \cdot \text{cm}^{-3} \cdot \text{sec}^{-1}$, the rapidity of a turbulent coagulation of this type is greater than that of a thermal coagulation. Yet, it would be expedient to indicate, that this is also so with regard to particles with $r = 10\mu$, whose $\epsilon = 10^3 \nu_R \approx 0.36 \text{ cm} \cdot \text{sec}^{-1}$ and $\text{Stk} = \nu_R \tau / 2r \approx 0.2$. Since the critical Stk value in a viscous by-passing of a sphere equals 0.6 (see page 193), then inertial precipitation is impossible under these conditions; a coagulation can only occur as a result of capture effect. Thus V. LEVICH'S evaluation of the effect of this type of turbulent coagulation is, according to data in table 32, somewhat exaggerated.

§56. Effectiveness of Collisions Between Aerosol Particles

Of basic importance in the theory of aerosol coagulation is the question of effectiveness of collisions between aerosol particles (i.e., the probability of their adhesion or fusion upon collision). The concepts of "collisions" and of "contact" of particles are not identical, as is evident from the statement below, collisions are possible without contact being made, because of an "air buffer" between particles (large drops). To begin with, we shall discuss the question of the effectiveness of contacts.

The solution of this question by way of direct ultramicroscopic observations is difficult for two reasons. Inasmuch as the depth of focus during ultramicroscopic examination of aerosols cannot be reduced for a number of reasons to more than approximately to 10μ , so the position of particles at a closer distance to each other along the direction of the particle's optical axis seems like being in one optical plane and thus the entry of particles into the same visual beam appears to an observer as a contact. It is obvious that in the given case stereoultramicroscopic observations are essential; yet up to this time they were not undertaken. Furthermore, the approach of two particles to a smaller distance than the resolvable capability of a microscope may also be regarded as a contact. Meanwhile, such particles, without prior contact with one another, may again become separated, i.e., a recognized part observed as being in contact will only appear so. These thoughts were not taken under consideration by some authors as they reported that all contacts between aerosol particles were ineffective when observed by them (497, 498).

It is somewhat easier to solve a similar question about the effectiveness of aerosol particle contacts made with the walls. To do this, the following method was used (499). A glass or a metal speculum was set up at an angle of 10-15° to the optical axis of the microscope. Simultaneously, with a dark-field illumination in the visual field, a mirror image of every particle was visible and at the same time particles contiguous with the speculum were perceived as contiguous with its image. The criterion of adhesion, in the case of liquid particles, was their disappearance, whereas in the case of solid particles, it was a discontinuation of Brownian movement.

Among contacts observed here, some were also apparent, because a contact was regarded as a particle's approach to the wall at a closer distance than $\delta/2$, i. e., at an average distance of $\delta/4$; where δ is the resolvable capability of the microscope. We shall denote by $w(x)$ a probability that a particle found at a distance x from a wall will withdraw from the wall (without making a contact with the latter) to a distance of x' , where the withdrawal will become noticeable to an observer. In accordance with the physical meaning of the function $w(x)$ it follows, that

$$w(x) = \frac{1}{2} w(x + \Delta x) + \frac{1}{2} w(x - \Delta x) \quad (56.1)$$

where Δx is a small displacement. If we analyze the right side of this equation according to TAYLOR'S equation, we obtain $\dot{w}(x) = 0$, i. e., the function of $w(x)$ is linear. Since $w(0) = 0$ and $w(x') = 1$, then it is obvious that $w(x) = x/x'$. In the discussed case, as we indicated above, x is equal to $\delta/4$; x' may be assumed to be approximately equal to δ . Thus, a probability that a contact will be an apparent one is of the magnitude of about 0.25

In experiments conducted with tobacco smoke (consisting of semi-liquid particles), also with smokes of magnesium oxide and ammonium chloride, whose average radius of particles was of the order of tenths of a micron, the apparent non-effective contacts found were in 10 to 25% volume. Their number, practically speaking, remained unchanged even after the slide was coated with glycerine. Meanwhile, if the non-effective contacts were real, their number according to all probabilities should have been noticeably reduced as the substitution of a solid wall by a liquid one took place. That NH_4Cl smoke showed a much higher percentage of apparent non-effective contacts (20-25%) than tobacco smoke and MgO smoke (10-15%) did, can probably be explained by this: that much higher electrical charges existed among the latter than among the former, and that the repulsive forces decreased the probability of the withdrawal of particles which did approach the wall.

These experiments show that the effectiveness of contacts of aerosol particles in the order of magnitude of $0.1 - 1\mu$ with walls is close to 1 and, according to all probabilities, is also equal to 1.

In principle, a magnitude of effectiveness of contacts between aerosol particles can be found by comparing experimentally and theoretically computed values of the aerosol coagulation constant. Yet, repeated contacts (see page 337) decrease considerably the dependence of the coagulation constant upon the effectiveness of a single contact α , whereas for purposes of determination it is necessary to know a rather exact magnitude of the ratio of $K_{\text{exp}}/K_{\text{theor}}$. On the other hand, the exact computation of K_{theor} is at the present time difficult due to the influence of polydispersion upon the velocity of coagulation (see page 341). Therefore, the only conclusion that can be drawn from the measurements of the coagulation constant is this, that α is of the order of magnitude of a unit. In so far as circumstantial evidence of the high effectiveness of contacts between particles may also serve the fact, that the coagulation constants of certain smokes and fogs, which have a close distribution of particle sizes (e.g., of oleic acid fog and of stearic acid smokes), are practically concurrent (428). Meanwhile, non-effective contacts among liquid droplets (in the absence of a solid film on their surfaces, considering, e.g., oxidized or impure mercury) are of very low probability. We should consider that during coagulation of fogs (except mercury), as a rule, not adhesion but a fusion of droplets takes place.

The discussed question may be approached from a theoretical standpoint in the following manner. We will estimate the magnitude of the potential of molecular forces at the time of contact of two spherical particles. For this purpose, equation (51.17) may be used, in which we assume that $\rho = 2r + \delta$; where δ is a length in the order of a molecular diameter. Assuming that $r \gg \delta$, we find that

$$\psi(2r + \delta) = - \frac{\pi^2 Q r}{12\delta}. \quad (56.2)$$

According to data contained on page 357, Q is of the order of magnitude of $10^{-13} - 10^{-14}$. It follows, hence, that the ratio of ψ/kT for particles with a radius of 10^{-5} cm is of the order of $10^2 - 10^3$, i.e., the potential of molecular forces in the given case exceeds considerably the particle's kinetic energy. Thus, even absolutely elastic particles are unable to break away from one another once a contact is made.

Analogous results can be obtained if one proceeds from the expression (derived by BRADLEY /443/ and B. BERYAGIN /500/) for the force which is essential for spherical particles (with radii r_1 and r_2) to break away from one another

$$F = 4\pi\sigma \frac{r_1 r_2}{r_1 + r_2} \quad (56.3)$$

or, in case of identical particles, ¹ for the force

$$F = 2\pi\sigma r, \quad (56.4)$$

where σ is the specific free surface energy of the particles. The energy of Brownian spinning of a doublet (formed of two particles) around the axis perpendicular to the line of centers is equal to

$$\Omega = \frac{1}{2} I \omega^2 = kT, \quad (56.5)$$

where $I = \frac{64}{15} \pi r^5$ is the moment of inertia of a doublet in proportion to its axis; where ω is the average angular velocity of spinning.

A centrifugal force striving to split a doublet is equal to

$$F' = \frac{4}{3} \pi r^4 \omega^2 = \frac{5kT}{8r}. \quad (56.6)$$

Thus, a splitting will result if $F' > F$, i. e., if $r < \left(\frac{5kT}{16\pi\sigma} \right)^{1/2}$. If we assume for σ an order of magnitude of several decades of $\text{erg} \cdot \text{cm}^{-2}$, we note that the splitting of the aggregates under the influence of molecular impulses is possible only if $r < 10^{-8} \text{ cm}$ (502). The centrifugal force is still smaller among much longer linear aggregates.

The theoretical considerations exposed here indicate that all contacts between aerosol particles have to be effective. This pertains, of

-
1. Of the same magnitude order are capillary forces during contacts made among humidified particles (e. g., in hygroscopic smokes). In this case σ denotes a surface tension of a liquid (501).

course, also to the particle contacts made with the walls. We want to emphasize that all this pertains exclusively to contacts caused by Brownian movement among particles. Some more or less large particles, when in motion under the influence of external forces, may bounce off after making a contact; then aggregates can be split by an aerial current, and so on (see pages 393, 398, 422)

A few words must also be said about a large amount of work undertaken by Soviet investigators such as E. RUMYANTSEVA (503), S. URAZOVSKIY and S. KUZMENKO (504), M. SAMOKHVALOV and O. KOZHUKHOVA (435), V. SAICHUK and O. NARSIKH (505), N. ANDREEV and S. KIBIRKSHTIS (506), L. SMIRNOV and V. SOLNTSEVA (507), on the question of the influence of various foreign vapors upon aerosol stability. These undertakings were intended to prepare records of the stabilizing as well as of the sensitizing influences of certain vapors upon aerosols. If we exclude the experiments during which the actual formation of a condensed aerosol proceeded in the presence of foreign vapors, which could have influenced the rapidity of formation and of growth of nuclei, thus the indicated effects are explainable by the basic influence of foreign vapors upon the form and structure of aggregates (see § 50). L. RADUSHKEVICH and O. CHUGUNOVA (508), also I. PETRYANOV, N. TUNITSKIY and M. TIKHOMIROV (509), as well as I. ARTEMOV (510) pointed out that in instances in which these complex phenomena do not occur, foreign vapors to all intents and purposes have no influence upon the velocity of coagulation. This fact is in full agreement with the afore-exposed considerations: a mono- or polymolecular adsorptive layer, formed on particle's surface, cannot lower the magnitude of molecular force potential between particles coming in contact to such an extent as to be comparable with the energy of their Brownian movement. But then, not all is clear as yet in this field: it is incomprehensible why, in proportion to the increase of humidity in the air, the rapidity of coagulation of ammonium chloride fumes decreases at first and then it increases (see page 351), also why linear aggregates are formed in the presence of certain vapors and so on.

Specifically one ought to pause at the phenomenon of large aqueous drops which rebound following their collisions in the air and this has been well known for a long time. The cause of this phenomenon is a thin layer of air present between colliding drops, which does not allow them to come in contact with one another. The same layer is also formed when more or less sizable drops are falling upon a flat surface of a liquid; at times drops float on such a surface without fusing with it. As large rain drops fall, they entrain an aerial layer deep into the water, whereupon the air emerges in the form of bubbles.

Soviet scientists attach great importance to the research on these phenomena. Thus, M. AGANIN (511) discovered a very important fact of the existence of a critical velocity among aqueous drops colliding with a flat surface of water; below this critical velocity, which is approximately equal to $1 \text{ m} \cdot \text{sec}^{-1}$ among drops with a radius of $0.3 - 0.4 \text{ mm}$, a rebound effect takes place, while above that velocity, a fusion occurs. S. GORBACHEV and E. MUSTEL (512) extended similar observations to collisions between free aqueous drops with a radius of 0.5 mm . In this case, the lower critical velocity is equal approximately to $5 \text{ cm} \cdot \text{sec}^{-1}$. The work of S. GORBACHEV and V. NIKIFOROVA (513), as well as that of N. TVERSKAYA (514), also uncovered the existence of an upper critical velocity among collisions. Although the methods in these two undertakings were dissimilar (in the first one, drops of water $/r = 0.3 \text{ mm}/$ were suspended to move on a little thread attached to a pendulum, while in the second one drops $/r = 0.5 - 1.5 \text{ mm}/$ were falling freely upon an immobile drop) the results of the two methods were very analogous; the upper critical rate depended very much upon the angle θ between the lines of the drop centers at the time of collision and the direction of the relative velocity. The larger the angle, the lower was the critical velocity. It equaled $\sim 80 \text{ cm} \cdot \text{sec}^{-1}$ at $\theta = 11^\circ$ and $\sim 20 \text{ cm} \cdot \text{sec}^{-1}$ at 77° . A critical velocity is defined with the exactness of $\pm 10 \text{ cm} \cdot \text{sec}^{-1}$, because between the regions of a full effectiveness and a full non-effectiveness of all collisions, there is an intermediate zone in which both types of collisions are observed.

Following the velocity which exceeds the upper critical value, a part of the liquid flows from one drop into another one (513) at the time of collision and then the formation of splash occurs ("a third drop") (514). It appears that at the moment of collision a connecting duct between the drops is formed; yet, with a higher rate of ricochet, drops fail to fuse and the duct becomes ruptured. Both drops become considerably flattened at the moment of collision. In order to explain these interesting phenomena, continued research is essential.

The work of B. DERYAGIN and P. PROKHOROV (515, 516) is of great importance in that it showed that if a vapor (of hexane, octane, ether, etc.) is present between liquid drops which are immobile and press against each other with considerable resiliency, a persistent gaseous layer can be obtained which remains well preserved for an indefinite time. Naturally, under these conditions, research on the layer would be greatly facilitated. It was discovered that the layer has a lens-shaped form whose thickness in the central part is in the order of 1μ and in the very thin part, in the order of several tenths of a micron. The average curvature of the surface of the

drops $\frac{1}{2} \left(\frac{1}{R_1} + \frac{1}{R_2} \right)$ decreases in the layer's center and it assumes here a negative value. This indicates, according to LAPLACE'S equation, that the excess of gas pressure in the layer increases from the periphery toward the center (it reaches here a magnitude of the order of $1000 \text{ dyn} \cdot \text{cm}^{-2}$). Consequently, the gaseous layer must constantly flow outwards.

If a nonvolatile liquid is involved, the effluence causes a rapid thinning of the layer and the fusion of drops. If there is a sufficiently high vapor pressure of the liquid employed, the diffusion of the liquid's vapor superimposes itself upon the hydrodynamic outflow from the layer toward the surrounding space. Thus, a well developed gradient of the partial pressure in the vapor is established in the layer and (almost the same in its absolute magnitude, but inversely directed) another gradient of the partial pressure of the air is established, which is thus diffusing deep into the layer. Inasmuch as the rapidity of diffusion is proportional to the depth of the layer and the velocity of the outflow to one third power of the depth, thus, with the thinning of the layer a stationary condition must follow whereby the diffusion of air inside the layer compensates its outflow. The higher the vapor pressure of the liquid, or the lower the air humidity, considering aqueous drops, the greater is the stationary thickness of the layer and its persistency. A quantitative theory of this phenomenon was prepared by B. DERYAGIN and P. PROKHOROV and it was later confirmed by them with the aid of replicate experiments. Thus, in accordance with the afore-said and in conformance with experiments of P. PROKHOROV and V. YASHIN (517), the lower critical rate of collisions of aqueous drops increases noticeably in proportion to the increase in the humidity's deficit. Let's assume that drops of non-volatile liquids, as well as drops of volatile liquids, fuse almost instantly upon collision in space saturated with their vapors. V. FEDOSEEV and A. POLYANSKIY (577) discovered a repulsion between aqueous drops which were vaporizing at a comparatively great distance between one another. The repulsion force comprised $1.6 \cdot 10^{-4}$ dynes among drops with one mm radius and at 0.1 mm clearance between them when relative humidity of air was 55 - 60%.

The work of P. PROKHOROV and L. LEONOV (518) included research on the influence of relative humidity's deficit upon the velocity of gravitational coagulation in aqueous fog. A fog with droplets of radii of $4 - 40 \mu$ was admitted into a vertical tube from below with a velocity of 20 or $40 \text{ cm} \cdot \text{sec}^{-1}$; at the same time, droplets with $r > 30$ or 40μ became separated from the fog, as their rate of fall exceeded the velocity of the current. As the fog flowed up, it passed through a micro-heat-exchanger (built in the tube), which changed the fog's temperature by several degrees

either up or down, changing at the same time the degree of saturation of the air by the fog. Thereupon, the fog passed by little windows which served for ultramicroscopic observations. The tube narrowed down considerably at the height of 5 cm above the little windows. Due to coagulation, the sufficiently large drops which were falling within the 5-cm space were recorded by an observer. It was found that in the presence of low supersaturation, the number of droplets falling per time unit did not change, but in the presence of a partial saturation, the number decreased almost proportionally to the humidity's deficit and this indicated the decrease in effectiveness of the collisions between the drops. In order to eliminate the possibility of drops falling out as they became enlarged due to the vapor's condensation, a small and partial expansion in the tube was provided, which separated the very large drops from the needed "reserve stock." Considering that a substantial deficit of humidity is scarcely probable in natural clouds, the effectiveness of collisions in the clouds should apparently be close to 1, as this was discovered during laboratory experiments of SHISHKIN and KHIMACH (see page 199) and of GUNN (see page 373), which were conducted with air saturated with aqueous vapor.

While examining the precipitation of a condensed aqueous fog and of a fog obtained by an atomized solution of an electrolyte on the bottom of a smoke chamber, V. FEDOSEEV, B. MANAKIN and Z. DOMENTIANOVA (519) discovered that when both fogs were combined, the sedimentation mass exceeded noticeably the amount of sedimentation obtained from the fogs individually. Yet, the natural supposition, that here on the droplets from the solution a condensation of vapor took effect, is rejected by the authors, who promote a less logical hypothesis, that the difference in the vapor pressure between the aqueous droplet vapor and that of the solution contributed to the droplet coagulation, eliminating the aerial layer. In order to confirm this opinion, the authors quote the following observation which they made. During the atomization of a weak solution of KCNS and of a strong solution of $\text{Fe}(\text{NO}_3)_3$ in a chamber, almost all drops in the fall-out were colored and then, as the concentrations of both solutions became equal, very few colored drops were observed. This strange phenomenon should be examined more thoroughly because it could also be explained in some other way.

In conclusion we shall pause at some questions important from a practical standpoint which refer to the influence of wetting agents upon the effectiveness of precipitation of aerosol particles if assisted by atomized water and also pertinently to the effect of adding wetting agents to water. There is a widespread opinion about low effectiveness of precipitation if aqueous vapors are applied on poorly-wettable dusts (e.g., of coal). In defending this opinion, a fact is cited that fused spherical particles of ashes

are retarded by atomized water better than particles of unburned coal (520). Yet, the main cause of a poor interception of coal particles, according to all probabilities, appears to be their flaky shape, due to which they orient themselves parallel to the surface of streamlined drops. At the same time the movement of particles toward a drop is greatly retarded and, furthermore, an aerial layer may be formed between large particles and the drops (see below). In his well-known book, DRINKER (215) explains the very low water absorbability in P_2O_5 fumes by the poorly-wettable peculiarities of the particles.

As we mentioned before, all contacts between small particles during thermal coagulation are apparently effective regardless of the nature of the particle surface. Yet, during kinematic coagulation of more or less large solid particles, with large drops among them, a similar layer of air may develop, as during collisions between large drops; especially so if a flaky particle with its flat side collides with a drop. In such case the surface tension of the liquid may have a substantial influence upon the rapidity with which the layer is pierced, and also may have an influence upon the ultimate result of the collision. It is possible that also the wetting of the particles by means of a liquid is of recognized importance here. Moreover, since the poorly-wettable particles remain on the surface of the drop and are not drawn into it, so, as a result of the high concentration of dust, the entire surface of a drop may become covered with a multi-layer of dust (202). In such a case, a dislodgement of particles by an aerial current may take place (see §57).

As to the effectiveness of adding wetting agents to water being atomized for the purpose of precipitation of aerosols, the existing data are very contradictory. Wetting agents provide a definite effect in a wet drilling, because they assist in spreading water over the walls of a bore hole as a uniform coating; in such a case solid particles colliding against the wall cannot be blown off the latter, as could happen on a dry wall. The effect of wetting agents on the settling of dust already formed is considerably more limited than that in drilling. In some instances, e. g., in the precipitation of an oil spray with the aid of atomized water, the effect amounts to zero (521) and in other instances, e. g., in settling quartz dusts, an important positive effect is recorded (580), so, as we already mentioned, in general, there is a great diversity in literature on this problem. The action of wetting agents may be of two kinds. Since they considerably lower the surface tension of water, much finer atomization is obtained which, under specific conditions (discussed in §54) may improve the effectiveness of precipitation. In addition, as we pointed out, the wetting agents can also improve directly the effectiveness of collisions of large dust particles with aqueous drops.

Chapter VIII

Transformation of Powdery Substances into the Aerosol Stage

§ 57. Transport of Particles and Their Dislodgements by Aerial Currents

In the preceding chapters, we discussed processes of precipitation and coagulation of aerosols, i. e., the adhesion of particles to walls and to each other. This chapter is dedicated to the converse processes, namely, to particles being dislodged from walls and to the dispersion of aggregates which appear to be powdery substances. As we indicated in the introduction these processes play a very important role in the universe and in man's life. Although some phenomena referred to here as of direct practical importance (e. g., fluidization of powders) were examined rather thoroughly, yet systematic theoretical and experimental studies of all the problems as a whole still remain in their initial stage.

Of greatest importance is certainly the dispersion of powders by aerial currents; therefore we shall confine ourselves to the discussion of the relevant problem of dispersion. Two difficulties arise here: the absence of pertinent data as to the magnitude of molecular forces which obstruct the dislodgement of particles from the walls and from each other, and also the difficulty of defining the forces which, on the part of an aerial current, influence the dust particles as they are engulfed by a current. Therefore, the material exposed in this chapter is preeminently of a qualitative type.

In the second half of this paragraph, we shall discuss the phenomenon of particles being dislodged from walls. As observations indicate, the dislodgement is almost always preceded by a certain phase of particle movement on a wall (sliding or rolling over). This is primarily explained so that the components of the tangential air current remain close to wall and likewise, the components of a hydrodynamic force; the latter influence small particles considerably more than the pertinent normal components do. The molecular cohesion of a moving particle on a wall is considerably less effective than that of an immobile particle; besides, new factors appear during the particle movement on a wall and they contribute to the particle dislodgement (see below). Therefore we shall begin to discuss the tangential transfer of particles on a wall by air currents, the process which is far better studied than the process of dislodgement. The transport of particles also represent an independent attraction, because it has a direct connection with the shifting of sands by winds and with the aerial transfer of free-flowing matter.

The most simple feature of this phenomenon, the transfer of particles resting on a horizontal smooth wall, was studied by S. SYRKIN (522) in an aerodynamic tube 10 cm in diameter. The results he obtained with a corundum dust are quoted in table 36, where r denotes the particle radius and \bar{U}_{cr} denotes (in the tube) the average air velocity with which particles deposited on an iron or a glass surface are carried away by the current. In actuality, some particles are carried away with a lower velocity and some with a higher velocity; therefore \bar{U}_{cr} , as such, represents a certain average magnitude.

Table 36

Corundum Particles Carried Away by Air Currents

	$r, \text{ cm}$							
	10^{-4}	10^{-3}	$3.5 \cdot 10^{-3}$	$5 \cdot 10^{-3}$	$8 \cdot 10^{-3}$	10^{-2}	$2 \cdot 10^{-2}$	$5 \cdot 10^{-2}$
\bar{U}_{cr} (exper) on iron wall, $\text{cm} \cdot \text{sec}^{-1}$	--	--	1140	1060	1080	1090	1270	1630
\bar{U}_{cr} (exper) on glass wall, $\text{cm} \cdot \text{sec}^{-1}$	--	--	860	680	650	650	750	870
$U_{r, cr}, \text{cm} \cdot \text{sec}^{-1}$	(0.016)	(1.65)	18.5	30	67	90	204	500
$U^*_{cr}, \text{cm} \cdot \text{sec}^{-1}$	(5.3)	(16.7)	30	32	37	39	41	41
\bar{U}_{cr} (theor) $\text{cm} \cdot \text{sec}^{-1}$	(76)	(280)	550	590	710	740	740	780

SYRKIN assumes, in the theoretical part of his work, that the transfer of particles is effected by their rolling over; thus, to permit a particle of a cubical shape of $2r$ dimensions to roll over, it is necessary that, at the height r , the following force be applied:

$$F > 8r^3\gamma g. \quad (57.1)$$

If the average velocity of the air flowing over a particle is equal to U_r , then the hydrodynamic force influencing a particle will be equal to

$$F_M = \psi 4r^2\gamma_g U_r^2/2, \quad (57.2)$$

where ψ is a coefficient of the drag resistance. Hence, it follows from the inequality of equation (57. 1) that a particle will roll over with

$$U_r > \left(\frac{4r\gamma g}{\gamma_g \psi} \right)^{1/2} \quad (57. 3)$$

No comparison of this equation with experiments was made in SYRKIN'S work. Inasmuch as the coefficient of friction between solid substances μ is less than 1, then the force needed for a particle to slide, $F = 8r^3\gamma g\mu$, is lower than that for rolling over, i. e., a particle of cubical shape will slide, but will not roll over. The fact that \bar{U}_{cr} is lower on a glass surface than on an iron surface points to this: that friction assumes an important role in SYRKIN'S experiments. Also, corundum particles are generally more rounded; therefore they need several times less force for rolling over than equation (57. 1) indicates. We consider, for computation purposes, that $\mu = 0.25$, i. e., we shall drop the coefficient 4 in equation (57. 3).

As follows from the theory of turbulent flow (§46), there is a laminar stratum near the wall and it maintains a velocity gradient expressed in equation (46. 11), i. e.,

$$U = \frac{U_*^2 z}{\nu} \quad (57. 4)$$

We shall see now that the magnitude of $U_* z / \nu$ in SYRKIN'S experiments does not exceed 12, i. e., in accordance with equation (46. 12), one may presume that in these experiments particles are "drowned" in the laminar stratum, and that they are by-passed by the air with the velocity expressed in equation (57. 4). Hence, with the aid of the Re number for the by-passing of a particle, $Re = 2rU_r / \nu$, one can represent the inequality in equation (57. 3) by dropping the coefficient 4

$$\psi Re^2 > \frac{4r^3\gamma g}{\nu^2 \gamma_g} \quad (57. 5)$$

Using table 5 (page 53), we found critical values of Re and of U_r pertinent to corundum ($\gamma = 4$). Subsequently, assuming in equation (57. 4) that $z = r$ and $U = U_r$, we determined the critical velocities of the drag velocity U_{*cr} . Thus, the maximal value of the nondimensional magnitude of $U_{*cr} r / \nu$ (at $r = 5 \cdot 10^{-2}$ cm) is at the same time equal to 12. Finally, with the aid of equation (46. 29), $U_* \approx 0.2 \bar{U} / Re_f^{1/8}$, the theoretical values of \bar{U}_{cr} were computed and are quoted in the table.

In the above conclusion, we made an allowance that the drag resistance of particles lying on a wall, and that of loose particles, are equal. Considering this circumstance, as well as the low accuracy in measurements of this type, one must acknowledge that the concurrence between the theory and the experiment is satisfactory.

According to the computation, the critical velocity must constantly decrease with a decrease in particle sizes. In actuality, as we see from table 36, the tendency toward an increase in \bar{U}_{cr} becomes already noticeable with a transition to particles with radii of $< 50\mu$. Although no systematic measurements were conducted among small particles, yet individual observations indicate that the critical velocity increases here proportional to the diminution of the particles (experiments with coal particles /581/ with radii 25 - 50μ). This is discussed in connection with experiments involving slit instruments (see page 186). Finally, we shall mention the observations of RUMPF (523). Dust, with $r = 0.5 - 6\mu$, lying on a lamina positioned parallel to the flow acquired, with low velocities of flow, a thick friable sediment containing particles of all sizes, whereas at high velocities it received a fine and dense sediment of particles with $r = 0.5 - 1\mu$; it is obvious, that much larger particles were blown away by the current. Usually, at still higher velocities of current no sediment was detected.

The point is that molecular forces between particles and a wall were not taken into account in the afore-quoted computations. It appears that in order to compute these forces, equation (56.3) could be used with $r_2 = \infty$ included in it. In this case, $F = 4\pi\sigma r$ is a force proportional to the first power of the radius of the particles. Unfortunately, this equation is applicable only to perfectly smooth particles as well as walls and it should not be used for practical computations. Actually, if we assume for σ a reasonable value within several decades of $\text{dyn}\cdot\text{cm}^{-1}$, we find according to this equation that the molecular forces must retain spherical particles with radii of several mm on the lower part of a horizontal wall. Naturally, the cohesive force is not determined by the macroscopic radius of a particle, but by the considerably smaller radius of curvature of submicroscopical protuberances with whose assistance a real contact between particles and a wall is made. In any case, this force decreases much slower in proportion to a decrease in the particle size than the force of gravity, i. e., slower than r^3 . This is verified by the fact that when a dust-covered lamina is rolling over, large particles become separated whereas the smaller ones remain. Inasmuch as among sufficiently small particles the hydrodynamic force is proportional to $U_r r$ and hence proportional to r^2 , it follows from the afore-said that the cohesive force decreases slower than r^2 .

S. SYRKIN also defined the "dynamic" critical velocity of flow in the presence of which corundum particles ejected into a current did not cohere to one another, but were carried away by the current. This velocity appears to be approximately 2.5-3 times lower than statistical critical velocity, namely, 3.5 to 5 m·sec⁻¹. According to experiments of YA. AVERBUKH and K. SHABALIN (524), a critical dynamic velocity for particles of aluminum hydroxide, with radii 25 - 30μ, equals 2 - 3 m·sec⁻¹.

We proceed to a very important instance: that of particle movement over the surface of a layer of particles. We refer here to the transport of sand and soil by wind, also to the aerial transport of free-flowing matter, etc. As N. SOKOLOV (525) determined for the first time, the discussed transport is effected in three ways: 1. particles roll over a surface; 2. particles are dislodged from a surface and immediately fall back, i.e., they travel by leaps; 3. particles travel as an aerosol.

The first two processes were thoroughly examined by BAGNOLD (526, 527) at an average air velocity up to 10 m·sec⁻¹ in an aerodynamic tube of square cross section 30 × 30 cm, provided with glass walls. A thick layer of sand was spread over the tube's bottom. The experiments of BAGNOLD were repeated by CHEPIL (528, 529) in testing various kinds of soil and precisely analogous results were obtained concurrently. Hence, the enunciations found below refer to experiments of both authors.

In one series of experiments a dynamic critical velocity of air was determined. In pursuance of this, a fire stream of sand was constantly poured into the frontal part of a tube. With the air velocity becoming lower than the critical one, sand particles falling upon the layer of sand on the stratum's surface developed certain movements which are described below; at a certain distance from the point of the flow's decrease (the distance becomes larger with the increase of air velocity), the movements were discontinued. With velocity exceeding the critical one, the movements expanded and did not diminish in the entire tube. The greater part of the sand particles remained in motion by means of leaping; the trajectories of the leaping sand particles are shown on figure 76. As the drawing shows, sand particles leaped up almost vertically,

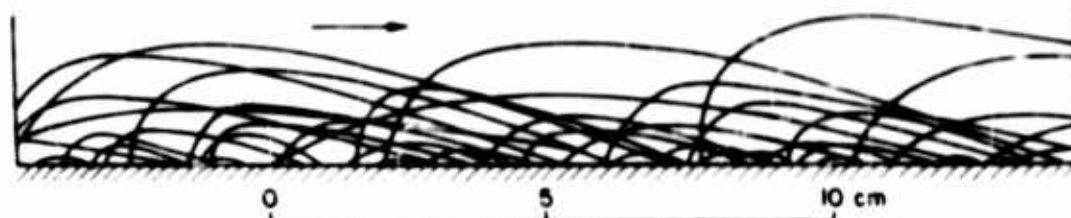


FIG 76 TRAJECTORIES OF LEAPING SAND PARTICLES

then they assumed a considerable horizontal velocity in the air stream, and they fell subsequently at a very sharp angle to the horizontal line. The height of

the leaps at the above-indicated air velocity reached several tens of centimeters. As falling sand particles struck the sand surface, they developed small cavities in it. Sometimes sand particles ricocheted from the surface and repeated their leaps and sometimes they buried themselves in sand and transmitted their impulses to other sand particles, which began to roll over, or to jump up in their turn. In this manner the transfer process assumed the character of a chain reaction.

If streamlines were not formed in sand, the following phenomena could be observed. Singly protruding sand particles began to roll over, as the air reached its definite velocity; yet, before long, they were stopped by falling, e.g., into a small cavity. As the air velocity was increased a little, a certain number of sand particles rolled over again and then stopped again, and so on. Then air velocity was sufficiently high, particles of sand rolling over collided with other large particles which protruded above the surface and at an opportune time they were able to gain a strong, upwards directed impulse to jump up. The entire subsequent conduct proceeded as described above, thus, when the air velocity exceeded the average critical velocity, the impulse from the air current which jumping particles received was sufficiently strong so that the process of jumping and dislodging new particles of sand did not stop, but was expanded much farther. Many jumping particles spun with a high velocity (200 - 1000 revolutions in one sec /528/); this indicates that prior to jumping they rolled over the surface. The number of sand particles with $r = 0.09 - 0.15$ mm carried by means of leaps was 4 - 5 times greater than that of sand carried by rolling over. Speaking of soils, this ratio could vary from 2 to 25 times, depending upon their condition of dispersion (528). Large particles of sand, with $r > 0.2 - 0.3$ mm, cannot leap if the wind velocity does not exceed 10 m sec^{-1} ; they can only roll over, whereas sand particles with $r > 1$ mm remain immobile. Thus, the wind blows out a fraction of much finer sand from polydispersed sands. Finally, the very fine fraction is transferred into aerosolic condition under the influence of an air stream (see below). BAGNOLD'S observation is significant in that, during his experiments conducted without sand being added, the movement of sand particles from without always began in the rearmost part of the tube and it expanded toward the current's direction. Evidently this is associated with a progressive development of turbulence in the air in proportion to air movement in the tube (BAGNOLD did not use any turbulency grid in his experiments).

Since the critical average velocity is greater than the dynamic velocity, then the carrying away of soil, once started, will expand at a greater distance. The process begins at low hills under the influence of

whirlwinds and due to accidental causes. The effectiveness of even low obstacles (corn stocks and such) in the struggle against dust storms could be explained by this: that soil particles cannot leap over the obstacles and thus the same process cannot be prolonged (528).

The results of measurements of the critical velocities of flow affecting sand in various conditions of dispersion are illustrated on figure 77, as prepared by BAGNOLD (527). The

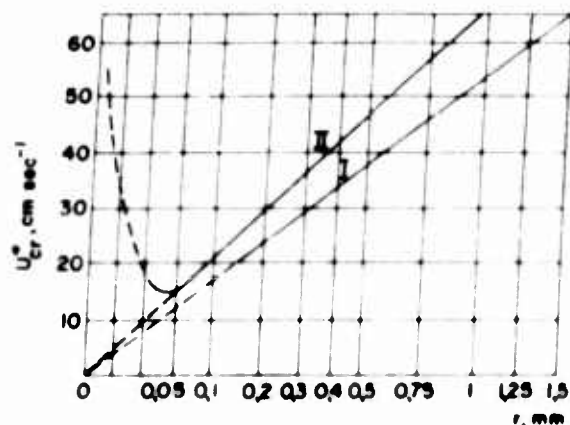


FIG 77 CRITICAL VELOCITIES OF FLOW FOR SAND

solid line I, for drag velocity, and II, for average velocity, were plotted according to experimental points; the broken part of both lines denotes extrapolation. The \sqrt{r} is plotted according to the axes of abscissae and the critical drag velocity is plotted according to the axes of ordinates. As the diagram shows, the U_{cr}^* is proportional to \sqrt{r} at $r > 50\mu$, namely,

$$(\text{dynam}) U_{cr}^* = 164 \sqrt{r} \text{ cm} \cdot \text{sec}^{-1}, \quad (57.6)$$

$$(\text{static}) U_{cr}^* = 208 \sqrt{r} \text{ cm} \cdot \text{sec}^{-1}. \quad (57.7)$$

If r is below 50μ , the U_{cr}^* increases at the time of transition to much smaller particles as a result of molecular forces between particles (this is in full agreement with the aforesaid).

In theoretical computations of critical velocities, it must be taken into account that in a given case the profile of the flow velocities corresponds to a current around rough walls, and this is expressed by the equation

$$U/U^* = 5.75 \lg \left(\frac{30z}{z_0} \right), \quad (57.8)$$

where z_0 is the approximate equivalent of the height of roughness, i. e., equal to the sand particle's diameter. According to BAGNOLD, the rolling

over of sand particles proceeds under the influence of a friction force between the air and the surface of the sand. Assuming that a friction force influencing any particle lying on a sand layer (figure 78) is the same as that applied to a particle from the upper layer of sand particles, i.e., equal to $\pi r^2 \tau_0$, we find the condition for a sand particle's rolling over by comparing the moment of gravitational force, F_2 , of the latter with the point of contact A, equal to $\frac{2}{3} \pi r^4 \gamma_g$, and by comparing the moment of hydrodynamic force, F_1 , around the same point, equal to $\frac{4}{3} \pi r^3 \tau_0$. The condition of rolling over is expressed by the inequality $\tau_0 > 0.5 r \gamma_g$, hence

$$U_{cr}^* = \left(\frac{r \gamma_g}{2 \tau_0} \right)^{1/2}. \quad (57.9)$$

Thus, we obtained the critical velocity's dependence upon the size of sand particles in conformity with BAGNOLD'S experiments; however, the absolute value of statistical U_{cr}^* appeared 4-1/2 times smaller than the one computed according to equation (57.9). Hence, the force influencing a

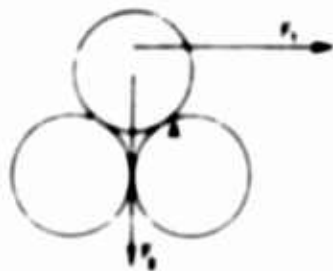


FIG 78 SCHEMATIC DRAWING OF SAND PARTICLES ROLLING OVER

particle lying on a sand layer is greater than that influencing the same particle lying flush with the layer's surface. We shall try to compute the U_{cr}^* by using the method of computation shown in the beginning of this paragraph, namely, according to the particle's drag resistance, and by assuming that the point of application of such resistance lies in the particle's center, and also that the flow velocity at the particle's center level is

expressed by equation (57.8), in which it is assumed that $z = 2z_0$ and consequently, $U_r = 10U^*$. Thus we arrive at the equation

$$U_{cr}^* = \left(\frac{0.013 r \gamma_g}{\psi \gamma_g} \right)^{1/2}. \quad (57.10)$$

Due to the presence of the coefficient ψ in this expression, the proportionality between U_{cr}^* and \sqrt{r} is disrupted here. In conjunction with BAGNOLD'S most careful studies on sand whose $r = 0.12$ mm, it can be computed that $\psi = 3.9$; thus, it follows from equation (57.10) that $U_{cr}^* = 8 \text{ cm} \cdot \text{sec}^{-1}$,

whereas the experimental value of statistical $U_{cr}^* = 23 \text{ cm} \cdot \text{sec}^{-1}$. Therefore, in the case of sliding on a smooth wall, we overestimated the magnitude of the particle drag resistance.

BAGNOLD'S observations conducted in a sandy desert on sand particles of the same size showed that, in this case, the $U_{cr}^* = 23 \text{ cm} \cdot \text{sec}^{-1}$; namely, it is equal to the statistical U_{cr}^* in an aerodynamic tube. This value of U_{cr}^* is appropriate to a wind velocity of $5.2 \text{ m} \cdot \text{sec}^{-1}$ at the height of 10 cm and to a wind velocity of $6.5 \text{ m} \cdot \text{sec}^{-1}$ at the height of one m. N. SOKOLOV (531) found that, pertinent to the same sand particles, the critical wind velocity is $4.5 - 6.7 \text{ m} \cdot \text{sec}^{-1}$ at the height of 10 cm; he also discovered the proportionality of U_{cr} and \sqrt{r} . According to GENZEL (see 532), sand movements begin with the following wind velocities (as table 37).

Table 37

Critical Wind Velocity for Sands of Various Sizes

$r, \text{ mm}$	0.087-0.12	0.12-0.25	0.25-0.5	0.5-1.0
$U_{cr}, \text{ cm} \cdot \text{sec}^{-1}$ (dry sand)	380	480	600	900
$U_{cr}, \text{ cm} \cdot \text{sec}^{-1}$ (sand with 2% humidity)	600	750	950	1200

Submitted here is also the approximate proportionality of U_{cr} and \sqrt{r} , which can thus be regarded as firmly determined.

According to CHEPIL (528), the easiest eroding soils are those with $r = 0.05 - 0.07 \text{ mm}$ when exposed to $U_{cr} = 3.6 \text{ to } 4 \text{ m} \cdot \text{sec}^{-1}$ at the height of 15 cm. Soils with $r < 25\mu$ and sands with $r > 0.5 \text{ mm}$ are practically not affected by erosion; the former, as we already mentioned, are not affected because of cohesive forces between particles.

Leaping sand particles, as a result of the impulse they received from the aerial current, slacken, in their turn, the current's speed in the stratum near the ground. BAGNOLD with an aerodynamic tube, conducted measurements of the distribution of current velocities above the layer of wet sand which remained immobile even at air velocities exceeding the critical velocity; later, he conducted measurements above the same layer after it

dried out and after the process of sand transfer by current began. The results of the discussed experiments are shown on figure 79, where the flow velocities are plotted according to the axes of abscissae, whereas the vertical distance from the sand's surface, being shown in logarithmic scale, is plotted according to the axes of ordinates. The broken lines of velocity contours refer to a wet sand and the continuous lines refer to a dry sand, with $r = 0.09 - 0.15$ mm; the two lines at the extreme left refer to both groups of sand, because the air velocity in this place is below the critical one. The pertinent drag velocity is indicated at each line. Shown on the chart is the distribution of the velocities over wet sand, which corresponds to the logarithmic profile in equation (57.8) with $z_0/30 = 0.0015$ cm. The contour lines cross one another at focal points with the coordinates $z = 0.0015$ cm and $U = 0$. The flow velocity at the height of 2 mm above dry sand is not dependent upon the average air velocity U in the tube and, as BAGNOLD points out, the flow velocity below 2 mm height even decreases as U increases. Generally speaking, the velocity of flow is considerably lower in the stratum near the ground than it would be in the absence of leaping sand particles. This is explained by considerable increase in the number of leaping particles of sand as the U increases and by a corresponding increase in losses of impulses within the current. In such a case, the focal point of contour lines has coordinates $z = 0.2$ cm and $U = 200 - 250$ cm·sec⁻¹.

The amount of sand carried per time unit of the afore-quoted dispersion by aerial current is, according to BAGNOLD, (527) expressed by the equation

$$q = 1.5 \cdot 10^{-9} (U - U'_{cr})^3, \quad (57.11)$$

where U is the flow velocity at the height of 1 m; where U'_{cr} is the critical velocity at the height of a focal point, i.e., 250 cm·sec⁻¹. Measurements

conducted by BAGNOLD in the Libyan desert brought highly conformable results.

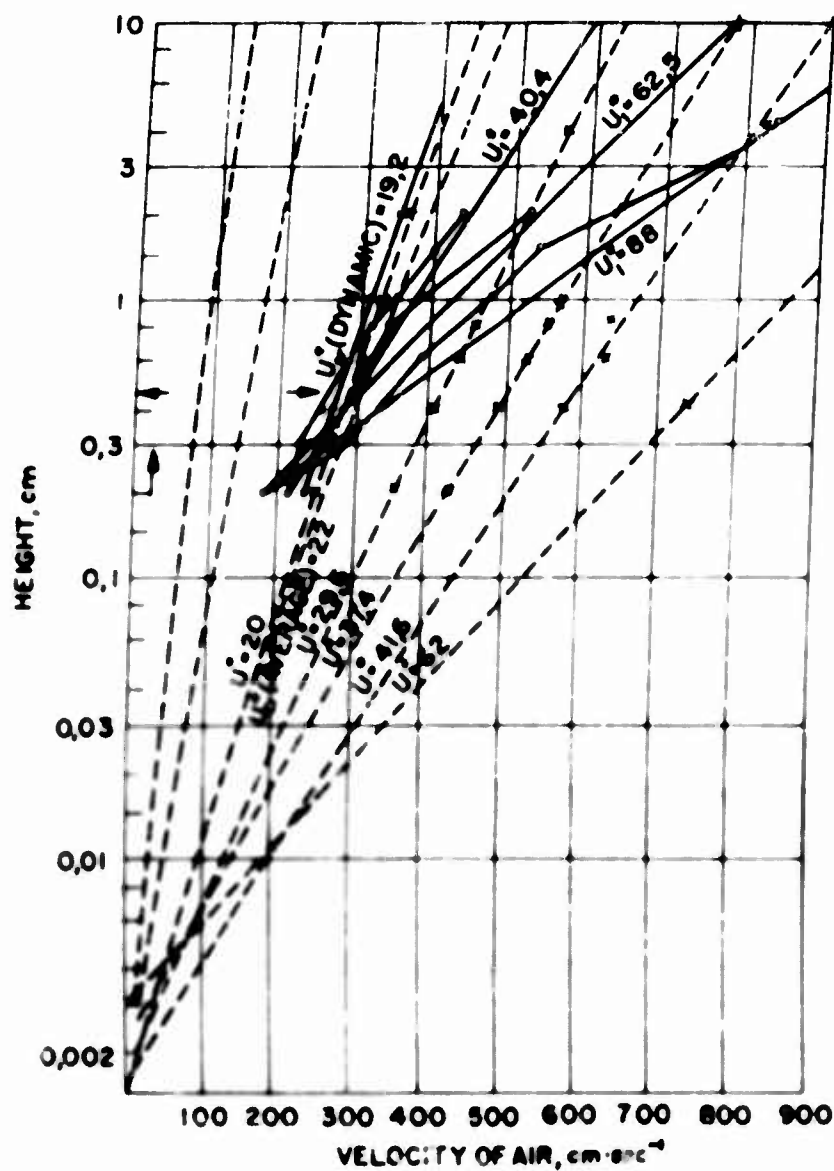


FIG. 79 THE INFLUENCE OF LEAPING SAND PARTICLES UPON PROFILE OF WIND VELOCITY

According to L. DANOVSIIY (533), a noticeable transport of snow begins with a wind strength of $4 - 5 \text{ m} \cdot \text{sec}^{-1}$ (on the ice it begins at $2 \text{ m} \cdot \text{sec}^{-1}$) and it grows rapidly proportional to the wind's intensity. If we adapt as a measuring unit the rapidity of snow transport at a wind velocity between $5 - 7 \text{ m} \cdot \text{sec}^{-1}$, then at a wind velocity of $8 - 10 \text{ m} \cdot \text{sec}^{-1}$, the transport will amount to 10, at $11 - 14 \text{ m} \cdot \text{sec}^{-1}$ it will amount to 30 and at $15 - 18 \text{ m} \cdot \text{sec}^{-1}$ it will amount to 70. Thus, the rapidity of snow transport

increases almost proportionally to $(U - U_{cr})^2$. Hence, a rapid increase in the transport of snow and sand, which follows upon the rising of wind strength, explains the dreadful nature of the phenomena during severe storms.

As we proceed to the question of particles being dislodged from a surface by an air current, we notice that so far the mechanism of this phenomenon is still not quite clear. N. ZHUKOVSKIY'S theorem can be applied to large particles by-passed by air and this resembles an ideal case. As to particles of semicylindrical shape, lying with their flat side on a wall, S. CHAPLYGIN (534) suggested that the lifting power be expressed per semicylinder's length unit according to the equation

$$F_M = \frac{8}{3} \gamma g r U_r^2, \quad (57.12)$$

where r is the radius of a semicylinder. According to JEFFREYS (535), the following analogous equation

$$F_M = \pi \left(\frac{1}{3} + \frac{\pi^2}{9} \right) \gamma g r U_r^2 \quad (57.13)$$

is obtained for cylindrical particles. Here, as above, U_r denotes the flow velocity at the level of a particle's center

That the lifting force influences a large particle on a wall or which is very close to wall, is also understood from the experiments of A. LOSIEVSKIY (536). He determined the presence of this force while experimenting on a rectangular plate, 3.8 mm thick placed in flowing water, parallel to, and 0.5 mm from the bottom. EINSTEIN and EL-SAMNI (537) measured the pressure effective at various points of hemispheres (with $r = 3.4$ cm) as the latter were lying with their flat side on the bottom of a duct; thus, they determined the presence of a lifting power which is proportional to γU_r^2 . In addition, they found out that the magnitude of this force is constant and highly fluctuating. According to the opinion of these authors, the dislodgement of particles from the bottom takes place at the very moment when the fluctuating force attains a definite, critical magnitude.

The origin of the lifting power can be explained graphically in the following way. At the time of by-passing an obstacle positioned on the ground's surface or on a wall, the field of flow appears as is illustrated on figure 67; the current's velocity increases at the upper part of the obstacle and it decreases at its lower part. Inasmuch as beyond the obstacle the

static pressure of air is constant within the vertical cross section close to the near-wall stratum, therefore, according to BERNOULLI'S theorem, the air pressure at the upper part of the obstacle must be more moderate than at the lower part. If the obstacle has a shape similar to a reclining cylinder, or that of a sphere or a similar shape, then the emerging resultant force is directed upwards. It must be emphasized that all the afore-said is not applicable to small particles which are buried in a laminar stratum, because in such a stratum the viscous forces exceed the inertial forces and thus it is impossible to apply BERNOULLI'S theorem.

A particle rolling over a vertical obstacle with a velocity lower than that of air is influenced by the MAGNUS effect, which is directed upwards and whose magnitude can be computed according to the same theorem of ZHUKOVSKI'S. In the opinion of some authors (B. TIRITSYN /538/, R. YOUNG /539/ and others), this effect is the main cause of particles being dislodged from the walls. The lifting power in the case of a cylindrical particle with a radius r (per cm of its length) is equal to

$$F_M = 2\pi r \gamma_g U_R V_r. \quad (57.14)$$

where U_R is the relative velocity of air and that of a particle; where V_r is the linear surface velocity of a rolling particle proportional to its axis and coinciding with the particle's progressive velocity. The U_R and V_r are lower than U_r , but the numerical coefficient in equation (57.14) is higher than that in equation (57.13). In general, the two equations provide approximately an identical order of magnitude for F_M . The equation (57.14) is also inapplicable to particles buried in a laminar stratum.

If, according to equation (57.13), one has to compute velocity of a current necessary for a particle to become dislodged from a horizontal wall, one will find that the said velocity is considerably lower than that needed for particles sliding or rolling over a surface. Meanwhile, as a matter of fact (e.g., in BAGNOLD'S experiments), particles begin to roll over first and then they break away. This points out to the inapplicability of equations (57.12) - (57.14) pertinent to small particles.

It is obvious that in very many instances the dislodgement of particles from horizontal walls by an air current is effected in the following way. At first, the particles begin to move (to slide or roll over) over the surface. After they have reached a sufficiently high velocity, the particle jumping is caused by slight elevations on the wall's surface, or even by the

particles themselves. If, at the same time, a particle jumps out of a laminar stratum, it is picked up by the turbulent vertical fluctuations and, in the case of a rolling particle, by the MOEBIUS force as well, whereupon the particle will be carried far off the wall. According to all probabilities, an analogous procedure also exists among small particles when they are dislodged from walls; these particles are, for the most part, held back by molecular forces. Supposing a plate dusted with any powder is set up vertically, then much larger particles would slide over it and much finer particles would be stopped on this plate. Now, if we gently turn its dusted side downward, then all adhering particles will remain on the plate. This indicates that the force needed for a particle's dislodgement in the direction perpendicular to the surface is in any case no smaller than the force needed for a particle to move over the surface.¹ Inasmuch as hydrodynamic forces along the surface are always greater than those set perpendicularly to it, so it is natural to expect that the beginning of the movement of a particle will be preceded by the latter's change of its position on the surface (sliding or rolling over). At the same time, a decrease in the number of contact points will inevitably take place between a particle and a wall with a decrease in the adhesion force as well. Meanwhile, the probability involving the particle's being dislodged from the wall will be increased considerably.

In addition to jumping up, the cause of the particle dislodgement may be eddies which locally break loose from a surface (e.g., at higher points in a layer of sand, or that of soil), as well as whirlwinds with vertical axes (tornados): both develop low pressure on the inside and as the air close to the ground is sucked in, it may also absorb particles of soil.

The capability of small particles to counteract their own dislodgement from walls is named the adherence, which is of great importance, especially to insecticidal powders (dusts). Inasmuch as the topic under discussion in the given case is the particle dislodgement from walls (foliage, etc.), then the natural weight of the particles does not complicate, but rather facilitates, the dislodgement of particles, inasmuch as adherence is exclusively dependent on the magnitude of molecular force. Therefore, the adherence improves with a decrease in the particle sizes in their entire range.

1. The work of B. DERYAGIN, S. RATNER and M. FUTRAN (540) discloses that the force of static friction between freshly extracted quartz fibers is, in the absence of extraneous weight, equal to the force which is essential to fibers to break away from each other.

of dispersion. Naturally, the size of particles, their shape and the kind of particles, as well as that of the walls, are also of importance, because in a similar type equation (56.3), the magnitude of σ is dependent upon them. Moreover, the pliability of the particle and that of the wall plays apparently an important role. At their contact point and with the influence of molecular forces occurs the flattening of surfaces where the contact is made. As B. DERYAGIN (500) pointed out, as long as this flattening bears the characteristics of a plastic deformation, it leads to a considerable increase of a force which is essential to the particle becoming dislodged. That is why particles of soft substances adhere better than those of hard substances. We want to call attention to an example: on a metallic plate, dusted with a pyrophyllite powder and then rapped lightly 20 times, more particles will remain than if one uses a powder with approximately the same degree of dispersion, but made from a considerably harder material, as e.g., bauxite (541). Moreover, it is understood that flat or needle-like particles adhere better than rounded particles of the same volume. At this point, the humidity is of enormous importance to the aqueous meniscus which forms at the point of contact of a spherical particle with a wall and draws a particle to the wall with a force of the order of $2\pi r\sigma$, where σ is a surface tension of water (501). Inasmuch as, generally speaking, a particle's radius is considerably larger than the radii of curvatures of these submicroscopic protuberances at which a real contact is made (see page 402), then the adherence rises very sharply with humidity. On the other hand, major electrostatic forces frequently emerge during adhesion of particles to walls; so, if such is the case, humidity can decrease adherence. We have to be reconciled to these improved considerations, because experimental data pertinent to adherence of various powders are very scanty.

§ 58. Atomization and Fluidization of Powders

In this paragraph, we shall examine the process of atomization of powdery substances, i.e., their transition from the state of aggregation into an aerosolic condition. In the preceding paragraph we frequently encountered the term, atomization; when air currents of comparatively low velocities flow over a layer of powder, the next result is that particles will become detached from the layer's surface and will be lifted upwards by a turbulent current. Apparently, such is in the nature of the basic mechanism for the transition of solid particles into an aerosolic state. Simultaneously, as the particles are carried away, a packing in the layer takes place with the aid of an air current; next follows the formation of well streamlined contour lines in the layer (522) and so on, whereupon the transport of the particles is stopped. Now in order to resume the process, a considerably higher flow velocity is necessary, and thus everything is repeated all over again. Yet, with very high flow velocities and with a simultaneous carrying away of individual

particles, whole aggregates are also pulled out; they are instantly atomized by the air stream and, as little cavities form on the layer's surface (526), the entire surface becomes more uneven; this facilitates a condition, so that the dislodgement of aggregates is continued. Thus one observes here a transition from a "superficial" to a "volumetric" atomization. The latter also occurs in atomizers for dust, such as are used for atomizing coal dust in fire chambers, during aerial separation of powdery materials (see page 65), and also in atomizing insecticidal compounds (dusts), as well as in carrying out chemical reactions in a "boiling stratum" and so on. Therefore, a volumetric atomization is of very great importance in technology. The knowledge about the mechanism of atomization of powders has improved considerably in recent times due to experimental studies conducted in the fluidization of powders (i. e., their transfer into a "boiling" state), which is of great interest from the standpoint of chemical technology. Therefore, we shall begin with a description of this phenomenon as has been examined in a gaseous fluid medium.

If a layer of powder is placed in a cylindrical vessel with a porous bottom, and water or gas is introduced from underneath, as the velocity of the water or gas is progressively increased, the following phenomena can be observed (see figure 80, which illustrates the fluidization by air of a vitreous powder with spherical particles of 0.135 mm (41/542/)). If the powder's particles remain immobile at low velocities, i. e., $U < U_{cr}$, and also if the layer's height L and the coefficient of space filling ϕ remain constant, then the layer's resistance Δp will be expressed by the well-known equation of Poiseuille:

$$\Delta p = L \text{grad } p = \frac{\alpha L U \eta \phi^2}{r^2 (1 - \phi)^3} \quad (58.1)$$

where $\text{grad } p$ is the pressure gradient of a medium in a layer; where r is the average particle's radius; where L is the layer's height; where U is the current's velocity above the layer; where α is a coefficient dependent upon the particle's shape. Whenever the medium's pressure gradient becomes equalized with the powder's hydrostatic pressure gradient, which is equal to $g\phi(\gamma - \gamma_g)$, i. e., when

$$\Delta p = L g \phi (\gamma - \gamma_g) = \frac{\alpha L U_{cr} \eta \phi^2}{r^2 (1 - \phi)^3} \quad (58.2)$$

then the equivalent of all forces influencing a particle becomes congruent with zero. With the attainment of the current's velocity U_{cr} corresponding to the

above equation, the layer begins to expand, but the resistance remains constant because the product of $L\phi$ is obviously constant.

Already, at this stage of the layer's expansion, the influence of the medium and that of dispersion begin to manifest themselves in the behavior of the powders. During fluidization of powders with $r > 0.15 - 0.20$ mm in a gaseous medium and then in an aqueous medium at a still considerably greater dispersion, the layer's resistance continues to conform with equation (58.1), whereas the layer's expansion, i.e., the decrease of ϕ proportional to the increase in the current's velocity, can be determined from the equation (58.2). This indicates that under these conditions the powder expands evenly, and also

the contact between adjacent particles is maintained although the powder adapts a more porous structure. Thus, in the case of isodispersed powders containing

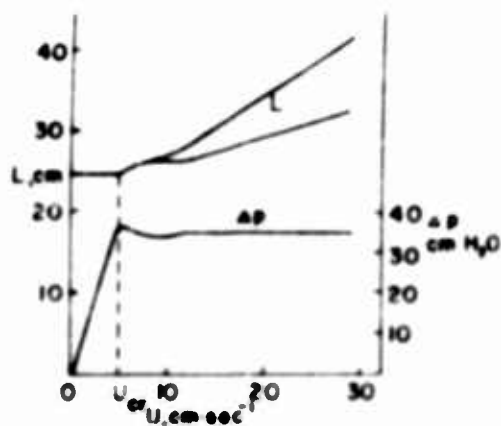


FIG 80 THE DEPENDENCE OF THE CURRENT VELOCITY, WITH PRESSURE AND HEIGHT OF LAYER DURING FLUIDIZATION

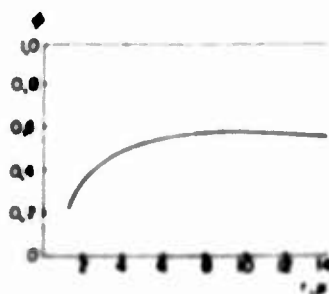


FIG 81 DISPERSION AND THE APPARENT DENSITY OF POWDERS

spherical particles, the ϕ decreases approximately from 0.66 to 0.54 (543). Inasmuch as with the most dense packing of spheres the $\phi = 0.74$, and with the most common cubical contents the $\phi = 0.52$, then in the discussed case the structure of the expanded layer remains close to the cubical contents.

Among more dispersed powders where the cohesive forces begin to play a noticeable role between particles, deviations from equation (58.1) are obvious. The ratio of $U / \Delta p$ increases more rapidly than according to the discussed equation and is no longer proportional to $(1 - \phi)^3 / \phi^2$, but to $[(1 - \phi^3) / \phi^2]^s$ ($s > 1$), whereas the coefficient s increases in proportion to the decrease in the particle sizes (544). This observation indicates that it is not an even expansion of powder which takes place here, but that the powder disintegrates into individual aggregates instead, and between the latter slot-like paths are formed. A considerable amount of gas passes through these paths; therefore the current's velocity is higher than one computed according to equation (58.1).

We shall note that the influence of cohesive forces upon the properties of powders manifests itself also under static conditions (in the absence of air movement). The so-called "apparent density" of a powder, equal to $\phi\gamma$, is almost non-dependent upon particle size among coarse powders because it is determined by the ratio of the particle weight to the (proportional to weight) friction force between particles. The molecular forces begin to manifest themselves in proportion to the increased dispersion of the powder; they increase the friction force between the particles and thereby contribute to the formation of a coarser structure. Thus, the apparent density begins to decrease (545) (see figure 81). The condition pertinent to the powder's angle of rest is analogous, which is also not dependent upon the particle size among very coarse powders, and it increases as the transition to small particles advances (546).

B. DERYAGIN states that the molecular forces, just as small or distinct, which exist between particles in an aqueous medium, disjoin the action of water so thoroughly that a uniform expansion occurs even among highly dispersed powders. But in a gaseous medium, the action that is consumed on overcoming molecular forces during a uniform expansion in a layer of small particles is considerably greater than the action which is essential to break up a powder into individual aggregates, and that is precisely the reason why this occurs.

In proportion to the layer's expansion, its fluidity (measured e. g., according to the resistance of rotatory stirring in a layer) increases several deca-times (547), whereas the side slope angle decreases considerably (542), i. e., a powder by its own characteristics approaches the peculiarities of a liquid. The side slope angle in an aqueous medium finally comes to zero and this indicates that a contact between particles is discontinued. This angle retains some ultimate magnitude in a gaseous medium.

It should be noted that the rule expressed in the equation (58. 2) is fulfilled in a gaseous medium provided the layer's height does not exceed by too much the diameter of the tube in which the powder is deposited. Otherwise the friction of powder against the walls of the tube begins to manifest itself and the layer begins to expand with the ratio of $\text{grad } p / g\phi\gamma$, which somewhat exceeds a unity (548).

Thereupon, when the layer's expansion has reached a definite magnitude of from 5 to 20% of the original volume, which depends upon the powder's properties and dispersion, the particles begin to move and the layer's resistance somewhat decreases (see page 16), probably due to a decrease in friction between the particles. Beyond this point, the picturization between an aqueous and a gaseous medium differs sharply. In the

first instance, a "complete" fluidization is observed: a layer continues to expand evenly as the particles are freely suspended in the current, whereas the dependence between the coefficient ϕ and that of the current's velocity remains the same as that between the ϕ and the velocity of precipitation of the suspension within a limited volume (542) (see §14).

Whether a complete fluidization can take place in a gaseous medium is not known, because no experiments were conducted on such powders which should fluidize particularly well, as, e.g., lycopodium does. At any rate, the conditions for a complete fluidization in a gaseous medium are very unfavorable due to the great magnitude of molecular forces and small viscosity of gases. Therefore, the following situation can be observed here. Taking under consideration coarse powders, the gas at certain flow velocity begins to bubble through a uniformly expanding layer as though through a liquid. Thus, the layer's height begins to rise, yet it varies sharply (see figure 80). The gas pockets create in the powder a very energetic stirring; it assumes the trend of a circulation as it rises in the tube's center and then drops down at the walls (544). A powder in this state very much resembles a boiling liquid. As the current's velocity increases, the entrainment from a "liquid" stage begins, namely, from a boiling stratum into a "gaseous" (aerosolic) stage of particles, whose precipitation velocity remains lower than the flow velocity above the layer, the concentration of particles in the aerosolic stage increases everywhere, finally, the border line between the two stages vanishes and the powder is completely air borne by the gas (549).

As to the structure of the expanded layer here described, it is obvious from the explanation which follows that a contact between particles is maintained but, due to equalization of the gravitational force by the gas pressure, the friction between particles remains very small and this explains the high fluidity in fluidized powders.

That a complete fluidization is not observed among coarse powders, where cohesive forces do not have to sustain an important part, is apparently explained by the action of hydrodynamic forces (§23) between the particles (550) which do not allow a layer of powder to expand evenly. These forces grow larger with the increase in particle size.

The so-called aggregate fluidization is observed among fine powders. With low velocities of flow, ducts are formed in a layer and the basic volume of gas passes through the ducts. As the flow velocity becomes accelerated, the ducts become wider and energetic stirring in the layer begins to take effect; also, a constant formation and disintegration of the aggregates is accompanied by individual particles being carried away into an

aerosolic stage. The smaller the particles, the stronger their aggregation manifests itself, and so much the worse their fluidization proceeds. Inasmuch as hydrodynamic forces grow stronger and the effect of molecular forces decreases as the particle sizes increase, one should anticipate that the conditions for a uniform fluidization are most favorable at some intermediate degree of dispersion of the powder. Actually, indications are that the most uniform fluidization of powders is observed with $r = 25\mu$ (551) and 20μ (552), and that the tendency toward formation of gas pockets in a layer improves with the increase of r among coarse powders and with the decrease of r among fine powders (553).

Inasmuch as the powder's friction against the walls of a tube decreases in proportion to the increase in particle size (the effect of molecular forces decreases) among coarse powders in tubes of small diameter one can observe a "bread-rising" phenomenon in a layer: the layer is lifted up by gas, then the gas breaks through the layer and the layer settles down again.

The use of fluidized catalyzers has the following advantages: a free access of reacting gases to the catalyzer's particle surface; a rapid elimination of heat, which averts overheating, and then the opportunity for uninterrupted transfer of the catalyzer from the reactor to the regenerator and vice versa. The coefficient of heat coming from gas flowing through a tube and transmitted to the walls is considerably increased in the absence of a fluidized powder as a result of a very intensive powder stirring by gas pockets (554). Fluidized catalyzers are mostly used for a vapor-phase cracking of hydrocarbons.

Upon the gradual decrease in the flow velocity and after a complete shutdown of the flow of gas, the powder's layer will remain in an expanded stage; it is necessary to shake it up in order to bring it back to its original, unexpanded stage (544). It follows, hence, that the contact between particles is maintained in an expanded layer and thus the assertion found in reports, that particles in an expanded layer are surrounded on all sides by a "gaseous coating" and consequently do not contact each other, is groundless. It was convenient to determine by the indicated method the ϕ_{\min} values, which corresponds to the expanded stage and which we submitted in table 38 (555). The table also shows the ϕ_0 values, which correspond to a quiescent, unexpanded layer. If we measure the ϕ_{\min} while gradually increasing the velocity of flow, the results obtained will be variable. In this case, the ϕ_{\min} will depend upon the initial packing of the particles (556), because they are unable to re-distribute themselves. Some authors measured the ϕ_{\min} by way of gas admittance, and they obtained considerably lower

values than those in the table due to the presence of gas pockets in a layer. We assume that the magnitude of ϕ_{\min} corresponding to a maximal possible porosity, or to a maximal possible volume of a given powder while contact between particles is maintained, is one of the most important physical characteristics of powdery materials.

Table 38
Coefficient Values of Apparent Volume
During Fluidization of Powders

	r, μ	ϕ_0	ϕ_{\min}
Vitreous globules	285	0.67	0.55
	115	0.66	0.54
Round sand	185	--	0.58
	80	--	0.56
	42	--	0.53
	25	--	0.46
Angular sand	160	--	0.50
	100	--	0.47
	42	--	0.43
	27	--	0.42
Ferric oxide	187	0.50	0.48
	100	0.48	0.44
	35	0.42	0.39

Table 33 shows that the degree of apparent volume decreases together with the particle size not only in a quiescent, but also in an expanded layer which fact also implies that molecular forces are preserved and, consequently, that a contact between particles, along with the layer's expansion, is also maintained.

We assume that certain powders can be brought to an expanded stage not only by way of passing gas through them, but also by a simple and careful interspersation (557). Some powders in this stage also possess a higher fluidity and, by their characteristics, they resemble a liquid. Evidently the air between particles retards their falling and assists in the

formation of porous structures. Inasmuch as in the given case gravitational force does not equalize itself, the fluidity of some powders can probably be explained by the smallness of molecular forces and thus by the smallness of the friction force between particles as well. The obviously high fluidity which lycopodium possesses promotes high isodispersion, the lightness and sphericity of its particles, as well as the presence of small ridges on the particle surfaces; this promotes porosity in the powder's structure.

Following the experiments in fluidization, we so far explained only the influence of the medium (aqueous or gaseous) and partly that of the dispersion of the powder upon its atomization, i. e., capability of transition into the aerosolic stage. The influence of the particle shape, as well as of the kind of substance, still remains wholly unexplained. Meanwhile, we know that certain powders "raise dust" vigorously during their interspersion, while others with the same degree of dispersion raise no dust. We also know that the question of atomization of powders is of great importance in technology, and particularly so in the dusting of crops with insecticidal compounds. At this point, much can be repeated about the adherence which we discussed in the preceding paragraph: atomization is determined in the first place by the magnitude of the cohesive forces between particles; it improves with the increase in particle size and it depends very much upon the powder's dampness. For this reason non-humidified hydrophobic powders (e. g., talcum) can be better atomized than purely hydrophilic powders (e. g., of quartz or limestone). According to ALBINSSON (481), the rapidity with which quartz powder, with $r = 25 - 50\mu$, is sieved, depends upon the humidity in the air where the powder was stored; it begins to decrease sharply in the presence of a relative humidity above 70%. Yet, some decrease in sieving velocity can also be noted in the presence of a relative humidity $< 10\%$, but this phenomenon can, at the same time, be eliminated if a radioactive substance is added to a powder, i. e., if charges are cleared off the particles. Evidently, when a very dry powder is sifted, nascent charges contribute to the formation of stable aggregates, or even to the adhesion of particles to the sieve.

It is more difficult to atomize powders derived from soft and flaky substances than those of solid substances; isodispersed powders are easier to atomize than polydispersed because the degree of apparent volume among the latter and, consequently, the number of contact points between particles is higher than among isodispersed powders.

Experimental data pertinent to atomization of various powders are very scanty. One can quote here only the data which ANDREASEN (558) obtained in the following way: 2 cm^3 of powder were poured through a narrow slot into a tube 250 cm high and 4.5 cm in diameter. The powder, in

course of dropping down, was to some extent atomized by air while falling. Then the percentage of powder which did not settle on the tube's bottom within 6 seconds was determined. Inasmuch as individual particles of the examined powders could not settle within this time, the author assumed that the figures thus obtained corresponds to the percentage of atomized powder, and he named this a magnitude of the powder's "atomization". Yet, actually, even small aggregates could have been included in the group which failed to settle. Some results of ANDREASEN'S experiments are submitted in table 39

Table 39
Atomization of Some Powders

Material	Particles' radius (range), μ	Atomization, %	Material	Particles' range (range), μ	Atomization, %
Lycopodium	12	100	Siliceous dust, poly-		
Charcoal dust	0-25	85	dispersed, coarse	--	21
Aluminum powder	0-15	66	The same, fine	--	8
Talcum	0-20	57	Siliceous dust, isodis-	11 5	68
Soot	0-15(?)	47	persed	8	83
Potato starch	0-35	27		5 6	45
Charcoal dust	0-7	23	Porcelain dust, rendered	7	50
Graphite dust	0-25	17	free from fine fractions	4 7	52
Pulverized slate	0-25	13		1. 1	21
Cement	0-45	5.5		0 45	12
Pulverized slate	0-17	5.5	Porcelain dust, not ren-		
Prepared (elutriated) chalk	0-6	1.5	dered free from fine		
			fractions	--	5

The question of atomization of powders is of great importance in the prevention of explosions in coal mines with the aid of inert powders. As dust (usually of limestone) is picked up the the explosion's wave, it checks the spreading of the explosion. It is important that the powders used for this purpose be suitable for a thorough atomization. It was found that if 0.5% of soot

is added to pulverized limestone to reduce the cohesive force between the limestone particles, the atomization of the latter by explosion wave is considerably improved (559).

As we mentioned already, a theoretical computation of the cohesive forces between particles is very unreliable. For this reason the experimental determination of these forces by way of measuring the stress required to disjoin thread-like aggregates is of great interest (BEISCHER /560/). Such aggregates, obtained from non-magnetic ferric oxide smoke, with particle radii of 0.25μ in an electrical field, were separated with a force equal to $4 - 6 \cdot 10^{-5}$ dyn. If we assume, according to equation (56.4), that the cohesive force is proportional to the particle radii, then we obtain for this force the following expression

$$F = (1.6 \div 2.4)r, \text{ dyn} \quad (58.3)$$

Having adapted a reasonable value of σ , we could obtain, according to equation (56.4), the absolute values for a disruptive force which would exceed experimental values many times. The aggregates of zinc oxide yield approximately the same magnitude of disruptive force as is present among aggregates of ferric oxide. Yet, the disruptive force is considerably greater among aggregates obtained in an electrical field from ammonium chloride smoke, and also from arsenous acid anhydride and from anthracene. BEISCHER explains that among the specified, more volatile substances, a cementation of aggregates takes effect because of diffusion and recrystallization. Finally, among aggregates formed in pyroelectric and magnetic smokes from aminoazobenzene or from magnetic ferric oxide in which, besides molecular forces between particles there are also electrostatic or magnetic forces which are active, the disruptive force is 100 - 1000 times greater than among aggregates from zinc oxide and from nonmagnetic ferric oxide.

In conclusion, we shall mention few words about rupture of aggregates of particles by an air current. There are two main rupturing mechanisms possible here. The first one resembles a bursting of liquid drops (see figure 15). Flat aggregates orient themselves perpendicularly to the current's direction. In the center of an aggregate, where the velocity of the by-passing is the lowest, the pressure (according to BERNOULI'S theorem) attains its maximal magnitude and there, an aggregate curves outwardly like a drop on figure 15; also a shearing force emerging there increases with the aggregate's size, as well as with the aggregate's relative velocity with the air. Thus, the larger the aggregate, the easier it breaks while falling through the air. Yet, generally speaking, during such a fall the relative velocity is not

high; a much more complete disaggregation is attained at greater momentary values of the relative velocity which occurs when the aggregates enter a swift aerial current. The action of atomizers of powders is probably based upon this factor, and so is the atomization of insecticides as the latter are blown out of an aeroplane, and so on.

The second rupture mechanism operates in the presence of a sufficiently high gradient of flow velocity, e. g., in slit instruments (see page 108) and, as such, it is well understood without additional explanations. Its effectiveness also increases with the elongation of aggregates. Apparently, the rupturing of aggregates during energetic stirrings, and while in a turbulent current, proceeds in this way. According to reference data, upon sufficiently intensive stirring in an aerosol containing solid particles, a stationary condition may follow whereby the velocity of coagulation and of disaggregation could become equalized (502). However, it must be noted that if the effort to grasp the meaning of the fluidization of powders was suspended, it would hardly be possible to approach the question of atomization mechanism in the scientific literature.

References

1. W GIBBS, J Soc. Chem. Ind., 51, 1042 (1932).
2. E. VIGDORCHIK Retarding of aerosols during respiration. LIOT, L., 1948, chapter I.
3. Handbuch der Physik. Berlin, Bd. 22 (I), Kap. 4 (1933).
4. Handbuch der Experimentalphysik. Leipzig, Bd. 13 (I), Kap. 5 (1929)
5. B. VONNEGUT. Chem. Rev., 44, 277 (1949).
6. D. SINCLAIR, V. LaMER Chem. Rev., 44, 245 (1949).
7. N. FIGUROVSKIY. Problems of kinetics and catalysis ONTI, M - L., 7, 9 (1949)
8. M. NEIBURGER, M. WURTELE. Chem. Rev., 44, 321 (1949)
9. P ROLLER. J. Frankl. Inst., 223, 609 (1937).
10. P ROSIN, E RAMMLER. Koll. Z., 67, 16 (1934)
11. HYKIAMA, TANASAVA. Quotations by H LEWIS Ind Eng Chem., 40, 67 (1948)
12. J. ZELENY, L. McKEEHAN Phys. Z., 11, 78 (1910).
13. L. LEVIN, DAN, USSR, 94, 1045 (1954)
14. T. HATCH, S. CHOATE J. Frankl. Inst., 207, 369 (1929).
15. C. VOEGTLIN, H. HODGE Pharmacology and toxicology of uranium compounds, New York, 1949, p. 468.
16. S. FRIEDMAN. Chem. Eng. Progr., 48, 118 (1952)
17. W. RANZ, J. WONG. Arch. Ind. Hyg. Occ. Med., 5, 464 (1952)
18. F. KOTTLER J. Frankl. Inst., 250, 339, 419 (1950).
19. A. KOLMOGOROV. DAN, USSR, 31, 99 (1941).
20. B. EPSTEIN. Ind. Chem., 40, 2289 (1948)
21. T. HATCH, S. CHOATE. J. Frankl. Inst., 215, 27 (1933)
22. G. ROMASHOV. Basic principles and methods in determination of dispersed consistency among industrial powders. LIOT, L., 1938, p. 16
23. ICHIDA. Nature, 140, 70 (1937).
24. G. PLACZEK Z. Phys., 55, 81 (1929).
25. P. SANZENBACHER Z. Phys., 39, 251 (1926)
26. J. MATTAUCH. Z. Phys., 32, 439 (1925).
27. O. TRAUNER. Z. Phys., 46, 237 (1928).
28. E. WASSER. Z. Phys., 27, 226 (1924)
29. R. BOWLING and others. Ind. Eng. Chem., News Ed., 19, 965 (1941)
30. I. ARTEMOV. New ideas in the realm of aerosol studies. Publ. AN, USSR, 1949, p. 68.
31. R. WHITLAW-GRAY, KH. PATTERSON. Smoke Goskhimtekhnizdat, M. 1934, chapter 10.
32. W. GERLACH. Phys. Z., 20, 298 (1919).
33. E. REGENER. Ber. Preuss. Akad. Wiss., 192, 632 (1920)
34. H. WADELL. J. Frankl. Inst., 217, 459 (1934)
35. YU. RANKO. Colloidal journal 10, 42 (1948)

36. E. HANSON, J. DANIEL. J. Appl. Phys., 18, 439 (1947).
37. P. EPSTEIN. Phys. Rev., 23, 710 (1924).
38. R. MILLIKAN. Phys. Rev., 21, 217 (1923).
39. R. MILLIKAN. Phys. Rev., 22, 1 (1923).
40. J. WEYSSENHOFF. Ann. Phys., 62, 1 (1920).
41. Handbuch der Experimentalphysik. Leipzig, Bd. 4 (II), 342 (1932).
42. C. OSEEN. Neuere Methoden und Ergebnisse in der Hydrodynamik. Leipzig, 1927, §16.
43. W. RYBCZINSKI. Anzeig. Akad. Krakau, s. 40 (1911).
44. G. LAMB. Hydrodynamics. Gostekhizdat, M. - L., 1947, §337.
45. G. LAMB. The same, §338.
46. E. CUNNINGHAM. Proc. Roy. Soc., 83 A, 357 (1910).
47. L. STACY. Phys. Rev., 21, 239 (1923).
48. E. WASSER. Phys. Z., 34, 257 (1938).
49. M. KNUDSEN, S. WEBER. Ann. Phys., 36, 382 (1911).
50. M. REISS. Z. Phys., 39, 623 (1926).
51. T. LABY. Nature, 150, 648 (1942).
52. Handbuch der Experimentalphysik. Leipzig, Bd. 4 (II), 339 (1932).
53. R. MILLIKEN. Electrons. Gosizdat, M., 1923, chapter 4 and 5.
54. G. KELLSTRÖM. Nature, 136, 682 (1935).
55. S. GOLDSTEIN. Proc. Roy. Soc., 123 A, 225 (1929).
56. J. SCHMIEDEL. Phys. Z., 29, 593 (1928).
57. H. MÖLLER. Phys. Z., 39, 57 (1938).
58. Handbuch der Experimentalphysik. Leipzig, Bd. 4 (II), Kap. 4, 13 (1932).
59. C. DAVIES. Proc. Phys. Soc., 57, 260 (1945).
60. L. KLYACHKO. Heating and ventilation. No. 4 (1934).
61. E. PETTIJOHN, E. CHRISTIANSEN. Chem. Eng. Progr., 44, 157 (1948).
62. J. McNOWN, J. MALAIKA. Trans. Am. Geoph. Union, 31, 74 (1950).
63. R. GANS. München. Ber., S. 191 (1911).
64. W. KUNKEL. J. Appl. Phys., 19, 1056 (1948).
65. G. LAMB. Hydrodynamics. Gostekhizdat, M. - L., 1947, §124.
66. A. KILB. Forsch. Ingen. Wesen, 58, 6, 89 (1934).
67. P. LYASHCHENKO. Gravitational methods of concentration. Gostoptekhizdat, M., 1940, p. 40.
68. A. PETERLIN, H. STUART. Z. Phys., 112, 1 (1939).
69. G. JEFFERY, Proc. Roy. Soc., 102 A, 161 (1923).
70. R. TREVELYAN, S. MASON. J. Coll. Sci., 6, 354 (1951).
71. C. OSEEN. Neuere Methoden und Ergebnisse in der Hydrodynamik. Leipzig, 1927, §18.
72. Handbuch der Experimentalphysik. Leipzig, Bd. 4 (II), 367 (1932).
73. G. LAMB. Hydrodynamics. Gostekhizdat, M. - L., 1947, p. 774.
74. R. FINN. J. Appl. Phys., 24, 771 (1953).

75. J. HEISS *J. Coull. Chem. Eng. Progr* , 48, 133 (1952).
76. Problems of purification of air from dust M. - The all-union scientific research publication for heat supply, heating systems and ventilation, 52 (1940).
77. H. GONELL *Z. Ver. Deutsch. Ing* , 72, 27 (1928).
78. H. HERWIG. *Feuerungstechnik*, 28, 122 (1940).
79. R. GUNN *J. Meteor* , 6, 243 (1949)
80. A. BEST *Quart. J. Roy. Meteor. Soc* , 76, 302 (1950)
81. D. BLANCHARD. *Trans. Am. Geoph. Union*, 31, 836 (1950).
82. M. SMOLUCHOWSKI *Proc. Internat. Mathem. Congr. Cambr* (1912)
83. J. BURGERS *Proc. Amsterd. Acad. Sci* , 44, 1177 (1941); 45, 126 (1942).
84. K. PROSAD, D. SEN. *Phil. Mag.* , 25, 993 (1938).
85. W. KERMAK and others. *Proc. Roy. Soc. Edinb.* , 49, 170 (1920).
86. P. HAWXLEY. Some aspects of fluid flow. 1950, p. 114.
87. E. LEWIS, E. BOWERMAN. *Chem. Eng. Progr.* , 48, 603 (1952)
88. J. RICHARDSON, W. ZAKI. *Chem. Eng. Sci.* , 3, 65 (1954)
89. E. REGENER. *Z. Phys. Chem.* , 139, 420 (1926).
90. R. MILLIKAN. *Phil. Mag.* , 19, 209 (1910)
91. F. EHRENHAFT. *Wien. Ber.* , 119, 11a (1910).
92. W. GERLACH. *Handbuch der Physik*, Berlin, Bd. 22 (1), Kap. 1 (1933)
93. N. N. SEMENOV. *Electronics' phenomena*. Publ. NIU VSNKH, M. - 1928, chapter 3.
94. E. MEYER, W. GERLACH. *Elster-Geitel Festschrift*, 1915, S. 196.
95. J. PARANKIEWITZ. *Phys. Z.* , 19, 280 (1918).
96. R. MILLIKEN. *The electron*. Gosizdat, M. - 1923, chapter 3
97. R. BÄR. *Ann. Phys.* , 67, 157 (1922).
98. B. ROTTSEIG, N. FUKS. *ZHFKH*, 9, 35 (1937)
99. R. BÄR. *Ann. Phys.* , 59, 393 (1919)
100. V. HOPPER, T. LABY. *Proc. Roy. Soc.* , 178 A, 243 (1941)
101. A. RUBINOWITZ. *Ann. Phys.* , 62, 695 (1920)
102. G. HETTNER. *Ann. Phys.* , 27, 12 (1924).
103. G. HETTNER. *Z. Phys.* , 37, 179 (1926)
104. J. MATTAUCH. *Ann. Phys.* , 85, 967 (1928)
105. P. EPSTEIN. *Z. Phys.* , 54, 537 (1929).
106. P. ROSENBLATT, V. LAMER. *Phys. Rev.* , 70, 385 (1946).
107. R. SAXTON, W. RANZ. *J. Appl. Phys.* , 23, 917 (1952)
108. D. NIELSEN. *Proc. Phys. Soc.* , No 4, 16 (1940).
109. R. WEBER. *Z. Naturforsch.* , 29, 48 (1947)
110. S. BLACKTIN. *J. Soc. Chem. Ind.* , 58, 334 (1939).
111. J. BREDL, T. GRIEVE. *J. Scient. Instr.* , 28, 23 (1951)
112. H. WATSON. *Trans. Farad. Soc.* , 32, 1073 (1936).
113. F. DEGUILLON. *C. R.* , 231, 274 (1950).

114. RAY. *Annal. Phys.*, 66, 71 (1921).
115. J. BOUSSINESQ. *Theorie analytique de chaleur*. Paris, 1903, t. II, p. 224.
116. L. LANDAU, E. LIFSHITS. *The mechanics of solid media*. Gostekhizdat, M. - L., 1944, p. 89.
117. T. BOGGIO. *Rend. conti*, 16, 613, 730 (1907).
118. V. VLADIMIRSKIY, YA. TERLETSKIY. *ZHETF*, 15, 258 (1945).
119. S. BERKOWITCH. *Helv. Phys. Acta* 7, 170 (1934).
120. F. SCHMIDT. *Ann. Phys.*, 61, 633 (1920).
121. R. LUNNON. *Proc. Roy. Soc.*, 110 A, 302 (1926).
122. G. KHUDYAKOV, Z. CHUKHANOV. *DAN, USSR*, 78, 681 (1951).
123. G. KHUDYAKOV. *Izvetiya A. N., USSR, Technical Series* 1022 (1953).
124. J. LAWS. *Trans. Am. Geophys. Union*, 22, 709 (1941).
125. W. HITSCHFELD. *Trans. Am. Geophys. Union*, 32, 697 (1951).
126. C. LAPPLE, C. SHEPHERD. *Ind. Eng. Chem.*, 32, 605 (1940).
127. G. LAMB. *Hydrodynamics*. Gostekhizdat, M. - L., 1947, § 356.
128. YÜ-Chen-Yang. *Ann. Phys.*, 76, 333 (1925).
129. H. ISRAEL. *Meteor. Z.*, S. 36, (1942).
130. W. KÖNIG. *Ann. Phys.*, 42, 353 (1891).
131. O. BRANDT, H. FREUND, E. HIEDEMANN. *Z. Physik*, 104, 511 (1937).
132. V. ZERNOV. *Ann. Phys.*, 26, 79 (1908).
133. M. WAGENSCHNEIDER. *Ann. Phys.*, 65, 461 (1921).
134. H. CASSEL, H. SCHULZ. "Air Pollution". New York, 635 (1952).
135. H. ST. CLAIR. *Ind. Eng. Chem.*, 41, 2434 (1949).
136. L. KING. *Proc. Roy. Soc.*, 147 A, 212, (1934).
137. J. RUDNICK. *J. Acoust. Soc. Am.*, 23, 633 (1951).
138. P. WESTERVELT. *The same*, p. 3.
139. E. da ANDRADE. *Proc. Roy. Soc.*, 134 A, 445 (1931).
140. G. LAMB. *Hydrodynamics*. Gostekhizdat, M. - L., 1947, § 362, 363.
141. C. SEWELL. *Phil. Trans.*, 210 A, 239 (1910).
142. S. RYTOV, V. VLADIMIRSKIY, M. GALANIN. *SHETF* 8, 614 (1938).
143. E. EPSTEIN, R. CARHART. *J. Acoust. Soc. Am.*, 25, 553 (1953).
144. V. ALTHERR, M. GOLTSMAN. *Phys. Z.*, 26, 149 (1925).
145. T. LAIDLIER, E. RICHARDSON. *J. Acoust. Soc. Am.*, 9, 217 (1938).
146. V. KNUDSEN, J. WILSON, N. ANDERSON. *J. Acoust. Soc. Am.*, 20, 849 (1948).
147. D. TINDAL. *Sound*. Gosizdat, Moscow, 1922.
148. H. INGARD. *J. Acoust. Soc. Am.*, 25, 405 (1953).
149. H. SIEG. *Elektr. Nachricht. Techn.*, 17, 193 (1940).
150. V. ARABADZHI. *Meteorology and hydrology*. No. 3, 11 (1947).
151. K. OSWATICH. *Phys. Z.*, 42, 365 (1941).
152. J. POYNTING, J. THOMSON. *Sound*. London, 1940, p. 169.
153. C. OSEEN. *Neuere Methoden und Ergebnisse in der Hydrodynamik*. Leipzig, 1927, § 14, 21.

154. Handbuch der Experimentalphysik. Leipzig, Bd. 4 (II), 344 (1932).
155. G. KIRCHHOFF. Mechanik. Leipzig, 1877, S. 251
156. G. LAMB. Hydrodynamics Gostekhizdat, M. - L. - 1947, § 137.
157. S. GORVACHEV, A. SEVERNYI. Koll., Z. 73, 146 (1935)
158. V. BJERKNES, J. BJERKNES, H. SOLBERG, T. BERGERON. Physikalische Hydrodynamik, Berlin, 1933
159. L. LANDAY, E. LIFSHITS. The mechanics of solid media. Gostekhizdat, M. - L., 1944, § 20
160. W. KÖNIG. Ann. Phys., 42, 549 (1891)
161. S. COOK. Phil. Mag., 3, 471 (1902)
162. V. BAZILEVICH. Coagulation phenomena in aqueous clouds and fogs. Dissertation GEOFI, AN, 1941 - 1943
163. G. THOMAS. Ann. Phys., 42, 1079 (1913).
164. J. TOWNSEND. Phil. Mag., 45, 471 (1898)
165. N. WOŁODKEWITCH. Z. Phys., 84, 593 (1933).
166. N. FUKS, I. PETRYANOV. ZHFKH, 7, 312 (1936).
167. R. WHYTLAW-GRAY, KH. PATTERSON. Smoke Goskhimtekhnizdat, M. 1934, p. 143
168. F. DESSAYER. Ionized air and its physiological actions. Tekhteorizdat. M. - L. - 1932
169. A. CHIZHEVSKIY. Treatment of pulmonary diseases by ionized air. The all-union association of physicians homeopaths. M. - 1930.
170. R. ABBOTT. Phys. Rev., 12, 381 (1918)
171. N. FUKS, I. PETRYANOV. Koll. Z., 65, 173 (1933)
172. P. WELLS, R. GERKE. J. Am. Chem. Soc., 41, 312 (1919)
173. L. WHITE, D. HILL. J. Coll. Sci., 3, 251 (1948)
174. N. ROZENBLYUM. Tech. Phys., USSR 4, 1. (1937).
175. S. TARC. Basic theories of laminar currents. Gostekhizdat. L. - 1951, chapter 6.
176. A. CHISTOV. Heating and ventilation. No. 11, 14 (1935). No. 11/12, 27 (1939)
177. P. LISOVSKIY. Acta physicochim. USSR, 13, 157 (1940).
178. N. FUKS. Izvestiya AN USSR, series of geography and geophysics 11, 341 (1947)
179. W. ZIMMERSCHMIED. Koll. Z., 72, 135 (1935)
180. S. CHAPMAN. Phys. Rev., 52, 184 (1937).
181. H. ISRAEL. Gerlands Beitr., 31, 173 (1931)
182. Handbuch der Experimentalphysik, 13 (I), Kap. 5 (1929).
183. I. PETRYANOV, N. TUNITSKIY. ZHFKH, 13, 1131 (1939).
184. P. NOLAN, P. KENNY. J. Atm. Terr. Phys., 3, 181 (1953).
185. R. COCHET. Rev. Gener. Electricité, 62, 113 (1953)
186. D. MUNDEN. - J. Appl. Chem., 2, 65 (1952).
187. W. Wells. Am. J. Publ. Health, 23, 58 (1933)
188. L. LANDAY, E. LIFSHITS. The mechanics of solid media. Gostekhizdat. M. - L. - 1944, p. 57.

189. A. SHAFIR. Hygienics and sanitation. No. 7/8, 1 (1944).
190. K. SAWYER, W. WALTON. J. Sci. Instr., 27, 272 (1950).
191. P. SMUKHNIN, P. KOUZOV. Centrifugal dust eliminating cyclones. Stroyizdat, M. - 1935.
192. P. KOUZOV. Purification of air from dust in cyclones. LIOT. L. - 1938.
193. H. Larcombe. Mining Mag., 77, 137, 208, 273, 346 (1947).
194. P. ROSIN, E. RAMMLER, W. INTELTMANN. Z. Ver. Deutsch. Ing., 76, 433 (1932).
195. W. MUHLRAD. Genie civile, 124, 152 (1947).
196. M. LISSMANN. Chem. Met. Eng., 37, 630 (1930).
197. C. SHEPHERD, C. LAPPLE. Ind. Eng. Che., 31, 972 (1939).
198. R. MELDAU. Z. Ver. Deutsch. Ing., 76, 1189 (1932).
199. N. BELYAEV. Chemical Industry, No. 5 (1949).
200. W. BRIGGS. Trans. Am. Inst. Chem. Eng., 42, 511 (1946).
201. L. FARBAR. Trans. Am. Soc. Mech. Eng., 75, 953 (1953).
202. N. ZALOGIN, S. SHUKHER. Purification of gases in smoke. Gosenergoizdat. M. - L. - 1948.
203. L. McCABE. Ind. Eng. Chem., 45, No. 12, 108 A (1953).
204. W. SELL. VDI Forschungsheft, No. 347 (1931).
205. F. ALBRECHT. Phys. Z., 32, 48 (1931).
206. I. MAZIN. Trudy. TSAO, publ. 7, 39 (1952).
207. S. SYRKIN. Theory about modeling trajectories of solid particles in a curvilinear current. Boiler-Turbine Institute, 1934.
208. D. ROSIN, H. KAYSER, E. RAMMLER. Z. techn. Phys., 16, 205 (1935).
209. R. BARTH, W. BARTH. Rauch und Staub, 22, 93 (1932).
210. P. VOLKOV. Exploitation of research methods as to movement of solid particles in models. Boiler-Turbine Institute, 1936.
211. W. WALTON. "Symposium on particle size analysis". London, 136 (1947).
212. C. DAVIES. The same, p. 25.
213. K. MAY, H. DRUETT. Brit. J. Ind. Med., 10, 93 (1953).
214. J. HIRST. Ann. Appl. Biol., 39, 257 (1952).
215. P. DRINKER, T. HATCH. Industrial dusts, 1936.
216. R. BOURDILLON. J. Hygiene, 41, 197 (1941).
217. K. MAY. J. Sci. Instr., 22, 187 (1947).
218. C. DAVIES, M. AYLWARD, D. LEACEY. Arch. Ind. Hyg. Occ. Med., 4, 354, 1951.
219. C. DAVIES, M. AYLWARD. Proc. Phys. Soc., 64 B, 889 (1951).
220. L. LEVIN. DAN USSR, 91, 1329 (1953).
221. J. WILCOX. Arch. Ind. Hyg. Occ. Med., 7, 376 (1953).
222. W. RANZ, J. WONG. Ind. Eng. Chem., 44, 1371 (1952).
223. V. PIK, L. SHURCHILOV. Industrial hygienics and safety, No. 4, 22 (1935).

224. D. JORDAN. Brit. J. Appl. Phys. Suppl., No. 3, 194 (1954).
225. E. BIRSE, J. ROBERTS. Trans. Farad. Soc., 44, 273 (1948).
226. J. FICKLEN, L. GOOLDEN. Science, 85, 587 (1937).
227. G. FAIRS. J. Soc. Chem. Ind., 60, 141 (1941).
228. G. LAMB. Hydrodynamics. Gostekhizdat. M - L. - 1947, § 68.
229. The same, § 343.
230. The same, § 96.
231. The same, § 337.
232. The same, § 171.
233. The same, § 342.
234. I. LANGMUIR, K. BLODGETT. Army Air Force. Techn. Rep., No. 5418, 1946.
235. C. LAPPLE. Fluid and particle mechanics. Newark, 1951, p. 304.
236. H. LANDAHL, K. HERMANN. J. Coll. Sci., 4, 103 (1949).
237. A. THOM. Proc. Roy. Soc., 141 A, 651 (1933).
238. J. GEIST, J. YORK, G. GRANGER. Ind. Eng. Chem., 43, 1371 (1951).
239. I. LANGMUIR. J. Meteor., 5, 175 (1948).
240. "Physics in settlements' formations" IL, Moscow, 153 (1951).
241. The same, p. 156.
242. The same, p. 159.
243. N. FUKS. DAN USSR, 81, 1043 (1951).
244. E. BRUN and others. C. R., 224, 1518 (1947).
245. H. DESSENS. Quart. J. Roy. Meteor. Soc., 75, 23 (1949).
246. "Contemporary stage of hydro-aero-dynamics in a viscous liquid" IL, M - L, 137 (1948).
247. H. Schlichting. Grenzschicht-Theorie. Karlsruhe, 1951.
248. A. YEOMANS and others. J. Econ. Entom., 42, 591 (1949).
249. M. KHIMACH, N. SHISHKIN. Trudy. GGO, publ. 31 (93), 29 (1951).
250. P. BOUCHER. Chal. et Industrie, 33, 363 (1952).
251. F. FRANK, R. MIZES. Differential and integral equations in physical mathematics. ONTI, M - L - 1937, chapter 13.
252. "Brownian movement". ONTI, M - L - 1936.
253. M. LEONTOVICH. "Physics' statistics" Gostekhizdat, M - L - 1944, chapter 6.
254. A. EINSTEIN. Ann. Phys., 17, 549 (1905).
255. P. FRANK. Ann. Phys., 52, 323 (1927).
256. M. SMOLUCHOWSKI. "Brownian movement" ONTI, M - L - 150 (1936).
257. Yu. KRUTKOV. The same, page 497.
258. L. ORNSTEIN. Proc. Amsterd. Acad. Sci., 21, 96 (1918).
259. B. BÄCKER. Z. Phys., 38, 609 (1926).
260. F. ZEILINGER. Ann. Phys., 75, 403 (1924).
261. R. FÜRTH. Ann. Phys., 59, 409 (1919).

262. S. LANDMANN. *Z. Phys.*, 27, 237 (1924).
263. E. SCHRÖDINGER. *Phys. Z.*, 16, 289 (1915).
264. H. FLETCHER. *Phys. Rev.*, 4, 440 (1914).
265. M. SMOLUCHOWSKI. "Brownian movement". *ONTI, M. - L.* - 315 (1936).
266. E. SCHMID. *Phys. Z.*, 22, 438 (1921).
267. E. SCHMID. *Wien. Ber.*, 129, IIa, 813 (1920).
268. A. WINKEL, H. WITZMANN. *Z. Elektrochem.*, 46, 181 (1940).
269. M. SMOLUCHOWSKI. "Brownian movement". *ONTI, M. - L.* - 320 and 324 (1936).
270. A. KOLMOGOROV. *Analytical methods of the theory of probabilities. Progress in the science of mathematics. Publ. 5* (1938).
271. A. KOLMOGOROV, M. LEONTOVICH. *Physik. Z. Sovjetunion*, 4, 1 (1933).
272. F. FRANK, R. MIZES. *Differential and integral equations in physical mathematics. ONTI, L. - M.* - 1937, chapter 13 § 2
273. M. SMOLUCHOWSKI. "Brownian movement". *ONTI, M. - L.* - 375, 381, 1936.
274. F. FRANK, R. MIZES. *Differential and integral equations in physical mathematics. ONTI, L. - M.* - 1937, chapter 13 § 3, 1.
275. The same, chapter 14, § 2, 5.
276. E. BUCHWALD. *Ann. Phys.*, 66, 1 (1921).
277. B. DERYAGIN, G. VILASENKO. *DAN USSR*, 63, 155 (1948).
278. L. RADUSHKEVICH. *DIFKH*, 13, 1322 (1939).
280. M. SMOLUCHOWSKI. "Brownian movement". *ONTI, M. - L.* - 376 (1936).
281. M. JAKOB. *Heat Transfer. New York*, 1949, t. 1, p. 267.
282. L. GRAETZ. *Ann. Phys.*, 18, 79 (1883).
283. W. NUSSELT. *Z. Ver. Deutsch. Ing.*, 54, 1154 (1910).
284. J. TOWNSEND. *Phil. Trans.*, 193, 129 (1900).
285. P. GORMLEY, M. KENNEDY. *Proc. Roy. Irish Acad.*, 52 A, 163 (1949).
286. M. LEVEQUE. *Ann. Mines*, 13, 276 (1928).
287. V. LEVICH. *Physical-chemical hydrodynamics. Publ. A. N. USSR, M.* - 1952, § 20.
288. L. RADUSHKEVICH. *Acta physicochim. USSR*, 6, 161 (1937).
289. J. NOLAN, N. GUERRINI. *Trans. FARAD. Soc.*, 32, 1175 (1936).
290. N. FRÖSSLING. *Gerlands Beitr.*, 52, 170 (1938).
291. D. FRANK-KAMENETSKIY. *Diffusion and heat transfer in chemical kinetics. Publ. A. N., USSR, M. - L.* - 1947, p. 162.
292. V. LEVICH. *Physical-chemical hydrodynamics. Publ. A. N., USSR, M.* - 1952, chapter 2.
293. The same, § 14.
294. O. ROBERTS. *Proc. Roy. Soc.*, 104 A, 640 (1923).

295. H. WITZMANN. Z. Elektrochem., 46, 313 (1940), VDI Verfahrenstechnik, No 4 107 (1940).
296. H. BORN, K. ZIMMER. Naturwiss., 28, 447 (1940).
297. S. KATZ, D. MACRAE. J. Phys. Coll. Chem., 52, 695 (1948).
298. V. KUCHERUK, V. SEROV. Industrial dust and dust removing ventilation. Stroyizdat, M - 1941
299. L. WEISCHHAUS. Chem. Eng., 54, No. 8, 113 (1947).
300. L. SILVERMAN. Chem. Eng. Progr., 47, 462 (1951).
301. R. PRING. "Air Pollution", New York, 1952, p. 280.
302. E. REKK. Heating and ventilation. No. 4, 20 (1934).
303. F. ROWLEY, R. JORDAN. Heat Pip. Air Cond., 1938, 469
304. A. KAUFMANN. Z. Ver. Deutsch. Ing., 80, 593 (1936)
305. Handbook on Aerosols. Washington, 1950.
306. V. LAMER. "Air Pollution". New York, 1952, p. 612
307. W. SMITH, E. STAFFORD. The same, p. 264.
308. A. Clayton and others. Ind. Eng. Chem., 46, 176 (1954).
309. J. PEROT. Paper Trade J., 124, No. 25, 54 (1947).
310. E. RAMSKILL, W. ANDERSON. J. Coll. Sci., 6, 416 (1951)
311. H. EISENBART. Die Gasmasken, 8, 72 (1936)
312. E. STAFFORD, W. SMITH. Ind. Eng. Chem., 43, 1346 (1951)
313. A. ROSSANO, L. SILVERMAN. Heat. Ventil., 51, No. 5, 102 (1954)
314. R. WEBER. Angew. Chem., 20 B, 335 (1948).
315. L. DAUTREBANDE and others. C. R., 205, 156, 240 (1937).
316. L. DAUTREBANDE and others. C. R., 205, 329 (1937)
317. T. TACHIBANA. Chem. Abstr., 41, 3343 (1947)
318. G. GOYER, R. GRUEN, V. LAMER. J. Phys. Chem., 58, 137 (1954)
319. G. FAIRS. J. Soc. Chem. Ind., 60, 141 (1941).
320. L. DAUTREBANDE and others. J. Ind. Hyg. Tox., 30, 103 (1948)
321. J. WILSON, V. LAMER. J. Ind. Hyg. Tox., 30, 265 (1948)
322. H. LANDAHL and others. Arch. Ind. Hyg. Occ. Med., 3, 359 (1951)
323. H. LANDAHL, S. BLACK. J. Ind. Hyg. Tox., 29, 269 (1947).
324. C. DAVIES. Proc. Roy. Soc., 133 B, 282 (1946).
325. M. GUTMANN. Die Pollenallergie, München, 1929.
326. L. DAUTREBANDE. Physiol. Rev., 32, 214 (1952)
327. F. BUCKLAND and others. Nature, 166, 354 (1950).
328. M. SHOSHKES and others. Arch. Ind. Hyg. Occ. Med., 1, 20 (1950)
329. A. VAN WIJK, H. PATTERSON. J. Ind. Hyg. Tox., 22, 31 (1940).
330. J. BROWN, T. HATCH. Am. J. Publ. Health., 40 A, 450 (1950)
331. C. DAVIES. Brit. J. Ind. Med., 9, 120 (1952).
332. I. LIFSHITS, E. LYKHINA, G. ERENBURG. Hygienics and sanitation. No. 10, 17 (1948)
333. W. FINDEISEN. Arch. Gesamt. Physiol., 236, 367 (1935).
334. H. LANDAHL. Bull. Mathem. Biophys., 12, 43, (1950).

335. J. WILSON. J. Coll. Sci., 2, 27 (1947).
336. L. DAUTREBANDE. Aerosols medicamenteux, Paris 1946.
337. N. TUNITSKIY, M. TIKHOMIROV, I. PETRYANOV. Industrial physics journal, 10, 1723 (1940).
338. V. LEVICH. Physical-chemical hydrodynamics. Publ. A. N. USSR, M. - 1952, chapter 6.
339. D. KREVELEN. Chem. Eng. Progr., 46, 29 (1950).
340. H. REMY, W. SEEMANN. Koll. Z., 72, 3 (1935).
341. H. REMY, K. RUHLAND. Z. anorg. Chem., 139, 51 (1924).
342. H. REMY, Trans. Farad. Soc., 32, 1185 (1936).
343. H. REMY, C. BEHRE. Koll. Z., 71, 129 (1935).
344. H. REMY, H. FINNERN. Z. anorg. Chem., 159, 241 (1926).
345. G. LUCHINSKIY. ZHFKH. 13, 302 (1939).
346. M. ALEKSEEVA, B. ANDRONOV. Factory laboratory. 16, 18 (1941).
347. D. BRONSKY, F. DIWOKY. Chem. Met. Eng., 47, 541 (1940).
348. M. POZIN. Gas-purifying installations and their introduction to electric power plants of industrial enterprises. Energoizdat, M. - L. - 98 (1953).
349. R. GANS. Ann. Phys., 86, 628 (1928).
350. F. PERRIN. C. R., 181, 514 (1925).
351. E. COHN. Das Elektromagnetische Field. Leipzig, 1900, S. 110.
352. K. BLOCH. C. R., 146, 970 (1908).
353. P. ZEEMANN, C. HOOGENBOOM. Phys. Z., 13, 913 (1912).
354. WATMSLEY. Phil. Mag., 7, 1097 (1927).
355. C. O'KONSKI, C. THACHER. J. Phys. Chem., 57, 955 (1953).
356. L. PRANDTL. Hydro-aeromechanics. IL, M. - 1949, §18.
357. T. GILLEPSIE, G. LANGSTROTH. Canad. J. Chem., 29, 133, 201 (1951).
358. E. VIGDORCHIK. Leningrad Labor Welfare Dept. 6, No. 7 (1933).
359. K. SHIFRIN, I. GORDON, M. FAINSTEIN. Izvestiya A. N. USSR. Geography and geophysics series, 3, 238 (1949).
360. T. GILLEPSIE. Proc. Roy. Soc., 216 A, 569 (1951).
361. G. LANGSTROTH, T. GILLEPSIE. Canad. J. Research, 25 B, 455 (1947).
362. A. KOLMOGOROV. DAN USSR, 30, 299 (1941).
363. L. SIMMONS, C. SALTER. Proc. Roy. Soc., 165 A, 73 (1938).
364. A. OBUKHOV, A. YAGLOM. Examples of the mechanics of mathematics. 15, 1 (1949).
365. A. OBUKHOV. DAN USSR, 67, 643 (1949).
366. C. PRIESTLEY, P. SHEPPARD. Quart. J. Roy. Meteor. Soc., 78, 488, (1952).
367. W. HEISENBERG. Z. Physik, 124, 628 (1948).
368. P. MACCREADY. J. Meteor., 10, 434 (1953).

369. W. SCHMIDT. Der Massenaustausch in frier Luft und verwandte Erscheinungen, 1925.
370. Ivestiya AN, USSR, Technical Series, 1742, 1831, 1848 (1952).
371. B. BROUNSHTEIN, C. TODES. Journal of industrial physics, 23, 119 (1953).
372. L. LANDAY, E. LIFSHITS. The mechanics of solid media. Gostekhizdat, M. - L. - 1944, p. 37.
373. V. VANONI. Proc. Am. Soc. Civil Eng., 70, 793 (1944).
374. A. KALINSKE, C. PIEN. Trans. Am. Geophys. Union, 24, 530 (1943).
375. M. KALINUSHKIN. Trudy. TSAGI, No. 266 (1936).
376. T. SHERWOOD, B. WOERTZ. Ind. Eng. Chem., 31, 1034 (1939).
377. E. LINDGREN. Arkiv Fysik, 7, 293 (1954).
378. B. FILATOV. Colloidal Journal 16, 65 (1954).
379. A. ter. LINDEN. Chemie-Ing. Techn., 25, 328 (1952).
380. N. FUKS. Industrial physics journal. 21, 704 (1951).
381. G. BARENBLATT. Examples of the mechanics of mathematics 17, 261 (1953); 19, 61 (1955).
382. A. FAGE, H. TOWNSEND. Proc. Roy. Soc., 135 A, 656 (1932).
383. E. MINSKIY. DAN USSR, 49, 329 (1945).
384. W. SCHMIDT. Ind. Eng. Chem., 41, 2418 (1949).
385. I. PRANDTL. Hydro-aero-mechanics. IL, M. - 1949, chapter 3, § 5.
386. L. PRANDTL. The same, p. 151.
387. "Contemporary stage of hydro-aero-dynamics in a viscous liquid". IL, M. - 1948, § 280.
388. V. LEVICH. Physical-chemical hydrodynamics. Publ. A. N. USSR, M. - 1952, chapter 3.
389. "Contemporary stage of hydro-aero-dynamics in a viscous liquid". IL, M. - 1948, § 154, 155.
390. L. ALEXANDER. C. COLDREN. Ind. Eng. Chem., 43, 1325 (1951).
391. H. TOWNSEND. Proc. Roy. Soc., 145 A, 180 (1934).
392. G. SCHUBAUER. J. Appl. Phys., 25, 188 (1954).
393. N. ZHUKOVSKIY. Snow drifts and silting in rivers. Kiev, 1911.
394. G. ASSET, D. PURY. Arch. Ind. Hyg. Occ. Med., 9, 273 (1954).
395. G. SHELEYKHOVSKIY. Smoke-clouded towns. Publ. of the Ministry of Communications, M. - L. - 1949.
396. P. ANDREEV. Gasses dispersed in the air discharged by industrial enterprises. Gosstroyizdat, M. - 1952.
397. O. SUTTON. Micrometeorology. New York, 1953.
398. O. SUTTON. Atmospheric turbulence. London, 1949.
399. G. DOBSON. Advis. Comm. Aeronaut., Rep. No. 67 (1949).
400. L. RICHARDSON. Proc. Roy. Soc., 104 A, 640 (1923).
401. M. YUDIN. DAN USSR, 51, 99 (1946).
402. P. ANDREEV. Gasses dispersed in the air discharged by industrial enterprises. Gosstroyizdat. M. - 1952, p. 40.

403. O. SUTTON. Proc. Roy. Soc., 135 A, 143 (1932).
404. K. CALDER. Quart. J. Mech. Appl. Math., 2, 153 (1949).
405. O. SUTTON. Quart. J. Roy. Meteor. Soc., 73, 257, 426 (1947).
406. D. LAIKHTMAN, A. CHUDNOVSKIY. Physics of the atmospheric stratum near the ground. Gostekhizdat. L. - M. - 1949, chapter 5.
407. E. TEVEROVSKIY. "New ideas in the realm of aerosol studies". Publ. AN USSR. M. - 1949, p. 108.
408. K. CALDER. "Air Pollution". New York, 1952, p. 787.
409. E. DEACON. Quart. J. Roy. Meteor. Soc., 75, 89 (1949).
410. F. PASQUILL. Proc. Roy. Soc., 202 A, 150 (1950).
411. R. FROST. Proc. Roy. Soc., 186 A, 20 (1946).
412. M. BUDYKO, D. LAIKHTMAN, M. TIMOFEEV. Meteorology and hydrology, No. 3, 27 (1953).
413. C. BOSANQUET, J. PEARSON. Trans. Farad. Soc., 32, 1249 (1936).
414. C. GOSLINE. Chem. Eng. Progr., 48, 165 (1952).
415. D. THOMAS, G. HILL. Ind. Eng. Chem., 41, 2403 (1949).
416. P. CHURCH. Ind. Eng. Chem., 41, 2753 (1949).
417. H. JOHNSTONE, W. WINSCH, L. SMITH. Chem. Rev., 44, 353 (1949).
418. C. DAVIES. Proc. Cambr. Phil. Soc., 46, 500 (1950).
419. M. SMOLUCHOWSKI. "Colloidal coagulation". ONTI, M. - L., 7 (1936).
420. W. HARPER. Trans. Farad. Soc., 30, 636 (1934).
421. N. FUKS. Z. phys. Chem., 171 A, 199 (1934).
422. M. SMOLUCHOWSKI. "Colloidal coagulation". ONTI, M. - L., 25 (1936).
423. G. MYULLER. The same, p. 61.
424. M. TIKHOMIROV, N. TUNITSKIY, I. PETRYANOV. Acta physicochim. URSS, 17, 185 (1942).
425. O. TODES. Problems of kinetics and catalysis. ONTI, M. - L., 7, 137. (1949).
426. S. PSHENAI-SEVERIN. DAN USSR, 94, 865 (1954).
427. R. WHITLAW-GRAY, KH. PATTERSON. Smoke. Goskhimtekhnizdat, M. - 1934, p. 48.
428. H. PATTERSON, W. CAWOOD. Proc. Roy. Soc., 136 A, 538 (1932).
429. M. SMOLUCHOWSKI. "Colloidal coagulation". ONTI, M. - L., 20 (1936).
430. N. TUNITSKIY. ZHETF, 8, 418 (1938).
431. G. MYULLER. "Colloidal coagulation". ONTI, M. - L., 79 (1936).
432. Handbuch der Physik. Berlin, 12, Kap. 4, §86 - 88 (1927).
433. The same, 8 (II), 703 (1929).
434. D. BEISCHER, A. WINKEL. Z. phys. Chem., 176 A, 1 (1936).
435. M. SAMOKHVALOV, O. KOZHUKHOVA. ZHFKH, 8, 420 (1936).
436. L. RADUSHKEVICH. ZHFKH, 9, 6 (1937).
437. R. WHITLAW-GRAY, KH. PATTERSON. Smoke. Goskhimtekhnizdat, M. - 1934, p. 159.

438. N. FUKS. ZHFKH, 6, 30 (1935).
439. Handbuch der Physik, Berlin. 12, §82 (1927).
440. R. WHYTLAW-GRAY, KH. PATTERSON. Smoke Goskhimizdat, M. - 1934, p. 144.
441. A. WIEGAND, E. FRANKENBERGER. Physik Z., 31, 204 (1930).
442. H. HAMAKER. Physica, 4, 1058 (1937).
443. R. BRADLEY. Phil. Mag., 13, 853 (1932).
444. B. DERYAGIN, I. ABRIKOSOVA. Faraday Society Discussion, 18, 36 (1954).
445. W. KRASNY-ERGEN. Ann. Phys., 27, 459 (1936).
446. A. WINKEL. VDI Verfahrenstechnik, 25 (1941).
447. R. GUNN. J. Geophys. Research, 55, 171 (1950).
448. O. SCHWECKENDIECK. Z. NATURFORSCH., 5a, 397 (1950).
449. A. WINKEL. Z. angew. Chem., 54, 152 (1941).
450. D. BEISCHER. Z. Elektrochem., 44, 375 (1938).
451. R. WHYTLAW-GRAY, KH. PATTERSON. Smoke Goskhimtekhnizdat, M. - 1934, p. 77 - 80.
452. A. WINKEL, R. HAUL. Z. Elektrochem., 44, 823 (1938).
453. D. BEISCHER, A. WINKEL. Naturwiss., 25, 420 (1937).
454. R. WHYTLAW-GRAY, KH. PATTERSON. Smoke Goskhimtekhnizdat, M. - 1934, p. 80.
455. J. DALLAVALLE and others. Brit. J. Appl. Phys. Suppl., No. 3, 194 (1954).
456. W. WOOD, A. LOOMIS. Phil. Mag., 4, 433 (1927).
457. Trans. Farad. Soc., 32, 1122 (1936).
458. O. BRANDT, H. FREUND, E. HIEDEMANN. Koll. Z., 77, 103, 168 (1936).
459. R. PARKER. Trans. Farad. Soc., 32, 1115 (1936).
460. E. daANDRADE. Trans. Farad. Soc., 32, 1111 (1936).
461. H. St. CLAIR. Bur. Mines. Rep. Investig. No. 3400 (1938).
462. H. DANSER, F. NEUMANN. Ind. Eng. Ch., 41, 4439 (1949).
463. O. BRANDT, E. HIEDEMANN. Trans. Farad. Soc., 32, 1101 (1936).
464. C. STOKES. Chem. Eng. Progr., 46, 423 (1950).
465. O. BRANDT. Koll. Z., 46, 272 (1936).
466. R. O'MARA. Combustion, 21, No. 4, 40 (1950).
467. C. SODERBERG. Iron, Steel Eng., 29, 87 (1952).
468. H. St. CLAIR. "Air Pollution". New York, 1952, p. 382.
469. P. KUBANSKIY. Industrial physics journal, 24, 1044 (1954).
470. Ya. FRENKEL. Theory about atmospheric electricity phenomena. Gostekhizdat. L. - M. - 1949, chapter 3.
471. W. FINDEISEN. Meteor. Z., 56, 356 (1939).
472. W. FINDEISEN. Gerlands Beitr., 35, 295 (1932).
473. "Physics in settlements' formation." IL, M. - 1951.

474. N. SHISHKIN. Collection of information No. 1 on hydromet. Gidrometizdat, M. - 47 (1951).
475. R. GUNN, W. HITSCHFELD. J. Meteor., 8, 7 (1951).
476. YA. FRENKEL, N. SHISHKIN. Izvestiya A.N. USSR, Geography and Geophysics Series 10, 301 (1946).
477. N. SHISHKIN. Clouds, precipitations and thunderbolt electricity Gostekhizdat, M. - 1954, chapter 6.
478. L. DAUTREBANDE and others. J. Ind. Hyg. Tox., 30, 108 (1948).
479. L. DAUTREBANDE, R. CAPPS. Arch. Internat. Pharmacodyn. Therap., 82, 512 (1950).
480. A. AVY. Arch. Malad. Profess., 14, 342 (1953).
481. A. ALBINSON. Arkiv Kemi, 6, 293 (1953).
482. L. DAUTREBANDE and others. Arch. Internat. Pharmacodyn. Therap., 80, 413 (1949).
483. H. JOHNSTONE, M. ROBERTS. Ind. Eng. Chem., 41, 2417 (1949).
484. H. JOHNSTONE and others. Ind. Eng. Chem., 46, 1601 (1954).
485. F. EKMAN, H. JOHNSTONE. Ind. Eng. Chem., 43, 1358 (1951).
486. P. SCHAUER. The same, p. 1532.
487. G. MYULLER. "Colloidal coagulation". ONTI, M. - L., - 91 (1936).
488. L. LEVIN. DAN USSR, 94, 467 (1954).
489. M. PAUTHENIER, R. COCHET. Rev. Gener. Electricite, 62, 255 (1953).
490. H. KÖHLER. Meteor. Z., 42, 137 (1925).
491. E. RICHARDSON. Acustica, 2, 141 (1952).
492. M. SMOLUCHOWSKI. "Colloidal coagulation". ONTI, M. - L. - 28 (1936).
493. R. MANLEY, S. MASON, J. Coll. Sci., 7, 354 (1952).
494. L. VEICH. DAN USSR, 94, 809 (1954).
495. N. TUNITSKIY. ZHFKH, 20, 1136 (1946).
496. V. LEVICH. DAN USSR, 94, 1041 (1954).
497. G. DADY. C. R., 225, 1349 (1937).
498. W. SWINBANK. Nature, 159, 849 (1947).
499. N. FUKS. ZHETF, 6, 139 (1936).
500. B. DERYAGIN. Koll. Z., 69, 155 (1934).
501. B. KIN. Physical properties of soils. Gostekhizdat. L. - M. - 1933 chapter 4.
502. R. BRADLEY. Trans. Farad. Soc., 32, 108A (1936).
503. E. RUMYANTSEVA. ZHFKH, 2, 293 (1931).
504. S. URAZOVSKIY, S. KUZMENKO. ZHFKH, 6, 897 (1935).
505. V. SAICHUK, O. NARSKIKH. Colloidal Journal 2, 841 (1936).
506. N. ANDREEV, S. KIBIRKSHITS. ZHOKH, 6, 1698 (1936).
507. L. SMIRNOV, V. SOLNTSEVA. Colloidal Journal 4, 401 (1938).
508. L. RADUSHKEVICH, O. CHUGUNOVA. ZHFKH, 12, 34 (1938).

509. I. PETRYANOV, N. TUNITSKIY, M. TIKHOMIROV. ZHFKH, 15, 811 (1941).
510. I. ARTEMOV. DAN USSR, 50, 289 (1945).
511. M. AGANIN. Geophysics Journal 5, 408 (1935); Izvestiya A. N. USSR, Geography-Geophysics Series 3, 305 (1940).
512. S. GORBACHEV, E. MUSTEL. Koll. Z., 73, 21 (1935).
513. C. GORBACHEV, V. NIKIFOROVA. The same, p. 14.
514. N. TVERSKAYA. Trudy GGO, Publ. 47 (109), 112 (1954).
515. B. DERYAGIN, P. Prokhorov. DAN USSR, 54, 511 (1946).
516. P. PROKHOROV. ZHFKH, 21, 1045 (1947).
517. P. PROKHOROV, V. YASHIN. Colloidal Journal 2, 122 (1948).
518. P. PROKHOROV, L. LEONOV. Colloidal Journal 14, 66 (1952).
519. V. FEDOSEEV, B. MANAKIN, Z. DOMENTIANOVA. Colloidal Journal, 14, 274, 470 (1952).
520. H. GONELL. Koll. Z., 71, 31 (1935).
521. J. BURGOGNE, D. RASBACH. Fuel, 28, 281 (1949).
522. S. SYRKIN. Study of conditions of dusts airborne through tubes. Boiler-Turbine Institute 1935.
523. H. RUMPF. Chemie-Ing. Techn., 25, 328 (1952).
524. YA. AVERBUKH, K. SHABALIN. Chemical Industry, 290 (1947).
525. N. SOKOLOV. Dunes, their formation, development and internal structure. SPb., 1894.
526. A. BAGNOLD. Proc. Roy. Soc., 157 A, 594 (1936).
527. A. BAGNOLD. The physics of blown sand and desert dunes. London, 1941.
528. W. CHEPIL. Soil. Sci., 60, 305, 395 (1945).
529. W. CHEPIL. Soil. Sci., 71, 141 (1951).
530. A. BAGNOLD. Proc. Roy. Soc., 167 A, 282 (1938).
531. N. SOKOLOV. Extracts of H. JEFFREYS' reports. Proc. Cambr. Phil. Soc., 25, 272 (1929).
532. T. YAKUBOV. Wind erosion of soil. Sekhorgiz, 1946.
533. L. DANOVSkiY. Snow fences by roads in Western Siberia. Novosibirsk, 1950.
534. S. CHAPLYGIN. Complete Scripts. Gostekhizdat, M. - L. - 1948, chapter 2, p. 537.
535. H. JEFFREYS. Proc. Cambr. Phil. Soc., 25, 272 (1920).
536. Extracts of reports of M. VELIKANOV. Movement of drifts. Rechizdat, M. - 1948, p. 59.
537. H. EINSTEIN. EL-SAMNI. Rev. Modern Phys., 21, 520 (1949).
538. B. TURITSYN. Heating and ventilation. No. 1 (1935).
539. R. YOUNG. Heat. Ventil. Eng., 26, 469 (1935).
540. B. DERYAGIN, S. RATNER, M. FUTRAN. DAN USSR, 92, 1137 (1953).
541. J. MILLER and others. Science, 107, 144 (1948).

542. R. WILHELM, M. KWAUK. Chem. Eng. Progr., 44, 195 (1948).
543. S. ERGUN, A. ORNING. Ind. Eng. Chem., 41, 1179 (1949).
544. M. LEVA and others. Chem. Eng. Progr., 44, 511, 619 (1948).
545. J. DALLAVALLE. Micromeritics. New York, 1943, p. 118.
546. F. GAN. Analysis of dispersion. Gokhimizdat. M. - 1940, §42.
547. G. AMTHESON, W. HERBST, H. HOLT. Ind. Eng. Chem., 41, 1099 (1949).
548. W. LEWIS, E. GILLILAND, W. BAUER. The same, p. 1104.
549. J. PARENT and others. Chem. Eng. Progr., 43, 429 (1947).
550. R. MORSE, C. BALLON. Chem. Eng. Progr., 47, 199 (1950).
551. E. WICKE, K. HEDDEN. Chemie-Ing. Techn., 24, 82 (1952).
552. G. MATHESON and others. Ind. Eng. Chem., 41, 1099 (1949).
553. W. BRÖTZ. Chemie-Ing. Techn., 24, 60 (1952).
554. M. LEVA, M. GRUMMER. Chem. Eng. Progr., 48, 307 (1952).
555. M. LEVA. Ind. Eng. Chem., 41, 1206 (1949).
556. C. VAN HEERDEN, A. NOBEL, D. van KREVELEN. Chem. Eng. Sci., 1, 37 (1951).
557. O. BRANDT. Koll. Z., 85, 24 (1938).
558. A. ANDREASEN. Koll. Z., 86, 70 (1939).
559. F. TIDESWELL, R. WHEELER. Trans. Inst. Min. Eng., 97, 176 (1938).
560. D. BEISCHER. Koll. Z., 89, 214 (1939); Z. angew. Chem., 52, 514 (1939).
561. T. AOI. J. Phys. Soc. Japan, 10, 119 (1955).
562. O. PREINING. Staub. No. 39, S. 45 (1955).
563. H. ROHATSCHKE. Acta phys. austriaca, 9, 151 (1955).
564. W. STASZEWSKI. Acta phys. polon., 13, 208 (1953).
565. C. N. DAVIES. Proc. Inst. Mech. Eng., IB, 185 (1952).
566. J. WONG, W. RANZ, H. JOHNSTONE. J. Appl. Phys., 26, 244 (1955).
567. C. CHEN. Chem. Rev., 55, 595 (1955).
568. L. KOVASZNAY. Proc. Cambr. Phil. Soc., 44, 58 (1948).
569. A. BLASEWITZ, B. JUDSON. Chem. Eng. Progr., 51, 6-J (1955).
570. L. SILVERMAN, M. FIRST. Ind. Eng. Chem., 14, 2777 (1952).
571. C. WHITE. Proc. Roy. Soc., 186 A, 472 (1946).
572. H. GREEN, D. THOMAS. Proc. Inst. Mech. Eng., IB, 203 (1952).
573. W. CROZIER, B. SEELY. Trans. Am. Geophys. Union, 36, 42 (1955).
574. J. TELFORD, N. THORNDIKE, E. BOWEN. Quart. J. Roy. Meteor. Soc., 81, 241 (1955).
575. D. SARTOR. J. Meteor., 11, 91 (1954).
576. T. EAST, J. MARSHALL. Quart. J. Roy. Meteor. Soc., 80, 26 (1954).
577. V. A. FEDOSEEV, A. I. POLYANSKIY. Trudy, publ. by Odessa Institute, Faculty of Physics and Mathematics, 5, 95 (1954).

578. J. NOLAN, P. NOLAN. Proc. Roy. Irish Acad. , 45 A. 47 (1939).
579. C. MAGONO. J. Meteorol., 11, 77 (1954).
580. W. CUMMINGS and others. J. Appl. Chem., 2, 413 (1952).
581. A. BRYAN, I. SMELLIE. J. Royal Techn. Collega, 4, 406 (1937).

---000---

Subject Index

- Absorption of aerosols
 - by foams 272
 - during bubbling 266
- Absorption of sound
 - by atmospheric fogs 122
 - by aerosols 118
- Adherence of powders 412
- Apparent length of particles free path 203
- Atomization of powders 420
 - influence of humidity 420
- Average Brownian displacement 204
- "Average" sizes of particles 26

- Border line stratum
 - influence upon coefficient of inertial precipitation 174, 197
- Breaking away of particles by air currents 410
- Breaking of aggregates
 - by Brownian spinning 393
 - in air current 188
 - in ultrasonic field 368
- Brownian movement 201
 - development of basic form 205
 - and diffusion 214
 - form of particles trajectories 203
 - characteristics of particles of various sizes 206
 - experimental testing of the theory 207
- Brownian spinning 272
- By-passing of objects of regular form 189

- Calculating concentration of aerosols 27
- Capture (enmeshing) effect 176
 - its influence upon coefficient of particle precipitation 196
- Capture of particles by charged drops 379
- Centrifuge, aerosolic 154
- Classification of aerosols 8, 12
- Cloud, 9
 - by-passed and air-swept 70
 - precipitation 68

- Coagulation of aerosols
 - in a turbulent current 388
 - in ultrasonic field 365
 - influence of molecular forces 355
 - gravitational 370
 - gradient 385
 - of charged aerosols 352
 - kinematic 370
 - directional (oriented) 358
 - during agitation (stirring) 383
 - with particles of irregular shape 347
 - thermal (Brownian) 329
- Coarsely dispersed aerosols 12
- Coefficient
 - of drag resistance 53
 - of precipitation 173, 371
 - of aerosol absorption during bubbling 268
 - of aerosol absorption by filters 243
- Concealment of actual distribution of sizes 18
- Concentration of aerosols, inertial 167
- Condensed aerosols 7
- Conifuge 157
- Curves of size distribution 13, 18
- Curvilinear movement of particles 132
- Cyclone 158
 - dependence of resistance upon dustiness of gas 165, 296
 - theory 160, 298
 - working with models 177
- Deflection of aqueous drops upon collisions 395
- Deformation of drops
 - in electrical field 278
 - in falling 66
- Density of aggregated particles
 - experimental determination 179
- Determination of particle trajectories in curvilinear flow 167
- Differential method of determination of mobilities 144
- Diffusible precipitation of aerosol
 - in a parallel-flat small vessel 226
 - in a parallel-flat duct 236
 - enclosed between two horizontal walls 229
 - from a laminar current in a round tube 234
 - on a vertical wall 220

- on a horizontal wall 226
- on a cylindrical surface 233
- on a spherical surface 232
- on walls of a cylindrical vessel 230
- on walls of a spheroidal vessel 230
- Diffusion
 - from a line and a point source 238
 - convective 280
 - turbulent 292
- Dispersed aerosols 7
- Dispersion of sound by aerosols 116
- Distribution
 - of particle charges 141
 - of particle sizes 12
 - in a coagulating aerosol 345
 - logarithmically-normal 25
- Dusts 8
- Dynamic coefficient of shape 61
- Effectiveness
 - of precipitation 12, 163, 181, 184, 246, 254, 260, 265
 - of collisions
 - between aqueous drops 395
 - between particles 390
 - between particles and a wall 391
- EINSTEIN-FOKKER'S equation 213
- Electrical mobility of particles 46, 140
- Electrofilters 153
- Electrostatic dispersion of aerosols 129
- Empirical equations of distribution 21
- Equivalent radius 35, 64
- "Expanded" powders' stage 415, 417
- Expansion of aerosols in the atmosphere 308
- Factors of polydispersion 341
- Falling of large drops 54, 66
- Filters
 - fibrous 241
 - experimental data 252
 - the role of electrical forces 256
 - resistance 249
 - theory 243, 248
 - granular 257
 - netted and cloth 240

Fluctuations, turbulent 290
 their degree of particles entrainment 292
 Fluidization of powders 414
 Fog 8
 Forces of cohesion in aggregates 415, 417

 Highly dispersed aerosols 12
 Histograms 16
 Hydrodynamic interaction in a sonic field 127
 between precipitating particles 127
 between aerosol particles 123

 Inertial precipitation of aerosols on substances of straight shape 159
 Inertial run 98
 of ultra-STOKES particles 103
 Integral method of determination of mobilities 145
 Ions, heavy 141

 Linear aggregates 34
 formed in electrical or magnetic field 363

 Method
 of vertical electrical field 74
 of horizontal electrical field 81
 Mobility of particles 433
 Motion of particles
 in a curvilinear current 167
 in a turbulent current 290

 Non-inertial motion of particles 98, 100, 114
 Non-spherical particles
 general type of motion 54
 orientation in a gradient current 56
 orientation in electrical field 274
 medium's resistance 58

 Orientation of particles 56, 274
 Oscillations of particles
 in sonic field 109
 in electrical field 108
 under the influence of external forces 104

Photophoresis 87
Polarization of particles in electrical field 274
Precipitation of aerosols
 in respiratory tracts 258
 in electrical field from a laminar current 140
 vortical, behind an obstacle 307
 from the atmosphere 325
 from a turbulent current 297
 inertial on substances of regular shape 189
 on a vertical wall 284
 on a chamber's bottom 280
 general rules 176
 under the influence of gravitational force from a laminar current 136
 during stirring (agitation) 287
 by means of atomized water 376, 397
Principle of similarity in the mechanics of aerosols 170
Probability of reaching
 a vertical or horizontal wall 220
 of a border line 217
 of appearance 215
 of transition 213

Quasi-fixed motion of particles 99

Radiometric forces in aerosols 82
Rapidity of settling
 of aqueous drops 67
 of spherical particles 39, 53
Rectilinear, non-uniform particles motion 93
 at higher Re numbers 101
Rectilinear, uniform motion of particles 99
Relaxation time of particles 40, 94, 96, 103
Resistance of the medium
 in a transitional region 42
 in ultra-STOKES' region 50
 to the motion of very small particles 37
 during variable velocity of motion 93

Sample taking of aerosols 177
Sedimentation (STOKES') radius 35, 61
Settling of aerosols within a limited space 72
Shape of aerosol particles 30
Size of particles in aerosols 9
 determination 35, 78

UNCLASSIFIED
AD

227876

FOR
MICRO-CARD
CONTROL ONLY

9

OF

9

Reproduced by

Armed Services Technical Information Agency

ARLINGTON HALL STATION; ARLINGTON 12 VIRGINIA

UNCLASSIFIED

"NOTICE: When Government or other drawings, specifications or other data are used for any purpose other than in connection with a definitely related Government procurement operation, the U.S. Government thereby incurs no responsibility, nor any obligation whatsoever; and the fact that the Government may have formulated, furnished, or in any way supplied the said drawings, specifications or other data is not to be regarded by implication or otherwise in any manner licensing the holder or any other person or corporation, or conveying any rights or permission to manufacture, use or sell any patented invention that may in any way be related to

Slit instruments 183
 experimental data 186
 stage of particles blowing off 187
 theory 184
Smoke stream in a turbulent atmosphere 309, 325
Smokes 8
Sonic pressure upon particles 114
Sound, its absorption by fogs 117
Spectrum of turbulent fluctuations 291
Sphericity's coefficient 35
STOKES' law 39
 experimental testing 48

Thermal coagulation of aerosols 329
 of highly dispersed aerosols 333
 of polydispersed aerosols 338
 with charged particles 352
 with particles of elongated shape 347
Thermal precipitation 86
Thermophoresis 82
Trajectories of particles, computation 168
Transport
 of sand by wind 403
 of particles by air currents 396
Turbulence
 in the atmosphere 308
 its influence on dispersed phase 296
Turbulent diffusion 292, 296

Unipolar charging of aerosols 130, 263

Vertical distribution of particles in atmosphere 328

Whirling precipitation of aerosols 306

---000---

Approved for printing
by the Institute for Scientific Information
of the Academy of Sciences of the USSR

- 0 -

Publishing Editor N.G. EGOROV
Technical Editor B.A. SOMOROV

- 0 -

RISO AN, USSR No. 1-102 B Released for typesetting 27 Nov. 1955
Approved for printing 12 Dec 1955. Paper size 70 x 108 1/116.
Pech. l. 22 = 30.14 Uch. - izd. list. 24.4. Circulation 3.000. T - 10229.
Publ. No. 1150 Type law 1853
Price 19 rubles

2d Printing Press, Publishing House of the Academy of Sciences of the
USSR Moscow, Shubinskiy Alley, House No. 10.

U. S. Army Chemical Corps Research and Development Command
U. S. ARMY CHEMICAL WARFARE LABORATORIES
Army Chemical Center, Maryland

Errata Sheet to CWL Special Publication 4-12

THE MECHANICS OF AEROSOLS

by

N. A. FUKS

Academy of Sciences of the U. S. S. R.
Institute of Scientific Information
1955

Translated from the Russian by
MSP. E. Lachowicz

Technical Information Division
Directorate of Technical Services
U. S. ARMY CHEMICAL WARFARE LABORATORIES
Army Chemical Center, Maryland

It is requested that the following editorial and typographical corrections as listed below be made.

Page no.	Line no.	As printed	Should read
x	6	probability of occurrence	probability of transition
xi	4	coefficient of apparent volume (volume of	volume coefficient of dispersed phase (volume of
9	27	$10^{-3}-10^{-4} \text{ cm}^2 \text{ B}^{-1} \text{ sec}^{-1}$	$10^{-3}-10^{-4} \frac{\text{cm}}{\text{sec}} \text{ per } \frac{\text{volt}}{\text{cm}}$
9	34	$10^{-3}-10^{-1} \text{ cm}^2 \text{ B}^{-1} \text{ sec}^{-1}$	$10^{-3}-10^{-1} \frac{\text{cm}}{\text{sec}} \text{ per } \frac{\text{volt}}{\text{cm}}$
9	36	$0.2 \text{ cm}^2 \text{ B}^{-1} \text{ sec}^{-1} (3, 4).$	$0.2 \frac{\text{cm}}{\text{sec}} \text{ per } \frac{\text{volt}}{\text{cm}} (3, 4).$
10	12	$0.2 \text{ cm}^2 \text{ B}^{-1} \text{ sec}^{-1}$ is equal	$0.2 \frac{\text{cm}}{\text{sec}} \text{ per } \frac{\text{volt}}{\text{cm}}$ is equal
11	37	$0.5 - 1 \cdot 10^{-5}$ to	$0.5 - 1 \cdot 10^{-5}$ to
12	9	$0.5 - 1 \cdot 10^{-5} \text{ cm},$	$0.5 - 1 \cdot 10^{-5} \text{ cm},$
12	28	$0.5 - 1 \cdot 10^{-5}$ to	$0.5 - 1 \cdot 10^{-5}$ to
13	9	$(r > 3 - 5 \cdot 10^{-5} \text{ cm}),$	$(r > 3 - 5 \cdot 10^{-5} \text{ cm}),$
13	15	$1 - 2 \cdot 10^{-7} \text{ cm}.$	$1 - 2 \cdot 10^{-7} \text{ cm}.$
15	20	$4\pi\gamma r^2 f(m) = f(r).$	$4\pi\gamma r^2 f, (m) = f(r).$
23	6	0 only $r \geq 0$, then	0 only when $r \geq 0$, then
25		Error in pagination.	Page 27 and then first 18 lines at top of page 26 should follow page 25.

Page no.	Line no.	As printed	Should read
26	1	As printed. From line 1, top, through line 18 from the top	Is the continuation of page 27, line 1, bottom.
28	18	value than that which	value, which
31	5	(see page 79),	(see page 74),
39	16	(6.3), see page 38.	(6.3), see page 48.
51	1	resistance changes proportionally to V_s and at the same time V_s increases	resistance is proportional to V^s and at the same time s increases
65	31	$Re_f = 2R\bar{U}y_g/\eta$	$Re_f = 2R\bar{U}y_g/\eta$
75	3	is $E = \pi/\hbar$; where π	is $E = \bar{\pi}/\hbar$; where $\bar{\pi}$
80	21	$F_E = 2\mathcal{K}_E v \text{grad } E^2$,	$F_E = 2\mathcal{K}_E v \text{grad } E^2$,
80	22	where v is the	where v is the
80	30	$F_E = 2\mathcal{K}_E v \text{EdE}/dz$.	$F_E = 2\mathcal{K}_E v \text{EdE}/dz$.
80	33	$\text{EdE}/dz = \frac{mg}{2\mathcal{K}_E v} = \frac{yg}{2\mathcal{K}_E}$	$\text{EdE}/dz = \frac{mg}{2\mathcal{K}_E v} = \frac{yg}{2\mathcal{K}_E}$
84	25	$\bar{\Gamma}_i = \frac{3\chi_a \bar{\Gamma}_a}{3\chi_a + \chi_i}$	$\bar{\Gamma}_i = \frac{3\chi_a \bar{\Gamma}_a}{2\chi_a + \chi_i}$
89	2	$\pi r^2 I - \frac{\chi_a}{r} \int_{\pi} \Delta T dS -$	$\pi r^2 I - \frac{\chi_a}{r} \int_{\pi} \Delta T dS -$
99	30	difference π_o was	difference $\bar{\pi}_o$ was

Page no.	Line no.	As printed	Should read
99	38	$-C_E \frac{d\pi}{dt} = \frac{\pi}{R_E}$	$-C_E \frac{d\Pi}{dt} = \frac{\Pi}{R_E}$
100	2	$\pi = \pi_0 e^{-t/C_E R_E}$	$\Pi = \Pi_0 e^{-t/C_E R_E}$
100	4	and $\pi_0 = 2500$ volts.	and $\Pi_0 = 2500$ volts.
100	8	$\frac{dx}{dt} = \frac{\pi_0 qB}{h} e^{-t/C_E R_E},$	$\frac{dx}{dt} = \frac{\Pi_0 qB}{h} e^{-t/C_E R_E},$
100	11	$x_\infty = \frac{\pi_0 qB}{h} \int_0^\infty e^{-t/C_E R_E} dt =$ $\frac{\pi_0 qB C_E R_E}{h}.$	$x_\infty = \frac{\Pi_0 qB}{h} \int_0^\infty e^{-t/C_E R_E} dt =$ $\frac{\Pi_0 qB C_E R_E}{h}.$
138	15	is equal to ψ and	is equal to Ψ and
138	18	$\partial = \psi_0 / \psi = V_s L / \psi$	$\partial = \psi_0 / \Psi = V_s L / \Psi$
138	20	$\psi = 2h\bar{U},$	$\Psi = 2h\bar{U},$
146	2	potential π within	potential Π within
146	3	taken of π and	taken of Π and
146	16	$V_\rho =$	$V_\rho =$
155	36	of 22 cu in. diameter	of 22 cm in diameter
169		$V_x = V_{xi} + (U_{xi} - V_{xi}) \frac{1}{T}$	$V_x = V_{xi} + (U_{xi} - V_{xi}) \frac{t}{T}$